WOJSKOWA AKADEMIA TECHNICZNA
im. Jarosława Dąbrowskiego

WYDZIAŁ INŻYNIERII MECHANICZNEJ

ROZPRAWA DOKTORSKA

Modelowanie niezawodności i gotowości pojazdów ciężarowo-osobowych funkcjonujących w wojskowych systemach transportowych

kpt. mgr inż. Mateusz Oszczypała

Promotor: **płk dr hab. inż. Jarosław Ziółkowski**

Promotor pomocniczy: **ppłk dr inż. Piotr Kędzierski**

Warszawa 2025

SPIS TREŚCI

STRESZCZENIE

W rozprawie doktorskiej przeprowadzono badania procesu eksploatacji pojazdów jako obiektów będących na wyposażeniu wojskowych systemów transportowych. Szczegółowej analizie poddano podstawowe miary procesu eksploatacji, w zbiorze których znajdują się niezawodność i gotowość. Głównym celem pracy było opracowanie modeli probabilistycznych i symulacyjnych, które mogą być wykorzystane do oceny procesu eksploatacji pojazdów na podstawie wskaźników niezawodności i gotowości. W celu odtworzenia empirycznego przebiegu podprocesów użytkowania, obsługiwania oraz napraw opracowano dwie bazy danych obejmujących próby o liczebnościach wynoszących odpowiednio 19 i 55 pojazdów z uwzględnieniem 3-letniego oraz 5-letniego okresu badań. Najliczniej reprezentowaną marką w grupie 1-szej struktury parku samochodowego (pojazdy ciężarowo-osobowe) był pojazd marki Honker 2000. Główne źródło informacji stanowiła dokumentacja eksploatacyjna obejmująca rozkazy wyjazdu, karty usług technicznych, plany eksploatacji i protokoły stanu technicznego. Podstawę rozprawy doktorskiej stanowi cykl sześciu powiązanych tematycznie publikacji naukowych, omówionych poniżej.

Analiza niezawodności i gotowości pojazdu ciężarowo-osobowego uwzględnia przedmiot badań postrzegany w trzech aspektach. Po pierwsze jako obiekt techniczny, po drugie jako system techniczny złożony z głównych podsystemów oraz po trzecie jako komponent (element) systemu transportowego. W modelach matematycznych opartych o rachunek prawdopodobieństwa i statystykę matematyczną po odtworzeniu badanego procesu eksploatacji oblicza się empiryczne jego miary. W pracy [P1] wykorzystując estymator Kaplana-Meiera wartości funkcji niezawodności zostały obliczone jako prawdopodobieństwa prawidłowej pracy obiektu. Następnie aproksymowano modele wykładnicze i Weibulla w celu wyznaczenia pozostałych charakterystyk niezawodnościowych z uwzględnieniem intensywności użytkowania wyrażanej jako przebieg pojazdu.

W pracach [P2, P3, P4] w dziedzinie czasu eksploatacji do oceny i analizy niezawodności i gotowości pojazdów opracowano modele semi-Markowa o zróżnicowanej przestrzeni stanów. Na podstawie prawdopodobieństw ergodycznych dla modeli 4- i 9-stanowych opisujących proces eksploatacji obliczono wartości wskaźników gotowości, które mieściły się w wąskim zakresie wynoszącym 0,90-0,91. Na podstawie analizy procesu stwierdzono, że stan oczekiwania na naprawę najbardziej obniża gotowość i zdatność pojazdów. Z tego względu przeprowadzono analizę wrażliwości 9-stanowego

modelu semi-Markowa, która wykazała, że redukcja czasu oczekiwania na naprawę o 50% spowodowałaby wzrost wskaźników gotowości i zdatności o około 0,04. Usprawnienie czynności administracyjnych i logistycznych, takich jak pozyskiwanie części zamiennych i materiałów eksploatacyjnych, pozwoliłoby skrócić oczekiwany czas przebywania pojazdów w stanie niezdatności. W efekcie wskaźnik gotowości pojazdów ciężarowo-osobowych spełniłby wymagania stawiane obiektom i systemom wojskowym na poziomie 0,95.

Model 4-stanowy został zastosowany do określenia wpływu intensywności użytkowania na gotowość pojazdu. W tym celu opracowano algorytm symulacyjny bazujący na wielokrotnym próbkowaniu metodą Monte Carlo. Wyselekcjonowano najlepiej dopasowane charakterystyki probabilistyczne poszczególnych podprocesów służące do przeprowadzenia symulacji dla 16 opracowanych modeli Monte Carlo. Wyniki algorytmu symulacyjnego zostały zweryfikowane na podstawie rezultatów modelu semi-Markowa. Następnie najlepiej dopasowany model Monte Carlo został zastosowany do analizy wrażliwości, w której określono wpływ wartości prawdopodobieństwa przydziału zadania transportowego dla pojazdu oraz oczekiwanego dziennego przebiegu na wskaźniki gotowości i zdatności technicznej. Wyniki analizy wykazały, że zwiększenie prawdopodobieństwa przydziału zadania transportowego o wartość 0,01 spowodowało zmniejszenie wartości wskaźników o około 0,002. Natomiast wzrost wartości oczekiwanej dobowego przebiegu o 1 km spowodował nieznaczną redukcję wartości wskaźników gotowości i zdatności technicznej wynoszącą zaledwie 0,0008. Zatem główną zaletą modelu symulacyjnego okazała się zdolność do badania efektywności procesu eksploatacji pojazdów dla różnych poziomów intensywności użytkowania.

W kolejnym etapie badań [P5] opracowano szeregową strukturę niezawodności pojazdu, zbudowaną z siedmiu głównych podsystemów, tj. silnika, układu przeniesienia napędu, układu hamulcowego, układu kierowniczego, zawieszenia, instalacji elektrycznej oraz nadwozia. Na podstawie dokumentacji dla próby liczącej 55 pojazdów marki Honker 2000 z 5-letniego okresu eksploatacji opracowano bazę danych zawierającą 575 kompletnych interwałów pomiędzy uszkodzeniami i 647 obserwacji cenzorowanych[1]. Dla każdego podsystemu aproksymowano dystrybuanty rozkładów granicznych czasów i przebiegów pomiędzy uszkodzeniami. Następnie wykorzystano je do wyznaczenia funkcji niezawodności w dwuwymiarowej dziedzinie za pomocą probabilistycznych

[1] Obserwacje cenzorowane - wartości danej zmiennej, które nie są w pełni znane w momencie zakończenia badania.

kopul Claytona. Następnie zmodyfikowane miary ważności niezawodnościowej zastosowano do identyfikacji podsystemów, które najbardziej obniżają niezawodność pojazdu jako systemu technicznego. Miara ważności Birnbauma oraz miara krytyczna wskazały silnik i instalację elektryczną jako podsystemy najbardziej awaryjne odpowiednio dla 29 i 6 punktów pomiarowych dwuwymiarowej dziedziny funkcji niezawodności. Natomiast miara ważności Barlowa-Proschana określiła najbardziej istotne podsystemy dla całej dziedziny czasu eksploatacji i przebiegu pojazdu, którymi były: silnik, układ przeniesienia napędu oraz instalacja elektryczna.

Ostatnim etapem badań [P6] była analiza gotowości systemu transportowego, zbudowanego z jednorodnych pojazdów reprezentujących progową strukturę niezawodnościową typu k z n. System transportowy obsługuje zmienny w czasie strumień zadań, który opisano za pomocą rozkładu logistycznego. Do opisu zmian stanów niezawodnościowych systemu opracowano model Markowa o $n+1$ stanach. Parametrami wpływającymi na zmianę stanów systemu były intensywności uszkodzeń oraz intensywności napraw pojazdów. Do oceny działania systemu zaproponowano wskaźniki gotowości i efektywności, określające prawdopodobieństwa realizacji zadań transportowych wpływających do systemu. Wartości wskaźników zostały obliczone dwutorowo, tj. stosując podejścia: probabilistyczne i symulacyjne. W przypadku obu wspomnianych metod otrzymano zgodność osiągniętych rezultatów, co spowodowało zmniejszenie ryzyka popełnionego błędu, a tym samym potwierdziło poprawność ich zastosowania. W wyniku analizy możliwości optymalizacji poziomów redundancji strukturalnej systemu wykazano, że przy redukcji floty transportowej z 19 do 10 pojazdów, gotowość i efektywność systemu utrzymuje wymagane poziomy wynoszące 0,95, przy jednoczesnym obniżeniu kosztów budowy i eksploatacji systemu aż o 47%. Ponadto zgodnie z analizą wrażliwości zoptymalizowanego systemu transportowego, przy utrzymaniu bieżącej intensywności napraw, nawet 10-krotny wzrost intensywności uszkodzeń nie spowodowałby obniżenia wartości wskaźników poniżej 0,90.

Opracowane w pracy metody i modele wraz z uzyskanymi wynikami analiz stanowią wartość dodaną w obszarze badanego procesu eksploatacji. Jej podstawowe miary rozumiane jako niezawodność i gotowość obiektów oraz systemów technicznych wpisują się w dziedzinę nauk inżynieryjno-technicznych. Ponadto stanowią oryginalny wkład Autora w dyscyplinę naukową inżynieria mechaniczna. Zaprezentowane wieloaspektowe podejścia, których efektem jest cykl sześciu opublikowanych prac naukowych uzupełniają stan literatury pod względem merytorycznym, metodologicznym i przedmiotowym. Szczegółowe opisy założeń, metodologii, wyników i analiz zostały opublikowane w ramach cyklu wydawniczego zawierającego 6 powiązanych tematycznie artykułów naukowych (Tab. 1.1) opublikowanych w międzynarodowych czasopismach z listy Journal Citation Reports (JCR).

STRESZCZENIE W J. ANGIELSKIM

The doctoral dissertation presents a study of the vehicle operation process as objects within military transport systems. A detailed analysis was conducted on the key measures of the operation process, including reliability and availability. The main purpose of the study was to develop probabilistic and simulation models that can be used to evaluate the vehicle operation process on the basis of reliability and readiness indicators. To empirically reconstruct the subprocesses of usage, maintenance, and repair, two types of databases were developed, comprising samples of 19 and 55 vehicles over 3-year and 5-year study periods, respectively. The most represented vehicle brand in the first group of the vehicle fleet (light utility vehicles) was the Honker 2000. The primary source of information was operational documentation, which included travel orders, technical service records, operation plans, and technical condition reports.

The analysis of the reliability and availability of light utility vehicles considers the subject of the research from three perspectives: first, as a technical object; second, as a technical system composed of major subsystems; and third, as a component of a transport system. In the mathematical models based on probability theory and mathematical statistics, empirical measures of the operation process were calculated after the reconstruction of the studied process. In [P1], using the Kaplan-Meier estimator, reliability functions were calculated as probabilities of correct operation of the object. Exponential and Weibull models were then approximated to determine the remaining reliability characteristics, taking into account usage intensity expressed as vehicle mileage. The dissertation is based on a series of six thematically interconnected scientific articles, which are discussed in detail below.

In studies [P2, P3, P4], semi-Markov models with varied state spaces were developed in the domain of operating time to evaluate and analyze vehicle reliability and availability. Based on ergodic probabilities for the 4- and 9-state models describing the operation process, availability indicators were calculated, ranging narrowly between 0.90 and 0.91. The analysis revealed that waiting for repairs significantly reduces vehicle readiness and operability. Therefore, a sensitivity analysis of the 9-state semi-Markov model was conducted, showing that reducing repair wait time by 50% would increase functional readiness and technical operability indices by approximately 0.04. Streamlining administrative and logistical processes, including the procurement of spare parts and consumables, would significantly reduce the expected downtime of vehicles. Consequently, the

readiness index of light utility vehicles would align with the required 0.95 standard for military facilities and systems.

The 4-state model was applied to assess the impact of usage intensity on vehicle readiness. A simulation algorithm based on Monte Carlo sampling was developed, selecting the best-fit probabilistic characteristics for each subprocess to perform simulations for 16 developed Monte Carlo models. The simulation algorithm's results were verified against those of the semi-Markov model. The best-fit Monte Carlo model was then utilized for sensitivity analysis, where the impact of the probability of task assignment and expected daily mileage on readiness and operability indices was determined. The analysis showed that increasing the probability of task assignment by 0.01 reduced the indices by approximately 0.002, while an increase in expected daily mileage by 1 km reduced the indices by about 0.0008. Thus, the main advantage of the simulation model proved to be its ability to evaluate the efficiency of the vehicle operation process for various levels of usage intensity.

In the next phase of the research [P5], a series-parallel reliability structure of the vehicle, consisting of seven major subsystems (engine, transmission system, brake system, steering system, suspension, electrical installation, and vehicle bodywork), was developed. Based on documentation from 55 Honker 2000 vehicles over a 5-year period, a database containing 575 complete intervals between failures and 647 censored observations was compiled. For each subsystem, the cumulative distribution functions of the times and mileages between failures were approximated. These were then used to determine the reliability functions in a two-dimensional domain using Clayton copulas. Modified reliability importance measures were then applied to identify the subsystems that most reduce the vehicle's reliability as a technical system. The Birnbaum and critical importance measures identified the engine and electrical installation as the most failure-prone subsystems in 29 and 6 measurement points, respectively, within the two-dimensional reliability function domain. The Barlow-Proschan measure determined the most significant subsystems across the entire operating time and mileage domain, identifying the engine, transmission system, and electrical installation.

The final stage of the research [P6] involved analyzing the availability of a transport system composed of homogeneous vehicles representing a threshold reliability structure of the k-out-of-n type. The transport system handles a time-varying stream of tasks, described by a logistic distribution. To describe changes in the system's reliability states, a Markov model with $n+1$ states was developed. Parameters affecting state changes included failure rates and repair rates of the vehicles. Availability and performance indicators, which describe the probability of completing incoming transport tasks, were proposed to evaluate the system's efficiency. These indicators were calculated using both probabilistic and simulation approaches, with both methods yielding consistent results, thereby reducing the risk of error and confirming their correctness. The analysis of the system's structural redundancy levels showed that reducing the fleet from 19 to 10 vehicles maintained the required availability and efficiency levels of 0.95 while reducing system construction and operational costs by as much as 47%. Moreover, the sensitivity analysis of the optimized transport system indicated that, even with a 10-fold increase in failure rates, the indices remained above 0.90, provided the current repair intensity was maintained.

The methods and models developed in the thesis, together with the analysis results, bring added value to research on the vehicle operation process. Its key measures, understood as the reliability and availability of technical objects and systems, fall within the field of engineering sciences. Additionally, they represent the author's original contribution to the scientific discipline of mechanical engineering. The presented multi-faceted approaches, resulting in a series of six published scientific papers, complement the current literature both methodologically and substantively. Detailed descriptions of the assumptions, methodologies, results, and analyses have been published in a series of six thematically related scientific articles (Tab. 1.1) in international journals listed in the Journal Citation Reports (JCR).

WYKAZ SKRÓTÓW

BIM – miara ważności Birnbuma (ang. *Birnbaum Importance Measure*)

BPIM – miara ważności Barlowa-Proschana (ang. *Barlow-Proschan Importance Measure*)

CIM – krytyczna miara ważności (ang. *Criticality Importance Measure*)

CTMC – ang. *Continuous-Time Markov Chain*

JCR – ang. *Journal Citation Reports*

KUT – Karta Usług Technicznych

MC – Monte Carlo

MLP – perceptron wielowarstwowy (ang. *Multilayer Perceptron*)

NATO – Sojusz Północnoatlantycki (ang. *North Atlantic Treaty Organization*)

PST – Park Sprzętu Technicznego

SpW – sprzęt wojskowy

SZ RP – Siły Zbrojne Rzeczpospolitej Polskiej

TPM – wskaźnik efektywności (ang. *Technical Performance Measure*)

1. WYKAZ PUBLIKACJI STANOWIĄCYCH PODSTAWĘ ROZPRAWY DOKTORSKIEJ

Tab. 1.1. Wykaz publikacji naukowych

Ozn.	Dane bibliograficzne	Punkty MNiSW[2]	Impact Factor[3]	Udział doktoranta
P1	**Oszczypała M.,** Ziółkowski J., Małachowski J., *Reliability Analysis of Military Vehicles Based on Censored Failures Data*, Applied Sciences 2022, Volume 12, Issue 5, 2622, DOI: 10.3390/app12052622	100	2,5	75%
P2	**Oszczypała M.,** Ziółkowski J., Małachowski J., *Analysis of Light Utility Vehicle Readiness in Military Transportation Systems Using Markov and Semi-Markov Processes*, Energies 2022, 15(14), 5062. DOI: 10.3390/en15145062	140	3,0	75%
P3	**Oszczypała M.,** Ziółkowski J., Małachowski J., *Modelling the Operation Process of Light Utility Vehicles in Transport Systems Using Monte Carlo Simulation and Semi-Markov Approach*, Energies 2023, 16(5), 2210. DOI: 10.3390/en16052210	140	3,0	75%
P4	**Oszczypała M.,** Ziółkowski J., Małachowski J., *Semi-Markov approach for reliability modelling of light utility vehicles*, Eksploatacja i Niezawodnosc – Maintenance and Reliability 2023, 25(2), DOI: 10.17531/ein/161859	140	2,2	80%
P5	**Oszczypała M.,** Konwerski J., Ziółkowski J., Małachowski J., *Reliability analysis and redundancy optimization of k-out-of-n systems with random variable k using continuous time Markov chain and Monte Carlo simulation*, Reliability Engineering and System Safety 2023, 109780, DOI: 10.1016/j.ress.2023.109780	140	9,4	45%
P6	**Oszczypała M.,** Konwerski J., Ziółkowski J., Małachowski J., *Copula-Based Reliability Analysis of Vehicles Based on Censored Failures Data Using Reliability Importance Measures*, IEEE Access 2024, DOI: 10.1109/ACCESS.2024.3450076	100	3,4	75%
Sumarycznie		**760**	**23,5**	**-**

[2] Lista MNiSW z dnia 05.01.2024 r.
[3] Wskaźniki IF podano na podstawie Journal Citation Reports 2024.

2. UZASADNIENIE PODJĘCIA TEMATYKI BADAWCZEJ

Obecna sytuacja geopolityczna oraz trwające konflikty mają wpływ na postrzeganie bezpieczeństwa rozumianego w skali globalnej. Trwała tendencja do wzrostu wydatków na obronność jest spowodowana zwiększonym zagrożeniem trwającego konfliktu Rosja-Ukraina oraz prawdopodobieństwem wybuchu kolejnych konfliktów lub szerzej ryzykiem wybuchu III wojny światowej. Zmiana mentalności elit politycznych i społeczeństw oraz opinie ekspertów z zakresu obronności prowadzą do skupienia uwagi na kwestiach przygotowania sił zbrojnych do odstraszania potencjalnego przeciwnika państw-członków Sojuszu Północnoatlantyckiego (NATO). Zdolności bojowe wojsk są ściśle związane z posiadaniem nowoczesnego i niezawodnego sprzętu wojskowego (SpW) oraz odpowiednim zabezpieczeniem logistycznym (szczególnie w aspekcie technicznym). System transportowy Sił Zbrojnych RP stanowi jeden z kluczowych elementów systemu logistycznego, a jego celem jest zabezpieczeniem potrzeb w zakresie szybkiego i skutecznego przemieszczania sił i środków do obszaru prowadzenia działań. Transport spełnia kluczową rolę dla zapewnienia dostaw zaopatrzenia, obejmujących amunicję, paliwo, żywność i inne istotne dla realizacji zadań zasoby. Posiadanie zdolności w sferze transportu umożliwia nie tylko szybki (strategiczny) przerzut wojsk, ale również skuteczne i elastyczne dostawy, a także dostosowanie się do różnorodnych scenariuszy działań bojowych. Należy jednocześnie podkreślić, że efektywność systemu transportowego zależy w głównej mierze od niezawodności i gotowości środków transportowych. Z tego względu właściwe planowanie i realizacja procesu eksploatacji pojazdów wojskowych stanowi ważne zadanie nie tylko dla specjalistów logistyki wojskowej, ale przede wszystkim dla analityków, projektantów i administratorów takich systemów oraz dla środowisk akademickich badających eksploatację SpW.

Utrzymywanie wysokich wartości wskaźników niezawodności i gotowości systemów wojskowych ma jednak swoją cenę. Powszechną praktykę stanowi stosowanie redundancji strukturalnej. Oznacza ona w przypadku systemów wojskowych wyposażanie jednostek wojskowych w nadmiarowe liczbowo jednostki sprzętowe (zwane rezerwą), które znacząco przekraczają potrzeby wynikające z bieżącego użytkowania w czasie pokoju. Ich przeznaczenie polega na zabezpieczaniu zadań zawiązanych z losowymi awariami obiektów i fluktuacjami obciążenia systemu. Z ekonomicznego punktu widzenia nadmiarowość taka jest zjawiskiem niepożądanym, generującym wysokie koszty zarówno budowy, jak i utrzymywania takich systemów. Problemów redundancji nie można jednak rozwiązać bez znajomości wielu miar (wskaźników) niezawodności i gotowości. Z tego względu niezwykle istotne jest opracowanie modeli niezawodnościowych, które odzwierciedlą specyfikę wojskowych systemów transportowych oraz stanowią przydatne narzędzie służące poprawie ich funkcjonowania.

W obecnym stanie literatury naukowej badania dotyczące wojskowych środków transportowych stanowią nieliczną grupę publikacji w czasopismach o zasięgu międzynarodowym. Główną przyczynę stanowią ograniczenia w dostępie do informacji, które są często objęte klauzulą niejawności. Pozyskanie szczegółowych danych eksploatacyjnych o sprzęcie wojskowym, który jest na bieżącym wyposażeniu sił zbrojnych danego państwa nie jest łatwe. Aktualna wiedza stosowana na temat sprzętu wojskowego jest bowiem starannie chronioną strategią rządów i korporacji. Ujawnia się ją dopiero wiele lat po jej dezaktualizacji. Dzieje się tak z powodu okresów karencji generujących dochody. W przypadku żołnierzy zawodowych istnieje możliwość pozyskania danych dotyczących SpW. Warunkami koniecznymi są jednak zgoda dowódcy jednostki i anonimizacja danych.

Dotychczasowe publikacje naukowe w obszarze eksploatacji pojazdów wskazują na przydatność modeli probabilistycznych w wyznaczaniu charakterystyk niezawodnościowych [1]. Do modelowania gotowości obiektów technicznych nadal często wykorzystywane są procesy Markowa i semi-Markowa, jednak ich aplikacyjność wymaga identyfikacji przestrzeni stanów, dostosowanych do przedmiotu badań i celów badawczych. W publikacji [2] Migawa zaproponował 16-stanowy model semi-Markowa do wyznaczenia wskaźników gotowości i optymalizacji zarządzania flotą transportową. Z kolei Girtler i Ślęzak [3] opracowali 4-stanowy model eksploatacji pojazdów, w którym zidentyfikowali stany o szczególnym znaczeniu dla ich niezawodności. W literaturze spotyka się również mniejsze przestrzenie stanowe procesów eksploatacyjnych, jak np. 3-stanowy model Markowa skonstruowany przez Kamlu i Laxmi [4] oraz 3-stanowy model semi-Markowa opracowany przez Borucką [5]. Mniejsza liczba stanów upraszcza złożoność obliczeniową, jednak wraz ze zwiększaniem przestrzeni stanowej pojawia się możliwość identyfikacji szeregu czynników, które wpływają na charakterystyki niezawodnościowe obiektu. Modele stochastyczne oparte na teorii procesów Markowa i semi-Markowa są powszechnie stosowanymi metodami badań eksploatacji, jednak ich uniwersalność jest ograniczona, ponieważ każdy rodzaj obiektu (z uwzględnieniem marki i wersji wyposażenia) posiada inną strategię eksploatacji, realizuje odmienne rodzaje zadań i w efekcie stanowi odrębny przedmiot badań. Jednocześnie ważnym aspektem aplikacyjności modeli Markowa opracowanych na rzeczywistych danych eksploatacyjnych obiektów są liczebności oraz częstotliwości przejść międzystanowych obliczone na podstawie danych empirycznych analizowanego procesu eksploatacji [6]. Dodatkowo w badaniach procesów eksploatacji wykorzystuje się symulacje Monte Carlo w dwóch aspektach, tj. po pierwsze, do walidacji modeli probabilistycznych, a po drugie, do badania hipotetycznych scenariuszy [7]. Ponadto znaczącym ograniczeniem dotychczasowych opracowań naukowych w obszarze badań niezawodności i gotowości pojazdów był brak uwzględnienia synergicznego wpływu czynników związanych z czasem eksploatacji (czas fizyczny) oraz wielkością wykonanej pracy (przebieg pojazdu) na wskaźniki niezawodności i gotowości [8–10].

Wybór pojazdów ciężarowo-osobowych jako przedmiotu badań był umotywowany w szczególności dwoma następującymi powodami. Po pierwsze, w dotychczasowych pracach naukowych brakuje opracowań dotyczących tego typu pojazdów, co skłania do podjęcia próby skonstruowania charakterystyk eksploatacyjnych (w tym niezawodnościowych) obejmujących tę grupę pojazdów. Stanowi to uzupełnienie luki przedmiotowej w literaturze naukowej. Po drugie, należy podkreślić aspekt utylitarny wynikający z faktu, iż pojazdy ciężarowo-osobowe stanowią znaczny odsetek całej floty transportowej Sił Zbrojnych RP. Zatem wnioski i spostrzeżenia wysunięte na bazie przeprowadzonych badań naukowych mogą mieć istotny wpływ na funkcjonowanie wojskowych systemów transportowych.

3. WPROWADZENIE, ZAKRES I CEL PRACY

3.1. Wprowadzenie

Przedmiotem rozważań naukowych podjętych w niniejszej rozprawie doktorskiej są pojazdy ciężarowo-osobowe, stanowiące znaczący odsetek środków transportowych będących na wyposażeniu Sił Zbrojnych RP. Obiektem badań był pojazd marki Honker 2000, którego sylwetkę zaprezentowano na Rys. 3.1. Pojazd z uwagi na przeznaczenie służy do transportu ludzi (maksymalnie 9 osób) oraz ładunków (do masy 1000 kg). Obiekt badań został sklasyfikowany do grupy 1, tj. pojazdów ciężarowo-osobowych wysokiej mobilności oraz podgrupy 1.1 według struktury parku samochodowego przedstawionego na Rys. 3.2. Zgodnie z instrukcją użytkowania jest on również przystosowany do holowania przyczepy o masie całkowitej do 750 kg (bez hamulca) lub do 1500 kg (z hamulcem najazdowym). Pojazd jest napędzany czterosuwowym, czterocylindrowym, rzędowym silnikiem o zapłonie samoczynnym z wtryskiem pośrednim. Pojemność silnika wynosi 2417 cm^3, co pozwala na wygenerowanie maksymalnej mocy na poziomie 75 kW przy prędkości obrotowej 4100 obr/min oraz maksymalnego momentu obrotowego równego 230 Nm dla 2000 obr/min [11].

Rys. 3.1. Przedmiot prowadzonych badań naukowych – Honker 2000 (Źródło: https://autokatalog.pl/intrall/honker-2000/i/dane-techniczne)

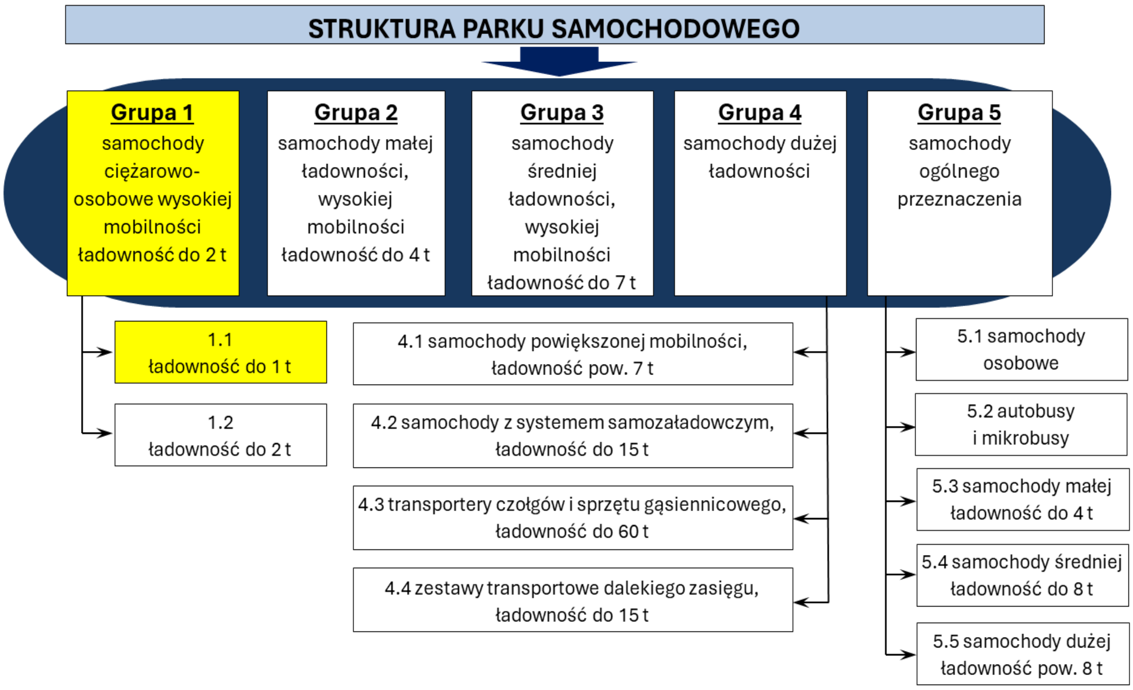

Rys. 3.2. Struktura parku samochodowego w SZ RP [12]

Proces eksploatacji pojazdów ciężarowo-osobowych w SZ RP jest realizowany według strategii planowo-zapobiegawczej. Zakłada ona przeprowadzanie obsług okresowych w ściśle zdeterminowanym zakresie czynności obsługowych. Obsługi są realizowane zgodnie z określonym interwałem czasu eksploatacji lub według zużytego resursu mierzonego wykonaną pracą (przebiegiem). Eksploatacja środków transportowych jest planowana na okres roku kalendarzowego. Jej podstawę stanowią plany eksploatacji i ewidencji sprzętu wojskowego na dany rok. Dokument ten jest opracowywany przez sekcję logistyczną jednostek wojskowych i monitorowany (nadzorowany) przez Wojskowe Oddziały Gospodarcze (WOG-i). Dokumentem rozliczeniowym każdorazowego użytkowania pojazdu jest rozkaz wyjazdu, który określa m. in. dane użytkownika, czas rozpoczęcia i zakończenia pracy, pokonany dystans, zużyte paliwo i inne materiały eksploatacyjne oraz przeprowadzone obsługiwania bieżące przed- i po wyjeździe. W razie wystąpienia niesprawności pojazdu i konieczności przeprowadzenia czynności diagnostycznych, wykonuje się pisemnie protokół stanu technicznego, który określa przyczyny wystąpienia awarii i wskazuje elementy niezbędne do naprawy lub wymiany. Do ewidencji przeprowadzonych obsług okresowych i napraw opracowywane są karty usług technicznych (KUT). Zawierają one zakres przeprowadzonych czynności obsługowo-naprawczych, czasy ich realizacji, części zamienne i materiały eksploatacyjne niezbędne do naprawy oraz pracochłonność.

W ramach realizacji badań pozyskano dokumentację eksploatacyjną z Wojskowych Oddziałów Gospodarczych oraz z Brygady Logistycznej. Na jej podstawie opracowano źródłowe bazy danych w celu odtworzenia procesu eksploatacji 19 pojazdów ciężarowo-osobowych marki Honker 2000. Badania dotyczyły trzyletniego okresu, obejmującego lata 2017, 2019 i 2020. Ponadto do badań nad niezawodnością pojazdu jako systemu technicznego złożonego z podstawowych podsystemów, zgromadzono informacje na temat uszkodzeń komponentów pojazdów występujących w okresie 5 lat dla próby o liczebności 55 obiektów. Obydwie próby badawcze były jednorodne, a proces ich eksploatacji był realizowany według analogicznej strategii użytkowania i obsługiwania.

3.2. Cel i zakres pracy

Przyjęta przez autora w niniejszej rozprawie koncepcja analizy przedmiotu badań została przedstawiona na Rys. 3.3. Pojazd ciężarowo-osobowy jest rozważany jako obiekt techniczny bez dekompozycji na elementy składowe wchodzące w jego budowę. Jest to najczęściej spotykane podejście do modelowania niezawodności pojazdów. Jednakże, aby zidentyfikować potencjalnie najbardziej i najmniej niezawodne jego elementy, należy opracować model odzwierciedlający strukturę niezawodnościową pojazdu, a zatem przyjąć, że jest on złożonym systemem technicznym. Ponadto, w ramach rozprawy przeanalizowano poprawność działania całego systemu transportowego jako floty, w której pojazd stanowi komponent realizujący strumień zadań wpływających do systemu. Przedstawione powyżej wieloaspektowe podejście do modelowania niezawodności i gotowości pojazdów ciężarowo-osobowych zostało zaimplementowane w ramach przeprowadzonych badań naukowych.

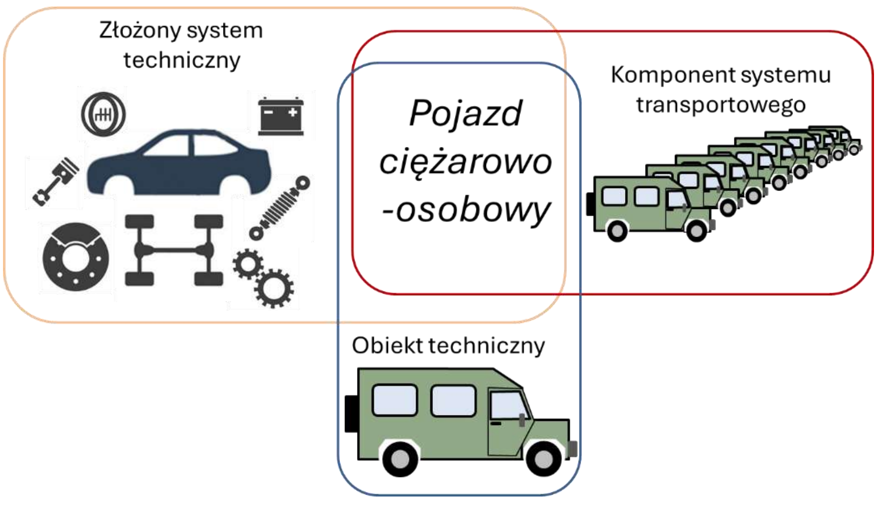

Rys. 3.3. Koncepcja analizy przedmiotu badań (Źródło: Opracowanie własne)

Na podstawie obecnego stanu wiedzy naukowej oraz praktyki inżynierskiej sformułowano w niniejszej rozprawie doktorskiej hipotezę badawczą, zgodnie z którą *zastosowanie metod probabilistycznych i symulacyjnych umożliwia opracowanie modeli służących do wieloaspektowej analizy i oceny niezawodności oraz gotowości pojazdów ciężarowo-osobowych eksploatowanych w systemach wojskowych*.

Zakres niniejszej rozprawy doktorskiej obejmuje:

- analizę literatury w zakresie metod modelowania niezawodności i gotowości obiektów oraz systemów technicznym ze szczególnym uwzględnieniem pojazdów mechanicznych;
- analizę procesu eksploatacji pojazdów ciężarowo-osobowych marki Honker 2000, realizujących zadania transportowe jednostki wojskowej w czasie pokoju;
- modele probabilistyczne, stochastyczne (Markowa) i symulacyjne (Monte Carlo) do wyznaczenia wskaźników niezawodności i gotowości obiektu technicznego;
- modele niezawodności podsystemów pojazdu z uwzględnieniem czasu eksploatacji i przebiegu pojazdu;
- analizę systemu transportowego wybranej jednostki wojskowej pod względem poziomów redundancji floty pojazdów ciężarowo-osobowych.

Głównym celem pracy było opracowanie oraz implementacja modeli probabilistycznych i symulacyjnych do wieloaspektowej analizy niezawodności i gotowości pojazdów ciężarowo-osobowych, będących na wyposażeniu wojskowych systemów transportowych. Realizacja celu głównego została zdekomponowana na następujące cele szczegółowe pracy:

- **[C1]** estymacja funkcji niezawodności na podstawie danych empirycznych pochodzących z obserwacji rzeczywistych procesów eksploatacji;
- **[C2]** opracowanie modelu niezawodnościowego uwzględniającego charakterystykę prowadzonych obsług okresowych w ramach planowo-zapobiegawczej strategii eksploatacyjnej;
- **[C3]** opracowanie oraz porównanie modeli gotowości pojazdów ciężarowo-osobowych jako obiektów technicznych o zróżnicowanej przestrzeni stanów;
- **[C4]** zbadanie wpływu intensywności użytkowania pojazdów na ich gotowość;
- **[C5]** identyfikacja podsystemów pojazdu o największej awaryjności i kluczowym znaczeniu dla niezawodności pojazdu;

— **[C6]** określenie gotowości systemu transportowego oraz wpływu parametrów procesów uszkodzeń i napraw na gotowość systemu obsługującego zmienny w czasie strumień zadań transportowych.

Na Rys. 3.4 przedstawiono schemat realizacji celów szczegółowych rozprawy doktorskiej z uwzględnieniem zastosowanych metod i modeli oraz empirycznych danych eksploatacyjnych niezbędnych do estymacji parametrów modeli. Szczegółowe opisy przeprowadzonych badań i osiągniętych wyników zostały zamieszczone w rozdziałach 4–6 niniejszej rozprawy.

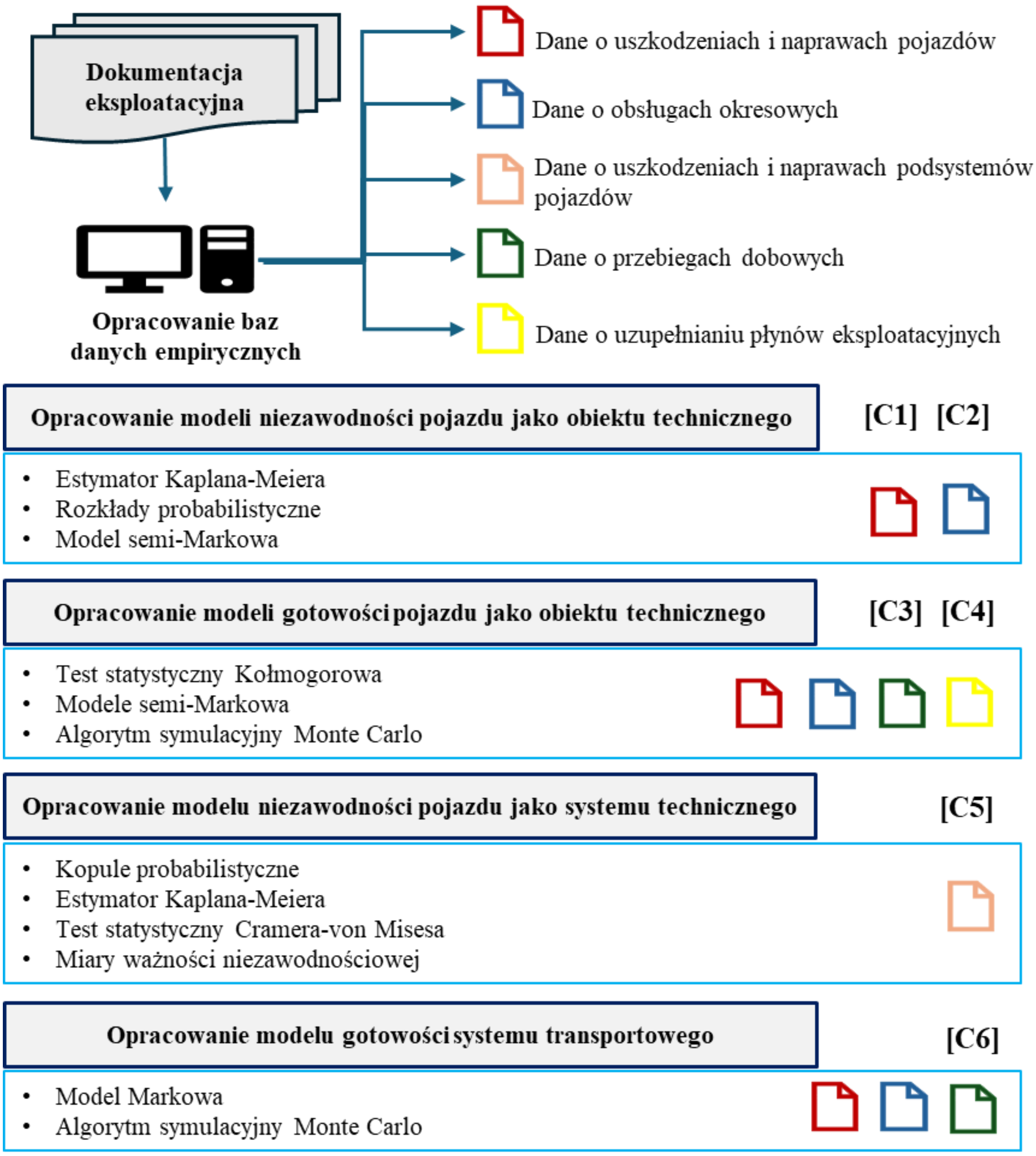

Rys. 3.4. Schemat realizacji szczegółowych celów rozprawy doktorskiej (Źródło: Opracowanie własne)

4. MODELOWANIE MATEMATYCZNE PROCESU EKSPLOATACJI POJAZDU CIĘŻAROWO-OSOBOWEGO Z UWZGLĘDNIENIEM NIEZAWODNOŚCI I GOTOWOŚCI

W niniejszym rozdziale zaprezentowano modele matematyczne umożliwiające analizę i ocenę niezawodności oraz gotowości pojazdów marki Honker 2000. Opisy szczegółowe zastosowanych metodologii, wyniki badań oraz wykonane analizy zostały zawarte w publikacjach **[P1]**, **[P2]**, **[P3]** i **[P4]**.

4.1. Wybrane aspekty analizy niezawodności pojazdu ciężarowo-osobowego

Niezawodność jako miara procesu eksploatacji reprezentuje charakterystykę obiektu lub systemu technicznego, definiującą jego zdolność do skutecznego wykonywania zadań zgodnie z określonym przeznaczeniem [13–15]. Analiza niezawodności w kontekście obiektów technicznych stanowi istotny aspekt w procesie zarządzania systemami technicznymi. Wystąpienie awarii w maszynach, urządzeniach lub obiektach negatywnie wpływa na efektywność procesów produkcyjnych i logistycznych, które wykorzystują te środki techniczne [16,17]. Modelowanie procesu eksploatacji, włączając prognozowanie potencjalnych uszkodzeń, umożliwia minimalizację strat w całym systemie. Ponadto, postrzeganie niezawodności w szerokim ujęciu stanowi istotne wsparcie dla planowania regularnych prac konserwacyjnych oraz zarządzania zapasami części zamiennych [18,19]. Z tego powodu w różnych dziedzinach nauki, techniki i gospodarki podejmowane są próby stworzenia modeli odzwierciedlających rzeczywiste procesy eksploatacji obiektów i urządzeń technicznych [20–22].

Niezawodność obiektu technicznego jest powszechnie rozumiana jako prawdopodobieństwo zdarzenia, że obiekt techniczny użytkowany w określonych warunkach, będzie przebywać nieprzerwanie w stanie sprawności technicznej do danej chwili *t* [23–26]. Można to opisać zależnością (4.1):

$$R(t) = P(T \geq t) \; dla \; t \geq 0. \tag{4.1}$$

Funkcja niezawodności $R(t)$ i funkcja zawodności $F(t)$ stanowią układ zupełny zdarzeń, z czego wynika poniższa własność (4.2):

$$R(t) + F(t) = 1. \tag{4.2}$$

Funkcja niezawodności jest nierosnąca, co w literaturze jest interpretowane jako zmniejszanie się wartości prawdopodobieństwa poprawnego działania obiektu technicznego wraz ze wzrostem wykonanej pracy. Zależność (4.2) implikuje zatem własność funkcji zawodności, jaką jest jej niemalejąca monotoniczność, która wynika również z założenia, że wraz z ilością wykonanej pracy przez dany obiekt wzrasta prawdopodobieństwo jego uszkodzenia [27,28].

Charakterystykami określającymi prawdopodobieństwo wystąpienia uszkodzenia w danej chwili t jest funkcja gęstości prawdopodobieństwa powstania uszkodzenia $f(t)$ oraz funkcja intensywności uszkodzeń $\lambda(t)$. Funkcja $f(t)$ oznacza przypadające na jednostkę resursu prawdopodobieństwo powstania uszkodzenia w chwili *t*. Z rachunku prawdopodobieństwa wynika, że gęstość powstania uszkodzenia $f(t)$ jest pochodną funkcji zawodności $F(t)$, co przedstawia równanie (4.3):

$$f(t) = \frac{dF(t)}{dt} = F'(t). \tag{4.3}$$

Funkcja intensywności uszkodzeń $\lambda(t)$ określa przypadającą na jednostkę resursu wartość prawdopodobieństwa warunkowego uszkodzenia obiektu technicznego w chwili t, pod warunkiem, że nie uległ on uszkodzeniu w przedziale $(0, t)$. Wartość funkcji $\lambda(t)$ w chwili *t* wyraża się zależnością (4.4):

$$\lambda(t) = \frac{f(t)}{R(t)}. \tag{4.4}$$

Dla znanego przebiegu funkcji niezawodności $R(t)$ oczekiwany czas (przebieg) poprawnej pracy obiektu technicznego bez uszkodzenia oblicza się jako całkę oznaczoną według wzoru [26,29] (4.5):

$$ET = \int_0^\infty R(t)dt. \tag{4.5}$$

4.1.1. Wyznaczenie niezawodności z uwzględnieniem intensywności użytkowania

W przypadku pojazdu wielkość wykonanej pracy jest mierzona za pomocą pokonanego dystansu (przebiegu) wyrażonego w kilometrach (km) [8]. W związku z tym w ramach przeprowadzonych badań, jednym z zastosowanych podejść jest opracowanie modeli niezawodnościowych w dziedzinie przebiegu od ostatniego uszkodzenia obiektu. Rozważania na ten temat przeprowadzono w publikacji **[P1]**. Według dokumentacji eksploatacyjnej badania eksploatacyjne polegające na obserwacji i akwizycji empirycznych danych pochodzących z realizacji rzeczywistych procesów eksploatacji były prowadzone przez cały okres. Cechą charakterystyczną takich danych jest występowanie obserwacji cenzorowanych (uciętych), tj. sytuacji, w których obiekt pracował poprawnie (przebywał w stanie zdatności) od chwili ostatniego uszkodzenia i naprawy aż do końca prowadzenia badań. Pominięcie tych danych byłoby równoważne z popełnieniem błędu metodologicznego, co w efekcie mogłoby skutkować niepełnym odwzorowaniem rzeczywistości i błędnymi wynikami z przeprowadzonych analiz. Z tego względu, zaimplementowano znany z analizy przeżycia estymator Kaplana-Meiera do estymacji wartości funkcji niezawodności dla danych zawierających obserwacje cenzorowane. Estymowane wartości są obliczane zgodnie z zależnością (4.6):

$$\hat{R}(t_i) = \prod_{j:t_i \leq t_j}^{i} \left(1 - \frac{d_j}{n_j}\right), \tag{4.6}$$

gdzie: d_j oznacza liczbę obiektów technicznych, które doznały awarii w chwili t_j, natomiast n_j oznacza liczbę wszystkich obiektów technicznych, które nie uległy awarii do momentu t_j.

Następnie przy wykorzystaniu nieliniowej metody najmniejszych kwadratów aproksymowano funkcję niezawodności dla dwóch zasadniczych niezawodnościowych rozkładów probabilistycznych: wykładniczego i Weibulla, których postacie analityczne przedstawiono za pomocą wzorów (4.7)-(4.8):

$$R(t) = e^{-0{,}000235t}, \tag{4.7}$$

$$R(t) = e^{-0{,}000574t^{0{,}889}}. \tag{4.8}$$

Aproksymowane modele probabilistyczne funkcji niezawodności pojazdów przedstawiono graficznie na Rys. 4.1 i 4.2. Model wykładniczy i Weibulla przechodzą blisko wartości estymowanych na podstawie estymatora Kaplana-Meiera, co potwierdziły wysokie wartości współczynników korelacji wynoszące odpowiednio $R = 0{,}9945$ i $R = 0{,}9971$.

W celu zwiększenia wiarygodności wyników otrzymanych za pomocą modelu wykładniczego i Weibulla, aproksymację funkcji niezawodności przeprowadzono również z wykorzystaniem algorytmów uczenia maszynowego. Do wytrenowania perceptronu wielowarstwowego (MLP) zastosowano algorytm uczenia Levenberga-Marquardta zaimplementowany w środowisku MATLAB. Wynik aproksymacji o dopasowaniu do wartości empirycznych na poziomie $R = 0{,}9975$ przedstawiono na Rys. 4.3.

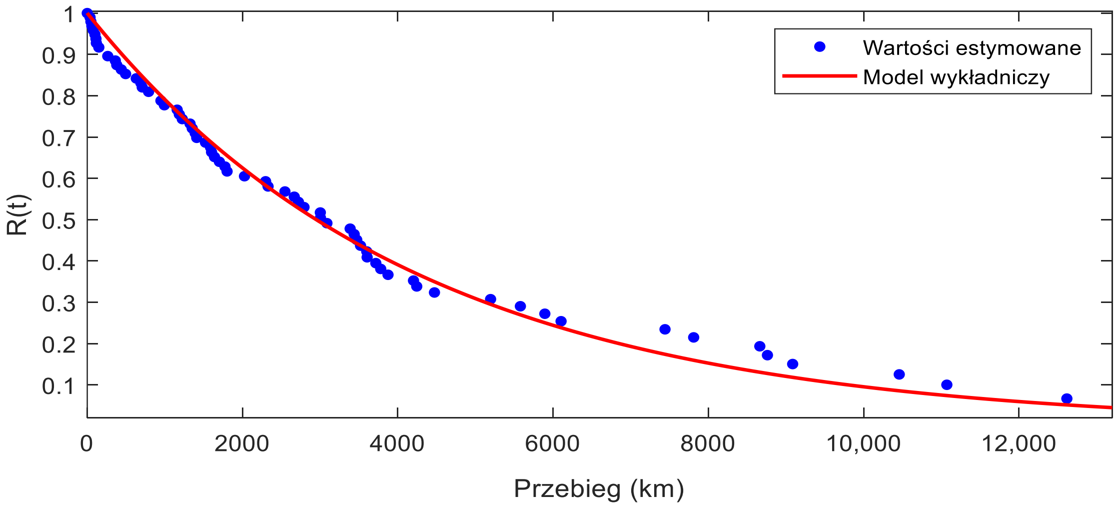

Rys. 4.1. Przebieg modelu wykładniczego funkcji niezawodności **[P1]**

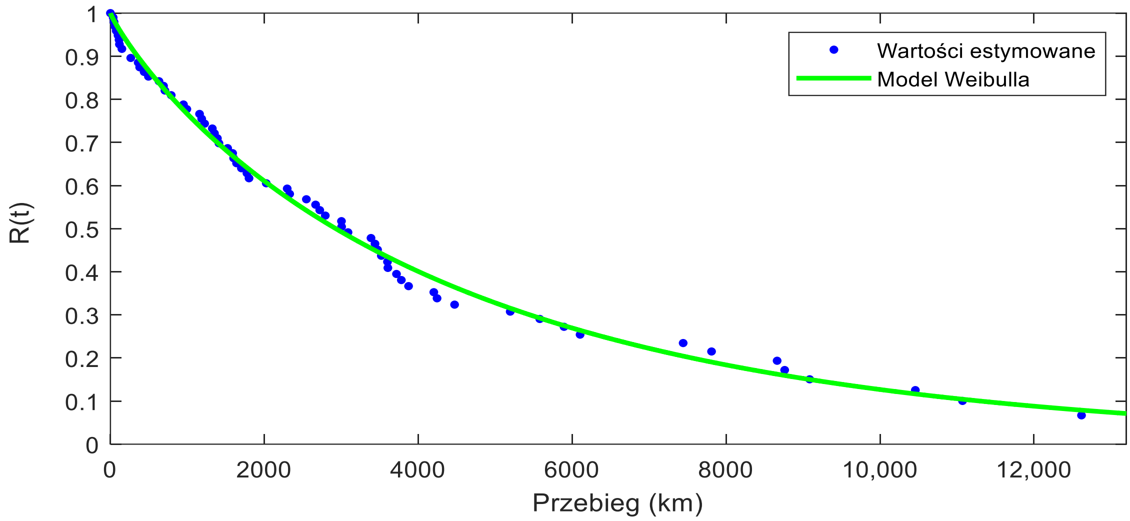

Rys. 4.2. Przebieg modelu Weibulla funkcji niezawodności **[P1]**

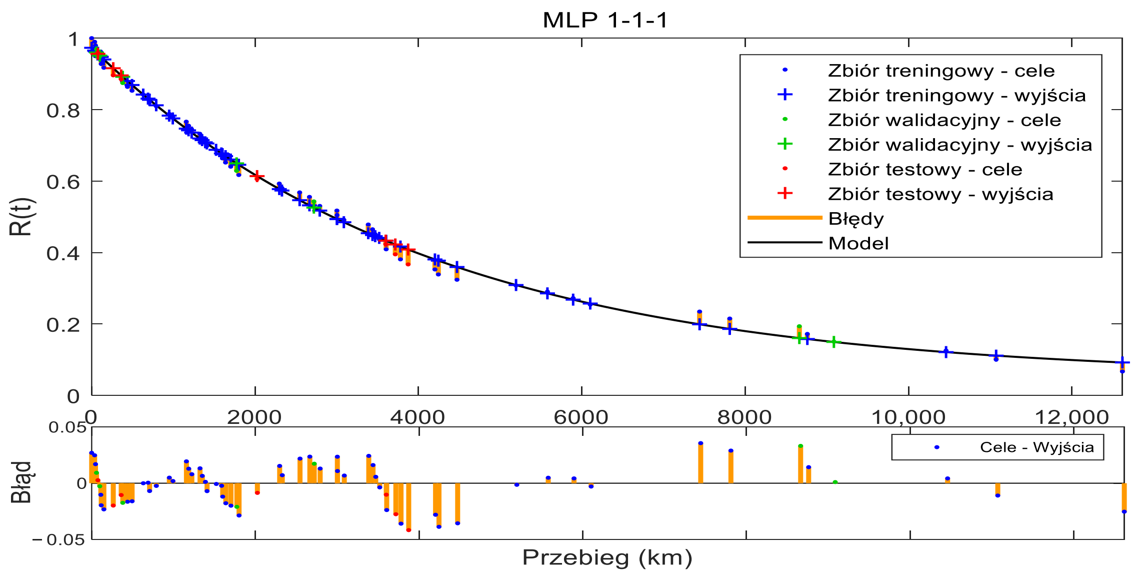

Rys. 4.3. Funkcja niezawodności aproksymowana przez sieć MLP 1-1-1 **[P1]**

Na podstawie wag połączeń synaptycznych modelu MLP 1-1-1 wyprowadzono postać analityczną funkcji niezawodności pojazdu opisaną zależnością (4.9):

$$R(t) = \frac{32{,}9 + 1{,}78e^{0{,}000249t}}{1 + 34{,}7e^{0{,}000249t}}. \tag{4.9}$$

Podsumowując, estymacja funkcji niezawodności w dziedzinie ilości wykonanej pracy przez pojazd ciężarowo-osobowy, oparta na cenzorowanych danych dotyczących uszkodzeń, została przeprowadzona z zastosowaniem estymatora Kaplana-Meiera. Bazując na estymatorach, można skutecznie wyznaczyć postać analityczną funkcji niezawodności jako modelu probabilistycznego lub za pomocą sieci neuronowych o prostej architekturze. Pozostałe charakterystyki takie jak: funkcja gęstości prawdopodobieństwa powstania uszkodzenia i intensywności uszkodzeń są możliwe do określenia na podstawie funkcji niezawodności. Model neuronowy okazał się lepiej dopasowany do danych empirycznych, jednakże z uwagi na wypłaszczony kształt jego wykresu na poziomie około 0,05 dla dużych wartości przebiegu pojazdu, jest on niezdolny do ekstrapolacji funkcji niezawodności. Z tego względu obliczenie wartości oczekiwanej przebiegu pojazdu pomiędzy jego uszkodzeniami było możliwe tylko na podstawie modeli probabilistycznych. Dla modelu wykładniczego oczekiwany przebieg pomiędzy uszkodzeniami wyniósł 4255,32 km, a dla modelu Weibulla 4686,22 km. Wartości te sugerują niewielki zasób bezawaryjnej pracy dla próby badawczej pojazdów ciężarowo-osobowych marki Honker 2000. Wyniki i wnioski z przeprowadzonych badań dokumentują realizację celu szczegółowego **[C1]**.

4.1.2. Opracowanie 3-stanowego modelu semi-Markowa w czasie ciągłym

Analiza niezawodności pojazdów ciężarowo-osobowych w dziedzinie czasu została opisana w publikacji **[P4]**. W celu identyfikacji przestrzeni stanowej procesu dla niezawodnościowego modelu semi-Markowa, metodą kolejnych przybliżeń dokonano agregacji modelu 9-stanowego do zawężonej przestrzeni fazowej obejmującej 3 główne stany eksploatacyjne, które uznano za istotne w aspekcie modelowania niezawodności. Przeprowadzenie agregacji stanów było spowodowane koniecznością zmniejszenia złożoności obliczeniowej dla transformaty Laplace'a i jej odwrotności. Stany takie jak: realizacja zadania, uzupełnianie paliwa, postój w garażu, obsługi przed wyjazdem i po realizacji zadania zostały zagregowane w jeden stan użytkowania. Obsługiwanie okresowe z uwag na fakt, że jest realizowane zgodnie z planowo-zapobiegawczą strategią eksploatacyjną oraz w oparciu o Katalog Norm Eksploatacji Techniki Lądowej i instrukcję pojazdu, pozostało wyodrębnionym stanem eksploatacyjnym. Własności techniczne stanu obsługi okresowej stanowią czynniki deterministyczne w procesie eksploatacji pojazdów. Czynności obsługowe są wykonywane w interwale jednego roku kalendarzowego lub co 10 tys. km. Natomiast stan niezdatności objął naprawę bieżącą, diagnozowanie i oczekiwanie na naprawę. Wynik przeprowadzonej agregacji przedstawiono na Rys. 4.4 zawartym w publikacji **[P4]**. Zastosowanie uogólnionego modelu stochastycznego wynikało z niespełnienia warunku wykładniczych rozkładów przez charakterystyki czasowe przejść międzystanowych.

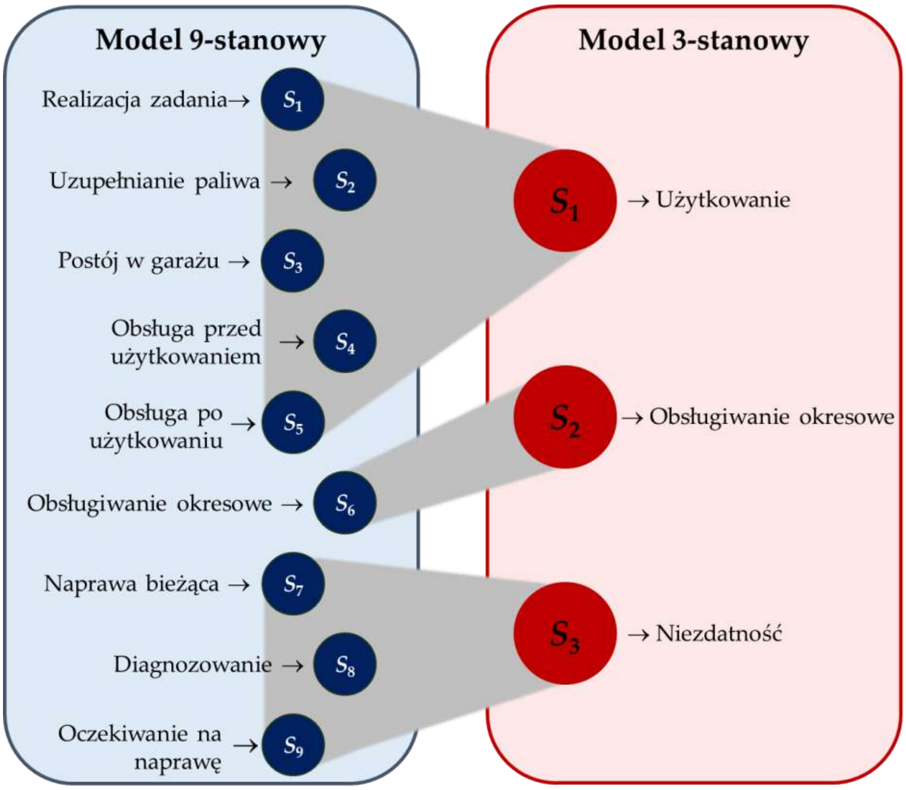

Rys. 4.4. Agregacja przestrzeni fazowej z modelu 9-stanowego do 3-stanowego **[P4]**

Matematycznym opisem modelu semi-Markowa jest macierz jądra odnowy, której elementy $Q_{ij}(t)$ są iloczynami prawdopodobieństw warunkowych p_{ij} włożonego łańcucha Markowa oraz dystrybuant $F_{ij}(t)$ czasów przejść międzystanowych. Dla 3-stanowego modelu opracowano graf przejść międzystanowych przedstawiony na Rys. 4.5. Zidentyfikowano przejście ze stanu S_2 (obsługiwanie okresowe) do stanu S_3 (niezdatność) jako niedozwolone, ponieważ tylko zdatny technicznie pojazd może być poddany czynności obsługiwania okresowego. Jeśli pojazd został uszkodzony i jednocześnie jego interwał międzyobsługowy się skończył, to w pierwszej kolejności jest on przywracany do stanu zdatności, a następnie realizowane są czynności obsługiwania okresowego. Macierz jądra odnowy dla 3-stanowego modelu jest zgodna ze wzorem (4.10):

$$Q(t) = \begin{bmatrix} 0 & Q_{12}(t) & Q_{13}(t) \\ Q_{21}(t) & 0 & 0 \\ Q_{31}(t) & Q_{32}(t) & 0 \end{bmatrix} = \begin{bmatrix} 0 & p_{12}F_{12}(t) & p_{13}F_{13}(t) \\ p_{21}F_{21}(t) & 0 & 0 \\ p_{31}F_{31}(t) & p_{32}F_{32}(t) & 0 \end{bmatrix}. \tag{4.10}$$

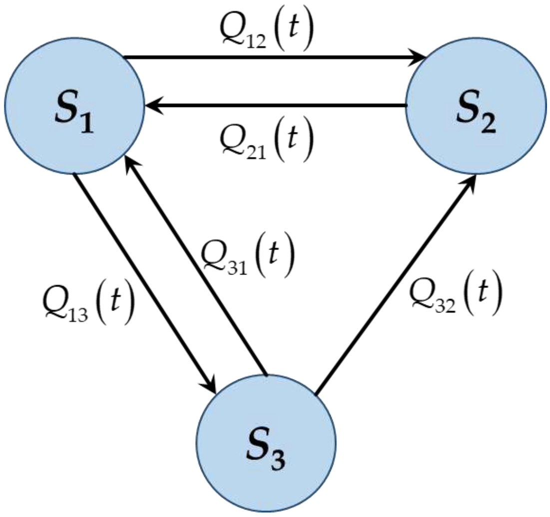

Rys. 4.5. Graf przejść międzystanowych w 3-stanowym modelu semi-Markowa wraz z ich charakterystykami **[P4]**

Dla modelu semi-Markowa funkcję niezawodności wyznaczono, używając dystrybuanty $\Phi_{iA}(t)$, która opisuje prawdopodobieństwa pierwszego przejścia obiektu z podzbioru stanów zdatności A' do podzbioru stanów niezdatności A, przy założeniu, że w chwili $t = 0$ obiekt znajduje się w jednym ze stanów zdatności. Jest to podejście zgodnie z rozważaniami przedstawionymi w [30]. Zatem funkcja niezawodności $R(t)$ została obliczona na podstawie równania (4.11):

$$R(t) = 1 - \Phi_{iA}(t) = 1 - P(\Theta_A \leq t | X(t = 0) = i). \tag{4.11}$$

Dystrybuantę $\Phi_{iA}(t)$ oblicza się za pomocą zależności (4.12):

$$\Phi_{iA}(t) = \sum_{j \in A} Q_{ij}(t) + \sum_{k \in A} \int_0^t \Phi_{kA}(t - x)\, dQ_{ik}(x). \tag{4.12}$$

Dla uproszczenia obliczeń zastosowano transformację Laplace'a, która przekształca równanie (4.12) do zależności:

$$\tilde{\varphi}_{iA}(s) = \sum_{j \in A} \tilde{q}_{ij}(s) + \sum_{k \in A} \tilde{q}_{ik}(s) \tilde{\varphi}_{ik}(s). \tag{4.13}$$

W opracowanym 3-stanowym modelu semi-Markowa, dwa stany eksploatacyjne, tj. S_1 (użytkowanie) oraz S_2 (obsługiwanie okresowe) tworzą podzbiór miary zdatności. W badaniach rozważono dwa możliwe warianty funkcji niezawodności, w zależności od stanu, w którym pojazd znajduje się w czasie $t = 0$. Pierwszy scenariusz zakładał stan początkowy obiektu jako S_1, natomiast drugi (scenariusz) jako S_2. Na podstawie równań macierzowych wyznaczono postacie analityczne funkcji $R_1(t)$ i $R_2(t)$, odpowiednio dla pierwszego i drugiego scenariusza. Ich bezpośrednia interpretacja jest praktycznie niemożliwa z uwagi na skomplikowany charakter zapisów zależności matematycznych. Z tego względu, wykorzystując oprogramowanie Wolfram Mathematica, opracowano wykresy funkcji niezawodności, przedstawione na Rys. 4.6.

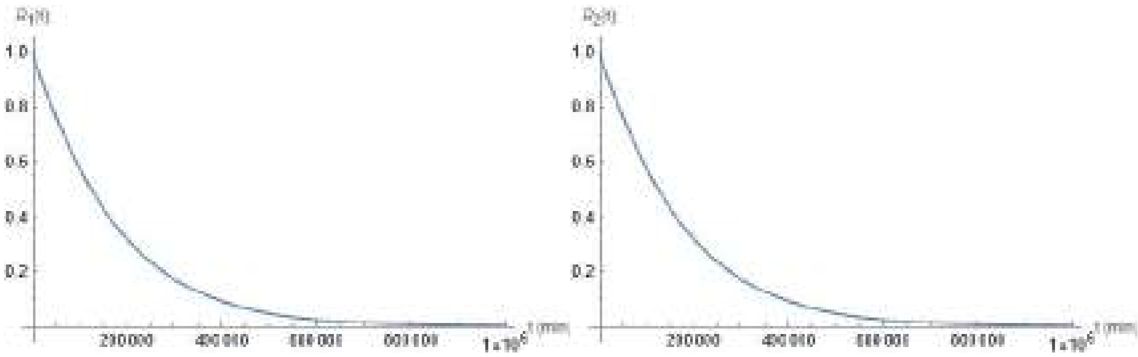

Rys. 4.6. Funkcje niezawodności $R_1(t)$ i $R_2(t)$ dla 3-stanowego modelu procesu eksploatacji pojazdu ciężarowo-osobowego **[P4]**

Na podstawie obliczonych różnic w wartościach funkcji niezawodności dla analizowanego zakresu dziedziny czasu od 0 do 1×10^6 (min), których wartości nie przekraczają 0,0014 stwierdzono, że przebieg funkcji niezawodności pojazdu wyznaczonych z zastosowaniem modelu semi-Markowa praktycznie nie zależy od stanu początkowego.

Wykorzystując funkcję niezawodności, wyznaczono pozostałe charakterystyki eksploatacyjne dla pojazdu ciężarowo-osobowego, tj. funkcję gęstości prawdopodobieństwa powstania uszkodzenia oraz intensywności uszkodzeń. Postać analityczna wyznaczonych charakterystyk, podobnie jak w przypadku funkcji niezawodności, nie jest interpretowalna w sposób bezpośredni, jednakże przy zastosowaniu zaawansowanego oprogramowania informatycznego, uzyskano graficzną ich postać. Funkcja gęstości prawdopodobieństwa powstania uszkodzenia jest malejąca, z kolei intensywność uszkodzeń posiada charakterystykę rosnącą, przy czym po czasie 5×10^5 (min) jej stabilizacja następuje na poziomie około $6{,}5\times10^{-6}$ (min^{-1}). Oczekiwany czas do uszkodzenia oznaczający miarę ilościową wynosił 119,44 dni i został obliczony za pomocą całki oznaczonej funkcji niezawodności w przedziale od 0 do ∞.

Opracowany 3-stanowy model semi-Markowa okazał się przydanym narzędziem w badaniu niezawodności pojazdów ciężarowo-osobowych z uwzględnieniem stanu eksploatacyjnego odnoszącego się do obsługiwania okresowego zgodnego z planowo-zapobiegawczą strategią eksploatacji w Siłach Zbrojnych RP. Przeprowadzone badania i analizy wypełniają założenia zgodne z realizacją celu szczegółowego **[C2]** niniejszej rozprawy. Należy jednak podkreślić, że model semi-Markowa ma zastosowanie tylko w przypadku analizy niezawodności w dziedzinie czasu. Natomiast jego wykorzystanie w modelowaniu odniesionym do dziedziny przebiegu jest niemożliwe z uwagi na naturalne ograniczenia wynikające z faktu, że tylko stan użytkowania można scharakteryzować jako proces stochastyczny realizowany w dziedzinie dystansu pokonanego przez pojazd, natomiast obsługiwanie okresowe oraz niezdatność są definiowane (mierzone) wyłącznie w dziedzinie czasu ciągłego lub dyskretnego.

4.2. Modelowanie gotowości pojazdu ciężarowo-osobowego

Gotowość jest istotną właściwością obiektu technicznego, szczególnie dla systemów, w których pojawiające się losowe zdarzenia odzwierciedlają naturę procesu stochastycznego. Utrzymywanie wysokich poziomów gotowości jest jednym z kluczowym warunków zapewnienia efektywnego działania pojedynczego obiektu i całego systemu. W literaturze gotowość jest definiowana jako zdolność obiektu do realizacji zadania zgodnego z jego przeznaczeniem w losowej chwili czasu t [5,22,31]. Najczęściej analizę gotowości przeprowadza się dla obiektów naprawialnych o niezerowym czasie odnowy, analizując kolejne przedziały czasów przebywania obiektu w stanach zdatności i niezdatności [32,33].

W obszarze modelowania gotowości środków transportowych zostało opublikowanych kilka artykułów naukowych, w których zastosowano teorię procesów Markowa i semi-Markowa oraz metody symulacyjne. Istotnym elementem opracowywania modelu stochastycznego jest identyfikacja przestrzeni fazowej, uwzględniającej specyfikę procesu eksploatacji danego obiektu technicznego. Należy przy tym uwzględnić założony cel modelowania oraz możliwość analizy i weryfikacji opracowanego modelu [34,35]. W publikacji [4] do obliczenia wskaźnika gotowości autobusów w systemie transportowym zaproponowano 3-stanowy ukryty model Markowa. Również w przypadku opisu matematycznego dotyczącego pojazdów specjalnych opracowano 3-stanowy model semi-Markowa [5]. Jednakże występują również znacznie bardziej złożone modele, jak np. 16-stanowy model semi-Markowa dla eksploatacji środków transportu zaproponowany w artykule [2]. Zaletą wielostanowych modeli jest możliwość wnikliwej analizy oraz wskazanie kierunków poprawy procesu poprzez usprawnienie realizacji wybranych czynności obsługowych i organizacyjnych [36,37]. Należy mieć jednak na uwadze, że wraz ze zwiększaniem przestrzeni fazowej wzrasta złożoność obliczeniowa modelu stochastycznego [38].

4.2.1. Modele semi-Markowa o zróżnicowanej przestrzeni stanów

W przeprowadzonych badaniach nad procesem eksploatacji pojazdów ciężarowo-osobowych zgodnie z przyjętymi celami modelowania dostosowano wielkości przestrzeni stanowych modeli. W podjętej problematyce modelowania gotowości pojazdów ciężarowo-osobowych, opracowano trzy modele o zróżnicowanych pod względem liczebności przestrzeniach fazowych, które tworzą:

1) Model 9-stanowy **[P2]** obejmujący poniżej wymienione stany eksploatacyjne:
   - S_1 – realizacja zadania,
   - S_2 – uzupełnienie paliwa,
   - S_3 – postój w garażu,
   - S_4 – obsługa przed użytkowaniem,
   - S_5 – obsługa po użytkowaniu,
   - S_6 – obsługiwanie okresowe,
   - S_7 – naprawa bieżąca,
   - S_8 – diagnozowanie,
   - S_9 – oczekiwanie na naprawę,
2) Model 4-stanowy **[P3]** zawierający stany jak poniżej:
   - S_1 – realizacja zadania,
   - S_2 – oczekiwanie na zadanie,
   - S_3 – obsługiwanie okresowe,
   - S_4 – niezdatność,
3) Model 3-stanowy **[P4]**, o następującej przestrzeni fazowej procesu:
   - S_1 – użytkowanie,
   - S_2 – obsługiwanie okresowe,
   - S_3 – niezdatność.

Skierowany graf procesu eksploatacji dla 9-stanowego modelu przedstawiono na Rys. 4.7. Przejścia międzystanowe zostały zidentyfikowane na podstawie trajektorii fazowych odzwierciedlających empiryczny przebieg procesu eksploatacji pojazdów ciężarowo-osobowych.

Wskaźniki gotowości dla modelu Markowa i semi-Markowa wyznacza się na podstawie prawdopodobieństw ergodycznych badanego procesu [39]. W przypadku modelu Markowa do obliczenia gotowości niezbędne jest oszacowanie poszczególnych elementów macierzy intensywności przejść międzystanowych. Należy jednak zaznaczyć, iż stosowalność modelu Markowa wymaga dopasowania rozkładów czasu trwania stanów do rozkładu wykładniczego [40,41]. Powyższy warunek stanowi znaczącą przeszkodę w modelowaniu procesów eksploatacji obiektów technicznych, w tym pojazdów ciężarowo-osobowych. W przeprowadzonych badaniach charakterystyki czasowe opracowanych trzech modeli o 3, 4 i 9 stanach w przestrzeni fazowej zostały zweryfikowane w aspekcie spełniania tego warunku przy użyciu testu statystycznego Kołmogorowa. Dla każdej przestrzeni stanów warunek ten nie został spełniony przez znaczną część charakterystyk. Zatem proces eksploatacji pojazdów ciężarowo-osobowych opisano za pomocą modelu semi-Markowa, będącego uogólnieniem modelu Markowa z uwagi na dowolność rozkładów czasów przejść międzystanowych.

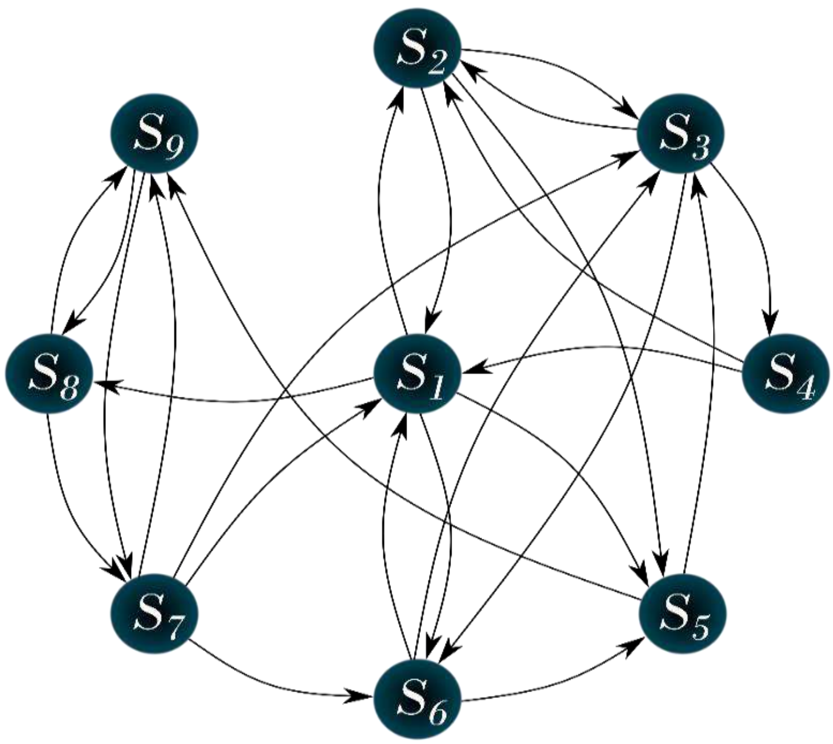

Rys. 4.7. Skierowany graf przejść międzystanowych dla 9-stanowego modelu semi-Markowa **[P2]**

Dla n-stanowego modelu przestrzeń fazowa została zdefiniowana jako $S = \{S_1, S_2, \dots, S_n\}$, przy czym zbiór stanów gotowości S_r obiektu jest podzbiorem zbioru S. Prawdopodobieństwa ergodyczne modelu semi-Markowa $P = \{p_1, p_2, \dots, p_n\}$ obliczono na podstawie prawdopodobieństw ergodycznych włożonego łańcucha Markowa $\Pi = \{\pi_1, \pi_2, \dots, \pi_n\}$ i oczekiwanych czasów $ET = \{E(T_1), E(T_2), \dots, E(T_n)\}$ przebywania pojazdu w poszczególnych stanach eksploatacyjnych. Zastosowano wzór (4.14):

$$p_j = \frac{\pi_j \cdot E(T_j)}{\sum_{i=1}^{n}(\pi_i \cdot E(T_i))} = \frac{\pi_j \cdot E(T_j)}{\sum_{i=1}^{n}\left(\pi_i \cdot \sum_{k=1}^{n}(p_{kj} \cdot T_{kj})\right)} \tag{4.14}$$

Łańcuch Markowa odzwierciedla dyskretny proces zmian stanów eksploatacyjnych pojazdu ciężarowo-osobowego bez uwzględnienia czasów przebywania w tych stanach. Dla wszystkich trzech modeli semi-Markowa obliczono wartości elementów macierzy prawdopodobieństw warunkowych przejść międzystanowych dla włożonego łańcucha Markowa na podstawie danych empirycznych i trajektorii fazowych, zgodnie z zależnością (4.15):

$$p_{ij} = \frac{n_{ij}}{\sum_{j=1}^{n} n_{ij}}, \tag{4.15}$$

gdzie: n_{ij} – liczebność przejść ze stanu S_i do stanu S_j, a p_{ij} – prawdopodobieństwo warunkowe przejścia ze stanu S_i do stanu S_j.

W Tab. 4.1 przedstawiono wyniki analiz gotowości pojazdów ciężarowo-osobowych dla trzech opracowanych modeli semi-Markowa. W modelu 3-stanowym tylko stan S_1 (użytkowanie) jest stanem gotowości funkcjonalnej (technicznej) obiektu. Natomiast dla modelu 4- i 9-stanowego podzbiory stanu gotowości są dwuelementowe, tj. stany S_1 i S_2 dla przestrzeni 4-stanowej oraz stany S_1 i S_3 dla przestrzeni 9-stanowej. Wskaźnik gotowości funkcjonalnej K_r jest równy sumie prawdopodobieństw ergodycznych wszystkich stanów tworzących podzbiór gotowości funkcjonalnej dla danego modelu semi-Markowa.

Wartości wskaźnika gotowości funkcjonalnej K_r uzyskane przy zastosowaniu 4- i 9-stanowych modeli semi-Markowa kształtują się na zbliżonym poziomie i w obu przypadkach przekraczają 0,90. Oznacza to, iż pojazd ciężarowy przez ponad 90% czasu przebywał w podzbiorze stanów gotowości funkcjonalnej, tzn. był gotowy do realizacji zadań transportowych zgodnie z jego przeznaczeniem. Model 3-stanowy uzyskał współczynnik K_r wynoszący niespełna 87%. Należy jednak zauważyć, że agregacja przestrzeni fazowej w praktyce prowadzi do uproszczenia modelu, które skutkuje zmniejszeniem dokładności odwzorowania rzeczywistego procesu eksploatacji. W odniesieniu do gotowości, modele o większej przestrzeni fazowej szczegółowiej odwzorowują proces, a tym samym dokładniej określają wartości jego wskaźników, zgodnie z przyjętym celem modelowania.

Tab. 4.1. Wyniki analiz gotowości pojazdów ciężarowo-osobowych **[P2], [P3], [P4]**

Model semi-Markowa	Model 3-stanowy	Model 4-stanowy	Model 9-stanowy
Prawdopodobieństwa ergodyczne włożonego łańcucha Markowa	$\pi_1 = 0{,}4882$ $\pi_2 = 0{,}2750$ $\pi_3 = 0{,}2368$	$\pi_1 = 0{,}4847$ $\pi_2 = 0{,}4895$ $\pi_3 = 0{,}0136$ $\pi_4 = 0{,}0121$	$\pi_1 = 0{,}2235$ $\pi_2 = 0{,}0775$ $\pi_3 = 0{,}2396$ $\pi_4 = 0{,}2161$ $\pi_5 = 0{,}2159$ $\pi_6 = 0{,}0063$ $\pi_7 = 0{,}0077$ $\pi_8 = 0{,}0053$ $\pi_9 = 0{,}0081$
Oczekiwane czasy przebywania w poszczególnych stanach eksploatacyjnych (min)	$E(T_1) = 84140{,}3$ $E(T_2) = 263{,}4$ $E(T_3) = 26121{,}3$	$E(T_1) = 755{,}5$ $E(T_2) = 4396{,}9$ $E(T_3) = 1196{,}8$ $E(T_4) = 21376{,}6$	$E(T_1) = 717{,}5$ $E(T_2) = 4{,}6$ $E(T_3) = 3956{,}6$ $E(T_4) = 5{,}0$ $E(T_5) = 8{,}1$ $E(T_6) = 272{,}0$ $E(T_7) = 174{,}6$ $E(T_8) = 36{,}11$ $E(T_9) = 13240{,}5$
Prawdopodobieństwa ergodyczne modelu semi-Markowa	$p_1 = 0{,}8678$ $p_2 = 0{,}0015$ $p_3 = 0{,}1307$	$p_1 = 0{,}1311$ $p_2 = 0{,}7704$ $p_3 = 0{,}0058$ $p_4 = 0{,}0927$	$p_1 = 0{,}1313$ $p_2 = 0{,}0003$ $p_3 = 0{,}7760$ $p_4 = 0{,}0009$ $p_5 = 0{,}0014$ $p_6 = 0{,}0014$ $p_7 = 0{,}0011$ $p_8 = 0{,}0002$ $p_9 = 0{,}0874$
Podzbiór stanów gotowości	S_1 – użytkowanie	S_1 – realizacja zadania S_2 – oczekiwanie na zadanie	S_1 – realizacja zadania S_3 – postój w garażu
Wartość wskaźnika gotowości	$K_r = 0{,}8693$	$K_r = 0{,}9015$	$K_r = 0{,}9073$

Z uwagi na szczegółowy opis eksploatacji reprezentowany przez 9-stanowy model semi-Markowa, zaproponowano dwa dodatkowe wskaźniki. Pierwszym z nich była sprawność techniczna K_e, która określa prawdopodobieństwo przebywania pojazdu w podzbiorze stanów, w których obiekt posiada odpowiednią wartość resursu technicznego do podjęcia realizacji zadań transportowych. Podzbiór stanów sprawności technicznej S_e obejmuje następujące stany: S_1 (realizacja zadania), S_2 (uzupełnienie paliwa), S_3 (postój w garażu), S_4 (obsługa przed użytkowaniem) oraz S_5 (obsługa po użytkowaniu). Natomiast S_e powiększony o stan S_6 (obsługiwanie okresowe), tworzy podzbiór stanów zdatności technicznej S_s, tzn. stanów, w których pojazd nie wymaga przeprowadzenia naprawy bieżącej. Uzyskane wartości wskaźników sprawności technicznej K_e i zdatności technicznej K_s są zbliżone do wskaźnika gotowości funkcjonalnej K_r, co jest spowodowane niewielkimi prawdopodobieństwami ergodycznymi stanów S_2, S_4, S_5 i S_6. Szczegółowe wyniki przeprowadzonej analizy przedstawiono w publikacji **[P2]**.

Model 9-stanowy został poddany analizie wrażliwości w aspekcie wpływu czasu przebywania pojazdu w stanie niezdatności (S_9) na wartość wskaźnika gotowości. Wybór tego stanu był podyktowany jego dominującym wpływem pojazdu ciężarowo-osobowego na gotowość funkcjonalną. Jest to związane z prawdopodobieństwem ergodycznym stanu S_9 dla modelu semi-Markowa, wynoszącym $p_9 = 0{,}0874$. Jednakże należy zauważyć, że prawdopodobieństwo ergodyczne łańcucha Markowa wynosi 0,0081, a wartość oczekiwana czasu przebywania pojazdu w stanie S_9 wynosi $E(T_9) = 13240{,}5$ (min). Powyższe wyniki wskazują na istotny wpływ wartości oczekiwanej $E(T_9)$ na prawdopodobieństwo ergodyczne stanu S_9, które zwiększa ponad dziesięciokrotnie wartość S_9 modelu semi-Markowa w stosunku do prawdopodobieństwa włożonego łańcucha Markowa. Na podstawie analizy wrażliwości wykazano, że skrócenie czasu oczekiwania pojazdu na naprawę o 50% skutkowałoby wzrostem gotowości, sprawności i zdatności o ponad 0,04 do wartości odpowiednio równych 0,9488, 0,9515 i 0,9530. Wyniki analizy wrażliwości 9-stanowego modelu semi-Markowa w aspekcie wpływu redukcji oczekiwanego czasu przebywania pojazdu w stanie S_9 na wskaźniki gotowości, sprawności i zdatności przedstawiono na Rys. 4.8.

Przedstawione modele semi-Markowa spełniają założenia przyjęte do realizacji celu szczegółowego **[C3]**.

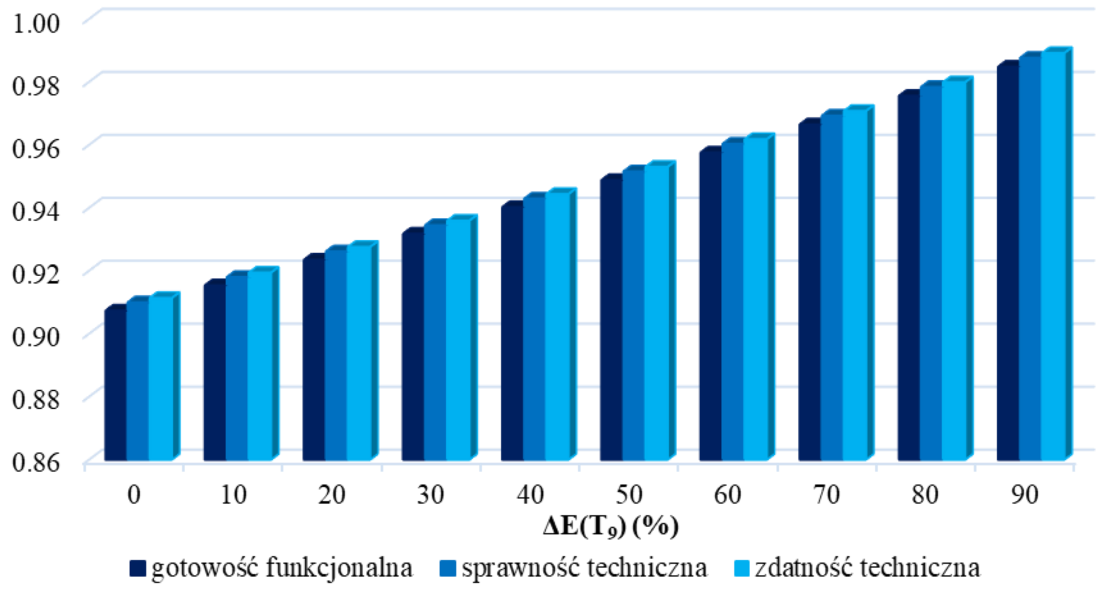

Rys. 4.8. Wyniki analizy wrażliwości 9-stanowego modelu semi-Markowa **[P2]**

4.2.2. Model symulacyjny Monte Carlo

Modele symulacyjne oparte na metodach Monte Carlo polegają na wielokrotnym przeprowadzeniu eksperymentu losowego [42–44]. Istnieje szereg prac naukowych, w których autorzy zastosowali modele Monte Carlo do badań niezawodnościowych [45–48]. Autorzy publikacji [49] opracowali 2-stanowy model niezawodności, który następnie został zweryfikowany za pomocą symulacji sekwencyjnej i niesekwencyjnej. W obszarze badań nad gotowością techniczną maszyn wiertniczych jako obiektów odnawialnych został opracowany model symulacyjny bazujący na metodzie Monte Carlo i teorii łańcuchów Markowa [50]. W pracy [51] autorzy zaproponowali metodę łączącą symulację Monte Carlo i próbkowanie kierunkowe do analizy wrażliwości dotyczącej niezawodności obiektów, która bazuje na strategii najbliżej odległości euklidesowej. Dokładność i skuteczność zaproponowanej metody udowodniono praktycznymi przykładami numerycznymi. Natomiast autorzy publikacji [52] przeprowadzili ocenę niezawodności stacji energoelektrycznej, przyjmując 4- i 5-stanowy model niezawodnościowy.

Modele stochastyczne oparte na teorii procesów Markowa i semi-Markowa odzwierciedlają proces eksploatacji w wymiarze czasu dyskretnego lub ciągłego, jednak nie uwzględniają intensywności użytkowania pojazdów, mierzonej przebytym przebiegiem wyrażonym w kilometrach [53]. Intensywność użytkowania wpływa na częstotliwość realizacji obsług okresowych przeprowadzanych w ramach planowo-zapobiegawczej strategii eksploatacji [54–56]. Ponadto, zgodnie z wynikami analizy niezawodności pojazdu, jego awaryjność może być odniesiona do wykonanej pracy wyrażonej jako przebyty dystans. Można zatem przypuszczać, że wzrost intensywności użytkowania może spowodować zwiększenie się częstotliwości występowania awarii oraz konieczność przeprowadzenia częstszych napraw bieżących. W celu odzwierciedlenia procesu eksploatacji pojazdu ciężarowo-osobowego opracowano model symulacyjny oparty na metodach Monte Carlo. Szczegółowe wyniki przeprowadzonych analiz przedstawiono w publikacji **[P3]**.

Model symulacyjny opracowano w dyskretnej przestrzeni stanowej, zaadaptowanej z 4-stanowego modelu semi-Markowa. Możliwe przejścia międzystanowe przedstawiono na Rys. 4.9. Zidentyfikowano dwa stany gotowości: S_1 – realizacja zadania i S_2 – oczekiwanie na zadanie transportowe, a także obsługiwanie okresowe (S_3) oraz naprawę (S_4). Są to stany o dużych wartościach oczekiwanych czasów przebywania pojazdu, co umożliwiło zastosowanie dyskretyzacji czasu jako przedziału jednodniowego.

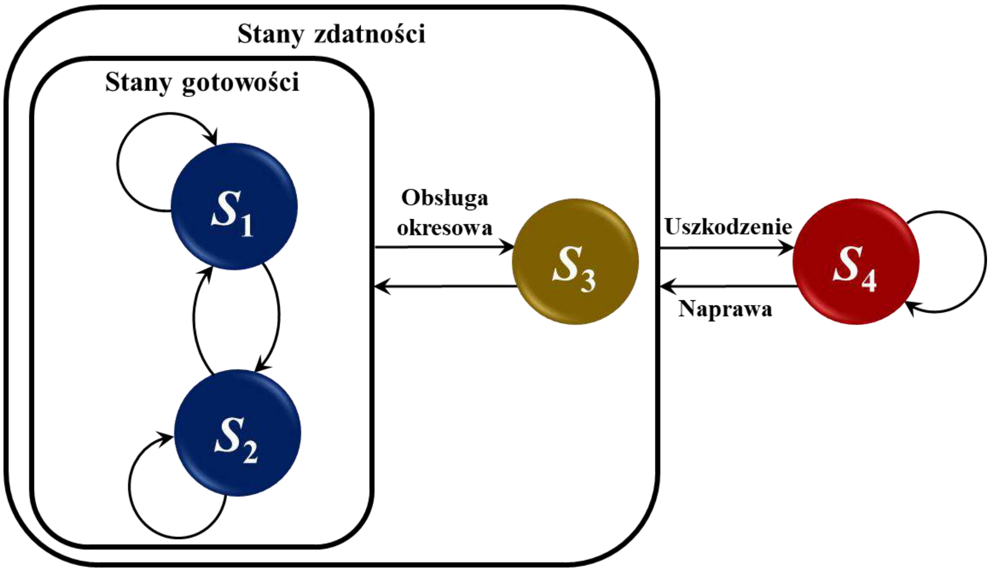

Rys. 4.9. Przestrzeń stanów dla modelu symulacyjnego Monte Carlo **[P3]**

Dla 4-stanowego modelu symulacyjnego zidentyfikowano cztery następujące podstawowe procesy realizowane w ramach eksploatacji pojazdu ciężarowo-osobowego, tj.:

- obsługiwanie okresowe,
- realizacja zadań transportowych,
- uszkodzenie/awaria pojazdu,
- naprawa uszkodzonego pojazdu.

W planowo-zapobiegawczej strategii zarządzania procesem eksploatacji pojazdów realizacja okresowych obsług odbywa się w ściśle określonych interwałach czasowo-przebiegowych. Zgodnie z jej założeniami czynności obsługowe są wykonywane po określonej ilości pracy (wyrażonej zazwyczaj w motogodzinach lub kilometrach). Dla pojazdu Honker 2000, zgodnie z zaleceniami producenta i przyjętymi normami eksploatacyjnymi, obsługiwanie okresowe odbywa się w interwale jednego roku kalendarzowego lub po przebiegu 10 tys. km. W opracowanym modelu symulacyjnym jest to jedyny proces mający deterministyczny charakter.

Przydział zadań transportowych dla poszczególnych pojazdów w systemie odbywa się na podstawie strumienia potrzeb oraz możliwości przewozowych. Na podstawie zgromadzonych danych empirycznych obliczono prawdopodobieństwo użytkowania pojazdu ciężarowo-osobowego, znajdującego się w stanie gotowości funkcjonalnej w danym dniu eksploatacji, które wynosiło 0,32. Badany proces opisano za pomocą rozkładu dwuwymiarowego o prawdopodobieństwach sukcesu i porażki równym odpowiednio 0,32 i 0,68.

Jeżeli pojazd ciężarowo-osobowy w danym dniu eksploatacji został przydzielony do realizacji zadań transportowych, to wartość jego dobowego przebiegu jest rozumiana jako zmienna losowa. Rozkłady probabilistyczne (wykładniczy, gamma, Weibulla i logarytmiczno-normalny) dobowego przebiegu zostały aproksymowane metodą najmniejszych kwadratów na podstawie danych empirycznych z okresu trzech lat eksploatacji dla próby 19 pojazdów.

Modele niezawodności pojazdu jako obiektu technicznego w odniesieniu do dziedziny przebiegu pojazdu od ostatniego uszkodzenia przyjęto na podstawie badań przeprowadzonych w ramach publikacji **[P1]**. W algorytmie symulacyjnym wykorzystano model wykładniczy i Weibulla. Model neuronowy odrzucono ze względu na jego właściwości osiągania wartości funkcji niezawodności znacznie powyżej 0 dla argumentów większych od 12 tys. km, co skutkowało brakiem możliwości obliczenia wartości oczekiwanej przebiegu pomiędzy uszkodzeniami jako całki oznaczonej od 0 do nieskończoności.

W celu przywrócenia zdatności technicznej pojazdu ciężarowo-osobowego realizowane są czynności diagnostyczne, identyfikujące mechanizmy i elementy do naprawy lub wymiany oraz czynności naprawcze. Czas odnowy niezdatnego obiektu jest zależny od zdolności naprawczych (moce przerobowe) i sprawności podsystemu zabezpieczenia materiałowego (dostępności lub/i czasu dostawy części zamiennych). Czas naprawy uszkodzonego pojazdu stanowi realizację procesu stochastycznego.

Opracowany model symulacyjny zakładał przeprowadzenie wielokrotnego próbkowania na podstawie 4-stanowej przestrzeni fazowej eksploatacji pojazdów oraz estymowanych charakterystykach opisujących realizowane procesy operacyjne, obsługowe i naprawcze. Przejścia pomiędzy stanami S_1 i S_2 były zgodne z rozkładem dwumianowym przydziału zadań transportowych. Przejście ze stanów gotowości do stanu obsługiwania okresowego S_3 odbywało się na podstawie deterministycznej zależności wynikającej ze strategii planowo-zapobiegawczej. Z kolei przejście ze stanów gotowości do stanu naprawy S_4 przebiegało na podstawie funkcji niezawodności, natomiast powrót ze stanu S_4 do podzbioru stanów zdatności następował zgodnie z dystrybuantą czasu naprawy.

Do przeprowadzenia symulacji procesu eksploatacji zastosowano wielokrotne próbkowanie metodą Monte Carlo. Przyjęto założenie, że w chwili $t = 0$ pojazd ciężarowo-osobowy był sprawny technicznie z losowym zasobem resursu technicznego. Każda iteracja odpowiadała jednej dobie procesu eksploatacji. Opracowany algorytm w pierwszej kolejności dokonywał sprawdzenia czy pojazd kwalifikuje się do przeprowadzenia obsługiwania okresowego. Jeśli czas lub przebieg od ostatniego obsługiwania był większy bądź równy interwałom międzyobsługowym określonym w normach eksploatacyjnych, wtedy pojazd w danej iteracji przechodził w stan S_3. Z danych empirycznych wynikało, że czas trwania czynności obsługi okresowej nie przekraczał 8 godzin pracy personelu, a zatem pojazd pozostawał w stanie S_3 tylko przez jedną iterację. Jeżeli obiekt techniczny posiadał odpowiedni zasób pracy, to następowało próbkowanie liczby losowej z przedziału [0, 1], która następnie została porównana z prawdopodobieństwem przydziału zadania transportowego. Jeśli wylosowana liczba była większa od tego prawdopodobieństwa to pojazd nie miał przydzielonego zadania i przechodził do stanu S_2. W przeciwnym razie następowało kolejne próbkowanie liczby losowej z przedziału [0, 1] i na podstawie dystrybuanty dobowego przebiegu została obliczona liczba kilometrów jaką musi pokonać pojazd, aby zrealizować zadanie transportowe. Istniało również ryzyko wystąpienia awarii podczas realizacji zadania, które było scharakteryzowane przez odpowiednie prawdopodobieństwo warunkowe i funkcję niezawodności pojazdu. Jeśli prawdopodobieństwo wystąpienia awarii pojazdu było większe niż wylosowana liczba z przedziału [0, 1], to pojazd przechodził do stanu S_4 (niezdatność), a w przeciwnym razie do stanu S_1 (realizacji zadania). Uszkodzony środek transportu podlegał naprawie, która została ukończona w przypadku, w którym liczba losowa z przedziału [0, 1] była mniejsza niż prawdopodobieństwo warunkowe naprawy pojazdu w danej iteracji symulacji.

Na podstawie aproksymowanych charakterystyk poszczególnych podprocesów zachodzących w eksploatacji pojazdów ciężarowo-osobowych opracowano 16 modeli symulacyjnych Monte Carlo, które zestawiono w Tab. 4.2. Następnie zostały one wykorzystane do przeprowadzenia 7300 iteracji, co w praktyce odpowiadało 20 letniemu okresowi przewidywanej eksploatacji dla tego typu środków transportu. W każdym modelu symulacje przeprowadzono dla próby 19 pojazdów, co odpowiadało liczebności empirycznej próby, na podstawie której opracowano modele.

Tab. 4.2. Charakterystyki podprocesów eksploatacyjnych dla opracowanych modeli symulacyjnych Monte Carlo **[P3]**

Model	Obsługiwanie okresowe	Przydział zadań	Dobowy przebieg	Niezawodność	Naprawa
MC1	Deterministyczny	Dwumianowy	Wykładniczy	Wykładniczy	Weibulla
MC2	Deterministyczny	Dwumianowy	Wykładniczy	Wykładniczy	Log-norm.
MC3	Deterministyczny	Dwumianowy	Wykładniczy	Weibulla	Weibulla
MC4	Deterministyczny	Dwumianowy	Wykładniczy	Weibulla	Log-norm.
MC5	Deterministyczny	Dwumianowy	Weibulla	Wykładniczy	Weibulla
MC6	Deterministyczny	Dwumianowy	Weibulla	Wykładniczy	Log-norm.
MC7	Deterministyczny	Dwumianowy	Weibulla	Weibulla	Weibulla
MC8	Deterministyczny	Dwumianowy	Weibulla	Weibulla	Log-norm.
MC9	Deterministyczny	Dwumianowy	Log-norm.	Wykładniczy	Weibulla
MC10	Deterministyczny	Dwumianowy	Log-norm.	Wykładniczy	Log-norm.
MC11	Deterministyczny	Dwumianowy	Log-norm.	Weibulla	Weibulla
MC12	Deterministyczny	Dwumianowy	Log-norm.	Weibulla	Log-norm.
MC13	Deterministyczny	Dwumianowy	Gamma	Wykładniczy	Weibulla
MC14	Deterministyczny	Dwumianowy	Gamma	Wykładniczy	Log-norm.
MC15	Deterministyczny	Dwumianowy	Gamma	Weibulla	Weibulla
MC16	Deterministyczny	Dwumianowy	Gamma	Weibulla	Log-norm.

Modele symulacyjne MC1-MC16 zaimplementowano jako skrypty algorytmów w środowisku programistycznym MATLAB 2022b. Schemat algorytmu i pseudokod przedstawiono w publikacji **[P3]**. Kod źródłowy symulacji zamieszczono w Załączniku

A1. Dla każdego z 16 modeli Monte Carlo przeprowadzono symulacje dla próby 19 pojazdów. W efekcie uzyskano sumarycznie 304 symulacje o łącznej liczbie przeprowadzonych iteracji wynoszącej 2 219 200. Przykładowe wyniki symulacji dla jednego pojazdu ciężarowo-osobowego przedstawiono na Rys. 4.10. Wykresy przedstawiają odpowiednio stany w jakich znajdował się pojazd w kolejnych iteracjach, sumaryczną liczebność obserwacji poszczególnych stanów, dobowy przebieg pojazdu w kolejnych iteracjach oraz całkowity przebieg pojazdu od początku symulacji do danej iteracji. Przykładowo pojazd nr 1 w modelu MC1 przebywał przez 1951 dni eksploatacji w stanie S_1, 4330 dni – w stanie S_2, 18 dni – w stanie S_3 oraz 1001 dni – w stanie S_4. Dobowe przebiegi pojazdu mieściły się w przedziale od 0 do 606 km, a całkowity przebieg przez cały okres symulowanej eksploatacji wyniósł 168 718 km.

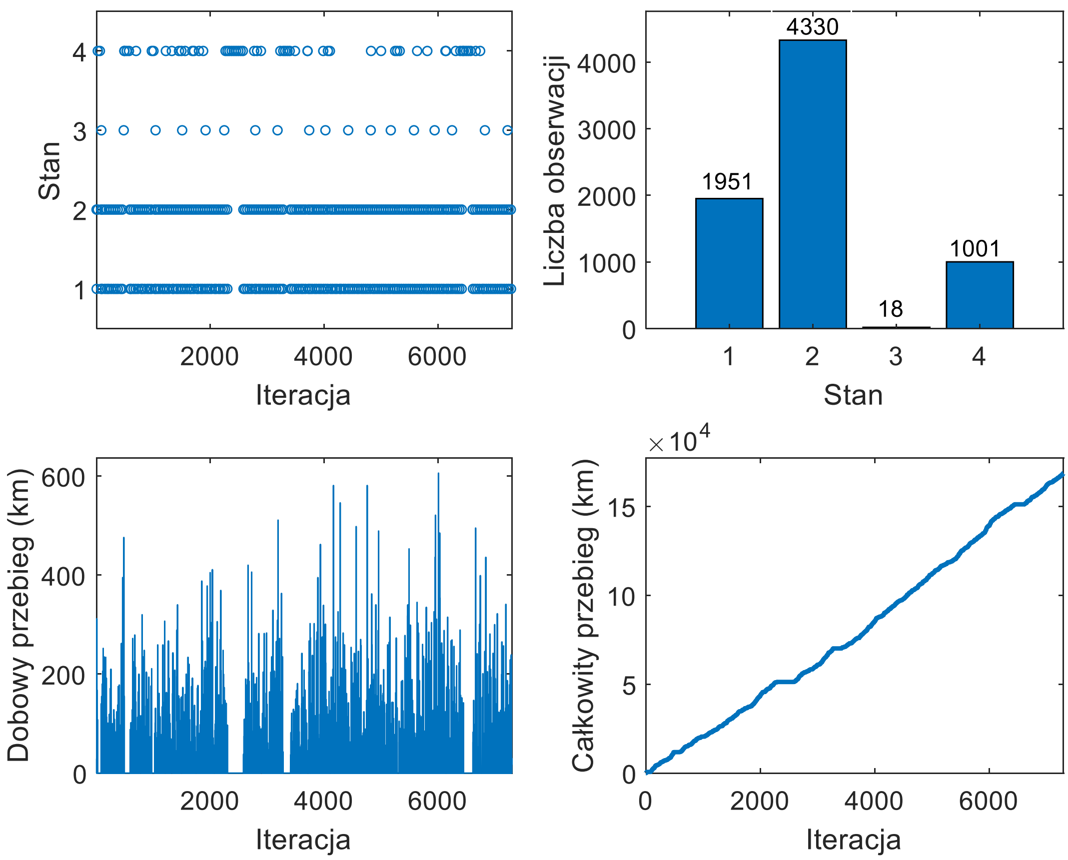

Rys. 4.10. Przykładowe wyniki symulacji modelu MC1 dla pojazdu nr 1 (Źródło: Opracowanie własne)

Wyniki przeprowadzonych symulacji wykorzystano do wyznaczenia wartości dwóch miar niezawodnościowych, tj. wskaźników: gotowości (K_r) i zdatności technicznej (K_s) próby pojazdów ciężarowo-osobowych. Wskaźnik gotowości K_r obliczono jako iloraz liczby obserwacji stanów S_1 i S_2 w stosunku do liczby iteracji algorytmu symulacyjnego. Natomiast wskaźnik zdatności technicznej K_s został zdefiniowany jako iloraz liczby obserwacji stanów S_1, S_2 i S_3 w stosunku do liczby iteracji algorytmu symulacyjnego. W celu walidacji modeli symulacyjnych porównano wyniki uzyskane tymi modelami oraz przy zastosowaniu 4-stanowego modelu semi-Markowa. Wyniki wszystkich modeli symulacyjnych nie odbiegały od modelu semi-Markowa o więcej niż 6%, co świadczy o dobrym odwzorowaniu rzeczywistego procesu eksploatacji. Biorąc pod uwagę powyższe, najlepszym modelem Monte Carlo okazał się model MC1. Jego wartości wskaźników gotowości i zdatności wyniosły odpowiednio 0,9078 i 0,9104 oraz różniły się od wyników modelu semi-Markowa odpowiednio o 0,70% i 0,34%. Stosunkowo niska częstotliwość obsługiwania okresowego prowadziła do niewielkich różnic występujących pomiędzy wskaźnikiem gotowości K_r a wskaźnikiem zdatności K_s. Wartości średnie wskaźnika gotowości od początku symulowanej eksploatacji do danej iteracji przedstawiono na Rys. 4.11.

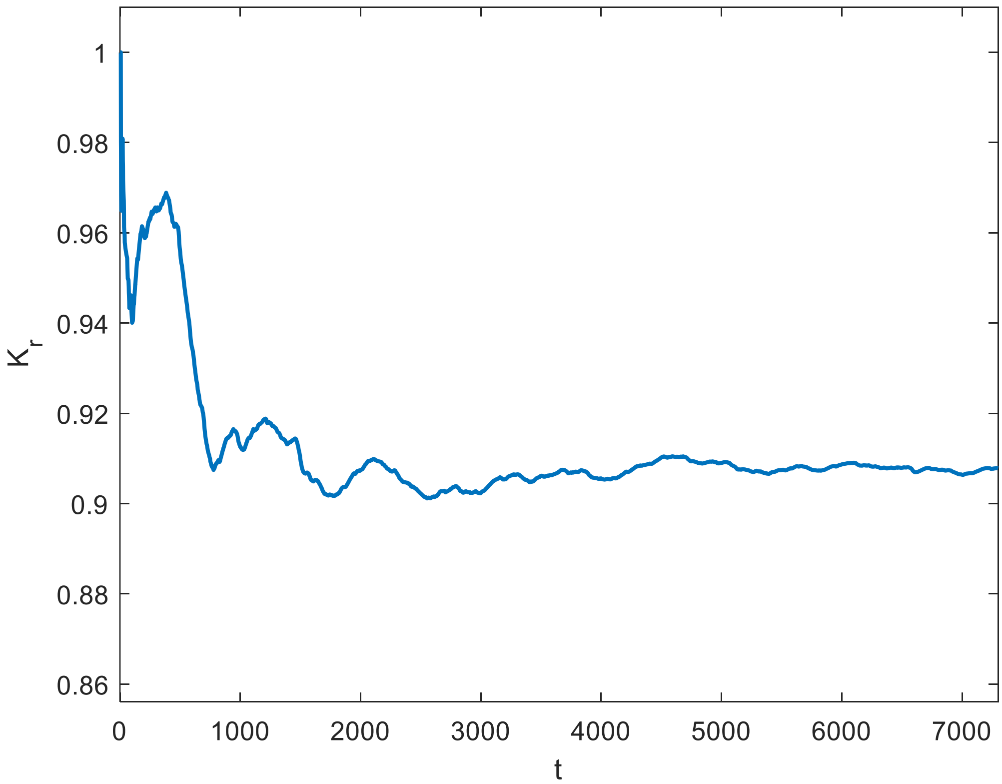

Rys. 4.11. Średnia wartość wskaźnika gotowości od początku eksploatacji do danej iteracji t **[P3]**

Aplikacyjność algorytmu symulacyjnego w modelowaniu procesu eksploatacji pojazdów ciężarowo-osobowych w aspekcie gotowości nie obejmuje jedynie określenia wartości przyjętych wskaźników. Główną przewagą symulacji Monte Carlo w stosunku do modelu semi-Markowa jest możliwość identyfikacji wpływu intensywności użytkowania pojazdów na ich gotowość i zdatność techniczną. Z tego względu przeprowadzono analizę wrażliwości modelu MC1 w celu wyznaczenia wpływu wartości wskaźników gotowości funkcjonalnej i zdatności technicznej w zależności od intensywności użytkowania pojazdów. Intensywność użytkowania jest określona poprzez prawdopodobieństwo przydziału zadania transportowego Θ oraz wartość oczekiwaną dobowego przebiegu l_d podczas realizacji zadań. Symulowany proces eksploatacji został zrealizowany dla określonych przedziałów rozważanych zmiennych przy zachowaniu rzeczywistych charakterystyk pozostałych podprocesów.

Wyniki przeprowadzonej analizy wrażliwości przedstawiono na Rys. 4.12 i Rys. 4.13. Przy minimalnym wykorzystaniu pojazdów na średnim poziomie 10%, dobowe wskaźniki gotowości funkcjonalnej i zdatności technicznej osiągnęły wartości wynoszące ok. 0,97. Wraz ze wzrostem liczby użytkowanych pojazdów do bieżących zadań wskaźniki te systematycznie zmniejszały się, aż do osiągnięcia wartości ok. 0,80 dla 90% prawdopodobieństwa przydziału zadania transportowego. Aproksymacje liniowe wskaźników K_r i K_s w zależności od parametrów Θ i l_d, przeprowadzono metodą najmniejszych kwadratów. Dopasowanie liniowych funkcji aproksymujących do symulowanych danych kształtowało się na bardzo wysokich poziomach współczynników determinacji wynoszących: $R^2 > 0{,}99$ dla parametru Θ i $R^2 > 0{,}95$ dla parametru l_d. Zgodnie z funkcjami aproksymującymi wzrost parametru Θ o wartość 0,01 spowodował zmniejszenie wartości wskaźników K_r i K_s o około 0,002. Natomiast wzrost wartości oczekiwanej dobowego przebiegu o 1 km wpłynął na redukcję wartości wskaźników gotowości i zdatności technicznej o ok. 0,0008.

Z przeprowadzonej analizy wynika, że wpływ intensywności użytkowania pojazdów marki Honker 2000 na wskaźniki gotowości i zdatności technicznej jest istotny. Zaobserwowane zmniejszenie się wartości wskaźników z poziomu ok. 0,97 do 0,80 przy wzroście intensywności użytkowania z 10% do 90% świadczy o znacznym pogorszeniu zdolności pojazdów do realizacji zadań transportowych. Pomimo pozornie niewielkich zmian wskaźników wynikających z przyrostów parametru Θ oraz dobowego przebiegu l_d, to zmiany te w dłuższej perspektywie czasu mogą kumulować się i w efekcie doprowadzić do obniżenia efektywności funkcjonowania wojskowych systemów transportowych.

Wyniki i wnioski z analizy modelu symulacyjnego Monte Carlo dają podstawę do stwierdzenia prawidłowej realizacji celu szczegółowego **[C4]**.

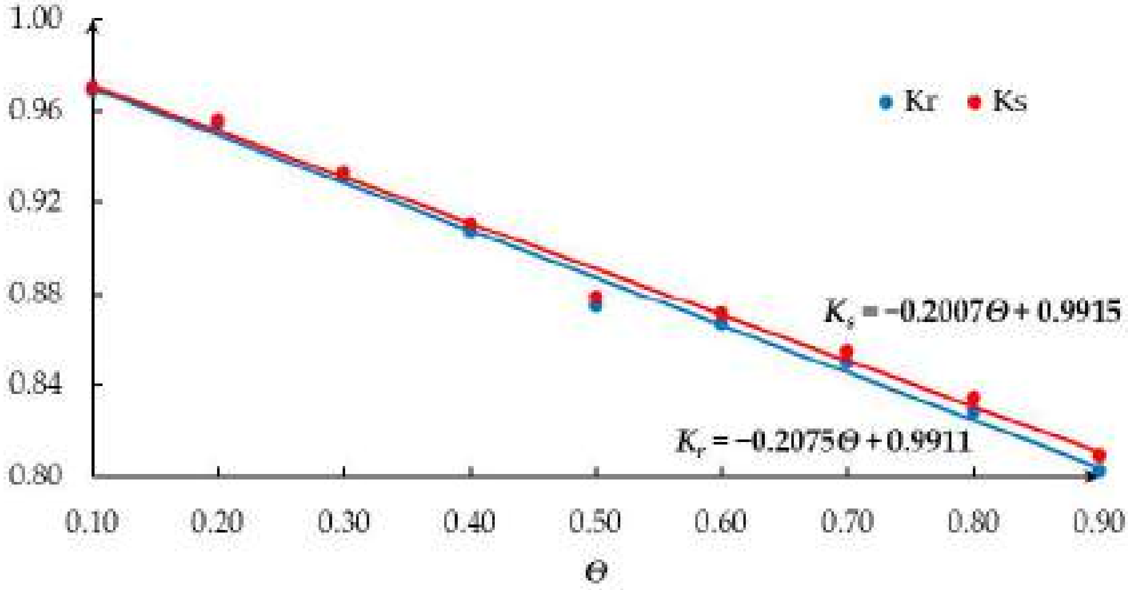

Rys. 4.12. Liniowe aproksymacje zależności wskaźników K_r i K_s od prawdopodobieństwa przydziału zadania transportowego (parametr Θ) **[P3]**

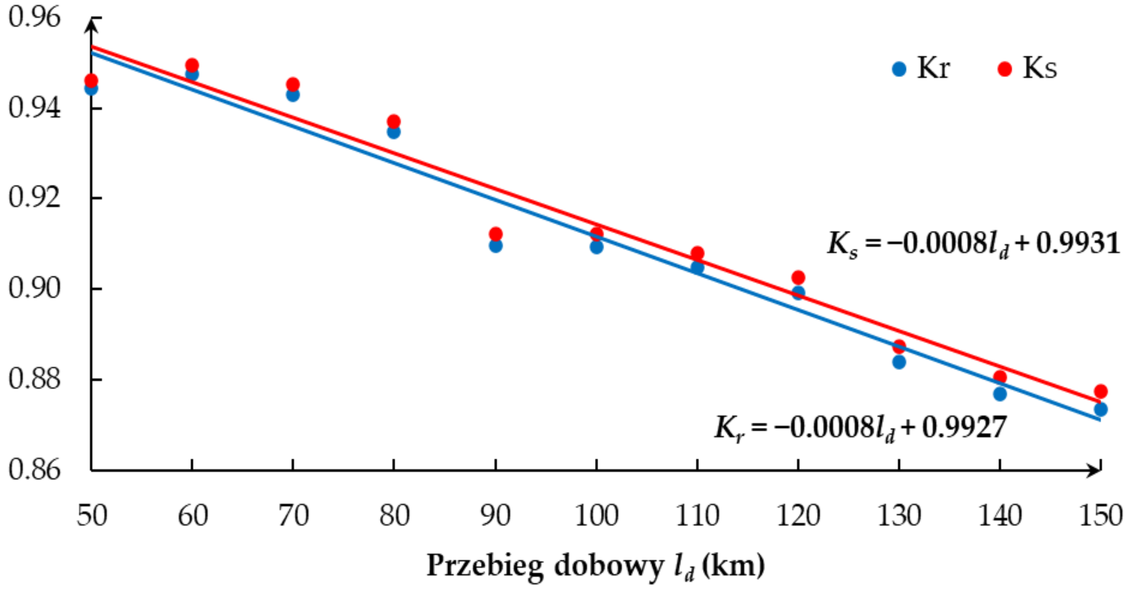

Rys. 4.13. Liniowe aproksymacje zależności wskaźników K_r i K_s od wartości oczekiwanej dobowego przebiegu l_d **[P3]**

5. ANALIZA NIEZAWODNOŚCI POJAZDU CIĘŻAROWO-OSOBOWEGO JAKO ZŁOŻONEGO SYSTEMU TECHNICZNEGO

W podrozdziale 4.1 przedstawiono analizę niezawodności pojazdów bez uwzględnienia ich wewnętrznej struktury niezawodnościowej. Oznacza to, że pojazd był interpretowany jako obiekt techniczny, a przeprowadzone analizy były skupione na odzwierciedleniu jego niezawodności w jednowymiarowych dziedzinach odnieszących się do czasu eksploatacji lub przebiegu. W rzeczywistości dla kompleksowej analizy awaryjności badanej próby pojazdów zaproponowano podejście, które określa prawdopodobieństwo uszkodzenia w dwuwymiarowej dziedzinie czasu fizycznego i wielkości pracy wykonanej przez pojazd. Oddziaływanie czynników fizyko-chemicznych, w tym przede wszystkim korozja elementów metalowych oraz utrata elastyczności elementów gumowych powoduje zużycie starzeniowe. Z kolei procesy tribologiczne stanowią główną przyczynę zużycia warstwy wierzchniej maszyn. Na skutek tarcia statycznego i kinetycznego występuje zużycie ścierne, adhezyjne i zmęczeniowe. Ponadto, w celu identyfikacji elementów pojazdu, które najbardziej wpływają na jego awaryjność, rozważono przedmiot badań jako złożony system techniczny o szeregowej strukturze niezawodnościowej.

Na podstawie zgromadzonej dokumentacji eksploatacyjnej obejmującej Karty Usług Technicznych (KUT) i Protokoły Stanu Technicznego (PST) dla próby 55 pojazdów Honker 2000 obejmujacej 5-cio letni okres badań, opracowano zbiorczą bazę danych dotyczących uszkodzeń podsystemów pojazdów ciężarowo-osobowych. Łącznie zgromadzono 575 kompletnych interwałów pomiędzy uszkodzeniami i 647 obserwacji cenzorowanych. Wszystkie interwały między uszkodzeniami i obserwacje cenzorowane zostały zarejestrowane zarówno w dziedzinie czasu eksploatacji, jak i w dziedzinie pokonanego dystansu (przebiegu) mierzonego w kilometrach. Dokładne statystyki przedstawiono na Rys. 5.1. Pojazd ciężarowo-osobowy został podzielony na siedem zasadniczych podsystemów, tj. silnik, układ przeniesienia napędu, układ hamulcowy, układ kierowniczy, zawieszenie, instalacja elektryczna i nadwozie. Najwięcej uszkodzeń zaobserwowano w przypadku silnika i układu przeniesienia napędu.

Zgromadzona baza danych została wykorzystana do przeprowadzenia badań nad niezawodnością pojazdu ciężarowo-osobowego jako złożonego systemu technicznego. Wyniki badań zostały przedstawione w publikacji **[P6]** i stanowią realizację celu szczegółowego **[C5]** niniejszej rozprawy doktorskiej.

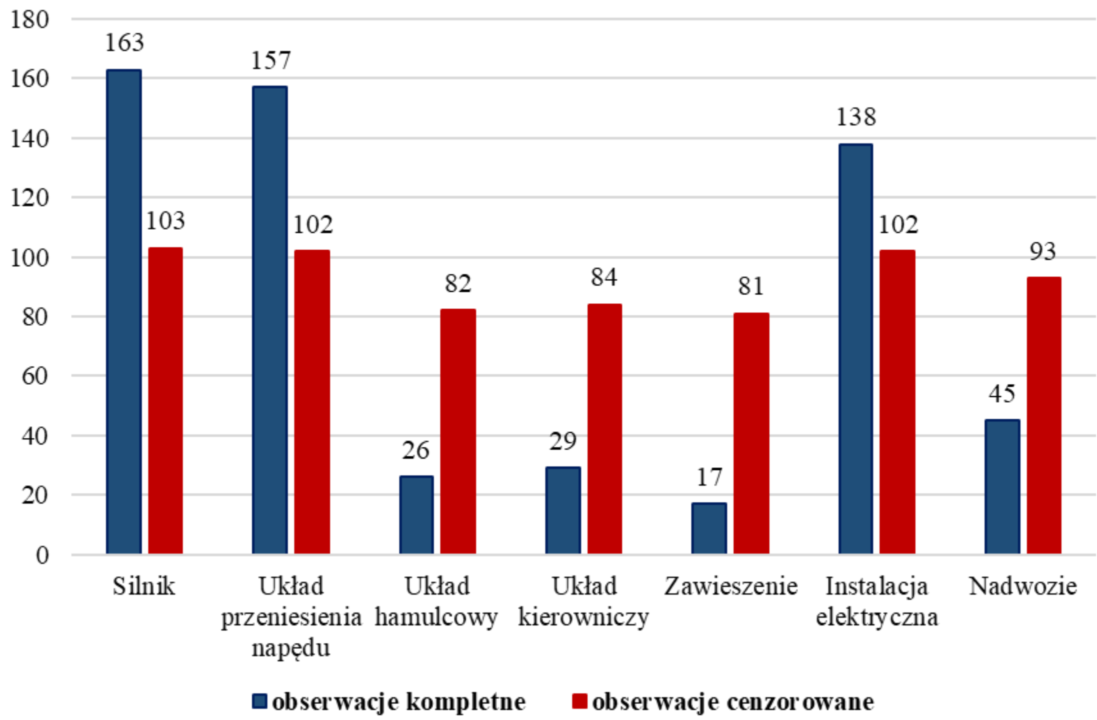

Rys. 5.1. Liczba danych empirycznych o uszkodzeniach podsystemów zgromadzonych na podstawie dokumentacji eksploatacyjnej (Źródło: Opracowanie własne)

5.1. Zastosowanie dwuwymiarowych kopul probabilistycznych do modelowania niezawodności podsystemów pojazdu

Kopule probabilistyczne w badaniach nad niezawodnością pojazdów zostały zastosowane w pracy [57]. Publikacja ta była jedną z pierwszych, w której określono zależność pomiędzy wiekiem samochodu osobowego i wielkością jego zużycia, co pozwoliło na opracowanie asymetrycznych kopul odzwierciedlających prawdopodobieństwo jego poprawnej pracy. Jednakże przytoczone rozważania traktowały pojazd jako prosty obiekt techniczny. Zatem przeprowadzone badania w ramach rozprawy doktorskiej stanowią nowatorskie podejście w modelowaniu niezawodności pojazdów.

W analizie niezawodności pojazdów ciężarowo-osobowych jako złożonych systemów technicznych zastosowano trzy najpopularniejsze dwuwymiarowe kopule archimedesowskie o następujących zależnościach matematycznych (5.1)-(5.3):

- kopula Franka:

$$C(u_1, u_2) = -\frac{1}{\theta} \ln\left(1 + \frac{(e^{-\theta\mu_1}-1)(e^{-\theta\mu_2}-1)}{e^{-\theta}-1}\right) \tag{5.1}$$

- kopula Claytona:

$$C(u_1,u_2) = \left[max\{\mu_1^{-\theta} + \mu_2^{-\theta} - 1{,}0\}\right]^{-\frac{1}{\theta}} \tag{5.2}$$

- kopula Gumbela:

$$C(u_1,u_2) = exp\left(-\left((-ln\mu_1)^{\theta} + (-ln\mu_2)^{\theta}\right)^{\frac{1}{\theta}}\right) \tag{5.3}$$

gdzie: u_1 i u_2 oznaczają dystrybuanty rozkładów granicznych zmiennych monotonicznie zależnych, natomiast θ jest parametrem kopuli.

Wszystkie trzy kopule probabilistyczne są jednoparametryczne, jednakże dopuszczalne zakresy wartości parametru θ są różne [58–60]. Parametr θ oblicza się na podstawie zależności monotonicznej opisanej za pomocą tau Kendalla (τ) [61,62]. Zakresy wartości parametru θ oraz sposoby ich wyznaczania dla kopul Franka, Claytona i Gumbela przedstawiono w Tab. 5.1.

Tab. 5.1. Charakterystyki kopul archimedesowskich zastosowanych do modelowania niezawodności podsystemów pojazdu **[P6]**

Kopula	Zakres wartości parametru θ	Zależność matematyczna pomiędzy τ i θ
Franka	$\theta \in (-\infty, 0) \cup (0, \infty)$	$\tau = 1 + \frac{4}{\theta}\left[\left(\int_0^{\theta} \frac{t}{e^t - 1}dt\right) - 1\right]$
Claytona	$\theta \in (-1{,}0) \cup (0, \infty)$	$\theta = \frac{2\tau}{1-\tau}$
Gumbela	$\theta \in [1, \infty)$	$\theta = \frac{1}{1-\tau}$

Na podstawie zgromadzonych danych o uszkodzeniach estymowano wartości *tau* Kendalla oraz aproksymowano rozkłady graniczne czasów i przebiegów pomiędzy uszkodzeniami dla wszystkich siedmiu podsystemów pojazdu. Metodologia przeprowadzonych obliczeń dla danych cenzorowanych została opisana w publikacji **[P6]**.

Na Rys. 5.2 przedstawiono wykresy rozrzutu realizacji dwuwymiarowych zmiennych losowych określających czas i przebieg pomiędzy uszkodzeniami poszczególnych podsystemów. Dane oznaczone kolorem czerwonym stanowią obserwacje cenzorowane. Dla wszystkich podsystemów wykazano znaczącą zależność monotoniczną mierzoną za pomocą *tau* Kendalla na poziomie od 0,5804 dla układu przeniesienia napędu do 0,8197 dla zawieszenia. Otrzymane wyniki wskazują na słuszność przyjętych założeń dotyczących możliwości zastosowania teorii kopul probabilistycznych w modelowaniu niezawodności podsystemów pojazdu ciężarowo-osobowego.

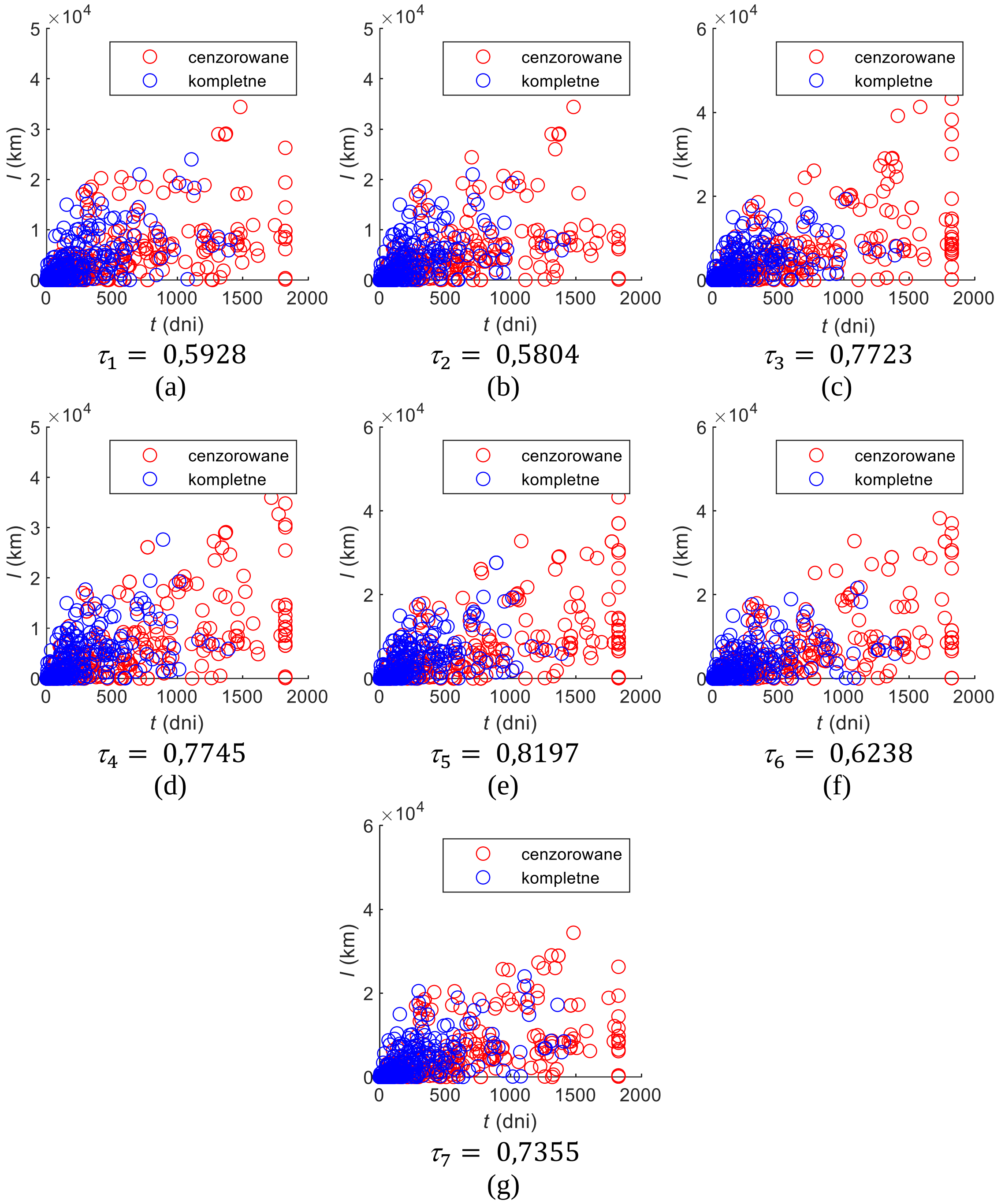

Rys. 5.2. Dane empiryczne dwuwymiarowych zmiennych losowych opisujących czas i przebieg pomiędzy uszkodzeniami dla podsystemów pojazdu: (a) silnik, (b) układ przeniesienia napędu, (c) układ hamulcowy, (d) układ kierowniczy, (e) zawieszenie, (f) instalacja elektryczna, (g) nadwozie **[P6]**

W przeprowadzonych badaniach opracowano modele probabilistyczne oparte na kopulach Franka, Claytona i Gumbela dla każdego podsystemu, a następnie wykorzystując statystykę Cramera-von Misesa, wyselekcjonowano modele najlepiej dopasowane do danych empirycznych. Im mniejsza wartość statystyki tym kopula jest lepiej dopsowana do empirycznej dystrybuanty zmiennej dwuwymiarowej. Dla wszystkich podsystemów pojazdu najlepszymi modelami probabilistycznymi okazały się kopule Claytona o wartościach paramterów przedstawionych w Tab. 5.2.

Tab. 5.2. Parametry rozkładów granicznych czasów i przebiegów pomiędzy uszkodzeniami dla podsystemów pojazdu **[P6]**

Podsystem	Czas (dni)		Przebieg (km)		Parametr kopuli
	Rozkład graniczny	Parametry	Rozkład graniczny	Parametry	
Silnik	Weibulla	$\alpha = 575{,}6$ $\beta = 0{,}7381$	Gamma	$k = 0{,}6204$ $\sigma = 1{,}348\times10^4$	$\theta = 2{,}9116$
Układ przeniesienia napędu	Weibulla	$\alpha = 597{,}4$ $\beta = 0{,}8043$	Gamma	$k = 0{,}6570$ $\sigma = 1{,}241\times10^4$	$\theta = 2{,}7664$
Układ hamulcowy	Wykładn.	$\lambda = 4{,}264\times10^{-4}$	Wykładn.	$\lambda = 3{,}372\times10^{-5}$	$\theta = 6{,}7835$
Układ kierowniczy	Weibulla	$\alpha = 6{,}873\times10^3$ $\beta = 0{,}5941$	Gamma	$k = 0{,}5169$ $\sigma = 1{,}809\times10^5$	$\theta = 6{,}8692$
Zawieszenie	Weibulla	$\alpha = 1{,}347\times10^4$ $\beta = 0{,}6272$	Wykładn.	$\lambda = 1{,}769\times10^{-5}$	$\theta = 9{,}0926$
Instalacja elektryczna	Weibulla	$\alpha = 705{,}1$ $\beta = 0{,}7952$	Weibulla	$\alpha = 8478$ $\beta = 0{,}6281$	$\theta = 3{,}3163$
Nadwozie	Weibulla	$\alpha = 2{,}778\times10^3$ $\beta = 0{,}7321$	Wykładn.	$\lambda = 4{,}577\times10^{-5}$	$\theta = 5{,}5614$

Kopule probabilistyczne Claytona o określonych rozkładach granicznych i wartościach parametrów są dystrybuantami uszkodzeń, a zatem odpowiadają funkcjom zawodności. Z tego powodu, aby wyznaczyć funkcje niezawodności podsystemów pojazdu posłużono się zależnością matematyczną (5.4):

$$R_i(t_i, l_i) = 1 - C\big(F(t_i), G(l_i)\big) = 1 - \big(F(t_i)^{-\theta} + G(l_i)^{-\theta} - 1\big)^{-\frac{1}{\theta}}, \qquad (5.4)$$

gdzie: $F(t_i)$ jest dystrybuantą graniczną czasu poprawnej pracy, a $G(l_i)$ dystrybuantą przebiegu pomiędzy uszkodzeniami.

Dla każdego z siedmiu podsystemów pojazdu ciężarowo-osobowego opracowano funkcję niezawodności $R_i(t_i, l_i)$. Na Rys. 5.3. przedstawiono graficzne postacie funkcji od R_1 do R_7, przyjmując taką samą skalę kolorów wykresu konturowego oraz analogiczne zakresy wartości dziedziny czasu i przebiegu. Taka prezentacja wyników umożliwia wstępną ocenę i porównanie awaryjności podsystemów. Wraz ze wzrostem dominacji odcieni ciepłych kolorów poprawia się niezawodność podsystemu. Na tej podstawie określono najbardziej niezawodne podsystemy, tj. układ kierowniczy i zawieszenie oraz najbardziej zawodne podsystemy, do których należały: silnik, układ przeniesienia napędu i instalacja elektryczna.

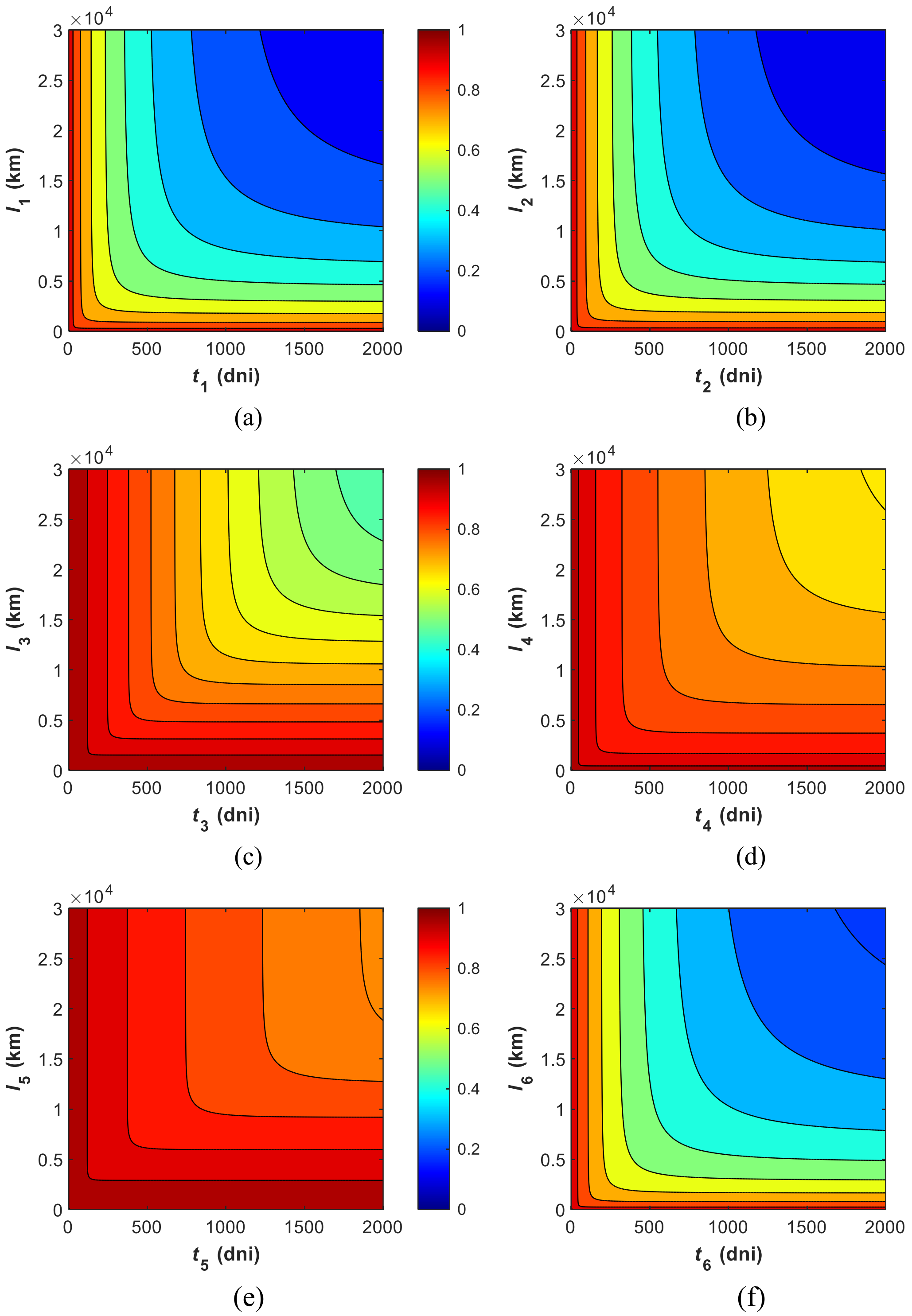

Rys. 5.3. Wykresy funkcji niezawodności podsystemów pojazdu: (a) silnik, (b) układ przeniesienia napędu, (c) układ hamulcowy, (d) układ kierowniczy, (e) zawieszenie, (f) instalacja elektryczna, (g) nadwozie **[P6]**

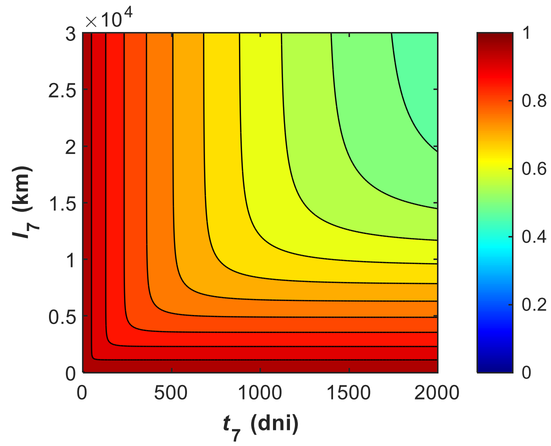

(g)

Rys. 5.3. (cd)

5.2. Model szeregowej struktury niezawodności pojazdu ciężarowo-osobowego

System o szeregowej strukturze niezawodnościowej przechodzi w stan niezdatności w momencie, gdy którykolwiek z jego elementów ulega uszkodzeniu [63–65]. Zatem w analizowanym studium przypadku, awaria jednego z siedmiu jego podsystemów skutkuje niezdatnością całego pojazdu. Z matematycznego punktu widzenia, funkcja niezawodności systemu szeregowego jest iloczynem wartości funkcji niezawodności jego komponentów. Adaptując tę właściwość do przedmiotu badań, opracowano zależność matematyczną opisującą niezawodność pojazdu $R_s(T,L)$, która wyraża się wzorem (5.5):

$$R_s(T,L) = \prod_{i=1}^{7} R_i(t_i,l_i), \tag{5.5}$$

gdzie: T i L są wektorami złożonymi z elementów t_i i l_i, opisującymi odpowiednio czasy i przebiegi od ostatniego uszkodzenia poszczególnych podsystemów.

Na podstawie funkcji niezawodności siedmiu podsystemów określono przebieg funkcji niezawodności pojazdu, który przedstawiono na Rys. 5.4. Funkcja niezawodności pojazdu szybko maleje, osiągając wartość 0,0908 dla $t_i = 500$ (dni) oraz $l_i = 5000$ (km), $i = 1, \dots, 7$. Oznacza to, że prawdopodobieństwo poprawnej i bezawaryjnej pracy przez okres 500 dni i przebieg na poziomie 5000 km wynosi niewiele ponad 9% przy założeniu, że wszystkie podsystemy zostały jednocześnie odnowione.

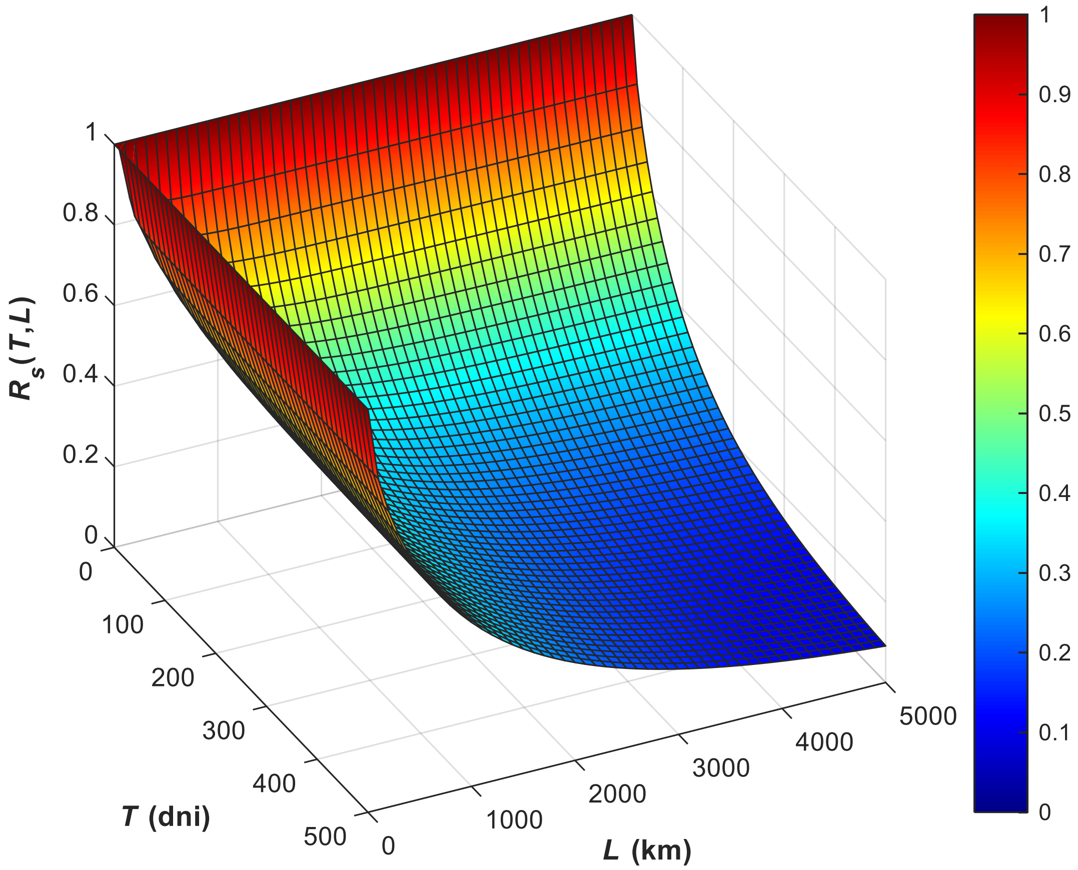

Rys. 5.4. Wykres funkcji niezawodności pojazdu w dwuwymiarowej dziedzinie czasu eksploatacji i przebiegu **[P6]**

5.3. Istotność podsystemów pojazdu ciężarowo-osobowego dla struktury niezawodnościowej

Wstępną ocenę awaryjności podsystemów dokonano na podstawie wykresów konturowych zamieszczonych na Rys. 5.3. Jednakże, aby precyzyjnie określić, który podsystem w danej chwili eksploatacji negatywnie wpływa na niezawodność pojazdu, wykorzystano miary ważności określające priorytety niezawodności [66]. Pierwszą z nich do literatury naukowej wprowadził Birnbaum w 1969 roku, która później została nazwana od nazwiska autora miarą ważności Birnbauma (ang. *Birnbaum Importance Measure* (BIM)) [67]. Wartość miernika BIM wskazuje na wpływ poszczególnych komponentów na niezawodność całego systemu i jest obliczana zgodnie ze wzorem (5.6):

$$I_i^B(t) = \frac{\partial R_s(t)}{\partial R_i(t)}. \tag{5.6}$$

Zależność (5.6) rozwinięto i dostosowano do modelu systemu pojazdu ciężarowo-osobowego w dwuwymiarowej dziedzinie funkcji niezawodności, otrzymując wzór (5.7):

$$I_i^B(t,l) = \frac{\partial R_S(T,L)}{\partial R_i(t,l)} = \prod_{\substack{j=1 \\ j \neq i}}^{m} R_j(t,l) = \prod_{\substack{j=1 \\ j \neq i}}^{m} \left(1 - C_j\left(F_j(t), G_j(l)\right)\right). \tag{5.7}$$

Rozszerzeniem miary ważności Birnbauma jest miara krytyczna (ang. *Criticality Importance Measure* (CIM)) [66,68–70], która uwzględnia zawodność komponentu i jest zapisywana jako (5.8):

$$I_i^{CR}(t) = I_i^B(t) \cdot \frac{Q_i(t)}{Q_S(t)}. \tag{5.8}$$

Po podstawieniu odpowiednich zależności opracowanego modelu niezawodności opartego na kopulach probabilistycznych otrzymano następujący wzór (5.9):

$$\begin{aligned} I_i^{CR}(t,l) &= I_i^B(t,l) \cdot \frac{Q_i(t,l)}{Q_S(t,l)} \\ &= \prod_{\substack{j=1 \\ j \neq i}}^{m} \left(1 - C_j\left(F_j(t), G_j(l)\right)\right) \cdot \frac{C_j\left(F_j(t), G_j(l)\right)}{\prod_{j=1}^{m}\left(1 - C_j\left(F_j(t), G_j(l)\right)\right)}. \end{aligned} \tag{5.9}$$

Stosując zmodyfikowane mierniki BIM i CIM dla modelu niezawodności pojazdu ciężarowo-osobowego, przeprowadzono obliczenia dla wybranych punktów dziedziny funkcji niezawodności. W tym celu określono pięć poziomów czasu eksploatacji, tj. 100, 200, 300, 400 i 500 dni, a także siedem poziomów przebiegu pojazdu, wynoszących 1000, 2000, 3000, 4000, 5000, 10000 i 20000 km. W ten sposób zdefiniowano 35 punktów pomiarowych dziedziny funkcji, będących kombinacjami czasu eksploatacji i przebiegu pojazdu. Na Rys. 5.5 i Rys. 5.6 przedstawiono odpowiednio podsystemy z największymi i najmniejszymi wartościami miar BIM i CIM. Im większa wartość miary ważności tym dany podsystem jest bardziej istotny z punktu widzenia niezawodności całego systemu, a co za tym idzie jest bardziej awaryjny. W analizowanym pojeździe ciężarowo-osobowym najbardziej awaryjnymi podsystemami były silnik (dla 29 punktów pomiarowych dziedziny) i instalacja elektryczna (dla 6 punktów pomiarowych). Natomiast najbardziej niezwodnymi podsystemami okazały się: zawieszenie (dla 30 punktów pomiarowych) oraz układ hamulcowy (dla 5 punktów pomiarowych).

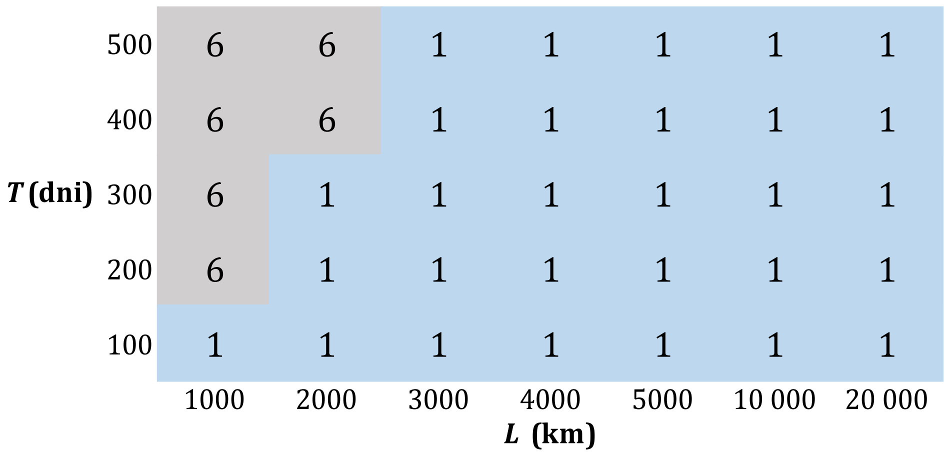

Rys. 5.5. Podsystemy z największymi wartościami miar BIM i CIM (1 – silnik, 6 – instalacja elektryczna) **[P6]**

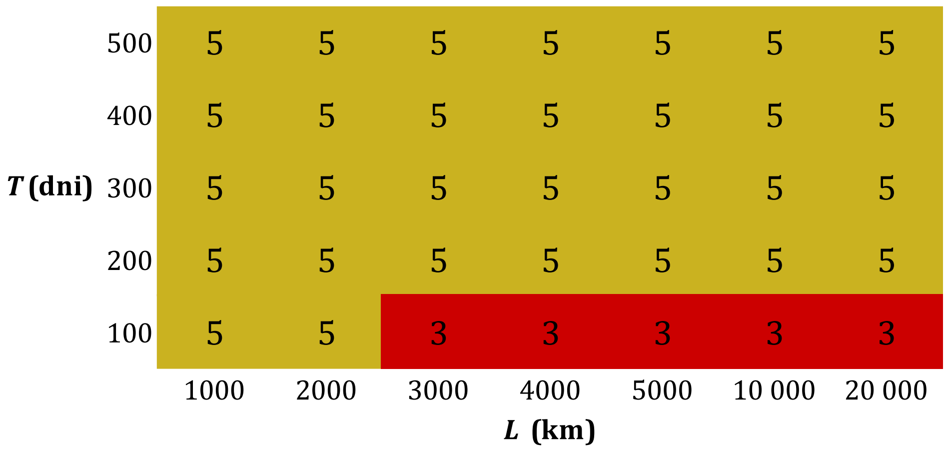

Rys. 5.6. Podsystemy z najmniejszymi wartościami miar BIM i CIM (3 – układ hamulcowy, 5 – zawieszenie) **[P6]**

Należy zaznaczyć, że mierniki BIM i CIM wyrażają ważność niezawodnościową podsystemu w odniesieniu do konkretnego punktu dziedziny funkcji niezawodności. Aby określić ważność niezawodnościową podsystemów dla całej dziedziny funkcji niezawodności, stosuje się miarę ważności Barlowa-Proschana (ang. *Barlow-Proschan Importance Measure* (BPIM)) [71]. Dla dziedziny czasu eksploatacji BPIM oblicza się jako całkę oznaczoną iloczynu miary Birnbauma i funkcji gęstości prawdopodobieństwa powstania uszkodzenia [72], zgodnie ze wzorem (5.10):

$$I_i^{BP}(t) = \int_0^{\infty} I_i^B(t) \cdot q_i(t)\, dt. \tag{5.10}$$

Natomiast dla opracowanego modelu niezawodności pojazdu opartego na dwuwymiarowych kopulach Claytona, wzór (5.11) przyjmuje postać:

$$I_i^{BP}(t,l) = \int_0^\infty \int_0^\infty I_i^B(t,l) \cdot q_i(t,l)\, dtdl = \int_0^\infty \int_0^\infty \left(\prod_{\substack{j=1 \\ j \neq i}}^{m} \left(1 - C_j\left(F_j(t), G_j(l)\right)\right)\right) \cdot c_i\big(F_i(t), G_i(l)\big) \cdot f_i(t) \cdot g_i(l)\, dtdl. \tag{5.11}$$

Zatem kolejnym krokiem badań było obliczenie wartości miar BPIM, aby zidentyfikować podsystemy, które w najbardziej znaczącym stopniu wpływają na awaryjność pojazdów ciężarowo-osobowych. Wyniki obliczeń przedstawiono na Rys. 5.7. Największą wartość BPIM, wynoszącą 0,3434, osiągnięto dla podsystemu silnika. Następnymi w kolejności hierarchii niezawodnościowej okazały się układ przeniesienia napędu i instalacja elektryczna, których wartości BPIM były względnie niższe odpowiednio o 5,68% i 8,91%. Pozostałe podsystemy uzyskały wartości mieszczące się w przedziale od 0,04 do 0,10. Oznacza to, że ich wpływ na niezawodność pojazdu można określić jako mało znaczący. Przedstawione rozważania odnoszą się do sytuacji, w której czasy i przebiegi od ostatniego uszkodzenia dla wszystkich podsystemów były równe.

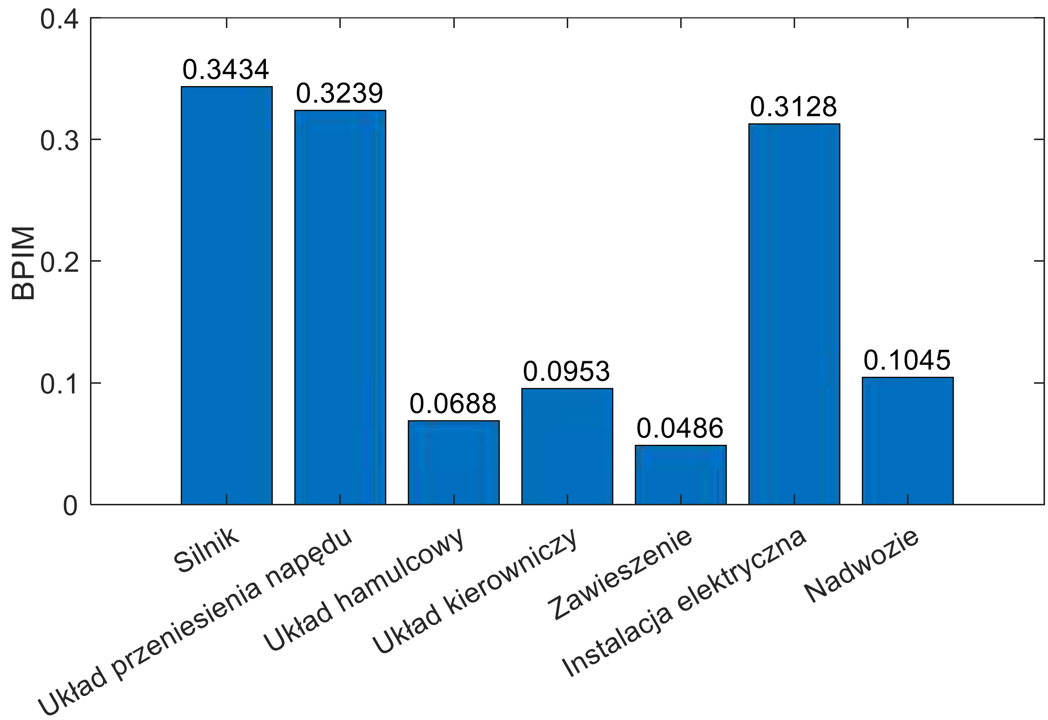

Rys. 5.7. Wartości miary ważności Barlowa-Proschana dla podsystemów pojazdu ciężarowo-osobowego **[P6]**

Zaproponowane podejście do modelowania niezawodności pojazdów stanowi użyteczne narzędzie do identyfikacji tzw. „słabych ogniw”. Określenie priorytetów dla poszczególnych komponentów systemu może być wartościową wskazówką do planowania i optymalizacji interwałów obsługowych odnoszących się do konkretnych elementów struktury niezawodnościowej. Takie rozwiązanie może przynieść korzyści w postaci zmniejszenia awaryjności systemu oraz redukcji ponoszonych kosztów. Analiza i wyniki przedstawione niniejszym rozdziale i publikacji **[P6]** stanowią realizację celu szczegółowego **[C5]**.

6. METODY WYZNACZANIA GOTOWOŚCI POJAZDU CIĘŻAROWO-OSOBOWEGO JAKO ELEMENTU WOJSKOWEGO SYSTEMU TRANSPORTOWEGO

W niniejszym rozdziale przedstawiono analizę i ocenę gotowości pojazdów ciężarowo-osobowych w ujęciu komponentów systemu transportowego. Szczegółowe założenia, metody, wyniki i wnioski zostały opisane w publikacji **[P5]**. Wojskowe systemy transportowe charakteryzują się wysokimi poziomami redundancji, co podnosi koszty ich budowy i eksploatacji. Rozpatrując system transportowy w sensie technicznym, zidentyfikowano jego progową strukturę niezawodnościową, określaną w literaturze jako k z n (ang. *k-out-of-n*). W takiej strukturze system działa poprawnie, jeśli co najmniej k komponentów jest zdatnych w odniesieniu do wszystkich n tworzących system [73–75]. Minimalna liczba pojazdów zdatnych do właściwego działania systemu transportowego jest zależna od wielkości strumienia napływających zadań w danym dniu eksploatacji. Jest to efekt zmiennego w czasie procesu stochastycznego, na który mają wpływ zarówno intensywność szkolenia wojsk, jak i konieczność zapewnienia odpowiednich zdolności transportowych. Zebrane dane empiryczne określające wielkość strumienia zadań transportowych na dany dzień eksploatacji systemu przedstawiono na Rys. 6.1.

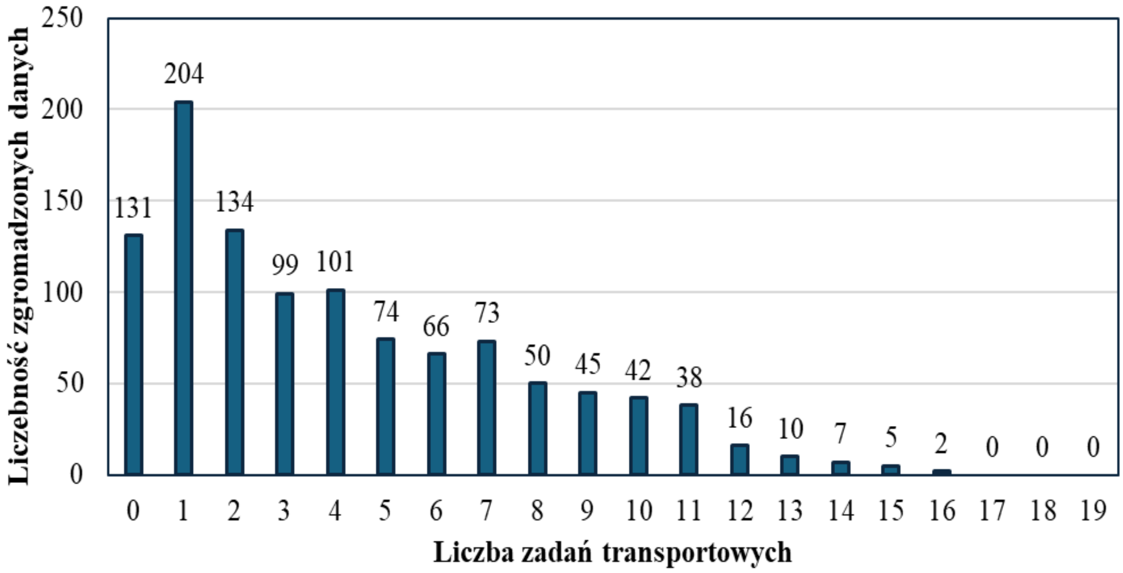

Rys. 6.1. Histogram danych empirycznych określających wielkość strumienia zadań transportowych w poszczególnych dniach eksploatacji systemu (Źródło: Opracowanie własne)

System transportowy złożony z 19 pojazdów maksymalnie użytkował zaledwie dwukrotnie w okresie badań 16 środków transportowych w tym samym czasie. Przez większość czasu eksploatacji użytkowanych było równocześnie od 0 do 11 pojazdów. Zgromadzone dane empiryczne wskazują zatem na wysoki poziom redundancji wojskowych systemów transportowych.

W publikacji **[P5]** przeanalizowano dwa rodzaje studium przypadku, dotyczące pojazdów ciężarowo-osobowych oraz pojazdów ciężarowych. Jednakże, w niniejszym rozdziale odniesiono się wyłączenie do analiz związanych z przedmiotem badań prowadzonych w ramach pracy doktorskiej (tj. pojazdów ciężarowo-osobowych).

6.1. Wielostanowy model Markowa dla systemu transportowego o strukturze progowej typu *k z n*

W badaniach przyjęto szereg założeń dotyczących charakterystyki systemu transportowego, które zostały szczegółowo opisane w publikacji **[P5]**. W badaniach zidentyfikowano wojskowy system transportowy jako redundantny system techniczny złożony z homogenicznych komponentów funkcjonujących w gorącym trybie rezerwowania (ang. *hot standby*) [76,77]. Pojazdy, które nie realizują w danym czasie zadań transportowych są utrzymywane w ciągłej gotowości. Z tego względu, zgodnie ze stanem literatury naukowej, intensywność uszkodzeń rezerwowych komponentów i aktywnych pozostaje na stałym poziomie [78–80]. Intensywności uszkodzeń i napraw pojazdów w prostym modelu dwustanowym są zgodne z rozkładem wykładniczym, co implikuje możliwość zastosowania modelu Markowa do opisu zmian stanów niezawodnościowych [81–83]. Dopasowanie rozkładów o parametrach $\lambda = 0{,}0048\ \frac{1}{dzie\acute{n}}$ i $\mu = 0{,}2607\ \frac{1}{dzie\acute{n}}$ dla pierwszego studium przypadku określono na podstawie błędu średniokwadratowego równego odpowiednio $MSE = 0{,}0004$ i $MSE = 0{,}0208$ oraz współczynnika korelacji Pearsona $\rho = 0{,}9956$ i $\rho = 0{,}9609$.

Dla systemu transportowego złożonego z n pojazdów opracowano model niezawodnościowy bazujący na procesie Markowa z liczebnością stanów równą $n + 1$. Graf przejść międzystanowych modelu przedstawiono na Rys. 6.2. Wartość każdego stanu odnosi się do liczby zdatnych pojazdów w systemie transportowym. Z dowolnego stanu, z wyjątkiem stanów $S = 0$ i $S = n$, system może przejść do dwóch stanów sąsiednich, w zależności od tego, który proces (uszkodzenie sprawnego pojazdu lub naprawa pojazdu uszkodzonego) zrealizuje się w pierwszej kolejności. Intensywność przejść międzystanowych zależy od dwóch parametrów: intensywności uszkodzeń λ i intensywności napraw μ.

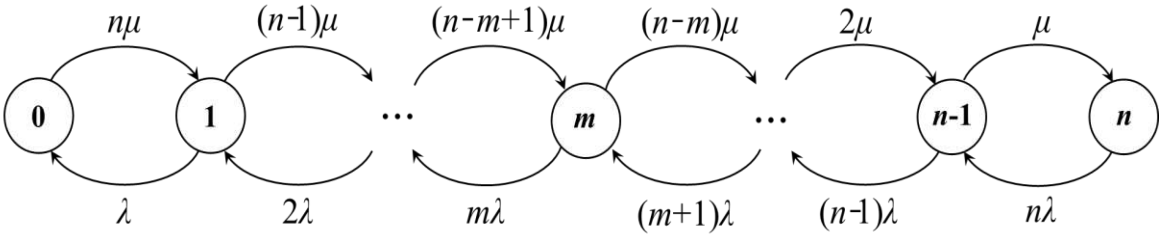

Rys. 6.2. Model niezawodności systemu złożonego z n komponentów **[P5]**

Do opisu zmian stanów niezawodnościowych opracowano ogólną macierz intensywności przejść międzystanowych Λ_S, której elementy opisuje równanie (6.1):

$$\Lambda_S = \begin{bmatrix} -n\mu & n\mu & 0 & \dots & 0 & 0 & 0 \\ \lambda & -(\lambda+(n-1)\mu) & (n-1)\mu & \dots & 0 & 0 & 0 \\ 0 & 2\lambda & -(2\lambda+(n-2)\mu) & \dots & 0 & 0 & 0 \\ \dots & \dots & \dots & \dots & \dots & \dots & \dots \\ 0 & 0 & 0 & \dots & -(2\mu+(n-2)\lambda) & 2\mu & 0 \\ 0 & 0 & 0 & \dots & (n-1)\lambda & -(\mu+(n-1)\lambda) & \mu \\ 0 & 0 & 0 & \dots & 0 & n\lambda & -n\lambda \end{bmatrix} \tag{6.1}$$

gdzie: λ – intensywność uszkodzeń, μ – intensywność napraw, n – liczba pojazdów w systemie, k – minimalna liczba sprawnych pojazdów do prawidłowego działania systemu.

Ogólna postać modelu Markowa pozwala na jego implementację dla systemu złożonego z dowolnej liczby komponentów i minimalnej liczby sprawnych komponentów do jego prawidłowej pracy. Dzięki tej uniwersalności, opracowano algorytm w formie skryptu w środowisku MATLAB, który umożliwia analizę wielu wariantów systemu transportowego. Kod źródłowy algorytmu przedstawiono w Załączniku A2.

6.2. Analiza gotowości i efektywności systemu transportowego

Do oceny efektywności funkcjonowania systemu transportowego zaproponowano dwa wskaźniki ilościowe. Pierwszym z nich jest gotowość systemu A_S, która określa prawdopodobieństwo zdarzenia, że w systemie transportowym liczba zdatnych pojazdów jest wystarczająca do realizacji wszystkich zadań transportowych przewidzianych na dany dzień eksploatacji. Specyfika funkcjonowania wojskowego systemu transportowego powoduje, że w sytuacji, w której wielkość strumienia zadań do niego wpływających przekracza jego możliwości, system realizuje najważniejsze z nich, pracując z odpowiednio mniejszą efektywnością w stosunku do zakładanych wymagań i celów. Aby ocenić odsetek zrealizowanych zadań zaproponowano wskaźnik efektywności TPM

(ang. *Technical Performance Measure*), który został zaadaptowany z armii USA [84] i dostosowany do warunków technicznych analizowanego systemu transportowego.

Do wyznaczenia wartości wskaźników opracowano dwa podejścia: probabilistyczne i symulacyjne. W podejściu probabilistycznym wykorzystano znany z literatury wzór (tzw. rozkład Bernoulliego) na gotowość systemu o strukturze progowej *k z n*, składający się z homogenicznych komponentów [85–87]:

$$A_S = \sum_{i=k}^{n} \binom{n}{i} p^i q^{n-i}, \tag{6.2}$$

gdzie: p – prawdopodobieństwo gotowości komponentu, q – prawdopodobieństwo niegotowości komponentu.

Wartości prawdopodobieństw p i q obliczono na podstawie wartości oczekiwanej liczby zdatnych pojazdów w systemie transportowym w stosunku do wielkości jego struktury. Natomiast wartość oczekiwana liczby zdatnych pojazdów wynika z prawdopodobieństw ergodycznych modelu Markowa czasu ciągłego.

Podejście symulacyjne oparto na próbkowaniu metodą Monte Carlo, bazując na dystrybuancie liczby zadań wpływających do systemu i na niezawodnościowym modelu Markowa. Założono, że każda iteracja i odpowiada jednemu dniowi funkcjonowania systemu transportowego, dla którego losowano minimalną liczbę pojazdów $k(i)$ wymaganych do realizacji zadań. Liczba zdatnych pojazdów w danej chwili t była wynikiem próbkowania czasów uszkodzeń i napraw. Jeśli system w iteracji i posiadał liczbę zdatnych pojazdów $m(i)$ większą lub równą minimalnej liczbie zdatnych pojazdów $k(i)$ to jego gotowość w tej iteracji wynosiła 1, a w przeciwnym razie 0, zgodnie ze wzorem (6.3):

$$A_S(i) = \begin{cases} 1 \; jeśli \; m(i) \geq k(i) \\ 0 \; w \; przeciwnym \; przypadku \end{cases}. \tag{6.3}$$

Natomiast wskaźnik efektywności TPM dla pojedynczej iteracji i, w której liczba pojazdów zdatnych $m(i)$ była mniejsza niż ich minimalna wymagana liczba $k(i)$ został obliczony jako iloraz $\frac{m(i)}{k(i)}$, zgodnie ze wzorem (6.4):

$$TPM(i) = \begin{cases} 1 \; jeśli \; m(i) \geq k(i) \\ \dfrac{m(i)}{k(i)} \; w \; przeciwnym \; przypadku \end{cases}. \tag{6.4}$$

Gotowość A_S i efektywność TPM systemu transportowego dla całego czasu symulacji T_S obliczono jako średnie arytmetyczne odpowiednio wartości $A_S(i)$ oraz $TPM(i)$.

W przeprowadzonym badaniu przeanalizowano 19 możliwych konfiguracji systemu transportowego, obejmujących od 1 do 19 pojazdów ciężarowo-osobowych. Konfiguracja obejmująca 19 pojazdów odpowiadała liczebności wyposażenia badanego systemu transportowego w momencie zbierania danych empirycznych. Dla każdej z konfiguracji przeprowadzono symulację metodą Monte Carlo, składającą się z 10 000 iteracji. Przykład symulacji dla systemu zawierającego 10 pojazdów przedstawiono na Rys. 6.3. Kod źródłowy algorytmu symulacyjnego przedstawiono w Załączniku A3.

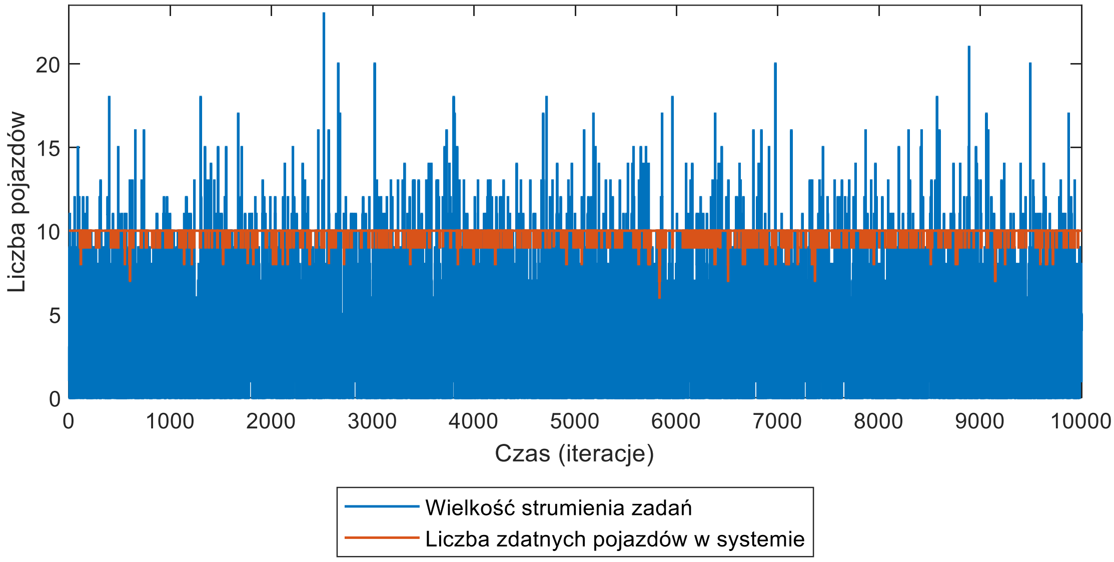

Rys. 6.3. Wyniki symulacji dla systemu transportowego złożonego z 10 pojazdów **[P5]**

Wykorzystując podejście probabilistyczne i symulacyjne, na Rys. 6.4 zobrazowano uzyskane wartości wskaźnika gotowości systemu transportowego A_S w zależności od liczby pojazdów ciężarowo-osobowych. Wykazano, że różnice dla wszystkich konfiguracji systemu pomiędzy wynikami obydwu podejść nie przekraczały 0,008, co stanowi potwierdzenie poprawnej weryfikacji opracowanych metod i modeli. Wymagana wartość gotowości systemu na poziomie 0,95 została osiągnięta dla systemu złożonego z 10 pojazdów, co odpowiadało ok. 52,6% wielkości bieżącej floty transportowej. Największy przyrost wartości wskaźnika A_S zaobserwowano w zakresie zwiększenia struktury systemu w zakresie od 1 do 8 pojazdów.

Średnia efektywność funkcjonowania systemu dla struktury złożonej z 10 pojazdów wyniosła $TPM = 0{,}9912$ co oznaczało, że system transportowy posiada zdolności do realizacji ponad 99% zadań, które napływały stochastycznie zgodnie z rozkładem logistycznym o parametrach położenia $\phi = 3{,}8344$ i skali $\sigma = 2{,}0762$. Zgodnie z przeprowadzoną symulacją wartości $TPM(i)$ dla poszczególnych symulacji mogą jednak przyjmować wartości nawet poniżej 0,50. Tego typu obserwacje są traktowane jako odstające (ang. *outliers*) i nie mają istotnego wpływu na średnią wartość wskaźnika efektywności. Dokładne wyniki dla systemów transportowych wyposażonych od 1 do 19 pojazdów ciężarowo-osobowych przedstawiono na Rys. 6.5.

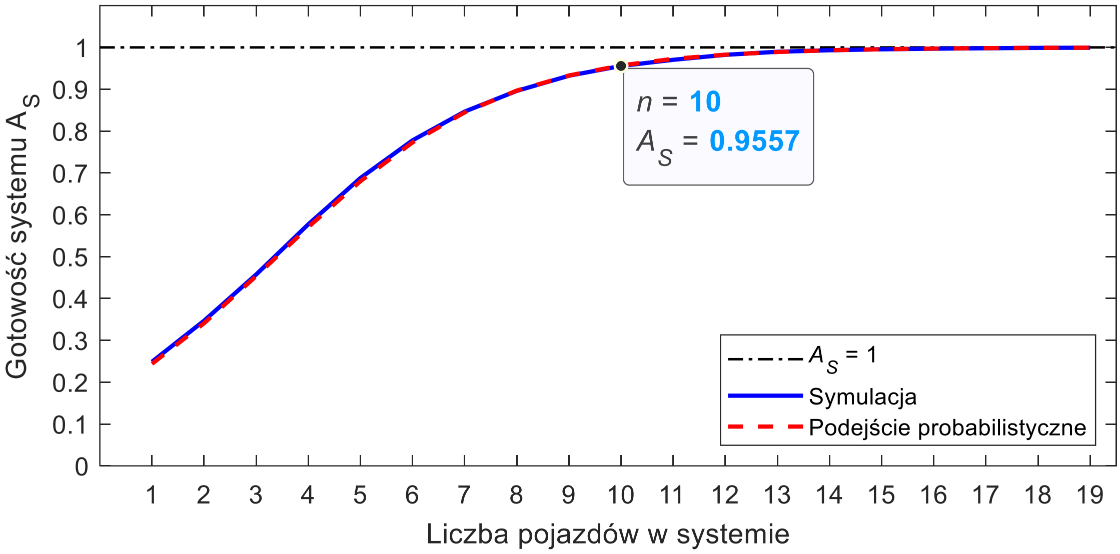

Rys. 6.4. Gotowość systemu transportowego w zależności od liczby pojazdów **[P5]**

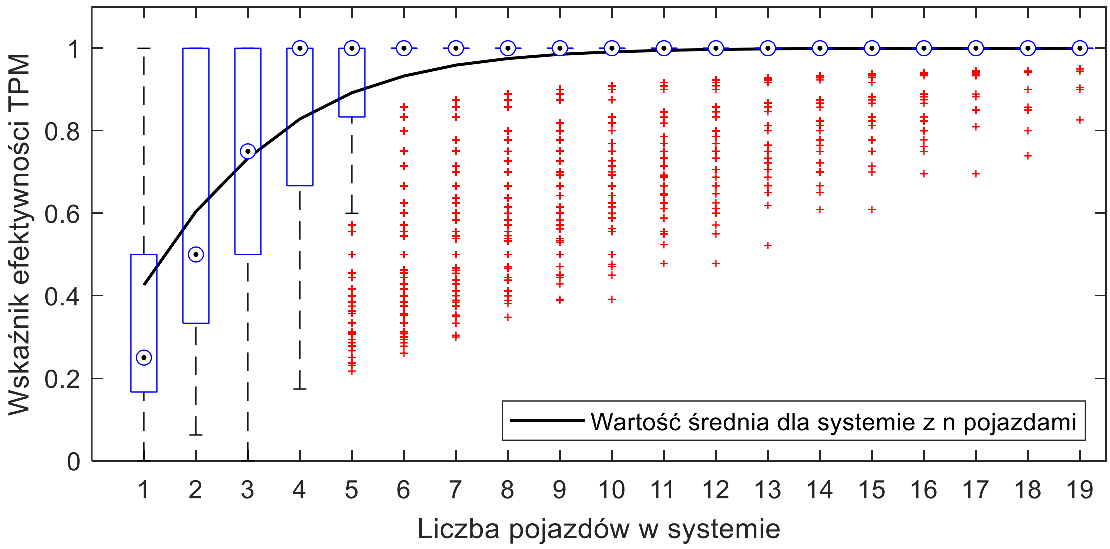

Rys. 6.5. Wskaźnik efektywności systemu transportowego w zależności od liczby pojazdów **[P5]**

6.3. Analiza wrażliwości i potencjalnej redukcji kosztów systemu transportowego

Opracowany model niezawodności oparty na procesie Markowa wykorzystano do przeprowadzenia analizy wrażliwości. Przyjęto założenie, że system transportowy wyposażony jest w zredukowaną do 10 liczbę pojazdów ciężarowo-osobowych. Przeanalizowano wpływ parametrów intensywności uszkodzeń i napraw pojazdów na wskaźniki gotowości i efektywności systemu transportowego. Zakres zmienności obu parametrów został przeanalizowany w przedziale 10-cio krotnego zmniejszenia i zwiększenia wartości parametrów estymowanych na podstawie zgromadzonych danych empirycznych. Dla wszystkich analizowanych punktów przeprowadzono obliczenia w oprogramowaniu MATLAB. Wyniki analizy wrażliwości przedstawiono na Rys. 6.6 i Rys. 6.7.

W przypadku utrzymania obecnego potencjału obsługowo-remontowego, którego naprawa uszkodzonego pojazdu była realizowana z intensywnością równą $\mu = 0{,}2607\ \frac{1}{dzień}$, nawet dziesięciokrotny wzrost intensywności uszkodzeń nie spowodował znacznego obniżenia się wartości wskaźnika gotowości systemu. Wskaźnik A_S osiągnął w takiej sytuacji poziom około 0,90. Jeżeli przy takim wzroście intensywności uszkodzeń nastąpi jednoczesne zmniejszenie się intensywności napraw, to gotowość systemu osiągnie wskaźnik wynoszący 0,50. Jednakże warto podkreślić, iż jest to skrajny scenariusz zdarzeń o znikomym prawdopodobieństwie realizacji. Wskaźnik efektywności funkcjonowania systemu transportowego podobnie jak jego gotowość przy zachowaniu obecnego poziomu intensywności napraw wykazuje dużą odporność na wzrost intensywności uszkodzeń pojazdów. Wartość TPM obniża się poniżej poziomu 0,90 dopiero w przypadku tak ekstremalnych wariantów jak np. czterokrotny wzrost intensywności uszkodzeń ($\lambda = 0{,}0192\ \frac{1}{dzień}$) przy jednoczesnym dziesięciokrotnym obniżeniu się intensywności napraw ($\mu = 0{,}0261\ \frac{1}{dzień}$). Taki scenariusz oznacza, że pojazd ciężarowo-osobowy uszkadza się średnio co 52 dni i jest naprawiany średnio przez ponad 38 dni.

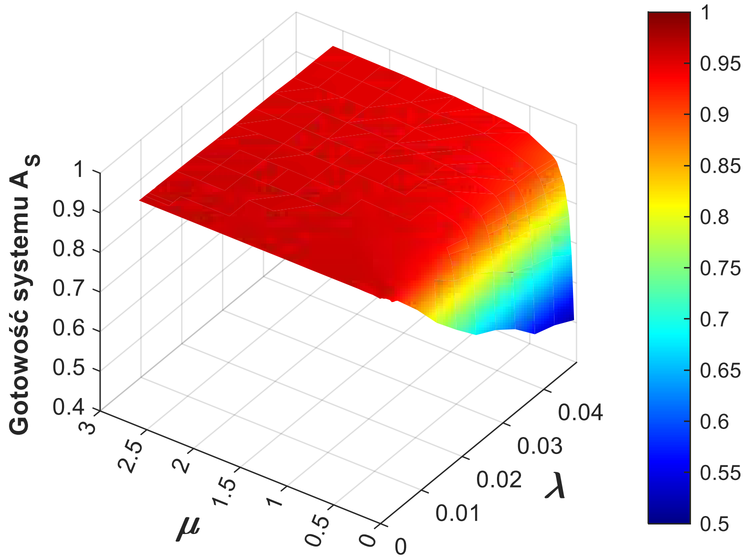

Rys. 6.6. Analiza wrażliwości gotowości systemu w zależności od parametrów uszkodzeń i napraw pojazdów **[P5]**

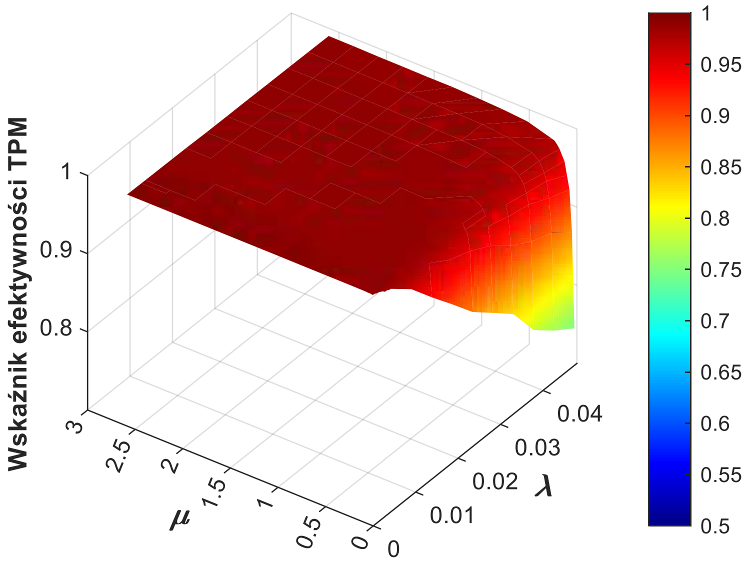

Rys. 6.7. Analiza wrażliwości wskaźnika efektywności systemu w zależności od parametrów uszkodzeń i napraw pojazdów **[P5]**

Finalnym etapem badań nad gotowością i efektywnością systemu transprotowego była analiza możliwości redukcji kosztów jego budowy i funkcjonowania. Koszty budowy systemu transportowego są zdeterminowane przez zakup pojazdów. Pojazd ciężarowo-osobowy Honker 2000 według danych wojskowych w momencie jego zakupu kosztował przeciętnie około 30 100 dolarów amerykańskich (USD)[4]. Wydatek ten jest

[4] Dane z wojskowego systemu PWE ZWSI RON.

ponoszony jednorazowo, przy czym jego potencjał eksploatacyjny zgodnie z Katalogiem Norm Eksploatacji Techniki Lądowej wynosi 20 lat, co w przeliczeniu na rok eksploatacji pojazdu daje koszt zakupu jednostki wynoszący 1505 USD. Wydatki na eksploatację systemu obejmują:

- naprawy główne o wartości około 18 940 USD, ponoszone co 8 lat;
- naprawy bieżące, których koszt oraz interwał czasowy estymowano na podstawie danych empirycznych i wynoszą odpowiednio 1090 USD i 0,58 lat (6,96 miesięcy);
- obsługiwania okresowe o wartości 160 USD rocznie.

Sumaryczny średnio-roczny koszt zakupu i eksploatacji (z pominięciem kosztów paliwa) jednego pojazdu ciężarowo-osobowego Honker 2000 wynosi zatem około 5911,81 USD. Na Rys. 6.8 przedstawiono stosunek przyrostu wartości wskaźników A_S i TPM do kosztów ponoszonych rocznie przy zwiększeniu struktury systemu transportowego o jeden pojazd. Przyrost efektywności systemu do przyrostu wartości ponoszonych kosztów ma przebieg malejący i dla optymalnej liczby pojazdów osiąga wartość bliską zero. Przyrost gotowości systemu do przyrostu wartości ponoszonych kosztów nie jest monotoniczny i osiąga wartość maksymalną równą $2{,}03\times10^{-5}$ (1/USD) dla struktury złożonej z 4 pojazdów.

Na tej podstawie określono potencjalną redukcję kosztów systemu transporotwego przy zmniejszeniu liczebności pojazdów z obecnego poziomu wynoszącego 19 obiektów do wartości równej 10. Zapewnia to osiągnięcie 0,95 i większej wartości wskaźników gotowości oraz efektywności systemu. Wartość bezwzględna redukcji kosztów wynosi ponad 53,2 tys. USD rocznie, co w efekcie przekłada się na procentową wartość względną równą 47%. Należy jednocześnie wskazać niewspółmierność znaczących zysków ekonomicznych uzyskanych przy optymalizacji systemu w stosunku do niewielkich strat gotowości oraz efektywności systemu równych odpowiednio 4,36% i 0,87%. Zatem optymalizacja wielkości floty transportowej ma bezpośrednie przełożenie na redukcję kosztów i wzrost efektywności ekonomicznej systemu. Oznacza to, że opracowany model systemu i algorytm jego optymalizacji posiadają znaczenie nie tylko w obszarze bezpieczeństwa państwa, ale również mają wpływ na gospodarkę kraju.

Przedstawione w niniejszym rozdziale modele, przeprowadzone analizy oraz sformułowane wnioski stanowią realizację celu szczegółowego **[C6]** rozprawy doktorskiej.

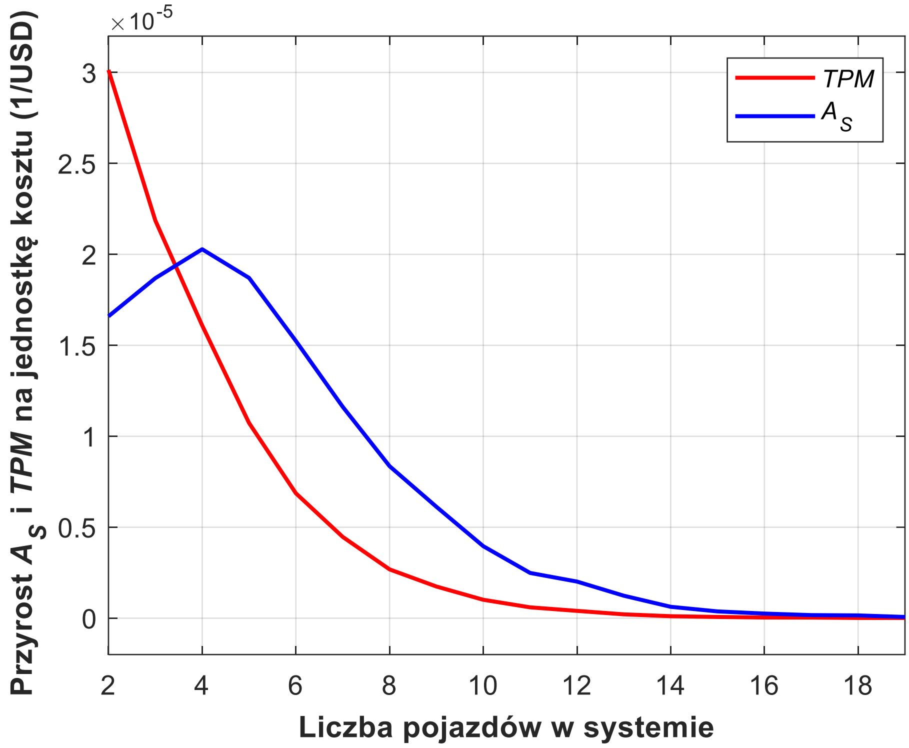

Rys. 6.8. Analiza wzrostu gotowości i efektywności systemu w stosunku do kosztu zwiększenia systemu transportowego o jeden pojazd **[P5]**

7. PODSUMOWANIE WYNIKÓW BADAŃ I WNIOSKI Z PRZEPROWADZONYCH ANALIZ

Celem niniejszej rozprawy doktorskiej było opracowanie oraz implementacja modeli probabilistycznych i symulacyjnych do wieloaspektowej analizy niezawodności i gotowości pojazdów ciężarowo-osobowych, będących na wyposażeniu wojskowych systemów transportowych. Badania naukowe zostały przeprowadzone na podstawie zgromadzonej, obszernej dokumentacji eksploatacyjnej dla prób o liczebnościach 19 i 55 pojazdów marki Honker 2000. Wszystkie założone szczegółowe cele pracy zostały zrealizowane w oparciu o przyjętą metodologię badawczą. Opracowane modele niezawodności i gotowości wraz z otrzymanymi wynikami zostały wydane w ramach cyklu publikacyjnego obejmującego 6 artykułów naukowych w czasopismach z listy MNiSW oraz Journal Citation Reports.

Na podstawie przeprowadzonych badań i analiz sformułowano następujące wnioski końcowe:

- Do estymacji funkcji niezawodności pojazdów użyteczny okazał się jest estymator Kaplana-Meiera. Dane o uszkodzeniach pochodzące z empirycznego procesu eksploatacji pojazdów wojskowych zawierają obserwacje cenzorowane. Wykorzystanie estymatora Kaplana-Meiera umożliwia uwzględnienie wpływu zarówno kompletnych, jak i cenzorowanych danych eksploatacyjnych na niezawodność obiektu technicznego. Na podstawie estymowanej i aproksymowanej funkcji niezawodności określono oczekiwany przebieg pomiędzy uszkodzeniami pojazdu ciężarowo-osobowego Honker 2000 wynoszący 4255,32 km dla modelu wykładniczego oraz 4686,22 km dla modelu Weibulla. Przedstawione wyniki i wnioski stanowią realizację celu szczegółowego **[C1]** rozprawy doktorskiej.
- Procesy semi-Markowa ze względu na dowolne rozkłady czasów przejść międzystanowych są właściwym modelem do odwzorowania procesu eksploatacji pojazdów ciężarowo-osobowych. Do analitycznego wyznaczenia funkcji niezawodności i pozostałych charakterystyk niezawodnościowych odpowiednim okazał się 3-stanowy model semi-Markowa i transformata Laplace'a. Modele o większej przestrzeni stanowej (4 i 9 stanów) stanowiły dokładniejsze odtworzenie badanego procesu, co przełożyło się również na wyższe wartości wskaźników gotowości obiektu. Wartości wskaźników gotowości pojazdów ciężarowo-osobowych marki Honker 2000 obliczone w oparciu o 4- i 9-stanowe modele semi-Markow mieściły

się w przedziale 0,90 – 0,91. Niniejsze wnioski odnoszą się do celów szczegółowych **[C2]** i **[C3]** rozprawy doktorskiej.

- Modele symulacyjne bazujące na wielokrotnym próbkowaniu losowym Monte Carlo są przydatne do prognozowania wartości wskaźników gotowości w zależności od intensywności użytkowania pojazdów. Model symulacyjny o 4-stanowej przestrzeni fazowej odzwierciedla cztery główne stany pojazdu w procesie eksploatacji, tj. realizację zadań transportowych, oczekiwanie na przydział zadania, realizację obsługiwania okresowego w ramach planowo - zapobiegawczej strategii eksploatacji oraz stan niezdatności. Wykazano, że zwiększenie wartości oczekiwanej dobowego przebiegu pojazdu o 1 km zmniejsza wartość wskaźników gotowości o ok. 0,0008. Przedstawiona konkluzja dotyczy celu szczegółowego **[C4]** rozprawy doktorskiej.
- Funkcja niezawodności pojazdu w dwuwymiarowej dziedzinie czasu eksploatacji i przebiegu odzwierciedla wpływ czynników związanych ze starzeniem i zużyciem układów i mechanizmów na prawdopodobieństwo prawidłowej pracy. Modele probabilistyczne niezawodności siedmiu podstawowych podsystemów pojazdu bazujące na dwuwymiarowych kopulach Claytona okazały się najskuteczniejsze ze względu na najlepsze dopasowanie do danych empirycznych mierzone z wykorzystaniem statystyki Craméra-von Misesa. Mierniki ważności niezawodnościowej wykazały, że najbardziej niezawodnymi podsystemami pojazdu Honker 2000 są zawieszenie i układ hamulcowy, natomiast najbardziej awaryjne okazały się silnik, instalacja elektryczna i układ przeniesienia napędu. Wyniki i wnioski z analizy opracowanych modeli niezawodności wypełniają cel szczegółowy **[C5]** rozprawy doktorskiej.
- Analiza poziomów redundancji za pomocą modelu Markowa oraz symulacji Monte Carlo opracowanych dla systemu transportowego o strukturze progowej *k z n* wykazała możliwość redukcji liczby pojazdów z 19 do 10 przy zachowaniu wartości wskaźników gotowości i efektywności systemu na poziomie powyżej 0,95. Na podstawie analizy wrażliwości modelu stwierdzono, że dziesięciokrotny wzrost intensywności uszkodzeń pojazdów przy zachowaniu bieżącej intensywności napraw spowodował obniżenie wartości wskaźników gotowości i efektywności do poziomu około 0,90. Zatem kluczowe dla systemu transportowego jest utrzymywanie odpowiednich zdolności do naprawy uszkodzonych komponentów. Przedstawiony wniosek odnosi się do celu szczegółowego **[C6]** rozprawy doktorskiej.

Badania naukowe przeprowadzone w ramach rozprawy doktorskiej były ukierunkowane na uzupełnienie istniejących luk w literaturze naukowej, które zostały zidentyfikowane w ramach obszernego przeglądu wielu najnowszych publikacji. Elementy nowatorskie, stanowiące wkład naukowy w rozwój dyscypliny naukowej inżynieria mechaniczna, zostały scharakteryzowane poniżej:

- W zakresie uzupełnienia luki przedmiotowej, przeprowadzono badania i opracowano analizy naukowe dotyczące niezawodności wojskowych pojazdów ciężarowo-osobowych. Stanowi to nowe podejście, ponieważ dotychczasowe publikacje naukowe nie obejmowały badań procesu eksploatacji tak specyficznych obiektów technicznych. Należy jednocześnie podkreślić, że dane eksploatacyjne obiektów i systemów wojskowych są w praktyce trudno dostępne, a ich pozyskanie jest procesem utrudnionym, długotrwałym i wymaga uzyskania szeregu zezwoleń od odpowiednich organów logistycznych.
- W obszarze implementacji procesów semi-Markowa, opracowano modele z trzema wariantami przestrzeni stanowej w zależności od założonego celu badawczego. Wykazano przydatność 3-stanowego modelu do wyznaczenia funkcji niezawodności pojazdu oraz modeli 4-stanowego i 9-stanowego służących do obliczenia wskaźników gotowości i zdatności technicznej.
- W zakresie podejścia metodologicznego, opracowano model symulacyjny oparty na metodach wielokrotnego próbkowania Monte Carlo, który stanowi innowacyjne podejście do analizy wpływu intensywności użytkowania na wartości wskaźników gotowości pojazdów, uwzględniając jednocześnie deterministyczne procesy obsługiwania okresowego.
- Niemniej istotne pozostaje rozwinięcie modeli probabilistycznych wykorzystujących dwuwymiarowe kopule Claytona do odwzorowania niezawodności podsystemów pojazdu. Rozwinięto również miary ważności niezawodnościowej do określania „słabych ogniw” systemów opisanych za pomocą modeli niezawodnościowych o dwuwymiarowej dziedzinie funkcji niezawodności.
- Ostatnim oryginalnym elementem merytorycznym było opracowanie metodyki służącej do wyznaczania gotowości i efektywności systemów technicznych o strukturze progowej *k z n*, obsługujących zmienne w czasie strumienie zadań. Autorska metoda jest uniwersalna i może być zastosowana do innych rodzajów

pojazdów o podobnej strategii eksploatacji. W rozprawie została zweryfikowana na przykładzie badanej próby wojskowych pojazdów ciężarowo-osobowych.

Poza naukowym aspektem rozprawy doktorskiej, opracowane metody i modele mogą zostać zaimplementowane w systemach informatycznych wspierających proces eksploatacji w SZ RP. Włączenie zaproponowanych w pracy narzędzi do modułu wsparcia eksploatacji PWE ZWSI RON umożliwi rozszerzenie funkcjonalności oprogramowania o kluczowe komponenty analityczne. Wykorzystanie modeli semi-Markowa, których parametry są estymowane na podstawie bieżących danych eksploatacyjnych, pozwala na precyzyjną ocenę gotowości pojazdów wojskowych. Dodatkowo, w kontekście planowania wymaganych zdolności transportowych na potrzeby ćwiczeń poligonowych, misji operacyjnych oraz innych przedsięwzięć skutkujących intensyfikacją użytkowania sprzętu wojskowego (SpW), prognoza gotowości może być realizowana przy użyciu symulacji Monte Carlo. Implementacja modeli probabilistycznych bazujących na kopulach umożliwia predykcję awarii podsystemów i komponentów w zadanych warunkach eksploatacyjnych, co może znacząco usprawnić proces planowania oraz zarządzania zapasami części zamiennych. Ostatnim istotnym aspektem, który może przyczynić się do zwiększenia efektywności funkcjonowania SZ RP, jest optymalizacja poziomów redundancji w systemach transportowych poprzez odpowiednie alokowanie pojazdów do jednostek wojskowych, uwzględniające ograniczenia budżetowe.

8. BIBLIOGRAFIA

[1] Macheret Y, Koehn P, Sparrow D. Improving reliability and operational availability of military systems. 2005 IEEE Aerospace Conference, Big Sky, Montana, USA: IEEE Operations Center; 2005, p. 3948–57. https://doi.org/10.1109/AERO.2005.1559700.

[2] Migawa K. Availability control for means of transport in decisive semi-markov models of exploitation process. Archives of Transport 2012;24:497–508. https://doi.org/10.2478/v10174-012-0030-4.

[3] Girtler J, Ślezak M. Four-state stochastic model of changes in the reliability states of a motor vehicle. Eksploatacja i Niezawodnosc 2013;15:156–60.

[4] Kamlu S, Laxmi V. Condition-based maintenance strategy for vehicles using hidden Markov models. Advances in Mechanical Engineering 2019;11:1–13. https://doi.org/10.1177/1687814018806380.

[5] Borucka A, Niewczas A, Hasilova K. Forecasting the readiness of special vehicles using the semi-Markov model. Eksploatacja i Niezawodnosc - Maintenance and Reliability 2019;21:662–9. https://doi.org/10.17531/ein.2019.4.16.

[6] Ziółkowski J. Stochastyczne modelowanie i optymalizacja gotowości w procesie eksploatacji śmigłowców. Podstawy teoretyczne, metodologia tworzenia, weryfikacja i implementacja modeli. Warszawa: Wojskowa Akademia Techniczna; 2019.

[7] Barde SRA, Yacout S, Shin H. Optimal preventive maintenance policy based on reinforcement learning of a fleet of military trucks. J Intell Manuf 2019;30:147–61. https://doi.org/10.1007/s10845-016-1237-7.

[8] Selech J, Andrzejczak K. An aggregate criterion for selecting a distribution for times to failure of components of rail vehicles. Eksploatacja i Niezawodnosc - Maintenance and Reliability 2019;22:102–11. https://doi.org/10.17531/ein.2020.1.12.

[9] Przybysz K, Dygnatowski S, Grzesik N. An Analysis of Reliability of Military Vehicles. Journal of KONBiN 2019;49:527–36. https://doi.org/10.2478/jok-2019-0070.

[10] Simiński P, Kończak J, Przybysz K. Analysis and Testing of Reliability of Military Vehicles. Journal of KONBiN 2018;47:87–95. https://doi.org/10.2478/jok-2018-0040.

[11] Ministry of National Defence,. HONKER 2000 light utility vehicle Data Sheet 2005.

[12] Sosnowicz R, Wachowiak P, Dorczuk M. Conception of Military Vehicle Classification. Journal of KONES 2011;18:585–94.

[13] Lyu H, Yang Z, Wang S, Zhao Y, Pecht M. Reliability modeling for multistage systems subject to competing failure processes. Quality and Reliability Engineering International 2021;37:2936–49. https://doi.org/10.1002/qre.2898.

[14] Woch M, Zieja M, Tomaszewska J. Analysis of the time between failures of aircrafts. 2017 2nd International Conference on System Reliability and Safety (ICSRS), 2017, p. 112–8. https://doi.org/10.1109/ICSRS.2017.8272805.

[15] Thijssens OWM, Verhagen WJC. Application of Extended Cox Regression Model to Time-On-Wing Data of Aircraft Repairables. Reliability Engineering & System Safety 2020;204:1–11. https://doi.org/10.1016/j.ress.2020.107136.

[16] Gołda P, Zawisza T, Izdebski M. Evaluation of efficiency and reliability of airport processes using simulation tools. Eksploatacja i Niezawodnosc - Maintenance and Reliability 2021;23:659–69. https://doi.org/10.17531/ein.2021.4.8.

[17] Chatterjee S, Bandopadhyay S. Reliability estimation using a genetic algorithm-based artificial neural network: An application to a load-haul-dump machine. Expert

Systems with Applications 2012;39:10943–51. https://doi.org/10.1016/j.eswa.2012.03.030.
[18] Kamruzzaman Md, Bhusal N, Benidris M. A convolutional neural network-based approach to composite power system reliability evaluation. International Journal of Electrical Power & Energy Systems 2022;135:1–10. https://doi.org/10.1016/j.ijepes.2021.107468.
[19] Song S, Coit DW, Feng Q. Reliability for systems of degrading components with distinct component shock sets. Reliability Engineering & System Safety 2014;132:115–24. https://doi.org/10.1016/j.ress.2014.06.020.
[20] Barabino B, Di Francesco M, Mozzoni S. An Offline Framework for the Diagnosis of Time Reliability by Automatic Vehicle Location Data. IEEE Transactions on Intelligent Transportation Systems 2017;18:583–94. https://doi.org/10.1109/TITS.2016.2581024.
[21] Barabino B, Di Francesco M, Mozzoni S. Time Reliability Measures in bus Transport Services from the Accurate use of Automatic Vehicle Location raw Data. Quality and Reliability Engineering International 2017;33:969–78. https://doi.org/10.1002/qre.2073.
[22] Ziółkowski J, Małachowski J, Oszczypała M, Szkutnik-Rogoż J, Lęgas A. Modelling of the Military Helicopter Operation Process in Terms of Readiness. Defence Science Journal 2021;71:602–11. https://doi.org/10.14429/dsj.71.16422.
[23] Alkaff A, Qomarudin MN, Purwantini E, Wiratno SE. Dynamic reliability modeling for general standby systems. Computers & Industrial Engineering 2021;161:1–21. https://doi.org/10.1016/j.cie.2021.107615.
[24] Hao S, Yang J, Ma X, Zhao Y. Reliability modeling for mutually dependent competing failure processes due to degradation and random shocks. Applied Mathematical Modelling 2017;51:232–49. https://doi.org/10.1016/j.apm.2017.06.014.
[25] Hong L, Zhai Q, Wang X, Ye Z-S. System Reliability Evaluation Under Dynamic Operating Conditions. IEEE Transactions on Reliability 2019;68:800–9. https://doi.org/10.1109/TR.2018.2869572.
[26] Żurek J, Machałowski J, Ziółkowski J, Szkutnik-Rogoż J. Reliability Analysis of Technical Means of Transport. Applied Sciences 2020;9:1–17. https://doi.org/10.3390/app10093016.
[27] Song C-Y. A Study on Learning Parameters in Application of Radial Basis Function Neural Network Model to Rotor Blade Design Approximation. Applied Sciences 2021;11:6133. https://doi.org/10.3390/app11136133.
[28] Kozłowski E, Borucka A, Świderski A. Application of the logistic regression for determining transition probability matrix of operating states in the transport systems. Eksploatacja i Niezawodnosc 2020;22:192–200. https://doi.org/10.17531/ein.2020.2.2.
[29] Wu B, Cui L. Reliability evaluation of Markov renewal shock models with multiple failure mechanisms. Reliability Engineering & System Safety 2020;202:107051. https://doi.org/10.1016/j.ress.2020.107051.
[30] Grabski F. Semi-Markov failure rates processes. Applied Mathematics and Computation 2011;217:9956–65. https://doi.org/10.1016/j.amc.2011.04.055.
[31] Zhao J, Jia Y, Shi L, Zhao X, Kong L. Research on Technical Readiness Evaluation Method in Model Development. 2015 8th International Symposium on Computational Intelligence and Design (ISCID), vol. 1, 2015, p. 392–6. https://doi.org/10.1109/ISCID.2015.234.

[32] Wang L, Cui L, Zhang J, Peng J. Reliability evaluation of a Semi-Markov repairable system under alternative environments. Communications in Statistics - Theory and Methods 2016;45:2938–57. https://doi.org/10.1080/03610926.2014.894062.
[33] Wu B, Cui L. Reliability of repairable multi-state two-phase mission systems with finite number of phase switches. Applied Mathematical Modelling 2020;77:1229–41. https://doi.org/10.1016/j.apm.2019.09.018.
[34] Żurek J, Zieja M, Ziółkowski J, Borucka A. Vehicle operation process analysis using the Markov processes, 2020, p. 2598–605. https://doi.org/10.3850/978-981-11-2724-3_0652-cd.
[35] Paś J, Klimczak T, Rosiński A, Stawowy M. The analysis of the operational process of a complex fire alarm system used in transport facilities. Build Simul 2022;15:615–29. https://doi.org/10.1007/s12273-021-0790-y.
[36] Migawa K, Borowski S, Neubauer A, Sołtysiak A. Semi-Markov Model of the System of Repairs and Preventive Replacements by Age of City Buses. Applied Sciences 2021;11:1–16. https://doi.org/10.3390/app112110411.
[37] Bai B, Zhang J, Wu X, wei Zhu G, Li X. Reliability prediction-based improved dynamic weight particle swarm optimization and back propagation neural network in engineering systems. Expert Systems with Applications 2021;177:1–13. https://doi.org/10.1016/j.eswa.2021.114952.
[38] Blasi A, Janssen J, Manca R. Numerical Treatment of Homogeneous and Non-homogeneous Semi-Markov Reliability Models. Communications in Statistics - Theory and Methods 2004;33:697–714. https://doi.org/10.1081/STA-120028692.
[39] Świderski A, Borucka A, Grzelak M, Gil L. Evaluation of Machinery Readiness Using Semi-Markov Processes. Applied Sciences 2020;10:1541. https://doi.org/10.3390/app10041541.
[40] Thomas O, Sobanjo J. Comparison of Markov Chain and Semi-Markov Models for Crack Deterioration on Flexible Pavements. Journal of Infrastructure Systems 2013;19:186–95. https://doi.org/10.1061/(ASCE)IS.1943-555X.0000112.
[41] Aït-Sahalia Y, Fan J, Jiang J. Nonparametric tests of the Markov hypothesis in continuous-time models. Ann Statist 2010;38:3129–63. https://doi.org/10.1214/09-AOS763.
[42] Liu C, Kramer A, Neumann S. Reliability assessment of repairable phased-mission system by Monte Carlo simulation based on modular sequence-enforcing fault tree model. Eksploatacja i Niezawodnosc - Maintenance and Reliability 2020;22:272–81. https://doi.org/10.17531/ein.2020.2.10.
[43] Novak M, Sangwongwanich A, Blaabjerg F. Monte Carlo Based Reliability Estimation Methods in Power Electronics. 2020 IEEE 21st Workshop on Control and Modeling for Power Electronics (COMPEL), 2020, p. 1–7. https://doi.org/10.1109/COMPEL49091.2020.9265685.
[44] Green RC, Wang L, Alam M, Singh C. Intelligent state space pruning for Monte Carlo simulation with applications in composite power system reliability. Engineering Applications of Artificial Intelligence 2013;26:1707–24. https://doi.org/10.1016/j.engappai.2013.03.006.
[45] Liu K, Wu J, Liu H, Sun M, Wang Y. Reliability analysis of thermal error model based on DBN and Monte Carlo method. Mechanical Systems and Signal Processing 2021;146:107020. https://doi.org/10.1016/j.ymssp.2020.107020.
[46] Jensen HA, Jerez DJ, Valdebenito M. An adaptive scheme for reliability-based global design optimization: A Markov chain Monte Carlo approach. Mechanical Systems and Signal Processing 2020;143:106836. https://doi.org/10.1016/j.ymssp.2020.106836.

[47] Zhang L, Dong L, Cheng S, Li W, Wang B, Liu H, et al. Efficient reliability assessment method for bridges based on Markov Chain Monte Carlo (MCMC) with Metropolis-Hasting Algorithm (MHA). IOP Conf Ser: Earth Environ Sci 2020;580:1–7. https://doi.org/10.1088/1755-1315/580/1/012030.
[48] Zhu H, Wang X, Xiao M, Yang Z, Tang X, Wen B. Reliability modeling for intermittent working system based on Wiener process. Computers & Industrial Engineering 2021;160:107599. https://doi.org/10.1016/j.cie.2021.107599.
[49] Roslan NNRB, Fauzi NFBM, Ridzuan MIM. Sequential and Nonsequential Monte Carlo in Assessing Reliability Performance of Distribution Network. 2020 Emerging Technology in Computing, Communication and Electronics (ETCCE), Malaysia: 2020, p. 1–6. https://doi.org/10.1109/ETCCE51779.2020.9350906.
[50] Ugurlu OF, Kumral M. Reliability-based performance analysis of mining drilling operations through Markov chain Monte Carlo and mean reverting process simulations. Simulation 2020;96:593–604. https://doi.org/10.1177/0037549720923751.
[51] Zhang X, Lu Z, Cheng K, Wang Y. A novel reliability sensitivity analysis method based on directional sampling and Monte Carlo simulation. Proceedings of the Institution of Mechanical Engineers, Part O: Journal of Risk and Reliability 2020;234:622–35. https://doi.org/10.1177/1748006X19899504.
[52] Zhang K, Du Z, Xiao F, Wang T, Zhang L. Improved Sequential Monte Carlo Method Approach to Substation Connection Reliability Assessment. 2020 IEEE 4th Conference on Energy Internet and Energy System Integration (EI2), Wuhan, China: 2020, p. 2357–62. https://doi.org/10.1109/EI250167.2020.9347301.
[53] Żurek J, Ziółkowski J, Borucka A. Application of markov processes to the method for analysis of combat vehicle operation in the aspect of their availability and readiness, 2017, p. 2343–52. https://doi.org/10.1201/9781315210469-294.
[54] Hu J, Shen J, Shen L. Periodic preventive maintenance planning for systems working under a Markovian operating condition. Computers & Industrial Engineering 2020;142:1–10. https://doi.org/10.1016/j.cie.2020.106291.
[55] Sbihi M, Varnier C. Single-machine scheduling with periodic and flexible periodic maintenance to minimize maximum tardiness. Computers & Industrial Engineering 2008;55:830–40. https://doi.org/10.1016/j.cie.2008.03.005.
[56] Liu P, Wang G. Optimal periodic preventive maintenance policies for systems subject to shocks. Applied Mathematical Modelling 2021;93:101–14. https://doi.org/10.1016/j.apm.2020.12.013.
[57] Wu S. Construction of asymmetric copulas and its application in two-dimensional reliability modelling. European Journal of Operational Research 2014;238:476–85. https://doi.org/10.1016/j.ejor.2014.03.016.
[58] Bolbolian Ghalibaf M. Relationship Between Kendall's tau Correlation and Mutual Information. Rev Colomb Estad 2020;43:3–20. https://doi.org/10.15446/rce.v43n1.78054.
[59] Fang G, Pan R, Hong Y. Copula-based reliability analysis of degrading systems with dependent failures. Reliability Engineering & System Safety 2020;193:106618. https://doi.org/10.1016/j.ress.2019.106618.
[60] Calabrese R, Osmetti SA. A new approach to measure systemic risk: A bivariate copula model for dependent censored data. European Journal of Operational Research 2019;279:1053–64. https://doi.org/10.1016/j.ejor.2019.06.027.
[61] Amini A, Abdollahi A, Hariri-Ardebili MA, Lall U. Copula-based reliability and sensitivity analysis of aging dams: Adaptive Kriging and polynomial chaos Kriging methods. Applied Soft Computing 2021;109:107524. https://doi.org/10.1016/j.asoc.2021.107524.

[62] Chen R, Zhang C, Wang S, Hong L. Bivariate-Dependent Reliability Estimation Model Based on Inverse Gaussian Processes and Copulas Fusing Multisource Information. Aerospace 2022;9:392. https://doi.org/10.3390/aerospace9070392.
[63] Jafary B, Mele A, Fiondella L. Component-based system reliability subject to positive and negative correlation. Reliability Engineering & System Safety 2020;202:107058. https://doi.org/10.1016/j.ress.2020.107058.
[64] Ye Z, Cai Z, Zhou F, Zhao J, Zhang P. Reliability analysis for series manufacturing system with imperfect inspection considering the interaction between quality and degradation. Reliability Engineering & System Safety 2019;189:345–56. https://doi.org/10.1016/j.ress.2019.05.005.
[65] Qiu S, Ming X. A fuzzy universal generating function-based method for the reliability evaluation of series systems with performance sharing between adjacent units under parametric uncertainty. Fuzzy Sets and Systems 2021;424:155–69. https://doi.org/10.1016/j.fss.2020.08.013.
[66] Espiritu JF, Coit DW, Prakash U. Component criticality importance measures for the power industry. Electric Power Systems Research 2007;77:407–20. https://doi.org/10.1016/j.epsr.2006.04.003.
[67] Birnbaum ZW. On the importance of different components in a multicomponent system. Multivariate Analysis II New York: Academic Press 1969:581-92.
[68] Amrutkar KP, Kamalja KK. An Overview of Various Importance Measures of Reliability System. Int J Math, Eng, Manag Sci 2017;2:150–71. https://doi.org/10.33889/IJMEMS.2017.2.3-014.
[69] Rausand M, Høyland A. System reliability theory: models, statistical methods, and applications. 2nd ed. Hoboken, NJ: Wiley-Interscience; 2004.
[70] He L, Lu Z, Xinyao Li. Failure-mode importance measures in structural system with multiple failure modes and its estimation using copula. Reliability Engineering & System Safety 2018;174:53–9. https://doi.org/10.1016/j.ress.2018.02.016.
[71] Yalcin F, Franko C. Computing Birnbaum and Barlow-Proschan importance measures using system signature. Communications in Statistics - Theory and Methods 2022;51:8446–57. https://doi.org/10.1080/03610926.2021.1986536.
[72] Eryilmaz S, Bozbulut AR. Computing marginal and joint Birnbaum, and Barlow–Proschan importances in weighted-k-out-of-n:G systems. Computers & Industrial Engineering 2014;72:255–60. https://doi.org/10.1016/j.cie.2014.03.025.
[73] Aghaei M, Zeinal Hamadani A, Abouei Ardakan M. Redundancy allocation problem for k-out-of-n systems with a choice of redundancy strategies. J Ind Eng Int 2017;13:81–92. https://doi.org/10.1007/s40092-016-0169-3.
[74] Bian L, Wang G, Liu P. Reliability analysis for k-out-of-n(G) systems subject to dependent competing failure processes. Computers & Industrial Engineering 2023;177:109084. https://doi.org/10.1016/j.cie.2023.109084.
[75] Fang S, Yu R, Wu D, Peng R. Reliability of a consecutive k-out-of-n: G system with protection blocks. International Journal of General Systems 2024:1–19. https://doi.org/10.1080/03081079.2024.2402308.
[76] Oszczypała M, Ziółkowski J, Małachowski J. Redundancy allocation problem in repairable k-out-of-n systems with cold, warm, and hot standby: A genetic algorithm for availability optimization. Applied Soft Computing 2024;165:112041. https://doi.org/10.1016/j.asoc.2024.112041.
[77] Sun H, Zhang Y, Zhao P. Allocating hot standbys to randomly weighted k-out-of-n: G systems. Proceedings of the Institution of Mechanical Engineers, Part O: Journal of Risk and Reliability 2022;236:37–54. https://doi.org/10.1177/1748006X211030812.

[78] Zheng J, Okamura H, Dohi T. Reliability Importance of Components in a Real-Time Computing System with Standby Redundancy Schemes. Int J Math, Eng, Manag Sci 2018;3:64–89. https://doi.org/10.33889/IJMEMS.2018.3.2-007.
[79] Sharifi M, Moghaddam TA, Shahriari M. Multi-objective Redundancy Allocation Problem with weighted-k-out-of-n subsystems. Heliyon 2019;5:e02346. https://doi.org/10.1016/j.heliyon.2019.e02346.
[80] Sharifi M, Taghipour S. Redundancy allocation problem of a Multi-State system with Binary-State continuous performance level components. Expert Systems with Applications 2022;200:117161. https://doi.org/10.1016/j.eswa.2022.117161.
[81] Levitin G, Xing L, Dai Y. Predetermined standby mode transfers in 1-out-of-N systems with resource-constrained elements. Reliability Engineering & System Safety 2023;229:108849. https://doi.org/10.1016/j.ress.2022.108849.
[82] Rykov V, Kozyrev D, Filimonov A, Ivanova N. On reliability function of a k-out-of-n system with general repair time distribution. Prob Eng Inf Sci 2021;35:885–902. https://doi.org/10.1017/S0269964820000285.
[83] Gao S. Reliability analysis and optimization for a redundant system with dependent failures and variable repair rates. Mathematics and Computers in Simulation 2023;208:637–59. https://doi.org/10.1016/j.matcom.2023.02.001.
[84] Sears, T. B. Taylor, E. P. Technical Performance Measurement Handbook 1984.
[85] Pham H, editor. Handbook of reliability engineering. London ; New York: Springer; 2003.
[86] Sharifi M, Shahriari M, Khajehpour A, Mirtaheri SA. Reliability Optimization of a k-out-of-n Series-Parallel System with Warm Standby Components. Scientia Iranica 2022;29:3523–41. https://doi.org/10.24200/sci.2021.56113.4591.
[87] Rykov VV, Sukharev MG, Itkin VYu. Investigations of the Potential Application of k-out-of-n Systems in Oil and Gas Industry Objects. JMSE 2020;8:928. https://doi.org/10.3390/jmse8110928.

9. ZAŁĄCZNIKI A – KODY ŹRÓDŁOWE MATLAB

Załącznik A1. Kod źródłowy symulacji Monte Carlo dla 4-stanowej przestrzeni procesu eksploatacji

```
vehicle = 19; % liczba pojazdów
readiness = zeros(vehicle,1);
suitability = zeros(vehicle,1);
L_m = 10000; % przebieg pomiędzy obsługami okresowymi (km)
T_m = 365; % czas pomiędzy obsługami okresowymi (dni)
max_iteration = 365*20; % liczba iteracji
s_1 = zeros(vehicle,1); % zadanie
s_2 = zeros(vehicle,1); % oczekiwanie na zadanie
s_3 = zeros(vehicle,1); % obsługa okresowa
s_4 = zeros(vehicle,1); % naprawa
failure = zeros(vehicle,1);
mileage = zeros(vehicle,max_iteration);
mileage_daily = zeros(vehicle,max_iteration);
l_max = 1000; % 1000 km maksymalny przebieg dzienny;
X = zeros(vehicle,max_iteration); % trajektoria zmian stanów
using_percentage = 0.32; % parametr intensywności użytkowania
mean_daily_mileage = 88.52; % parametr intensywności użytkowania
mean_mileage_between_failure = 4255.33; % MTBF
alfa_repair = 5.0784; % parametr naprawy
beta_repair = 0.4612; % parametr naprawy
K_r = zeros (max_iteration,1);
K_t = zeros (max_iteration,1);
for z = 1:vehicle
l_r = randi([0 5000],1,1);
l_m = randi([0 L_m],1,1);
t_m = randi([0 T_m],1,1);
t = 0;
while t < max_iteration
    if L_m <= l_m
       s_3(z,1) = s_3(z,1) + 1;
       t_m = 0;
       l_m = 0;
       X(z,t+1) = 3;
       mileage_daily(z,t+1) = 0;
       mileage(z,t+2) = mileage(z,t+1);
       t = t+1;
       elseif T_m <= t_m
             s_3(z,1) = s_3(z,1) + 1;
             t_m = 0;
             l_m = 0;
             X(z,t+1) = 3;
             mileage_daily(z,t+1) = 0;
             mileage(z,t+2) = mileage(z,t+1);
             t = t+1;
             else
               p_1 = rand;
               if p_1 > using_percentage
                  s_2(z,1) = s_2(z,1) + 1;
                  X(z,t+1) = 2;
                  mileage_daily(z,t+1) = 0;
                  mileage(z,t+2) = mileage(z,t+1);
                  t = t+1;
```

```
                else
                  p_2 = rand;
                  l = round(expinv(p_2,mean_daily_mileage));
                  l(l>l_max) = l_max;
                  p_3 = rand;
                    if p_3 > 1-(exp(-(l_r+l)/mean_mileage_between_fail-
ure)/((exp(-(l_r)/mean_mileage_between_failure))))
                      s_1(z,1) = s_1(z,1) + 1;
                      X(z,t+1) = 1;
                      l_r = l_r+l;
                      l_m = l_m+l;
                      t_m = t_m+1;
                      mileage_daily(z,t+1) = l;
                      mileage(z,t+2) = mileage(z,t+1) + l;
                      t = t+1;
                    else
                      s_4(z,1) = s_4(z,1) + 1;
                      X(z,t+1) = 4;
                      lf = randi([0 l],1,1);
                      mileage_daily(z,t+1) = lf;
                      mileage(z,t+2) = mileage(z,t+1)+lf;
                      l_m = l_m+lf;
                      t_m = t_m+1;
                      failure(z,1) = failure(z,1)+1;
                      p_4 = rand(1,1);
                      tau = 0;
                      while p_4 > 1-(exp(-((tau+1)/alfa_repair)^beta_re-
pair)/((exp(-((tau)/alfa_repair)^beta_repair))))
                           if t < max_iteration-1
                             tau = tau+1;
                             s_4(z,1) = s_4(z,1) + 1;
                             X(z,t+1) = 4;
                             mileage_daily(z,t+1) = 0;
                             mileage(z,t+2) = mileage(z,t+1);
                             t_m = t_m+1;
                             p_4 = rand;
                             t = t+1;
                           else
                             p_4=0;
                           end
                       end
                       l_r = 0;
                       X(z,t+1) = 4;
                       mileage_daily(z,t+1) = 0;
                       mileage(z,t+2) = mileage(z,t+1);
                       t = t+1;
                    end
                end
    end
end
% wykresy dla jednego pojazdu
h = figure;
n = 1:1:max_iteration;
m = 0:1:max_iteration;
subplot (2,2,1); plot(n,X(z,:),'o','MarkerSize',3);
xlabel('Day');
ylabel('State');
yticks([1 2 3 4]);
yticklabels([1 2 3 4]);
```

```
axis([1 max_iteration 0.5 4.5]);
N_s = [s_1(z,1) s_2(z,1) s_3(z,1) s_4(z,1)];
S = [1 2 3 4];
subplot (2,2,2); bar(S,N_s);
xlabel('State');
ylabel('Number of observation');
axis([0 5 0 1.1*max(N_s)]);
subplot (2,2,3); plot(n,mileage_daily(z,:));
xlabel('Day');
ylabel('Daily mileage (km)');
axis([1 max_iteration 0 1.05*max(mileage_daily(z,:))]);
subplot (2,2,4); plot(m, mileage(z,:), LineWidth=1.5);
xlabel('Day');
ylabel('Total mileage (km)');
axis([0 max_iteration 0 1.05*max(mileage(z,:))]);
saveas(h,sprintf('Vehicle_%d.fig',z));
close(h);
readiness(z,1) = (s_1(z,1)+s_2(z,1))/(s_1(z,1)+s_2(z,1)+s_3(z,1)+s_4(z,1));
suitability(z,1) =
(s_1(z,1)+s_2(z,1)+s_3(z,1))/(s_1(z,1)+s_2(z,1)+s_3(z,1)+s_4(z,1));
end
mean_readiness = mean(readiness);
mean_suitability = mean(suitability);
% wykresy dla całej próby 19 pojazdów
v = 1:1:vehicle;
total_mileage = mileage(:,max_iteration+1);
subplot (2,2,1); bar(v,total_mileage,'FaceColor', [0.4940 0.1840 0.5560],
'EdgeColor',[0.4940 0.1840 0.5560]); % przebiegi całtkowite pojazdów
xlabel('Vehicle');
ylabel('Total mileage (km)');
axis([0.5 vehicle+0.5 0 1.05*max(total_mileage)]);
subplot (2,2,2); bar(v,failure(:), 'FaceColor', [0.6350 0.0780 0.1840],
'EdgeColor',[0.6350 0.0780 0.1840]); % uszkodzenia pojazdów
xlabel('Vehicle');
ylabel('Number of failures');
axis([0.5 vehicle+0.5 0 max(failure)+1]);
subplot (2,2,3); bar(v,readiness(:), 'FaceColor', [0.4660 0.6740 0.1880],
'EdgeColor',[0.4660 0.6740 0.1880]); % gotowość pojazdów
xlabel('Vehicle');
ylabel('Readiness');
axis([0.5 vehicle+0.5 0.9*min(readiness) 1.05*max(readiness)]);
hold on
w = 0:1:vehicle+1;
mr = mean_readiness*ones(1,vehicle+2);
plot(w,mr, 'b', 'LineWidth',2);
legend('','Mean readiness', 'Location', 'southeast');
hold off
subplot (2,2,4); bar(v,suitability(:), 'FaceColor', [0.3010 0.7450 0.9330],
'EdgeColor',[0.3010 0.7450 0.9330]); % zdatność pojazdów
xlabel('Vehicle');
ylabel('Suitability');
axis([0.5 vehicle+0.5 0.9*min(suitability) 1.05*max(suitability)]);
hold on
ms = mean_suitability*ones(1,vehicle+2);
plot(w,ms, 'r', 'LineWidth',2);
legend('','Mean suitablity', 'Location', 'southeast');
hold off
saveas(gcf, 'Simulation');
close(gcf);
```

```
% obliczanie gotowości
iter = 1:1:max_iteration;
K = zeros(max_iteration, 4);
for a = 1:1:max_iteration
    for b =1:1:vehicle
if X(b,a) == 1
    K(a,1) = K(a,1)+1;
elseif X(b,a) == 2
    K(a,2) = K(a,2)+1;
elseif X(b,a) == 3
    K(a,3) = K(a,3)+1;
elseif X(b,a) == 4
    K(a,4) = K(a,4)+1;
end
    end
end
for c=1:1:max_iteration
    K_r (c,1) =
(sum(K(1:c,1))+sum(K(1:c,2)))/(sum(K(1:c,1))+sum(K(1:c,2))+sum(K(1:c,3))+sum(
K(1:c,4)));
end
plot(iter,K_r, 'LineWidth',1.5);
xlabel('t');
ylabel('K_r');
axis([0 max_iteration 0.95*min(K_r) 1.01*max(K_r)]);
saveas(gcf, 'K_r');
close(gcf);
for d=1:1:max_iteration
    K_t (d,1) = ((K(d,1))+(K(d,2)))/((K(d,1))+(K(d,2))+(K(d,3))+(K(d,4)));
end
plot(iter,K_t);
xlabel('t');
ylabel('K_r (t)');
axis([0 max_iteration 0.95*min(K_t) 1.01*max(K_t)]);
saveas(gcf, 'K_t');
close(gcf);
```

Załącznik A2. Kod źródłowy modelu Markowa dla systemu k-out-of-n

```
lambda = 0.0048; % intensywność uszkodzeń
mu = 0.2607; % intensywność napraw
n = 19; % maksymalna liczba pojazdów w systemie
X = zeros(n+1, n+1, n); % tensor macierzy intensywności przejść
for i = 1:n
markov_matrix = zeros(i+1,i+1); % macierz przejść międzystanowych modelu Mar-
kowa dla systemu złożonego z i pojazdów
for j = 1:i+1
    for k = 1:i+1
        if k == j
           markov_matrix(j,k) = -((i - j + 1)*mu + (j - 1)*lambda);
        end
        if k == j - 1
           markov_matrix(j,k) = (j - 1)*lambda;
        end
        if k == j + 1
           markov_matrix(j,k) = (i - j + 1)*mu;
        end
    end
```

```
        k = 1;
end
X(1:i+1,1:i+1,i) = markov_matrix;
end
P = zeros(n, n); % macierz prawdopodobieństw ergodycznych
for a = 1:n
    Lambda_matrix = X(1:a+1,1:a+1,a); % pobranie fragmentu tensora dla sys-
temu złożonego z a pojazdów jako macierzy przejść modelu Markowa
    Lambda_matrix_transp = Lambda_matrix.'; % transponowanie macierzy
    Lambda_matrix_transp(a+1,1:a+1) = 1;
    Z = zeros(a+1,1); % wektor elementów zerowych
    Z(a+1,1) = 1;
    P(1,1:a+1) = (Lambda_matrix_transp^(-1))*Z;
    clear("Z");
    ergodic_probabilities(a:a,1:a+1) = P(1,1:a+1); % obliczenie prawdopodo-
bieństw ergodycznych modelu Markowa
end
ergodic_probabilities = ergodic_probabilities.'; % transponowanie macierzy
for j = 1:1:n+1
    for i = 1:1:n
        if j - 2>i
            ergodic_probabilities(j,i) = NaN;
        end
    end
end
```

Załącznik A3. Kod źródłowy symulacji Monte Carlo dla systemu k-out-of-n

```
% dane wejściowe
time_simulation = 10000; % liczba iteracji
num_vehicles = 19; % maksymalna liczba pojazdów w systemie
lambda = 0.0048; % intensywność uszkodzeń
mu = 0.2607; % intensywność napraw
location_parameter = 3.8344; % parametr rozkładu strumiania zadań
scale_parameter = 2.0762; % parametr rozkładu strumiania zadań
for n = 1:num_vehicles
    time = 0;
    S = n;
    X_t(n,1) = S; % stan początkowy
    T_t(n,1) = 0; % czas
    t = 1; % numer przejścia
    while time < time_simulation
        t = t + 1;
        if S == n % uszkodzenie
           p = rand(1,1);
           time_failure = -log(1-p)/(lambda*S);
           time = time + time_failure;
           S = S - 1;
        elseif S == 0 % naprawa
           q = rand(1,1);
           time_repair = -log(1-q)/(mu*(n-S));
           time = time + time_repair;
            S = S + 1;
        else % uszkodzenie lub naprawa
           p = rand(1,1);
           q = rand(1,1);
           time_failure = -log(1-p)/(lambda*S);
           time_repair = -log(1-q)/(mu*(n-S));
```

```
            if time_failure > time_repair
               time = time + time_repair;
               S = S + 1;
            else
              time = time + time_failure;
              S = S - 1;
            end
         end
         T_t(n,t) = time;
         X_t(n,t) = S;
     end
end
 I = 1:1:time_simulation; % czas dyskretny symulacji
 for j = 1:time_simulation % próbkowanie wielkości strumienia zadań
       p_sample = rand(1,1);
       task_stream = icdf('Logistic',p_sample, location_parameter, scale_pa-
rameter);
       if task_stream < 0
           task_stream = 0;
       end
       task_stream(j) = round(task_stream); % zaokrąglanie do wartości całko-
witych
 end
for m = 1:num_vehicles
    for i = 1:length(T_t)-1
        if T_t(m,length(T_t)-i+1) <= T_t(m,length(T_t)-i)
            T_t(m,length(T_t)-i+1) = NaN;
            X_t(m,length(T_t)-i+1) = NaN;
        end
    end
X_discrete = num_vehicles.*ones(num_vehicles,time_simulation);
for i = 1:num_vehicles
    j = 1;
    for m = 1:length(X_t(i,:))
        while j < time_simulation + 1
            if T_t(i,m) < j
                if T_t(i,m+1) > j - 1
                    X_t_discrete(i,j) = X_t(i,m);
                    if X_t_discrete(i,j) < X_discrete(i,j)
                        X_discrete(i,j) = X_t_discrete(i,j);
                    end
                end
            end
            j = j + 1;
        end
        j = 1;
    end
end
% Technical Performance Measure
for a = 1:num_vehicles
    for b = 1:time_simulation
        if X_discrete(a,b) >= task_stream(b)
            TPM(a,b) = 1;
        else
            TPM(a,b) = X_discrete(a,b)/task_stream(b);
        end
    end
end
% gotowość systemu
```

```
for a = 1:num_vehicles
    for b = 1:time_simulation
        if X_discrete(a,b) >= task_stream(b)
            R(a,b) = 1;
        else
            R(a,b) = 0;
        end
    end
    system_availability(a) = sum(R(a,:))/time_simulation;
end
```

10. ZAŁĄCZNIKI B – ARTYKUŁY NAUKOWE

Publikacje naukowe [P1] – [P6] będące zbiorem sześciu powiązanych tematycznie artykułów naukowych stanowią rozprawę doktorską. Wszystkie opublikowane prace wraz z oświadczeniami współautorów o ich procentowym wkładzie zostały zgrupowane w formie załączników Z1 – Z6:

Z1. Oszczypała M., Ziółkowski J., Małachowski J., *Reliability Analysis of Military Vehicles Based on Censored Failures Data*, Applied Sciences 2022, Volume 12, Issue 5, 2622, DOI: 10.3390/app12052622

Z2. Oszczypała M., Ziółkowski J., Małachowski J., *Analysis of Light Utility Vehicle Readiness in Military Transportation Systems Using Markov and Semi-Markov Processes*, Energies 2022, 15(14), 5062. DOI: 10.3390/en15145062

Z3. Oszczypała M., Ziółkowski J., Małachowski J., *Modelling the Operation Process of Light Utility Vehicles in Transport Systems Using Monte Carlo Simulation and Semi-Markov Approach*, Energies 2023, 16(5), 2210. DOI: 10.3390/en16052210

Z4. Oszczypała M., Ziółkowski J., Małachowski J., *Semi-Markov approach for reliability modelling of light utility vehicles*, Eksploatacja i Niezawodnosc – Maintenance and Reliability 2023, 25(2), DOI: 10.17531/ein/161859

Z5. Oszczypała M., Konwerski J., Ziółkowski J., Małachowski J., *Reliability analysis and redundancy optimization of k-out-of-n systems with random variable k using continuous time Markov chain and Monte Carlo simulation*, Reliability Engineering and System Safety 2023, 109780, DOI: 10.1016/j.ress.2023.109780

Z6. Oszczypała M., Konwerski J., Ziółkowski J., Małachowski J., *Copula-Based Reliability Analysis of Vehicles Based on Censored Failures Data Using Reliability Importance Measures*, IEEE Access 2024, DOI: 10.1109/ACCESS.2024.3450076

Oświadczenie głównego autora oraz współautorów o wkładzie procentowym w publikację [P1]

Niniejszym oświadczam, że wkład autorski w powstanie publikacji o poniższych danych bibliometrycznych przedstawia się następująco:

Mateusz Oszczypała, Jarosław Ziółkowski, Jerzy Małachowski

„Reliability Analysis of Military Vehicles Based on Censored Failures Data"

Applied Sciences, 2022, Volume 12, Issue 5, 2622

DOI: 10.3390/app12052622

Autor	Udział procentowy [%]	Podpis
Mateusz Oszczypała	75	
Jarosław Ziółkowski	20	Jarosław Ziółkowski
Jerzy Małachowski	5	

Udział doktoranta w powstaniu niniejszej publikacji obejmował następujące czynności:

- Realizacja przeglądu literatury;
- Zgromadzenie i opracowanie bazy danych badawczych dotyczących uszkodzeń pojazdów;
- Opracowanie koncepcji badań i dobór metod badawczych;
- Opracowanie kodu programistycznego w środowisku MATLAB do aproksymacji modeli probabilistycznych i uczenia sieci neuronowych;
- Wykonanie wykresów i schematów graficznych;
- Ocena uzyskanych wyników i opracowanie wniosków końcowych;
- Opracowanie pierwotnej wersji manuskryptu i współudział w jego edycji;
- Współudział w odpowiedziach do recenzentów manuskryptu.

Oświadczenie głównego autora oraz współautorów o wkładzie procentowym w publikację [P2]

Niniejszym oświadczam, że wkład autorski w powstanie publikacji o poniższych danych bibliometrycznych przedstawia się następująco:

Mateusz Oszczypała, Jarosław Ziółkowski, Jerzy Małachowski

„Analysis of Light Utility Vehicle Readiness in Military Transportation Systems Using Markov and Semi-Markov Processes"

Energies, 2022, 15(14), 5062

DOI: 10.3390/en15145062

Autor	Udział procentowy [%]	Podpis
Mateusz Oszczypała	75	
Jarosław Ziółkowski	20	Jarosław Ziółkowski
Jerzy Małachowski	5	

Udział doktoranta w powstaniu niniejszej publikacji obejmował następujące czynności:

- Analiza bieżącego stanu literatury;
- Zgromadzenie danych badawczych dotyczących szczegółowego przebiegu procesu eksploatacji pojazdów w okresie trzech lat i opracowanie baz danych w formie arkuszy MS Excel;
- Opracowanie koncepcji badań i dobór metod badawczych;
- Identyfikacja 9 stanów eksploatacyjnych pojazdu ciężarowo-osobowego oraz opracowanie modeli Markowa i semi-Markowa;
- Przeprowadzenie analiz statystycznych próby badawczej;
- Obliczenia wskaźników gotowości i analiza wrażliwości modelu;
- Wykonanie wykresów i schematów graficznych;
- Ocena uzyskanych wyników i opracowanie wniosków końcowych;
- Opracowanie pierwotnej wersji manuskryptu i współudział w jego edycji;
- Współudział w odpowiedziach do recenzentów manuskryptu.

Oświadczenie głównego autora oraz współautorów o wkładzie procentowym w publikację [P3]

Niniejszym oświadczam, że wkład autorski w powstanie publikacji o poniższych danych bibliometrycznych przedstawia się następująco:

Mateusz Oszczypała, Jarosław Ziółkowski, Jerzy Małachowski

„Modelling the Operation Process of Light Utility Vehicles in Transport Systems Using Monte Carlo Simulation and Semi-Markov Approach"

Energies 2023, 16(5), 2210

DOI: 10.3390/en16052210

Autor	Udział procentowy [%]	Podpis
Mateusz Oszczypała	75	Mateusz Oszczypała
Jarosław Ziółkowski	20	Jarosław Ziółkowski
Jerzy Małachowski	5	

Udział doktoranta w powstaniu niniejszej publikacji obejmował następujące czynności:

- Analiza bieżącego stanu literatury;
- Zgromadzenie danych badawczych dotyczących szczegółowego przebiegu procesu eksploatacji pojazdów w okresie trzech lat i opracowanie baz danych w formie arkuszy MS Excel;
- Opracowanie koncepcji badań i dobór metod badawczych;
- Agregacja przestrzeni fazowej procesu z 9 do 4 stanów eksploatacyjnych pojazdu ciężarowo-osobowego;
- Wyznaczenie charakterystyk probabilistycznych podprocesów procesu eksploatacji;
- Opracowanie kodu źródłowego w środowisku MATLAB do przeprowadzenia symulacji Monte Carlo;
- Obliczenia wskaźników gotowości i weryfikacja modeli symulacyjnych w oparciu o model semi-Markowa;
- Wykonanie wykresów i schematów graficznych;
- Ocena uzyskanych wyników i opracowanie wniosków końcowych;
- Opracowanie pierwotnej wersji manuskryptu i współudział w jego edycji;
- Współudział w odpowiedziach do recenzentów manuskryptu.

Oświadczenie głównego autora oraz współautorów o wkładzie procentowym w publikację [P4]

Niniejszym oświadczam, że wkład autorski w powstanie publikacji o poniższych danych bibliometrycznych przedstawia się następująco:

Mateusz Oszczypała, Jarosław Ziółkowski, Jerzy Małachowski

„Semi-Markov approach for reliability modelling of light utility vehicles"

Eksploatacja i Niezawodnosc – Maintenance and Reliability, 2023, 25(2)

DOI: 10.17531/ein/161859

Autor	Udział procentowy [%]	Podpis
Mateusz Oszczypała	80	
Jarosław Ziółkowski	15	
Jerzy Małachowski	5	

Udział doktoranta w powstaniu niniejszej publikacji obejmował:

- Realizacja przeglądu literatury;
- Zgromadzenie danych badawczych dotyczących szczegółowego przebiegu procesu eksploatacji pojazdów w okresie trzech lat i opracowanie baz danych w formie arkuszy MS Excel;
- Opracowanie koncepcji badań i dobór metod badawczych;
- Agregacja przestrzeni fazowej procesu z 9 do 3 stanów eksploatacyjnych pojazdu ciężarowo-osobowego i opracowanie 3-stanowego modelu semi Markowa;
- Przeprowadzenie analiz statystycznych;
- Przeprowadzenie analiz matematycznych w celu wyznaczenia charakterystyk niezawodnościowych na podstawie transformaty Laplace'a i przy wykorzystaniu oprogramowania Mathematica;
- Wykonanie wykresów i schematów graficznych;
- Ocena uzyskanych wyników i opracowanie wniosków końcowych;
- Opracowanie pierwotnej wersji manuskryptu i współudział w jego edycji;
- Współudział w odpowiedziach do recenzentów manuskryptu.

Oświadczenie głównego autora oraz współautorów o wkładzie procentowym w publikację [P5]

Niniejszym oświadczam, że wkład autorski w powstanie publikacji o poniższych danych bibliometrycznych przedstawia się następująco:

Mateusz Oszczypała, Jakub Konwerski, Jarosław Ziółkowski, Jerzy Małachowski

„Reliability analysis and redundancy optimization of k-out-of-n systems with random variable k using continuous time Markov chain and Monte Carlo simulation"

Reliability Engineering and System Safety, 2023, 109780

DOI: 10.1016/j.ress.2023.109780

Autor	Udział procentowy [%]	Podpis
Mateusz Oszczypała	45	
Jakub Konwerski	40	Konwerski Jakub
Jarosław Ziółkowski	10	Jarosław Ziółkowski
Jerzy Małachowski	5	

Udział doktoranta w powstaniu niniejszej publikacji obejmował następujące czynności:

- Współudział w analizie bieżącego stanu literatury;
- Współudział w tworzeniu bazy danych empirycznych;
- Opracowanie koncepcji badań i dobór metod badawczych;
- Współudział w opracowaniu modeli niezawodności systemu i wyznaczeniu wartości parametrów;
- Opracowanie kodu źródłowego w środowisku MATLAB do przeprowadzenia symulacji Monte Carlo oraz do obliczenia wskaźników gotowości i wydajności systemu;
- Wykonanie wykresów i schematów graficznych;
- Ocena uzyskanych wyników i opracowanie wniosków końcowych;
- Współudział w opracowaniu pierwotnej wersji manuskryptu i w jego edycji;
- Współudział w odpowiedziach do recenzentów manuskryptu.

Oświadczenie głównego autora oraz współautorów o wkładzie procentowym w publikację [P6]

Niniejszym oświadczam, że wkład autorski w powstanie publikacji o poniższych danych bibliometrycznych przedstawia się następująco:

Mateusz Oszczypała, Jakub Konwerski, Jarosław Ziółkowski, Jerzy Małachowski

„Copula-Based Reliability Analysis of Vehicles Based on Censored Failures Data Using Reliability Importance Measures"

IEEE Access, 2024

DOI: 10.1109/ACCESS.2024.3450076

Autor	Udział procentowy [%]	Podpis
Mateusz Oszczypała	75	Mateusz Oszczypała
Jakub Konwerski	10	Konwerski Jakub
Jarosław Ziółkowski	10	Jarosław Ziółkowski
Jerzy Małachowski	5	

Udział doktoranta w powstaniu niniejszej publikacji obejmował następujące czynności:

- Analiza bieżącego stanu literatury;
- Współudział w tworzeniu bazy danych empirycznych;
- Opracowanie koncepcji badań i dobór metod badawczych;
- Analiza matematyczna i wyprowadzenie zależności na miary ważności niezawodnościowych dla modeli niezawodności opartych na kopulach probabilistycznych;
- Opracowanie kodu źródłowego w środowisku MATLAB do przeprowadzenia analiz statystycznych oraz wyznaczenia charakterystyk niezawodnościowych pojazdu i jego podsystemów;
- Wykonanie wykresów i schematów graficznych;
- Ocena uzyskanych wyników i opracowanie wniosków końcowych;
- Opracowanie pierwotnej wersji manuskryptu i współudział w jego edycji;
- Współudział w odpowiedziach do recenzentów manuskryptu.

applied sciences

MDPI

Article

Reliability Analysis of Military Vehicles Based on Censored Failures Data

Mateusz Oszczypała, Jarosław Ziółkowski and Jerzy Małachowski *

Institute of Mechanics and Computational Engineering, Faculty of Mechanical Engineering, Military University of Technology, 00-908 Warsaw, Poland; mateusz.oszczypala@wat.edu.pl (M.O.); jaroslaw.ziolkowski@wat.edu.pl (J.Z.)
* Correspondence: jerzy.malachowski@wat.edu.pl

Abstract: The paper proposes a methodology of reliability testing as applied to vehicles used in military transport systems. After estimating the value of the reliability function using the Kaplan–Meier estimator, reliability models were developed and analysed. The neural model, which achieved the value of the correlation coefficient R exceeding 0.99, was determined to fit the empirical data the best. On the basis of the approximated reliability function of several models, the reliability characteristics of the tested sample of vehicles were determined. Plots of the failure probability density function for all three models had similar courses over a significant part of the function domain. A failure intensity function was also determined, which varied between models. For the exponential and Weibull model, the expected mileage between failures was calculated, which proved impossible for the neural model. The proposed methodology is capable of modelling reliability characteristics based on the observation of an assumed period of the exploitation process of the selected group of military vehicles.

Keywords: reliability analysis; artificial neural networks; military vehicles; censored data

Citation: Oszczypała, M.; Ziółkowski, J.; Małachowski, J. Reliability Analysis of Military Vehicles Based on Censored Failures Data. *Appl. Sci.* **2022**, *12*, 2622. https://doi.org/10.3390/app12052622

Academic Editors: Chang Yong Song, Wu Deng and Jérôme Morio

Received: 7 February 2022
Accepted: 28 February 2022
Published: 3 March 2022

1. Introduction

Modelling and reliability analysis of technical objects should be an important element in the process of technical systems management. Any failure can result in a decrease in the efficiency of production and logistics processes carried out using technical means [1,2]. Modelling of a technical object operation while taking failure prediction into account makes it possible to minimise losses resulting from such failures. In addition, advanced knowledge of reliability should support the planning process for periodic maintenance and spare parts supply. Therefore, in many fields of science and technology, as well as branches of the economy, attempts are made to create models reflecting the real operational processes of exploitation of technical objects and devices [3–5].

Effective operation of military transport systems requires a fleet of reliable vehicles. The occurrence of failures to the means of transport during the task almost always results in greater or lesser losses for the entire system. In order to meet the challenges posed to the armed forces and the requirements for the efficient implementation of transport processes, appropriate maintenance, diagnostic and repair systems must be organised. Reliability models are useful tools for forecasting and evaluating the maintenance and repair needs of military vehicles [6–8]. Therefore, the development of accurate reliability models is critical to maintaining the assumed readiness and effectiveness of military transport systems.

Research fields dealing with reliability problems are frequently addressed in the scientific literature [9–12]. In the article [13], a reliability assessment method was developed as a decision support in the selection of a vehicle fleet for a transport company. The developed indicator took into account reliability characteristics such as mileages to the first failure, mileages between failures and the intensity of failures. The authors of the publication [14] presented a method for determining the reliability function using the

Kaplan–Meier estimator and a modified Kolmogorov–Smirnov statistical test. The case study consisted of 5 years of data on the driver's door locks usage for a sample size of 45 rail vehicles. Whereas in the study [15], an analysis of aircraft reliability was carried out. Several reliability models were analysed using statistical tests. The log-normal model proved to be the closest fitting model for the empirical data collected. In the paper [16], a Cox regression model was developed to account for the relationship between operational and maintenance conditions affecting aircraft reliability.

Modelling the reliability of technical objects using artificial neural networks remains the subject of many scientific publications. Xu et al. [17] proposed regression models based on Multilayer Perceptron (MLP) and Radial Basis Function (RBF) networks, which they then implemented to describe and predict the reliability of turbochargers and engines. The standardised roots of mean square error for the analysed objects reached acceptably low values. The authors of the paper [18], on the other hand, developed a model using the Support Vector Regression method combined with genetic algorithms, whose accuracy was an order of magnitude better than the model based on RBF networks for data taken from the publication [17]. In contrast, the Support Vector Machines-based model, when applied to the time series of failure occurrences presented in the paper [19], achieved accuracy similar to MLP and RBF models.

A significant improvement in prediction accuracy occurred for models presented in publications [20,21]. The first was developed as a hybrid of artificial neural networks and genetic algorithms, for which the magnitude of the time series delay was determined using the Shannon entropy. The smallest error, close to zero, for the datasets from the article [17] was obtained by the one presented in the paper [21]. Its design is based on a hybridisation of dynamic weight particle swarm optimisation-based sine map and back propagation neural network.

In publication [22], a reliability prediction model was developed based on a cascade neural network. A sigmoidal hidden layer activation function along with linear output neuron activation was proposed. The model predicted the value of the reliability function for Computerized Numerical Control (CNC) machines depending on the mean time between failures (MTBF) with an accuracy measured through Mean Absolute Percentage Error (*MAPE*), ranging from 1.56% to 2.53%. An approach based on the use of a three-layer neural network and remanufacturing coefficients is presented in [23]. Reliability indices for the individual components of the technical system were determined based on the average times between failures. The flexibility of artificial neural networks in fitting degradation paths has been highlighted in publications [24,25]. The authors of these studies used MLP supported by a stochastic process [24] and a Weiner process [25]. Validations of both models were performed using simulated data and spindle systems wear data. For the actual data, the mean absolute relative error for all test trials did not exceed 0.13 in [24] and 0.06 in [25].

A much more structurally complex convolutional neural network was developed by the authors of [26]. The proposed model, when validated with data from three power systems, achieved significantly better fitting results than MLP, SVM (Support Vector Machine) and KNN (K-Nearest Neighbors) models.

In Table 1, the models discussed above, which have been tested using turbocharger and engine datasets, as well as models for predicting the reliability of other technical objects, are summarised in chronological order.

Table 1. Neural modelling of reliability—literature review.

Model	Case Study	Results	Paper
Regressive models based on neural networks (MLP and RBF)	Turbocharges in diesel engine (time to failure) Car engines (miles to failure)	Normalized Root Mean Square Error *NRMSE* = 3.9×10^{-3} (RBF) for turbocharges *NRMSE* = 1.22×10^{-2} (MLP Gaussian activation) for engines	[17]
Model (GA-SVR) based on Support Vector Regression (SVR) and Genetic Algorithm (GA)	Turbocharges in diesel engine (data from [17])	*MAPE* = 0.0387% *NRMSE* = 4×10^{-4}	[18]
Neural model with one and two hidden layers	Vehicles (mileage to failure)	Correlation Coefficient R = 0.80 Error = 9%	[27]
Model based on Support Vector Machines (SVM) (time series regression as an alternative to probability distribution models)	Turbocharges in diesel engine Car engines (data from [17])	*NRMSE*: 2.4×10^{-3} for turbocharges *NRMSE* = 1.25×10^{-2} for engines	[19]
PSO+SVM (Particle Swarm-optimized Support Vector Machine)	Turbocharges in diesel engine and car engines (data from [17]) Submarine diesel engines	*NRMSE* = 2.0303×10^{-4} for turbocharges *NRMSE* = 7.1126×10^{-3} for car engines *NRMSE* = 2.0305×10^{-4} for submarine engines	[28]
Hybrid model: neural networks and Genetic Algorithm (GA) (Number of lag data calculated using Shannon entropy)	Turbocharges in diesel engine and car engines (data from [17]) Load-haul-dump (LHD) machines	*NRMSE* = 2.52×10^{-4} for turbocharges *NRMSE* = 1.195×10^{-2} for engines R^2: 0.94–0.99 and *NRMSE* = 8.36×10^{-3} for LHD machines	[20]
Neural model based on time series data	Control, operating and military systems	R: 0.82–0.99	[29]
Hybrid model based on metaheuristics and neural networks	Validation on simulated data	Values of Reliability Index and probability of failure are the same as those obtained with other methods	[30]
Model SDWPSO-BPNN (hybrid of dynamic weight particle swarm optimisation-based sine map and back propagation neural network)	Turbocharges in diesel engine (data from [17]) and industrial robot systems	*NRMSE* = 6.9×10^{-5} for turbocharges *NRMSE* = 2.3×10^{-6} for industrial robot systems	[21]
Cascade feedforward neural network	CNC machine tool spindles	*MAPE*: 1.56–2.53%	[22]
ANN supported stochastic process	Simulated data and degradation dataset of spindle systems	Mean absolute relative error < 0.13 for all samples of real degradation data	[24]
ANN supported Wiener process	Simulated data and degradation dataset of spindle systems	Mean absolute relative error < 0.06 for all samples of real degradation data	[25]
Model based on convolutional neural networks	IEEE Reliability Test Systems and Saskatchewan Power Corporation	Root Mean Square Error *RMSE* = 0.1038 for IEEE RTS *RMSE* = 0.047 for SPC	[26]
Three-layer feedforward artificial neural network	Reliability of machine tools	Reliabilty of the machine components obtained values 0.8966–0.9840	[23]

Military vehicles are technical objects which are submitted to the renewal of their technical worthiness after its loss due to the failure incurred. The system of operation also entails periodic maintenance to renew the technical service life. This is an action aimed at maintaining the technical readiness of vehicles at a sufficiently high level. However, due to the extreme operating conditions and long service life, unplanned periods of technical inoperability of the vehicle fleet due to frequent breakdowns are a real problem for the transport system of military units.

To date, reliability studies of military-technical facilities have mainly been conducted using mathematical statistics and probability calculation. This publication proposes a reliability testing methodology based on the use of numerical methods and artificial neural networks. With the developed algorithm, it is possible to model and analyse the reliability characteristics of a specific set of technical objects on the basis of observations of a certain period of exploitation with consideration of censored data. The research was conducted on a selected sample of military vehicles carrying out transport tasks within the transport system of a given military unit.

The proposed study focuses on technical objects and, from that point of view, is original research and have not yet been the subject of research in the present approach published by other authors. The methodology involving the use of artificial neural networks with a low complexity structure to approximate reliability functions is also an innovation. This allows the neural model to be presented as a relationship that can form the basis for determining the other reliability characteristics. The authors of the publications summarised in Table 1 focused on maximising the precision of representation of the estimated values of the reliability function, creating very complex models for this purpose. The complex structures of neural networks complicate the analysis of the developed models, making more difficult the calculation of the failure intensity function, the failure probability density function and the expected time (mileage) to failure or between failures functions.

This publication consists of four main sections. Following the introduction, Section 2 presents the methodology developed for conducting reliability studies, with a particular focus on means of transport. Classical reliability models known from previous scientific studies and advanced neural models based on the use of MLP networks have been proposed. Section 3 presents the validation of the models using the example of military light utility vehicles in service within the military transport system. The developed models were then compared in terms of fitting accuracy with the empirical data. Section 4 formulates conclusions from the analyses carried out regarding the usefulness and limitations of the proposed methodology for carrying out vehicle reliability tests.

2. Methodology

Reliability of a technical object is commonly understood as the probability that the technical object, when used under specified conditions, will remain continuously in a state of operational condition until a given moment t [12,31–33]. This can be described using the relation:

$$R(t) = P(T \geq t) \text{ for } t \geq 0. \tag{1}$$

The reliability function $R(t)$ and the unreliability function $F(t)$ constitute a complete system of events.

The reliability function is non-increasing, which is interpreted in the literature as a decrease in the value of the probability of a correct operation of a technical object as the amount of work executed increases. Thus, relation (2) implies the property of the failure function, which is its non-decreasing monotonicity, which also results from the assumption that the probability of failure of a technical object increases with the increase in the service life [34].

The characteristics that determine the probability of failure occurring at a given time t are the failure probability density function $f(t)$ and the failure intensity function $\lambda(t)$. The function $f(t)$ represents the probability per unit of service life of a failure occurring at time t. From the probability calculus, it follows that the failure density $f(t)$ is a derivative of the failure function $F(t)$, as shown in the following equation:

$$f(t) = \frac{dF(t)}{dt} = F'(t). \tag{2}$$

The failure intensity function $\lambda(t)$ defines the conditional probability of failure of the technical object at time t per unit of service life, provided that the object has not failed within the interval $(0, t)$. The value of the function $\lambda(t)$ at time t is expressed by the relation:

$$\lambda(t) = \frac{f(t)}{R(t)}. \tag{3}$$

For a known course of the reliability function $R(t)$, the expected time (mileage) of reliable operation without failure of the technical object is calculated according to the formula [35,36]:

$$ET = \int_{0}^{\infty} R(t)dt. \tag{4}$$

Figure 1 shows the author's algorithm for analysing and modelling the reliability of technical objects. According to the given assumptions, the reliability study of technical objects begins with the identification of a representative group of objects working under indistinguishable operating conditions and performing the same work. The starting point for modelling reliability characteristics is the estimation of the value of the reliability function using empirical data. This is followed by an approximation of the reliability function using analytical and neural models. On the basis of the created reliability function models, the remaining characteristics are created, i.e., the failure probability density function and the failure intensity function.

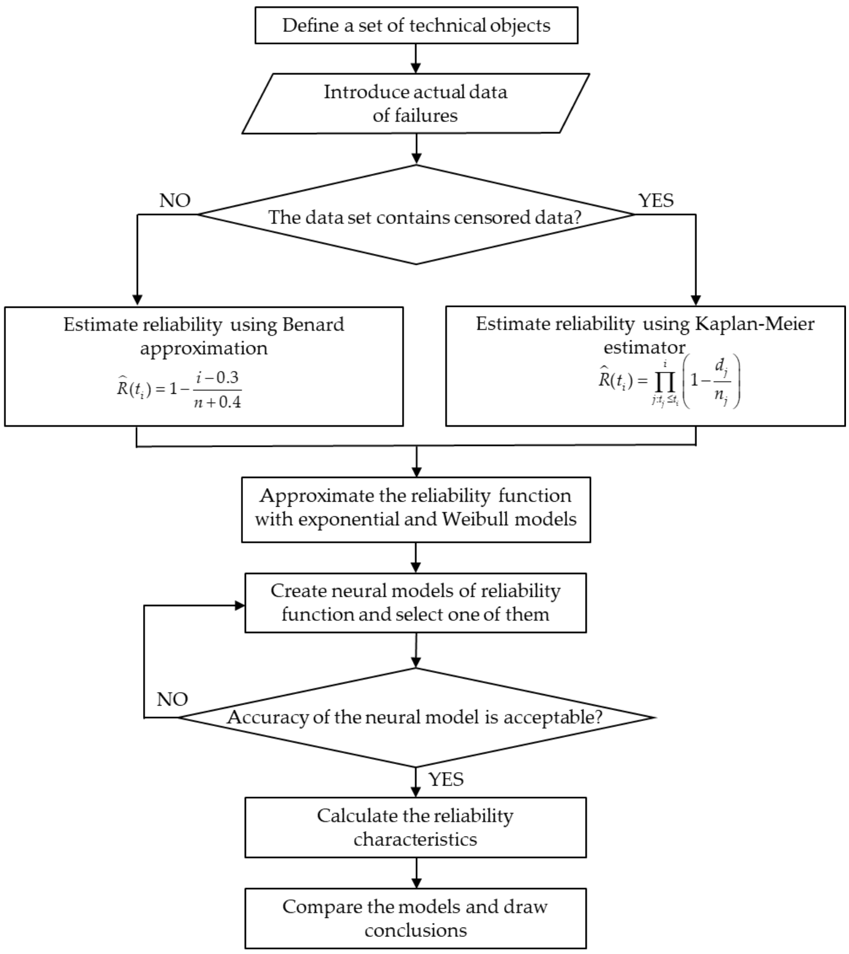

Figure 1. Flowchart of reliability modelling.

2.1. Reliability Estimation

During the operation of technical facilities, the failure records form the basis for the development of reliability models. From this perspective, indices defining intervals to failure or between failure are useful [11,37]. These intervals can be expressed in operational units referring to the operating time of the object (h, mth) or to the mileage [km] in the case of vehicles. The following reliability indicators are identified [38–41]:

- Time to failure (TTF),
- Time between failures (TBF),
- Mileage to failure (MTF),
- Mileage between failures (MBF).

Based on a statistically significant sample of technical objects, an empirical reliability function is determined. The following equation can be used to determine it [35]:

$$\widehat{R}(t_i) = 1 - \frac{i}{n}, \tag{5}$$

where t_i is the time of occurrence of the i-th failure, i is the number of failed technical objects up to time T_i, and n is the number of all technical objects belonging to the study sample.

However, this form of the empirical reliability function may cause distortion for values of i close to 0 and n. The solution to this problem is the Benard approximation commonly used in the literature [17–19,42], the form of which is shown in the equation:

$$\widehat{R}(t_i) = 1 - \frac{i - 0.3}{n + 0.4}. \tag{6}$$

The above estimators are applicable to scientific studies of a specified sample of technical objects, assuming equal intensity of use of all objects and complete knowledge of the exploitation process. In real technical systems, including transport systems involving military vehicles, there are significant differences in the mileage achieved, despite the aim of even usage. It is therefore proposed to adopt the Kaplan–Meier estimator used in survival analysis to estimate the value of the reliability function. It allows the analysis of censored data, useful for studying certain periods of the exploitation process, in which, after having performed a certain amount of work expressed in exploitation units, did not suffer from failure until now or ceased to operate in a given system [14]. Figure 2 shows a graphical interpretation of the study period of the exploitation process, taking into account the censored data. The Kaplan–Meier estimator for the reliability function [14,43] is presented in the following equation:

$$\widehat{R}(t_i) = \prod_{j:t_j \le t_i}^{i} \left(1 - \frac{d_j}{n_j}\right), \tag{7}$$

where d_j is the number of technical objects that have sustained failure at time t_j, and n_j is the number of all technical objects that have lasted until time t_j.

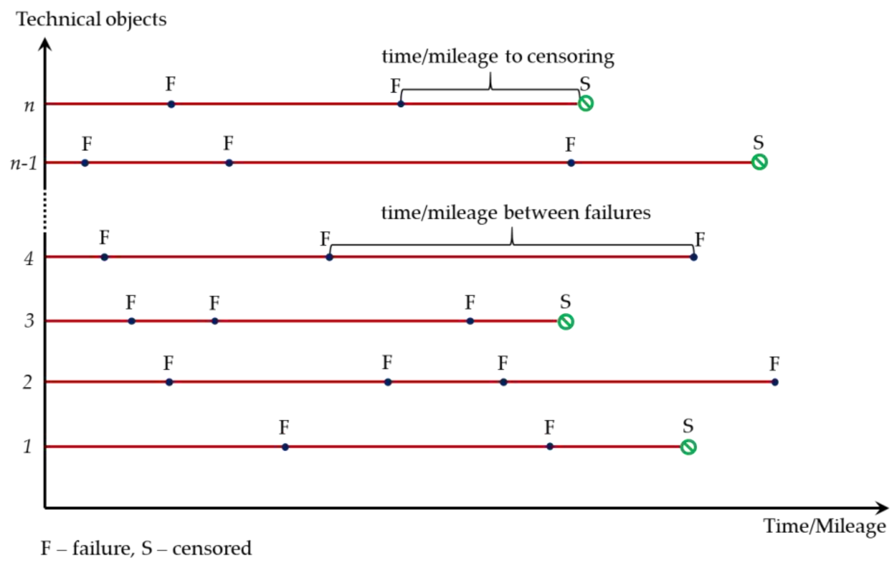

Figure 2. Schematic of exploitation process with censored data.

The standard error [44,45] has been obtained by the Greenwood Formula (8):

$$SE\left\{\widehat{R}(t_i)\right\} = \widehat{R}(t_i)\sqrt{\sum_{j=1}^{i}\frac{d_j}{n_j(n_j-d_j)}}. \tag{8}$$

2.2. Exponential Model

The exponential model is a single-parameter distribution, described by the failure intensity λ, assuming $\lambda = \lambda(t) = \text{const}$. This model is applicable when describing the reliability of technical objects with a constant intensity of failure, which occurs as a result of random causes and not as a result of changes in technical conditions during the operation process. The reliability function for the exponential model takes the form:

$$R(t) = e^{-\lambda t}. \tag{9}$$

The failure probability density function for the exponential model takes the form:

$$f(t) = \lambda e^{-\lambda t}. \tag{10}$$

2.3. Weibull Model

The Weibull model is a two-parameter distribution used to describe the reliability of a technical object for which the failure intensity is time-varying. The reliability function in the Weibull model [42,46] is expressed by the relation:

$$R(t) = e^{-\beta t^{\alpha}}. \tag{11}$$

where α is the shape factor and β is the scale factor of the distribution.

After calculating the derivative from the failure function, a relation representing the failure probability density function is obtained:

$$f(t) = \alpha\beta t^{\alpha-1}e^{-\beta t^{\alpha}}. \tag{12}$$

After substituting the characteristics determined for the Weibull model into Equation (4), the failure intensity [47] can be expressed by the following equation:

$$\lambda(t) = \alpha\beta t^{\alpha-1}. \tag{13}$$

The parameter α determines the course of the failure intensity function of the technical object. For $0 < \alpha < 1.0$ the failure intensity function is decreasing, for $\alpha > 1.0$ it is increasing, while for $\alpha = 1.0$ it is constant and the distribution has the character of an exponential distribution.

2.4. Neural Modelling

Artificial neural networks are an advanced tool for modelling, classification and prediction of processes, phenomena and objects based on a set of data [48]. Multilayer Perceptron (MLP) is a neural network based on three types of neuron layers: input, hidden (or several hidden) and output [27,49,50]. The input layer neurons are responsible for sending input signals to the hidden layer neurons. For predictive models, the input signals are the normalised values of the explanatory variables. Hidden neurons aggregate the received input signals multiplied by the weights of the synaptic connections. The aggregated signal is the argument of the activation function, whose value is passed to the neurons of the next hidden layer or to the neurons of the output layer. The output layer neurons perform the same actions as the hidden neurons, except that the value obtained is equated to the value of the explanatory variable in the model [51–53].

The use of a simple neural network to approximate functions on the basis of estimated values obtained from empirical studies makes it possible to develop models that fit real data with a very high accuracy. Additionally, a regression network with an uncomplicated structure allows the approximating function to be written in analytical form.

Figure 3 shows a flowchart illustrating the operation of the proposed neural network used to approximate the reliability function. The input signal is the mileage between failures, for which the value of the reliability function has been estimated. The output signal is the value of the reliability function. In the proposed neural model, the activation function of the hidden layer is a hyperbolic tangent, which ensures a fast learning process of the neural network [54,55]. For the output layer, on the other hand, activation occurs using a linear function.

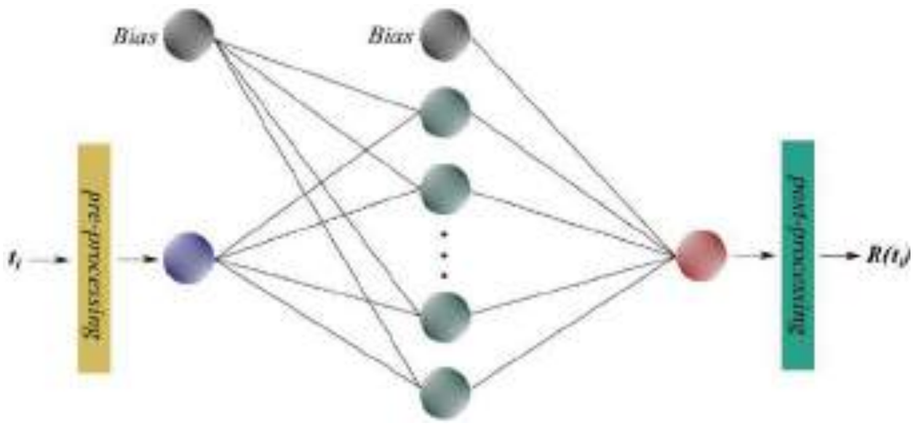

Figure 3. Graph of neural network for reliability modelling.

If the variables x and y represent the normalised values of the variables t and $R(t)$ according to the following relations:

$$x = \frac{2(t - t_{\min})}{t_{\max} - t_{\min}} - 1, \tag{14}$$

$$y = \frac{2\left(\widehat{R}(t) - \widehat{R}(t)_{\min}\right)}{\widehat{R}(t)_{\max} - \widehat{R}(t)_{\min}} - 1. \tag{15}$$

Then the analytical form of the neural model is represented by the relation:

$$y = \left[\sum_{n=1}^{h}\left(\left(\frac{2}{1 + e^{-2(xw_{1n} + w_{0n})}} - 1\right) \cdot v_{n1}\right)\right] + v_{01}, \tag{16}$$

where h is the number of hidden neurons, w represents weights of synaptic connections between the input layer and the hidden layer, and v are weights of synaptic connections between the hidden layer and the output layer.

During the training process, the neural network, using the Levenberg–Marquardt algorithm, seeks to minimise the value of its error function, which is calculated according to the following formula:

$$E(n) = \frac{1}{2}\sum_{i=1}^{n}\left(\widehat{R}(t_i) - R_{out}(t_i)\right)^2, \tag{17}$$

where $\widehat{R}(t_i)$ denotes the estimated value of the reliability function at point t_i, while $R_{out}(t_i)$ is the value obtained at the output of the neural network.

2.5. Accuracy of Fitting

An important part of carrying out reliability studies is assessing the accuracy of the developed models. In the literature, a number of measures and indicators are used to determine how accurately the model fits the empirical or estimated values. The authors of this publication used two indices in their reliability studies to completely assess the accuracy of the developed models in relation to the estimated values for a selected group of military vehicles. The first is the correlation coefficient R calculated according to the formula [56]:

$$R = \sqrt{1 - \frac{\sum_{i=1}^{n}\left(\widehat{R}(t_i) - R_d(t_i)\right)^2}{\sum_{i=1}^{n}\left(\widehat{R}(t_i) - \frac{1}{n}\left(\sum_{i=1}^{n}\widehat{R}(t_i)\right)\right)^2}}, \tag{18}$$

where $\widehat{R}(t_i)$ is the estimated value of reliability function by Equation (7) and $R_d(t_i)$ is the fit value of the approximation model.

The second measure [56–58] is the Mean Squared Error (MSE) expressed per the formula:

$$MSE = \frac{1}{n}\sum_{i=1}^{n}\left(\widehat{R}(t_i) - R_d(t_i)\right)^2. \tag{19}$$

3. Results and Discussion

A selected sample of Honker military vehicles operated by a military unit of the Armed Forces of the Republic of Poland was used to carry out research on reliability characteristics. These are military vehicles with a maximum load capacity of approximately 1000.0 kg. Their tasks include transporting passengers and cargo on public roads as well as in off-road conditions.

Table 2 summarises the empirical data on mileages between failures. The data comes from the analysis of operational records and covers a 3-year study period in which 99 observations were recorded. The designation F refers to the mileage between failures, while S is the amount of mileage that the vehicle has completed until the end of the observation of a certain period of the service process without sustaining failure.

Table 2. Data set of mileages between failures of military vehicles.

No.	Mileage (km)	F/S	No.	Mileage (km)	F/S	No.	Mileage (km)	F/S	No.	Mileage (km)	F/S
1	18	S	26	949	F	51	2297	F	76	4418	S
2	36	F	27	993	F	52	2329	F	77	4472	F
3	38	S	28	1034	S	53	2546	F	78	4904	S
4	47	F	29	1066	S	54	2592	S	79	5177	S
5	59	F	30	1158	F	55	2666	F	80	5195	F
6	76	F	31	1159	S	56	2720	F	81	5387	S
7	80	S	32	1186	F	57	2792	F	82	5579	F
8	99	F	33	1224	F	58	2829	S	83	5664	S
9	112	F	34	1324	F	59	3002	F	84	5894	F
10	117	F	35	1352	F	60	3004	F	85	6103	F
11	148	S	36	1367	S	61	3087	F	86	6526	S
12	149	F	37	1390	F	62	3259	S	87	7442	F
13	264	F	38	1410	F	63	3386	F	88	7811	F
14	264	F	39	1523	F	64	3438	F	89	8252	S
15	273	S	40	1527	S	65	3457	S	90	8663	F
16	351	S	41	1588	F	66	3471	F	91	8761	F
17	361	F	42	1601	F	67	3515	S	92	9086	F
18	380	F	43	1639	F	68	3520	F	93	9653	S
19	438	F	44	1702	F	69	3600	F	94	10,459	F
20	494	F	45	1774	F	70	3605	F	95	11,072	F
21	631	F	46	1801	F	71	3717	F	96	11,404	S
22	690	F	47	2025	F	72	3780	F	97	12,618	F
23	708	F	48	2074	S	73	3874	F	98	14,977	S
24	790	F	49	2109	S	74	4202	F	99	21,477	S
25	949	F	50	2112	S	75	4244	F			

3.1. Kaplan–Meier Estimation

The Kaplan–Meier estimator was used to estimate the values of the unreliability and reliability functions. The study was based on the data in Table 2 and the relations (7) and (8). The results are presented in Table 3. The range of estimated values that will be used for approximation with reliability models includes the values of mileage at which the failure occurred and the initial value of 0.0. A graphical interpretation of the estimated values of the reliability function is presented using a staircase diagram in Figure 4.

Table 3. Estimated values of unreliability and reliability functions.

Mileage (km)	$F(t)$	$R(t)$	$SE\{R(t)\}$	Mileage (km)	$F(t)$	$R(t)$	$SE\{R(t)\}$
0	0.0000	1.0000	0.0000	2025	0.3948	0.6052	0.0512
36	0.0102	0.9898	0.0102	2297	0.4071	0.5929	0.0515
47	0.0205	0.9795	0.0144	2329	0.4195	0.5805	0.0519
59	0.0308	0.9692	0.0175	2546	0.4318	0.5682	0.0523
76	0.0411	0.9589	0.0201	2666	0.4444	0.5556	0.0526
99	0.0516	0.9484	0.0225	2720	0.4571	0.5429	0.0530
112	0.0620	0.9380	0.0245	2792	0.4697	0.5303	0.0532
117	0.0724	0.9276	0.0264	3002	0.4826	0.5174	0.0535
149	0.0829	0.9171	0.0281	3004	0.4956	0.5044	0.0537
264	0.1040	0.8960	0.0297	3087	0.5085	0.4915	0.0539
361	0.1148	0.8852	0.0311	3386	0.5218	0.4782	0.0541
380	0.1256	0.8744	0.0326	3438	0.5351	0.4649	0.0542
438	0.1364	0.8636	0.0339	3471	0.5487	0.4513	0.0543
494	0.1472	0.8528	0.0352	3520	0.5628	0.4372	0.0544
631	0.1580	0.8420	0.0364	3600	0.5769	0.4231	0.0545
690	0.1688	0.8312	0.0375	3605	0.5910	0.4090	0.0545
708	0.1796	0.8204	0.0385	3717	0.6051	0.3949	0.0545
790	0.1904	0.8096	0.0395	3780	0.6192	0.3808	0.0544
949	0.2120	0.7880	0.0404	3874	0.6333	0.3667	0.0543
993	0.2228	0.7772	0.0413	4202	0.6474	0.3526	0.0541
1158	0.2339	0.7661	0.0421	4244	0.6615	0.3385	0.0538
1186	0.2451	0.7549	0.0429	4472	0.6763	0.3237	0.0535
1224	0.2564	0.7436	0.0437	5195	0.6925	0.3075	0.0531
1324	0.2677	0.7323	0.0445	5579	0.7095	0.2905	0.0529
1352	0.2789	0.7211	0.0452	5894	0.7277	0.2723	0.0526
1390	0.2904	0.7096	0.0459	6103	0.7458	0.2542	0.0524
1410	0.3018	0.6982	0.0466	7442	0.7654	0.2346	0.0519
1523	0.3133	0.6867	0.0472	7811	0.7849	0.2151	0.0515
1588	0.3249	0.6751	0.0478	8663	0.8065	0.1935	0.0508
1601	0.3366	0.6634	0.0484	8761	0.8280	0.1720	0.0500
1639	0.3482	0.6518	0.0490	9086	0.8495	0.1505	0.0489
1702	0.3598	0.6402	0.0495	10,459	0.8746	0.1254	0.0473
1774	0.3715	0.6285	0.0500	11,072	0.8996	0.1004	0.0456
1801	0.3831	0.6169	0.0504	12,618	0.9331	0.0669	0.0428

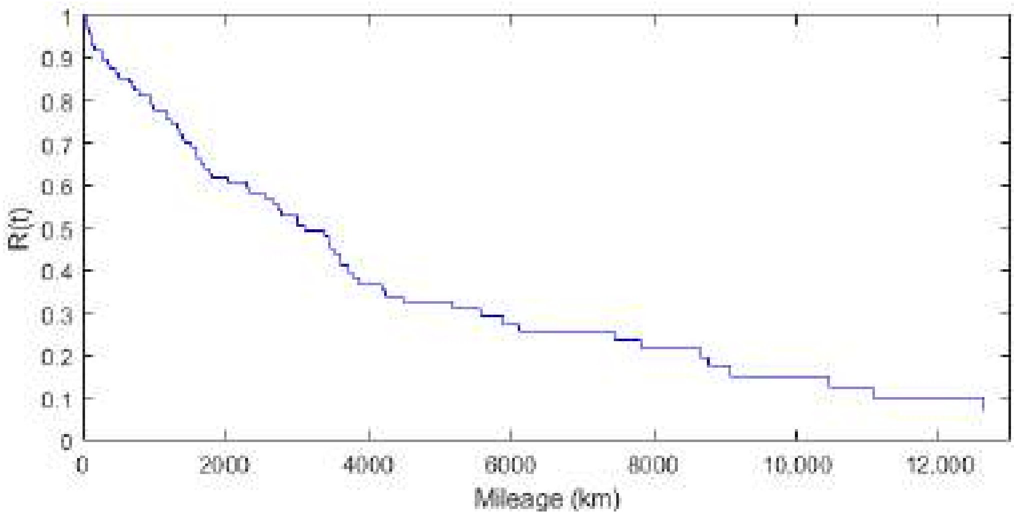

Figure 4. Kaplan–Meier reliability estimation graph.

3.2. Exponential Model of Reliability

An approximation using Matlab software was used to determine the reliability function of military vehicles as a function of the mileage between failures. The parameter determination λ for the exponential model was done using the nonlinear least-squares method. The objective function is to minimise the sum of squares of the differences between the true values and the values achieved by the approximating function, according to the following equation [59–61]:

$$S_n(\lambda) = \sum_{i=1}^{n} \left(\widehat{R}(t_i) - f(t_i, \lambda)\right)^2, \tag{20}$$

where $f(t_i,\lambda)$ is the value of the exponential reliability function $R(t)$ with parameter λ for the value of t_i.

$S_n(\lambda)$ takes the minimum value for the critical point, for which the following expression exists:

$$\frac{\partial S_n(\lambda)}{\partial \lambda} = 0. \tag{21}$$

After transformations according to the chain rule, the above relation can be written by the equation:

$$\sum_{i=1}^{n} \left[\widehat{R}(t_i) - f(t_i, \lambda)\right] \left(-\frac{\partial f(t_i, \lambda)}{\partial \lambda}\right) = 0. \tag{22}$$

Model fitting was performed using the Trust Region algorithm [62,63] in the Curve Fitting Tool application (Matlab). The models were matched to the estimated values of functions presented in Table 3. The exponential model for approximating the reliability function of the studied sample of technical objects is presented in Equation (26):

$$R(t) = e^{-0.000235t}. \tag{23}$$

Figure 5 shows a graphical interpretation of how the exponential model fits the estimated values of the reliability function.

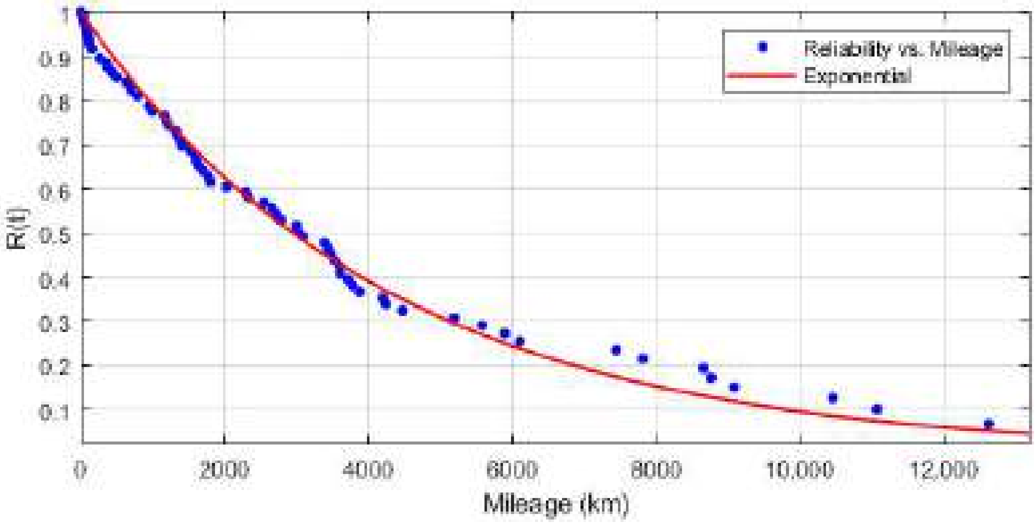

Figure 5. Graph presenting exponential model fitting to estimated values of reliability function.

3.3. Weibull Model of Reliability

The approximation of the reliability function $R(t)$ with the Weibull model was performed using the nonlinear least-squares method, analogous to the exponential model. Selection of optimal values of parameters α and β was carried out with minimisation of the objective function according to the relation [59–61]:

$$S_n(\alpha,\beta) = \sum_{i=1}^{n}\left(\widehat{R}(t_i) - f(t_i,\alpha,\beta)\right)^2, \quad (24)$$

where $f(t_i,\alpha,\beta)$ is the value of the Weibull model of the reliability function $R(t)$ with parameters α and β for the value of t_i.

$S_n(\alpha,\beta)$ takes the minimum value for the critical point for which the following relations are valid:

$$\frac{\partial S_n(\alpha,\beta)}{\partial \alpha} = 0, \quad (25)$$

$$\frac{\partial S_n(\alpha,\beta)}{\partial \beta} = 0. \quad (26)$$

Transforming the above relations, analogous to the case of the exponential model, the following two conditions are obtained:

$$\sum_{i=1}^{n}\left[\widehat{R}(t_i) - f(t_i,\alpha,\beta)\right]\left(-\frac{\partial f(t_i,\alpha,\beta)}{\partial \alpha}\right) = 0, \quad (27)$$

$$\sum_{i=1}^{n}\left[\widehat{R}(t_i) - f(t_i,\alpha,\beta)\right]\left(-\frac{\partial f(t_i,\alpha,\beta)}{\partial \beta}\right) = 0. \quad (28)$$

After the approximation by the nonlinear least-squares method, using the Trust Region algorithm [62,63], the two-parameter Weibull model was obtained, which is represented by the formula:

$$R(t) = e^{-0.000574t^{0.889}}. \quad (29)$$

Figure 6 shows the course of the approximation curve with the points corresponding to the values obtained from the estimation. The small distances between the curve and the points indicate a good fit of the Weibull model.

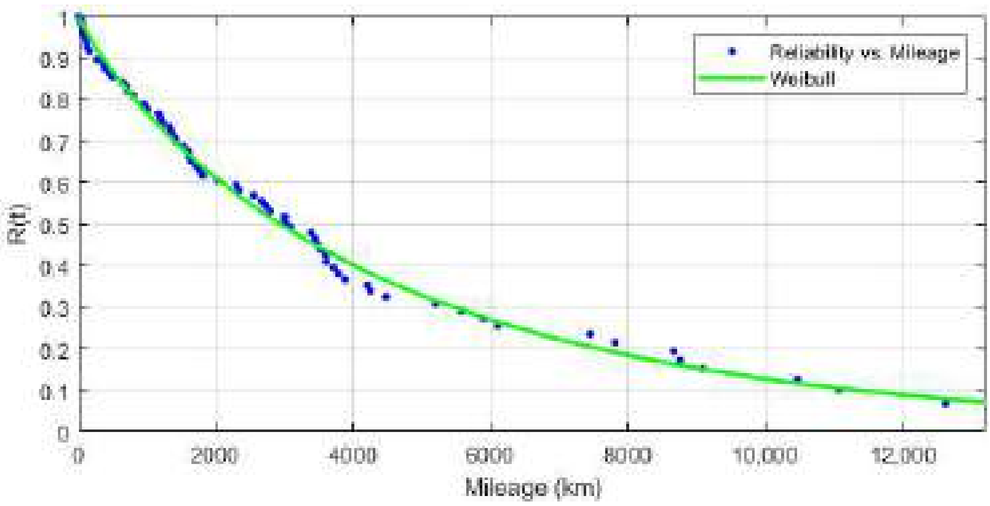

Figure 6. Graph presenting Weibull model fitting to estimated values of reliability function.

3.4. Neural Model of Reliability

Neural modelling was carried out using IT support in the form of the Neural Net Fitting application in Matlab. The database was divided into three sets: training (80%), validation (10%) and test (10%). As part of the research conducted, 10 neural networks were created with varying numbers of neurons in the hidden layer. The results of model fitting are shown in Table 4 and in Figures 7 and 8. Each of the trained neural networks showed very high prediction accuracy.

Table 4. *R* values of artificial neural networks.

MLP	Hidden Neurons	Training	Validation	Test
1-1-1	1	0.9974	0.9988	0.9990
1-2-1	2	0.9973	0.9989	0.9985
1-3-1	3	0.9991	0.9993	0.9983
1-4-1	4	0.9990	0.9983	0.9992
1-5-1	5	0.9991	0.9996	0.9988
1-6-1	6	0.9988	0.9991	0.9960
1-7-1	7	0.9993	0.9991	0.9987
1-8-1	8	0.9995	0.9995	0.9994
1-9-1	9	0.9996	0.9997	0.9985
1-10-1	10	0.9992	0.9997	0.9991

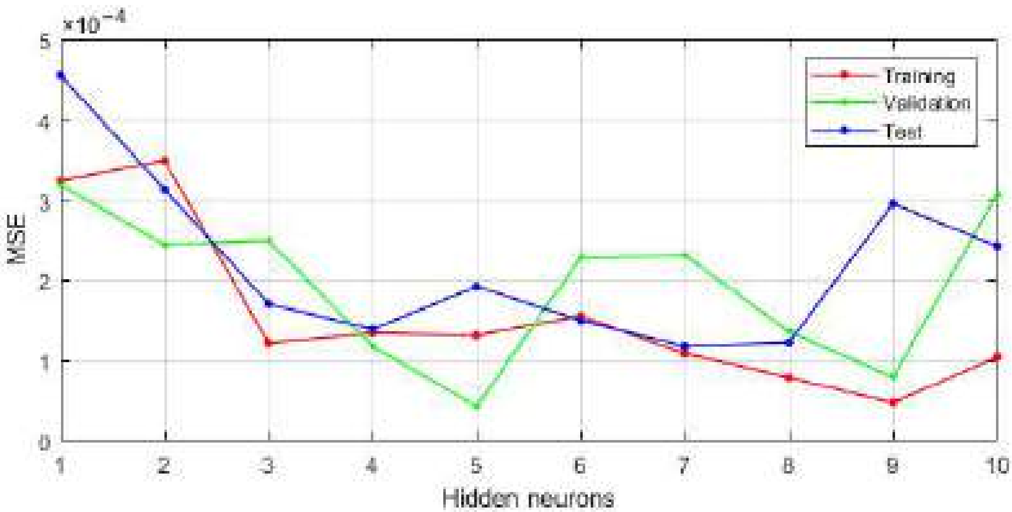

Figure 7. Sensitivity analysis of *MSE* error of neural model as a function of hidden neurons number.

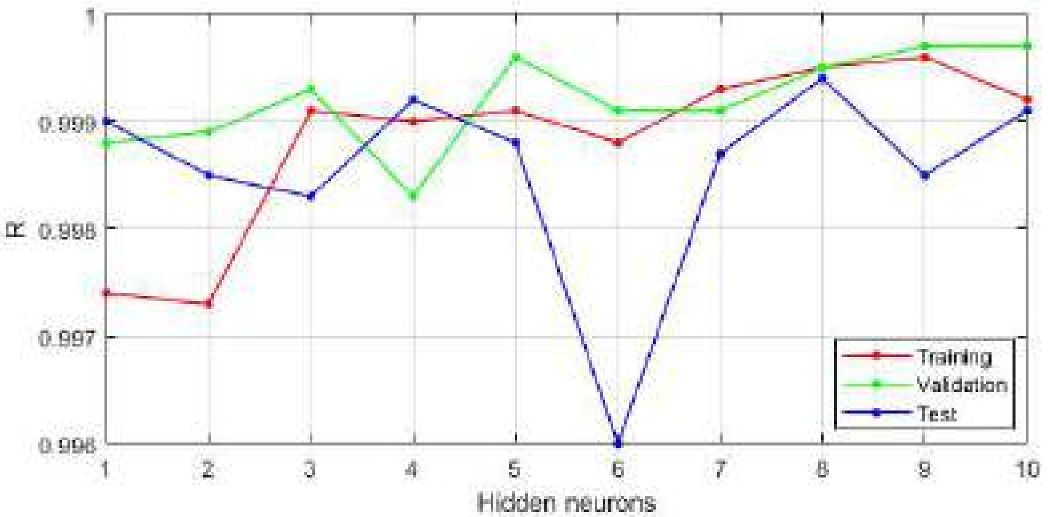

Figure 8. Analysis of sensitivity of *R* correlation coefficient in neural model as a function of hidden neurons number.

The analysis of the *MSE* error values and the *R* correlation coefficient presented in Figures 7 and 8 show a slight improvement in the degree of fitting of the neural model to the estimated values of the reliability function. The graphs shown in Figures 9 and A1–A9 (Appendix A) illustrate the approximation of the reliability function by neural models with a number of neurons in the hidden layer ranging from 1 to 10. While the number of hidden neurons increases, the model tends to interpolate the function. For a developed model based on 9 and 10 neurons, the approximating function takes a non-monotonic form and therefore does not satisfy the condition of non-increasing reliability function. The uncomplicated form and good fit of the MLP 1-1-1 model led us to choose this neural network as the suitable one for further analyses and considerations.

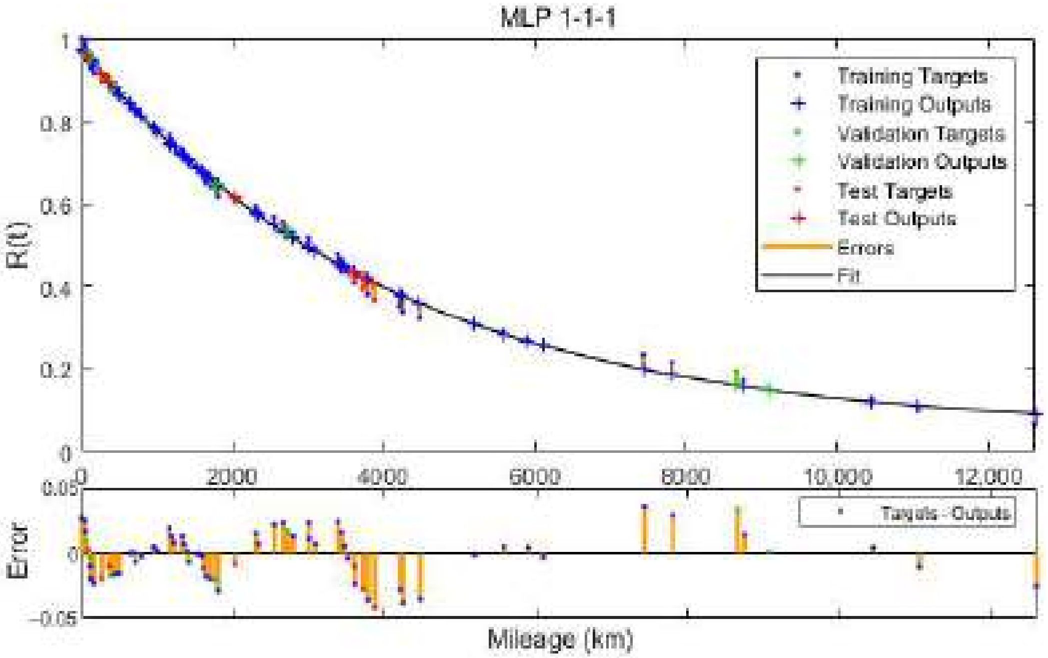

Figure 9. Reliability function approximated by MLP 1-1-1.

Figure 9 shows the course of the reliability function approximation curve in the MLP 1-1-1 neural model together with the estimated values and the difference between the estimated value and the modelled value. The degree of fitting in each dataset together with scatter plots are shown in Figure 10. The similar values of the R correlation coefficient indicate a valid approximation, without the occurrence of network overtraining and fitting only to the data from the training set.

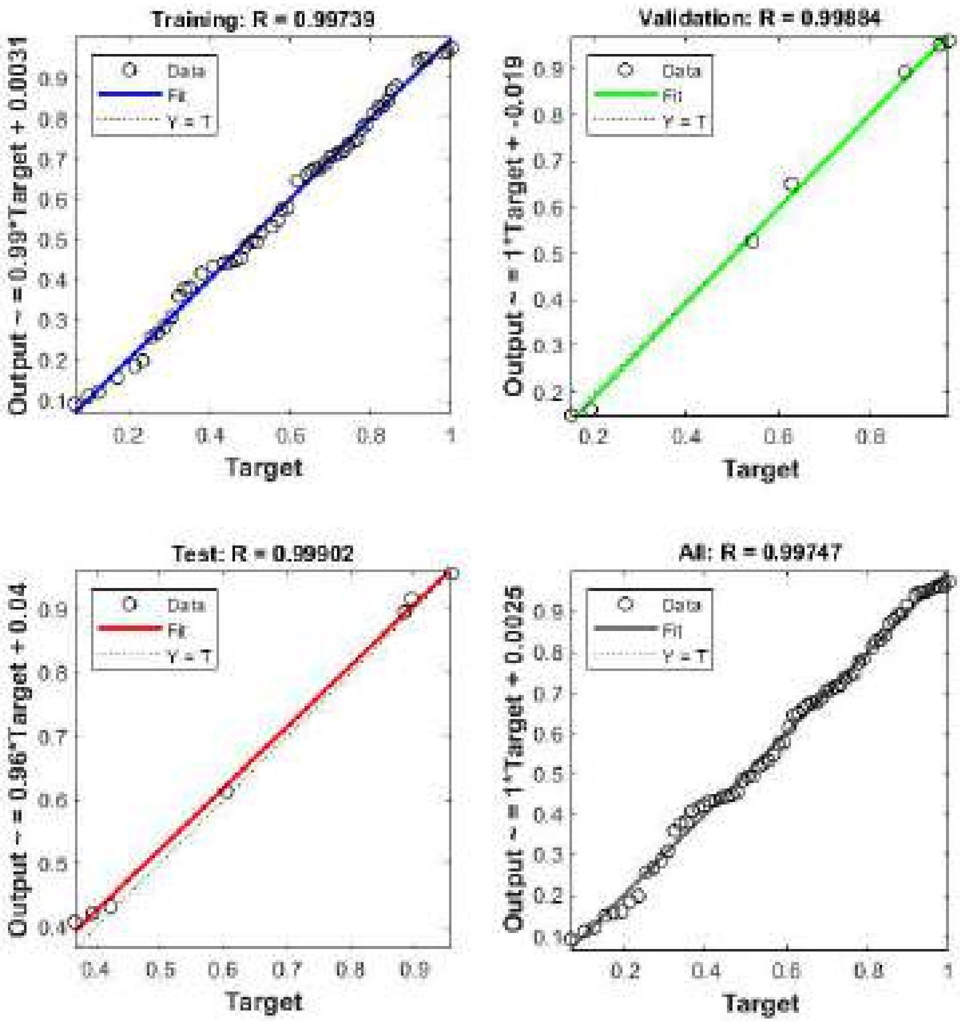

Figure 10. MLP 1-1-1 regression plot.

The low complexity of the MLP 1-1-1 neural model makes it easy to obtain its analytical form. For the analysed example, the MLP 1-1-1 model can be represented by relation (29):

$$R(t) = \frac{32.925260 + 1.786689e^{0.000249t}}{1 + 34.674828e^{0.000249t}}. \quad (30)$$

3.5. Analysis of Reliability Models

The reliability function models developed as a result of the study showed a high degree of match with the estimated values. Table 5 summarises the values of the linear correlation coefficient R and the MSE error to compare the neural model with the exponential and Weibull models commonly used in literature. For all three models, the R correlation coefficient reached a value exceeding 0.99. However, the best fitting model is the neural model. The MSE error made by the MLP 1-1-1 is more than 2 times smaller than for the exponential model and about 14% smaller than the Weibull model.

Table 5. Accuracy of models.

Model	*R*	*MSE*
Exponential	0.9945	7.32×10^{-4}
Weibull	0.9971	3.92×10^{-4}
Neural	0.9975	3.37×10^{-4}

The use of exponential and linear activation functions in the neural model allows for the utilisation of the differentiability of the analytical form of the approximating reliability function to calculate the relationships describing the failure probability density $f(t)$ and the failure intensity $\lambda(t)$. For the exponential and Weibull models, these relationships were developed according to the equations available in the literature. Table 6 shows the function $f(t)$, while Table 7 presents the failure intensity $\lambda(t)$ for each reliability model.

Table 6. Probability density functions.

Model	Probability Density Function
Exponential	$f(t) = 0.000235e^{-0.000235t}$
Weibull	$f(t) = 0.000510t^{-0.111} \cdot e^{-0.000574t^{0.889}}$
Neural	$f(t) = \frac{0.000236e^{0.000249t}}{(0.028839+e^{0.000249t})^2}$

Table 7. Failure intensity functions.

Model	Failure Intensity Function
Exponential	$\lambda(t) = 0.000235$
Weibull	$\lambda(t) = 0.000510t^{-0.111}$
Neural	$\lambda(t) = \frac{0.297572e^{0.000498t}+0.008621e^{0.000249t}}{1+65.246821e^{0.000747t}+1206.137388e^{0.000498t}+69.404797e^{0.000249t}}$

To compare the courses of the individual reliability characteristics, their graphical interpretations are shown in Figures 11 and 12. The probability density function has a very similar course for all three models. The Weibull model for the mileage in the $0.0 \div 1000.0$ km range is an exception, for which the function $f(t)$ significantly deviates from the values achieved by the other models. For all models, the function $f(t)$ is decreasing.

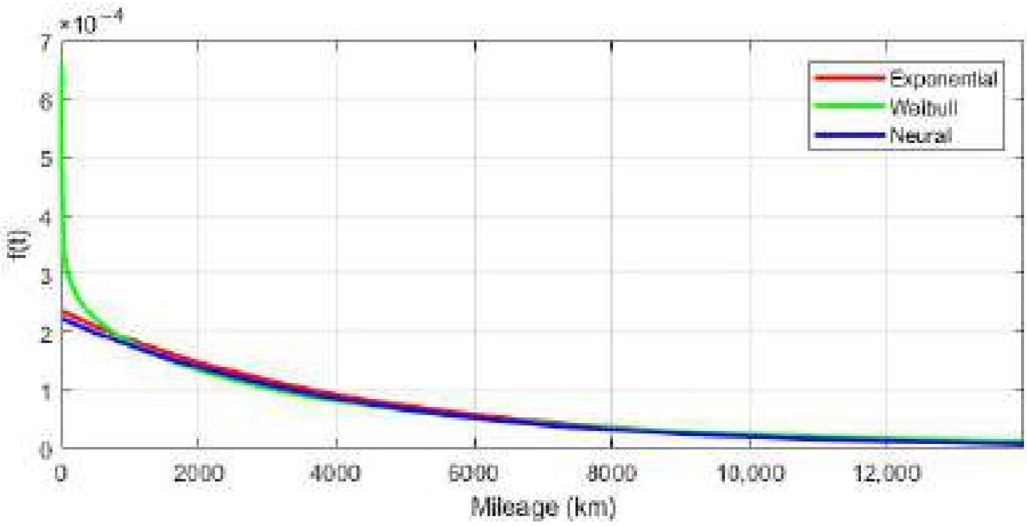

Figure 11. Probability density functions of reliability models.

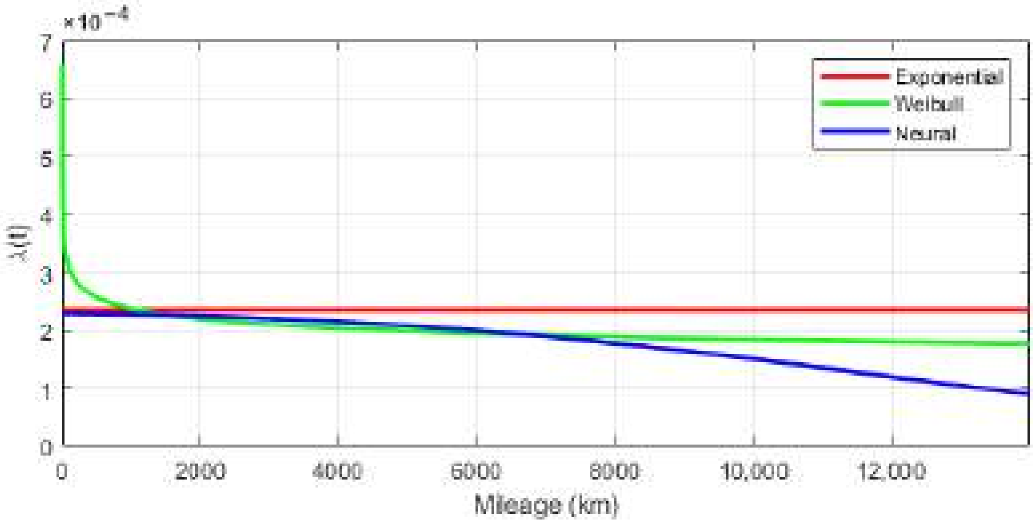

Figure 12. Failure intensity functions of reliability models.

The failure intensity function, which is the quotient of the failure probability density value and the reliability value, takes different courses for each of the three reliability models developed. For the exponential model, according to the theoretical assumptions, the function is constant and takes the value 0.000235 [1/km] for the studied sample of vehicles. For the Weibull model, the course of the function $\lambda(t)$ for arguments 0.0 ÷ 1000.0 km is similar to that of the function $f(t)$. This is due to the reliability function taking values close to one for these arguments. The further course of the intensity function for the Weibull model is flattened and reaches values smaller than in the exponential model. In the neural model, the function $\lambda(t)$ is decreasing, with values smaller than in the exponential model for the whole domain resulting from the model constraints.

Figure 13 presents a plot showing the value of the integral of the reliability function over the integration interval [0.0, t] for $t \leq$ 100,000.0 km. The calculated definite integral in the interval from 0.0 to infinity corresponds to the expected value of the mileage between failures. For the exponential and Weibull model, the expected value of ET is finite and is 4255.32 km and 4686.22 km, respectively (Table 8). For the neural model, the expected value of the mileage between failures approaches infinity. The use of the model, therefore, requires the implementation of appropriate constraints due to the inability of the neural network to extrapolate the value of the reliability function beyond the known data range. The empirical data for which the value of the reliability function was estimated range between [0.0; 21,477.0 km]. In this range, the ET value for the neural model attains similar levels to the Weibull model.

The value of the expected mileage between failures can be an indicator that determines the intervals between periodic inspections and maintenance of technical objects. Appropriate adjustment of the maintenance intervals according to the determined reliability characteristics can positively influence the readiness of the technical object and can increase the probability of a task being properly carried out without failure occurring.

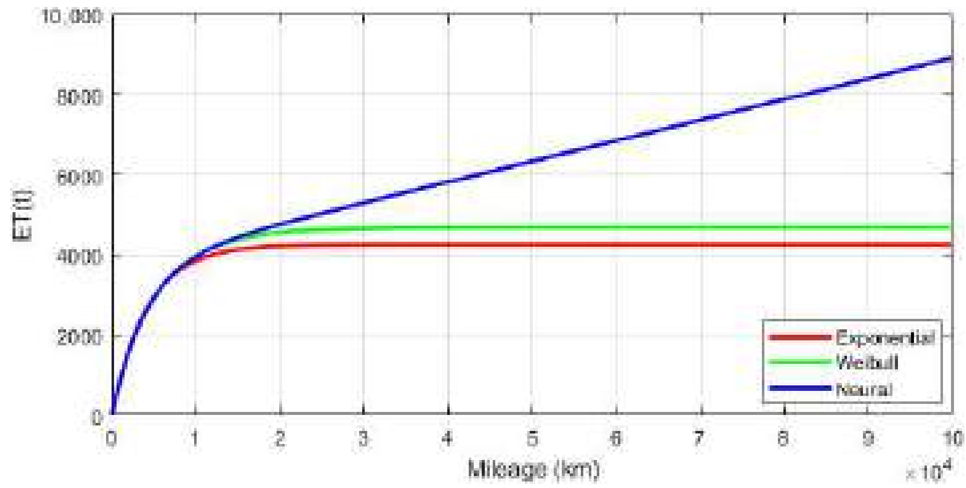

Figure 13. Definite integral graph of reliability function depending on integration interval.

Table 8. Expected mileage between failures.

Model	*ET* (km)
Exponential	4255.32
Weibull	4686.22
Neural	-

4. Conclusions

In this publication, research has been carried out concerning the reliability modelling of military vehicles. A methodology based on the use of non-parametric estimation and reliability function approximation has been proposed. The estimation of the reliability function values was carried out using the Kaplan–Meier estimator. As opposed to the Benard approximation, it enables the study to be carried out on censored data. The estimated values of the reliability function were used to develop mathematical and neural models. From the set of developed neural models, based on the analysis of the *MSE* error values and the correlation coefficient *R* and taking into account the low complexity of the model form, the MLP 1-1-1 model was selected. Then, the analytical form of the neural model was created, which allowed its further analysis. After comparing the exponential, Weibull and MLP 1-1-1 models, the neural model proved to be the best match for the estimated reliability function values. This confirms the feasibility of using artificial neural networks for accurate function approximation.

Based on the approximated reliability functions, the reliability characteristics have been developed, i.e., the failure probability density functions, the failure intensity functions and the expected values of the mileage between failures. The plot of the failure probability density function was similar for all 3 models for mileage values exceeding 1000.0 km. The failure intensity function for the exponential model, according to the theoretical assumptions, is constant. For the Weibull and neural models, the course of the function $\lambda(t)$ showed a decreasing monotonicity, but with different values.

The expected mileage between failures, calculated as the definite integral of the reliability function, took a finite value for the exponential and Weibull models, reaching 4255.32 km and 4686.22 km, respectively. For the neural model, the expected value approached infinity. The above fact indicates the inability of the neural network to extrapolate the reliability function. Thus, when using a neural model, it is necessary to impose constraints derived from the empirical data set. The practical aspect of determining the *ET* (expected mileage between failures) value can be to use it as an indicator for planning periodic vehicle maintenance. The purpose of periodic servicing is to restore the technical life and minimise the risk of failure and malfunction. The technical system, in which the analysed group of vehicles operates, assumes the realisation of preventive maintenance at intervals of 1 calendar year or every 5000.0 km of the mileage. Comparing this value to the expected mileage between failures, it can be concluded that the periodic services are carried out too rarely, which causes frequent failures and negatively affects the reliability of military vehicles.

So far, the applications of artificial neural networks for modelling the reliability of technical objects have been focused mainly on the precise predictions of reliability function values and the times of subsequent failure occurrences. This study goes beyond these areas of application, as the focus is on creating an accurate neural model that can be expressed in terms of analytical relationships. This approach allows further analysis of the model and determination of the remaining reliability characteristics.

The presented reliability testing methodology allows for the analysis and assessment of the reliability of military vehicles based on the observation of a certain period of operation in natural conditions, without the need for costly experiments and time-consuming simulations. This helps to avoid excessive costs associated with the implementation of experimental studies while ensuring the reliability of the analyses carried out.

Author Contributions: Conceptualisation, M.O. and J.Z.; methodology, M.O.; software, M.O.; validation, M.O. and J.Z.; formal analysis, M.O and J.Z.; investigation, M.O.; resources, M.O.; data curation, M.O.; writing—original draft preparation, M.O.; writing—review and editing, M.O.; visualisation, M.O.; supervision, M.O. and J.M.; project administration, M.O. and J.M.; funding acquisition, J.M. All authors have read and agreed to the published version of the manuscript.

Funding: This research was funded by the Military University of Technology, grant number UGB 771/2022.

Institutional Review Board Statement: Not applicable.

Informed Consent Statement: Not applicable.

Data Availability Statement: Not applicable.

Conflicts of Interest: The authors declare no conflict of interest. The funders had no role in the design of the study; in the collection, analyses, or interpretation of data; in the writing of the manuscript, or in the decision to publish the results.

Appendix A

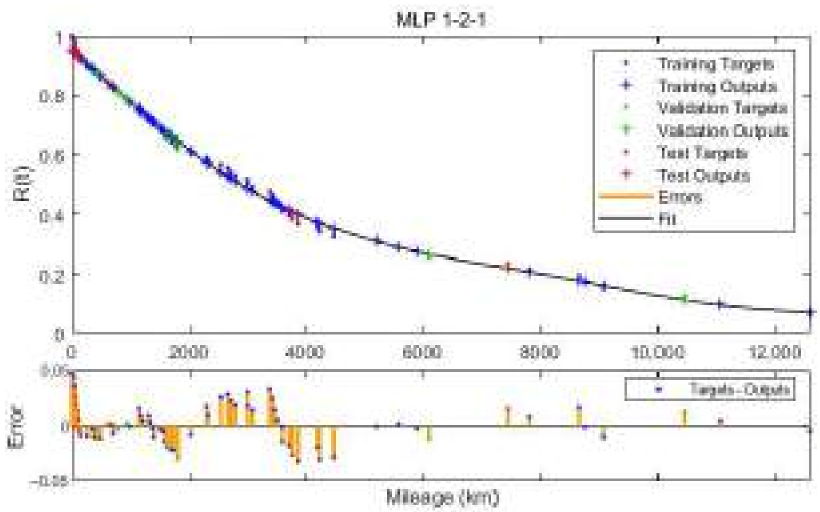

Figure A1. Reliability function approximated by MLP 1-2-1.

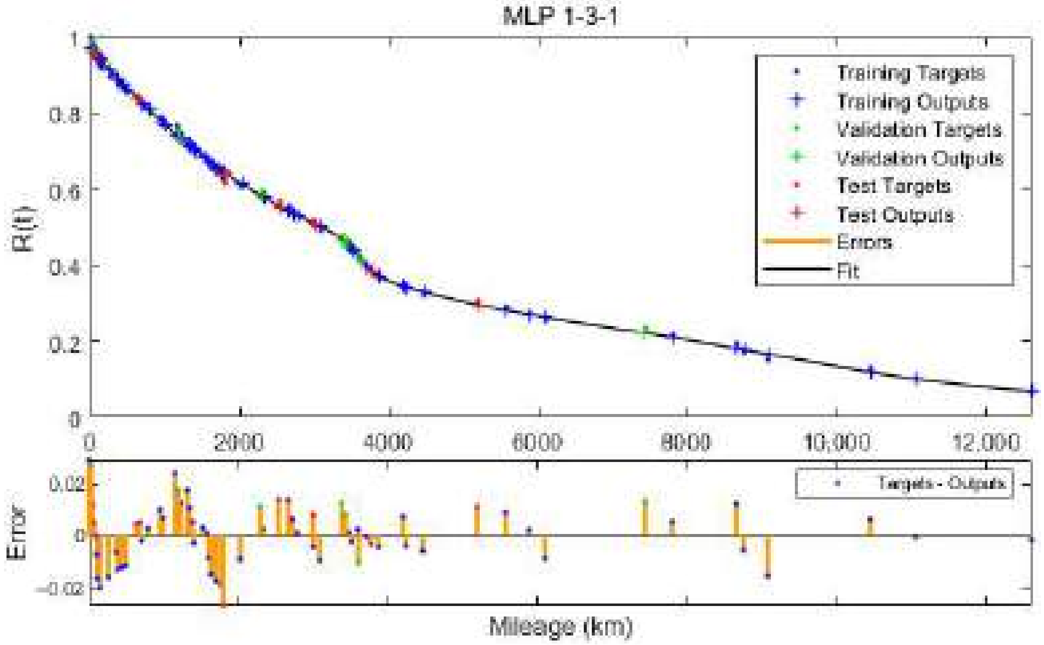

Figure A2. Reliability function approximated by MLP 1-3-1.

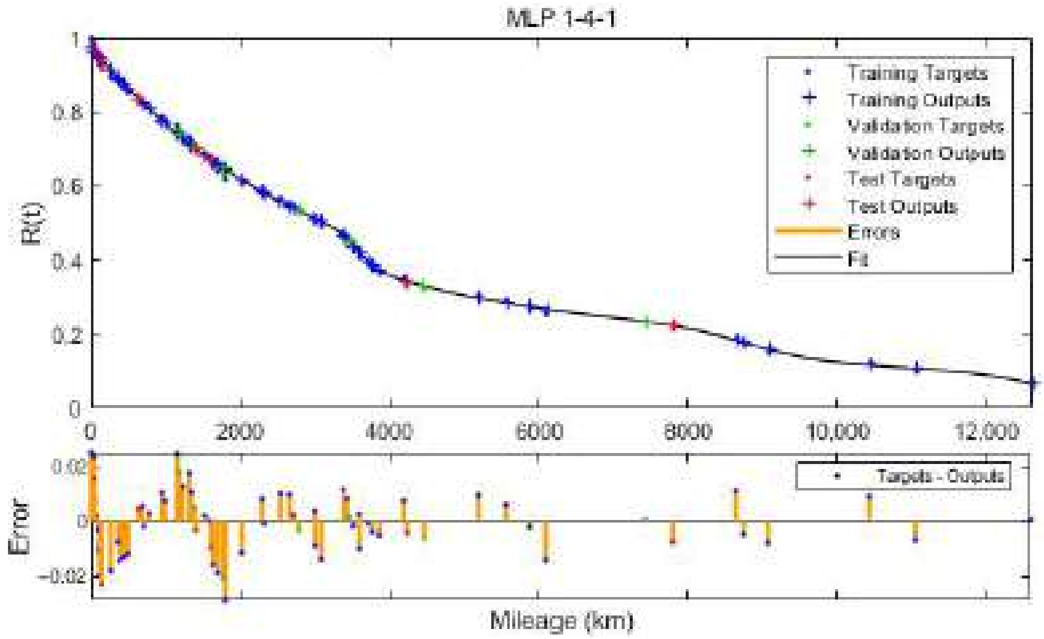

Figure A3. Reliability function approximated by MLP 1-4-1.

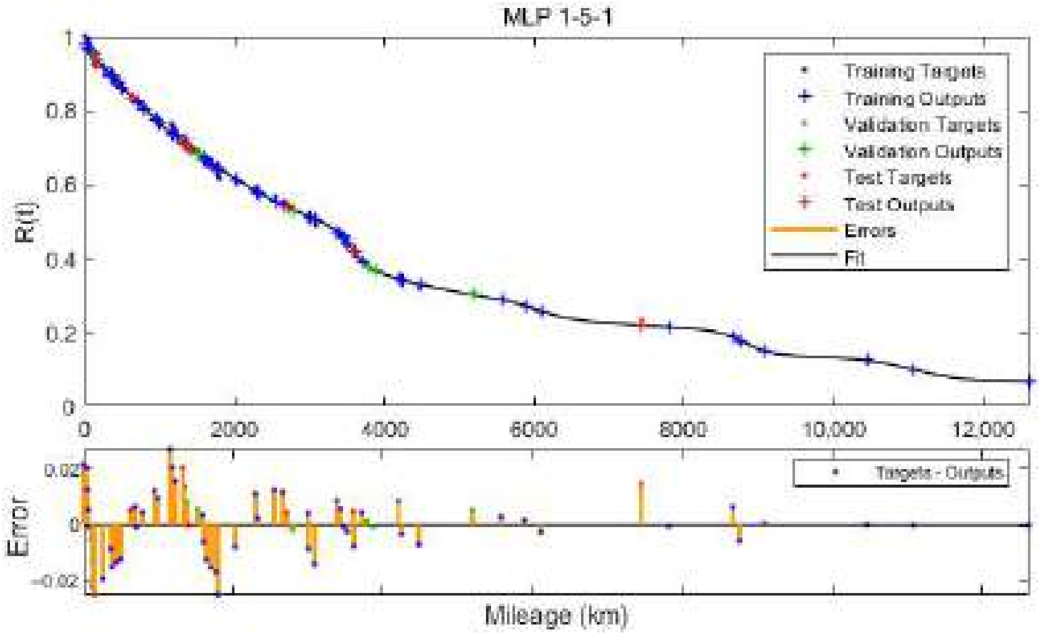

Figure A4. Reliability function approximated by MLP 1-5-1.

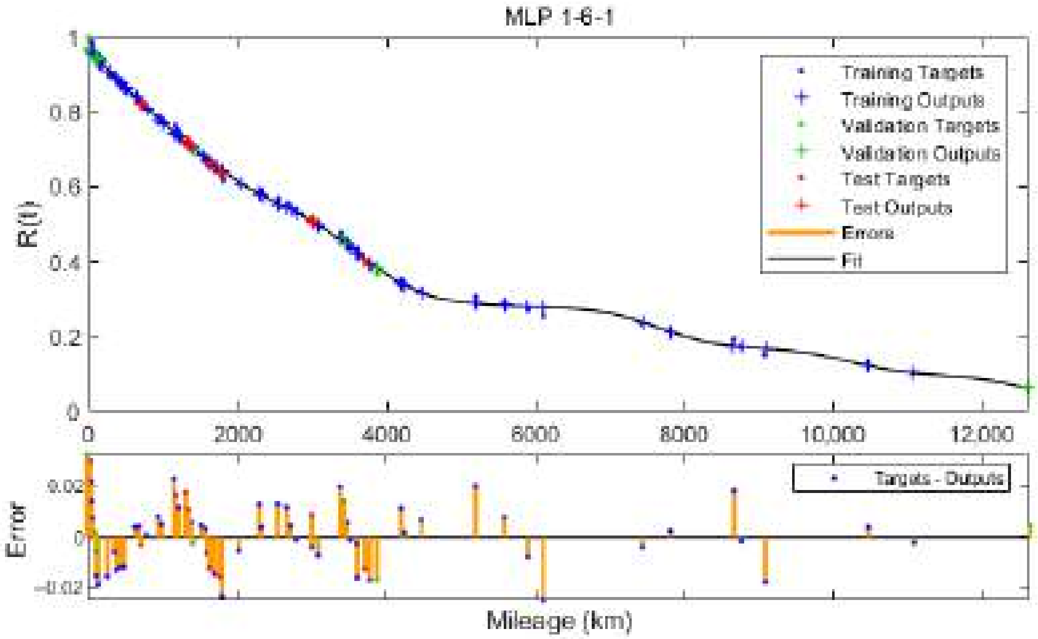

Figure A5. Reliability function approximated by MLP 1-6-1.

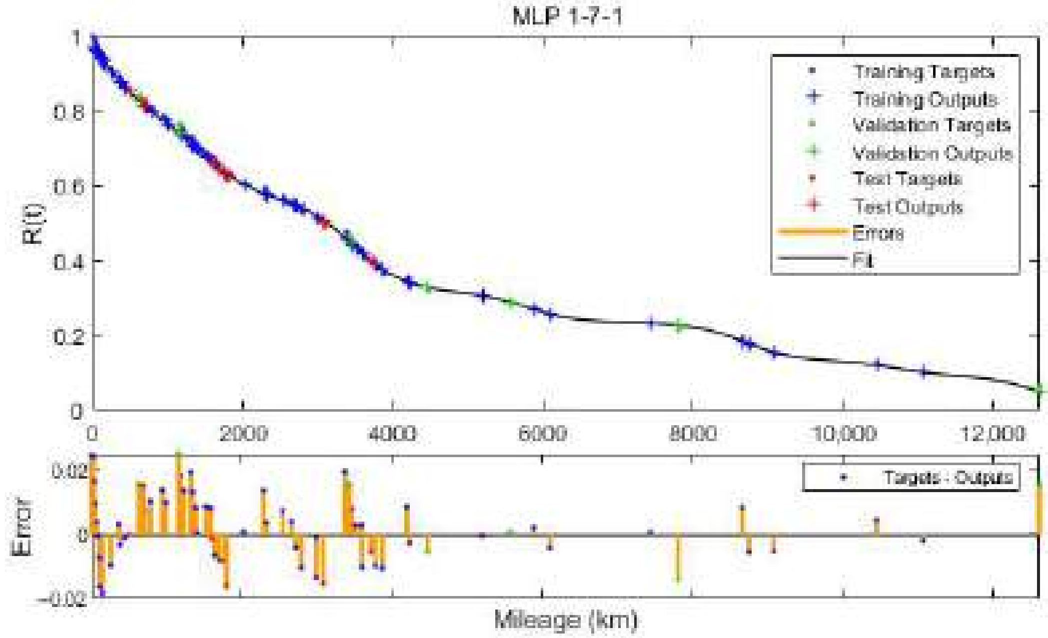

Figure A6. Reliability function approximated by MLP 1-7-1.

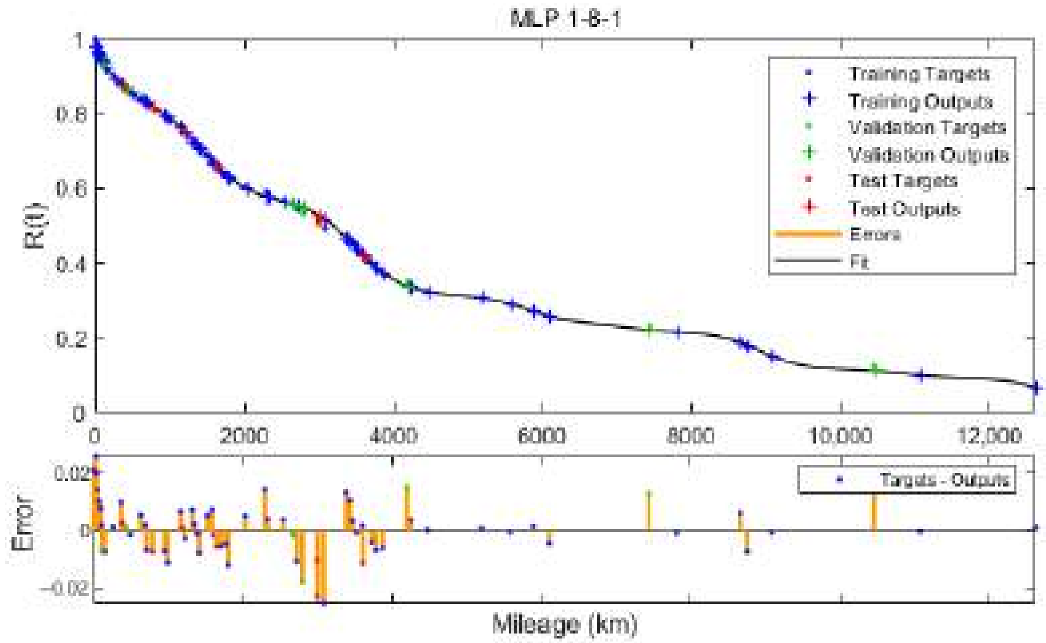

Figure A7. Reliability function approximated by MLP 1-8-1.

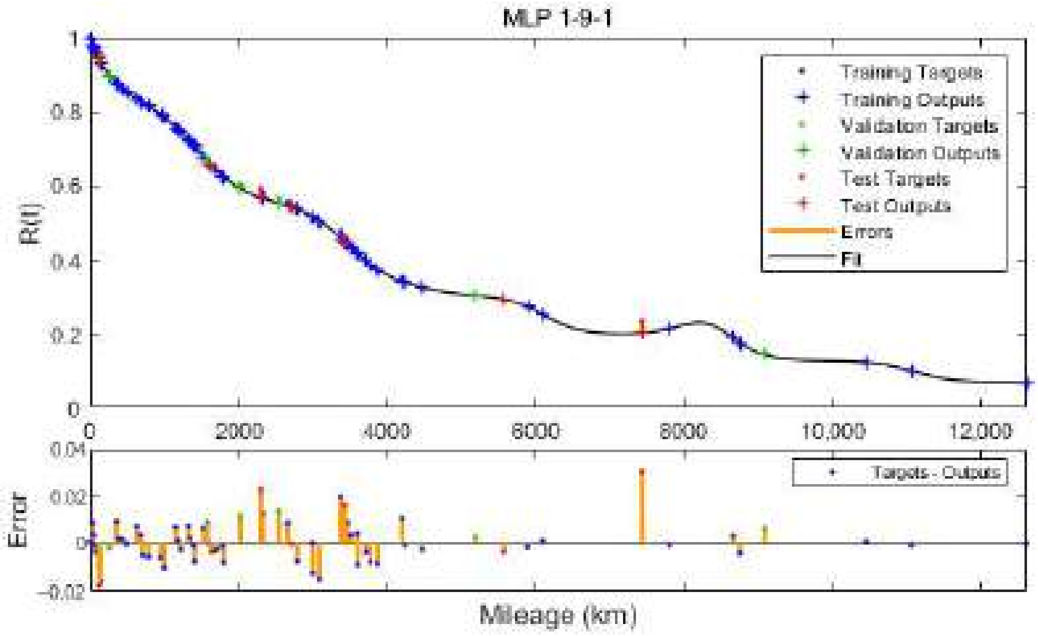

Figure A8. Reliability function approximated by MLP 1-9-1.

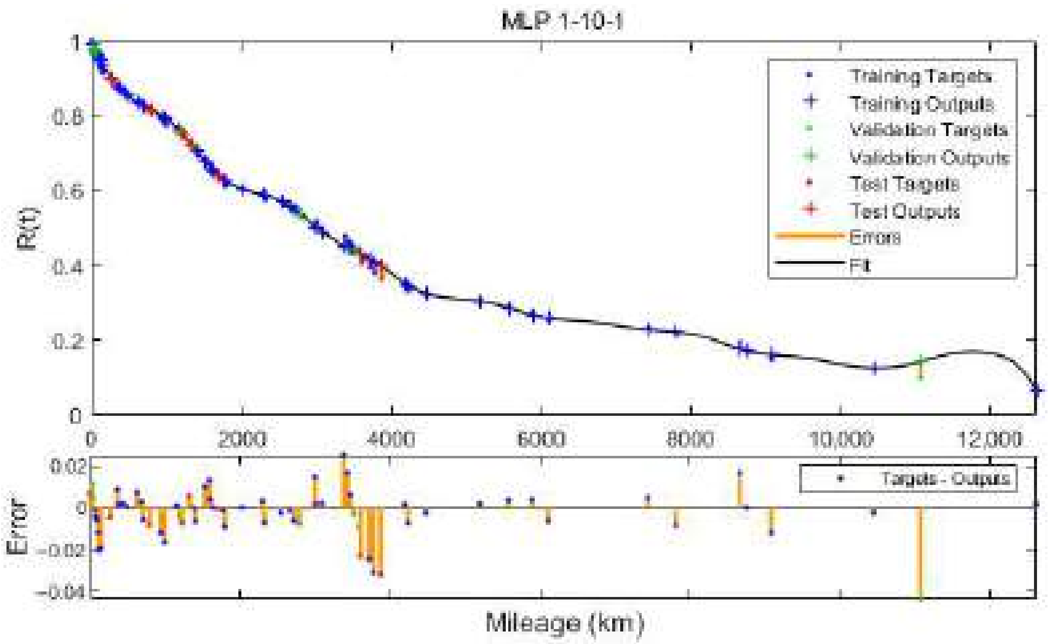

Figure A9. Reliability function approximated by MLP 1-10-1.

References

1. Li, X.; Zhao, X.; Pu, W. Knowledge-Oriented Modeling for Influencing Factors of Battle Damage in Military Industrial Logistics: An Integrated Method. *Def. Technol.* **2020**, *16*, 571–587. [CrossRef]
2. Wróblewski, P.; Drożdż, W.; Lewicki, W.; Miązek, P. Methodology for Assessing the Impact of Aperiodic Phenomena on the Energy Balance of Propulsion Engines in Vehicle Electromobility Systems for Given Areas. *Energies* **2021**, *14*, 2314. [CrossRef]
3. Barabino, B.; Di Francesco, M.; Mozzoni, S. An Offline Framework for the Diagnosis of Time Reliability by Automatic Vehicle Location Data. *IEEE Trans. Intell. Transp. Syst.* **2017**, *18*, 583–594. [CrossRef]
4. Barabino, B.; Di Francesco, M.; Mozzoni, S. Time Reliability Measures in Bus Transport Services from the Accurate Use of Automatic Vehicle Location Raw Data. *Qual. Reliab. Eng. Int.* **2017**, *33*, 969–978. [CrossRef]
5. Ziółkowski, J.; Małachowski, J.; Oszczypała, M.; Szkutnik-Rogoż, J.; Łęgas, A. Modelling of the Military Helicopter Operation Process in Terms of Readiness. *Def. Sci. J.* **2021**, *71*, 602–611. [CrossRef]
6. Simiński, P.; Kończak, J.; Przybysz, K. Analysis and Testing of Reliability of Military Vehicles. *J. KONBiN* **2018**, *47*, 87–95. [CrossRef]

7. Dobrzinskij, N.; Fedaravicius, A.; Pilkauskas, K.; Slizys, E. Impact of Climatic Conditions on the Parameters of Failure Flow of Military Vehicles. *Proc. Inst. Mech. Eng. Part D J. Automob. Eng.* **2021**, *236*, 753–762. [CrossRef]
8. Żurek, J.; Zieja, M.; Ziółkowski, J.; Borucka, A. Vehicle Operation Process Analysis Using the Markov Processes. In Proceedings of the 29th European Safety and Reliability Conference (ESREL), Hannover, Germany, 22–26 September 2019; pp. 2598–2605.
9. Li, Z.; Hensher, D.A.; Rose, J.M. Willingness to Pay for Travel Time Reliability in Passenger Transport: A Review and Some New Empirical Evidence. *Transp. Res. Part E Logist. Transp. Rev.* **2010**, *46*, 384–403. [CrossRef]
10. Żurek, J.; Zieja, M.; Ziółkowski, J. Reliability of Supplies in a Manufacturing Enterprise. In *Safety and Reliability–Safe Societies in a Changing World*; CRC Press: Boca Raton, FL, USA, 2018; pp. 3143–3148.
11. Jakkula, B.; Govinda, R.; Murthy, C.S.N. Maintenance Management of Load Haul Dumper Using Reliability Analysis. *J. Qual. Maint. Eng.* **2019**, *26*, 290–310. [CrossRef]
12. Alkaff, A.; Qomarudin, M.N.; Purwantini, E.; Wiratno, S.E. Dynamic Reliability Modeling for General Standby Systems. *Comput. Ind. Eng.* **2021**, *161*, 107615. [CrossRef]
13. Dziubak, T.; Wysocki, T.; Dziubak, S. Selection of Vehicles for Fleet of Transport Company on the Basis of Observation of Their Operational Reliability. *Eksploat. I Niezawodn. Maint. Reliab.* **2021**, *23*, 184–194. [CrossRef]
14. Selech, J.; Andrzejczak, K. An Aggregate Criterion for Selecting a Distribution for Times to Failure of Components of Rail Vehicles. *Maint. Reliab.* **2019**, *22*, 102–111. [CrossRef]
15. Woch, M.; Zieja, M.; Tomaszewska, J. Analysis of the Time between Failures of Aircrafts. In Proceedings of the 2017 2nd International Conference on System Reliability and Safety (ICSRS), Milan, Italy, 20–22 December 2017; pp. 112–118.
16. Thijssens, O.W.M.; Verhagen, W.J.C. Application of Extended Cox Regression Model to Time-On-Wing Data of Aircraft Repairables. *Reliab. Eng. Syst. Saf.* **2020**, *204*, 107136. [CrossRef]
17. Xu, K.; Xie, M.; Tang, L.C.; Ho, S.L. Application of Neural Networks in Forecasting Engine Systems Reliability. *Appl. Soft Comput.* **2003**, *2*, 255–268. [CrossRef]
18. Chen, K.-Y. Forecasting Systems Reliability Based on Support Vector Regression with Genetic Algorithms. *Reliab. Eng. Syst. Saf.* **2007**, *92*, 423–432. [CrossRef]
19. Da Chagas Moura, M.; Zio, E.; Lins, I.D.; Droguett, E. Failure and Reliability Prediction by Support Vector Machines Regression of Time Series Data. *Reliab. Eng. Syst. Saf.* **2011**, *96*, 1527–1534. [CrossRef]
20. Chatterjee, S.; Bandopadhyay, S. Reliability Estimation Using a Genetic Algorithm-Based Artificial Neural Network: An Application to a Load-Haul-Dump Machine. *Expert Syst. Appl.* **2012**, *39*, 10943–10951. [CrossRef]
21. Bai, B.; Zhang, J.; Wu, X.; Zhu, G.W.; Li, X. Reliability Prediction-Based Improved Dynamic Weight Particle Swarm Optimization and Back Propagation Neural Network in Engineering Systems. *Expert Syst. Appl.* **2021**, *177*, 114952. [CrossRef]
22. Yan, W.X.; Pin, W.; He, L. Reliability Prediction of CNC Machine Tool Spindle Based on Optimized Cascade Feedforward Neural Network. *IEEE Access* **2021**, *9*, 60682–60688. [CrossRef]
23. Du, Y.; Wu, G.; Tang, Y.; Liu, S. A Two-Stage Reliability Allocation Method for Remanufactured Machine Tools Integrating Neural Networks and Remanufacturing Coefficient. *Comput. Ind. Eng.* **2022**, *163*, 107834. [CrossRef]
24. Liu, D.; Wang, S. An Artificial Neural Network Supported Stochastic Process for Degradation Modeling and Prediction. *Reliab. Eng. Syst. Saf.* **2021**, *214*, 107738. [CrossRef]
25. Liu, D.; Wang, S.; Cui, X. An Artificial Neural Network Supported Wiener Process Based Reliability Estimation Method Considering Individual Difference and Measurement Error. *Reliab. Eng. Syst. Saf.* **2022**, *218*, 108162. [CrossRef]
26. Kamruzzaman, M.; Bhusal, N.; Benidris, M. A Convolutional Neural Network-Based Approach to Composite Power System Reliability Evaluation. *Int. J. Electr. Power Energy Syst.* **2022**, *135*, 107468. [CrossRef]
27. Lolas, S.; Olatunbosun, O.A. Prediction of Vehicle Reliability Performance Using Artificial Neural Networks. *Expert Syst. Appl.* **2008**, *34*, 2360–2369. [CrossRef]
28. Lins, I.D.; das Chasgas Moura, M.; Zio, E.; Droguett, E.L. A Particle Swarm-Optimized Support Vector Machine for Reliability Prediction. *Qual. Reliab. Eng. Int.* **2012**, *28*, 141–158. [CrossRef]
29. Krishna Mohan, G.; Yoshitha, N.; Lavanya, M.L.N.; Krishna Priya, A. Assessment and Analysis of Software Reliability Using Machine Learning Techniques. *Int. J. Eng. Technol. (UAE)* **2018**, *7*, 201–205. [CrossRef]
30. Hraiba, A.; Touil, A.; Mousrij, A. Artificial Neural Network Based Hybrid Metaheuristics for Reliability Analysis. *IFAC-Pap.* **2020**, *53*, 654–660. [CrossRef]
31. Hao, S.; Yang, J.; Ma, X.; Zhao, Y. Reliability Modeling for Mutually Dependent Competing Failure Processes Due to Degradation and Random Shocks. *Appl. Math. Model.* **2017**, *51*, 232–249. [CrossRef]
32. Hong, L.; Zhai, Q.; Wang, X.; Ye, Z.-S. System Reliability Evaluation Under Dynamic Operating Conditions. *IEEE Trans. Reliab.* **2019**, *68*, 800–809. [CrossRef]
33. Qi, S.; Huang, G.; Zhi, X.; Fan, F.; Flay, R.G.J. External Blast Load Factors for Dome Structures Based on Reliability. *Def. Technol.* **2021**, *18*, 170–182. [CrossRef]
34. Dong, Y.; Lu, H.; Li, L. Reliability Sensitivity Analysis Based on Multi-Hyperplane Combination Method. *Def. Technol.* **2014**, *10*, 354–359. [CrossRef]
35. Żurek, J.; Machałowski, J.; Ziółkowski, J.; Szkutnik-Rogoż, J. Reliability Analysis of Technical Means of Transport. *Appl. Sci.* **2020**, *9*, 3016. [CrossRef]

36. Wu, B.; Cui, L. Reliability Evaluation of Markov Renewal Shock Models with Multiple Failure Mechanisms. *Reliab. Eng. Syst. Saf.* **2020**, *202*, 107051. [CrossRef]
37. Tsarouhas, P. Reliability, Availability, and Maintainability (RAM) Study of an Ice Cream Industry. *Appl. Sci.* **2020**, *10*, 4265. [CrossRef]
38. Stavropoulos, C.N.; Fassois, S.D. Non-Stationary Functional Series Modeling and Analysis of Hardware Reliability Series: A Comparative Study Using Rail Vehicle Interfailure Times. *Reliab. Eng. Syst. Saf.* **2000**, *68*, 169–183. [CrossRef]
39. Wu, X.; Chang, Y.; Mao, J.; Du, Z. Predicting Reliability and Failures of Engine Systems by Single Multiplicative Neuron Model with Iterated Nonlinear Filters. *Reliab. Eng. Syst. Saf.* **2013**, *119*, 244–250. [CrossRef]
40. Dai, Y.; Zhou, Y.; Jia, Y. Distribution of Time between Failures of Machining Center Based on Type I Censored Data. *Reliab. Eng. Syst. Saf.* **2003**, *79*, 377–379. [CrossRef]
41. Petritoli, E.; Leccese, F.; Ciani, L. Reliability and Maintenance Analysis of Unmanned Aerial Vehicles. *Sensors* **2018**, *18*, 3171. [CrossRef]
42. Rajpal, P.S.; Shishodia, K.S.; Sekhon, G.S. An Artificial Neural Network for Modeling Reliability, Availability and Maintainability of a Repairable System. *Reliab. Eng. Syst. Saf.* **2006**, *91*, 809–819. [CrossRef]
43. Kaplan, E.L.; Meier, P. Nonparametric Estimation from Incomplete Observations. *J. Am. Stat. Assoc.* **1958**, *53*, 457–481. [CrossRef]
44. Pokhrel, A.; Dyba, T.; Hakulinen, T. A Greenwood Formula for Standard Error of the Age-Standardised Relative Survival Ratio. *Eur. J. Cancer* **2008**, *44*, 441–447. [CrossRef]
45. Cantor, A.B. Projecting the Standard Error of the Kaplan-Meier Estimator. *Statist. Med.* **2001**, *20*, 2091–2097. [CrossRef] [PubMed]
46. Santhosh, T.V.; Gopika, V.; Ghosh, A.K.; Fernandes, B.G. An Approach for Reliability Prediction of Instrumentation & Control Cables by Artificial Neural Networks and Weibull Theory for Probabilistic Safety Assessment of NPPs. *Reliab. Eng. Syst. Saf.* **2018**, *170*, 31–44. [CrossRef]
47. Wang, P.; Fan, J.; Li, Z. Study on Mean Time Between Failures Prediction Algorithms Based on Weibull Distribution. *IOP Conf. Ser. Earth Environ. Sci.* **2020**, *440*, 22083. [CrossRef]
48. Li, Z.; Li, Z.; Li, Y.; Tao, J.; Mao, Q.; Zhang, X. An Intelligent Diagnosis Method for Machine Fault Based on Federated Learning. *Appl. Sci.* **2021**, *11*, 12117. [CrossRef]
49. He, F.; Qi, H. A Method of Estimating Network Reliability Using an Artificial Neural Network. In Proceedings of the 2008 IEEE Pacific-Asia Workshop on Computational Intelligence and Industrial Application, Wuhan, China, 19–20 December 2008; Volume 2, pp. 57–60.
50. Song, C.-Y. A Study on Learning Parameters in Application of Radial Basis Function Neural Network Model to Rotor Blade Design Approximation. *Appl. Sci.* **2021**, *11*, 6133. [CrossRef]
51. Yang, R.; Zhang, L.; Cai, W.; Liu, Y.; Huang, H.-Z. Using Neural Network to Predict Reliability of Lithography Machine. In Proceedings of the 2013 International Conference on Quality, Reliability, Risk, Maintenance, and Safety Engineering (QR2MSE), Chengdu, China, 15–18 July 2013; pp. 308–311.
52. Ziółkowski, J.; Oszczypała, M.; Małachowski, J.; Szkutnik-Rogoż, J. Use of Artificial Neural Networks to Predict Fuel Consumption on the Basis of Technical Parameters of Vehicles. *Energies* **2021**, *14*, 2639. [CrossRef]
53. Aminisharifabad, M.; Yang, Q.; Wu, X. A Deep Learning-Based Reliability Model for Complex Survival Data. *IEEE Trans. Reliab.* **2021**, *70*, 73–81. [CrossRef]
54. Izquierdo, J.; Crespo Márquez, A.; Uribetxebarria, J. Dynamic Artificial Neural Network-Based Reliability Considering Operational Context of Assets. *Reliab. Eng. Syst. Saf.* **2019**, *188*, 483–493. [CrossRef]
55. Ching, T.; Zhu, X.; Garmire, L.X. Cox-Nnet: An Artificial Neural Network Method for Prognosis Prediction of High-Throughput Omics Data. *PLoS Comput. Biol.* **2018**, *14*, e1006076. [CrossRef]
56. Li, X.-Y.; Tao, Z.; Wu, J.-P.; Zhang, W. Uncertainty Theory Based Reliability Modeling for Fatigue. *Eng. Fail. Anal.* **2021**, *119*, 104931. [CrossRef]
57. Yangzhen, F.; Hong, Z.; Chenchen, Z.; Chao, F. A Software Reliability Prediction Model: Using Improved Long Short Term Memory Network. In Proceedings of the 2017 IEEE International Conference on Software Quality, Reliability and Security Companion (QRS-C), Prague, Czech Republic, 25–29 July 2017; pp. 614–615.
58. Zheng, H.; Kong, X.; Xu, H.; Yang, J. Reliability Analysis of Products Based on Proportional Hazard Model with Degradation Trend and Environmental Factor. *Reliab. Eng. Syst. Saf.* **2021**, *216*, 107964. [CrossRef]
59. Wu, C.-F. Asymptotic Theory of Nonlinear Least Squares Estimation. *Ann. Stat.* **1981**, *9*, 501–513. [CrossRef]
60. Kemmer, G.; Keller, S. Nonlinear Least-Squares Data Fitting in Excel Spreadsheets. *Nat. Protoc.* **2010**, *5*, 267–281. [CrossRef]
61. Gill, P.E.; Murray, W. Algorithms for the Solution of the Nonlinear Least-Squares Problem. *SIAM J. Numer. Anal.* **1978**, *15*, 977–992. [CrossRef]
62. Helfrich, H.-P.; Zwick, D. A Trust Region Algorithm for Parametric Curve and Surface Fitting. *J. Comput. Appl. Math.* **1996**, *73*, 119–134. [CrossRef]
63. Jiang, R.; Li, D. Novel Reformulations and Efficient Algorithms for the Generalized Trust Region Subproblem. *SIAM J. Optim.* **2019**, *29*, 1603–1633. [CrossRef]

energies

Article

Analysis of Light Utility Vehicle Readiness in Military Transportation Systems Using Markov and Semi-Markov Processes

Mateusz Oszczypała , Jarosław Ziółkowski * and Jerzy Małachowski

Institute of Mechanics and Computational Engineering, Faculty of Mechanical Engineering, Military University of Technology, gen. Sylwestra Kaliskiego Street 2, 00-908 Warsaw, Poland; mateusz.oszczypala@wat.edu.pl (M.O.); jerzy.malachowski@wat.edu.pl (J.M.)
* Correspondence: jaroslaw.ziolkowski@wat.edu.pl

Abstract: This paper presents the issues of modeling the operation process of light utility vehicles operating in military transport systems. The required condition for the effective operation of the system is to maintain the means of transport at the appropriate level of technical readiness. For this purpose, it is necessary to equip the technical system with appropriate resources enabling the efficient implementation of fuel refilling, maintenance and repair processes. Each failure of the means of transport causes a significant reduction in transport capacity, which then results in the inability to perform the planned tasks. Quality control and vehicle operation process management require advanced mathematical methods and tools. Three indicators have been proposed as quantitative characteristics for assessing and optimizing the availability of military vehicles: functional readiness, technical efficiency and airworthiness. To determine their value, a stochastic exploitation model was developed based on the application of the theory of Markov processes. Based on the collected empirical data, a nine-state phase space of the studied process was identified. Operating states were distinguished relating to the implementation of the transport task, refueling, parking in the garage, as well as maintenance and repairs. As part of the considerations for the continuous time, verification of the distributions of time characteristics led to the development of a semi-Markov model. The ergodic probabilities calculated based on the conditional probability matrix of interstate transitions and the expected values of the time spent in the states were used to determine the indicators of functional availability, efficiency and technical suitability. In order to determine the possibility of optimizing the process, a sensitivity analysis was performed. Reducing the amount of time the vehicles must wait for repair by about 50% can improve the values of the indexes from 0.91 to 0.95.

Keywords: exploitation process modeling; semi-Markov model; readiness; maintenance analysis; transportation system

Citation: Oszczypała, M.; Ziółkowski, J.; Małachowski, J. Analysis of Light Utility Vehicle Readiness in Military Transportation Systems Using Markov and Semi-Markov Processes. *Energies* **2022**, *15*, 5062. https://doi.org/10.3390/en15145062

Academic Editors: Marek Stawowy, Adam Rosiński and Zbigniew Kasprzyk

Received: 17 June 2022
Accepted: 7 July 2022
Published: 11 July 2022

1. Introduction

Military transport systems aim to ensure that transport capacity corresponds to the existing needs. The determinants of the level of transport needs include combat operations, training plans and the current activity of military units. The fleet of reliable vehicles is one of the main factors determining the high quality and timely implementation of processes in modern transport systems. The condition for the effective operation of the system is to maintain the means of transport in a state of technical efficiency and be ready to perform tasks [1,2]. The fulfilment of this condition is possible thanks to the organization of operating systems with appropriate technical resources to carry out processes of diagnosis, servicing and repair of vehicles. Along with the increase in the intensity of the use of means of transport, the demand for fuel and other consumables increases significantly, especially in the case of military vehicles traveling outside the area of public roads [3–5].

Military exploitation systems are largely based on a plan-preventive maintenance strategy, aiming to maximize the technical availability of facilities [6–9]. This strategy assumes the implementation of maintenance with a specific labor intensity, in accordance with the required scope. The guidelines for maintenance activities, time intervals and the size of the service life between maintenance are defined based on the manufacturer's technical specifications and the knowledge and experience of specialists dealing with planning and standardization of operation at individual management levels. The main disadvantages of this strategy are its cost-intensive nature and low flexibility.

The operation process covers activities related to a technical object from the moment of its production to its liquidation. During this period, there are essentially two overlapping sub-processes usage and maintenance. The rational use of machines and devices allows for extending the intervals between subsequent maintenance services, recreating the technical service life of the facility, and also reducing the current operating costs. The model of the operation process should, on the one hand, reflect the basic technical characteristics of the object consistent with the modeling objective, and on the other hand, it should be used for the rational forecasting of use and maintenance [10–13].

Markov's theory has found applications in many fields of science and technology. There are many scientific studies in the literature on the use of Markov processes for reliability modeling [14,15], the operation of objects [16–19] and technical systems [20,21]. Depending on the case study and the purpose of modeling, the authors constructed models based on a diverse number of operational states in the phase space. The least complicated Markov chain model was presented in [22] and applied to simulate and optimize energy savings for machines operating in production systems. Models with three states were constructed to analyze and assess the technical availability of buses [23], special vehicles [24], operational readiness of wind turbine elements [17], working time of production machines [25], the time interval of preventive maintenance [26] and the reliability of technical facilities [27]. In [28], the authors developed a five-state semi-Markov model with the Weibull distribution of the residence times of four types of buses in the states of the renewal process. This model allowed for profit optimization per unit of time and availability depending on the duration of preventive maintenance.

The comparison of the values obtained by the six-state Markov and semi-Markov models, which the authors of the publication [29] developed for production machines, indicated that the unverified assumption of the exponential distribution of the time the object stays in states may lead to significant errors in the calculation of the readiness indices. In the presented case study, the difference between the results of the semi-Markov model and the erroneous Markov model was as much as 0.40, which is less than half of the actual value of the readiness index.

Markov models with 9- and 16-state phase spaces are presented in [8,30] with much more elaborate models. The increased number of states allows a detailed analysis of the process and factors affecting the technical readiness of the facility. The multi-state models presented in [31] accurately reflected the stochastic nature of the electric vehicle driving cycle during their use in urban areas, outside the city, on the motorway and during road congestion. Table 1 summarizes the literature review containing the latest publications in the field of modeling the exploitation process with the use of Markov theory.

In this publication, the authors addressed the issue related to the operation of light utility vehicles operating in military transport systems. The research sample consisted of 19 Honker vehicles for which detailed data were collected during the three-year research period. The operating system is focused on maintaining the high reliability of vehicles through an appropriately planned and implemented maintenance strategy. The plan-preventive system each time assumes the scope of maintenance works after a specified amount of work (mileage) or time elapsed. Unfortunately, the records of operation are still kept in the form of traditional documentation registered on an ongoing basis by direct users (drivers) and in relation to inspections and repairs by service and repair workshops.

Source documents that create departure orders, technical service cards and operation plans were used to prepare detailed databases individually for each facility.

Table 1. Literature review of Markov and semi-Markov modeling in engineering.

Paper	Case Study	Model	Results and Conclusions
[22]	Machines in manufacturing system	Two-state Markov chain	The model was developed to simulate and optimize energy saving.
[8]	Military helicopters	Nine-state Markov model	Boundary probabilities were calculated for all states and the functional readiness index reached 0.9223.
[17]	Spring shock absorber in wind turbine system	Three-state semi-Markov model of maintenance	Erlang distribution of sojourn time. The system operational availability reached 0.6354–0.6497.
[25]	Machines in wafer fabrication work centre	Three-state hidden semi-Markov model	Accuracy of the machine condition recognition was 95.56% and prediction accuracy of job processing time was 94.91%.
[29]	Production machines	Six-state Markov and semi-Markov models	Readiness index: 0.85 (semi-Markov model) and 0.45 (Markov model). Groundless assumption of exponential distribution lead to incorrect results.
[24]	Special vehicles	Three-state semi-Markov model	Technical readiness factor was 0.95.
[30]	Means of transport	16-state semi-Markov model of exploitation process	Genetic algorithm was proposed for determining the optimal strategy to control availability.
[23]	Buses in transportation system	Three-state hidden Markov model	Probability of availability reached values in the range 0.896–0.969.
[28]	Four types of city bus renewal processes	Five-state semi-Markov model (Weibull distribution)	The model allows to optimize the profit per unit time and readiness to carry out transport tasks depending on the time to preventive maintenance.
[27]	Reliability of technical objects	Three-state semi-Markov model	Reliability function for Poisson and Furry-Yule failure rate processes.
[26]	Marine diesel engines	Three-state semi-Markov model (Weibull distribution)	The optimal preventive maintenance interval was 1095 h.
[31]	Driving cycles of electric vehicles	Multistate Markov models of acceleration	The models describe the stochastic nature of driving cycles in four scenarios: rural, highway, urban and congestion.
[19]	Offshore wind farms	Six-state Markov model	The proposed method allows for improving maintenance efficiency of offshore wind farms.
[10]	Transformers	Five-state Markov chain	Prediction of maintenance cost in 20-year forecast horizon.

The current review of the literature allows the authors to state there are no studies on the analysis and evaluation of the operation of heavy goods vehicles with the use of the Markov theory. It was a premise for conducting scientific research and developing an exploitation model for the aforementioned group of military vehicles. In addition, Honker vehicles have a significant share in the structure of the military transport fleet of the Polish Armed Forces. Carrying out the modeling of the operation process based on the application of the Markov theory requires a thorough understanding of the examined process and enables the analysis and assessment of the basic operational indicators of the studied object.

This article presents the original methodology for creating a stochastic model of Honker vehicles based on the Markov theory. An algorithm for creating a mathematical model was developed, the practical usefulness of which was verified on the actual operation process of the said sample of vehicles. An event model covering the nine-state phase space of the process was developed. The determined values of ergodic probabilities for individual operational states constituted the basis for calculating the values of functional availability, efficiency and technical suitability indicators. From the point of view of the transport capacity of the entire system as well as economic and technical conditions, the personnel managing the vehicle operation process aim to maximize the presented readiness and/or reliability measures. The proposed methodology makes it possible to indicate possible components influencing the improvement of exploitation indicators. The performed sensitivity analysis of the model allows for the examination of the impact of improving the organization of the repair subsystem, consisting of the shortening/elimination of waiting time for spare parts, on the readiness indicators of the tested sample of vehicles.

The nine-state model adds to the current state of the literature both in terms of the subject of the study and the application of sensitivity analysis to identify opportunities for improving process efficiency. No previous scientific studies have addressed the issue of modeling the operation of light utility vehicles (trucks) using Markov and semi-Markov process theory. In addition, a completely novel way of analyzing the sensitivity of the semi-Markov model in terms of the dependence of the values of ergodic probabilities on the values of expected dwell times was proposed.

The article has been divided into the following main chapters. The introduction reviews the current state of knowledge on the application of Markov theory to the exploitation process. Section 2 describes the methodology of creating event-based models of the operation process using the Markov theory. Section 3 provides a statistical analysis of the source data constituting the basis for the development of the model. In Section 4, the semi-Markov model is described, and the process research results are presented together with the model sensitivity analysis. The values of ergodic probabilities of the semi-Markov model were confronted with the standard Markov model. Finally, the Section 5 includes the conclusions from the conducted research.

2. Methods

The actual operation processes are a composition of deterministic and random subprocesses. Random components are usually interpreted as stochastic processes *X(t)* reflecting changes in the operational states of the tested object in discrete or continuous time. In the processes of exploitation at a random moment t, the object is only in one of the states identified in the phase space $S = X(t)$. This assumption requires precise determination of all possible operational states in which vehicles may be in the course of the operation process. The stochastic processes fulfilling the Markov property are essential in terms of applicability. According to Markov's theory, the conditional probabilities of reaching the future states $X(t_{z+1})$ result only from the current state $X(t_z)$ [32]. Mathematically, this property is consistent with Equation (1) [33–35]:

$$P\{X(t_z) = x_z | X(t_{z-1}) = x_{z-1}, X(t_{z-2}) = x_{z-2}, \ldots, X(t_0) = x_0\} = P\{X(t_z) = x_z | X(t_{z-1}) = x_{z-1}\}. \quad (1)$$

The literature is dominated by the division of Markov processes with regard to time and state space, which distinguishes four types of processes, i.e., processes:

1. Discrete in time and discrete in states;
2. Continuous in time and discrete in states;
3. Discrete in time and continuous in states;
4. Continuous in time and continuous in states.

In operation, the most frequently used models are based on discrete processes in states, developed for both discrete and continuous time [8,16,24,28,29].

2.1. Markov Chains

The Markov chain assumes the discretization of time into specific Δt intervals, the width of which depends on the characteristics of the process, measurement technique, and, above all, the adopted modeling objective [36]. With the increase in the dynamics of the process course, the possibility, and, at the same time, the necessity to perform frequent measurements and the focus on creating a very accurate model, the values of time Δt decrease. The dynamics of changes in the operational states identified in the phase space for the operation of light utility vehicles determine the assumption of the duration of moments Δt for the time interval equal to 1 min. Increasing this value could cause the undesirable omission of registering the occurrence of conditions, which are usually short-lived. At the same time, reducing the time intervals is practically impossible due to recording the course of operation processes of vehicles operating in military transport systems.

Constructing the Markov Chain Model based on an empirical process flow requires acquiring data on interstate transitions. For this purpose, it is reasonable to create a matrix of the number of interstate transitions according to the Formula (2):

$$\boldsymbol{N} = \begin{bmatrix} n_{11} & n_{12} & \cdots & n_{1(k-1)} & n_{1k} \\ n_{21} & n_{22} & \cdots & n_{2(k-1)} & n_{2k} \\ \vdots & \vdots & \ddots & \vdots & \vdots \\ n_{(k-1)1} & n_{(k-1)2} & \cdots & n_{(k-1)(k-1)} & n_{(k-1)k} \\ n_{k1} & n_{k2} & \cdots & n_{k(k-1)} & n_{kk} \end{bmatrix}. \tag{2}$$

The values of the $\boldsymbol{N}$ matrix correspond to the total number of observed interstate transitions in the analyzed period of the process implementation, where n_{ij} is the transition from the i state to the j state.

For a homogenous Markov chain, the conditional probability p_{ij} of transition from state i to state j in one step is the same for every moment t. The homogeneity of the process indicates the invariability of the rules affecting the state changes at any time of its implementation. If the analyzed realizations of the process are included in the same phase of operation, then the course of the process should be homogenous. The probability values of the conditional interstate transitions are presented by means of the stochastic matrix $\boldsymbol{P}$, according to the Formula (3) [33,37,38]:

$$\boldsymbol{P} = \begin{bmatrix} p_{11} & p_{12} & \cdots & p_{1(k-1)} & p_{1k} \\ p_{21} & p_{22} & \cdots & p_{2(k-1)} & p_{2k} \\ \vdots & \vdots & \ddots & \vdots & \vdots \\ p_{(k-1)1} & p_{(k-1)2} & \cdots & p_{(k-1)(k-1)} & p_{(k-1)k} \\ p_{k1} & p_{k2} & \cdots & p_{k(k-1)} & p_{kk} \end{bmatrix}, \tag{3}$$

provided that the following formula [37] is fulfilled:

$$\sum_{j=1}^{k} p_{ij} = 1. \tag{4}$$

The probabilities of the interstate transitions of the $\boldsymbol{P}$ stochastic matrix can be obtained using the values of the $\boldsymbol{N}$ interstate number matrix by estimation [31,35,39] according to the relationship:

$$p_{ij} = \frac{n_{ij}}{\sum\limits_{j=1}^{k} n_{ij}}, \tag{5}$$

where the standard error of the conditional probability estimation [40,41] is calculated according to the formula:

$$SE(p_{ij}) = \sqrt{\frac{p_{ij}(1-p_{ij})}{\sum_{j=1}^{k} n_{ij}}}. \tag{6}$$

The values of ergodic probabilities π_j are calculated by solving the following matrix Equation (7) [37]:

$$(\boldsymbol{P}^T - \boldsymbol{I}) \cdot \boldsymbol{\Pi} = 0, \tag{7}$$

assuming that the normalization condition is met, according to the formula:

$$\sum_{j=1}^{n} \pi_j = 1. \tag{8}$$

2.2. Markov and Semi-Markov Processes

Discrete Markov models in states and continuous in time allow for the analysis of the operation process under constant supervision and monitoring of the course of changes in operational states. This approach excludes the influence of the size of the time moments Δt on the values of the instantaneous and ergodic characteristics of the process. In principle, the change of state from S_i to S_j can take place at any time during the process. It is also assumed that only one state change can occur at any time t. The Markov process assumes the presence of exponential distributions of the characteristics of individual states describing the analyzed process [42–44].

The transition intensity matrix $\boldsymbol{\Lambda}$ is the quantitative characteristic of the Markov process:

$$\boldsymbol{\Lambda} = \begin{bmatrix} \lambda_{11} & \lambda_{12} & \cdots & \lambda_{1(k-1)} & \lambda_{1k} \\ \lambda_{21} & \lambda_{22} & \cdots & \lambda_{2(k-1)} & \lambda_{2k} \\ \vdots & \vdots & \ddots & \vdots & \vdots \\ \lambda_{(k-1)1} & \lambda_{(k-1)2} & \cdots & \lambda_{(k-1)(k-1)} & \lambda_{(k-1)k} \\ \lambda_{k1} & \lambda_{k2} & \cdots & \lambda_{k(k-1)} & \lambda_{kk} \end{bmatrix}, \tag{9}$$

whose elements meet the following dependencies:

$$\forall i, j, i \neq j, \lambda_{ij} = \frac{d}{dt} p_{ij} = \lim_{\Delta t \to 0} \frac{p_{ij}(t + \Delta t) - p_{ij}(t)}{\Delta t}, \tag{10}$$

$$\forall i, \lambda_{ii} = -\frac{d}{dt} p_{ii} = \lim_{\Delta t \to 0} \frac{1 - (p_{ii}(t + \Delta t) - p_{ii}(t))}{\Delta t}. \tag{11}$$

All elements of the matrix on the main diagonal have non-positive values, while all other elements are non-negative and the sum of all elements for each row of the transition intensity matrix is equal to 0.

In the operation processes of objects, the estimators of the values of the elements λ_{ij} of the interstate intensity matrix are the reciprocal of the average residence times in the S_i state before the transition to the S_j state. On the other hand, the value of λ_{ii} is taken as the reciprocal of the sum of the remaining elements in the i row. The presented description of the estimation of the intensity matrix elements can be written using the relationship:

$$\lambda_{ij} = \frac{1}{T_{ij}}, \tag{12}$$

$$\lambda_{ii} = -\sum_{j \neq i} \lambda_{ij}, \tag{13}$$

where T_{ij} is the average transition time from state S_i to state S_j.

The condition of exponential distributions of the stochastic process characteristics narrows the spectrum of applications of the Markov model in continuous time. Some characteristics of the operation process may not meet it. From the point of view of the reliability of the mapping, this excludes the possibility of applying the Markov model [29,45]. The generalization of the Markov process is the semi-Markov process, which does not require the fulfilment of the condition of exponential distributions of interstate transition times. In the semi-Markov process, the durations of states are independent random variables with any distribution function [27,43,46].

The basic characteristic of the semi-Markov process is the matrix of the renewal kernel $\boldsymbol{Q(t)}$, the elements of which are the products of the probability p_{ij} and the transition between the states S_i and S_j and the distribution function of the conditional duration distribution of the state S_i before the transition to S_j, according to the equation [30,47]:

$$\boldsymbol{Q}(\boldsymbol{t}) = \begin{bmatrix} 0 & Q_{12}(t) & \cdots & Q_{1(k-1)}(t) & Q_{1k}(t) \\ Q_{21}(t) & 0 & \cdots & Q_{2(k-1)}(t) & Q_{2k}(t) \\ \vdots & \vdots & \ddots & \vdots & \vdots \\ Q_{(k-1)1}(t) & Q_{(k-1)2}(t) & \cdots & 0 & Q_{(k-1)k}(t) \\ Q_{k1}(t) & Q_{k2}(t) & \cdots & Q_{k(k-1)}(t) & 0 \end{bmatrix}, \quad (14)$$

wherein:

$$Q_{ij}(t) = p_{ij} \cdot F_{ij}(t), \quad (15)$$

where p_{ij} is the probability of transition from the S_i state to S_j, and $F_{ij}(t)$ is the distribution function of the residence time in state S_i before the transition to state S_j.

An embedded Markov chain is formulated for a semi-Markov process in continuous time, which represents changes in the process state without taking into account the residence times in individual states.

The embedded Markov chain assumes the possibility of transition from the S_i state to $S_{j,}$ assuming that $i \neq j$. The interstate transition probability matrix for such a chain can have non-zero elements only outside the main diagonal, which can be written by the formula:

$$\boldsymbol{P} = \begin{bmatrix} 0 & p_{12} & \cdots & p_{1(k-1)} & p_{1k} \\ p_{21} & 0 & \cdots & p_{2(k-1)} & p_{2k} \\ \vdots & \vdots & \ddots & \vdots & \vdots \\ p_{(k-1)1} & p_{(k-1)2} & \cdots & 0 & p_{(k-1)k} \\ p_{k1} & p_{k2} & \cdots & p_{k(k-1)} & 0 \end{bmatrix}. \quad (16)$$

If the embedded Markov chain is ergodic and there are expected $E(T_i)$ values of the times in individual states, then the ergodic values of the probabilities π_j for the semi-Markov process can be determined using the following dependencies:

$$\pi_j = \frac{p_j \cdot E(T_j)}{\sum\limits_{i=1}^{k} p_i \cdot E(T_i)}, \quad (17)$$

$$E(T_j) = \sum_{i=1}^{k} p_{ij} T_{ij}, \quad (18)$$

where p_i is the ergodic probability of the embedded Markov chain for state S_i, and T_{ij} is the average transition time from state S_i to state S_j.

Figure 1 shows a block diagram of creating a model of the exploitation process based on the theory of Markov and semi-Markov. The first stages of stochastic modeling are the identification of the technical object, the selection of a statistical sample, and the collection of empirical data in the form of databases. Then a choice is made between discrete-time and continuous-time models. In the case of discrete-time, a model is constructed based on a Markov chain. When analyzing a process in continuous time, verification of the exponential distribution of time characteristics, a condition for the possibility of using a Markov model, is carried out. Two non-parametric consistency tests are proposed as statistical verification tools: χ^2 and Kolmogorov, depending on the size of the research samples. For empirical data containing statistical samples less than 80, the Kolmogorov test is recommended, while otherwise, there is no contraindication to using the χ^2 test [48,49]. For processes satisfying the condition of the exponential distribution, Markov models are used, while otherwise, a semi-Markov model is an appropriate solution. The calculation of the values of operating indicators is carried out on the basis of the ergodic probabilities of the corresponding model.

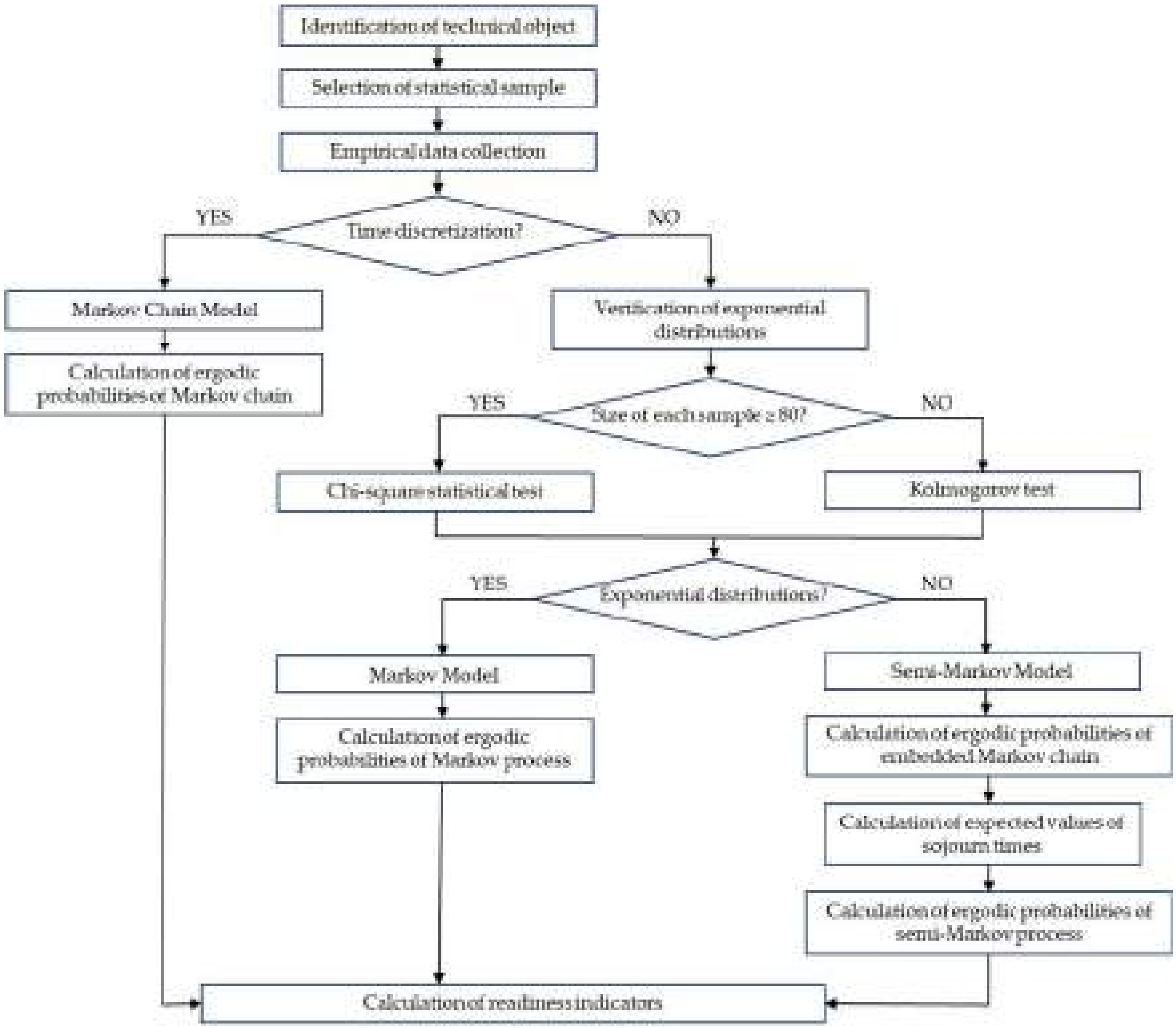

Figure 1. Flowchart of stochastic modeling.

2.3. Functional Readiness, Technical Efficiency and Technical Suitability

Functional readiness is usually understood as the ability of a technical system or object to undertake and perform tasks consistent with its intended use in the required time [50,51]. The availability index Kr reflects the quantitative characteristic of functional availability, which for the Markov model is expressed as the sum of the probabilities of ergodic operational states $k \in S_r$, in which the object can start the task or is in the process of its implementation. The mathematical notation of this relationship is presented by the formula:

$$K_r = \sum_{k \in S_r} \pi_k, \tag{19}$$

where π_k is the ergodic probability of the desired (from the standpoint of readiness) set of operational states $k \in S_r$.

In functional readiness, the vehicle is technically fully operational, i.e., it has an adequate supply of fuel and consumables and is not being serviced. The functional availability indicator shows the share of time that can be allocated to the implementation of tasks by the technical object during its operation period.

The concept of technical efficiency refers to a wider set of operational states than in the case of functional availability. The technically efficient facility has a technical resource to perform the tasks. However, it may require refueling or short-term maintenance before or after use. For the Markov model, the technical efficiency coefficient K_e is the sum of the ergodic probabilities of operational states $l \in S_e$ in which the technical object has a technical service life and does not require periodic maintenance, which is shown in the relationship:

$$K_e = \sum_{l \in S_e} \pi_l, \tag{20}$$

where π_l is the ergodic probability of the desired set of operational states $l \in S_e$.

Technical suitability expresses the condition of a technical object, in which it is not damaged, or there is no need to repair it. The technical suitability condition is an extension of the technical efficiency by the time needed to perform periodic maintenance in order to restore its technical life. The technical suitability index K_s for the Markov model is therefore, the sum of the probabilities of ergodic operational states $m \in S_s$, in which the object is not damaged. This is expressed in the equation:

$$K_s = \sum_{m \in S_s} \pi_m, \tag{21}$$

where π_m is the ergodic probability of the set of operational states $m \in S_s$.

There is the following relationship between the sets defining the states of functional readiness, technical efficiency and technical suitability:

$$S_r \subset S_e \subset S_s. \tag{22}$$

3. Object of Analysis

3.1. Case Study

The case study of the conducted research is a trial of Honker light utility vehicles, constituting a fleet of vehicles of the military unit transport system. The analyzed technical facilities perform tasks related to the transport of people and small loads weighing up to 1000 kg.

Determining the phase space of the studied process requires the reproduction of a detailed phase trajectory for each object in the three-year research period. In the case of the operation process, one should also take into account the conditions resulting from the operation organization system as well as standards and guidelines for the maintenance subsystem of technical facilities. In the case of military transport systems, the implementation of the vehicle operation process depends on both instructions and procedures developed by the operators of military equipment as part of the adopted operational strategy. As a result of the analysis of the process of light utility vehicles carried out by the authors of this study, a nine-state phase space was identified, for which the possible interstate transitions were specified in Table 2.

Table 2. State space of the light utility vehicles operation process.

State	Name	Possible Transition from	Possible Transition to
S_1	Task execution	S_2, S_4, S_6, S_7	S_2, S_5, S_6, S_8
S_2	Refueling	S_1, S_3, S_4	S_1, S_3, S_5
S_3	Parking in garage	S_2, S_5, S_6, S_7	S_2, S_4, S_6
S_4	Pre-task service	S_3	S_1, S_2
S_5	Service after task	S_1, S_2, S_6	S_3, S_9
S_6	Periodic maintenance	S_1, S_3, S_7	S_1, S_3, S_5,
S_7	Repair	S_8, S_9	S_1, S_3, S_6, S_9
S_8	Diagnostics	S_1, S_9	S_7, S_9
S_9	Awaiting repair	S_5, S_7, S_8	S_7, S_8

The distinguished operating states are mutually disjoint subsets, which means that at any time t the object may be in only one of them. For example, the vehicle is in the S_3 garage state while waiting to be used. Before starting the task, it is necessary for the direct user to check the correct operation of the systems and mechanisms that determine the safe use of the vehicle. These activities correspond to state S_4. State S_1 means completion of the transportation task, upon completion of which the object should be serviced after use (S_5). Its purpose is to re-check its operational condition, including the removal of minor defects and cleaning the body. The implementation of the S_2 refueling state may occur before, during, or after the task commencement, depending on the identified needs. State S_6 corresponds to the performance of periodic vehicle maintenance in accordance with the operational strategy as well as instructions and guidelines. S_7, S_8 and S_9 states are undesirable from the standby point of view, as they symbolize damage to the object and the need for repair.

The database was developed on the basis of operational documentation covering a three-year research period. Its fragment is presented in Table 3. In the following rows of the database, the transitions between the various operational states were identified, along with detailed records in the following system: transition number, date, hour and minute. The accuracy of the measurement in the order of 1 min is determined by the occurrence of short-term states and is necessary to verify the correctness of the time balance over the entire research period.

Table 3. Example of a part of database sheet.

No.	Date	Time	S_1	S_2	S_3	S_4	S_5	S_6	S_7	S_8	S_9
267	30.03.2020	08:40:00				1					
268	30.03.2020	08:45:00	1								
269	30.03.2020	13:31:00		1							
270	30.03.2020	13:35:00					1				
271	30.03.2020	13:40:00									1
272	31.03.2020	07:00:00								1	
273	31.03.2020	07:30:00							1		
274	31.03.2020	11:30:00			1						
275	04.04.2020	07:20:00				1					
276	04.04.2020	07:25:00	1								
277	05.04.2020	08:40:00					1				
278	05.04.2020	08:45:00			1						

3.2. Statistical Analysis of Data

For the verification of the empirical distribution with the theoretical distribution, non-parametric consistency tests are commonly used [52–54]. The choice of test depends on the type of distribution being verified, the random variable and the sample size. The most common test χ^2 requires a sample size of at least 80 realizations of a random variable. For a small number of interstate transitions in the operation process, this condition may not be met. In this case, the verification of the assumptions of the Markov process is performed using the Kolmogorov test.

The condition for the exponential distribution of transition times between states was verified with the use of the Kolmogorov conformance test (Table 4). As the H_0 hypothesis, it was assumed that the distribution of T_{ij} times for individual allowed interstate transitions is consistent with the exponential distribution. The alternative hypothesis (H_1) contradicts this assumption. The U_y statistic of the Kolmogorov test has the form (23):

$$U_y = \max_{1 \le i \le y}\left(d_y^-, d_y^+\right), \tag{23}$$

wherein:

$$d_y^- = \max_{1 \le i \le y}\left|F(x_i) - \frac{i-1}{y}\right|, \tag{24}$$

$$d_y^+ = \max_{1 \le i \le y}\left|\frac{i}{y} - F(x_i)\right|, \tag{25}$$

where $F(x_i)$ is the cumulative value of the theoretical distribution according to the H_0 hypothesis, and y is the sample size.

Table 4. Results of Kolmogorov test.

T_{ij}	y	U_y Statistics	Critical Range	Hypothesis
T_{12}	798	0.2585	<0.0479, 1>	H_1
T_{15}	3340	0.2019	<0.0234, 1>	H_1
T_{16}	32	0.1834	<0.2343, 1>	H_0
T_{18}	32	0.3587	<0.2343, 1>	H_1
T_{21}	396	0.4773	<0.0678, 1>	H_1
T_{23}	366	0.4970	<0.0705, 1>	H_1
T_{25}	695	0.4731	<0.0513, 1>	H_1
T_{32}	365	0.1428	<0.0706, 1>	H_1
T_{34}	4063	0.2867	<0.0213, 1>	H_1
T_{36}	76	0.2907	<0.1534, 1>	H_1
T_{41}	3769	0.6316	<0.0221, 1>	H_1
T_{42}	294	0.6151	<0.0786, 1>	H_1
T_{53}	3988	0.4533	<0.0215, 1>	H_1
T_{59}	70	0.5071	<0.1598, 1>	H_1
T_{61}	11	0.4395	<0.3914, 1>	H_1
T_{63}	84	0.2843	<0.1461, 1>	H_1
T_{65}	23	0.4757	<0.2750, 1>	H_1
T_{71}	27	0.2320	<0.2544, 1>	H_0
T_{73}	67	0.3295	<0.1632, 1>	H_1
T_{76}	10	0.4754	<0.4094, 1>	H_1
T_{79}	44	0.4082	<0.2006, 1>	H_1
T_{87}	63	0.3348	<0.1683, 1>	H_1
T_{89}	39	0.2445	<0.2128, 1>	H_1
T_{97}	85	0.2186	<0.1452, 1>	H_1
T_{98}	70	0.5196	<0.1598, 1>	H_1

For the U_y statistic values within the range of critical values <$D(y;\alpha)$, 1> for the significance level α, the H_0 hypothesis is rejected and H_1 is accepted. Otherwise, there is no reason to reject the H_0 hypothesis. For the significance level α = 0.05, the value $D(y;\alpha)$ can be approximated using the formula:

$$D(0.05; y) = \frac{1.358}{\sqrt{y} + 0.12 + \frac{0.11}{\sqrt{y}}}. \tag{26}$$

At the adopted significance level of α = 0.05, only two time characteristics, T_{16} and T_{71}, achieved the values of the Kolmogorov test statistics, which are not included in the critical intervals. This means there are no grounds to reject the null hypothesis assuming the exponential distribution of the times of stay in individual states. Thus, for the remaining time characteristics, the null hypothesis was rejected and an alternative was adopted. The results of the statistical test for all variables are presented in Table 4. Figure 2 presents the frequency graphs for two exemplary times T_{16} and T_{34} and the course of the exponential distribution with the parameter estimated on the basis of the reciprocal of the mean values from both statistical samples. The number of histogram intervals was determined using the square root method.

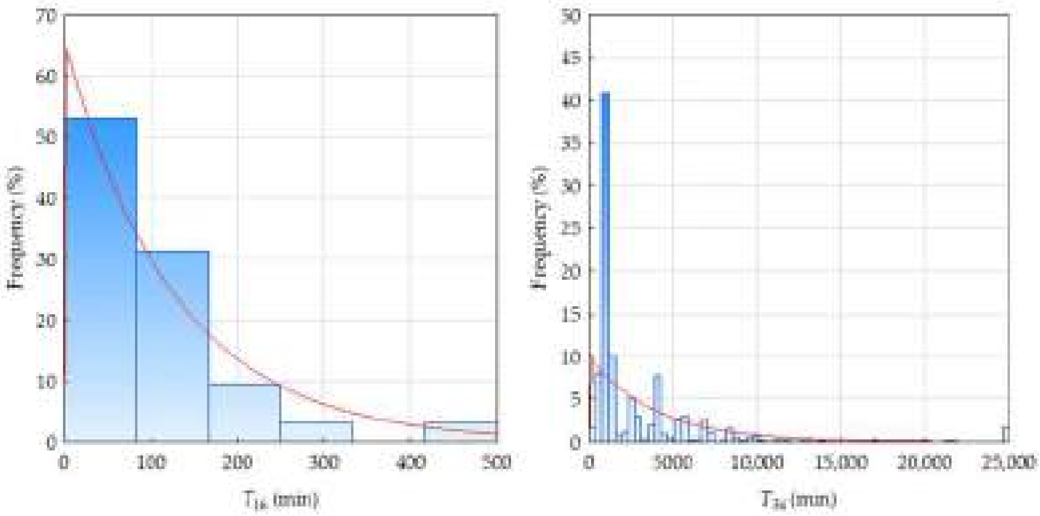

Figure 2. Fitting exponential distributions to sojourn times.

The exploitation process does not fulfill the condition of exponential distributions and, therefore, cannot be considered a Markov process in continuous time. In this case, semi-Markov processes should be used for modeling.

4. Results and Discussions

4.1. Semi-Markov Model (SMM)

The embedded Markov chain in the semi-Markov process, in accordance with the adopted assumptions, does not allow for the possibility of returns (transition from the S_i state to the S_i state). This assumption adopts that every change of the process state is recorded, while its absence means that the object is in the S_i state before transitioning to the next S_j state for a period of time equal to T_{ij} [26,28–30]. The matrix (27) shows the empirical numbers of transitions between particular exploitation states as a result of observation of the process. On the other hand, matrix (28) represents the probabilities of transitions between states estimated on the basis of the matrix of the number of transitions.

$$\boldsymbol{N} = \begin{bmatrix} 0 & 798 & 0 & 0 & 3340 & 32 & 0 & 32 & 0 \\ 396 & 0 & 366 & 0 & 695 & 0 & 0 & 0 & 0 \\ 0 & 365 & 0 & 4063 & 0 & 76 & 0 & 0 & 0 \\ 3769 & 294 & 0 & 0 & 0 & 0 & 0 & 0 & 0 \\ 0 & 0 & 3988 & 0 & 0 & 0 & 0 & 0 & 70 \\ 11 & 0 & 84 & 0 & 23 & 0 & 0 & 0 & 0 \\ 27 & 0 & 67 & 0 & 0 & 10 & 0 & 0 & 44 \\ 0 & 0 & 0 & 0 & 0 & 0 & 63 & 0 & 39 \\ 0 & 0 & 0 & 0 & 0 & 0 & 85 & 70 & 0 \end{bmatrix}, \tag{27}$$

$$P = \begin{bmatrix} 0 & 0.189910 & 0 & 0 & 0.794860 & 0.007615 & 0 & 0.007615 & 0 \\ 0.271791 & 0 & 0.251201 & 0 & 0.477008 & 0 & 0 & 0 & 0 \\ 0 & 0.081039 & 0 & 0.902087 & 0 & 0.016874 & 0 & 0 & 0 \\ 0.927640 & 0.072360 & 0 & 0 & 0 & 0 & 0 & 0 & 0 \\ 0 & 0 & 0.982750 & 0 & 0 & 0 & 0 & 0 & 0.017250 \\ 0.093220 & 0 & 0.711864 & 0 & 0.194915 & 0 & 0 & 0 & 0 \\ 0.182432 & 0 & 0.452703 & 0 & 0 & 0.067568 & 0 & 0 & 0.297297 \\ 0 & 0 & 0 & 0 & 0 & 0 & 0.617647 & 0 & 0.382353 \\ 0 & 0 & 0 & 0 & 0 & 0 & 0.548387 & 0.451613 & 0 \end{bmatrix}. \quad (28)$$

Table 5 summarizes the values of the standard error for the conditional probabilities (28) estimated on the basis of the matrix of the number of interstate transitions (27). According to Formula (6), with the increase in the number of transitions from the S_i state, the standard error $SE(p_{ij})$ decreases. For this reason, the values of the standard error are higher for operational states in which the technical object is relatively rare. Nevertheless, for all conditional probabilities, the $SE(p_{ij})$ did not exceed the value of 0.05 [55,56]. The result at this level is considered acceptable.

Table 5. Standard errors of probabilities estimation.

$SE(p_{ij})$	S_1	S_2	S_3	S_4	S_5	S_6	S_7	S_8	S_9
S_1	0	0.0061	0	0	0.0062	0.0013	0	0.0013	0
S_2	0.0117	0	0.0114	0	0.0131	0	0	0	0
S_3	0	0.0041	0	0.0044	0	0.0019	0	0	0
S_4	0.0041	0.0041	0	0	0	0	0	0	0
S_5	0	0	0.0020	0	0	0	0	0	0.0020
S_6	0.0268	0	0.0417	0	0.0365	0	0	0	0
S_7	0.0317	0	0.0409	0	0	0.0206	0	0	0.0376
S_8	0	0	0	0	0	0	0.0481	0	0.0481
S_9	0	0	0	0	0	0	0.0400	0.0400	0

Figure 3 presents a graph illustrating possible transitions between states during the implementation of the operation process. According to the assumptions made for the embedded Markov chain, the fact that the object remains in the same state is not treated as a $S_i \rightarrow S_i$ transition. For this reason, the SMM model graph does not have connections coming from the S_i state and going directly to the S_i state. This means a lack of return to the same state, which is commonly used in modeling the operation processes.

Assuming that at $t = 0$, the vehicle is technically efficient and awaits the appearance of the task, it is possible to determine the instantaneous probabilities of the embedded Markov chain. This assumption reflects the initiation of the operation process for a vehicle included in the transport system. The instantaneous probabilities are the matrix product of the initial distribution matrix $\boldsymbol{p_0}$ and the n-th power of the conditional probability matrix $\boldsymbol{P}$, where n corresponds to the number of transitions between states. The development of the dependence of the instantaneous probabilities on the number of interstate transitions allows us to determine the period after which their values stabilize at a certain level and the stochastic process reaches the equilibrium state.

Figures 4 and 5 show changes in the value of the instantaneous probabilities of the embedded Markov chain in the semi-Markov process. In the range from $t = 0$ to $t = 30$, there are fluctuations with a large amplitude of changes in the values, which decrease with time and after overcoming about 50 transitions, the probability values remain constant.

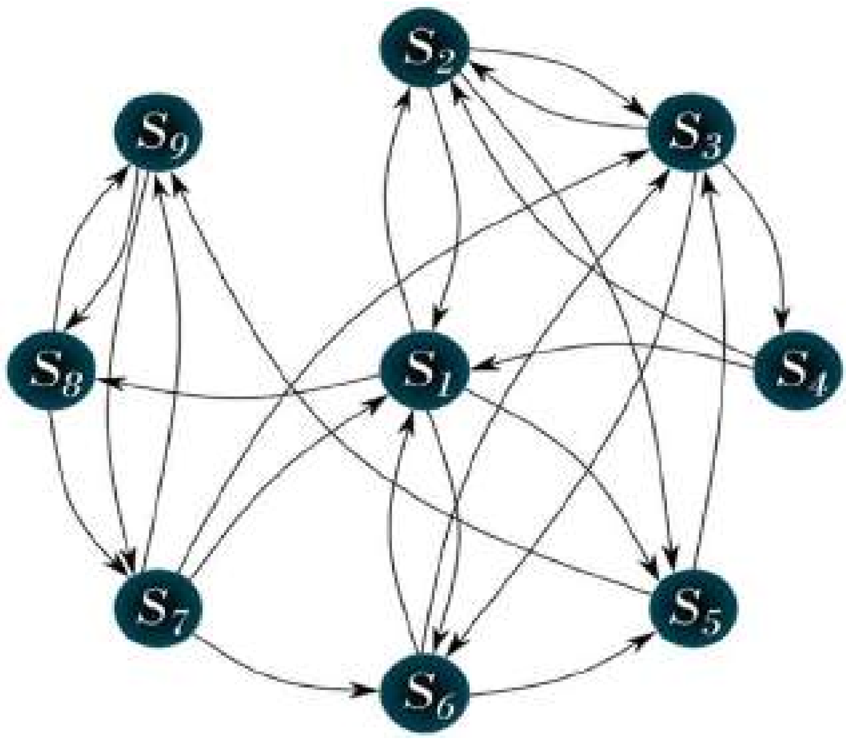

Figure 3. Transition diagram for nine-state semi-Markov model of light utility vehicle operations process.

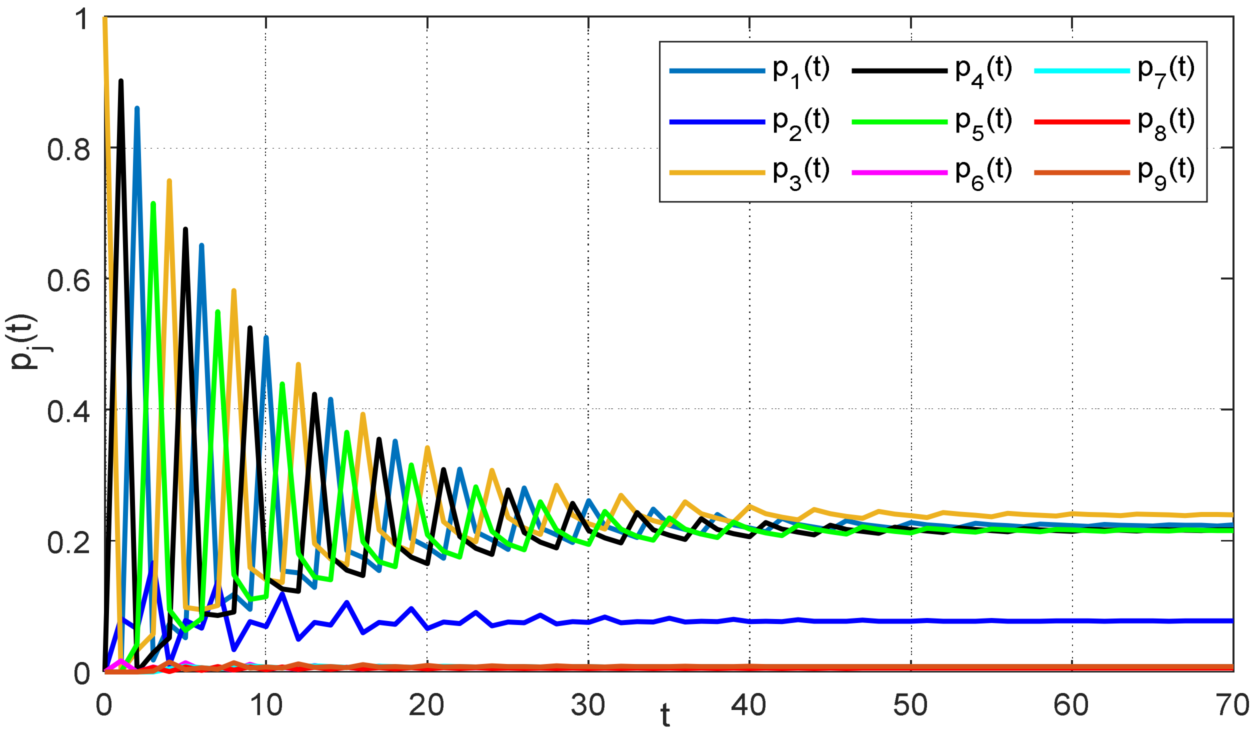

Figure 4. The course of changes in the probabilities of the states of the embedded Markov chain for the initial vector p_0 = [0,0,1,0,0,0,0,0,0].

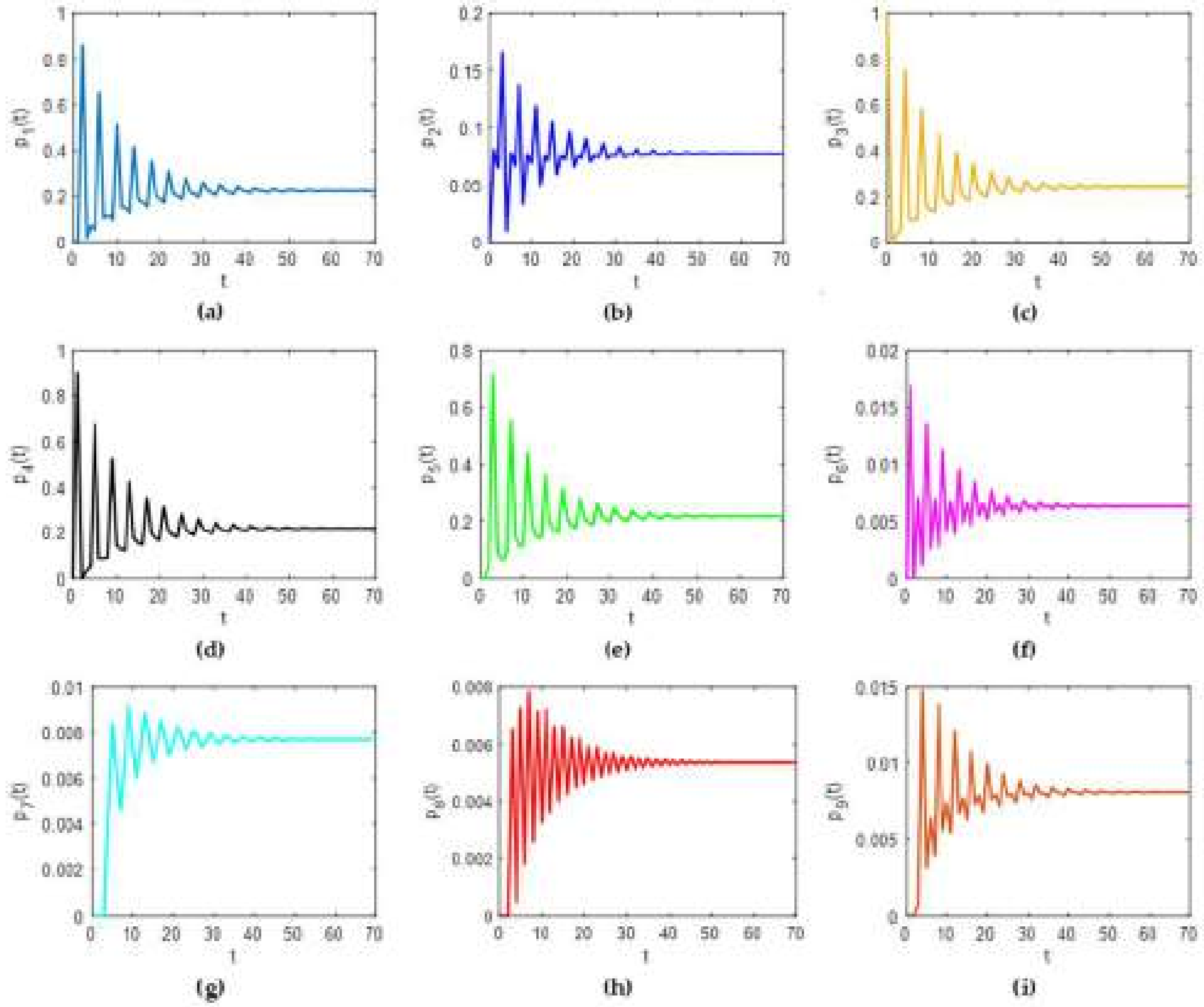

Figure 5. The course of changes in the probabilities of S_1–S_9 states for the initial vector $\boldsymbol{p_0}$ = [0,0,1,0,0,0,0,0,0]. (**a**) $p_1(t)$; (**b**) $p_2(t)$; (**c**) $p_3(t)$; (**d**) $p_4(t)$; (**e**) $p_5(t)$; (**f**) $p_6(t)$; (**g**) $p_7(t)$; (**h**) $p_8(t)$; (**i**) $p_9(t)$.

4.2. Ergodic Probabilities of SMM

The ergodic probabilities of the semi-Markov process are determined on the basis of the probabilities of the embedded Markov chain and the values of the expected time in individual states of the process. For the embedded Markov chain, the ergodic probabilities are computed using the matrix equation:

$$(\boldsymbol{P}^T - \boldsymbol{I}) \cdot \boldsymbol{P_j} = \begin{bmatrix} -1 & p_{21} & 0 & p_{41} & 0 & p_{61} & p_{71} & 0 & 0 \\ p_{12} & -1 & p_{32} & p_{42} & 0 & 0 & 0 & 0 & 0 \\ 0 & p_{23} & -1 & 0 & p_{53} & p_{63} & p_{73} & 0 & 0 \\ 0 & 0 & p_{34} & -1 & 0 & 0 & 0 & 0 & 0 \\ p_{15} & p_{25} & 0 & 0 & -1 & p_{65} & 0 & 0 & 0 \\ p_{16} & 0 & p_{36} & 0 & 0 & -1 & p_{76} & 0 & 0 \\ 0 & 0 & 0 & 0 & 0 & 0 & -1 & p_{87} & p_{97} \\ p_{18} & 0 & 0 & 0 & 0 & 0 & 0 & -1 & p_{98} \\ 0 & 0 & 0 & 0 & p_{59} & 0 & p_{79} & p_{89} & -1 \end{bmatrix} \cdot \begin{bmatrix} p_1 \\ p_2 \\ p_3 \\ p_4 \\ p_5 \\ p_6 \\ p_7 \\ p_8 \\ p_9 \end{bmatrix} = \begin{bmatrix} 0 \\ 0 \\ 0 \\ 0 \\ 0 \\ 0 \\ 0 \\ 0 \\ 0 \end{bmatrix}, \quad (29)$$

which can be written as a system of Equation (30) together with the condition (31) of system normalization:

$$\begin{cases} -p_1 + 0.271791p_2 + 0.927640p_4 + 0.093220p_6 + 0.182432p_7 = 0 \\ 0.189910p_1 - p_2 + 0.081039p_3 + 0.072360p_4 = 0 \\ 0.251201p_2 - p_3 + 0.982750p_5 + 0.711864p_6 + 0.452703p_7 = 0 \\ 0.902087p_3 - p_4 = 0 \\ 0.794860p_1 + 0.477008p_2 - p_5 + 0.194915p_6 = 0 \\ 0.007615p_1 + 0.016874p_3 - p_6 + 0.067568p_7 = 0 \\ -p_7 + 0.617647p_8 + 0.548387p_9 = 0 \\ 0.007615p_1 - p_8 + 0.451613p_9 = 0 \\ 0.017250p_5 + 0.297297p_7 + 0.382353p_8 - p_9 = 0 \end{cases}, \quad (30)$$

$$\sum_{j=1}^{9} p_j = 1. \quad (31)$$

After solving the system of equations, the values of ergodic probabilities p_j of the inserted Markov chain were obtained. The expected $E(T_j)$ times of staying in individual operating states were determined as average values based on empirical data. The values of p_j and $E(T_j)$ were used to calculate the values of ergodic probabilities in the semi-Markov model. The results of the conducted analyses are summarized in Table 6.

Table 6. Ergodic probabilities of states in embedded Markov chain and SMM.

State	S_1	S_2	S_3	S_4	S_5	S_6	S_7	S_8	S_9
p_j	0.223537	0.077505	0.239575	0.216117	0.215872	0.006267	0.007722	0.005343	0.008063
$E(T_j)$ (min)	717.52	4.60	3956.58	5.00	8.13	271.95	174.63	36.11	13,240.50
π_j	0.131311	0.000292	0.776024	0.000885	0.001436	0.001395	0.001104	0.000158	0.087396
π_j (%)	13.1311	0.0292	77.6024	0.0885	0.1436	0.1395	0.1104	0.0158	8.7396

The garage state S_3 had the highest value of the ergodic probability of over 77%. On the basis of the calculated values of probabilities, it can be concluded that the trucks and passenger cars stay together in other states for approximately 13% of the time during the entire three-year research period. The S_9 state also obtained a significant level of ergodic probability, which indicates that the vehicles remain in a state of waiting for repair for almost 9% of their operational time. The remaining operational states obtained probability values below 1% and do not have a significant impact on the availability rates.

4.3. Calculations of Indicators in SMM

In the nine-state exploitation model, state subsets were distinguished corresponding to the functional readiness S_r, technical efficiency S_e and technical suitability S_s. The mathematical notation is presented by the Formulas (32)–(34):

$$S_r = \{S_1, S_3\}, \quad (32)$$

$$S_e = \{S_1, S_2, S_3, S_4, S_5\}, \quad (33)$$

$$S_s = \{S_1, S_2, S_3, S_4, S_5, S_6\}. \quad (34)$$

Functional readiness corresponds to the vehicle being in the task (S_1) or garage (S_3) state. Technical efficiency extends the set of these states with fuel refilling (S_2) and the implementation of maintenance before starting the task (S_4) and after its completion (S_5). On the other hand, technical suitability also takes into account the implementation of periodic maintenance (S_6), the purpose of which is to restore the technical service life. The graphical diagram of the division of the operating conditions set into individual subsets is shown in Figure 6.

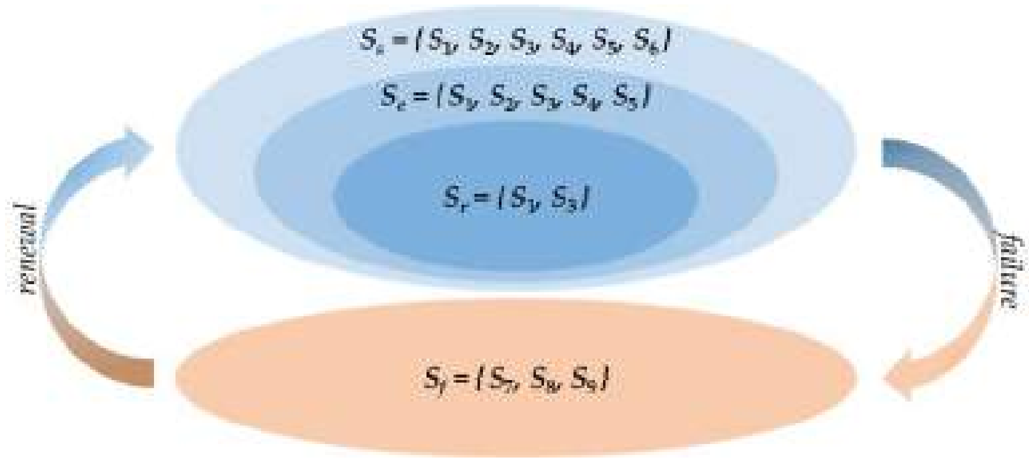

Figure 6. Subsets of light utility vehicle exploitation states.

For such defined subsets, the values of functional availability, technical efficiency and technical suitability indicators were calculated. The results are presented in Table 7. The values of all three indicators are similar, which means a small share of the time of current and periodic maintenance and refueling in the entire test period.

Table 7. Values of K_r, K_e and K_s indicators in SMM.

Indicator	Value
Functional readiness K_r	0.907334
Technical efficiency K_e	0.909947
Technical suitability K_s	0.911343

The high probability value of the S_9 ergodic state has the greatest impact on the reduction of the indicators of functional availability, technical efficiency and technical suitability of vehicles. This state corresponds to the situation when the vehicle has suffered a breakdown, is out of order and requires repair. Due to the lack of technical possibilities, it is not in the repair state (S_7) and is not in the diagnosis phase (S_8). The main reasons for such a situation are logistic delays related to the limited availability of spare parts and the lack of qualified technical personnel within the specified time.

4.4. Sensitivity Analysis of SMM

The calculated ergodic probability π_9 of the S_9 state has the strongest impact on the values of the K_r, K_e and K_s indicators. Due to this fact, the sensitivity analysis of the SMM model was carried out in order to investigate the impact of the presence of objects in the S_9 state on the ergodic probabilities and technical readiness rates. The parameter against which the variability analysis was performed is the expected value of the duration of the S_9 state. For the change of this parameter, expressed as a percentage and amounting to $\Delta E(T_9)$, the values of the ergodic probabilities of the semi-Markov process can be determined using the relationship:

$$\pi_j = \frac{p_j \cdot E(T_j)}{\sum_{i=1}^{8} p_i \cdot E(T_i) + p_9 \cdot E(T_9) \cdot (1 - \Delta E(T_9))} \text{ for } j = \{1, 2, 3, \ldots, 8\}, \quad (35)$$

$$\pi_9 = \frac{p_9 \cdot E(T_9) \cdot (1 - \Delta E(T_9))}{\sum_{i=1}^{8} p_i \cdot E(T_i) + p_9 \cdot E(T_9) \cdot (1 - \Delta E(T_9))}. \quad (36)$$

The undoubted advantage of the SMM model is the ability to perform a sensitivity analysis for a wide range of changes in the $E(T_9)$ parameter without the need to solve many matrix equations. Table 8 shows the results of the analysis for selected $\Delta E(T_9)$ values.

Figure 7 presents a graph of changes in ergodic probabilities for continuous changes in the value of $\Delta E(T_9)$.

Table 8. Ergodic probabilities obtained in sensitivity analysis of SMM.

$\Delta E(T_9)$ (%)	π_1	π_2	π_3	π_4	π_5	π_6	π_7	π_8	π_9
0	0.131311	0.000292	0.776024	0.000885	0.001436	0.001395	0.001104	0.000158	0.087396
10	0.132468	0.000294	0.782865	0.000893	0.001449	0.001407	0.001114	0.000159	0.079350
20	0.133646	0.000297	0.789828	0.000901	0.001462	0.001420	0.001124	0.000161	0.071162
30	0.134846	0.000300	0.796916	0.000909	0.001475	0.001433	0.001134	0.000162	0.062826
40	0.136067	0.000302	0.804133	0.000917	0.001488	0.001446	0.001144	0.000164	0.054339
50	0.137310	0.000305	0.811481	0.000926	0.001502	0.001459	0.001154	0.000165	0.045698
60	0.138577	0.000308	0.818965	0.000934	0.001515	0.001472	0.001165	0.000167	0.036897
70	0.139867	0.000311	0.826588	0.000943	0.001530	0.001486	0.001176	0.000168	0.027932
80	0.141181	0.000314	0.834354	0.000952	0.001544	0.001500	0.001187	0.000170	0.018799
90	0.142520	0.000317	0.842268	0.000961	0.001559	0.001514	0.001198	0.000171	0.009492

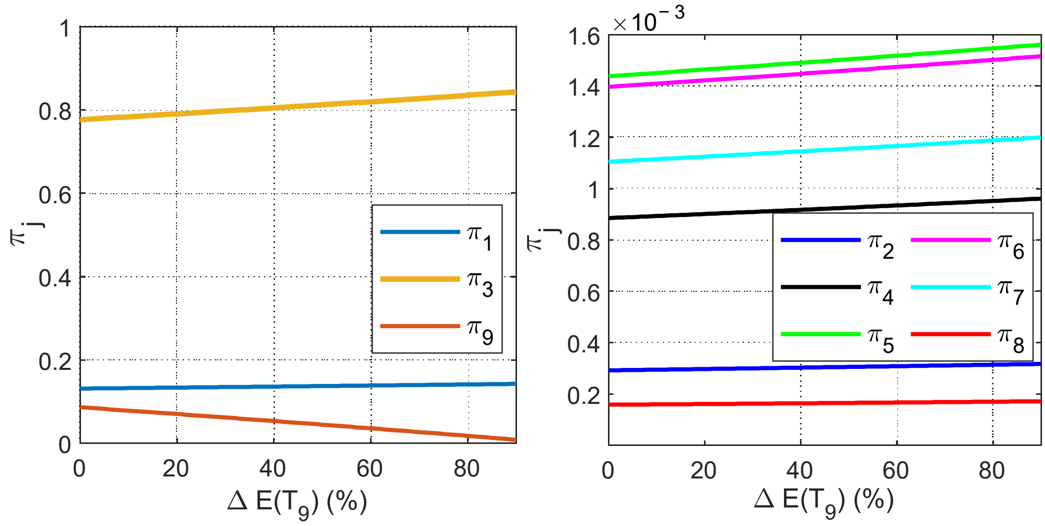

Figure 7. Ergodic probabilities of SMM obtained in simulation by reduction of the expected value of sojourn time $E(T_9)$.

On the basis of the determined ergodic probabilities, the possibilities of improving the values of the readiness ratios were carried out at the assumed levels of reduction of the time spent in the state of incapacity and waiting for repair. The results are presented in Table 9 and Figure 8.

Table 9. Indicators values obtained in sensitivity analysis of SMM.

$\Delta E(T_9)$ (%)	K_r	ΔK_r	K_e	ΔK_e	K_s	ΔK_s
0	0.907334	0.000000	0.909947	0.000000	0.911343	0.000000
10	0.915334	0.008000	0.917970	0.008023	0.919377	0.008035
20	0.923476	0.016142	0.926135	0.016188	0.927555	0.016213
30	0.931764	0.024430	0.934447	0.024500	0.935880	0.024538
40	0.940202	0.032868	0.942910	0.032962	0.944356	0.033013
50	0.948794	0.041460	0.951527	0.041580	0.952986	0.041643
60	0.957545	0.050211	0.960303	0.050356	0.961775	0.050433
70	0.966459	0.059125	0.969243	0.059295	0.970729	0.059386
80	0.975541	0.068206	0.978350	0.068403	0.979850	0.068508
90	0.984794	0.077460	0.987630	0.077683	0.989145	0.077802

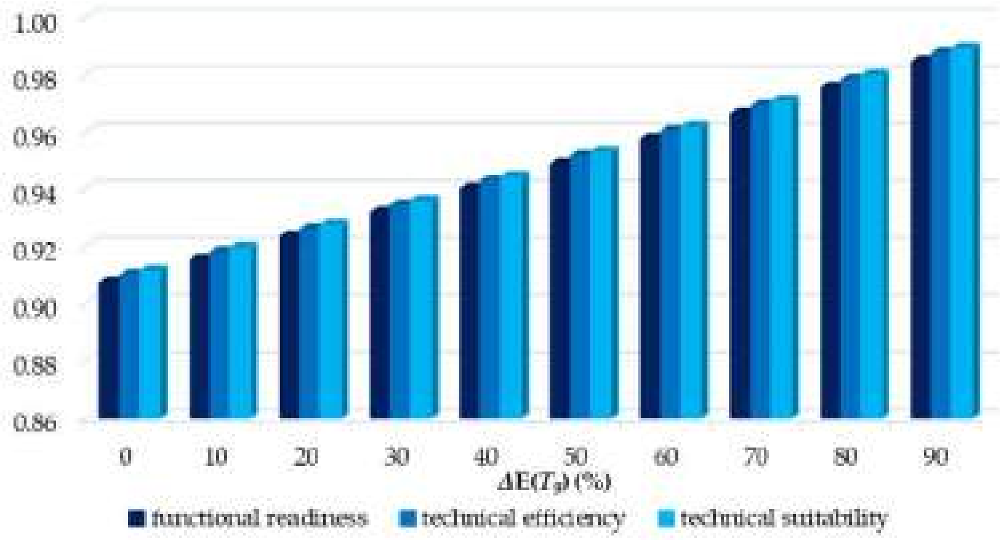

Figure 8. Readiness indicators values obtained in sensitivity analysis of SMM.

Reducing the waiting time for repairs by 50% would result in an increase in the values of the K_r, K_e and K_s indicators to the level of about 0.95, which at the same time means their improvement by over 0.04. The sensitivity analysis of the SMM model was carried out with regard to the impact of changes in the expected value of the time of staying in the S_9 state.

4.5. Markov Model (MM)

Markov models, assuming exponential distributions of time characteristics, often use stochastic models to describe the operation processes of machines, devices and technical systems. For small deviations of empirical distributions of interstate times from the theoretical assumptions of the Markov theory, the results obtained for Markov and semi-Markov models may be similar or even negligibly small.

For the analyzed sample of means of transport, the non-parametric Kolmogorov test showed grounds for rejecting the null hypothesis about exponential distributions. However, the authors of the publication conducted an analysis of the applicability of the Markov model as a simplification of the generalized SMM presented in Sections 4.1–4.4. The basic characteristic of the Markov model is the matrix of interstate transition intensity $\mathbf{\Lambda}$. In the case study under consideration, the value of the $\mathbf{\Lambda}$ matrix presented in the matrix, which were estimated on the basis of the mean values of the transition times between the states according to the Equations (11) and (12).

$$\mathbf{\Lambda} = \begin{bmatrix} -0.012136 & 0.000890 & 0 & 0 & 0.001593 & 0.007880 & 0 & 0.001773 & 0 \\ 0.214402 & -0.657021 & 0.229036 & 0 & 0.213583 & 0 & 0 & 0 & 0 \\ 0 & 0.000241 & -0.000650 & 0.000257 & 0 & 0.000152 & 0 & 0 & 0 \\ 0.199841 & 0.200000 & 0 & -0.399841 & 0 & 0 & 0 & 0 & 0 \\ 0 & 0 & 0.122711 & 0 & -0.270079 & 0 & 0 & 0 & 0.147368 \\ 0.003216 & 0 & 0.003819 & 0 & 0.003446 & -0.010481 & 0 & 0 & 0 \\ 0.007004 & 0 & 0.005194 & 0 & 0 & 0.010753 & -0.028343 & 0 & 0.005392 \\ 0 & 0 & 0 & 0 & 0 & 0 & 0.045652 & -0.062586 & 0.016934 \\ 0 & 0 & 0 & 0 & 0 & 0 & 0.000068 & 0.000088 & -0.000156 \end{bmatrix}. \quad (37)$$

Ergodic probabilities of the Markov process for the entire set of operational states are calculated by solving the matrix Equation (38) together with the system normalization condition (39).

$$\boldsymbol{\Pi}^T \cdot \boldsymbol{\Lambda} = \begin{bmatrix} \pi_1 \\ \pi_2 \\ \pi_3 \\ \pi_4 \\ \pi_5 \\ \pi_6 \\ \pi_7 \\ \pi_8 \\ \pi_9 \end{bmatrix}^T \cdot \begin{bmatrix} -\lambda_{11} & \lambda_{21} & 0 & \lambda_{41} & 0 & \lambda_{61} & \lambda_{71} & 0 & 0 \\ \lambda_{12} & -\lambda_{22} & \lambda_{32} & \lambda_{42} & 0 & 0 & 0 & 0 & 0 \\ 0 & \lambda_{23} & -\lambda_{33} & 0 & \lambda_{53} & \lambda_{63} & \lambda_{73} & 0 & 0 \\ 0 & 0 & \lambda_{34} & -\lambda_{44} & 0 & 0 & 0 & 0 & 0 \\ \lambda_{15} & \lambda_{25} & 0 & 0 & -\lambda_{55} & \lambda_{65} & 0 & 0 & 0 \\ \lambda_{16} & 0 & \lambda_{36} & 0 & 0 & -\lambda_{66} & \lambda_{76} & 0 & 0 \\ 0 & 0 & 0 & 0 & 0 & 0 & -\lambda_{77} & \lambda_{87} & \lambda_{97} \\ \lambda_{18} & 0 & 0 & 0 & 0 & 0 & 0 & -\lambda_{88} & \lambda_{98} \\ 0 & 0 & 0 & 0 & \lambda_{59} & 0 & \lambda_{79} & \lambda_{89} & -\lambda_{99} \end{bmatrix} = \begin{bmatrix} 0 \\ 0 \\ 0 \\ 0 \\ 0 \\ 0 \\ 0 \\ 0 \\ 0 \end{bmatrix}^T, \tag{38}$$

$$\sum_{j=1}^{9} \pi_j = 1. \tag{39}$$

Mathematica and MS Excel software were used for the presented calculations. The results for MM are summarized in Table 10 and Figure 9, comparing them with the values of ergodic probabilities obtained for SMM. Percentage differences between the models reached significant values, with the most similar probabilities occurring for the S_2 state and differing by over 41.0%. The greatest discrepancies in the results occurred for the S_6 state, for which the ergodic probability obtained in MM was as much as 1153.69% higher than in SMM. In addition, the S_6, S_7, S_8 and S_9 states, which are a subset of the technical inoperability and failure states, achieved positive differences. The use of MM to evaluate the operation process would result in a significant reduction of the values of the K_r, $K_{e,}$ and K_s indices, inconsistent with the actual state.

Table 10. Comparison of results obtained by MM and SMM.

	π_1	π_2	π_3	π_4	π_5	π_6	π_7	π_8	π_9
SMM	0.131311	0.000292	0.776024	0.000885	0.001436	0.001395	0.001104	0.000158	0.087396
MM	0.012784	0.000172	0.275931	0.000177	0.000435	0.017489	0.003780	0.001325	0.687906
difference	−0.118527	−0.000120	−0.500093	−0.000708	−0.001001	0.016094	0.002676	0.001167	0.600510
difference in %	−90.26	−41.10	−64.44	−80.00	−69.71	1153.69	242.39	738.61	687.11

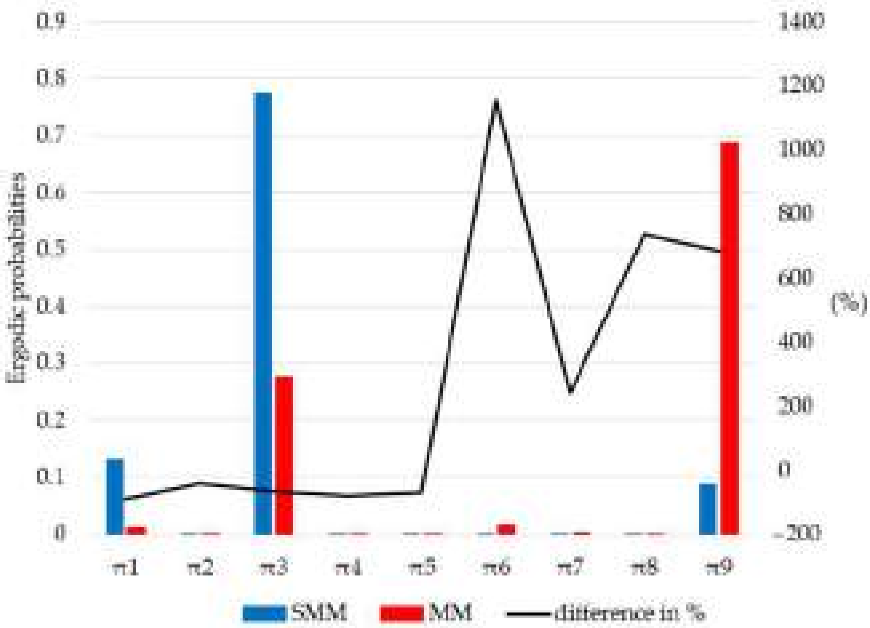

Figure 9. Differences of ergodic probabilities in Markov and semi-Markov models.

Compared to SMM, the Markov model achieved a mean absolute percentage error (MAPE) of 351.92%. Therefore, the hypothesis about the possibility of using the Markov process to describe state changes by the analyzed technical objects in the considered nine-element set of operational states should be unambiguously rejected.

5. Conclusions

The theory of Markov processes was used to model the operation of light utility vehicles. The paper presents a semi-Markov model that allows for the assessment the technical readiness of means of transport operating in a real system. On the basis of the systems of Chapman–Kolmogorov equations and the values of the expected times of stay in operating states, the values of the ergodic probabilities of the process were determined. The main reason for the reduction of functional availability, technical efficiency and technical suitability indicators was the high probability value of the S_9 state (Awaiting repair). This indicates the occurrence of significant delays in the implementation of repairs of damaged vehicles. Therefore, in eliminating the reasons for the presence of technical objects in the S_9 state, the operating system does not have sufficient technical resources to carry out repairs without unnecessary time delay. Repair delays are mainly caused by the unavailability of spare parts and a shortage of qualified technical personnel. In order to maximize the technical readiness of vehicles, it is necessary to focus on improving the organization of the spare parts delivery system, which will significantly reduce the time spent by technical facilities in the S_9 state.

For the current state of the operation system, the functional availability ratio K_r has reached the value of 0.907334, which should be interpreted as follows: for more than 90% of the duration of the operation process, vehicles in good technical condition await the appearance of a task or are in the process of its implementation. A slight difference between the technical efficiency index K_e and the functional readiness index K_r indicates that the process of refueling and servicing is carried out efficiently. The aforementioned processes constitute a set of activities preparing a technically efficient vehicle to perform the task, as well as control and check after its completion. On the other hand, the technical suitability index K_s amounting to 0.911343 means that for over 91% of the duration of the operation process, the vehicles are fit for use. Its high value indicates a well-thought-out and proper implementation of the exploitation strategy. The small value of the ergodic probability for the S_6 state resulted in a slight difference between the technical efficiency index K_e and the technical suitability index K_s. The above-mentioned results show that the capabilities of the technical subsystem, which carries out the periodic maintenance process, are adjusted to the requirements of the plan-preventive strategy used.

The ergodic probability π_2 of 0.000292 and the expected residence time in the S_2 state of 4.60 (min) indicate an efficiently implemented refueling process. For the current level of intensity of use of vehicles, in which over 13.0% of the operation time is during the implementation of transport tasks, the technical system provides sufficient resources of diesel oil and appropriate distribution equipment.

Despite the assumed high level of readiness, efficiency and suitability indicators of the tested military vehicles, an attempt was made to optimize the process by determining the impact of a potential reduction in the duration of the S_9 state, equipped with logistic delays occurring in the operation system. An analysis of the optimization possibilities was carried out on the basis of changes in the expected time of stay in the S_9 state based on analytical relationships, which enabled the analysis based on a continuous reduction of changes in $E(T_9)$ in the percentage range of 0.0–90.0%. As a result, the reduction of the expected time of the vehicle's stay in the S_9 state by 50.0% resulted in the increase of all indicators by over 0.041, and the reduction by 90% increased the values of the indicators by over 0.077.

The attempt to use the Markov process, despite not meeting the condition of exponential time characteristics, showed significant discrepancies between MM and SMM. The high degree of mismatch between the Markov model and the actual process is evidenced by the value of the MAPE error amounting to 351.92%. Therefore, it is inappropriate to use

MM to describe the nine-state process of operation of heavy goods vehicles operating in the military transport system. The performed non-parametric Kolmogorov test resulted in the rejection of the hypothesis concerning the compatibility of empirical distributions of the duration of individual states with the theoretical exponential distribution.

The proposed method allows a detailed analysis of vehicle operation as a stochastic process with a multi-state phase space. The unquestionable advantage of the nine-state semi-Markov model is the possibility of evaluating the operation process using indicators of functional readiness, efficiency, and technical efficiency, calculated based on the basis of ergodic probabilities of the process. Additionally, the model sensitivity analysis makes it possible to determine the impact of reducing the values of expected vehicle dwell times in each state on the efficiency of the operation process. However, a disadvantage of the proposed method is the inability to predict the values of indicators for the increased or decreased intensity of vehicle use expressed by means of average daily mileage. This is due to the condition of determining the characteristics of all states in the same time domain.

The proposed methodology for creating stochastic exploitation models can be applied to a wide range of facilities and technical devices. The developed model can be used to analyze and evaluate the operation process of other vehicles operating in technical systems with an analogous or similar operation strategy.

Author Contributions: Conceptualization, M.O.; methodology, M.O. and J.Z.; software, M.O. and J.Z.; validation, M.O.; formal analysis, M.O.; investigation, M.O.; resources, M.O.; data curation, M.O. and J.Z.; writing—original draft preparation, M.O.; writing—review and editing, M.O., J.Z. and J.M.; visualization, M.O.; supervision, J.Z. and J.M.; project administration, J.Z. and J.M.; funding acquisition, J.M. All authors have read and agreed to the published version of the manuscript.

Funding: This research was funded by the Military University of Technology, grant number UGB 22-771.

Institutional Review Board Statement: Not applicable.

Informed Consent Statement: Not applicable.

Data Availability Statement: Not applicable.

Conflicts of Interest: The authors declare no conflict of interest.

References

1. Oszczypała, M.; Ziółkowski, J.; Małachowski, J. Reliability Analysis of Military Vehicles Based on Censored Failures Data. *Appl. Sci.* **2022**, *12*, 2622. [CrossRef]
2. Betkier, I.; Mitkow, S.; Kijek, M. Analysis of Vehicle Stability Loss Due to Strong Crosswind Gusts Using Web Services in the Route Planning Process. *Arch. Transp.* **2019**, *52*, 47–56. [CrossRef]
3. Betkier, I.; Zak, J.K.; Mitkow, S. Parking Lots Assignment Algorithm for Vehicles Requiring Specific Parking Conditions in Vehicle Routing Problem. *IEEE Access* **2021**, *9*, 161469–161487. [CrossRef]
4. Wróblewski, P.; Lewicki, W. A Method of Analyzing the Residual Values of Low-Emission Vehicles Based on a Selected Expert Method Taking into Account Stochastic Operational Parameters. *Energies* **2021**, *14*, 6859. [CrossRef]
5. Dziubak, T. The Effects of Dust Extraction on Multi-Cyclone and Non-Woven Fabric Panel Filter Performance in the Air Filters Used in Special Vehicles. *Eksploat. Niezawodn.* **2016**, *18*, 348–357. [CrossRef]
6. Wang, L.; Yang, Q.; Tian, Y. Reliability Analysis of 6-Component Star Markov Repairable System with Spatial Dependence. *Math. Probl. Eng.* **2017**, *2017*, 9728019. [CrossRef]
7. Galiev, I.F.; Sabitov, A.E. Analysis of the Reliability and Efficiency of Local Power Supply Systems at Major International Events. *Lect. Notes Civ. Eng.* **2022**, *190*, 269–278. [CrossRef]
8. Ziółkowski, J.; Małachowski, J.; Oszczypała, M.; Szkutnik-Rogoż, J.; Lęgas, A. Modelling of the Military Helicopter Operation Process in Terms of Readiness. *Def. Sci. J.* **2021**, *71*, 602–611. [CrossRef]
9. Ziółkowski, J.; Żurek, J.; Małachowski, J.; Oszczypała, M.; Szkutnik-Rogoż, J. Method for Calculating the Required Number of Transport Vehicles Supplying Aviation Fuel to Aircraft during Combat Tasks. *Sustainability* **2022**, *14*, 1619. [CrossRef]
10. Yahaya, M.; Azis, N.; Mohd Selva, A.; Ab Kadir, M.; Jasni, J.; Kadim, E.; Hairi, M.; Yang Ghazali, Y. A Maintenance Cost Study of Transformers Based on Markov Model Utilizing Frequency of Transition Approach. *Energies* **2018**, *11*, 2006. [CrossRef]
11. Dziubak, T.; Dziubak, S.D. A Study on the Effect of Inlet Air Pollution on the Engine Component Wear and Operation. *Energies* **2022**, *15*, 1182. [CrossRef]
12. Wróblewski, P.; Drożdż, W.; Lewicki, W.; Miązek, P. Methodology for Assessing the Impact of Aperiodic Phenomena on the Energy Balance of Propulsion Engines in Vehicle Electromobility Systems for given Areas. *Energies* **2021**, *14*, 2314. [CrossRef]

13. Paś, J.; Rosiński, A.; Wiśnios, M.; Stawowy, M. Assessing the Operation System of Fire Alarm Systems for Detection Line and Circuit Devices with Various Damage Intensities. *Energies* **2022**, *15*, 3066. [CrossRef]
14. Mengistu, T.M.; Che, D.; Alahmadi, A.; Lu, S. Semi-Markov Process Based Reliability and Availability Prediction for Volunteer Cloud Systems. In Proceedings of the 2018 IEEE 11th International Conference on Cloud Computing (CLOUD), San Francisco, CA, USA, 2–7 July 2018; IEEE: Piscataway, NJ, USA; pp. 359–366.
15. Zhang, T.; Liu, T.; Liu, D.; Sun, F. Reliability Evaluation of Modular Multilevel Converter System Based on Semi-Markov Model. In Proceedings of the 2021 IEEE 4th International Conference on Electronics Technology (ICET), Chengdu, China, 7–10 May 2021; pp. 513–517.
16. Papadopoulos, C.T.; Li, J.; O'Kelly, M.E.J. A Classification and Review of Timed Markov Models of Manufacturing Systems. *Comput. Ind. Eng.* **2019**, *128*, 219–244. [CrossRef]
17. Wang, J.; Miao, Y. Optimal Preventive Maintenance Policy of the Balanced System under the Semi-Markov Model. *Reliab. Eng. Syst. Saf.* **2021**, *213*, 107690. [CrossRef]
18. Zhiyong, G.; Jiwu, L.; Rongxi, W. Prognostics Uncertainty Reduction by Right-Time Prediction of Remaining Useful Life Based on Hidden Markov Model and Proportional Hazard Model. *Eksploat. Niezawodn.* **2021**, *23*, 154–165. [CrossRef]
19. Seyr, H.; Muskulus, M. Use of Markov Decision Processes in the Evaluation of Corrective Maintenance Scheduling Policies for Offshore Wind Farms. *Energies* **2019**, *12*, 2993. [CrossRef]
20. Li, Y.; Cui, L.; Lin, C. Modeling and Analysis for Multi-State Systems with Discrete-Time Markov Regime-Switching. *Reliab. Eng. Syst. Saf.* **2017**, *166*, 41–49. [CrossRef]
21. El-Awady, A.; Ponnambalam, K. Integration of Simulation and Markov Chains to Support Bayesian Networks for Probabilistic Failure Analysis of Complex Systems. *Reliab. Eng. Syst. Saf.* **2021**, *211*, 107511. [CrossRef]
22. Wang, J.; Feng, Y.; Fei, Z.; Li, S.; Chang, Q. Markov Chain Based Idle Status Control of Stochastic Machines for Energy Saving Operation. In Proceedings of the 2017 13th IEEE Conference on Automation Science and Engineering (CASE), Xi'an, China, 20–23 August 2017; IEEE: Piscataway, NJ, USA; pp. 1019–1023.
23. Kamlu, S.; Laxmi, V. Condition-Based Maintenance Strategy for Vehicles Using Hidden Markov Models. *Adv. Mech. Eng.* **2019**, *11*, 1–13. [CrossRef]
24. Borucka, A.; Niewczas, A.; Hasilova, K. Forecasting the Readiness of Special Vehicles Using the Semi-Markov Model. *Eksploat. Niezawodn.-Maint. Reliab.* **2019**, *21*, 662–669. [CrossRef]
25. Yang, W.; Chen, L. Machine Condition Recognition via Hidden Semi-Markov Model. *Comput. Ind. Eng.* **2021**, *158*, 107430. [CrossRef]
26. Sánchez-Herguedas, A.; Mena-Nieto, A.; Rodrigo-Muñoz, F. A New Analytical Method to Optimise the Preventive Maintenance Interval by Using a Semi-Markov Process and z-Transform with an Application to Marine Diesel Engines. *Reliab. Eng. Syst. Saf.* **2021**, *207*, 107394. [CrossRef]
27. Grabski, F. Semi-Markov Failure Rates Processes. *Appl. Math. Comput.* **2011**, *217*, 9956–9965. [CrossRef]
28. Migawa, K.; Borowski, S.; Neubauer, A.; Sołtysiak, A. Semi-Markov Model of the System of Repairs and Preventive Replacements by Age of City Buses. *Appl. Sci.* **2021**, *11*, 10411. [CrossRef]
29. Świderski, A.; Borucka, A.; Grzelak, M.; Gil, L. Evaluation of Machinery Readiness Using Semi-Markov Processes. *Appl. Sci.* **2020**, *10*, 1541. [CrossRef]
30. Migawa, K. Availability Control for Means of Transport in Decisive Semi-Markov Models of Exploitation Process. *Arch. Transp.* **2012**, *24*, 497–508. [CrossRef]
31. Zhao, L.; Li, K.; Zhao, W.; Ke, H.-C.; Wang, Z. A Sticky Sampling and Markov State Transition Matrix Based Driving Cycle Construction Method for EV. *Energies* **2022**, *15*, 1057. [CrossRef]
32. Wang, Y.; Xie, B.; E, S. Adaptive Relevance Vector Machine Combined with Markov-Chain-Based Importance Sampling for Reliability Analysis. *Reliab. Eng. Syst. Saf.* **2022**, *220*, 108287. [CrossRef]
33. Şahin, İ. Markov Chain Model for Delay Distribution in Train Schedules: Assessing the Effectiveness of Time Allowances. *J. Rail Transp. Plan. Manag.* **2017**, *7*, 101–113. [CrossRef]
34. Rajarshi, M.B. *Statistical Inference for Discrete Time Stochastic Processes*; Springer Briefs in Statistics; Springer: Delhi, India, 2013; ISBN 978-81-322-0762-7.
35. Shepero, M.; Munkhammar, J. Spatial Markov Chain Model for Electric Vehicle Charging in Cities Using Geographical Information System (GIS) Data. *Appl. Energy* **2018**, *231*, 1089–1099. [CrossRef]
36. Pourmousavi Kani, S.A.; Ardehali, M.M. Very Short-Term Wind Speed Prediction: A New Artificial Neural Network–Markov Chain Model. *Energy Convers. Manag.* **2011**, *52*, 738–745. [CrossRef]
37. Karakaya, E.; Vinel, A.; Smith, A.E. Relocations in Container Depots for Different Handling Equipment Types: Markov Models. *Comput. Ind. Eng.* **2021**, *157*, 107311. [CrossRef]
38. González-Domínguez, J.; Sánchez-Barroso, G.; García-Sanz-Calcedo, J. Scheduling of Preventive Maintenance in Healthcare Buildings Using Markov Chain. *Appl. Sci.* **2020**, *10*, 5263. [CrossRef]
39. Iversen, E.B.; Morales, J.M.; Madsen, H. Optimal Charging of an Electric Vehicle Using a Markov Decision Process. *Appl. Energy* **2014**, *123*, 1–12. [CrossRef]
40. Brayer, E.F. Calculating the Standard Error of a Proportion. *Appl. Stat.* **1957**, *6*, 67–68. [CrossRef]

41. Gurland, J.; Tripathi, R.C. A Simple Approximation for Unbiased Estimation of the Standard Deviation. *Am. Stat.* **1971**, *25*, 30–32. [CrossRef]
42. van Staden, H.E.; Boute, R.N. The Effect of Multi-Sensor Data on Condition-Based Maintenance Policies. *Eur. J. Oper. Res.* **2021**, *290*, 585–600. [CrossRef]
43. Jafari, L.; Makis, V.; Gb, A.K. Optimal Maintenance Policy for a Partially Observable Two-Unit System. *World Acad. Sci. Eng. Technol. Int. J. Mech. Aerosp. Ind. Mechatron. Manuf. Eng.* **2014**, *8*, 1612–1619.
44. Agrawal, A.K.; Murthy, V.M.S.R.; Chattopadhyaya, S. Investigations into Reliability, Maintainability and Availability of Tunnel Boring Machine Operating in Mixed Ground Condition Using Markov Chains. *Eng. Fail. Anal.* **2019**, *105*, 477–489. [CrossRef]
45. Kampitsis, D.; Panagiotidou, S. A Bayesian Condition-Based Maintenance and Monitoring Policy with Variable Sampling Intervals. *Reliab. Eng. Syst. Saf.* **2022**, *218*, 108159. [CrossRef]
46. Girtler, J. Physical Aspects of Application and Usefulness of Semi-Markovian Processes for Modelling the Processes Occurring in Operational Phase of Technical Objects. *Pol. Marit. Res.* **2004**, *11*, 25–30.
47. Ivanchenko, O.; Kharchenko, V.; Moroz, B.; Kabak, L.; Smoktii, K. Semi-Markov Availability Model Considering Deliberate Malicious Impacts on an Infrastructure-as-a-Service Cloud. In Proceedings of the 2018 14th International Conference on Advanced Trends in Radioelecrtronics, Telecommunications and Computer Engineering (TCSET), Lviv-Slavske, Ukraine, 20–24 February 2018; pp. 570–573.
48. Conover, W.J. A Kolmogorov Goodness-of-Fit Test for Discontinuous Distributions. *J. Am. Stat. Assoc.* **1972**, *67*, 591–596. [CrossRef]
49. Quine, M.P.; Robinson, J. Efficiencies of Chi-Square and Likelihood Ratio Goodness-of-Fit Tests. *Ann. Stat.* **1985**, *13*, 727–742. [CrossRef]
50. Shepelev, S.; Shepelev, V.; Cherkasov, Y. Differentiation of the Seasonal Loading of Combine Harvester Depending on Its Technical Readiness. *Procedia Eng.* **2015**, *129*, 161–165. [CrossRef]
51. Zhao, J.; Jia, Y.; Shi, L.; Zhao, X.; Kong, L. Research on Technical Readiness Evaluation Method in Model Development. In Proceedings of the 2015 8th International Symposium on Computational Intelligence and Design (ISCID), Hangzhou, China, 12–13 December 2015; Volume 1, pp. 392–396.
52. Selech, J.; Andrzejczak, K. An Aggregate Criterion for Selecting a Distribution for Times to Failure of Components of Rail Vehicles. *Eksploat. Niezawodn.-Maint. Reliab.* **2019**, *22*, 102–111. [CrossRef]
53. Fadhil, R.M.; Unami, K. A Multi-State Markov Chain Model to Assess Drought Risks in Rainfed Agriculture: A Case Study in the Nineveh Plains of Northern Iraq. *Stoch. Environ. Res. Risk Assess.* **2021**, *35*, 1931–1951. [CrossRef]
54. Huang, X.-W.; Emura, T. Model Diagnostic Procedures for Copula-Based Markov Chain Models for Statistical Process Control. *Commun. Stat. Simul. Comput.* **2021**, *50*, 2345–2367. [CrossRef]
55. Roy, V.; Tan, A.; Flegal, J.M. Estimating Standard Errors for Importance Sampling Estimators with Multiple Markov Chains. *Stat. Sin.* **2018**, *28*, 1079–1101. [CrossRef]
56. Rosychuk, R.J.; Sheng, X.; Stuber, J.L. Comparison of Variance Estimation Approaches in a Two-State Markov Model for Longitudinal Data with Misclassification. *Stat. Med.* **2006**, *25*, 1906–1921. [CrossRef]

Eksploatacja i Niezawodnosc – Maintenance and Reliability

Volume 25 (2023), Issue 2

journal homepage: http://www.ein.org.pl

Article citation info:
Oszczypała M, Ziółkowski J, Małachowski J, Semi-Markov approach for reliability modelling of light utility vehicles. Eksploatacja i Niezawodnosc – Maintenance and Reliability 2023: 25(2), http://doi.org/10.17531/ein/161859

Semi-Markov approach for reliability modelling of light utility vehicles

Indexed by:

Mateusz Oszczypała[a], Jarosław Ziółkowski[a,*], Jerzy Małachowski[a]

[a] Institute of Mechanics & Computational Engineering, Military University of Technology, Faculty of Mechanical Engineering, Poland

Highlights

- The 3-state model has been developed for reliability modelling.
- Based on the semi-Markov model, the reliability characteristics were calculated.
- Readiness and suitability indicators were used to assess the operational process.
- The results of the 3-state model have been compared with those of the 9-state model.

Abstract

Vehicles are important elements of military transport systems. Semi-Markov processes, owing to the generic assumption form, are a useful tool for modelling the operation process of numerous technical objects and systems. The suggested approach is an extension of existing stochastic methods employed for a wide spectrum of technical objects; however, research on light utility vehicles complements the subject gap in the scientific literature. This research paper discusses the 3-state semi-Markov model implemented for the purposes of developing reliability analyses. Based on an empirical course of the operation process, the model was validated in terms of determining the conditional probabilities of interstate transitions for an embedded Markov chain, as well as parameters of time distribution functions. The Laplace transform was used to determine the reliability function, the failure probability density function, the failure intensity, and the expected time to failure. The readiness index values were calculated on ergodic probabilities.

Keywords

semi-Markov model, reliability modelling, readiness, maintenance analysis, transportation system.

1. Introduction

The operation of transport means primarily involves three main processes, that is, the implementation of transport tasks together with regular technical activities aimed at verifying correct vehicle functionality; conducting periodic maintenance and servicing; and diagnosing the causes of technical unsuitability and their removal through repair or replacement of spare parts with new ones. The intensity of vehicle operation affects the wear rate of subassemblies and consumables, which directly translates into the frequency of maintenance activities. The duration during which these vehicles remain in these states is strictly correlated with the capacities of a technical subsystem that supports the transport system and the effectiveness of logistics processes associated with the supply chain of consumables and spare parts. In the case of many technical systems, due to the unavailability of fast and flexible material requirements, the unsuitability time of faulty means of transport constitutes a significant factor reducing the values of readiness indices [33].

Technical availability and reliability of vehicles are two of the main determinants of operational effectiveness in modern and advanced transport systems. The appearance of a means of transport failure in the course of the implementation of transport processes generates functional interference with respect to the entire system [10, 23]. For this reason, the operational strategy of many objects and systems assumes periodic preventive maintenance, whose interval and scope depend on both technical and economic factors [18]. The result of such actions is a reduced number of unplanned shutdown periods of machinery and equipment. However, to precisely determine the optimal intervals between subsequent maintenance cycles, it is necessary to develop appropriate reliability models to describe the probability of object failure within a specified period and volume of work [24, 36].

The objective of this publication is to develop an operation process model for light utility vehicles that enables analysing their reliability through determining basic reliability

(*) Corresponding author.
E-mail addresses: M. Oszczypała (ORCID: 0000-0002-1194-6913) mateusz.oszczypala@wat.edu.pl, J. Ziółkowski (ORCID: 0000-0001-8880-5142) jaroslaw.ziolkowski@wat.edu.pl, J. Małachowski (ORCID: 0000-0003-1300-8020) jerzy.malachowski@wat.edu.pl

characteristics, such as the reliability function, failure probability density function, failure intensity, expected time to failure and readiness indices. A novel contribution to the current state of the source literature is the expansion of existing stochastic modelling methods in terms of their applications within the field of engineering and technical sciences [3, 5, 13]. In addition, the presented research complements the subject matter niche, because none of the previously published papers applied to the reliability of military light utility vehicles based on the semi-Markov model. The research subject matter is wheeled vehicles owned by the Polish Armed Forces. Currently (Russia's aggression against Ukraine), the research topic positions the importance of the content presented taking into account domestic (and international) security issues. Furthermore, it is possible to apply the method discussed in studies within the defence industry.

The research paper has been divided into five chapters. The further part of the article reviews the current state of knowledge in terms of the methods employed and approaches towards modelling the reliability of technical objects and systems. The third chapter contains a description of semi-Markov processes with a method for their implementation in reliability and operational studies. Then, in chapter four, the authors presented the application of the proposed approach with respect to analysing the operation process and reliability of light utility vehicles, based on empirical operational data obtained from an actual military transport system. The results of the studies and analyses presented enable the evaluation of vehicle reliability and readiness, which reflects the technical aspect of the functional effectiveness of transport means. The reliability characteristics developed may be grounds for planning the maintenance and repair potential of a technical system. The article ends with conclusions drawn from the performed computations and indications of future research directions.

2. Literature review

Table 1 contains an overview of the source literature on modelling the reliability of technical objects and systems in the transport, industry, and energy sector.

Statistical methods are some of the basic methods applied when developing reliability models. Selech and Andrzejczak [43] studied the reliability of the cabin door lock reliability in rail vehicles, using the Kaplan-Meier estimator. Next, using an original indicator, they selected a Generalized Gamma distribution as the best fitting of the empirical distribution function. In turn, Wawrzyński et al. [53] used statistical methods to develop a reliability model for aircraft commutators, under the assumption of a serial reliability structure of a tested object.

The results obtained by statistical methods also constitute the foundation for the evaluation of advanced models developed based on the application of fuzzy logic and neural networks. Żyluk et al. [60] developed statistical reliability models for lightweight combat aircraft, with the Weibull model turning out to be the best match. A fuzzy model with a similar accuracy reflected the values of an empirical reliability function. In turn, in [34], the multilayer perceptron (MLP) neural model was slightly better at approximating the light utility vehicle reliability function relative to the exponential and Weibull distributions. Whereas, in the case of fluid filling equipment in the automotive manufacturing industry, Soltanali et al. [45] demonstrated a significant improvement in the accuracy of reliability predictions using the Adaptive Neuro-Fuzzy Inference System model, compared to Weibull and Non-Homogeneous Poisson Process models.

The high accuracy of artificial neural networks in reliability modelling has prompted numerous researchers to employ them, without the need for their verification with other methods. Lolas and Olatunbosun [25] developed models based on MLP networks, used to predict the reliability of motor vehicles. In turn, Du et al. [11] used neural models to allocate reliability to components of industrial machines. On the other hand, Chang [7] suggested a method based on the ordered weighted averaging operator to allocate reliability and applied the developed model to study the liquid crystal display of thin-film transistors. Neural models can be improved by hybridization with other methods. Bai et al. [2] combined an artificial neural network with partial swarm optimization to develop a reliability model that was used to analyse industrial robot systems.

Macheret et al. [27] applied methods based on probabilistic dependencies and Monte Carlo simulations to study the reliability of military vehicles. A resulting exponential model was satisfactory in describing the time between failures (TBF). In turn, the authors of studies on micro-electro-mechanical system devices [37, 46] proposed the application of probabilistic methods to develop hard and soft failure models. The same failure classification was used by Lyu et al. [26] in relation to multi-state systems. They used probabilistic methods and dispersion to develop a reliability model. Another solution suggested by Miziuła and Navarro [31] is based on the Birnbaum importance measure and was implemented to evaluate the impact of the reliability of individual components on the reliability of the entire system.

The Bayesian approach to estimating the reliability of multi-component systems was presented by Guo and Wilson in [14]. The logistic regression, Weibull and degradation models were applied to describe the reliability of three components of a serial system. Next, using the Bayesian method, the authors developed a combined model that determined the reliability of the entire system.

The models most commonly employed for reliability analyses are Markov and semi-Markov processes. Depending on the complexity of a technical object or system and its operation processes, researchers and engineers develop stochastic models of a diverse number of states. Stawowy et al. [47] presented a 3-state Markov model to analyse power supply systems in transport telematics devices. In reliability studies related to other case studies, researchers constructed more complex models, such as a 4-state bearing model [22], a 5-state model for microelectromechanical systems [54], and a 10-state model for GPS receivers [41]. For a complex port distribution power system, Fang et al. [12] developed several Markov models to describe the reliability of individual subsystems, that is, 8-state models for a solar system, a wind system, and an energy storage system, a 4-state model for a combined cooling, heating and power system, and a 2-state model for a commercial power system.

Semi-Markov models have a significant advantage over Markov models in that they offer a considerably greater scope of possible applications. The applicability of Markov processes is limited due to the need to satisfy the conditions of exponential distributions for the time characteristics of the modelled processes [35]. However, semi-Markov processes are a generalization of Markov processes and allow for any characteristic distributions [9, 49].

Models with a phase space containing 3 operational states dominate the field of application of semi-Markov models. One of the most important 3-state semi-Markov models is the generalized object reliability model developed by Grabski [13], validated with assumed parameter values, without specified references to technical data. In the course of the research, the authors developed original 3-state models applicable to specific objects and systems, e.g., four types of repairable systems [8], single-use systems [9], special vehicles [5], lithium-ion batteries [55] and repairable systems [3]. Mengistu et al. [28] identified a five-state phase space of the semi-Markov model for volunteer cloud systems and Wu et al. [56] for power stations. L. Wang et al. [50] developed 6- and 4-state models to analyse the reliability of repairable systems in alternative environments, which turned out to be more reliable compared to Markov models. More complex models were proposed by Zhang et al. [57], who developed a 7-state model to analyse the reliability of a multilevel modular converter system. Whereas Blasi et al. [4] presented a 9-state semi-Markov model to evaluate the reliability of two machines operating in parallel.

The wide spectrum of applications demonstrated in Table 1 proves the usefulness of Markov and semi-Markov theories in modelling the reliability of technical objects and systems. Diversification of the number of states in the phase space proves the need to adapt the model to the analysed case study, the specificity of the technical object, and the assumptions of the operational strategy in particular. Therefore, the authors of this paper developed a specialized semi-Markov model to analyse the reliability of light utility vehicles. Based on assumptions adopted in military technical systems and the 9-state model [33] developed for a detailed analysis of vehicle readiness. The phase space aggregation was carried out in 3 main operational states.

Table 1. Review of literature on reliability modelling.

Methods	Models	Case study	Paper
Statistical methods	Generalized Gamma distribution	Cabin door lock on rail vehicles	[43]
	Reliability series structure model	Aircraft commutators	[53]
Statistical methods and fuzzy logic	Weibull and fuzzy models	Light combat aircraft	[60]
Statistical methods and neural networks	Exponential, Weibull and MLP models	Light utility vehicles	[34]
	Weibull, Non-Homogeneous Poisson Process and Adaptive Neuro-Fuzzy Inference System models	Fluid filling equipment in automotive manufacturing industry	[45]
Neural networks	Neural models (MLP)	Vehicles	[25]
	Neural model of reliability allocation	Machine tools	[11]
Neural networks and partial swarm optimization	Hybrid model	Industrial robot systems	[2]
Ordered weighted averaging aggregation operator	Reliability allocation model	Thin-film transistor liquid-crystal display	[7]
Probabilistic methods	Reliability models including hard and soft failures	Micro-electro-mechanical systems devices	[46][37]
	Models based on Birnbaum importance measure	2-, 3- and 5-component systems	[31]
Probabilistic methods and Monte Carlo simulation	Exponential model	Military vehicles	[27]
Probabilistic and dispersion methods	Reliability models including hard and soft failures	Multi-state systems	[26]
Bayesian methods	Combined model of component reliability	Multi-component complex system	[14]
Markov processes	3-state model	Power supply systems in transport telematics devices	[47]
	4-state model	Bearings	[22]
	5-state model	Micro-electro-mechanical systems	[54]
	2-, 4- and 8-state model	Port distribution power system	[12]
	10-state model	GPS Receivers	[41]
Semi-Markov processes	3-state model	Technical objects (general)	[13]
		Four types of repairable systems	[8]
		Single-use system	[9]
		Special vehicles	[5]
		Lithium-ion batteries	[55]
		Repairable systems	[3]
	5-state model	Volunteer cloud systems	[28]
		Power station	[56]
	4- and 6-state models	Repairable systems under alternative environments	[50]
	7-state model	Modular multilevel converter system	[57]
	9-state model	Two machines operating in parallel	[4]

3. Methods

Operation processes are a complex composition of deterministic and random processes, whereas random components are interpreted as stochastic processes $X(t)$ reflecting changes in the operational states of the technical object studied in discrete or continuous time. At any time t, an object is only in one of the states identified within the phase space $S = X(t)$. This assumption requires a precise identification of all possible operational states in which vehicles may remain during the operation process [33]. Stochastic processes that satisfy the Markov property are important in terms of applicability. According to Markov theory, the conditional probabilities of reaching future states $X(t_{n+1})$ result solely from the current state $X(t_n)$ [51]. In mathematical notation, the property presented [38, 42, 44] is consistent with the dependence (1):

$$P\begin{Bmatrix} X(t_n) = x_n | X(t_{n-1}) = x_{n-1}, \\ X(t_{n-2}) = x_{n-2}, \dots, X(t_0) = x_0 \end{Bmatrix} = P\{X(t_n) = x_n | X(t_{n-1}) = x_{n-1}\} \quad (1)$$

The source literature is dominated by the division of Markov processes based on state space and time, which distinguishes the following process types, i.e.:

1) discrete in states and discrete over time,
2) discrete in states and continuous over time,
3) continuous in states and discrete over time,
4) continuous in states and continuous over time,

Models based on discrete-state processes developed for both the discrete [30] and continuous times [42]–[45].

3.1. Semi-Markov processes

Semi-Markov processes are a generalization of Markov processes in terms of time characteristic distributions. Markov models assume exponential distributions of transition times between individual states within the phase space, which significantly narrows down their applicability when modelling reliability. Furthermore, their use without verifying the adopted assumptions may lead to significant errors in the obtained results [33, 48]. Semi-Markov models are a solution to this problem. They allow any distribution of time characteristics [13]. The values of sojourn times in states are calculated as time intervals from the moment an object entered the S_i state until it transitioned to the next S_j state. On the basis of the realization set of these variables, an approximation of the distributions is conducted based on the nonlinear least squares method.

The basic description of the semi-Markov process is the $\boldsymbol{Q}(t)$ renewal kernel matrix, consisting of products of the conditional probability of transition from the S_i state to the S_j state and distribution functions of the condition duration distribution of the S_i state before transition to the S_j state, according to the equation [19, 29]:

$$\boldsymbol{Q}(t) = \begin{bmatrix} 0 & Q_{12}(t) & \cdots & Q_{1(k-1)}(t) & Q_{1k}(t) \\ Q_{21}(t) & 0 & \cdots & Q_{2(k-1)}(t) & Q_{2k}(t) \\ \vdots & \vdots & \ddots & \vdots & \vdots \\ Q_{(k-1)1}(t) & Q_{(k-1)2}(t) & \cdots & 0 & Q_{(k-1)k}(t) \\ Q_{k1}(t) & Q_{k2}(t) & \cdots & Q_{k(k-1)}(t) & 0 \end{bmatrix} \quad (2)$$

whereas:

$$Q_{ij}(t) = p_{ij}F_{ij}(t), \quad (3)$$

where p_{ij} means the probability of transition from the S_i state to the S_j state, and $F_{ij}(t)$ is the distribution function of time spent in the S_i state befor transitioning to the S_j state.

An embedded Markov chain is constructed for a semi-Markov process over continuous time. It describes changes in process states, not taking into account the times of residence in individual states. The possibility of a transition from the S_i state to the S_j state is assumed for an embedded Markov chain, provided that $i \neq j$. The matrix of conditional probabilities of interstate transitions $\boldsymbol{P}$ may have non-zero elements, except only for the main diagonal, which can be written using the formula:

$$\boldsymbol{P} = \begin{bmatrix} 0 & p_{12} & \cdots & p_{1(k-1)} & p_{1k} \\ p_{21} & 0 & \cdots & p_{2(k-1)} & p_{2k} \\ \vdots & \vdots & \ddots & \vdots & \vdots \\ p_{(k-1)1} & p_{(k-1)2} & \cdots & 0 & p_{(k-1)k} \\ p_{k1} & p_{k2} & \cdots & p_{k(k-1)} & 0 \end{bmatrix}, \quad (4)$$

under the assumption of meeting the condition of the stochastic matrix [21, 32]:

$$\sum_{j=1}^{k} p_{ij} = 1. \quad (5)$$

Constructing an embedded Markov chain based on an empirical process waveform implies the need to acquire numerical data on interstate transitions. For this purpose, it is justified to construct a population matrix of interstate transitions $\boldsymbol{N}$, according to (6):

$$\boldsymbol{N} = \begin{bmatrix} 0 & n_{12} & \cdots & n_{1(k-1)} & n_{1k} \\ n_{21} & 0 & \cdots & n_{2(k-1)} & n_{2k} \\ \vdots & \vdots & \ddots & \vdots & \vdots \\ n_{(k-1)1} & n_{(k-1)2} & \cdots & 0 & n_{(k-1)k} \\ n_{k1} & n_{k2} & \cdots & n_{k(k-1)} & 0 \end{bmatrix}. \quad (6)$$

The elements n_{ij} of the empirical matrix $\boldsymbol{N}$ count the transitions in one step between all combinations of states S_i and S_j of the empirical embedded Markov chain. The process of transitions between states should be recorded for so long that all possible transitions can be observed. Based on the empirical data obtained contained in the matrix $\boldsymbol{N}$, the unknown elements p_{ij} of the transition matrix $\boldsymbol{P}$ are estimated, according to the formula (7):

$$\hat{p}_{ij} = \frac{n_{ij}}{\sum_{j=1}^{k} n_{ij}}, \quad (7)$$

where $\hat{p}_{ij}$ is the maximum likelihood estimator of the unknown value of p_{ij}. This estimator is consistent and unbiased, and the standard error of this estimator decreases rapidly as the number of transitions n_{ij} increases. The standard error $SE(p_{ij})$ of the estimation of the transition probability p_{ij} is given by the formula (8) [6, 15]:

$$SE(p_{ij}) = \sqrt{\frac{\hat{p}_{ij}(1-\hat{p}_{ij})}{\sum_{j=1}^{k} n_{ij}}}. \quad (8)$$

Estimating the probabilities of transitions p_{ij} with an acceptable error may require long-term observations for each state S_i.

3.2. Reliability modelling

The reliability function $R(t)$ determines the probability of an event, in which a technical object operated under assumed conditions remains continuously in a state of technical suitability from time 0 to time t [1, 16, 17, 34]. The mathematical reliability function description is presented by the dependence (9):

$$R(t) = P(T \geq t) \text{for } t \geq 0, \quad (9)$$

where T is the failure time of the technical object.

For an n-state semi-Markov model, if at time $t = 0$ an object is in state S_i belonging to a subset of suitability states A', its first time reaching state S_j belonging to a subset of unsuitability states A means losing suitability and the appearance of failure [13]. The probability of reaching a subset of states A up to time t corresponds to the value of the unreliability function $F_i(t)$.

$$F_i(t) = \Phi_{iA}(t) = P(\Theta_A \leq t | X(t=0) = i), \quad (10)$$

where Θ_A is a random variable that determines the time when the object reaches a subset of states A.

Using the formula (11):

$$R_i(t) = 1 - F_i(t), \quad (11)$$

the reliability function $R(t)$ is determined as (12):

$$R_i(t) = 1 - \Phi_{iA}(t) = 1 - P(\Theta_A \leq t | X(t=0) = i). \quad (12)$$

The cumulative distribution function $\Phi_{iA}(t)$ is calculated using the equation (13):

$$\Phi_{iA}(t) = \sum_{j\in A} Q_{ij}(t) + \sum_{k\in A} \int_0^t \Phi_{kA}(t-x) dQ_{ik}(x), \quad (13)$$

which, after a Laplace – Stieltjes transform, takes the form:

$$\tilde{\phi}_{iA}(s) = \sum_{j\in A} \tilde{q}_{ij}(s) + \sum_{k\in A} \tilde{q}_{ik}(s)\tilde{\phi}_{kA}(s), \quad (14)$$

where:

$$\tilde{\phi}_{iA}(s) = \int_0^\infty e^{-st} d\Phi_{iA}(t), \quad (15)$$

$$\tilde{q}_{ij}(s) = \int_0^\infty e^{-st} dQ_{ij}(t). \quad (16)$$

Equation (13) can be written in matrix form as (17):

$$\left(\boldsymbol{I} - \tilde{\boldsymbol{q}}_{A'}(s)\right)\tilde{\boldsymbol{\phi}}_{A'}(s) = \tilde{\boldsymbol{b}}(s), \quad (17)$$

where $\boldsymbol{I}$ is an identity matrix, $\tilde{\boldsymbol{q}}_{A'}$ is a square submatrix of the transform matrix $\tilde{\boldsymbol{q}}(s)$, while matrices $\tilde{\boldsymbol{\phi}}_{A'}(s)$ and $\tilde{\boldsymbol{b}}(s)$ are single-column matrices of relevant transforms, according to dependencies (18) and (19):

$$\tilde{\Phi}_{A'}(s) = \left[\tilde{\phi}_{iA}(s) : i \in A'\right]^{\mathrm{T}}, \quad (18)$$

$$\tilde{b}(s) = \left[\sum_{j\in A} \tilde{q}_{ij}(s) : i \in A'\right]^{\mathrm{T}}. \quad (19)$$

3.3 Instantaneous probabilities of states

Instantaneous probabilities that an object remains in the S_j states can be used to determine readiness indices at a given time t. Knowing the matrix $\boldsymbol{P} = p_j(t)$ of the $S_i \rightarrow S_j$ transition probabilities for the semi-Markov process and the initial distribution vector of the state probability $p_j(0)$, the matrix of instantaneous probabilities $p_j(t)$ is calculated as a matrix product according to formula (20):

$$\mathrm{p}_j(t) = \mathrm{p}_j(0) \cdot \mathrm{p}(t), \quad (20)$$

The probability matrix $\boldsymbol{p}_j(t)$ can be calculated by solving the matrix equation (21):

$$\tilde{\mathrm{p}}(s) = \frac{1}{s}\left(\mathrm{I} - \tilde{\mathrm{q}}(s)\right)^{-1}\left(\mathrm{I} - \tilde{\mathrm{h}}(s)\right), \quad (21)$$

whereas the matrix elements are calculated according to the dependencies [52] (22-30):

$$\tilde{p}_{ij}(s) = \int_0^\infty e^{-st} dP_{ij}(t), \quad (22)$$

$$\tilde{q}_{ij}(s) = \int_0^\infty e^{-st} dQ_{ij}(t), \quad (23)$$

$$q_{ij}(t) = \frac{dQ_{ij}(t)}{dt} = p_{ij}\frac{dF_{ij}(t)}{dt} = p_{ij} f_{ij}(t), \quad (24)$$

$$\tilde{h}_{ij}(s) = \int_0^\infty e^{-st} dH_{ij}(t), \quad (25)$$

$$h_{ij}(t) = \delta_{ij} \sum_{j=1}^{n} q_{ij}(t) = \delta_{ij} g_i(t), \quad (26)$$

$$g_i(t) = \frac{dG_i(t)}{dt}, \quad (27)$$

$$G_i(t) = \sum_{k\in S} Q_{ik}(t), \quad (28)$$

$$\tilde{g}_i(s) = \int_0^\infty e^{-st} dG_i(t), \quad (29)$$

where δ_{ij} are elements of the identity matrix (30):

$$\delta_{ij} = \begin{cases} 0 & \text{if } i \neq j \\ 1 & \text{if } i = j \end{cases}. \quad (30)$$

3.4. Ergodic probabilities of states

Ergodic probabilities values of an embedded Markov chain π_j are calculated by solving the matrix equation (31) [21]:

$$(\boldsymbol{P}^T - \boldsymbol{I}) \cdot \boldsymbol{\Pi} = 0, \quad (31)$$

assuming that the standardization condition is met, according to the formula (32):

$$\sum_{j=1}^{n} \pi_j = 1. \quad (32)$$

The random variable T_i determines the sojourn time in state S_i before the transition to another state. In turn, the variable T_{ij} determines the sojourn time in the S_i state before the direct transition to the S_j state. If at time $t = 0$, the object is in the state $S_i \in A'$, then the sum of the times T_{ij} until the transition to the state $S_k \in A$ is equal to the value of Θ_A, as described by the formula (33):

$$\Theta_A = \sum_{j:S_j\in A'}^{k} T_{ij}, \; S_k \in A. \quad (33)$$

If an embedded Markov chain exhibits ergodicity and there are expected values $E(T_i)$ of state sojourn times, the values of ergodic probabilities p_j for a semi-Markov process are determined using the dependence (34-35):

$$p_j = \frac{\pi_j E(T_j)}{\sum_{i=1}^{k} \pi_i E(T_i)}, \quad (34)$$

$$E(T_j) = \sum_{i=1}^{k} p_{ij} E(T_{ij}), \quad (35)$$

where π_i is the ergodic probability of an embedded Markov chain for the S_i state, and $E(T_{ij})$ is the expected time for the direct transition from the S_i state to the S_j state.

4. Results and discussions

4.1. 3-state Semi-Markov model of operation process

The operation process of light utility vehicles functioning within military transport systems is executed within a multi-state phase space. The identification of a phase-space state set should take into account the objectives of a developed stochastic model.

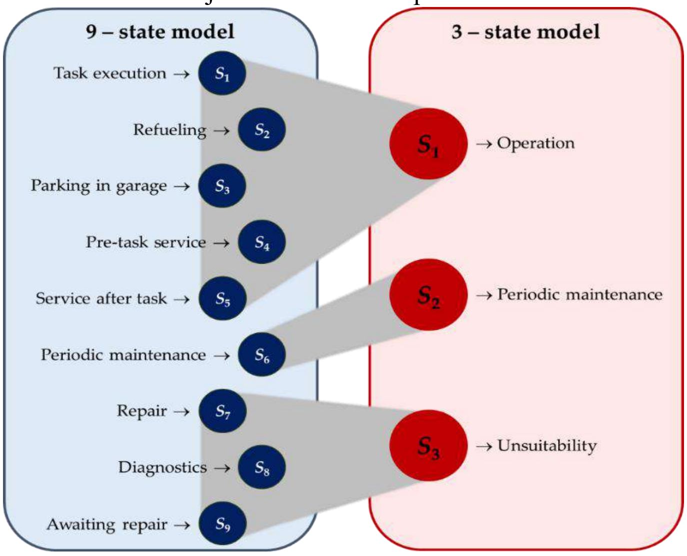

Figure 1. Aggregation of states of the 9-state model [33] modified to the 3-state model

For the purposes of a thorough analysis and evaluation of the operation process in terms of functional readiness indices, technical readiness, and technical suitability, the authors of this publication developed the 9-state semi-Markov model [33]. The calculation of instantaneous probabilities and probabilities of first-time reaching a given state subset by a technical object within a multi-state model requires having significant computing power suitable for complex mathematical operations. A solution to this problem is the aggregation of process phase space states.

The semi-Markov 3-state model was developed, which is a modification of the 9-state model proposed in [33] for reliability analyses. Reducing the number of operational states enabled us to achieve a 3-state phase space containing: S_1 – Operation, S_2 – Periodic maintenance, S_3 – Unsuitability. The state aggregation diagram is shown in Fig. 1.

In the 3-state operation model, the S_1 state defines technical readiness of a vehicle, which is implementing a task or awaiting a transport task as part of the analysed transport system. Short-term activities associated with daily vehicle maintenance and refuelling are frequently assumed. The S_2 state refers to periodic maintenance associated with the checking of the correct functioning of essential vehicle mechanisms, the replacement of specified parts and operating liquids according to the vehicle manual, and maintenance activities. The S_3 state means the unsuitability of a technical object and the need to conduct diagnostic activities in order to identify the causes behind the failure and to repair or replace damaged parts, mechanisms, subassemblies or assemblies. It also includes the time to wait for the availability of qualified personnel as well as materials and technical resources of the system to carry out diagnostic and repair activities. A directed graph of interstate transitions shown in Fig. 2 has been developed for such an identified phase space.

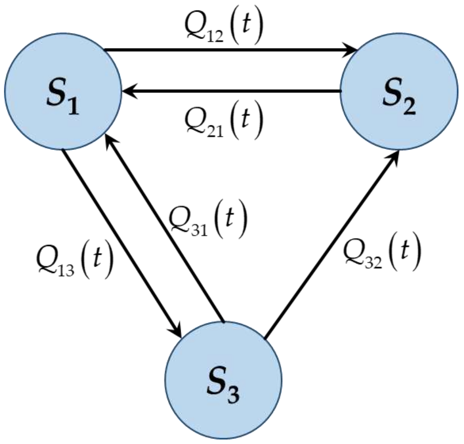

Figure 2. Transition graph of the 3-state semi-Markov model.

According to the assumptions of the operational strategy adopted within the analysed transport system, reaching state S_3 is possible only from state S_1. Periodic maintenance activities may cover only a vehicle in a state of technical suitability. If a vehicle is damaged during operation and is qualified to perform periodic maintenance due to completing a standard interval between subsequent maintenance cycles, it is first brought to a state of technical suitability through repair activities, followed by periodic maintenance. In the 3-state model, this principle has been implemented as an inability of a transition from state S_2 to state S_3.

A mathematical description of the 3-state semi-Markov model is a renewal kernel matrix $\boldsymbol{Q}(t)$, the elements of which are the products of conditional probabilities of the embedded Markov chain and distribution functions of conditions times of residence in individual states, as represented by formula (36):

$$\boldsymbol{Q}(t)=\begin{bmatrix} 0 & Q_{12}(t) & Q_{13}(t) \\ Q_{21}(t) & 0 & 0 \\ Q_{31}(t) & Q_{32}(t) & 0 \end{bmatrix}=$$
$$=\begin{bmatrix} 0 & p_{12}F_{12}(t) & p_{13}F_{13}(t) \\ p_{21}F_{21}(t) & 0 & 0 \\ p_{31}F_{31}(t) & p_{32}F_{32}(t) & 0 \end{bmatrix}. \tag{36}$$

An alternative model definition is the matrix $\mathbf{q}(t)$, the elements of which are products of conditional probabilities of an embedded Markov chain and densities of conditional probabilities of state residence times, according to the dependence (37):

$$\boldsymbol{q}(\mathrm{t})=\begin{bmatrix} 0 & q_{12}(t) & q_{13}(t) \\ q_{21}(t) & 0 & 0 \\ q_{31}(t) & q_{32}(t) & 0 \end{bmatrix}=$$
$$=\begin{bmatrix} 0 & p_{12}f_{12}(t) & p_{13}f_{13}(t) \\ p_{21}f_{21}(t) & 0 & 0 \\ p_{31}f_{31}(t) & p_{32}f_{32}(t) & 0 \end{bmatrix}. \tag{37}$$

4.2. Estimation of model parameters

The 3-state semi-Markov model was validated on the basis of the empirical waveform of the operation process of a sample of 19 Honker 2000 vehicles. These vehicles are part of a military unit transport system and are intended for transporting people and cargo weighing up to 1000 kg. A collective empirical database has been developed based on operating documents that cover a 3-year study period. The graphical visualization of the database can be found in Fig. 3, where each month is marked with a relevant colour, referring to the vehicles staying in specified operational states. The periods in which a vehicle remained in an unsuitable state were expressed in days. The total number of interstate transitions for the entire sample was 416. This was used as a base to estimate interstate transition probabilities for an embedded Markov chain presented by the formula (38):

$$\boldsymbol{P}=[p_{ij}]=\begin{bmatrix} 0 & 0.51 & 0.49 \\ 1 & 0 & 0 \\ 0.9 & 0.1 & 0 \end{bmatrix}, \tag{38}$$

whereas standard estimation errors amounted to:

$$\boldsymbol{SE}=\begin{bmatrix} 0 & 0.0352 & 0.0352 \\ 0 & 0 & 0 \\ 0.0300 & 0.0300 & 0 \end{bmatrix}. \tag{39}$$

$SE(p_{ij})$ values did not exceed 0.04, which can be adopted as a satisfactory and acceptable level in engineering applications [33, 39, 40].

The next model validation stage involves matching distributions to process time characteristics and estimating the parameters of these distributions. Matlab software was used for this purpose. The results are presented in Fig. 4 and Table 2. The four characteristics T_{12}, T_{13}, T_{31} and T_{32} were matched with an exponential distribution with parameter λ (λ_{12}, λ_{13}, λ_{31} and λ_{32}, respectively). Whereas the characteristic T_{21} was described by a gamma distribution with the shape k_{21} and the scale θ_2 parameters. The R^2 coefficient of determination was used as a measure of the quality of the match between the empirical and theoretical distribution functions. For characteristics T_{12}, $T_{13,}$ and T_{21}, coefficient R^2 adopted values above 0.96, while for characteristics T_{31} and T_{32}, it ranged from 0.85 to 0.86.

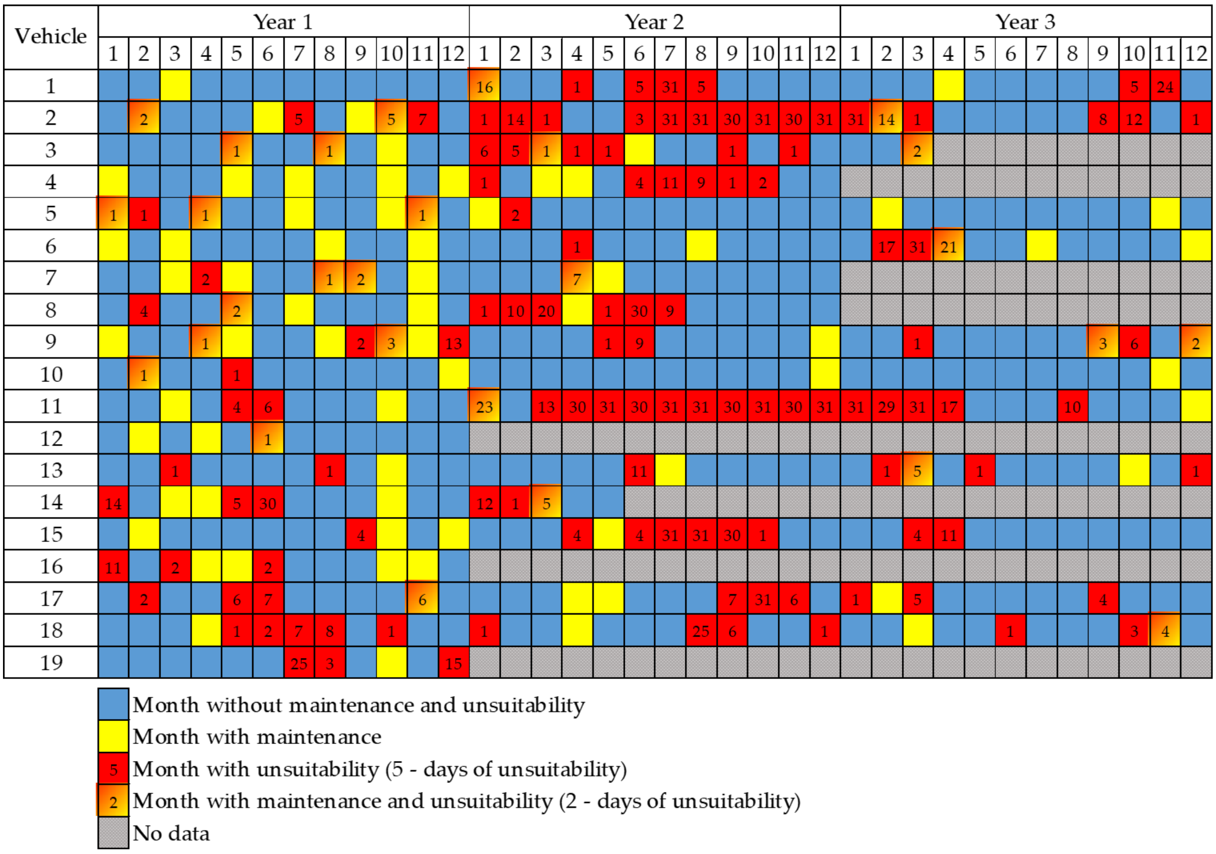

Figure 3. Graphical visualization of database.

Table 2. Estimation of distribution parameters.

Variable	**Distribution**	**Equation**	**Parameters**	R^2
T_{12}	Exponential	$F_{12}(t) = 1 - e^{-\lambda_{12}t}$	$\lambda_{12} = 1.33\times10^{-5}$	0.9909
T_{13}	Exponential	$F_{13}(t) = 1 - e^{-\lambda_{13}t}$	$\lambda_{13} = 1.07\times10^{-5}$	0.9961
T_{21}	Gamma	$F_{21}(t) = \frac{1}{\Gamma(k_{21})}\gamma\left(k_{21}, \frac{t}{\theta_{21}}\right)$	$k_{21} = 4$ $\theta_{21} = 65.85$	0.9630
T_{31}	Exponential	$F_{31}(t) = 1 - e^{-\lambda_{31}t}$	$\lambda_{31} = 4.67\times10^{-5}$	0.8560
T_{32}	Exponential	$F_{32}(t) = 1 - e^{-\lambda_{32}t}$	$\lambda_{32} = 1.46\times10^{-4}$	0.8662

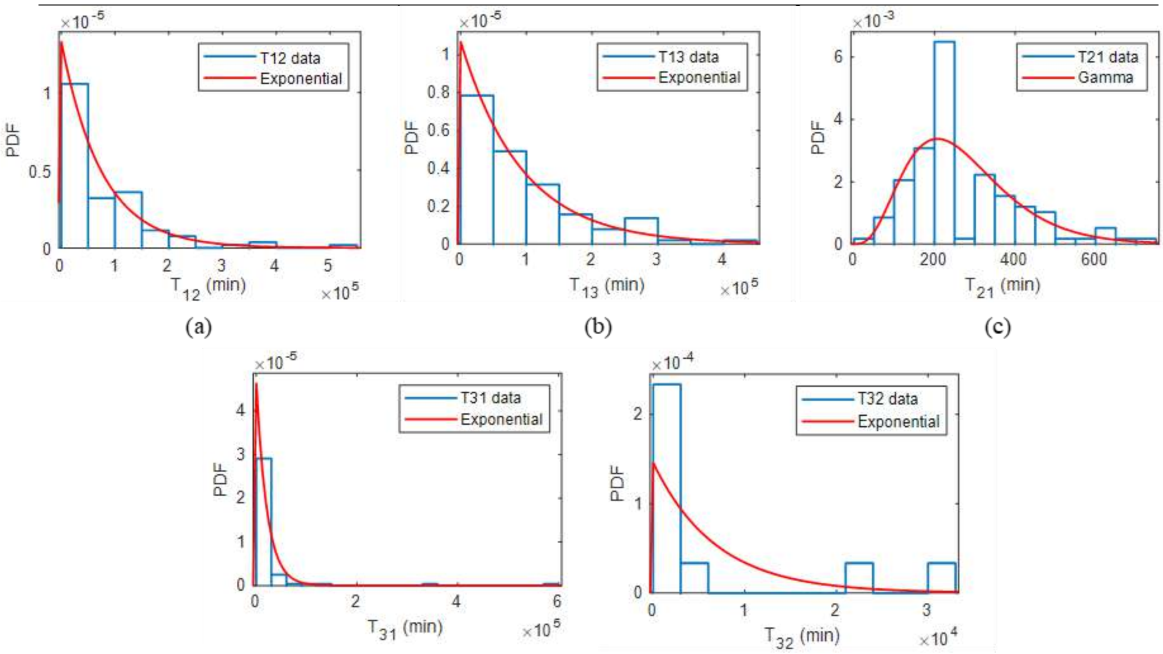

(d) (e)

Figure 4. PDFs of the time of sojourn T_{ij} in state S_i before transitioning to state S_j: (a) – T_{12}, (b) – T_{13}, (c) – T_{21}, (d) – T_{31}, (e) – T_{32}.

4.3. Reliability assessment of light utility vehicles

Based on empirical data and the estimated parameters of the 3-state semi-Markov model, calculations were performed according to the dependencies presented in Section 3 to assess the reliability characteristics of light utility vehicles. The reliability function $R(t)$ was determined using Equation (17), assuming that a vehicle at time $t = 0$ is in one of the technical suitability states, namely, S_1 or S_2. In the case of such initial conditions, the form of the square matrix $\tilde{\boldsymbol{q}}_{A'}(s)$ is shown by the formula (40). While single-column matrices $\tilde{\boldsymbol{\phi}}_{A'}(s)$ and $\tilde{\boldsymbol{b}}(s)$ are consistent with formulas (41) and (42).

$$\tilde{\mathbf{q}}_{A'}(s) = \begin{bmatrix} 0 & \tilde{q}_{12}(s) \\ \tilde{q}_{21}(s) & 0 \end{bmatrix}, \tag{40}$$

$$\tilde{\boldsymbol{\Phi}}_{A'}(s) = \begin{bmatrix} \tilde{\phi}_{13}(s) \\ \tilde{\phi}_{23}(s) \end{bmatrix}, \tag{41}$$

$$\tilde{\mathbf{b}}(s) = \begin{bmatrix} \tilde{q}_{13}(s) \\ 0 \end{bmatrix}. \tag{42}$$

Substituting the aforementioned dependencies into formula (17) provided the equation:

$$\begin{bmatrix} 1 & -\tilde{q}_{12}(s) \\ -\tilde{q}_{21}(s) & 1 \end{bmatrix} \cdot \begin{bmatrix} \tilde{\phi}_{13}(s) \\ \tilde{\phi}_{23}(s) \end{bmatrix} = \begin{bmatrix} \tilde{q}_{13}(s) \\ 0 \end{bmatrix}. \tag{43}$$

Using Mathematica software, the authors obtained the solutions to Equation (43), which are the values of the variables $\tilde{\phi}_{13}(s)$ and $\tilde{\phi}_{23}(s)$ presented using the formula (44):

$$\begin{cases} \tilde{\phi}_{13}(s) = \frac{\tilde{q}_{13}(s)}{1-\tilde{q}_{12}(s)\tilde{q}_{21}(s)} \\ \tilde{\phi}_{23}(s) = \frac{\tilde{q}_{13}(s)\tilde{q}_{21}(s)}{1-\tilde{q}_{12}(s)\tilde{q}_{21}(s)} \end{cases}. \tag{44}$$

Solutions to Equation (42) are Laplace transforms of the density function of the probability of the first transition from states S_1 and S_2, respectively, to the state of technical unsuitability S_3. The probability of a transition from any given time t to state S_3 depends on the initial state of the process. Therefore, the form of the reliability function also depends on the initial state. The authors adopted the designation of the reliability function $R_1(t)$ for an object that stayed at time $t = 0$ in state S_1 and $R_2(t)$ for the initial state S_2. The Laplace transforms $\tilde{R}_1(s)$ and $\tilde{R}_2(s)$ for the reliability functions $R_1(t)$ and $R_2(t)$, respectively, have been determined using the dependence (45):

$$\begin{cases} \tilde{R}_1(s) = \frac{1-\tilde{\phi}_{13}(s)}{s} = \frac{1-\tilde{q}_{12}(s)\tilde{q}_{21}(s)-\tilde{q}_{13}(s)}{s(1-\tilde{q}_{12}(s)\tilde{q}_{21}(s))} \\ \tilde{R}_2(s) = \frac{1-\tilde{\phi}_{23}(s)}{s} = \frac{1-(\tilde{q}_{12}(s)+\tilde{q}_{13}(s))\tilde{q}_{21}(s)}{s(1-\tilde{q}_{12}(s)\tilde{q}_{21}(s))}, \end{cases} \tag{45}$$

while transforms $\tilde{q}_{ij}(s)$ are expressed through formulas (46):

$$\begin{cases} \tilde{q}_{12}(s) = p_{12}\left(\frac{\lambda_{12}}{s+\lambda_{12}}\right) \\ \tilde{q}_{13}(s) = p_{13}\left(\frac{\lambda_{13}}{s+\lambda_{13}}\right) \\ \tilde{q}_{21}(s) = p_{21}\left(\frac{1}{1+\theta_{21}s}\right)^{k_{21}} \\ \tilde{q}_{31}(s) = p_{31}\left(\frac{\lambda_{31}}{s+\lambda_{31}}\right) \\ \tilde{q}_{32}(s) = p_{32}\left(\frac{\lambda_{32}}{s+\lambda_{32}}\right) \end{cases}. \tag{46}$$

In turn, $q_{ij}(t)$ values for the analysed case study have been determined as dependencies (47):

$$\begin{cases} q_{12}(t) = p_{12}\lambda_{12}e^{-\lambda_{12}t} \\ q_{13}(t) = p_{13}\lambda_{13}e^{-\lambda_{12}t} \\ q_{21}(t) = p_{21}\frac{1}{\Gamma(k_{21})\theta_{21}{}^{k_{21}}}t^{k_{21}-1}e^{-\frac{t}{\theta_{21}}} \\ q_{31}(t) = p_{31}\lambda_{31}e^{-\lambda_{31}t} \\ q_{32}(t) = p_{32}\lambda_{32}e^{-\lambda_{32}t} \end{cases}. \tag{47}$$

After substituting estimated values of the time characteristic distribution parameters for the semi-Markov process, the authors determined the formulas of the reliability functions $R_1(t)$ and $R_2(t)$ in the time domain t, using the inverse Laplace transforms of the functions $\tilde{R}_1(s)$ and $\tilde{R}_2(s)$:

$$\begin{aligned} &R_1(t) = \mathcal{L}^{-1}\{\tilde{R}_1\}(t) = \\ &(8.2271 \times 10^{-6} + 5.2308 \times 10^{-6}i)e^{(-0.01674170-0.00148814i)t} \\ &+(8.2271 \times 10^{-6} - 5.2308 \times 10^{-6}i)e^{(-0.01674170+0.00148814i)t} \\ &-(7.4578 \times 10^{-6} - 1.4309 \times 10^{-5}i)e^{(-0.01363380-0.00164869i)t} \\ &-(7.4578 \times 10^{-6} + 1.4309 \times 10^{-5}i)e^{(-0.01363380+0.00164869i)t} \\ &-0.3032e^{-0.00001070t} + 1.3032e^{-6.50536\times10^{-6}t} \\ &-2.0773 \times 10^{-16}, \end{aligned} \tag{48}$$

$$\begin{aligned} &R_2(t) = \mathcal{L}^{-1}\{\tilde{R}_2\}(t) = \\ &-(0.0194 + 0.0147i)e^{(-0.01674170-0.00148814i)t} \\ &-(0.0194 - 0.0147i)e^{(-0.01674170+0.00148814i)t} \\ &+(0.0185 - 0.0269i)e^{(-0.01363380-0.00164869i)t} \\ &+(0.0185 + 0.0269i)e^{(-0.01363380+0.00164869i)t} \\ &-0.3040e^{-0.0000107t} + 1.3054e^{-6.50536\times10^{-6}t} \\ &-2.0773 \times 10^{-16}. \end{aligned} \tag{49}$$

Fig. 5 shows graphical waveforms of the reliability functions $R_1(t)$ and $R_2(t)$ for the range of $0 - 10^6$ (min). They satisfy the assumptions about the monotonicity of the reliability function. The function limit at infinity is -2.0773×10^{-16}, which is a value negligibly different from zero.

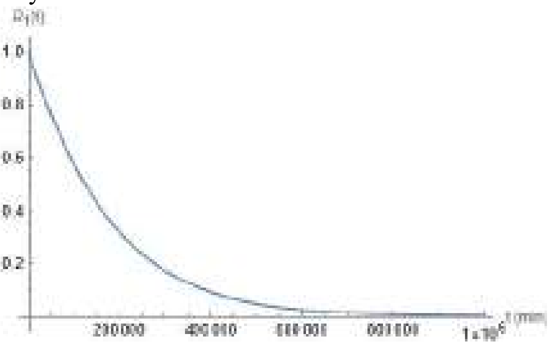

(a)

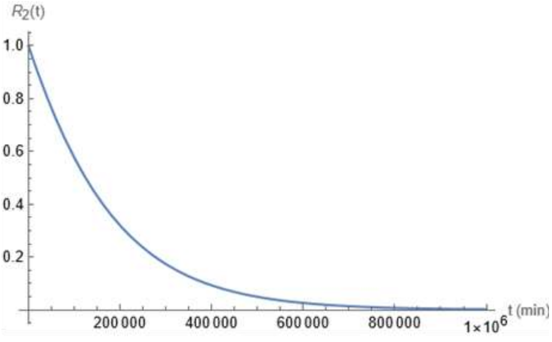

(b)

Figure 5. Reliability functions: (a) – $R_1(t)$, (b) – $R_2(t)$.

Fig. 6 shows the difference in the values between the determined reliability functions $R_1(t)$ and $R_2(t)$ for the time domain range of 0 to 10^6 (min). The maximum observed difference in this value does not exceed 0.0014, which means almost identical waveforms of both reliability functions for the analysed time interval. This conclusion prompts the selection of one function as a basis for further reliability analyses. Due to the operational strategy in military transport systems assuming the assignment of fully operational vehicles to the system, it was assumed that at time $t = 0$ the technical object under study was in the S_1 state. This implies determining the remaining reliability characteristics based on the reliability function $R_1(t)$.

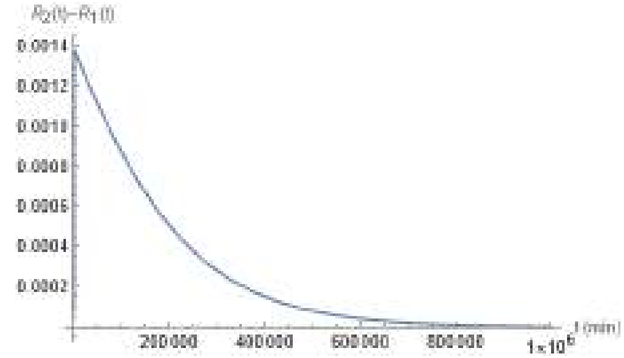

Figure 6. Difference value between reliability functions: $R_2(t) - R_1(t)$.

The failure probability density function $f(t)$ and the failure intensity function $\lambda(t)$ are identity reliability characteristics, which are related to the probability of a failure at a given time t. The function $f(t)$ defines the failure probabilities at time t [34] per unit of time. The probability calculus defines that the failure occurrence density $f(t)$ is a derivative of the unreliability function $F(t)$, as demonstrated by dependence:

$$f(t) = \frac{dF(t)}{dt} = \frac{d(1-R(t))}{dt}. \qquad (50)$$

After substituting the function $R_1(t)$ into the formula (50), the authors obtained the following $f_1(t)$:

$$\begin{aligned} f_1(t) = {} & (1.2995 \times 10^{-7} + 9.9815 \times 10^{-8} i)e^{(-0.01674169-0.00148813i)t} + \\ & (1.2995 \times 10^{-7} - 9.9815 \times 10^{-8} i)e^{(-0.01674169+0.00148813i)t} - \\ & (1.2527 \times 10^{-7} + 1.8279 \times 10^{-7} i)e^{(-0.01363376+0.00164869i)t} - \\ & (1.2527 \times 10^{-7} - 1.8279 \times 10^{-7} i)e^{(-0.01363376-0.001648692i)t} - \\ & (3.2440 \times 10^{-6} + 4.6129 \times 10^{-22} i)e^{-0.00001070t} + \\ & (8.4776 \times 10^{-6} + 1.6602 \times 10^{-21} i)e^{-0.00000651t} \end{aligned} \qquad (51)$$

Whereas the function $\lambda(t)$ defines the value of conditional probability for a technical object failure at time t, provided that it was not damaged during the interval $(0, t)$. According to the properties of conditional probability, the value of function $\lambda(t)$ at time t is expressed through the formula (52):

$$\lambda(t) = \frac{f(t)}{R(t)}. \qquad (52)$$

After substituting the function $R_1(t)$ and $f_1(t)$ into the formula (52), the authors obtained the following form of function $\lambda_1(t)$:

$$\lambda_1(t) = \begin{pmatrix} (1.2995 \times 10^{-7} + 9.9815 \times 10^{-8} i)e^{(-0.01674169-0.00148813i)t} + \\ (1.2995 \times 10^{-7} - 9.9815 \times 10^{-8} i)e^{(-0.01674169+0.00148813i)t} - \\ (1.2527 \times 10^{-7} + 1.8279 \times 10^{-7} i)e^{(-0.01363376+0.00164869i)t} - \\ (1.2527 \times 10^{-7} - 1.8279 \times 10^{-7} i)e^{(-0.01363376-0.001648692i)t} - \\ (3.2440 \times 10^{-6} + 4.6129 \times 10^{-22} i)e^{-0.00001070t} + \\ (8.4776 \times 10^{-6} + 1.6602 \times 10^{-21} i)e^{-0.00000651t} \end{pmatrix} \Big/ \begin{pmatrix} (8.2271 \times 10^{-6} + 5.2308 \times 10^{-6} i)e^{(-0.01674170-0.00148814i)t} + \\ (8.2271 \times 10^{-6} - 5.2308 \times 10^{-6} i)e^{(-0.01674170+0.00148814i)t} - \\ (7.4578 \times 10^{-6} - 1.4309 \times 10^{-5} i)e^{(-0.01363380-0.00164869i)t} - \\ (7.4578 \times 10^{-6} + 1.4309 \times 10^{-5} i)e^{(-0.01363380+0.00164869i)t} - \\ 0.3032e^{-0.00001070t} + 1.3032e^{-6.50536\times 10^{-6}t} - 2.0773 \times 10^{-16} \end{pmatrix}. \qquad (53)$$

Function waveforms $f_1(t)$ and $\lambda_1(t)$ have been graphically presented using graphs within the time domain range of 0 – 10^6 (min) in Fig. 7. The function $f_1(t)$ decreases and asymptotically tends to 0, while function $\lambda_1(t)$ is increasing and stabilizes at a level of approximately 6.5×10^{-6} (min^{-1}) after 5×10^5 (min).

The mean time to failure (*MTTF*) is an important measure of the reliability of technical objects that defines the correct operating time of the vehicle. It is determined as a definite integral of the reliability function, within a range from 0 to ∞, which is expressed in mathematical notation by equation (54):

$$MTTF = \int_0^\infty t \cdot f(t)dt = \int_0^\infty R(t)dt. \qquad (54)$$

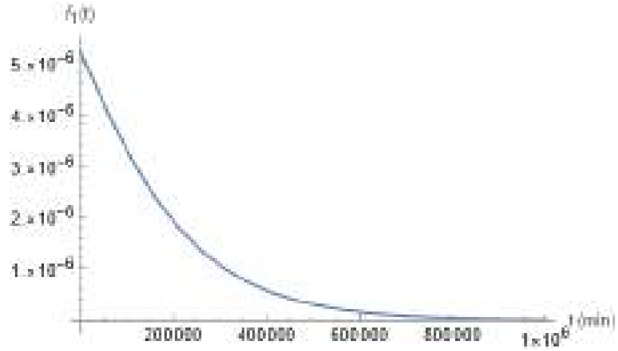

(a)

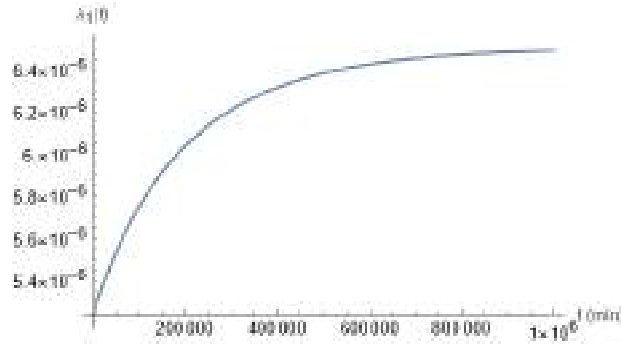

(b)

Figure 7. Reliability characteristics: (a) – PDF of failure $f_1(t)$, (b) – intensity of failure $\lambda_1(t)$.

In the analysed case study of light utility vehicles, the calculated *MTTF* based on the base of the $R_1(t)$ function is 171,989.0 (min). Converted to calendar days, this amounts to a value of 119.44 (days).

4.4. Readiness and suitability

According to the methodology adopted to determine vehicle readiness and suitability indices, the authors studied the developed 3-state semi-Markov model. The conditional probability matrix $\tilde{\boldsymbol{p}}(s)$ in the domain of the Laplace operator s is calculated using equation (55):

$$\tilde{\mathbf{p}}(s) = \frac{1}{s}\left(\mathbf{I} - \tilde{\mathbf{q}}(s)\right)^{-1}\left(\mathbf{I} - \tilde{\mathbf{h}}(s)\right), \tag{55}$$

where elements of the matrix $\tilde{\boldsymbol{q}}(s)$ are represented by the formula (46), while non-zero elements of the matrix $\tilde{\boldsymbol{h}}(s)$ have been determined based on systems of equations (56) and (57):

$$\begin{cases} G_1(t) = Q_{12}(t) + Q_{13}(t) = p_{12}\left(1 - e^{-\lambda_{12}t}\right) + p_{13}\left(1 - e^{-\lambda_{13}t}\right) \\ G_2(t) = Q_{21}(t) = p_{21}\frac{1}{\Gamma(k_{21})}\gamma\left(k_{21}, \frac{t}{\theta_{21}}\right) \\ G_3(t) = Q_{31}(t) + Q_{32}(t) = p_{31}\left(1 - e^{-\lambda_{31}t}\right) + p_{32}\left(1 - e^{-\lambda_{32}t}\right) \end{cases} \tag{56}$$

$$\begin{cases} h_{11}(t) = g_1(t) = \frac{dG_1(t)}{dt} = p_{12}\lambda_{12}e^{-\lambda_{12}t} + p_{13}\lambda_{13}e^{-\lambda_{13}t} \\ h_{22}(t) = g_2(t) = \frac{dG_2(t)}{dt} = p_{21}\frac{1}{\Gamma(k_{21})\theta_{21}{}^{k_{21}}}t^{k_{21}-1}e^{-\frac{t}{\theta_{21}}} \\ h_{33}(t) = g_3(t) = \frac{dG_3(t)}{dt} = p_{31}\lambda_{31}e^{-\lambda_{31}t} + p_{32}\lambda_{32}e^{-\lambda_{32}t} \end{cases} \tag{57}$$

and take the form consistent with the set of equations (58):

$$\begin{cases} \tilde{h}_{11}(s) = \mathcal{L}\{h_{11}\}(s) = p_{12}\left(\frac{\lambda_{12}}{s+\lambda_{12}}\right) + p_{13}\left(\frac{\lambda_{13}}{s+\lambda_{13}}\right) \\ \tilde{h}_{22}(s) = \mathcal{L}\{h_{22}\}(s) = p_{21}\left(\frac{1}{1+\theta_{21}s}\right)^{k_{21}} \\ \tilde{h}_{33}(s) = \mathcal{L}\{h_{33}\}(s) = p_{31}\left(\frac{\lambda_{31}}{s+\lambda_{31}}\right) + p_{32}\left(\frac{\lambda_{32}}{s+\lambda_{32}}\right) \end{cases} \tag{58}$$

The elements of the values of the conditional probability matrix in the time domain t are calculated as the inverse Laplace transform of matrix elements $\tilde{\boldsymbol{p}}(s)$, as demonstrated by the formula (59):

$$\mathrm{p}(t) = \mathcal{L}^{-1}\{\tilde{\mathrm{p}}\}(t). \tag{59}$$

Instantaneous probabilities of a technical object staying in individual states are determined as a product of the initial distribution vector and conditional probability matrices for the semi-Markov process. It was assumed that at time $t = 0$ a vehicle was in full technical suitability, therefore, it remained in state S_1. The initial distribution vector $\boldsymbol{p}_j(0)$, which describes the assumed adopted, has been presented using formula (60):

$$\mathbf{p}_j(0) = [1 \quad 0 \quad 0]. \tag{60}$$

Fig. 8 shows the waveform of changes in the values of instantaneous probabilities $p_j(t)$ over the range from 0 to 5×10^5 (min). After 10^5 (min), the value stabilizes, and the probabilities $p_j(t)$ tend to ergodic values.

The approximate values of instantaneous probabilities $p_1(t)$, $p_2(t)$ and $p_3(t)$ are represented by formulas (61-63):

$$\begin{aligned} p_1(t) &= 0.0912e^{-0.00005131t} + 0.0177e^{-0.00001486t} + 0.0226e^{-0.00001233t} + 0.8667e^{9.84533644\times10^{-22}t} + \\ &e^{(-0.01674167-0.00148812i)t}\left((0.0248 + 0.0190i) + (0.0248 - 0.0190i)e^{0.00297623it}\right) + \\ &e^{(-0.01363379-0.00164865i)t}\left((-0.0239 + 0.0349i) - (0.0239 + 0.0349i)e^{(0.00329731i)t}\right), \end{aligned} \tag{61}$$

$$\begin{aligned} p_2(t) &= 0.7277 + 1.6486\times10^{-4}e^{-0.00005131t} - 2.8573\times10^{-5}e^{-0.00001486t} + 1.3228\times10^{-4}e^{-0.00001233t} - \\ &0.7262e^{9.84533644\times10^{-22}t} + e^{(-0.016741665-0.00148811i)t}\left((-0.0248 - 0.0190i) - (0.0248 - 0.0190i)e^{(0.00329731i)t}\right) + \\ &e^{(-0.01363379-0.00164865i)t}\left((0.0239 - 0.0349i) + (0.0239 + 0.0349i)e^{(0.00329731i)t}\right), \end{aligned} \tag{62}$$

$$p_3(t) = 5.2430\times10^{-6}\begin{pmatrix} -148274.1947 - 17434.5692e^{-0.00005131t} - 3349.5998e^{-0.00001486t} - \\ 4360.4149e^{-0.00001233t} + 173419.0738e^{9.84533644\times10^{-22}t} + \\ e^{(-0.01674167i)t}\left((-1.5734 - 0.9999i) - (1.5734 - 0.9999i)e^{(0.00297623i)t}\right) + \\ e^{(-0.01363379-0.00164865i)t}\left((1.4259 - 2.7382i) + (1.4259 + 2.7382i)e^{(0.00329731i)t}\right) \end{pmatrix}. \tag{63}$$

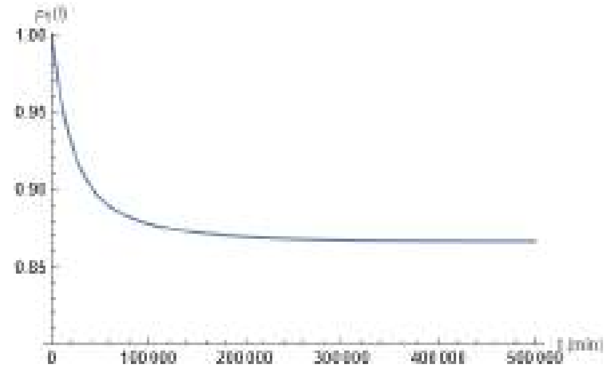

(a)

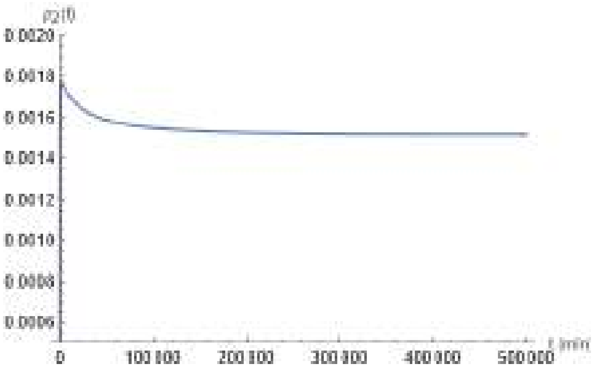

(b)

Figure 8. Instantaneous probabilities of states: (a) – $p_1(t)$, (b) – $p_2(t)$, (c) – $p_3(t)$.

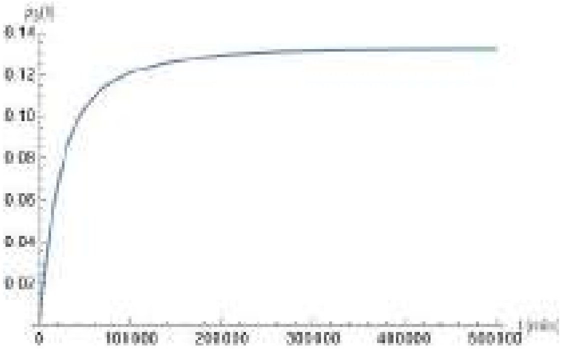

(c)

Figure 8. (continued)

Dependence (31) was used to determine the ergodic probabilities π_j for an embedded Markov chain. The dependence, after substituting appropriate values for the developed model, adopted the form of a matrix equation (64):

$$\left(\begin{bmatrix} 0 & p_{12} & p_{13} \\ p_{21} & 0 & 0 \\ p_{31} & p_{32} & 0 \end{bmatrix}^{\mathrm{T}} - \begin{bmatrix} 1 & 0 & 0 \\ 0 & 1 & 0 \\ 0 & 0 & 1 \end{bmatrix}\right) \cdot \begin{bmatrix} \pi_1 \\ \pi_2 \\ \pi_3 \end{bmatrix} = \begin{bmatrix} 0 \\ 0 \\ 0 \end{bmatrix}, \qquad (64)$$

assuming that the sum π_j is equal to 1.

The solution of Equation (64) is shown in Table 3. Based on Equation (35), the authors calculated the expected durations for the vehicle to stay in individual operational states. The system should tend to maximize the duration of the S_1 state. The time $E(T_2)$ depends on the adopted periodic maintenance strategy, the scope of maintenance activities, and the technical capabilities of the system. The S_3 state is undesirable, since it reduces the capabilities of a transport system, and, thus, tends to minimize its duration.

Table 3. Ergodic probabilities of embedded Markov chain and semi-Markov process.

	S_1	S_2	S_3
π_j	0.4882	0.2750	0.2368
$E(T_j)$ (min)	84140.3	263.4	26121.3
$E(T_j)$ (days)	58.43	0.18	18.14
p_j	0.8678	0.0015	0.1307

Probabilities π_j and the expected times $E(T_j)$ were used to determine the ergodic probabilities of the semi-Markov process p_j. They are the basis for calculating technical suitability and readiness indices.

Readiness means that a vehicle reamins in the S_1 state and the value of the readiness coefficient corresponds to the ergodic probability $p_1 = 0.8678$. In turn, the set $\{S_1, S_2\}$ is a subset of the technical suitability states, which implies a value of the technical suitability coefficient equal to $p_1+p_2 = 0.8693$.

5. Conclusions

The operational process of light utility vehicles was modelled using the semi-Markov process theory. The phase space was identified on the basis of the analysis of the empirical waveform of operation and previously developed models. The 9-state model was aggregated into 3 main operational states. S_1 – operation, S_2 – periodic maintenance, S_3 – unsuitability. Based on actual data acquired from a military transport system, the authors estimated the values of interstate transition conditional probability matrices of an embedded Markov chain and matched time characteristic distribution functions. The standard estimation errors of the $SE(p_{ij})$ probabilities and the determination coefficient R^2 between the empirical and theoretical distribution functions obtained values that were satisfactory from the engineering applicability perspective. Given all the above, it can be concluded that the 3-state semi-Markov model is a credible representation of the studied military vehicle operation process. Reliability functions were determined as complements to the variable distribution function Θ_A, which denotes the time of the first transition to the subset of unsuitable states. The considerations were carried out under two assumptions regarding a technical object that remained at time $t = 0$ in states S_1 and S_2, respectively. Based on the graph showing the difference between functions $R_1(t)$ and $R_2(t)$, it was concluded that the waveform of the reliability function negligibly depends on the initial state of the operation process (assuming that this state belongs to a subset of states of technical suitability). The reliability function was used to determine other characteristics of the objects studied, that is, the failure probability density function and the failure intensity. The analytical form of the determined characteristics was not directly interpreted. However, using advanced IT software, the authors obtained their graphical form, which facilitated the interpretation of results in the form of dependence graphs in the time domain. The failure probability density function is decreasing, while the failure intensity is increasing, and stabilizes after 5×10^5 (min) at a level of approx. 6.5×10^{-6} (min^{-1}). The expected time to failure was calculated using a definite integral reliability function in the range from 0 to ∞ and amounted to approx. 119.44 (days).

The final stage of the research involved determining instantaneous probabilities that a vehicle would remain in the operational state. The solution of a matrix equation in the domain of the Laplace operator s, followed by the implementation of an inverse Laplace transform, allowed us to obtain the analytical form of instantaneous probabilities $p_j(t)$ in the time domain t. Based on graphical interpretations, the authors concluded that the process stabilizes after a time of approximately 10^5 (min). The ergodic probabilities of the semi-Markov process have been determined using the ergodic probabilities of the embedded Markov chain and values of expected times of residence in operational states. The vehicle technical suitability and readiness indices adopted values of 0.8678 and 0.8693, respectively, which, however, compared to the 9-state model [33] means a reduction of approximately 4.6%. Therefore, the 3-state model is a less accurate reflection of the actual operation process. However, it significantly reduces and simplifies the computations performed in relation to reliability analyses.

The proposed approach enables a comprehensive reliability analysis of technical systems and objects for a multi-state phase space of the operation process. This paper presents all the stages of developing a semi-Markov model, its validation, and its application to determine the most important reliability characteristics and readiness indices of an object. In turn, the potential for further research directions may be the employing of a 3-state semi-Markov model to optimize the periodic maintenance and repair process.

Acknowledgements
This research was funded by the Military University of Technology, grant number UGB 835/2023.

Author Contributions
Conceptualization, M.O.; methodology, M.O. and J.Z.; software, M.O.; validation, M.O.; formal analysis, M.O.; investigation, M.O.; resources, M.O. and J.Z.; data curation, M.O. and J.Z.; writing—original draft preparation, M.O.; writing—review and editing, M.O., J.Z. and J.M.; visualization, M.O.; supervision, J.Z. and J.M.; project administration, M.O., J.Z. and J.M.; funding acquisition, J.M. All authors have read and agreed to the published version of the manuscript.

References:
1. Alkaff A, Qomarudin M N, Purwantini E, Wiratno S E. Dynamic reliability modeling for general standby systems. Computers & Industrial Engineering 2021; 161: 1–21, https://doi.org/10.1016/j.cie.2021.107615.
2. Bai B, Zhang J, Wu X et al. Reliability prediction-based improved dynamic weight particle swarm optimization and back propagation neural network in engineering systems. Expert Systems with Applications 2021; 177: 1–13, https://doi.org/10.1016/j.eswa.2021.114952.
3. Barbu V S, D'Amico G, Gkelsinis T. Sequential Interval Reliability for Discrete-Time Homogeneous Semi-Markov Repairable Systems. Mathematics 2021; 9(16): 1997, https://doi.org/10.3390/math9161997.
4. Blasi A, Janssen J, Manca R. Numerical Treatment of Homogeneous and Non-homogeneous Semi-Markov Reliability Models. Communications in Statistics - Theory and Methods 2004; 33(3): 697–714, https://doi.org/10.1081/STA-120028692.
5. Borucka A, Niewczas A, Hasilova K. Forecasting the readiness of special vehicles using the semi-Markov model. Eksploatacja i Niezawodnosc - Maintenance and Reliability 2019; 21(4): 662–669, https://doi.org/10.17531/ein.2019.4.16.
6. Brayer E F. Calculating the Standard Error of a Proportion. Applied Statistics 1957; 6(1): 67–68, https://doi.org/10.2307/2985858.
7. Chang K-H. A novel reliability allocation approach using the OWA tree and soft set. Annals of Operations Research 2016; 244(1): 3–22, https://doi.org/10.1007/s10479-016-2178-4.
8. Chryssaphinou O, Limnios N, Malefaki S. Multi-State Reliability Systems Under Discrete Time Semi-Markovian Hypothesis. IEEE Transactions on Reliability 2011; 60(1): 80–87, https://doi.org/10.1109/TR.2010.2104210.
9. D'Amico G. Single-use reliability computation of a semi-Markovian system. Applications of Mathematics 2014; 59(5): 571–588, https://doi.org/10.1007/s10492-014-0072-4.
10. Dobrzinskij N, Fedaravicius A, Pilkauskas K, Slizys E. Impact of climatic conditions on the parameters of failure flow of military vehicles. Proceedings of the Institution of Mechanical Engineers, Part D: Journal of Automobile Engineering 2021; 236(4): 753–762, https://doi.org/10.1177/09544070211020228.
11. Du Y, Wu G, Tang Y, Liu S. A two-stage reliability allocation method for remanufactured machine tools integrating neural networks and remanufacturing coefficient. Computers & Industrial Engineering 2022; 163: 1–12, https://doi.org/10.1016/j.cie.2021.107834.
12. Fang L, Tarasiuk T, Xia J, Xu X-Y. Reliability assessment of the port power system based on integrated energy hybrid system. Bulletin of the Polish Academy of Sciences: Technical Sciences 2022; 70(2): e140372.
13. Grabski F. Semi-Markov failure rates processes. Applied Mathematics and Computation 2011; 217(24): 9956–9965, https://doi.org/10.1016/j.amc.2011.04.055.
14. Guo J, Wilson A G. Bayesian Methods for Estimating System Reliability Using Heterogeneous Multilevel Information. Technometrics 2013; 55(4): 461–472, https://doi.org/10.1080/00401706.2013.804441.
15. Gurland J, Tripathi R C. A Simple Approximation for Unbiased Estimation of the Standard Deviation. The American Statistician 1971; 25(4): 30–32, https://doi.org/10.2307/2682923.
16. Hao S, Yang J, Ma X, Zhao Y. Reliability modeling for mutually dependent competing failure processes due to degradation and random shocks. Applied Mathematical Modelling 2017; 51: 232–249, https://doi.org/10.1016/j.apm.2017.06.014.
17. Hong L, Zhai Q, Wang X, Ye Z-S. System Reliability Evaluation Under Dynamic Operating Conditions. IEEE Transactions on Reliability 2019; 68(3): 800–809, https://doi.org/10.1109/TR.2018.2869572.
18. Hu J, Shen J, Shen L. Periodic preventive maintenance planning for systems working under a Markovian operating condition. Computers & Industrial Engineering 2020; 142: 106291, https://doi.org/10.1016/j.cie.2020.106291.
19. Ivanchenko O, Kharchenko V, Moroz B et al. Semi-Markov availability model considering deliberate malicious impacts on an Infrastructure-as-a-Service Cloud. 2018 14th International Conference on Advanced Trends in Radioelecrtronics, Telecommunications and Computer Engineering (TCSET), 2018: 570–573, https://doi.org/10.1109/TCSET.2018.8336266.
20. Iversen E B, Morales J M, Madsen H. Optimal charging of an electric vehicle using a Markov decision process. Applied Energy 2014; 123: 1–12, https://doi.org/10.1016/j.apenergy.2014.02.003.
21. Karakaya E, Vinel A, Smith A E. Relocations in container depots for different handling equipment types: Markov models. Computers & Industrial Engineering 2021; 157: 1–18, https://doi.org/10.1016/j.cie.2021.107311.
22. Kou L, Chu B, Chen Y, Qin Y. An Automatic Partition Time-Varying Markov Model for Reliability Evaluation. Applied Sciences 2022; 12(12): 5933, https://doi.org/10.3390/app12125933.
23. Li X, Zhao X, Pu W. Knowledge-oriented modeling for influencing factors of battle damage in military industrial logistics: An integrated method. Defence Technology 2020; 16(3): 571–587, https://doi.org/10.1016/j.dt.2019.09.001.
24. Liu P, Wang G. Optimal periodic preventive maintenance policies for systems subject to shocks. Applied Mathematical Modelling 2021; 93: 101–114, https://doi.org/10.1016/j.apm.2020.12.013.
25. Lolas S, Olatunbosun O A. Prediction of vehicle reliability performance using artificial neural networks. Expert Systems with Applications 2008; 34(4): 2360–2369, https://doi.org/10.1016/j.eswa.2007.03.014.
26. Lyu H, Yang Z, Wang S et al. Reliability modeling for multistage systems subject to competing failure processes. Quality and Reliability Engineering International 2021; 37(6): 2936–2949, https://doi.org/10.1002/qre.2898.
27. Macheret Y, Koehn P, Sparrow D. Improving reliability and operational availability of military systems. 2005 IEEE Aerospace Conference, Big Sky, Montana, USA, IEEE Operations Center: 2005: 3948–3957, https://doi.org/10.1109/AERO.2005.1559700.
28. Mengistu T M, Che D, Alahmadi A, Lu S. Semi-Markov Process Based Reliability and Availability Prediction for Volunteer Cloud Systems. 2018 IEEE 11th International Conference on Cloud Computing (CLOUD), San Francisco, CA, USA, IEEE: 2018: 359–366, https://doi.org/10.1109/CLOUD.2018.00052.
29. Migawa K. Availability control for means of transport in decisive semi-markov models of exploitation process. Archives of Transport 2012;

24(4): 497–508, https://doi.org/10.2478/v10174-012-0030-4.
30. Migawa K, Borowski S, Neubauer A, Sołtysiak A. Semi-Markov Model of the System of Repairs and Preventive Replacements by Age of City Buses. Applied Sciences 2021; 11(21): 10411, https://doi.org/10.3390/app112110411.
31. Miziuła P, Navarro J. Birnbaum Importance Measure for Reliability Systems With Dependent Components. IEEE Transactions on Reliability 2019; 68(2): 439–450, https://doi.org/10.1109/TR.2019.2895400.
32. Oniszczuk W. Loss tandem networks with blocking - a semi-Markov approach. Bulletin of the Polish Academy of Sciences: Technical Sciences; 2010; 58; No 4; 673-681 2010; 58(4): 673–681, https://doi.org/10.2478/v10175-010-0072-9.
33. Oszczypała M, Ziółkowski J, Małachowski J. Analysis of Light Utility Vehicle Readiness in Military Transportation Systems Using Markov and Semi-Markov Processes. Energies 2022; 15(14): 5062, https://doi.org/10.3390/en15145062.
34. Oszczypała M, Ziółkowski J, Małachowski J. Reliability Analysis of Military Vehicles Based on Censored Failures Data. Applied Sciences 2022; 12(5): 1–25, https://doi.org/10.3390/app12052622.
35. Papadopoulos C T, Li J, O'Kelly M E J. A classification and review of timed Markov models of manufacturing systems. Computers & Industrial Engineering 2019; 128: 219–244, https://doi.org/10.1016/j.cie.2018.12.019.
36. Park M, Jung K M, Park D H. Optimization of periodic preventive maintenance policy following the expiration of two-dimensional warranty. Reliability Engineering & System Safety 2018; 170: 1–9, https://doi.org/10.1016/j.ress.2017.10.009.
37. Rafiee K, Feng Q, Coit D W. Reliability assessment of competing risks with generalized mixed shock models. Reliability Engineering & System Safety 2017; 159: 1–11, https://doi.org/10.1016/j.ress.2016.10.006.
38. Rajarshi M B. Statistical Inference for Discrete Time Stochastic Processes. India, Springer India: 2013. doi:10.1007/978-81-322-0763-4, https://doi.org/10.1007/978-81-322-0763-4.
39. Rosychuk R J, Sheng X, Stuber J L. Comparison of variance estimation approaches in a two-state Markov model for longitudinal data with misclassification. Statistics in Medicine 2006; 25(11): 1906–1921, https://doi.org/10.1002/sim.2367.
40. Roy V, Tan A, Flegal J M. Estimating standard errors for importance sampling estimators with multiple markov chains. Statistica Sinica 2018; 28(2): 1079–1101, https://doi.org/10.5705/ss.202016.0378.
41. Rychlicki M, Kasprzyk Z, Rosiński A. Analysis of Accuracy and Reliability of Different Types of GPS Receivers. Sensors 2020; 20(22): 6498, https://doi.org/10.3390/s20226498.
42. Şahin İ. Markov chain model for delay distribution in train schedules: Assessing the effectiveness of time allowances. Journal of Rail Transport Planning & Management 2017; 7(3): 101–113, https://doi.org/10.1016/j.jrtpm.2017.08.006.
43. Selech J, Andrzejczak K. An aggregate criterion for selecting a distribution for times to failure of components of rail vehicles. Eksploatacja i Niezawodnosc - Maintenance and Reliability 2019; 22(1): 102–111, https://doi.org/10.17531/ein.2020.1.12.
44. Shepero M, Munkhammar J. Spatial Markov chain model for electric vehicle charging in cities using geographical information system (GIS) data. Applied Energy 2018; 231: 1089–1099, https://doi.org/10.1016/j.apenergy.2018.09.175.
45. Soltanali H, Rohani A, Abbaspour-Fard M H, Farinha J T. A comparative study of statistical and soft computing techniques for reliability prediction of automotive manufacturing. Applied Soft Computing 2021; 98: 106738, https://doi.org/10.1016/j.asoc.2020.106738.
46. Song S, Coit D W, Feng Q. Reliability for systems of degrading components with distinct component shock sets. Reliability Engineering & System Safety 2014; 132: 115–124, https://doi.org/10.1016/j.ress.2014.06.020.
47. Stawowy M, Rosiński A, Siergiejczyk M, Perlicki K. Quality and Reliability-Exploitation Modeling of Power Supply Systems. Energies 2021; 14(9): 2727, https://doi.org/10.3390/en14092727.
48. Świderski A, Borucka A, Grzelak M, Gil L. Evaluation of Machinery Readiness Using Semi-Markov Processes. Applied Sciences 2020; 10(4): 1541, https://doi.org/10.3390/app10041541.
49. Wang J, Miao Y. Optimal preventive maintenance policy of the balanced system under the semi-Markov model. Reliability Engineering & System Safety 2021; 213: 1–10, https://doi.org/10.1016/j.ress.2021.107690.
50. Wang L, Cui L, Zhang J, Peng J. Reliability evaluation of a Semi-Markov repairable system under alternative environments. Communications in Statistics - Theory and Methods 2016; 45(10): 2938–2957, https://doi.org/10.1080/03610926.2014.894062.
51. Wang Y, Xie B, E S. Adaptive relevance vector machine combined with Markov-chain-based importance sampling for reliability analysis. Reliability Engineering & System Safety 2022; 220: 1–11, https://doi.org/10.1016/j.ress.2021.108287.
52. Warr R L, Collins D H. A comprehensive method for solving finite-state semi-Markov processes. International Journal of Simulation and Process Modelling 2015; 10(1): 89–99, https://doi.org/10.1504/IJSPM.2015.068522.
53. Wawrzyński W, Zieja M, Tomaszewska J, Michalski M. Reliability Assessment of Aircraft Commutators. Energies 2021; 14(21): 7404, https://doi.org/10.3390/en14217404.
54. Wu B, Cui L. Reliability of multi-state systems under Markov renewal shock models with multiple failure levels. Computers & Industrial Engineering 2020; 145: 106509, https://doi.org/10.1016/j.cie.2020.106509.
55. Wu B, Cui L. Reliability of repairable multi-state two-phase mission systems with finite number of phase switches. Applied Mathematical Modelling 2020; 77: 1229–1241, https://doi.org/10.1016/j.apm.2019.09.018.
56. Wu B, Cui L, Fang C. Reliability analysis of semi-Markov systems with restriction on transition times. Reliability Engineering & System Safety 2019; 190: 106516, https://doi.org/10.1016/j.ress.2019.106516.
57. Zhang T, Liu T, Liu D, Sun F. Reliability Evaluation of Modular Multilevel Converter System Based on Semi-markov Model. 2021 IEEE 4th International Conference on Electronics Technology (ICET), 2021: 513–517, https://doi.org/10.1109/ICET51757.2021.9450902.
58. Zhao L, Li K, Zhao W et al. A Sticky Sampling and Markov State Transition Matrix Based Driving Cycle Construction Method for EV. Energies 2022; 15(3): 1057, https://doi.org/10.3390/en15031057.
59. Ziółkowski J, Małachowski J, Oszczypała M et al. Modelling of the Military Helicopter Operation Process in Terms of Readiness. Defence Science Journal 2021; 71(5): 602–611, https://doi.org/10.14429/dsj.71.16422.
60. Żyluk A, Kuźma K, Grzesik N et al. Fuzzy Logic in Aircraft Onboard Systems Reliability Evaluation—A New Approach. Sensors 2021; 21(23): 7913, https://doi.org/10.3390/s21237913.

energies

Article

Modelling the Operation Process of Light Utility Vehicles in Transport Systems Using Monte Carlo Simulation and Semi-Markov Approach

Mateusz Oszczypała , Jarosław Ziółkowski * and Jerzy Małachowski

Institute of Mechanics and Computational Engineering, Faculty of Mechanical Engineering, Military University of Technology, Gen. Sylwestra Kaliskiego Street 2, 00-908 Warsaw, Poland
* Correspondence: jaroslaw.ziolkowski@wat.edu.pl

Abstract: This research paper presents studies on the operation process of the Honker 2000 light utility vehicles that are part of the Polish Armed Forces transport system. The phase space of the process was identified based on the assumption that at any given moment the vehicle remains in one of four states, namely, task execution, awaiting a transport task, periodic maintenance, or repair. Vehicle functional readiness and technical suitability indices were adopted as performance measures for the technical system. A simulation model based on Monte Carlo methods was developed to determine the changes in the operational states. The occurrence of the periodic maintenance state is strictly determined by a planned and preventive strategy of operation applied within the analysed system. Other states are implementations of stochastic processes. The original source code was developed in the MATLAB environment to implement the model. Based on estimated probabilistic characteristics, the authors validated 16 simulation models resulting from all possible cumulative distribution functions (CDFs) that satisfied the condition of a proper match to empirical data. Based on the simulated operation process for a sample of 19 vehicles over the assumed 20-year forecast horizon, it was possible to determine the functional readiness and technical suitability indices. The relative differences between the results of all simulation models and the results obtained through the semi-Markov model did not exceed 6%. The best-fit model was subjected to sensitivity analysis in terms of the dependence between functional readiness and technical suitability indices on vehicle operation intensity. As a result, the proposed simulation system based on Monte Carlo methods turned out to be a useful tool in analysing the current operation process of means of transport in terms of forecasts related to a current environment, as well as when attempting its extrapolation.

Keywords: Monte Carlo algorithm; simulation approach; semi-Markov process; transport system; reliability analysis; maintenance

Citation: Oszczypała, M.; Ziółkowski, J.; Małachowski, J. Modelling the Operation Process of Light Utility Vehicles in Transport Systems Using Monte Carlo Simulation and Semi-Markov Approach. *Energies* **2023**, *16*, 2210. https://doi.org/10.3390/en16052210

Academic Editors: Adam Rosiński, Marek Stawowy and Zbigniew Kasprzyk

Received: 1 February 2023
Revised: 22 February 2023
Accepted: 23 February 2023
Published: 24 February 2023

1. Introduction

Simulation models based on Monte Carlo methods involve repeated performances of a certain random experiment. Initially, they were used to numerically determine the number value of π, calculate the integrals of complex functions as the area under the graph, and determine the probability of random events [1,2]. Developing an algorithm that depicts the course of changes in complex processes and implementing it within software enables the solution of a complex analytical problem using simulation methods [3–7].

Markov models [8,9] and semi-Markov models [10,11] are often used to analyse and evaluate the operation processes. They require a thorough analysis of the stochastic process through the identification of possible states and the description of probabilistic characteristics for interstate transition times. The elements of the transition intensity matrix for Markov models are identified as reciprocals of the expected times of transition between individual states. However, in the case of mechanical vehicles, the probabilistic characteristics determined within a time domain describe the intensity of the operation sub-process in a rather vague manner. The value of the vehicle with technical service life exhaustion is a reflected unit of measure of the work performed, expressed by the covered mileage (distance). Furthermore, probabilistic characteristics that describe the correct operating intervals of the vehicle between successive failures can be expressed within the mileage domain [12,13].

This study is a continuation of the research in the field of reliability and readiness of light utility vehicles. Previous publications in this field focused on analysing reliability based on censored failure damage [12] and modelling readiness through the application of Markov theory [14] and semi-Markov process theory [15]. After analysing a true operation's process, the authors developed a four-state simulation model employing Monte Carlo methods. It was assumed that the operation of light utility vehicles is a mixed process, that is, random-deterministic. Consequently, operation plans reflect the deterministic nature, which is, however, interrupted by random events of a stochastic character [6]. This result is from the planned and preventive technical maintenance strategy applied within the operating system of the studied vehicle population. The proposed innovative simulation model was verified based on determined probabilistic characteristics of individual operation, maintenance, and overhaul sub-processes. The model's undoubted advantage is its held ability to determine the values of functional readiness and technical suitability indices not only relative to current operating conditions but also to enable forecasting of their values in the case of hypothetically possible scenarios.

The approach to modelling an operation process presented in this paper supplements the current state of knowledge, which is discussed in the form of a source literature review. The iterative algorithm developed for the model based on Monte Carlo methods enables simulating a process composed of both stochastic and deterministic sub-processes. The achievement of particular operating states by vehicles in a transport system is carried out according to probabilistic characteristics. The cumulative distribution functions of daily mileage, repair time, and reliability function determine the course of the realisation of stochastic processes in the system. Periodic maintenance is a process strictly determined by the operating strategy. The numerical analyses carried out that make up part of this study refer to the operation of a selected population of light utility vehicles; however, the proposed model can also be applied to the analysis of other technical objects after appropriate modifications. It should also be stressed that the presented approach to simulation modelling, as well as the analysis of other technical objects, has not previously been the subject of research by other authors. The iterative algorithm developed is designed both to assess the efficiency of the operation of the transport system under current conditions and to forecast its performance under hypothetical conditions.

Additionally, the choice of the Honker 2000 as the subject of this study is justified by the significant importance of light utility vehicles in military transport systems. Assessment and prediction of the readiness and suitability of these technical objects are necessary for the planning of training and combat operations. In the reality of constant change and the emergence of new challenges, the proposed iterative Monte Carlo algorithm and the four-state operation model are valuable tools in engineering and military practise. The superiority of the proposed simulation approach over Markov and semi-Markov models is the extrapolation of the model over a wide range of variability in the intensity of the operation processes.

The purpose of this work is to develop a simulation model for the analysis, evaluation, and prediction of the efficiency and reliability of vehicle operating processes in transport systems. The main contributions of this paper are as follows:

- Development of a simulation model based on Monte Carlo methods;
- Implementation of the Monte Carlo model in the MATLAB environment;
- Validation of simulation models based on the analytical approach of a four-state semi-Markov process;

- Evaluation of the operation and maintenance processes of light utility vehicles using the proposed indicators and sensitivity analysis resulting from changes in the intensity parameters of the operational process.

This paper is divided into six sections. The literature review covers the current state of knowledge and shows the research published by other authors. In section three, several assumptions are made, and the simulation model based on Monte Carlo methods is presented with estimations of the probabilistic characteristics of sub-processes that determine whether a vehicle remains in individual operating states. The semi-Markov approach was developed in section four. Section five presents the results of the simulations and stochastic models. The Monte Carlo and semi-Markov models had almost the same functional readiness and technical suitability indicators, which is why the sensitivity analysis was developed for the above-mentioned models. In the end, the research is summarised and our final conclusions are formulated.

2. Literature Review

Several research papers employ Monte Carlo models for reliability studies [16–20]. Zhang et al. [21] used the Monte Carlo simulation to estimate the optimal parameters of a fault location model for wind turbines. Kallen [22] suggested a simulation model for a renewable object repair process with characteristics consistent with the exponential and Weibull distributions. Durczak et al. [23] used Monte Carlo techniques, Latin hypercube sampling, and Iman–Conover methods to generate time-to-failure data from the Weibull distribution. In contrast, the application of simulations within reliability studies of computer networks by Benson and Kellner [1] enables estimating the mean time-to-failure in an easier manner than with traditional methods. Simulation and computational methods relative to power supply systems are compared in [24]. In the case of both methods, the waveforms of the reliability function are very similar. Studies on the reliability of boat positioning systems involve developing a Monte Carlo model based on the probabilistic characteristics of its individual components [25]. A similar approach is presented in relation to photovoltaic systems when determining the reliability function for the entire system [26]. Green et al. [27] developed a complex simulation algorithm based on the Monte Carlo method and intelligent state space pruning (ISSP) combined with genetic algorithms (GA), particle swarm optimisation (PSO), ant colony optimisation (ACO), and artificial immune system optimisation (AIS). This solution reduced computational time by 50-90% compared to the non-sequential Monte Carlo simulation in the reliability analysis of electrical power systems.

Roslan et al. [28] developed a two-state reliability model, which was then verified through sequential and non-sequential simulations. In terms of reliability index estimation accuracy, the sequential Monte Carlo model turned out to be more effective than the non-sequential version. Research on the technical readiness of rotary drilling machines as renewable objects involved developing a simulation model based on Monte Carlo methods and Markov chain theory [29]. Here, the parameters of the reliability function were estimated based on times between failures. In their paper, for each 10 h period, it was determined with an 80% probability that a system composed of ten drilling machines will have five to eight such objects ready for operation. Whereas in [30], Monte Carlo sequential algorithms were used to determine the remaining useful life. The Monte Carlo Markov chain simulation algorithm [31] was developed to optimise maintenance policy and resulted in a 10% reduction in total costs for every mile of track.

Zhang et al. [32] proposed a method combining Monte Carlo simulations and directional sampling to analyse object reliability sensitivity. This method is based on the nearest Euclidean distance strategy. The accuracy and effectiveness of the proposed method were proved through practical numerical examples. In turn, Zhang et al. [33] evaluated the reliability of a power station by adopting a four- and five-state reliability model. They demonstrate that an approach based on the sequential Monte Carlo method is more rigorous than classical methods and that the calculated reliability indices adopt lower values.

A novel method for evaluating the reliability of renewable objects is proposed in [5]; the authors combined Monte Carlo methods with fault trees. In relation to the field of readiness and reliability of military structures, the authors of [34] conducted Monte Carlo simulations for three strategies for managing the platform operation processes, namely, replacing as needed, re-inspection at a specified interval, and prognostics. The prognostic approach optimised the operational readiness of military equipment by forecasting damage and reducing logistics delays. In addition, determining the remaining functional period of structures supports commanders in selecting appropriate platforms to implement future missions, resulting in a reduced failure risk.

The issues related to the simulation modelling of transport systems are presented in [35]. The authors analysed mass transit that provides transport services on 20 routes. The performance characteristics of individual drivers and vehicle reliability were used to optimise transport processes. Performing 10,000 simulation steps enable one to estimate the expected number of unrealized trips and the level of reduction in operating costs within a transport system, depending on the availability and reliability of the driver. The same number of simulations were conducted in the case of the Markov Chain Monte Carlo (MCMC) in [36], developed for a four-state phase space of the electrical vehicle operation process. In another paper [37], a Monte Carlo simulation based on the probability distribution function of the travel time was used to estimate the expected secondary delays of the trips. In Table 1, some selected works on the application of the Monte Carlo approach to reliability and readiness research for a spectrum of technical facilities and systems are summarised.

Table 1. Review of literature on the Monte Carlo approach for reliability and availability analysis.

Methods	Purposes of Research	Case Studies	Simulations	Papers
Monte Carlo	Reliability analysis	Coated surface	Sampling of inter-repair time (500 samples)	[22]
Monte Carlo, Latin hypercube sampling (LHS) and Iman-Conover methods	Reliability analysis	Agricultural tractors	Sampling of time-to-failure data	[23]
Markov Chain Monte Carlo	Reliability and availability analysis	Rotary drilling machines	Simulation of Markov Chain transitions	[29]
Markov Chain Monte Carlo	Global minimization of the system failure probability	Structural dynamic systems under stochastic excitation: linear single-degree of freedom system, linear eight-story two dimensional frame structure and a nonlinear three dimensional bridge structural	Random sampling of many variables	[17]
Markov Chain Monte Carlo	Modelling of vehicle use patterns	Electric vehicles	Random sampling of daily driving time (10^5 trials)	[36]
Markov Chain Monte Carlo and Sequential Monte Carlo	Assessment of remaining useful life	Milling machine	Sampling from posteriori distribution of states	[30]
Markov Chain Monte Carlo with the Metropolis–Hasting Algorithm	Reliability assessment	Bridge health monitoring	Sampling of points to estimate failure probability	[18]

Table 1. *Cont.*

Methods	Purposes of Research	Case Studies	Simulations	Papers
Sequential Markov Chain Monte Carlo	Optimisation of preventive maintenance schedule	Isolated Distributed Cuban Power System (wind turbines)	Simulation of wind speed	[38]
Sequential and Non-sequential Monte Carlo	Reliability assessment	Distribution network	Simulation by sampling of time-to-failure and time-to-repair	[28]
Monte Carlo and Copula	Power demand prediction	Electric vehicles	Simulation by sampling start time, end time, and distance travelled	[39]
Monte Carlo and directional sampling	Reliability sensitivity analysis	Headless rivet and wing box structure	Random sampling data (1×10^6 and 2×10^6)	[32]
Deep Belief Network and Monte Carlo	Calculate the reliability of the model	Physically-based thermal error model of the servo axis in machine tool	Random sampling data (10^7 trials) of the thermal characteristic parameters	[16]
Iterative Monte Carlo and semi-Markov approach	Assessing readiness and forecasting in various operational scenarios	Transportation system equipped with light utility vehicles	Sampling of task assignments, daily mileages, failures, and repairs based on CDFs and reliability function	This paper

Unlike previous studies, this publication presents a simulation model that takes into account random-deterministic processes. In the process of vehicle operation, periodic maintenance was adopted according to the documentation, taking into account time intervals or the amount of work performed in order to reliably reflect the phase trajectory for the vehicle. A novelty in this publication is the development of a four-state model adapted to the specificity of the Honker 2000 light utility vehicles, in accordance with the adopted modelling goal. Furthermore, the intention of the authors was to check which research method would prove to be more effective. Our findings suggest that the Monte Carlo simulation model turned out to be a slightly better forecasting tool compared to the semi-Markov model.

3. Monte Carlo Approach

All variables used for simulation modelling are listed in Table 2. A four-state vehicle operation process space was assumed for the proposed modelling method. The importance and description of individual states can be found in Table 3. Vehicle operation can be understood in this case as a process of changes in the operational states implemented within a calendar time. These changes are determined through operational strategy, operation processes, reliability of system components, and the organisation and efficiency of a technical system responsible for maintenance and operation. Due to the functional specificity of military transport systems (in the case of a defined state space), the authors adopted the assumption that on a given day, the vehicle is in exactly one operational state. The phase space of the process contains states that are significant from the perspectives of functional readiness and technical suitability. Compared to a nine-state model [15], the four-state model is simplified by eliminating short-term operational states, such as refuelling and maintenance performed both before and after the execution of the task. Furthermore, operational states that involve a vehicle staying in a technical unsuitability state, i.e., diagnosis (searching for damage causes) or awaiting repair or repair, are aggregated into a single state defined as 'repair'.

Table 2. Notations and definitions.

Notations	Definitions
$X(t)$	Stochastic process
T_m	Normative period between maintenance
L_m	Normative mileage between maintenance
$t_m(t)$	Time since last periodic maintenance
$l_m(t)$	Mileage since last periodic maintenance
Θ	Probability of assignment task
κ	Redundancy
l_d	Daily mileage
l_{dmax}	Maximum daily mileage
l_r	Mileage since last failure
l_f	Mileage on the day of failure
$G(l_d)$	Cumulative distribution function (CDF) of daily mileage
$R(l_r)$	Reliability function
$F(l_r)$	Cumulative distribution function (CDF) of failures
$f(l_r)$	Probability density function (PDF) of failures
$H(i)$	Cumulative distribution function (CDF) of repair time
q_1, q_2, q_3, q_4	Random values of the uniform distribution on the interval (0, 1)
$T(S_1), T(S_2), T(S_3), T(S_4)$	Sojourn times of state S_1, S_2, S_3, S_4
K_r	Readiness indicator
K_s	Suitability indicator
N_v	Number of vehicles
Z_i	Number of iterations

Table 3. Operation process state space.

State	Meaning	Description
S_1	Task execution	Vehicle is assigned to perform transportation tasks.
S_2	Awaiting a transport task	Vehicle in reserve is waiting for a task.
S_3	Periodic maintenance	Periodic maintenance is required. Vehicle is being serviced.
S_4	Repair	Vehicle has failed. Repair is completed or vehicle is pending repair.

Developing probabilistic characteristics is the basis for constructing a proposed simulation model based on Monte Carlo methods. The analysis was conducted through operational testing covering a sample of 19 Honker 2000 vehicles operated by the transport system of a military unit. These vehicles are intended to transport passengers and cargo weighing less than 1000 kg. They constitute a significant component of the transport capabilities of the Polish Armed Forces.

A three-element subset of technical suitability states, where an object is not damaged and does not require repair, was distinguished in the four-state operation model. This subset contains a two-element subset of functional readiness states, where the vehicle is ready or is performing transport tasks. Figure 1 is a graphical representation of the operational state distribution, together with vectors symbolising possible inter-state transitions.

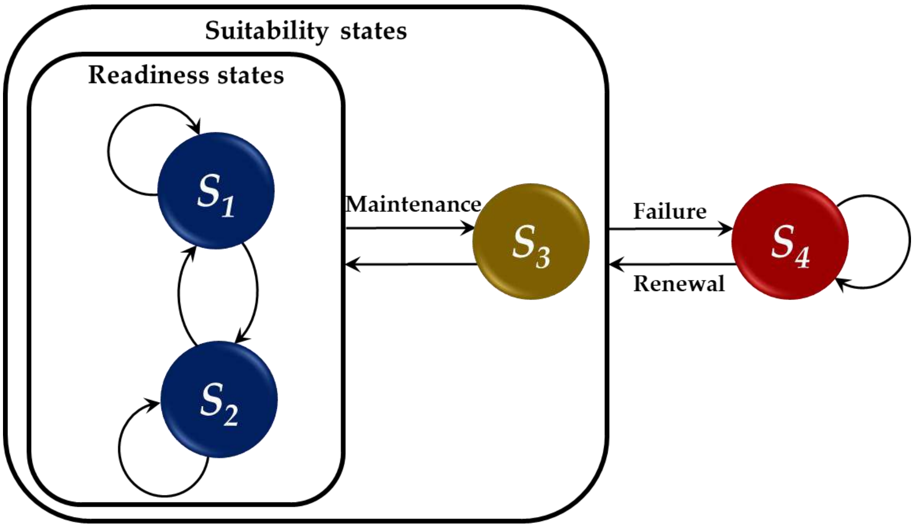

Figure 1. State transition within the operation process.

On the basis of the simulation results, the efficiency of the operation processes is assessed on the basis of suitably selected indicators. For the four-state model, two indicators were proposed to describe vehicle readiness: availability and suitability. The readiness index K_r corresponds to the probability that a technical object is in a subset of readiness states, which for the four-state model refers to states S_1 and S_2. Technical suitability expresses the condition of an object in which it is not damaged and repair is not required [15]. The technical suitability index K_s is the probability that the vehicle is in a subset of technical suitability states, i.e., states S_1, S_2, and S_3. The values of these indices are calculated according to the following relationships:

$$K_r = \frac{T(S_1) + T(S_2)}{\sum_{i=1}^{4} T(S_i)}, \tag{1}$$

$$K_s = \frac{T(S_1) + T(S_2) + T(S_3)}{\sum_{i=1}^{4} T(S_i)}. \tag{2}$$

3.1. Periodic Maintenance

Within the planned and preventive strategy for vehicle operation process management, periodic maintenance tasks are implemented at strictly specified time and mileage intervals. According to its assumptions, strictly defined maintenance tasks are performed after completing a specified amount of work, usually expressed in engine hours or kilometres [40,41]. However, it should be noted that all types of chemical, biological, and climatic factors acting on technical objects favour the physical ageing of assemblies, subassemblies, mechanisms and machinery components, as well as operating fluids [42,43]. This implies the need to define maximum intervals between successive maintenance tasks, usually expressed in months or years [44–48].

Such an organisation of vehicle maintenance circumscribes the deterministic nature of implementing this sub-process. A mathematical description of an event involving process $X(t)$ reaching state S_3 is expressed by the following relationship:

$$(t_m(t) \geq T_m \vee l_m(t) \geq L_m) \Rightarrow X(t) = S_3. \tag{3}$$

The incidence of state S_3 is mainly affected by the intensity of the operation process, which is determined by the probability of assigning a transport task to a vehicle and the daily mileage of vehicles. In the case of vehicles operated with low intensity, the frequency of carrying out periodic maintenance tasks is mainly based on the intervals specified via the T_m characteristic.

An undoubted advantage of the planned and preventive strategy is the possibility of adapting a technical system to enable efficient implementation of periodic maintenance [49–51]. Due to the determined interval of their implementation and a standardised scope of maintenance activities, the duration of a vehicle's stay in the state of S_3 falls within a single day of work.

Maintenance principles for military vehicles are laid out in a catalogue of operational standards [52], as well as manufacturer manuals. The interval between successive periodic maintenance and servicing of Honker light utility vehicles has been determined by two parameters: T_m = 365 days and L_m = 10,000 km. Vehicles are factory protected against weather factors; however, the manufacturer indicates that periodic maintenance is required at least once a year in the course of operation. In the case of lower operation intensity, the determining factor in performing periodic maintenance is the loss of physicochemical properties of operating fluids over time, resulting from the action of external factors.

In this study, we evaluated the operation and maintenance processes within the planned and preventive strategy of operational management. Herein, the appearance of state S_3 in a simulation model is the result of the t_m or l_m variables reaching permissible values.

3.2. Operational Process

The magnitude of transport demand within an operation system determines the operational intensity of the means of transport; ensuring an adequate level of reliability and security of transport process implementation requires maintaining a certain number of vehicles in a state of technical readiness—as backup for objects operated at a given time. This state enables us to respond actively to unwanted vehicle failures [47]. This feature is a particularly important functional aspect of military transport systems. However, an increasing number of standby vehicles entails the costs of acquiring and maintaining a fleet of cars [53,54].

The proposed method involves an introduced coefficient of operation task allocation Θ, which describes the probability that a task is executed by a vehicle with an alignment on a given day of operation. The Θ coefficient takes values from the range [0.0–1.0], and its high value implies a significant percentage of the exploitation of transport resources within an operation process and a low backup resource simultaneously. The mean redundancy within a transport system can be expressed using the Θ coefficient in (4) as follows:

$$\kappa = \frac{1 - \Theta}{\Theta}. \tag{4}$$

During successive iterations in a Monte Carlo simulation, a computer-based random number generator defines a certain number q_1 from the range [0.0–1.0]. Drawing a q_1 number lower than the Θ coefficient results in allocating a transport task at a given step of a simulated operation process. Otherwise, a roadworthy vehicle remains as backup and switches to the S_2 state:

$$q_1 > \Theta \Rightarrow X(t) = S_2. \tag{5}$$

In our study, a cumulative distribution function (CDF) G was used for the daily mileage of vehicles that perform transport tasks to enable a stochastic description of the intensity of technical service life exhaustion. Therefore, the probability distribution is fit on the basis of operational needs knowledge.

At this step of the simulation, the generator draws a q_2 number from the range [0.0–1.0]. The expected l_d distance that the vehicle will cover on a given day is an argument for which the value of the G CDF is q_2 as follows:

$$l_d = G^{-1}(q_2). \tag{6}$$

The assumption presented through formula (5) is burdened with a certain risk. Drawing a q_2 number very close to 1.0 may lead to a situation in which the l_d argument takes on an unrealistically high value. In reality, the maximum daily mileage value is limited by technical and road conditions. Therefore, maintaining the credibility of a simulated operation process requires introducing restrictions in the form of a maximum daily mileage value, depending on the types of means of transport, infrastructure, and other conditions.

The operation process of military vehicles was analysed based on empirical data collected as a part of operational studies covering a sample of 19 vehicles. These were operated on an actual military transport system for a period of 3 years. The operation process is particularly well documented, which enabled its reliable reconstruction.

Military transport systems are characterised by maintaining a high-level means of transport reserve. Based on the observations of the operation process, the authors estimated the value of the transport task allocation coefficient Θ to be 0.32. This value suggests that, statistically, an average of 32% of operational vehicles are intended for task execution on a single day, and more than two-thirds function as reserve vehicles and await being used in an emergency situation. Accordingly, the probabilistic description of the functioning of the task allocation system is a binomial distribution in which an event that involves the allocation of a task to a vehicle is implemented with a probability equal to 0.32. On the contrary, the probability that an operational vehicle will not perform any tasks on a given day is 0.68.

The execution leads to the end of service life. Service life is measured in mileage expressed in units of length. The variety of tasks within a system implies the random nature of the daily mileage. In mathematical terms, the value of daily mileage is a random variable that is described through an appropriate distribution. To determine probabilistic characteristics, 4620 implementations of the random variable l_d were used. These 4620 daily miles were recorded during the 3-year operation period. They constituted the basis for estimating the value of the empirical cumulative distribution function. The fit of exponential, Weibull, gamma, and lognormal cumulative distribution functions to the empirical cumulative distribution function value is shown in Figure 2; Table 4 lists CDFs for probabilistic models describing the intensity of the vehicle operation process, together with the assessed fit using Pearson's correlation coefficient R. According to our results, the lognormal model performed slightly better than the other models, obtaining a value of R = 0.9994.

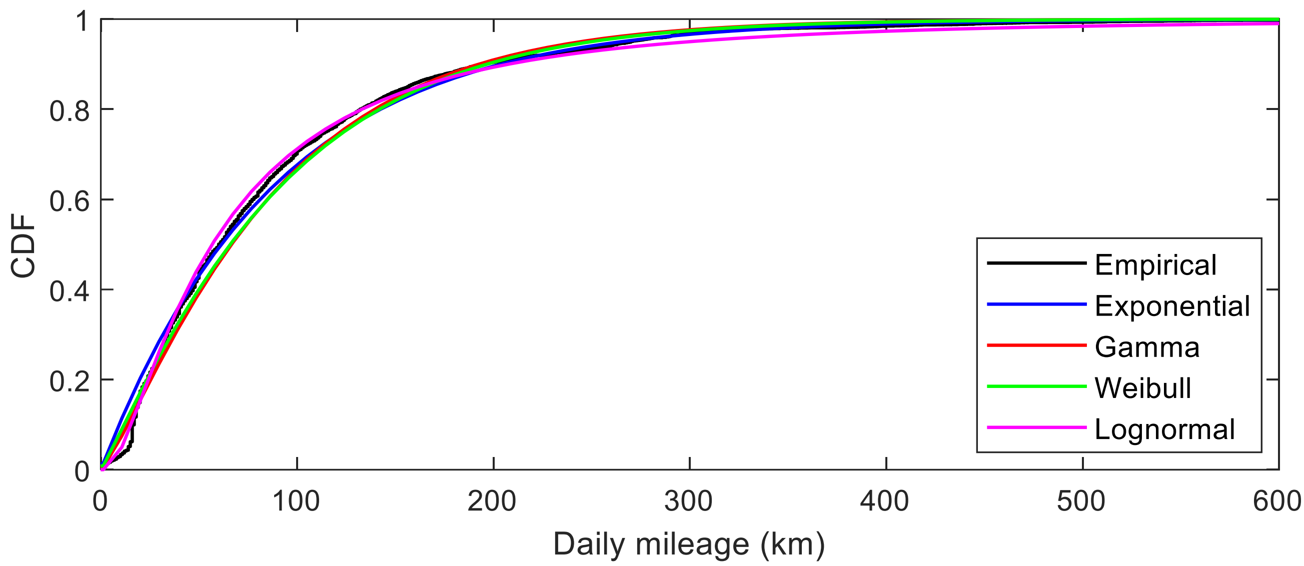

Figure 2. Empirical and fit mileage CDFs.

Table 4. Estimation of CDFs' parameters of daily mileage.

Model	CDF	Parameters	Estimation	R
Exponential	$G(l_d) = 1 - \exp(-\lambda l_d)$	λ—scale	λ = 0.0113	0.9976
Weibull	$G(l_d) = 1 - \exp\left[-\left(\frac{l_d}{\alpha}\right)^{\beta}\right]$	α—scale β—shape	α = 91.9967 β = 1.0984	0.9970
Gamma	$G(l_d) = \frac{1}{\Gamma(k)}\gamma\left(k, \frac{l_d}{\theta}\right)$	k—shape θ—scale	k = 1.2618 θ = 70.1488	0.9975
Lognormal	$G(l_d) = \frac{1}{2}\left[1 + \mathrm{erf}\left(\frac{\ln l_d - \mu}{\sigma\sqrt{2}}\right)\right]$	μ—log location σ—log scale	μ = 4.0373 σ = 1.0131	0.9994

The domain of the operating intensity model CDFs is the range (0,+∞). In the event of a Monte Carlo simulation drawing, a q_2 number with a value very close to 1 and its corresponding argument l_d can take an unrealistic value. This issue requires setting the maximum value of the l_d variable at a level of 1000 km per day, based on empirical data and the technical capabilities of the vehicles.

3.3. Reliability

The reliability of a technical object characterises its ability to operate correctly and its resistance to failures and damage [55–57]. Within the proposed four-state operational model, an object can switch from states S_1–S_3 to state S_4—provided that it was assigned on a given day with a transport task during the execution of which it experienced damage to at least one of its mechanisms or elements. Mechanical vehicles, as renewable objects, can be characterised through reliability models related to mileage between successive failures [12].

The reliability function reflects the probability of correct functioning from moment 0 to t [58–61]. In relation to vehicles subject to refurbishment, the function $R(l_r)$ is related to the mileage l_r, covered since the last repair, according to the relationship (7) [12] as follows:

$$R(l_r) = P(L > l_r). \tag{7}$$

If at time t, the mileage of a vehicle since the last recorded failure is l_r, while the assigned transport task requires covering a distance l_d, then the probability of its failure during the execution of the task is expressed by Formula (8) as follows:

$$P\{(L \le l_r + l_d)|(L > l_r)\} = \frac{P(L \le l_r + l_d, L > l_r)}{P(L > l_r)} = \frac{\int_{l_r}^{l_r+l_d} f(l)\mathrm{d}l}{1 - \int_0^{l_r} f(l)\mathrm{d}l} = 1 - \frac{1 - F(l_r + l_d)}{1 - F(l_r)} = 1 - \frac{R(l_r + l_d)}{R(l_r)}. \tag{8}$$

Monte Carlo simulation involves drawing a q_3 number from the range [0.0–1.0]. The probability that an event q_3 is lower or equal to the value obtained from formula (8) corresponds to the probability of a vehicle failure during the execution of a transport task under the presented conditions. In such a situation, the means of transport switch to state S_4. Otherwise, the vehicle remains in state S_1 and executes an assigned task according to the plan. The rules for the occurrence of vehicle failure (S_4) during the execution of a transportation task consisting of covering the distance l_d are described by Equation (9) as follows:

$$q_3 \le 1 - \frac{R(l_r + l_d)}{R(l_r)} \Rightarrow X(t) = S_4. \tag{9}$$

Otherwise, at time t, the stochastic process $X(t)$ assumes state S_1 according to Equation (10) as follows:

$$q_3 > 1 - \frac{R(l_r + l_d)}{R(l_r)} \Rightarrow X(t) = S_1. \tag{10}$$

The authors of this study conducted research on the reliability of light utility vehicles and published it in [12]. In this current work, the reliability function was estimated using the Kaplan–Meier estimator based on the empirical data on mileages between failures. This method is applied to determine the probability of the correct operation of the device based on information that contains censored data. Figure 3a shows the results of the estimation using a step graph.

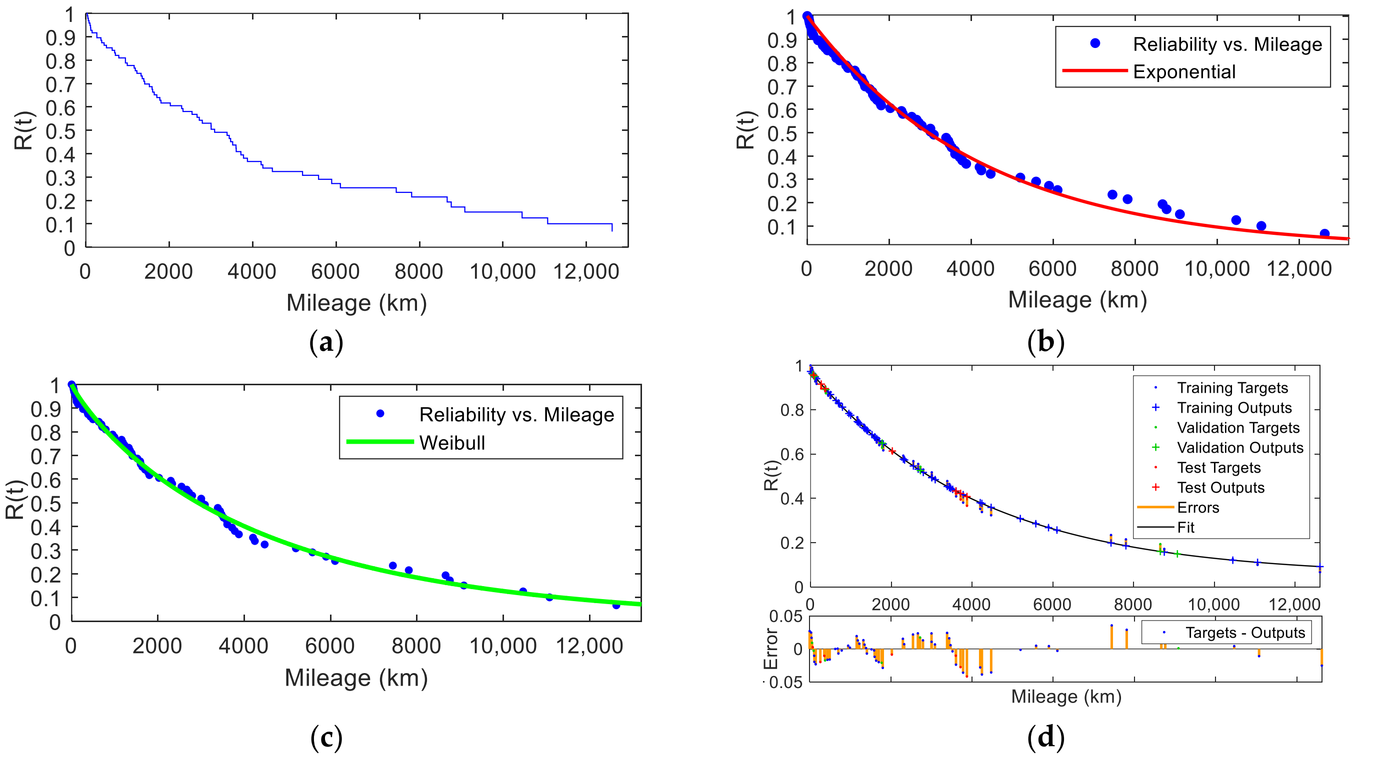

Figure 3. Estimation and approximation of the reliability function: (**a**)—Kaplan–Meier estimation, (**b**)—exponential model, (**c**)—Weibull model, and (**d**)—neural model [12].

The reliability function was approximated using the exponential, Weibull, and neural models. Figure 3b–d is a graphical representation of function waveforms with reference to estimated values. The accuracy of the fit measured through the correlation coefficient R was greater than 0.99 for all models. Table 5 lists the analytical forms of the reliability models used to perform the Monte Carlo simulation.

Table 5. Reliability functions [12].

Model	Reliability Function	*R*
Exponential	$R(l_r) = \exp(-0.000235\, l_r)$	0.9945
Weibull	$R(l_r) = \exp\left(-0.000574\, {l_r}^{0.889}\right)$	0.9971
Neural	$R(l_r) = \frac{32.925260+1.786689\exp(0.000249\, l_r)}{1+34.674828\ \exp(0.000249\, l_r)}$	0.9975

Despite the best-fit of the neural model to the empirical values of the reliability function, it is only an interpolation in terms of the known miles between the failures observed during the operation process. Outside this range, the approximating function is flattened. For this reason, the expected value of the mileage between subsequent failures cannot be calculated [12]. The application of a neural model for a Monte Carlo simulation may also lead to the implementation of an unreal process after the vehicle exceeds the right-hand boundary of the interval between failures, which constitutes a model limitation.

3.4. Failure Diagnostics and Repair

In the four-state operational model, S_4 corresponds to a situation where a vehicle is not suitable for the execution of transport tasks. Restoring the technical suitability of an object requires diagnostic actions that identify the mechanisms or elements to be repaired or replaced, followed by repair activities. Unfit object recovery time depends on repair capabilities (capacity) and the effectiveness of the material supply subsystem (part delivery, availability, and time).

A probabilistic description of the S_4 implementation is the cumulative distribution function of H for the duration that a vehicle remains in a technically unsuitable state [62,63]:

$$H(i) = P(I \leq i). \tag{11}$$

The probability of an event involving vehicle repair on an i-day after failure is calculated according to formula (12) as follows:

$$P\{(I \leq i)|(I > i-1)\} = \frac{P(I \leq i, I > i-1)}{P(I > i-1)} = \frac{\int_{i-1}^{i} h(u)\mathrm{d}u}{1 - \int_{0}^{i-1} h(u)\mathrm{d}u} = \frac{H(i) - H(i-1)}{1 - H(i-1)} = 1 - \frac{1 - H(i)}{1 - H(i-1)}. \tag{12}$$

The course of a Monte Carlo simulation involves a sequence of successive iterations within the technical recovery sub-process. Each subsequent step includes drawing a number q_4 from a standard range of [0.0–1.0] based on comparing the values of q_4 with the probability of completing a repair process in the i-step of the simulation, which corresponds to successive calendar days. The technical recovery process is completed at the i iteration, in the event of relationship (13):

$$q_4 \leq 1 - \frac{1 - H(i)}{1 - H(i-1)}. \tag{13}$$

Otherwise, the vehicle remains in state S_4.

$$q_4 > 1 - \frac{1 - H(i)}{1 - H(i-1)} \Rightarrow X(t) = S_4. \tag{14}$$

The time-to-repair the vehicle after it reaches a state of unsuitability primarily depends on the complexity of the repair process and numerous factors occurring within the technical system. The total duration of a vehicle remaining in state S_4 is the total time to diagnose the causes of the failure, the physical implementation of the repair process, and the logistic time associated with acquiring spare parts and waiting for the availability of technical personnel. Within the proposed four-state model, all actions involving an unfit vehicle are classified as state S_4.

The probabilistic characteristic required for conducting a Monte Carlo simulation is the cumulative distribution function (CDF) for the time a technical object remains in state S_4. For this purpose, as part of the operational study of light utility vehicles, the authors gathered documentation and used it to develop an empirical database that includes technical recovery times. In our study, 100 repairs were recorded during the 3-year operation period. They constituted a basis for estimating the value of the empirical cumulative distribution function. Figure 4 shows the fit of exponential, Weibull, gamma, and logarithmic normal cumulative distribution functions to the empirical cumulative distribution function value. Table 6 lists estimated CDFs parameters with an assessed fit using Pearson's correlation coefficient R.

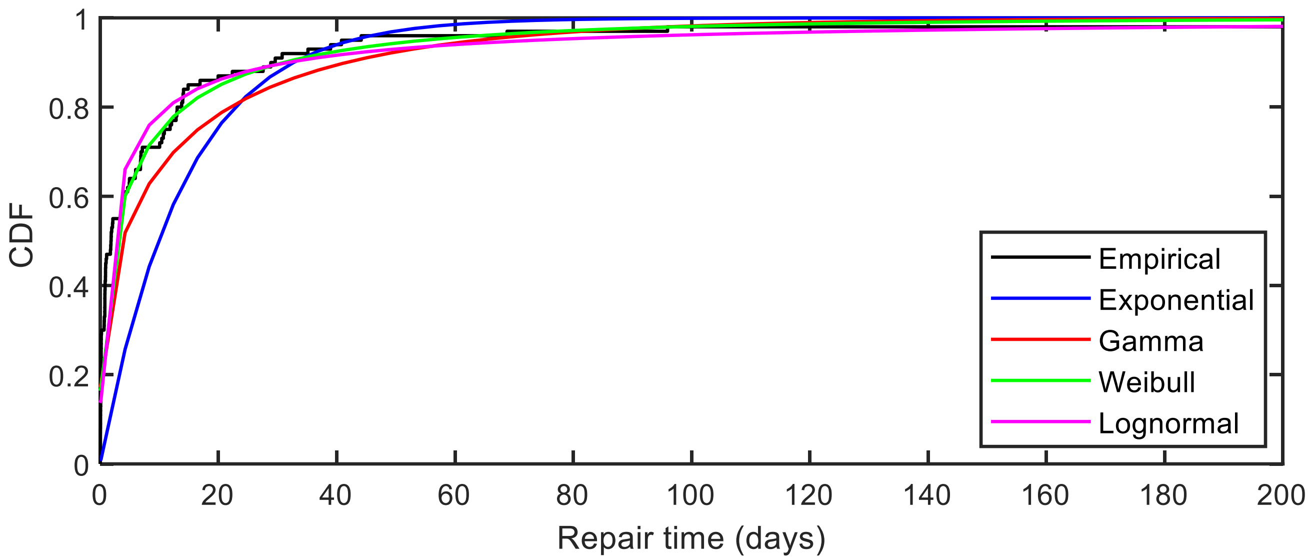

Figure 4. Empirical and fit CDFs of repair time.

Table 6. Estimation of repair time CDFs parameters.

Model	CDF	Parameters	Estimation	*R*
Exponential	$H(i) = 1 - \exp(-\lambda i)$	λ—scale	λ = 0.0704	0.9207
Weibull	$H(i) = 1 - \exp\left[-\left(\frac{i}{\alpha}\right)^{\beta}\right]$	α—scale β—shape	α = 5.0784 β = 0.4612	0.9924
Gamma	$H(i) = \frac{1}{\Gamma(k)}\gamma\left(k, \frac{i}{\theta}\right)$	k—shape θ—scale	k = 0.3144 θ = 45.1562	0.9846
Lognormal	$H(i) = \frac{1}{2}\left[1 + \mathrm{erf}\left(\frac{\ln i - \mu}{\sigma\sqrt{2}}\right)\right]$	μ—log location σ—log scale	μ = 0.4768 σ = 2.3254	0.9907

3.5. Monte Carlo Models of Light Utility Vehicle Operation Process

Probabilistic characteristics with a coefficient representing the quality-of-fit to empirical values of at least R = 0.99 were selected to validate the simulation model. Periodic maintenance is the only determined process within the operation system. Transport tasks are assigned according to a binomial distribution with a success probability equal to the value of the Θ coefficient. The exhaustion process of the technical life of the service is measured by the distance covered by a vehicle. Daily mileage is understood as a random variable and is presented as a cumulative distribution function for the exponential, Weibull, lognormal, and gamma distributions. The reliability function is the result of previous research discussed in [12], which involved developing three reliability models. Due to the limitations of the neural model, two other distributions, i.e., exponential and Weibull, are applied to describe the vehicle failure process. On the other hand, the repair process was characterised by Weibull and lognormal distribution functions for the random variable of the time the vehicle was in a state of technical unsuitability.

The general Monte Carlo model developed was validated on the basis of all possible combinations of characteristics exhibited by individual processes that occur within a military transport system. Table 7 lists sixteen models with assigned characteristics.

Table 7. Monte Carlo models of military vehicle operation processes.

Monte Carlo Model	Maintenance	Assignment of Tasks	Operational Process	Reliability	Repair
MC1	Deterministic	Binomial	Exponential	Exponential	Weibull
MC2	Deterministic	Binomial	Exponential	Exponential	Lognormal
MC3	Deterministic	Binomial	Exponential	Weibull	Weibull
MC4	Deterministic	Binomial	Exponential	Weibull	Lognormal
MC5	Deterministic	Binomial	Weibull	Exponential	Weibull
MC6	Deterministic	Binomial	Weibull	Exponential	Lognormal
MC7	Deterministic	Binomial	Weibull	Weibull	Weibull
MC8	Deterministic	Binomial	Weibull	Weibull	Lognormal
MC9	Deterministic	Binomial	Lognormal	Exponential	Weibull
MC10	Deterministic	Binomial	Lognormal	Exponential	Lognormal
MC11	Deterministic	Binomial	Lognormal	Weibull	Weibull
MC12	Deterministic	Binomial	Lognormal	Weibull	Lognormal
MC13	Deterministic	Binomial	Gamma	Exponential	Weibull
MC14	Deterministic	Binomial	Gamma	Exponential	Lognormal
MC15	Deterministic	Binomial	Gamma	Weibull	Weibull
MC16	Deterministic	Binomial	Gamma	Weibull	Lognormal

3.6. Software Implementation

A diagram of the proposed method is illustrated in Figure 5. A preliminary stage of simulation implementation is to define the characteristics of processes associated with vehicle operation and to determine the basic simulation parameters, that is, the number of vehicles and the number of iterations conducted. The simulation is then started while the initial value randomisation is maintained for each vehicle.

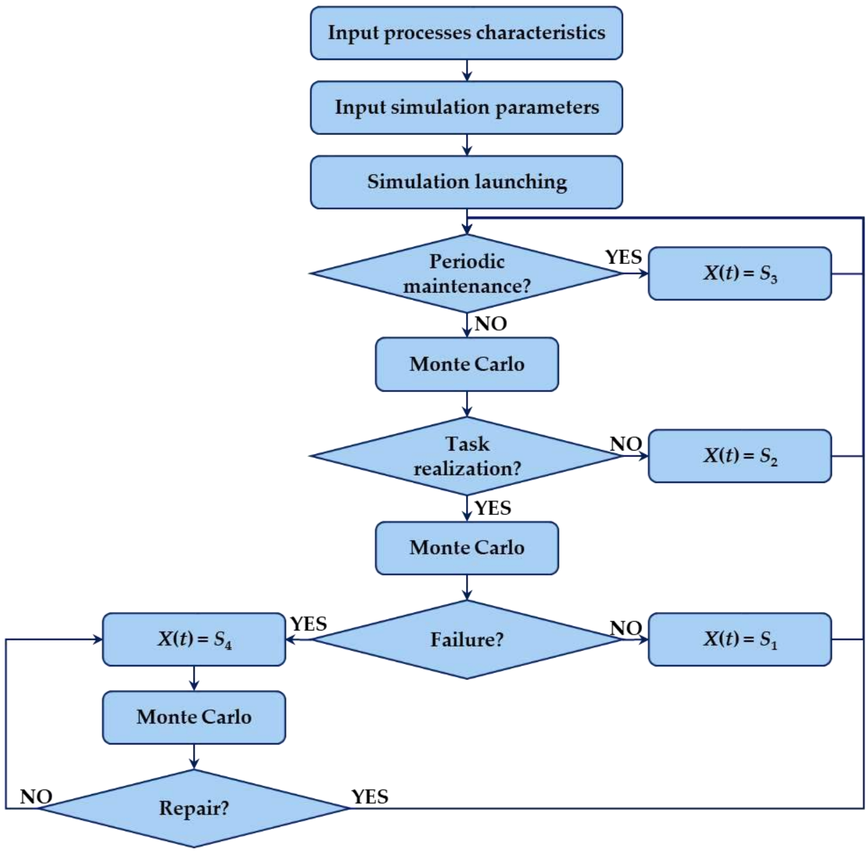

Figure 5. Proposed method flowchart.

The first simulation phase involves verifying whether vehicle operating parameters determine periodic maintenance. If this condition is satisfied, the vehicle switches to the S_3 state. Otherwise, a Monte Carlo draw takes place, and it is determined whether a transport task has been assigned for this vehicle to be executed in the simulated step. If such a task is not assigned, the vehicle enters the S_2 state. Otherwise, the simulation draws the daily mileage that the vehicle needs to cover to perform the assigned task. In the next phase, the algorithm checks if there was any vehicle failure during the execution of the task. If such a failure does not occur, the object enters the S_1 state. The appearance of a failure results in classifying the vehicle as being in the S_4 state, where it remains until the repair sub-process is completed.

The proposed method for modelling simulation of a vehicle operation process was implemented within the MATLAB environment. The application pseudocode is shown as Algorithm 1.

Algorithm 1: Pseudocode of Monte Carlo simulation for the four-state operation process.

Input: Reliability function $R(l_r)$, CDF of daily mileage $G(l_d)$, probability of assignment task Θ, CDF of repair time $H(i)$, maintenance parameters L_m and T_m, maximum of daily mileage l_{dmax}, number of vehicles N_v, and number of iterations for each vehicle Z_i
Output: Trajectory $X(t)$, sojourn times $T(S_1)$, $T(S_2)$, $T(S_3)$, $T(S_4)$, readiness K_r, and suitability K_s

for $z = 1{:}\ Z_i$ **do**
  set $t = 1$, set random integer values of l_m, t_m, l_r
  while $t \leq Z_i$ **do**
    if $l_m \geq L_m$ **then**
      Periodic maintenance $X(t) = S_3$, $T(S_3) = T(S_3) + 1$
      $l_m = 0$, $t_m = 0$
      $t = t + 1$
    elseif $t_m \geq T_m$ **then**
      Periodic maintenance $X(t) = S_3$, $T(S_3) = T(S_3) + 1$
      $l_m = 0$, $t_m = 0$
      $t = t + 1$
    else
      q_1 = rand
      if $q_1 > \Theta$ **then**
        Awaiting for task $X(t) = S_2$, $T(S_2) = T(S_2) + 1$
        $t = t + 1$
      else
        q_2 = rand
        $G(l_d) = q_2$, find l_d,
        l_d $(l_d > l_{dmax}) = l_{dmax}$
        q_3 = rand
        if q_3 > probability of failure **then**
          Task realization $X(t) = S_1$, $T(S_1) = T(S_1) + 1$
          $l_r = l_r + l_d$, $l_m = l_m + l_d$, $t_m = t_m + 1$
          $t = t + 1$
        else
          Failure $X(t) = S_4$, $T(S_4) = T(S_4) + 1$
          set random value $l_f \rightarrow [0.0, l_d]$
          $l_m = l_m + l_f$, $t_m = t_m + 1$
          $t = t + 1$
          q_4 = rand
          $i = 1$

```
            while q4 > probability of repair in i-th iteration do
              if t < Z_i then
                Repair of vehicle in progress X(t) = S4, T(S4) = T(S4) + 1
                t_m = t_m + 1
                i = i +1
                q4 = rand
                t = t + 1
              else
                End of simulation; vehicle inoperable
              end if
            end while
            Vehicle repaired in i-th iteration
            l_r = 0
            t = t + 1
          end if
        end if
      end if
    end while
end for
Calculate readiness K_r = [T(S1) + T(S2)]/[T(S1) + T(S2) + T(S3) + T(S4)]
Calculate suitability K_s = [T(S1) + T(S2) + T(S3)]/[T(S1) + T(S2) + T(S3) + T(S4)]
return X(t), T(S1), T(S2), T(S3), T(S4), K_r, K_s
```

4. Semi-Markov Approach

Semi-Markov processes are a generalisation of homogeneous Markov processes in terms of distributions of the individual states' durations. Markov models assume exponential distributions, significantly narrowing the spectrum of their applications [64]. Furthermore, their use without statistical verification may lead to significant errors in the results obtained, as demonstrated by real case studies in [11,15]. Semi-Markov models are a solution to this problem because they permit distributions of time characteristics [15,65].

The basic description of the semi-Markov process is the $\mathbf{Q}(t)$ renewal kernel matrix, consisting of products of the conditional probability p_{ij} and distribution functions of the condition duration distribution of state S_i prior to transition to state S_j, according to the dependence [66,67]:

$$\mathbf{Q}(t) = \begin{bmatrix} 0 & Q_{12}(t) & \cdots & Q_{1(k-1)}(t) & Q_{1k}(t) \\ Q_{21}(t) & 0 & \cdots & Q_{2(k-1)}(t) & Q_{2k}(t) \\ \vdots & \vdots & \ddots & \vdots & \vdots \\ Q_{(k-1)1}(t) & Q_{(k-1)2}(t) & \cdots & 0 & Q_{(k-1)k}(t) \\ Q_{k1}(t) & Q_{k2}(t) & \cdots & Q_{k(k-1)}(t) & 0 \end{bmatrix}, \tag{15}$$

whereas:

$$Q_{ij}(t) = p_{ij}F_{ij}(t). \tag{16}$$

where p_{ij} means the probability of transition from the S_i state to the S_j state and $F_{ij}(t)$ is the distribution function of time in the S_i state prior to the transition to the S_j state.

An embedded Markov chain is constructed for a semi-Markov process over continuous time. It is a description of the transition states of the process without taking into account the real time in each state. The possibility of a transition from the S_i state to the S_j state is assumed for an embedded Markov chain, provided that $i \neq j$. The matrix of conditional probabilities of interstate transitions $\boldsymbol{P}$ may have elements greater than zero only for allowed transitions, which can be written with the formula:

$$\boldsymbol{P} = \begin{bmatrix} 0 & p_{12} & \cdots & p_{1(k-1)} & p_{1k} \\ p_{21} & 0 & \cdots & p_{2(k-1)} & p_{2k} \\ \vdots & \vdots & \ddots & \vdots & \vdots \\ p_{(k-1)1} & p_{(k-1)2} & \cdots & 0 & p_{(k-1)k} \\ p_{k1} & p_{k2} & \cdots & p_{k(k-1)} & 0 \end{bmatrix}, \tag{17}$$

under the assumption of meeting the condition of the stochastic matrix [68,69]:

$$\sum_{j=1}^{k} p_{ij} = 1. \tag{18}$$

Figure 6 shows the transition diagram of the embedded Markov chain for the four-state phase space of operational light utility vehicles. The designations of the states correspond to the assumptions shown in Table 3.

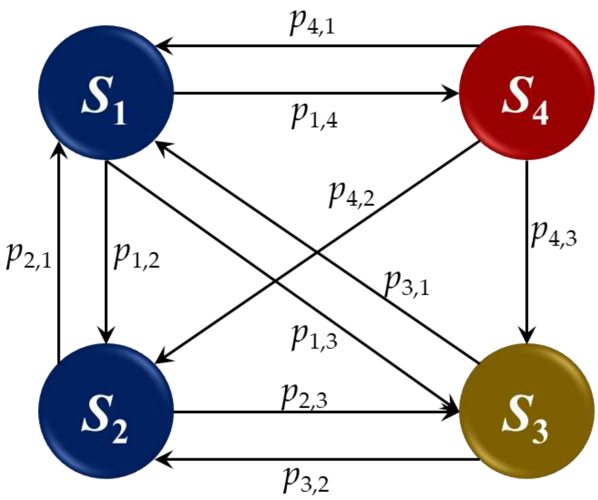

Figure 6. Transition diagram for the embedded Markov chain in the four-state semi-Markov model.

Constructing an embedded Markov chain based on an empirical process waveform implies the need to acquire numerical data on interstate transitions. For this purpose, it is justified to construct a population matrix of interstate transitions $\boldsymbol{N}$, according to Equation (19) as follows:

$$\boldsymbol{N} = \begin{bmatrix} 0 & n_{12} & \cdots & n_{1(k-1)} & n_{1k} \\ n_{21} & 0 & \cdots & n_{2(k-1)} & n_{2k} \\ \vdots & \vdots & \ddots & \vdots & \vdots \\ n_{(k-1)1} & n_{(k-1)2} & \cdots & 0 & n_{(k-1)k} \\ n_{k1} & n_{k2} & \cdots & n_{k(k-1)} & 0 \end{bmatrix}. \tag{19}$$

Values in $\boldsymbol{N}$ matrix correspond to the total number of observed interstate transitions over the analysed process execution time, while n_{ij} means a transition from S_i to S_j state.

The probability of transitions p_{ij} in the stochastic matrix $\boldsymbol{P}$ can be acquired by using the values of the population matrix for interstate transitions $\boldsymbol{N}$ by estimating [70–72] according to Equation (20) as follows:

$$p_{ij} = \frac{n_{ij}}{\sum\limits_{j=1}^{k} n_{ij}}, \tag{20}$$

whereas, the standard estimation errors $SE(p_{ij})$ of the probabilities p_{ij} [73,74] were calculated from formula (21) as follows:

$$SE\left(p_{ij}\right) = \sqrt{\frac{p_{ij}\left(1 - p_{ij}\right)}{\sum_{j=1}^{n} n_{ij}}}. \tag{21}$$

The values of ergodic probabilities for an embedded Markov chain π_j are calculated by solving the matrix Equation (22) [68] as follows:

$$\left(\boldsymbol{P}^T - \boldsymbol{I}\right) \cdot \boldsymbol{\Pi} = 0, \tag{22}$$

assuming that the standardization condition is met:

$$\sum_{j=1}^{n} \pi_j = 1. \tag{23}$$

If an embedded Markov chain exhibits ergodicity and there are expected values $E(T_i)$ of state residence times, the values of ergodic probabilities p_j for a semi-Markov process are determined using expression (24) as follows:

$$p_j = \frac{\pi_j E\left(T_j\right)}{\sum\limits_{i=1}^{n} \pi_i E(T_i)} = \frac{\pi_j \sum\limits_{k=1}^{n} p_{jk} E\left(T_{jk}\right)}{\sum\limits_{i=1}^{n} \left(\pi_i \sum\limits_{k=1}^{n} p_{ik} E(T_{ik})\right)}, \tag{24}$$

where π_i is the ergodic probability of an embedded Markov chain for the S_i state and $E(T_{ik})$ is the expected value of the direct transition time from the S_i state to the S_k state.

5. Results and Discussion

5.1. Monte Carlo Simulations

Simulations were performed for the real operating conditions of the transport system analysed. The operation processes of 19 light utility vehicles were simulated over a predicted 20-year operation period as set out in operational standards for each of the 16 Monte Carlo models [52]. Figure 7 shows sample waveforms of the simulated operation process for selected vehicles and Monte Carlo models.

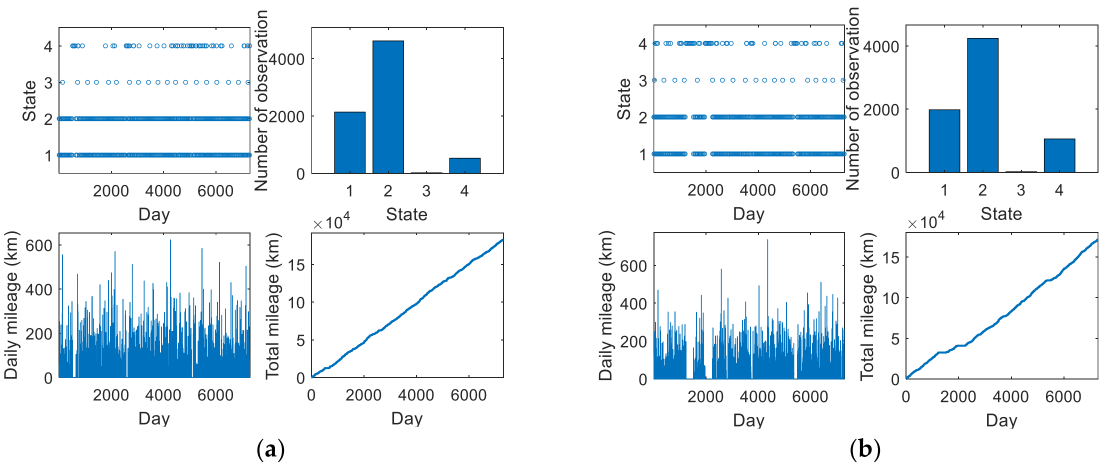

Figure 7. *Cont.*

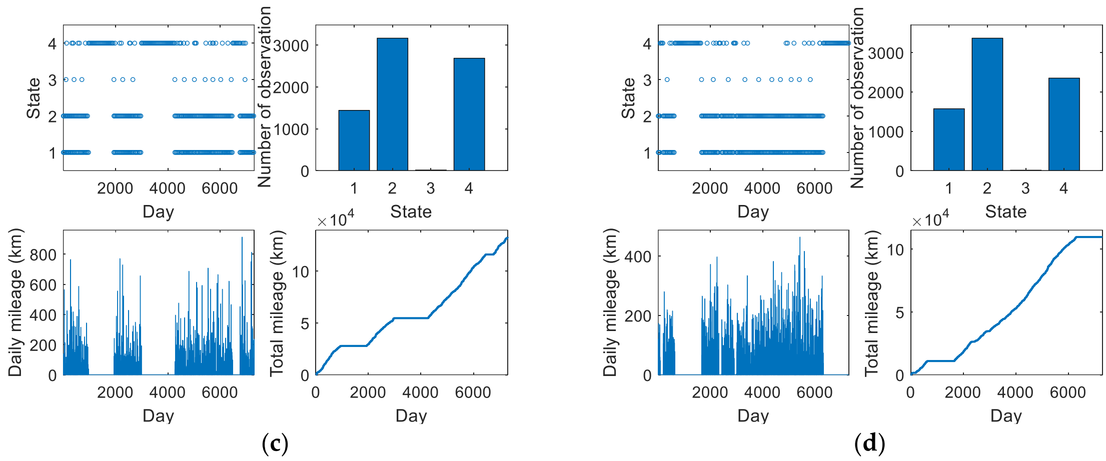

Figure 7. Examples of simulation results: (**a**)—vehicle No. 4 in MC1, (**b**)—vehicle No. 13 in MC6, (**c**)—vehicle No. 19 in MC10, and (**d**)—vehicle No. 14 in MC14.

The simulated operation of individual vehicles may show clearly different courses. Repairs of vehicles No. 4 in MC1 and No. 13 in MC6 took place shortly after a failure occurred. On the contrary, vehicle No. 19 in MC10 and No. 14 in MC14, after several failures, remained in an unsuitable state for a prolonged time, which adversely affected the object readiness index values.

Figure 8a–d shows detailed simulation results of the MC1 model. During a 20-year operation period, all vehicles must cover distances in the range of 150,000.0 to 200,000.0 km, which is shown in Figure 8a. In reference to the operational potential specified in the Catalogue of Operational Standards at a level of 230,000.0 km, our work reveals that the current operation intensity can be maintained for the entire estimated operation period. Furthermore, the number of failures for individual objects (Figure 8b) fell within the range of 30 to 60, while the average number of failures per vehicle was 45.68. Functional readiness and technical suitability were quite varied, with each vehicle exhibiting values of the K_r and K_s indices greater than 0.80, as illustrated in Figure 8c,d. The simulation results of all models (MC1–MC16) are presented in Appendix A.

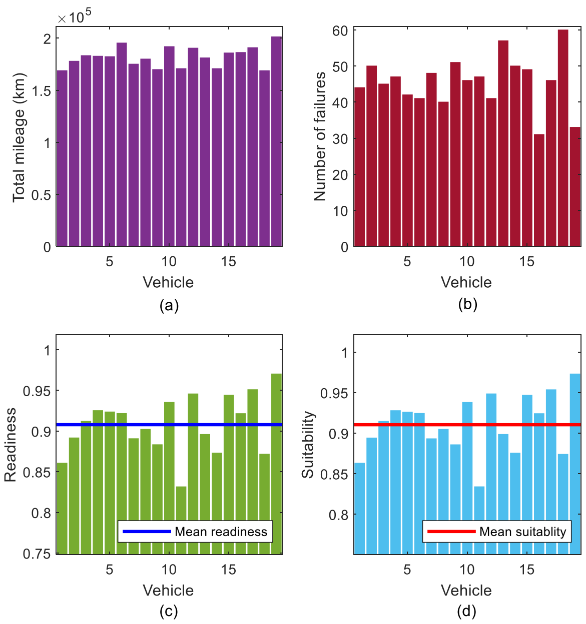

Figure 8. MC1 simulation results: (**a**)—total vehicle mileages, (**b**)—number of failures, (**c**)—vehicle readiness indicator values, and (**d**)—vehicle suitability indicator values.

5.2. Semi-Markov Model

An estimation of the conditional transition probability matrix was carried out using Equations (17)–(20), based on data collected from the real operation process of 19 light utility vehicles. During a 3-year period of operation, 7763 interstate transitions were observed for the study sample, whereas the numbers of transitions between states were represented by the $\boldsymbol{N}$ matrix:

$$\boldsymbol{N} = \begin{bmatrix} 0 & 3641 & 27 & 94 \\ 3729 & 0 & 70 & 0 \\ 9 & 97 & 0 & 0 \\ 24 & 63 & 9 & 0 \end{bmatrix}. \tag{25}$$

The result of the estimation is the $\boldsymbol{P}$ matrix presented below:

$$\boldsymbol{P} = \begin{bmatrix} 0 & 0.9678 & 0.0072 & 0.0250 \\ 0.9816 & 0 & 0.0184 & 0 \\ 0.0849 & 0.9151 & 0 & 0 \\ 0.2500 & 0.6562 & 0.0938 & 0 \end{bmatrix}. \tag{26}$$

According to Equation (21), with an increase in the number of transitions from the $S_{\rm i}$ state, the standard error $SE(p_{ij})$ decreases. For this reason, the standard error is higher for operational states in which the technical object has been observed to be relatively rare. However, for all conditional probabilities, the $SE(p_{ij})$ did not exceed the value of 0.05, as shown in Equation (27), so the results are considered acceptable [15,75,76].

$$\boldsymbol{SE} = \begin{bmatrix} 0 & 0.0029 & 0.0014 & 0.0025 \\ 0.0022 & 0 & 0.0022 & 0 \\ 0.0271 & 0.0271 & 0 & 0 \\ 0.0442 & 0.0485 & 0.0297 & 0 \end{bmatrix}. \tag{27}$$

The expected values of the interstate transition times $E(T_{ij})$ were estimated as arithmetic averages of the empirical transition times, which are represented by the $\boldsymbol{T}$ matrix (28):

$$\boldsymbol{T} = \begin{bmatrix} 0 & 12.63 & 2.23 & 14.00 \\ 72.23 & 0 & 129.5 & 0 \\ 187.03 & 4.44 & 0 & 0 \\ 16.28 & 518.84 & 124.98 & 0 \end{bmatrix}. \tag{28}$$

The ergodic probabilities π_j of the embedded Markov chain were calculated using the matrix equation (29) with the normalisation condition (23) as follows:

$$\left(\boldsymbol{P}^T - \boldsymbol{I}\right) \cdot \boldsymbol{\Pi} = \begin{bmatrix} -1 & 0.9678 & 0.0072 & 0.0250 \\ 0.9816 & -1 & 0.0184 & 0 \\ 0.0849 & 0.9151 & -1 & 0 \\ 0.2500 & 0.6562 & 0.0938 & -1 \end{bmatrix} \cdot \begin{bmatrix} \pi_1 \\ \pi_2 \\ \pi_3 \\ \pi_4 \end{bmatrix} = \begin{bmatrix} 0 \\ 0 \\ 0 \\ 0 \end{bmatrix}. \tag{29}$$

Then, based on the probabilities p and the times $E(T_{ij})$, the ergodic probability values p_j of the semi-Markov model were calculated using the relation (24). Figure 9a,b shows the results of the calculations for the embedded Markov chain and the SMM, respectively.

The π_j values of the embedded Markov chain contain information about the frequency of occurrence of states in the operation process without taking into account the time duration. In these terms, the most frequent states are S_1 and S_2, each above 48%. The SMM p_j values refer to the temporal stay of vehicles in states S_1–S_4, which is the basis for the calculation of readiness and suitability indices. At random time t, the vehicle will be in state S_2 with the highest probability (more than 77%).

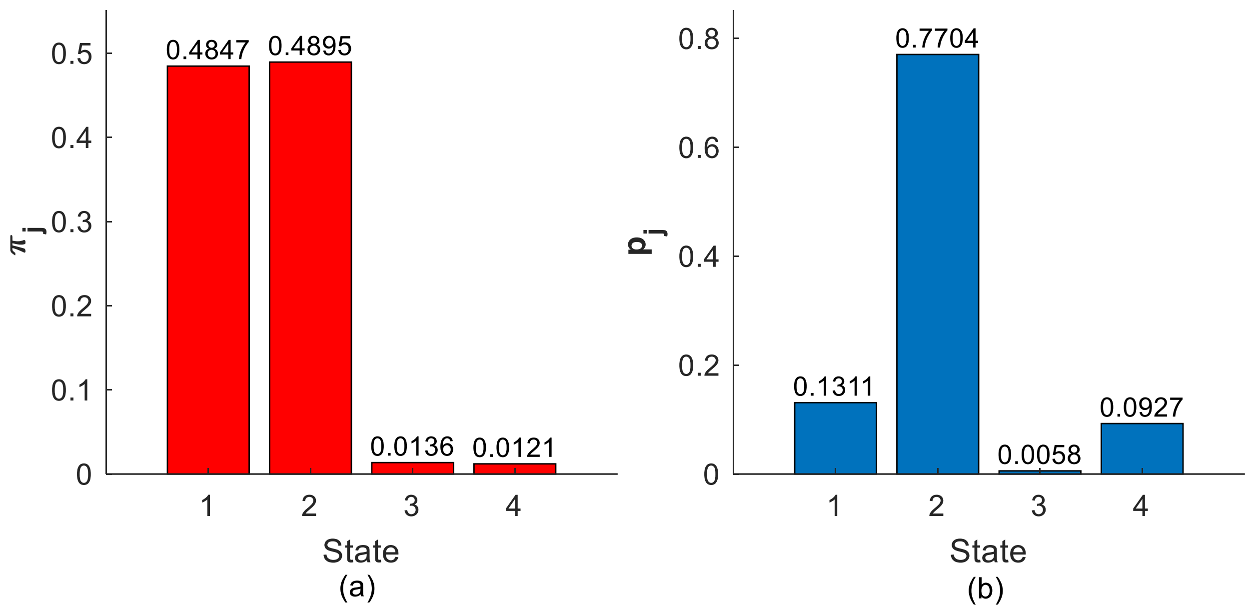

Figure 9. Ergodic probabilities of states for: (**a**)—embedded Markov Chain and (**b**)—semi-Markov model.

5.3. Comparison of the Results

The results of all the simulations are in Table 8. The values of the readiness and technical suitability indicators were compared with the results of the semi-Markov models (SMM). The ergodic probabilities determined for a four-state SMM constituted grounds to determine functional readiness and technical suitability indices, which reached values of 0.9015 and 0.9073, respectively. The results of all simulation models did not differ from SMM by more than 6%, which demonstrates the high precision of the developed models. Given the above, MC1 turned out to be the best four-state model. Its readiness and suitability indices differed from the boundary values of the semi-Markov model by 0.70% and 0.34%, respectively.

Table 8. Simulation and results of the semi-Markov model.

Simulation	Readiness K_r			Suitability K_s		
	Monte Carlo	Semi-Markov	Percentage Error (%)	Monte Carlo	Semi-Markov	Percentage Error (%)
MC1	0.9078	0.9015	0.70	0.9104	0.9073	0.34
MC2	0.8766	0.9015	−2.76	0.8790	0.9073	−3.12
MC3	0.9337	0.9015	3.57	0.9363	0.9073	3.20
MC4	0.9195	0.9015	2.00	0.9221	0.9073	1.63
MC5	0.9142	0.9015	1.41	0.9167	0.9073	1.04
MC6	0.8735	0.9015	−3.11	0.8760	0.9073	−3.45
MC7	0.9329	0.9015	3.48	0.9355	0.9073	3.11
MC8	0.8791	0.9015	−2.48	0.8816	0.9073	−2.83
MC9	0.9163	0.9015	1.64	0.9189	0.9073	1.28
MC10	0.8545	0.9015	−5.21	0.8571	0.9073	−5.53
MC11	0.9257	0.9015	2.68	0.9284	0.9073	2.33
MC12	0.8727	0.9015	−3.19	0.8753	0.9073	−3.53
MC13	0.9393	0.9015	4.19	0.9414	0.9073	3.76
MC14	0.8895	0.9015	−1.33	0.8916	0.9073	−1.73
MC15	0.9419	0.9015	4.48	0.9440	0.9073	4.04
MC16	0.8597	0.9015	−4.64	0.8617	0.9073	−5.03

The relatively low frequency of maintenance and service leads to minor differences between the K_r readiness index and the K_s suitability index. From the perspective of vehicle operation and satisfying transport needs, the K_r readiness index is very important.

5.4. Functional Readiness

Functional readiness defines the probability that a technical object will remain in a state of technical suitability where it can fully implement tasks according to its intended use. Figure 10 shows a functional readiness graph for a car fleet on individual days throughout a simulated operation process. It was defined as a percentage of vehicles in either state S_1 or S_2. Maintaining the $K_r(t)$ indices at an adequately high level is significant from the perspective of safely providing the transport capacity for the operational system. Within the simulation, this index took on a value of 0.55–0.70 through its several iterations. Therefore, more than 70% of the vehicles were ready for operation within the transport system for most of the operation period.

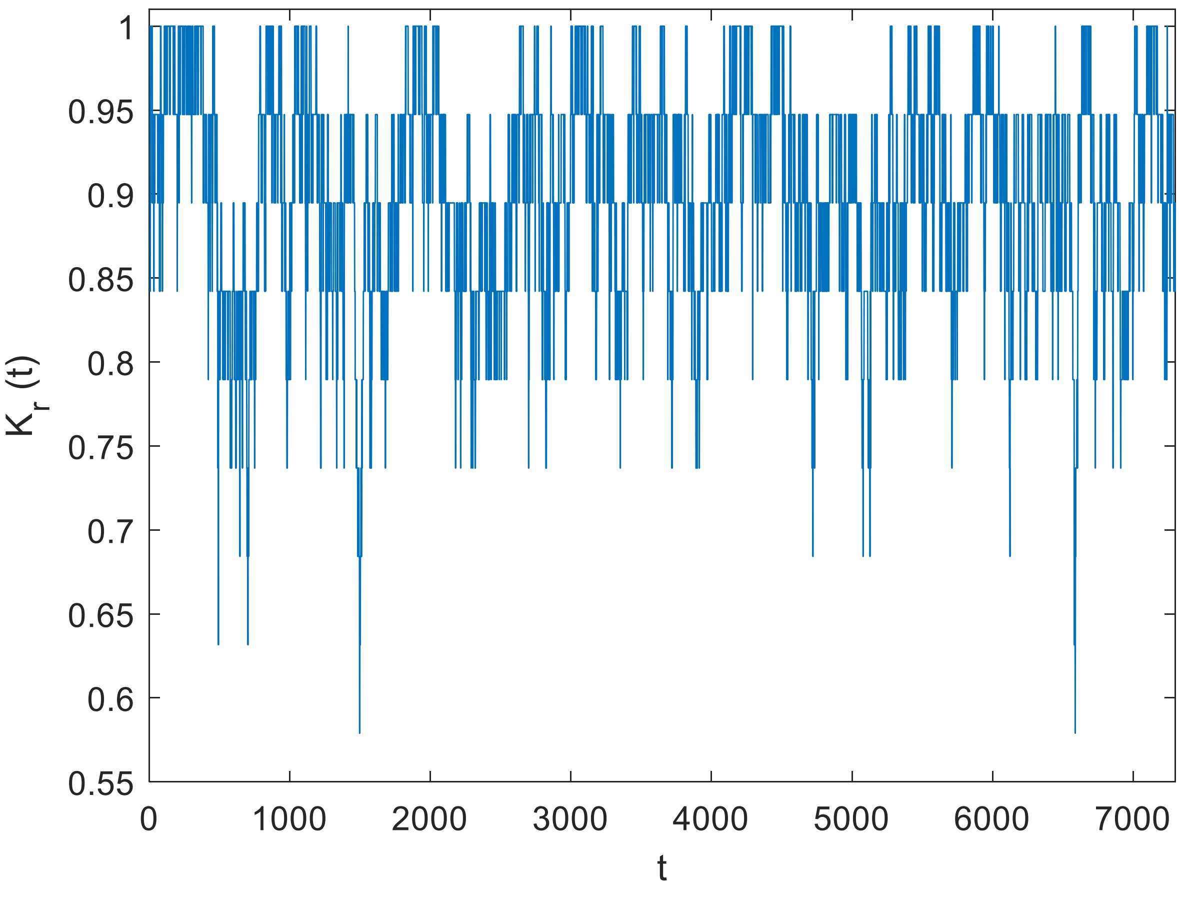

Figure 10. Instantaneous readiness index $K_r(t)$ obtained via simulation of MC1.

The analysis covered the impact of the number of iterations of the simulated process of operating 19 vehicles that form a transport system according to functional readiness. Figure 11 shows the mean value of the K_r index within the measured iteration range $[0, t]$, while t consecutively takes the values of integers in the range of [1, 7300]. At the initial stage of the simulation, functional readiness was found to remain high and then started to decline. After conducting more than 1000 iterations, the K_r index began to gradually stabilise at a level of approximately 0.91. This value came about due to the occurrence of recorded failures and, consequently, damaged vehicles remaining in the state of technical unsuitability.

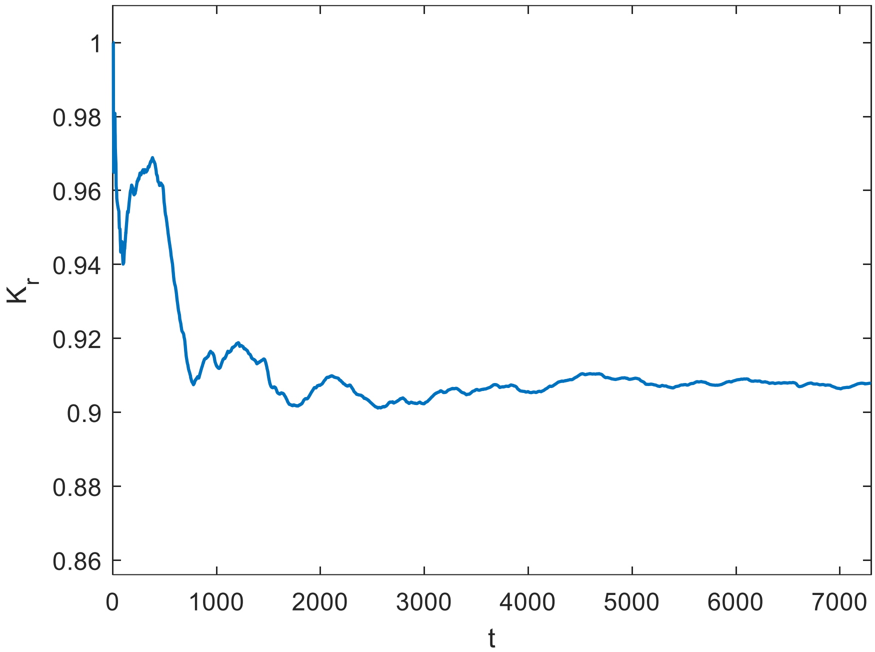

Figure 11. Mean values of the K_r readiness index within the range [0, t] obtained by MC1 simulation.

5.5. Sensitivity Analysis of Monte Carlo Model

A sensitivity analysis of the MC1 model was conducted in order to determine the impact of functional readiness and technical suitability indices depending on the intensity of vehicle operation. The intensity operation is defined by the probability of assigning the transport task Θ and the expected daily mileage value during the execution of the task. The simulated operation process was implemented for specified ranges of considered variables, while at the same time, maintaining the true characteristics of other sub-processes.

Table 9 shows the results of the sensitivity analysis for the Θ coefficient, which takes values from the range [0.10–0.90]. With the minimum vehicle utilisation rate at an average level of 10% of vehicles per day, the daily functional readiness and technical suitability indices reached values of approximately 0.97. However, with an increase in the number of daily operated vehicles, these indices decline until reaching values of approximately 0.80 for a probability of 90% for transport task allocation. Figure 12 shows linear approximations of the K_r and K_s indices depending on the Θ coefficient, carried out using the least squares method. The match of linear approximating functions with simulated data was $R^2 = 0.9916$ for the K_r index and $R^2 = 0.9910$ for the K_s index. According to the approximate functions, an increase in the Θ coefficient by 0.01 leads to a reduction in the values of the indices K_r and K_s by approximately 0.002.

Table 9. Readiness and suitability indicators obtained by sensitivity analysis of the Θ index.

Θ	K_r	K_s
0.10	0.9695	0.9704
0.20	0.9547	0.9564
0.30	0.9309	0.9333
0.40	0.9073	0.9104
0.50	0.8750	0.8788
0.60	0.8670	0.8715
0.70	0.8501	0.8553
0.80	0.8289	0.8347
0.90	0.8031	0.8094
0.10	0.9695	0.9704

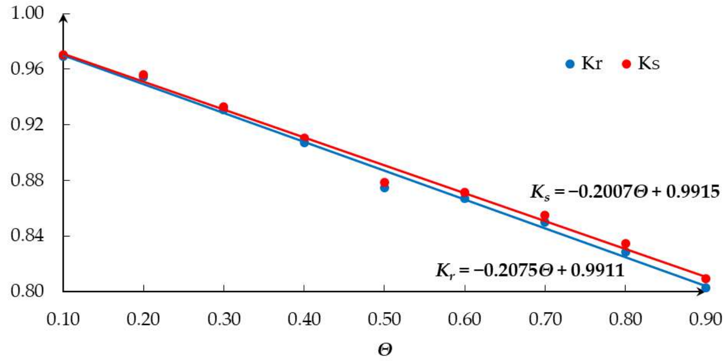

Figure 12. Linear approximations of the dependencies between the K_r and K_s indices and the Θ coefficient.

Table 10 lists the results of the sensitivity analysis for the expected daily mileage l_d over a variability range of 50.0–150.0 km. Figure 13 shows linear approximations of the K_r and K_s indices depending on the expected daily mileage l_d, which exhibited fit to the simulated data at a level of R^2 = 0.9580 and R^2 = 0.9554, respectively. In this paper, an increase in the expected daily mileage by 1.0 km leads to a decrease in the value of the functional readiness and technical suitability indices by approximately 0.0008.

Table 10. Readiness and suitability indicators obtained by sensitivity analysis of expected daily mileage.

Expected Daily Mileage (km)	K_r	K_s
50	0.9445	0.9461
60	0.9476	0.9495
70	0.9431	0.9452
80	0.9348	0.9371
90	0.9097	0.9123
100	0.9094	0.9122
110	0.9049	0.9080
120	0.8993	0.9027
130	0.8838	0.8873
140	0.8768	0.8806
150	0.8735	0.8775

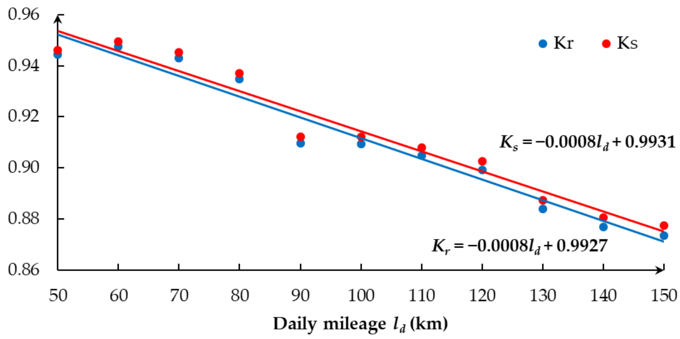

Figure 13. Linear approximations of the dependence between the K_r and K_s indices on the expected value of the daily mileage l_d.

6. Conclusions

This article presents an original Monte Carlo operation process simulation model for light utility vehicles operated by a military transport system. Based on an analysis of the empirical course of the process and the results of previous research, the authors identified a four-state phase space. The planned and preventive strategy for operational management introduces a deterministic element occurring within the stochastic process of changes in the operational state. In the case of military vehicles, the deterministic element is the frequency of periodic maintenance and service defined in the vehicle operation manual and the catalogue of operational standards.

The theoretical simulation model was implemented within the MATLAB software. Its validation was based on probabilistic characteristics estimated on the basis of empirical data. In this work, the simulated course of a stochastic process for 19 vehicles over a predicted 20-year operation period allowed the estimation of the functional readiness index and technical suitability index values in the range of [0.8545–0.9419] and [0.8571–0.9440], respectively. The relative differences between the results of 16 simulation models and the semi-Markov model were less than 6%. Therefore, this minor disproportion confirms the high usefulness of Monte Carlo methods for modelling the operation process.

Moreover, unlike Markov and semi-Markov models, Monte Carlo methods enable consideration of the behaviour of a technical object in hypothetical scenarios that are different from standard operating conditions. This consideration allows for extrapolating the obtained results. The case study involved analysing the sensitivity of the best-fit MC1 model in terms of the impact of vehicle operation intensity on the values of the K_r and K_s coefficients. Based on the spot results of the analyses, the authors performed an approximation with linear functions using the least squares method. Accordingly, an increase in the operation utilisation coefficient of 0.01 entails a decrease in the K_r and K_s coefficient by an average of approximately 0.002. On the other hand, an increase in expected daily mileage according to an exponential distribution of 1.0 km generates a decrease in the K_r and K_s coefficients of approximately 0.008.

An undoubted advantage of the proposed model is the relatively small set of empirical data required for its validation. The assumption of process discretization related to both states (four states) and time (single-day time intervals) implies the need to learn the probabilistic characteristics that determine changes in operational states. The adopted assumptions lead to a simplification of the analysed process, which results in omitting short-term situations and states that are insignificant from the perspectives of both functional readiness and technical suitability.

The proposed approach based on the iterative Monte Carlo algorithm can be implemented in both military and civilian transport systems, as well as industrial machinery. A practical aspect of the algorithm's application is the ability to assess and predict the readiness and suitability of technical objects and systems.

The developed simulation model does not take into account the seasonality of the operation process. Seasonal fluctuations may concern the sub-process of operation, periodic maintenance, and repair implementation. In addition, the social life cycle significantly impacts the intensity of vehicle operation on non-working days (Saturdays and Sundays) relative to other days of the week. A similar phenomenon is associated with maintenance and repair sub-processes, which are implemented primarily from Monday to Friday. The proposed Monte Carlo model does not classify successive iterations as individual days of the week. Expanding the developed model will be the direction of further research within this field.

Author Contributions: Conceptualization, M.O.; methodology, M.O. and J.Z.; software, M.O.; validation, M.O.; formal analysis, M.O.; investigation, M.O.; resources, M.O. and J.Z.; data curation, M.O. and J.Z.; writing—original draft preparation, M.O.; writing—review and editing, M.O., J.Z. and J.M.; visualization, M.O.; supervision, J.Z. and J.M.; project administration, M.O., J.Z. and J.M.; funding acquisition, J.M. All authors have read and agreed to the published version of the manuscript.

Funding: This research received no external funding.

Institutional Review Board Statement: Not applicable.

Informed Consent Statement: Not applicable.

Data Availability Statement: Not applicable.

Acknowledgments: This research was funded by the Military University of Technology, grant number UGB 22-835. This support is gratefully acknowledged.

Conflicts of Interest: The authors declare no conflict of interest.

Appendix A

Figure A1. Results of simulations: (**a**)—MC1, (**b**)—MC2, (**c**)—MC3, (**d**)—MC4, (**e**)—MC5, (**f**)—MC6.

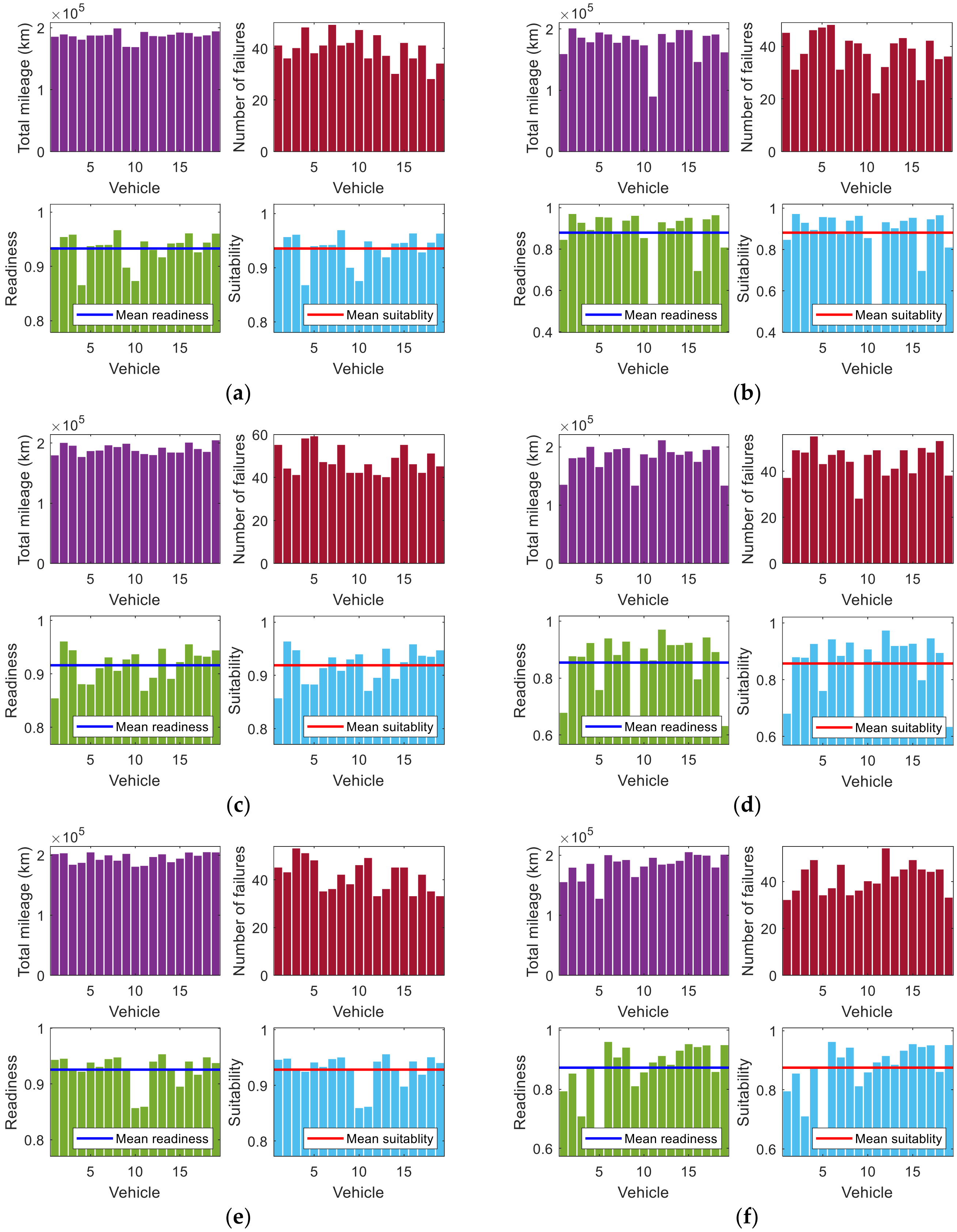

Figure A2. Results of simulations: (**a**)—MC7, (**b**)—MC8, (**c**)—MC9, (**d**)—MC10, (**e**)—MC11, (**f**)—MC12.

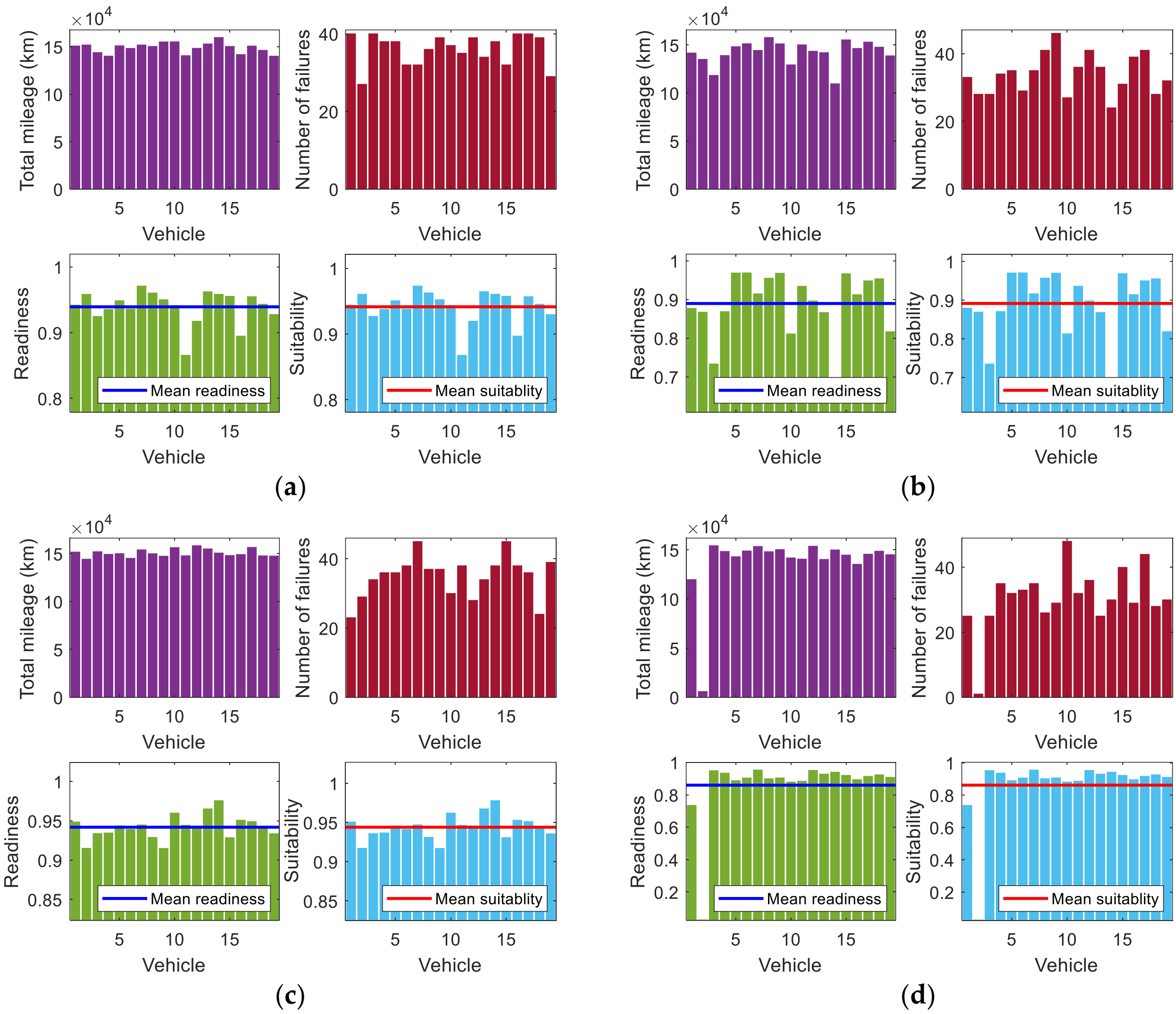

Figure A3. Results of simulations: (**a**)—MC13, (**b**)—MC14, (**c**)—MC15, (**d**)—MC16.

References

1. Benson, R.; Kellner, D. Monte Carlo Simulation for Reliability. In Proceedings of the 2020 Annual Reliability and Maintainability Symposium (RAMS), Palm Springs, CA, USA, 27–30 January 2020; pp. 1–6.
2. Acebes, F.; Poza, D.; González-Varona, J.M.; López-Paredes, A. Stochastic Earned Duration Analysis for Project Schedule Management. *Engineering* **2022**, *9*, 148–161. [CrossRef]
3. Dąbrowska, E. Monte Carlo Simulation Approach to Reliability Analysis of Complex Systems. *J. Konbin* **2020**, *50*, 155–170. [CrossRef]
4. Ren, W.; Ma, L.; Wang, Y. Monte Carlo Analysis for Safety and Reliability of Rail Transit Signal System Based on Cloud Computing. *J. Phys. Conf. Ser.* **2020**, *1654*, 012065. [CrossRef]
5. Liu, C.; Kramer, A.; Neumann, S. Reliability Assessment of Repairable Phased-Mission System by Monte Carlo Simulation Based on Modular Sequence-Enforcing Fault Tree Model. *Eksploat. I Niezawodn. Maint. Reliab.* **2020**, *22*, 272–281. [CrossRef]
6. Amjad, M.; Ahmad, I.; Ahmad, M.; Wróblewski, P.; Kamiński, P.; Amjad, U. Prediction of Pile Bearing Capacity Using XGBoost Algorithm: Modeling and Performance Evaluation. *Appl. Sci.* **2022**, *12*, 2126. [CrossRef]
7. Janekova, J.; Fabianova, J.; Kadarova, J. Selection of Optimal Investment Variant Based on Monte Carlo Simulations. *Int. J. Simul. Model.* **2021**, *20*, 279–290. [CrossRef]
8. Żurek, J.; Zieja, M.; Ziółkowski, J.; Borucka, A. Vehicle Operation Process Analysis Using the Markov Processes. In Proceedings of the 29th European Safety and Reliability Conference, Hannover, Germany, 22–26 September 2019; pp. 2598–2605.
9. Ziółkowski, J.; Borucka, A. Markov Model in Logistic Management of Enterprise. *J. Konbin* **2016**, *38*, 271–290. [CrossRef]
10. Borucka, A.; Niewczas, A.; Hasilova, K. Forecasting the Readiness of Special Vehicles Using the Semi-Markov Model. *Eksploat. Niezawodn. Maint. Reliab.* **2019**, *21*, 662–669. [CrossRef]

11. Świderski, A.; Borucka, A.; Grzelak, M.; Gil, L. Evaluation of Machinery Readiness Using Semi-Markov Processes. *Appl. Sci.* **2020**, *10*, 1541. [CrossRef]
12. Oszczypała, M.; Ziółkowski, J.; Małachowski, J. Reliability Analysis of Military Vehicles Based on Censored Failures Data. *Appl. Sci.* **2022**, *12*, 2622. [CrossRef]
13. Dziubak, T.; Wysocki, T.; Dziubak, S. Selection of Vehicles for Fleet of Transport Company on the Basis of Observation of Their Operational Reliability. *Eksploat. Niezawodn. Maint. Reliab.* **2021**, *23*, 184–194. [CrossRef]
14. Żurek, J.; Ziółkowski, J.; Borucka, A. Application of Markov Processes to the Method for Analysis of Combat Vehicle Operation in the Aspect of Their Availability and Readiness. In Proceedings of the 2nd International Conference on Engineering Sciences and Technologies, Kerbala, Iraq, 26–28 March 2018; pp. 2343–2352.
15. Oszczypała, M.; Ziółkowski, J.; Małachowski, J. Analysis of Light Utility Vehicle Readiness in Military Transportation Systems Using Markov and Semi-Markov Processes. *Energies* **2022**, *15*, 5062. [CrossRef]
16. Liu, K.; Wu, J.; Liu, H.; Sun, M.; Wang, Y. Reliability Analysis of Thermal Error Model Based on DBN and Monte Carlo Method. *Mech. Syst. Signal Process.* **2021**, *146*, 107020. [CrossRef]
17. Jensen, H.A.; Jerez, D.J.; Valdebenito, M. An Adaptive Scheme for Reliability-Based Global Design Optimization: A Markov Chain Monte Carlo Approach. *Mech. Syst. Signal Process.* **2020**, *143*, 106836. [CrossRef]
18. Zhang, L.; Dong, L.; Cheng, S.; Li, W.; Wang, B.; Liu, H.; Chen, K. Efficient Reliability Assessment Method for Bridges Based on Markov Chain Monte Carlo (MCMC) with Metropolis-Hasting Algorithm (MHA). *IOP Conf. Ser. Earth Environ. Sci.* **2020**, *580*, 012030. [CrossRef]
19. Zhu, H.; Wang, X.; Xiao, M.; Yang, Z.; Tang, X.; Wen, B. Reliability Modeling for Intermittent Working System Based on Wiener Process. *Comput. Ind. Eng.* **2021**, *160*, 107599. [CrossRef]
20. Shahtaheri, Y.; Flint, M.M.; De la Garza, J.M. A Multi-Objective Reliability-Based Decision Support System for Incorporating Decision Maker Utilities in the Design of Infrastructure. *Adv. Eng. Inform.* **2019**, *42*, 100939. [CrossRef]
21. Zhang, K.; Tang, B.; Deng, L.; Yu, X.; Wei, J. Fault Source Location of Wind Turbine Based on Heterogeneous Nodes Complex Network. *Eng. Appl. Artif. Intell.* **2021**, *103*, 104300. [CrossRef]
22. Kallen, M.J. Modelling Imperfect Maintenance and the Reliability of Complex Systems Using Superposed Renewal Processes. *Reliab. Eng. Syst. Saf.* **2011**, *96*, 636–641. [CrossRef]
23. Durczak, K.; Rybacki, P.; Sujak, A. Application of a Selected Pseudorandom Number Generator for the Reliability of Farm Tractors. *Appl. Sci.* **2022**, *12*, 12452. [CrossRef]
24. Singh, C.; Mitra, J. Monte Carlo Simulation for Reliability Analysis of Emergency and Standby Power Systems. In Proceedings of the IAS '95. Conference Record of the 1995 IEEE Industry Applications Conference Thirtieth IAS Annual Meeting, Orlando, FL, USA, 8–12 October 1995; Volume 3, pp. 2290–2295.
25. Souza-Franco, R.L.; Clavijo, V.; Schleder, M.; Martins, R. Monte Carlo Simulation to Consider Uncertainty in the Reliability Analysis of Dynamic Positioning Systems. In Proceedings of the 29th European Safety and Reliability Conference (ESREL), Hannover, Germany, 22–26 September 2019; Research Publishing Services: Hannover, Germany, 2019; pp. 2446–2453.
26. Novak, M.; Sangwongwanich, A.; Blaabjerg, F. Monte Carlo Based Reliability Estimation Methods in Power Electronics. In Proceedings of the 2020 IEEE 21st Workshop on Control and Modeling for Power Electronics (COMPEL), Aalborg, Denmark, 9–12 November 2020; pp. 1–7.
27. Green, R.C.; Wang, L.; Alam, M.; Singh, C. Intelligent State Space Pruning for Monte Carlo Simulation with Applications in Composite Power System Reliability. *Eng. Appl. Artif. Intell.* **2013**, *26*, 1707–1724. [CrossRef]
28. Roslan, N.N.R.B.; Fauzi, N.F.B.M.; Ridzuan, M.I.M. Sequential and Nonsequential Monte Carlo in Assessing Reliability Performance of Distribution Network. In Proceedings of the 2020 Emerging Technology in Computing, Communication and Electronics (ETCCE), Dhaka, Bangladesh, 21–22 December 2020; pp. 1–6.
29. Ugurlu, O.F.; Kumral, M. Reliability-Based Performance Analysis of Mining Drilling Operations through Markov Chain Monte Carlo and Mean Reverting Process Simulations. *Simulation* **2020**, *96*, 593–604. [CrossRef]
30. Hu, Y.-W.; Zhang, H.-C.; Liu, S.-J.; Lu, H.-T. Sequential Monte Carlo Method Toward Online RUL Assessment with Applications. *Chin. J. Mech. Eng.* **2018**, *31*, 5. [CrossRef]
31. Sharma, S.; Cui, Y.; He, Q.; Mohammadi, R.; Li, Z. Data-Driven Optimization of Railway Maintenance for Track Geometry. *Transp. Res. Part C Emerg. Technol.* **2018**, *90*, 34–58. [CrossRef]
32. Zhang, X.; Lu, Z.; Cheng, K.; Wang, Y. A Novel Reliability Sensitivity Analysis Method Based on Directional Sampling and Monte Carlo Simulation. *Proc. Inst. Mech. Eng. Part O J. Risk Reliab.* **2020**, *234*, 622–635. [CrossRef]
33. Zhang, K.; Du, Z.; Xiao, F.; Wang, T.; Zhang, L. Improved Sequential Monte Carlo Method Approach to Substation Connection Reliability Assessment. In Proceedings of the 2020 IEEE 4th Conference on Energy Internet and Energy System Integration (EI2), Wuhan, China, 30 October–1 November 2020; pp. 2357–2362.
34. Macheret, Y.; Koehn, P.; Sparrow, D. Improving Reliability and Operational Availability of Military Systems. In Proceedings of the 2005 IEEE Aerospace Conference, Big Sky, MT, USA, 5–12 March 2003; IEEE Operations Center: Big Sky, MT, USA, 2005; pp. 3948–3957.
35. Andrade-Michel, A.; Ríos-Solís, Y.A.; Boyer, V. Vehicle and Reliable Driver Scheduling for Public Bus Transportation Systems. *Transp. Res. Part B Methodol.* **2021**, *145*, 290–301. [CrossRef]

36. Wang, Y.; Infield, D. Markov Chain Monte Carlo Simulation of Electric Vehicle Use for Network Integration Studies. *Int. J. Electr. Power Energy Syst.* **2018**, *99*, 85–94. [CrossRef]
37. Ricard, L.; Desaulniers, G.; Lodi, A.; Rousseau, L.-M. Predicting the Probability Distribution of Bus Travel Time to Measure the Reliability of Public Transport Services. *Transp. Res. Part C Emerg. Technol.* **2022**, *138*, 103619. [CrossRef]
38. Salgado Duarte, Y.; Szpytko, J.; Del Castillo Serpa, A.M. Monte Carlo Simulation Model to Coordinate the Preventive Maintenance Scheduling of Generating Units in Isolated Distributed Power Systems. *Electr. Power Syst. Res.* **2020**, *182*, 106237. [CrossRef]
39. Lojowska, A.; Kurowicka, D.; Papaefthymiou, G.; van der Sluis, L. Stochastic Modeling of Power Demand Due to EVs Using Copula. *IEEE Trans. Power Syst.* **2012**, *27*, 1960–1968. [CrossRef]
40. Paś, J.; Klimczak, T.; Rosiński, A.; Stawowy, M. The Analysis of the Operational Process of a Complex Fire Alarm System Used in Transport Facilities. *Build. Simul.* **2022**, *15*, 615–629. [CrossRef]
41. Stawowy, M.; Rosiński, A.; Siergiejczyk, M.; Perlicki, K. Quality and Reliability-Exploitation Modeling of Power Supply Systems. *Energies* **2021**, *14*, 2727. [CrossRef]
42. Borowski, S.; Szubartowski, M.; Migawa, K.; Sołtysiak, A.; Neubauer, A.; Hujo, L.; Nosian, J. Mathematical Model for Determining the Time of Preventive Replacements in the Agricultural Machinery Service System with Minimal Repair. *Appl. Sci.* **2023**, *13*, 640. [CrossRef]
43. Migawa, K.; Borowski, S.; Neubauer, A.; Sołtysiak, A. Semi-Markov Model of the System of Repairs and Preventive Replacements by Age of City Buses. *Appl. Sci.* **2021**, *11*, 10411. [CrossRef]
44. Liu, P.; Wang, G. Optimal Periodic Preventive Maintenance Policies for Systems Subject to Shocks. *Appl. Math. Model.* **2021**, *93*, 101–114. [CrossRef]
45. Park, M.; Jung, K.M.; Park, D.H. Optimization of Periodic Preventive Maintenance Policy Following the Expiration of Two-Dimensional Warranty. *Reliab. Eng. Syst. Saf.* **2018**, *170*, 1–9. [CrossRef]
46. Hu, J.; Shen, J.; Shen, L. Periodic Preventive Maintenance Planning for Systems Working under a Markovian Operating Condition. *Comput. Ind. Eng.* **2020**, *142*, 106291. [CrossRef]
47. Wang, W.; Wu, Z.; Xiong, J.; Xu, Y. Redundancy Optimization of Cold-Standby Systems under Periodic Inspection and Maintenance. *Reliab. Eng. Syst. Saf.* **2018**, *180*, 394–402. [CrossRef]
48. Adekitan, A.I.; Bukola, A.; Kennedy, O. A Data-Based Investigation of Vehicle Maintenance Cost Components Using ANN. *IOP Conf. Ser. Mater. Sci. Eng.* **2018**, *413*, 012009. [CrossRef]
49. Chen, C.; Liu, Y.; Wang, S.; Sun, X.; Di Cairano-Gilfedder, C.; Titmus, S.; Syntetos, A.A. Predictive Maintenance Using Cox Proportional Hazard Deep Learning. *Adv. Eng. Inform.* **2020**, *44*, 101054. [CrossRef]
50. Hu, J.; Wang, Y.; Pang, Y.; Liu, Y. Optimal Maintenance Scheduling under Uncertainties Using Linear Programming-Enhanced Reinforcement Learning. *Eng. Appl. Artif. Intell.* **2022**, *109*, 104655. [CrossRef]
51. Sbihi, M.; Varnier, C. Single-Machine Scheduling with Periodic and Flexible Periodic Maintenance to Minimize Maximum Tardiness. *Comput. Ind. Eng.* **2008**, *55*, 830–840. [CrossRef]
52. Ministry of Defense of Poland. *DTU-4.22.13.1(A). Catalog of Operating Norms for Land Machinery*; Ministry of Defense of Poland; Armed Forces Support Inspectorate: Bydgoszcz, Poland, 2019.
53. Redmer, A. Optimisation of the Exploitation Period of Individual Vehicles in Freight Transportation Companies. *Transp. Res. Part E Logist. Transp. Rev.* **2009**, *45*, 978–987. [CrossRef]
54. Betkier, I.; Macioszek, E. Characteristics of Parking Lots Located along Main Roads in Terms of Cargo Truck Requirements: A Case Study of Poland. *Sustainability* **2022**, *14*, 15720. [CrossRef]
55. Soltanali, H.; Rohani, A.; Abbaspour-Fard, M.H.; Farinha, J.T. A Comparative Study of Statistical and Soft Computing Techniques for Reliability Prediction of Automotive Manufacturing. *Appl. Soft Comput.* **2021**, *98*, 106738. [CrossRef]
56. Gołda, P.; Zawisza, T.; Izdebski, M. Evaluation of Efficiency and Reliability of Airport Processes Using Simulation Tools. *Eksploat. Niezawodn.* **2021**, *23*, 659–669. [CrossRef]
57. Wang, J.; Gao, X.; Sun, Z. An Importance Sampling Framework for Time-Variant Reliability Analysis Involving Stochastic Processes. *Sustainability* **2021**, *13*, 7776. [CrossRef]
58. Alkaff, A.; Qomarudin, M.N.; Purwantini, E.; Wiratno, S.E. Dynamic Reliability Modeling for General Standby Systems. *Comput. Ind. Eng.* **2021**, *161*, 107615. [CrossRef]
59. Hao, S.; Yang, J.; Ma, X.; Zhao, Y. Reliability Modeling for Mutually Dependent Competing Failure Processes Due to Degradation and Random Shocks. *Appl. Math. Model.* **2017**, *51*, 232–249. [CrossRef]
60. Hong, L.; Zhai, Q.; Wang, X.; Ye, Z.-S. System Reliability Evaluation Under Dynamic Operating Conditions. *IEEE Trans. Reliab.* **2019**, *68*, 800–809. [CrossRef]
61. Torii, A.J.; Novotny, A.A. A Priori Error Estimates for Local Reliability-Based Sensitivity Analysis with Monte Carlo Simulation. *Reliab. Eng. Syst. Saf.* **2021**, *213*, 107749. [CrossRef]
62. Angus, J.; Ding, Y. On the Ratio of Current Age to Total Life for Null Recurrent Renewal Processes. *Stat. Probab. Lett.* **2020**, *162*, 399. [CrossRef]
63. Vassiliou, P.-C.G. Non-Homogeneous Semi-Markov and Markov Renewal Processes and Change of Measure in Credit Risk. *Mathematics* **2020**, *9*, 55. [CrossRef]
64. Ziółkowski, J.; Małachowski, J.; Oszczypała, M.; Szkutnik-Rogoż, J.; Lęgas, A. Modelling of the Military Helicopter Operation Process in Terms of Readiness. *Def. Sci. J.* **2021**, *71*, 602–611. [CrossRef]

65. Grabski, F. Semi-Markov Failure Rates Processes. *Appl. Math. Comput.* **2011**, *217*, 9956–9965. [CrossRef]
66. Migawa, K. Availability Control for Means of Transport in Decisive Semi-Markov Models of Exploitation Process. *Arch. Transp.* **2012**, *24*, 497–508. [CrossRef]
67. Ivanchenko, O.; Kharchenko, V.; Moroz, B.; Kabak, L.; Smoktii, K. Semi-Markov Availability Model Considering Deliberate Malicious Impacts on an Infrastructure-as-a-Service Cloud. In Proceedings of the 2018 14th International Conference on Advanced Trends in Radioelectronics, Telecommunications and Computer Engineering (TCSET), Lviv-Slavske, Ukraine, 20–24 February 2018; pp. 570–573.
68. Karakaya, E.; Vinel, A.; Smith, A.E. Relocations in Container Depots for Different Handling Equipment Types: Markov Models. *Comput. Ind. Eng.* **2021**, *157*, 107311. [CrossRef]
69. Oniszczuk, W. Loss Tandem Networks with Blocking—A Semi-Markov Approach. *Bull. Pol. Acad. Sci. Tech. Sci.* **2010**, *58*, 673–681. [CrossRef]
70. Shepero, M.; Munkhammar, J. Spatial Markov Chain Model for Electric Vehicle Charging in Cities Using Geographical Information System (GIS) Data. *Appl. Energy* **2018**, *231*, 1089–1099. [CrossRef]
71. Iversen, E.B.; Morales, J.M.; Madsen, H. Optimal Charging of an Electric Vehicle Using a Markov Decision Process. *Appl. Energy* **2014**, *123*, 1–12. [CrossRef]
72. Zhao, L.; Li, K.; Zhao, W.; Ke, H.-C.; Wang, Z. A Sticky Sampling and Markov State Transition Matrix Based Driving Cycle Construction Method for EV. *Energies* **2022**, *15*, 1057. [CrossRef]
73. Brayer, E.F. Calculating the Standard Error of a Proportion. *Appl. Stat.* **1957**, *6*, 67–68. [CrossRef]
74. Gurland, J.; Tripathi, R.C. A Simple Approximation for Unbiased Estimation of the Standard Deviation. *Am. Stat.* **1971**, *25*, 30–32. [CrossRef]
75. Roy, V.; Tan, A.; Flegal, J.M. Estimating Standard Errors for Importance Sampling Estimators with Multiple Markov Chains. *Stat. Sin.* **2018**, *28*, 1079–1101. [CrossRef]
76. Rosychuk, R.J.; Sheng, X.; Stuber, J.L. Comparison of Variance Estimation Approaches in a Two-State Markov Model for Longitudinal Data with Misclassification. *Stat. Med.* **2006**, *25*, 1906–1921. [CrossRef]

Reliability Engineering and System Safety 242 (2024) 109780

Contents lists available at ScienceDirect

Reliability Engineering and System Safety

journal homepage: www.elsevier.com/locate/ress

Reliability analysis and redundancy optimization of *k*-out-of-*n* systems with random variable *k* using continuous time Markov chain and Monte Carlo simulation

Mateusz Oszczypała, Jakub Konwerski, Jarosław Ziółkowski *, Jerzy Małachowski

Institute of Mechanics and Computational Engineering, Faculty of Mechanical Engineering, Military University of Technology, gen. Sylwestra Kaliskiego Street 2, Warsaw 00-908, Poland

A R T I C L E I N F O

Keywords:
K-out-of-*n*
Reliability modeling
Maintenance analysis
Transportation system
Probability of system failure
Markov chains
Monte Carlo simulation

A B S T R A C T

This article discusses the problems associated with the redundancy of structures *k*-out-of-*n* as a method of increasing system availability. A parallel *k*-out-of-*n* system was considered, with *k* repairable and homogeneous components. The other ($n - k$) objects are in hot redundancy mode. Failures and repairs are independent processes, and each repaired object is treated as full-fledged in terms of operation. The system operates under dynamically changing conditions, so the minimum number of operable components essential for its proper operation is a random variable with a specific distribution. Component damages and repairs are independent stochastic processes. A probabilistic and simulation approach based on Continuous Time Markov Chain and Monte Carlo simulation is proposed. This study aims to optimize the number of components in the *k*-out-of-*n* structure, which will ensure the system operation with a certain availability and performance. The proposed methods were applied to real transport systems, for which models were developed with parameters estimated on the basis of empirical data. The convergence of the results obtained, using two methods, testifies to the correctness of the methodology used and the reliability of the models developed. The risk to system performance associated with changing input parameters was assessed using model sensitivity analysis. As indicated, the model is not susceptible to changes in the damage and repair intensity. It has also been shown that optimization of the *k*-out-of-*n* structure brings a significant reduction in the costs incurred for system development and operation.

1. Introduction

With the development and application of modern technologies, objects and systems used today are extremely complex. Proper operation along with usage is to maintain the technical operability of the object for a certain time [1]. To ensure proper operation of the system, various forms of redundancy are used, often as soon as at the design stage, which reduce the importance of failure of a single object to ensure the system's assumed reliability and availability indicators.

Fig. 1 shows the most commonly used redundancy types [2–4]. Structural redundancy is the introduction of additional structural elements into the system. In the event of damage, it allows the re-assignment (often automatic) of the tasks performed by the basic element to a backup element. Parametric redundancy is that the object has better physical properties (e.g. strength) than those necessary to ensure the assumed reliability. Functional redundancy refers to the case where suitability is lost by one element in the system, and its tasks are taken over by another, which, in addition to its basic role in emergency situations is capable of performing additional functions.

Through the application of appropriate redundancy strategies, the maximum safety, durability, and reliability of facilities are constantly sought. In active redundancy, the components operate all the time, and in passive redundancy, until the failure, all redundant components are in standby mode. The mixed system [5–7] is a combination of the above two strategies.

In practice, three main redundancy methods are distinguished, i.e. cold, warm, and hot [8–10]. Cold redundancy consists in having a spare (identical) object nearby that takes a relatively long time to activate, e.g. lighting system in a manufacturing workshop and discrete signal transmission system [11]. It works wherever downtime and human intervention are acceptable. The standby components in cold redundant systems do not fail until they are switched to the working system [12].

* Corresponding author.
E-mail address: jaroslaw.ziolkowski@wat.edu.pl (J. Ziółkowski).

https://doi.org/10.1016/j.ress.2023.109780
Received 28 March 2023; Received in revised form 18 September 2023; Accepted 2 November 2023
Available online 4 November 2023

Warm redundancy is used in systems where the response time and duration of the failure are important, but despite this, a temporary interruption in operation is permissible, for example, the use of backup generators [13]. In warm standby mode, standby components are less likely to fail than during the operational period [14].

Hot redundancy provides an immediate process correction after a failure is detected, so the method is used as a solution for critical processes that cannot afford any downtime, for example, power supply in a hospital, air traffic control, and nuclear power plant operation [15]. In hot-standby redundant systems, the reliability characteristics of the working and standby components are the same [16].

Moreover, a system may have a serial, parallel, series-parallel, parallel-serial and k-out-of-n type structure, which is the most popular configuration currently used in redundant systems. The parallel system k-out-of-n consists of n components or subsystems, of which only k it must be operable for the system to operate properly. Such a system can be described in two ways. The k-out-of-n:G [17,18] structure defines it as one in which the parameter k represents the number of components that must be operable in order for the entire system to operate properly. However, if k is the number of the system components that must fail before the entire system fails, this structure is considered as k-out-of-n:F [19–21]. Of course, these descriptions are closely connected and each of them is dual to another. The parallel configuration allows us to increase the reliability of the system without changing the reliability of the individual components that make up the system [22].

The k-out-of-n systems are used in telecommunications [23], navigation [24] radar systems [25], oil products transport installations [26], transport [27–29], energy [30,31], health service [32], smart manufacturing systems [33], smart street light systems [34], industry [35] monitoring of undersea pipelines [36], and the army [37]. The wide range of k-out-of-n system applications justifies attempting to find methods appropriate for their analysis and evaluation. A specific type of system are dynamic k-out-of-n structures dedicated to handling time-varying task streams. They are encountered in real-world conditions in many areas of industry, including: fire safety systems [38], power systems [39,40], wireless networks [41], fuel supply systems [42], unmanned vehicles [43,44]. Depending on the volume of the task stream, the systems work with different performance. Therefore, the system configuration may require various configurations that are adapted to the changing needs of the users.

Depending on the reliability structure and component types, different approaches to modeling technical systems are used in practice. The aim of looking for suitable redundancy methods and the number of components in the structure is to optimize reliability and reduce the cost of system deployment and maintenance [45]. The operating costs of defense systems are significant and should be taken into account at the stages of facility design and management alike. Due to budgetary constraints, the economic performance of public spending is sought. For the sake of safety and the maintenance of assumed technical readiness, military systems, as a rule, are characterized by high structural redundancy. When using technical facilities, considerable attention is therefore paid to the reliability of the individual elements that make up the system. The process of driving vehicles in transport systems aims to perform tasks or wait for tasks to appear at random moments in time [46,47]. In peacetime, in times of direct threat of armed conflict, and in times of war, backup facilities are maintained in the state of readiness according to the assumptions of the passive hot redundancy strategy.

The aim of this paper is to develop methods for assessing and improving the availability and performance of dynamic technical systems with a k-out-of-n structure. The measurable effect of the model will be the optimal number of necessary components, which translates into a reduction in operating costs of the system in question. Due on constraints to the resources required for production, research on redundant systems can contribute to solving current economic and security problems. Taking into account the above and using the proposed methodology, these authors researched two transport systems in place in the Polish Armed Forces.

The main contribution to the article consists of the development of a simulation model based on CTMC and MC methods and the proposal of indicators to assess the availability and performance of dynamic technical systems with variable intensity of operation. The research and analyses were done in the MATLAB environment to solve the optimization problem in two military transport systems. The proposed models were validated on the basis of probabilistic methods for the number of components in the k-out-of-n system. An additional element was the analysis of the sensitivity of the model input parameters to the A_S and TPM indicators. The final stage was an assessment of the risk of a decrease in the availability and performance of the system operation in the event of changes in the system environment and the size of the task stream.

The article is divided into six sections. Section 2 presents the current state of knowledge of the applied redundant systems and reliability modeling of technical objects and systems. Then, on the basis of the accepted assumptions, the system and the applied mathematical model based on the Monte Carlo and Markov Chain Monte Carlo methods are described (Section 3). Based on empirical operational data obtained

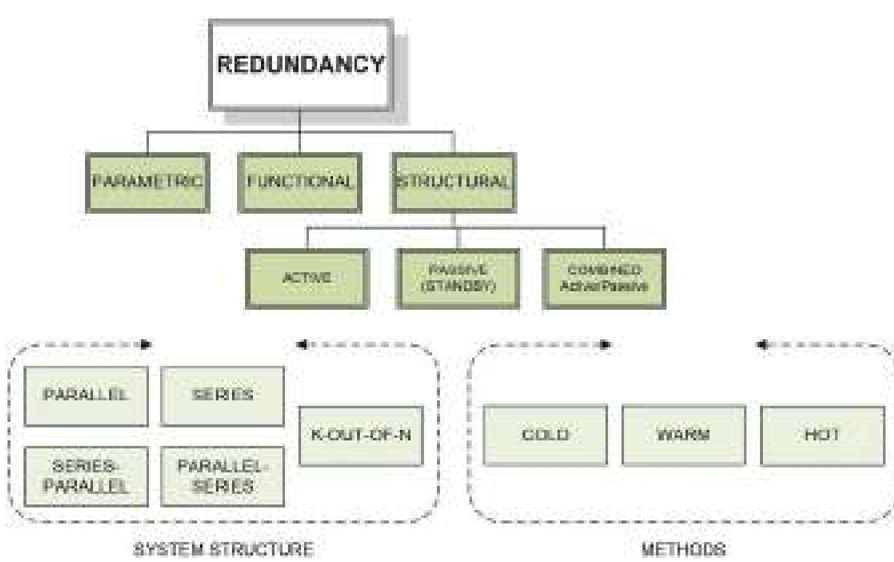

Fig. 1. Types of redundancy.

from actual military transport systems, Section 4 presents the practical application of the proposed approach to the analysis of the operation process and the availability of light utility vehicles and trucks. Based on real data, parameters of the intensity of damage λ and repair μ were determined, and the parameter of the cumulative distribution function of variable k. Then a simulation was performed to evaluate the indicators and assess the risk of reducing the number of components in the system. The results obtained, along with cost analysis are discussed in Section 5. The entire publication is summarized in the final conclusions contained in Section 6.

2. Literature review

This part reviews the literature on reliability modeling and optimization of technical k-out-of-n systems using redundant systems. Table 1 summarizes the methods used to date and the test objectives for systems equipped with homogeneous or heterogeneous and repairable or non-repairable components.

Rykov et al. [36] based on mathematical methods and numerical experiments with exponential, Gamma, Gnedenko-Weibull, and log-normal distributions, evaluated the reliability and compared the effectiveness of various preventive maintenance (PM) strategies for a redundant system using the active and hot redundancy method. They proposed an algorithm for choosing the strategy that ensures the greatest availability of the system. The applicability of the proposed modeling framework for the reliability of the system was illustrated by underwater transport pipeline monitoring equipment.

The Bayesian approach to reliability analysis was proposed by Saberzadeh et al. in [8]. The Monte Carlo algorithm (MC) was used to estimate the unknown parameters of the passive and hot redundancy models. The reliability of the system and its credible interval were estimated using the Bayesian method. An example of the applications of such kind of systems are wind turbines.

One method of describing redundancy systems is probabilistic dependencies. In the article [48], when using them, the reliability properties of k-out-of-n structured systems consisting of heterogeneous, irreparable components with discrete lifetimes are described. Passive and hot redundancies were applied. Similarly, Ling and Wei [52] and Zhang [59] optimized the redundancy allocation in terms of system reliability. Furthermore, it was inspected in [52] how heterogeneity affects k-out-of-n system reliability. Based on the common bus performance sharing (CBPS) system, in [63] a probabilistic model based on discrete stochastic processes in continuous time is proposed to evaluate the momentary availability of repairable objects. The presented methodology is applicable to any time-to-failure and time-to-repair schedules for system components. Hamdan et al. [61] extended this method with multicriteria optimization and presented optimal preventive maintenance models for the class of weighted k-out-of-n systems based on the average cost and availability criteria.

Markov chains and Markov Chain Monte Carlo (MCMC) are widely used approaches to reliability analysis. Sharifi et al. [3,49], in the numerical example (2-out-of-4 system) and the real case study of water transition system, used Markov processes to describe and optimize the expected total cost and minimize inspection interval. Parallel, repairable components with k-out-of-n redundancy were used to develop cost-effective inspection and maintenance policy [55]. Studying the same type of system Rykov et al. [26] using the complementary variables Markov chain method proved that at a low frequency of objects inoperability the system becomes virtually insensitive to the shape of the distributions of individual component repair times. In the article [30] the Markov chain model extension with Binary Indicator Universal Generating Function (BIUGF) has been shown to provide high accuracy reliability ratings.

It should be noted that in the modeling of reliability systems, the authors often use Genetic Algorithms (GA). In [54] GA extended Markov chain methods and used them to describe the preventive replacement (PR) schedule i.e. maximizing of mission success probability (MSP) and minimizing expected mission cost (EMC) homogeneous components. In publications [57,60], using the methods of Multi-objective Evolutionary Algorithm (MOEA), Universal Generating Function (UGF), Non-dominated Sorting Genetic Algorithm II (NSGA-II) and Non-dominated Ranked Genetic Algorithm (NRGA), a Redundancy Allocation Problem (RAP) model for optimizing the reliability and cost of k-out-of-n parallel and series-parallel systems was presented. Furthermore, in [60], weighed subsystem k-out-of-n was considered, with heterogeneous components in which its performance is the sum of the different values of all components. The system operates properly, if the sum of these values is not less than k.

In weighted k-out-of-n systems [65] the number of operable components required for the system to operate properly is not a fixed number. For each structure, a set can be specified of variants of operable components, the total value of which is greater than or equal to the assumed number k. However, there are technical systems operating with a variable intensity, which can be expressed as a random variable k with some assumed or approximated distribution. Dynamic k-out-of-n structures are a current subject of research by scientists. Lin et al. [41] developed an FMCI-based model for reliability analysis and replacement interval optimization for wireless sensor networks composed of non-repairable, homogeneous components. For this type of components, a reliability analysis of power transmission systems was performed in [39] based on a multi-valued decision diagram. This method was used by Wang et al. for heterogeneous components. They performed reliability analysis for numerical examples [64] and for real case studies of unmanned aerial vehicles [43] and performance assessment for smart home lighting control system and oil supply system [42]. An extension of the multi-valued decision diagram method to binary decision diagrams is included in [44]. The problem of reliability evaluation and RAP for a cold-standby system with homogeneous, non-repairable components was solved using semi-Markov process and MC simulation and validated using a satellite power supply system as an example [40]. The reduction of component and system cost for redundant warm fire detection systems using GA was proposed by Eslami Baladeh and Taghipour [38].

The proposed approach fills a methodological gap in the current state of the scientific literature. Reliability modeling of k-out-of-n structures in related work did not address systems handling variable task stream intensity. Dynamically varying task stream intensity is encountered, for example in commercial and military transport systems. The size of the stream determines the number of components (technical means) required to handle it. The realizations of this stochastic process can be described by probabilistic distributions. This publication proposes a method based on CTMC and MC for assessing availability and performance and optimizing the number of components in dynamic k-out-of-n systems. The simulation model was verified on the basis of a modified probabilistic approach related to the type of redundancy structure analyzed. These considerations represent the next stage in the development of methods for modeling and optimizing technical systems.

Table 1 lists the main research objectives of other authors, which can be divided into the following groups:

(1) Reliability analysis of technical systems [8,11–13,19,20,26,30,36,48,53,62],
(2) Optimization of redundancy allocation (RAP) [15,52,57,59,60],
(3) Indication of the optimal maintenance intervals [36,49,54,61,66],
(4) Cost reduction [15,49,51,55,57,60,61].

This publication analyzes the research problems addressed in the literature related to the analysis of the reliability of k-out-of-n systems. Previous models refer to systems that operate with constant intensity. The novelty presented by the authors is the development of original probabilistic and simulation models based on CTMC for the reliability

Table 1
A comparative summary of the literature review.

Type of system	Repairability of components	Homogeneity of components	Type of redundancy	Methods and models	Case study	Purpose of research	Papers
k-out-of-*n*	Non-repairable	Heterogeneous	Passive, hot	Probabilistic methods, joint discrete distribution of lifetimes of components	Numerical example (2-out-of-4 system)	Reliability analysis	Dembińska [48]
	Repairable		Active, passive, cold	Markov process		Optimization of the expected total cost and minimize inspection interval	Sharifi and Taghipour [49]
k-out-of-*n* load-sharing system	Non-repairable	Heterogeneous	Passive, hot	Combined MC and binary decision diagram method, Failure Mechanism Cumulative	Voltage stabilizing system	Reliability analysis	Chen et al. [50]
	Repairable	Homogeneous	Mixed-redundancy strategy	Markov process, heuristic algorithm	Water transition system	Optimization of the inspection interval	Sharifi et al. [3]
			Hybrid mixed-redundancy strategy	Matrix-based algorithm, HFE technique, GA	Case study from [3]	Minimization of the expected daily inspection cost	Sharifi et al. [51]
Series system composed of *k*-out-of-*n* subsystems	Non-repairable	Heterogeneous	Hot	Probabilistic methods	Not applicable to the real case study	Optimization of redundancy allocation in terms of system reliability	Ling and Wei [52]
	Repairable	Heterogeneous	Mixed passive (warm and cold)	CTMC	Not applicable to the real case study	Optimal system structure considering both system availability and system running cost	Gong et al. [15]
		Homogeneous	Passive, warm	Gumbel–Hougaard copula, supplementary variable method and Laplace transform	Numerical example (*k*-out-of-*n* and 2-out-of-4), not a real case study	Reliability, availability, mean time to failure and profit analysis	Poonia et al. [53]
		Homogeneous and heterogeneous	Mixed passive (warm and cold)	Probabilistic methods and GA	Subsystem with seven components (with configurations 3-out-of-7) and series system	Determine PR schedule i.e. maximizing of MSP and minimizing EMC	Levitin et al. [54]
Parallel components with *k*-out-of-*n* redundancy	Repairable	Heterogeneous	Active, hot	Mathematical methods and numerical experiments with distributions: exponential, Gamma, Gnedenko-Weibull and log-normal	Underwater pipeline monitoring systems (unmanned multi-functional underwater vehicle), combination of 3 + 1-out-of-6: *F* and 5-out-of-6: F systems	Reliability assessment and comparison of the effectiveness of different PM strategies	Rykov et al. [36]
		Homogeneous	Passive, warm	Multiphase Markov process and MC simulation	Feedwater subsystem in the multi-unit NPPs	Develop cost-effective inspection and maintenance policy	Wu et al. [55]
				Fuzzy reliability and availability are calculated using an algorithm based on α-cut technique	Three power supply systems (3-out-of-5)	A study of fuzzy availability and the fuzzy reliability system with common-cause failure	El-Ghamry et al. [13]
			Passive, hot	The supplementary variables method Markov chain	Objects in the oil and gas industry 3-out-of-4 model	A study of the *k*-out-of-*n* mathematical model with arbitrary repair time distributions	Rykov et al. [26]
Series-parallel system composed of *k*-out-of-*n* subsystems	Non-repairable	Heterogeneous	Active, passive-cold, and mixed redundancy strategy	MOEA and NSGA-II	Numerical example from [56]	RAP in terms of reliability and cost of system	Eshraghniaye Jahromi and Feizabadi [57]
			Active, cold	Probabilistic methods	Not applicable to the real case study	Stochastic precedence order with respect to the optimal redundancy allocation	Kuiti et al. [58]
		Homogeneous	Passive, cold	CTMC, sequential MC model and GA	Subsystem with four components (with configurations 1-out-of-4 and 2-out-of-4) and series-parallel system	Reliability assessment and reduction in calculation time	Peiravi et al. [12]
Weighted *k*-out-of-*n* system	Non-repairable	Heterogeneous	Active	Probabilistic methods	Numerical example,not a real case study	Optimization of redundancy allocation	Zhang [59]
				UGF, NSGA-II and NRGA	Numerical example from [56] with some changes	RAP in terms of availability and cost of system for to determine type and number of components in each sub-system	Sharifi et al. [60]

(*continued on next page*)

Table 1 (*continued*)

Type of system	Repairability of components	Homogeneity of components	Type of redundancy	Methods and models	Case study	Purpose of research	Papers
	Repairable		Passive, hot	Probabilistic methods and multi-criteria optimization	Gas pipeline network, numerical examples of 6- and 15-component weighted systems	PM optimization on the basis of cost and availability analysis	Hamdan et al. [61]
				Markov process UGF, and NSGA-II	Pumping system (weighted k-out-of-3 system)	Evaluation of system availability and optimization of component design	Chen et al. [62]
Consecutive k-out-of-n:F system with load sharing	Repairable Non-repairable	Heterogeneous	Passive, hot Passive hot, warm and cold	UGF FMC	Heating system Drone swarm (6 unmanned aerial vehicles with 4 rotors containing 4 engines)	Reliability analysis	Wu et al. [19] Wu et al. [20]
Consecutive k-out-of-n:G system	Non-repairable	Homogeneous	Passive, cold	FMCI	Lighting system in a manufacturing workshop and discrete signal transmission system	Reliability analysis	Gao et al. [11]
	Repairable	Homogeneous	Passive, hot	Markov chain model and BIUGF	Two power supply systems	Reliability evaluation with high accuracy	Cheng et al. [30]
Complex k-out-of-n:l system (series and parallel)	Non-repairable	Heterogeneous	Non-redundancy (series) and passive, hot redundancy (parallel)	Copula function, Bayesian approach, Bayesian bootstrap method, Hamiltonian Monte Carlo algorithm and MCMC simulation	Numerical example of complex 4-out-of-10:2 series and parallel systems. Real case study of wind turbine	Reliability analysis	Saberzadeh et al. [8]
CBPS systems	Repairable	Heterogeneous	Non-redundancy	Probabilistic methods and UGF	Numerical example of the system with 5 components and 3 lines	Instantaneous availability evaluation	Levitin et al. [63]
Dynamic k-out-of-n	Non-repairable	Homogeneous	Warm	FMCI	Wireless sensor networks	Reliability analysis and optimization of replacement interval	Lin et al. [41]
			Hot	Multi-valued decision diagram	Power transmission systems	Reliability analysis	Jia et al. [39]
		Heterogeneous	Warm	GA	Fire detection systems	Reduction of component and system costs	Eslami Baladeh and Taghipour [38]
			Hot	Multi-valued decision diagram	Numerical example of the system with different parameter configurations	Reliability analysis	Wang et al. [64]
					Smart home lighting control system and oil supply system	Performance assessment	Wang et al. [42]
					Unmanned aerial vehicles	Reliability analysis	Wang et al. [43]
				Binary decision diagrams and multi-valued decision diagram	Unmanned aerial vehicles	Reliability analysis	Wang et al. [44]
		Homogeneous	Cold standby	Semi-Markov process and MC simulation	Satellite power supply system	Reliability evaluation and RAP	Xu et al. [40]
	Repairable	Homogeneous	Passive, hot	CTMC, MC and MCMC simulation, probabilistic methods, Kaplan-Meier estimation	Two real case study of military transportation systems (equipped with light utility vehicles and truck vehicles)	Reliability, availability and technical performance analysis, optimization of vehicles number in transportation system, cost reduction	This paper

and availability analysis of systems operating with varying intensity. Cost minimization is achieved by reducing structural redundancy to the optimal number of components for which the assumptions of acceptable system availability and performance levels are met.

3. Methods

3.1. Assumptions

The article assumes the following:

We consider a repairable, homogeneous, parallel k-out-of-n system with k working components, and the other $(n - k)$ objects are in hot-standby mode [65],

(1) At any time t, only one event can occur in the system: failure or repair [60],
(2) A k-out-of-n system works if $m \geq k$ (m is a number of usable components) [15],
(3) The system is in downtime condition when $k = 0$,
(4) There cannot be more than one independent failure at the same time [60,65],
(5) In the event of a failure of an operated component, it is handed over for repair, and its tasks are taken over by an object in the hot-standby state (if available) [60],
(6) Each repaired object is as functionally resourceful as the new device [15,55],
(7) Component failures and repairs are independent processes [49],
(8) All failure and repair rates are treated as constants resulting from the exponential distribution [65],

(9) The system operates under dynamically changing conditions, which, in practice, results in the variability of the minimum number of operable components needed for its proper operation.
(10) The cost related parameters are constant [51,60].

3.2. Continuous time Markov chain (CTMC)

This subsection presents a CTMC approach to modeling the reliability and state changes of an object and a system composed of n homogeneous components. The Markov process is a stochastic process, characteristic of the memoryless property, which means that successive states of the process depend only on their direct predecessors [12,46]. Many events, including damage and restoration of objects and technical systems, fulfill this property. For this reason, Markov models have a versatile application in the field of reliability analysis of a wide range of real systems [67] and devices [68]. The proposed approach uses processes that are continuous in time, and evolve in a discrete state space. In the literature they are referred to as Continuous Time Markov Chains.

3.2.1. CTMC for component

As set out in Section 3.1, each component of the k-out-of-n system may be in a state of suitability ($S = 1$) or unsuitability ($S = 0$). The times of transition between these states are in accordance with the exponential distribution, with the suitability transition from the state to the state of unsuitability with constant intensity λ, whereas the transition in the opposite direction occurs with constant intensity μ. The Markov model for a repairable component is shown graphically in Fig. 2.

The failure rate λ of real technical objects depends on the quality of the materials of which they are made, the safety indicators selected properly, the proper operation and maintenance, and the intensity of their usage (operation). The repair rate μ reflects the performance of the technical system in terms of the implementation of repair and maintenance processes. In addition, the processes of supplying spare parts and consumables of the analyzed technical system also have a significant impact.

The process of changing the states of a component is described by the Markov process with an intensity matrix of transitions $\mathbf{\Lambda}_C$, the value of which is represented by the formula (1):

$$\mathbf{\Lambda}_C = \begin{pmatrix} -\mu & \mu \\ \lambda & -\lambda \end{pmatrix}, \tag{1}$$

subject to the assumption that CDF of time to failure $F(t)$ CDF of time to repair $G(t)$ are described by dependencies (2)-(3):

$$F(t) = 1 - e^{-\lambda t}, \tag{2}$$

$$G(t) = 1 - e^{-\mu t}. \tag{3}$$

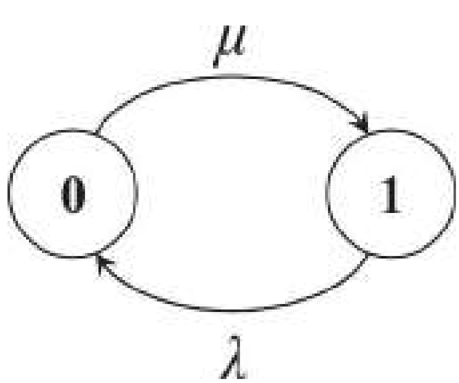

Fig. 2. Markov model for a repairable component.

3.2.2. CTMC for system

Assuming that the system is composed of n homogeneous components, its reliability model includes $n + 1$ possible states, where the state number specifies the number of properly operated components. Transitions between successive states proceed according to an exponential distribution. If at the time t the system includes m operable components ($S = m$) and $n - m$ inoperable, then the system can directly go to one of two states: $S = m - 1$ (if another component is damaged) or $S = m + 1$ (if one damaged component is repaired). The state change occurs in this case with intensity respectively $m\lambda$ to go to the state $S = m - 1$ and $(n - m)\mu$ to go to the state $S = m + 1$.

Fig. 3 graphically shows a CTMC-compliant model of interstate transition for a system composed of n components.

The process of changing the states of a system composed of n homogeneous components is described by the Markov process with a transition intensity matrix $\mathbf{\Lambda}_S$, the value of which is calculated by the formula (4):

$$\mathbf{\Lambda}_S = \begin{pmatrix} -n\mu & n\mu & 0 & \dots & 0 & 0 & 0 \\ \lambda & -(\lambda + (n-1)\mu) & (n-1)\mu & \dots & 0 & 0 & 0 \\ 0 & 2\lambda & -(2\lambda + (n-2)\mu) & \dots & 0 & 0 & 0 \\ \vdots & \vdots & \vdots & \ddots & \vdots & \vdots & \vdots \\ 0 & 0 & 0 & \dots & -(2\mu + (n-2)\lambda) & 2\mu & 0 \\ 0 & 0 & 0 & \dots & (n-1)\lambda & -(\mu + (n-1)\lambda) & \mu \\ 0 & 0 & 0 & \dots & 0 & n\lambda & -n\lambda \end{pmatrix} \tag{4}$$

For example, if the system is composed of 5 components and at time t each of them is usable then the system is in the state $S = 5$. The next state will be $S = 4$, to which the system will transition with an intensity equal to 5λ, where λ denotes the failure rate of one homogeneous component. From the state $S = 4$ the system can transition to the state $S = 3$ with intensity 4λ or to the state $S = 5$ with intensity μ (where μ is the repair rate of one homogeneous component). If all components are failed then the system is in state $S = 0$ and the next transition will be to state $S = 1$ with an intensity 5μ. Thus, the process of state transitions of a system composed of 5 components can be described by a transition intensity matrix represented by Eq. (5):

$$\mathbf{\Lambda}_S = \begin{pmatrix} -5\mu & 5\mu & 0 & 0 & 0 & 0 \\ \lambda & -(\lambda + 4\mu) & 4\mu & 0 & 0 & 0 \\ 0 & 2\lambda & -(2\lambda + 3\mu) & 3\mu & 0 & 0 \\ 0 & 0 & 3\lambda & -(3\lambda + 2\mu) & 2\mu & 0 \\ 0 & 0 & 0 & 4\lambda & -(4\lambda + \mu) & \mu \\ 0 & 0 & 0 & 0 & 5\lambda & -5\lambda \end{pmatrix}. \tag{5}$$

The Chapman-Kolmogorov equation determines the following relationship between the vector of instantaneous probabilities $\mathbf{P}(t)$ of the process states and intensity matrices $\mathbf{\Lambda}_S$ [69]:

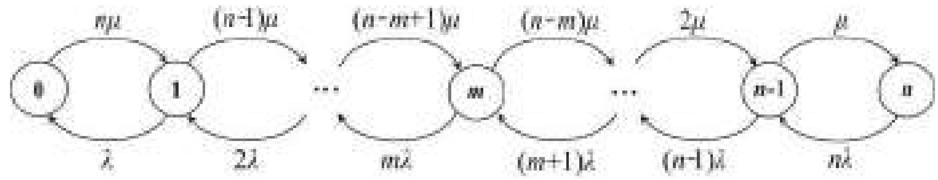

Fig. 3. Reliability CTMC model of n-component system.

$$\frac{d}{dt}\mathbf{P}(t) = \mathbf{P}(t)\cdot\mathbf{\Lambda}_\mathbf{S}. \tag{6}$$

The initial distribution vector CTMC denoted as $\mathbf{P}(0)$ for the k-out-of-n system where at the time $t = 0$ all components retain the state of suitability, takes the form of (7):

$$\mathbf{P}(0) = (0, 0, ..., 0, 1). \tag{7}$$

The distribution $\mathbf{P}$ of ergodic probabilities [46] CTMC describes the boundary values of the state probabilities at $t\to\infty$ and is calculated using the Eq. (8):

$$\mathbf{P}\cdot\mathbf{\Lambda}_\mathbf{S} = \mathbf{0}, \tag{8}$$

taking into account the normalization condition:

$$\sum_{j=0}^{n} p_j = 1. \tag{9}$$

3.3. Monte Carlo and Markov chain Monte Carlo

Simulation methods are useful tools for mathematical modeling of complex processes and complement analytical approaches. Monte Carlo models are widely used in the analysis of the reliability of objects [47,70,71] and technical systems [72,73]. This subsection describes an approach based on repeatedly sampling the values of random variables based on the cumulative distribution function of probabilities.

3.3.1. Monte Carlo

Monte Carlo simulation methods are based on repeated sampling of random values from a certain distribution. In the proposed method, the randomization is assumed of numbers a from continuous uniform distribution $U(0, 1)$:

$$a \in U(0, 1). \tag{10}$$

It is then assumed that variable a corresponds to the CDF value of the variable k:

$$a = K(k_i). \tag{11}$$

Using dependencies (11), a continuous value of the variable k is calculated, which in the next step is discretized to values belonging to the set of natural numbers, according to the dependencies (12) and (13):

$$k_i = K^{-1}(a), \tag{12}$$

$$k(i) = \begin{cases} 0 & \text{for } k_i \le 0 \\ \lfloor k_i \rfloor & \text{for } k_i > 0 \text{ and } k_i - \lfloor k_i \rfloor < 0.5 \\ \lceil k_i \rceil & \text{for } k_i > 0 \text{ and } k_i - \lfloor k_i \rfloor \ge 0.5 \end{cases}. \tag{13}$$

3.3.2. Markov chain Monte Carlo

Based on a CTMC system composed of n components, sampling is carried out from the uniform distribution $U(0, 1)$. Two values a and b are drawn simultaneously:

$$a, b \in U(0, 1), \tag{14}$$

which are assigned to the CDFs of failure and repair respectively, assuming that the system is in the $S = m$ state:

$$a = F_m(t_f) = 1 - e^{-m\lambda t_f}, \tag{15}$$

$$b = G_m(t_r) = 1 - e^{-(n-m)\mu t_r}. \tag{16}$$

An exception is when the system is in the state $S = 0$ or $S = n$. In these special cases, there is only one process (repair or failure). For $m \in \{1, 2, \ldots, n-1\}$ the direct transition of the system to the state $S = m - 1$ or $S = m + 1$ is decided by the relationship between the simulated times t_f i t_r which are calculated based on inverse CDFs of time to failure and repair time:

$$t_f = F_m^{-1}(a) = \frac{\ln(1-a)}{-m\lambda}, \tag{17}$$

$$t_r = G_m^{-1}(b) = \frac{\ln(1-b)}{-(n-m)\mu} \tag{18}$$

If the time of failure of any of the operable components is longer than the time of repair of any of the damaged components, then the system transits into the state $S = m + 1$ after time t_r (the damaged component is repaired.) Otherwise, the system reaches $S = m - 1$ after time t_f. The rules of interstate transition in MCMC simulation are described by the dependencies (19):

$$X(i) = (S(t) = m) \Rightarrow \begin{cases} X(i+1) = (S(t+t_r) = m+1) & \text{if } t_f > t_r \\ X(i+1) = (S(t+t_f) = m-1) & \text{otherwise} \end{cases}. \tag{19}$$

3.4. Indicators

Two indicators have been proposed to assess the proper operation of the k-out-of-n system:

- System Availability (A_S),
- Technical Performance Measure (*TPM*).

System Availability (A_S) has been defined as the ability of the device to perform specified functions under certain operating conditions, while maintaining operational indicators in the prescribed intervals of the required time or the required amount of work performed [74]. The A_S indicator for a single iteration is calculated as a binary value, which is especially useful for systems operating in a dichotomous (zero-one) manner. It takes values according to the following relationship:

$$A_S(i) = \begin{cases} 1 & \text{if } m(i) \ge k(i) \\ 0 & \text{otherwise} \end{cases}, \tag{20}$$

where the A_S value for the entire simulation period is calculated as the arithmetic mean of $A_S(i)$ for all iterations, according to Eq. (21):

$$A_S = \frac{1}{T_S}\sum_{i=1}^{T_S} A_S(i), \tag{21}$$

where $m(i)$ is a number of operable components in the system at time i and $k(i)$ is a minimum number of operable components.

A transport system can operate with performance measured as a value of the continuous interval [0, 1]. Therefore, it is important to determine the value of the *TPM* indicator, which expresses the system performance for a single iteration and the mean value for the entire simulation time. The implementation of the *TPM* indicator may be useful for all *k*-out-of-*n* systems that may operate at partial capacity, handling part of the incoming task stream. In such cases, the *TPM* indicator would provide much more complete information than the A_S indicator.

TPM is a term coined by Sears and Taylor [75] in the US Army to define the technical requirements that the system must meet in order to properly perform the tasks properly. It is a tool that facilitates efficient management, elimination of unnecessary costs that may occur throughout the facility's life cycle, and improvement of its performance. *TPM* is defined as the continued prediction and demonstration of the degree of expected or actual achievement of selected technical objectives [75]. Value of *TPM*(i) for a dynamic *k*-out-of-*n* in iteration *i*th of the simulation is calculated based on the dependence (22):

$$TPM(i) = \begin{cases} 1 & \text{if } m(i) \geq k(i) \\ \dfrac{m(i)}{k(i)} & \text{otherwise} \end{cases} . \tag{22}$$

The generalized value *TPM* for the entire period operation of the simulated system is calculated as the arithmetic mean *TPM*(i) for all iterations, according to the Eq. (23):

$$TPM = \frac{1}{T_S} \sum_{i=1}^{T_S} TPM(i). \tag{23}$$

Eqs. (20)–(23) imply the relationships $\underset{i>0}{\forall} TPM(i) \geq A_S(i)$ and $TPM \geq A_S$.

3.5. Description of research

The method proposed for modeling the reliability of a structured technical system and the optimization of the number of its components can be applied to theoretical considerations and actual case studies. Fig. 4 presents the proposed block diagram describing the implementation stages of the presented approach.

The first step involves studying the process of failure and repair in relation to the components that make up the system. For empirical data obtained from real-world systems, two tools have been proposed to estimate the value of cumulative distribution functions (CDF). The values F (t) and $G(t)$ for censored data are calculated on the basis of the Kaplan-Meier estimator [76–78], according to dependencies (24) and (25):

$$F(t) = 1 - \prod_{i:t_i \leq t} \left(1 - \frac{d_i}{D_i}\right), \tag{24}$$

$$G(t) = 1 - \prod_{i:t_i \leq t} \left(1 - \frac{r_i}{R_i}\right), \tag{25}$$

where d_i is the number of objects that failed at the time t_i, D_i is the number of objects that worked properly until t_i, and r_i is the number of objects that were repaired at t_i, and R_i is the number of objects that remained failed until t_i.

For uncensored data, Benard's approximation is used [79–82], whose form is represented by the Eqs. (26) and (27):

$$F(t) = \frac{d_i - 0.3}{D + 0.4}, \tag{26}$$

$$G(t) = \frac{r_i - 0.3}{R + 0.4}, \tag{27}$$

where D is the total number of failures and R is the total number of repairs (renewals).

Based on estimated values of CDFs $F(t)$ and $G(t)$ a least squares approximation is performed, resulting in exponential distributions with parameters equal to the intensity of damage and the intensity of repairs (failure rate λ and repair rate μ) of the components.

The next stage of research is the development of a CTMC model for a system composed of n components. The matrix of Interstate transition intensities $\mathbf{\Lambda_S}$ takes the form according to formula (4), and the ergodic probabilities of the space of states with numbers $n + 1$ is calculated in accordance with the formulas (b-8) and (9). Based on the vector $\mathbf{P}$, the expected number of operable components in the system is determined. With the use of an original computer script, the process of changing the states of the system as a result of failure and repair of its objects is simulated.

A dynamic technical system is characterized by variability in the intensity of operation, which is reflected by a variable minimum number of components necessary to perform the tasks assigned to the system. To assess the availability and performance of the system, simulations of the

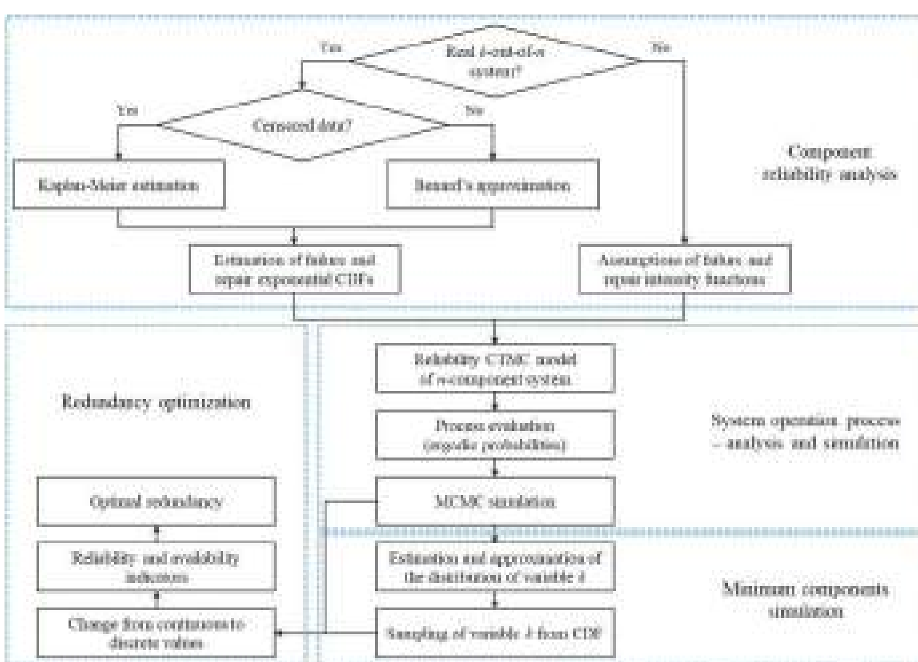

Fig. 4. Flowchart of the proposed method.

variable k as Monte Carlo sampling of the cumulative distribution function K according to models (10)-(13).

Evaluation of the A_S and *TPM* requires discretization of the simulated process progress accomplished with CTMC so that it relates to variable k sampling iterations. Therefore, the system state assigned to iteration i is defined as the minimum number of operable components in the interval $(i - 1, i)$ of continuous time. This means that for iteration $i = 1$, the system is in $S(i) = m$, where m is the minimum of all state of the system in the full first day of CTMC simulation, that is, in the interval (0, 1) of continuous time. The A_S and *TPM* indicators form the basis for determining the optimal number of elements for which the availability and performance of the system meet the assumed requirements.

3.6. Algorithms and implementations

The proposed simulation methods based on MCMC and variable k sampling with CDF have been implemented in MATLAB software. The application pseudocodes were presented as Algorithm 1 and Algorithm 2.

For the needs of each creation of a matrix of interstate transition intensities and calculation of the ergodic probabilities for a system composed of n components a pseudocode was developed, presented as Algorithm 3 and implemented in the MATLAB environment. Algorithm 3 introduces the tensor Λ_T, which consists of n intensity matrices Λ_S for systems composed of 1 to n components.

3.7. Probabilistic approach

In the probabilistic approach to k-out-of-n system availability modeling, if k is a specified constant that defines the minimum number of operable components for the proper operation of the system [2,83], the formula (28) applies:

Algorithm 1
Pseudocode for Markov Chain Monte Carlo simulation for reliability analysis k-out-of-n system.

```
Input: Failure intensity λ, repair intensity μ, number of component n, simulation time T_S
Output: Trajectory of stochastic process X(i), times of state transition T(i)
for z = 1: n do
  set t = 0, i = 1, S(i) = n, X(i) = S(i)
  while t ≤ T_s do
    i = i + 1
    if S(t) == n then
      a = rand
      t_f = – ln(1 – a)/(nλ)
      t = t + t_f
      S(t) = S(t) – 1
    elseif S(t) == 0 then
      b = rand
      t_r = – ln(1 – b)/(nμ)
      t = t + t_r
      S(t) = S(t) + 1
    else
      a = rand
      b = rand
      t_f = – ln(1 – a)/(S(t)·λ)
      t_r = – ln(1 – b)/((n – S(t))·μ)
      if t_f > t_r then
        t = t + t_r
        S(t) = S(t) + 1
      else
        t = t+t_f
        S(t) = S(t) – 1
      end if
    end if
    X(i) = S(t)
    T(i) = t
  end while
end for
return X(i), T(i)
```

Algorithm 2
Pseudocode for sampling variable k from CDF.

```
Input: CDF of variable k, simulation time T_s
Output: Array of minimum working components in j-th iteration k(j)
for j = 1: T_S do
    a = rand
    k = inverse CDF of a
    if k < 0 then
        k = 0
    else
        k = round(k)
    end if
    k(j) = k
end for
return k(j)
```

Algorithm 3
Pseudocode for computation of ergodic probabilities.

```
Input: Failure intensity λ, repair intensity μ, maximum number of component n,
Output: Matrix of ergodic probabilities P
Create a tensor Λ_T (n + 1, n + 1, n)
for i = 1: n do
    Create a matrix Λ_S (i + 1, i + 1)
    for j = 1: i + 1 do
        for k = 1: i + 1 do
            if k == j then
                Λ_S (j, k) = – (i – j + 1)·μ + (j – 1)·λ
            elseif k == j – 1 then
                Λ_S (j, k) = (j – 1)·λ
            elseif k == j + 1 then
                Λ_S (j, k) = (i – j + 1)·μ
            end if
        end for
        k = 1
    end for
    Λ_T (1:i + 1, 1:i + 1, i) = Λ_S
end for
Create a matrix J (n, n)
for c = 1: n do
    Create a matrix L from tensor Λ_T
    L = Λ_T (1:c + 1, 1:c + 1, c)
    Transpose matrix L
    L' = Transpose(L)
    L'(c + 1, c + 1) = 1
    Create a vector Z
    for d = 1: c + 1 do
        if d == c + 1 then
            Z(d) = 1
        else
            Z(d) = 0
        end if
    end for
    Compute the ergodic probabilities
    P(c, 1:c + 1) = ((L')^(–1))·Z
return P
```

$$A(k,n) = \sum_{i=k}^{n} \binom{n}{i} p^i q^{n-i}, \tag{28}$$

where p is availability of each component q is unavailability of each component. It should be noted that the formula (28) is applicable for a system with homogeneous components For CTMC p and q are calculated on the basis of ergodic probabilities, according to the formulas (29) and (30):

$$p = \frac{E(m)}{n} = \frac{\sum_{i=0}^{n} p_i \cdot i}{n}, \tag{29}$$

$$q = 1 - p, \tag{30}$$

where $E(m)$ is the expected number of operable components in the system, p_i is the ergodic probability of state $S = i$, and n is the number of components that make up the system.

However, in a dynamic system with a variable k number, which is described by the cumulative distribution function K, the probability of the intensity of the task stream entering the system should be considered. Due to the discrete set of variable k values, these probabilities have been determined using the continuous cumulative distribution function K according to the dependencies:

$$\Pr(k = 0) = K(0.5), \tag{31}$$

$$\Pr(k = j) = K(j + 0.5) - K(j - 0.5) \text{ for } j > 0. \tag{32}$$

Therefore the availability of the system A_S is equal to the sum of availability indicators $A(k, n)$ and the probabilities of subsequent variable k values, which was presented as the formula (33):

$$A_S = \sum_{j=0}^{n} \Pr(k = j) \cdot A(k, n), \tag{33}$$

which, when substituted, takes the form of (34):

$$A_S = K(0.5) \cdot \sum_{i=0}^{n} \binom{n}{i} p^i q^{n-i} + \sum_{j=1}^{n} \left((K(j+0.5) - K(j-0.5)) \cdot \sum_{i=j}^{n} \binom{n}{i} p^i q^{n-i} \right). \tag{34}$$

4. Results

In this section, two computational examples are presented, based on transport systems in place in the Polish Armed Forces. System means a dynamic k-out-of-n set in which the operated vehicles are treated as its homogeneous components. Empirical data was obtained on the basis of the operational documentation covering 3-year periods of operation of both mentioned systems. Due to the assumptions regarding the technical readiness (hardware) in force in the Polish Armed Forces, acceptable levels of the availability indicator A_S and performance indicator TPM for the tested systems were specified at the level of 0.95.

4.1. Case study no. 1

Case study no. 1 is a transport system with 19 HONKER vehicles, which according to the structure of road transport of the Polish Armed Forces are classified as light utility vehicles [84]. They were first launched in 2000 and are designed to transport people and cargo up to 1000 kg [85].

Table 2 lists the costs of light utility vehicle purchase, repair and maintenance. Construction and operation of the system are borne at different time intervals. The type of cost associated with Major repairs depends on the time periods and is based on the operating instructions. Component parts are renewed or replaced according to the manufacturer's recommendations after a certain period of usage. This applies to major systems such as engine, suspension, gearbox, etc. The cost of minor repairs is a random variable, and the average value of empirical repair costs extracted from operating records was used for the calculations. The cost of minor repair was estimated based on the average value of used spare parts and materials, while the time interval refers to the mean time between failures (MTBF). According to the adopted operational strategy, maintenance is carried out once a year, and its cost is equivalent to the expenditure on consumables.

Table 2
Costs of light utility vehicle purchase, repair and maintenance.

Type of cost	Value (USD)	Interval (years)
Purchase	30 100	20
Major repair	18 940	8
Minor repair	1 090	0.58
Maintenance	160	1
Average cost	5 911.81 (USD/year)	

Based on the displayed values of costs and time intervals, the average annual cost of operating one technical object was calculated at $ 5911.81.

4.1.1. Parameters estimation

The cumulative distribution functions of empirical damages and repairs were estimated according to the Kaplan-Meier estimator formula. Fig. 5(a) and (b) presents step graphs of the empirical CDF values, based on which the exponential distributions were adjusted. The light utility vehicle failure process intensity $\lambda = 0.0048$ (day^{-1}), with the distribution matching accuracy determined by $MSE = 0.0004$ and Pearson correlation coefficient $\rho = 0.9956$. The repair process intensity amounted to $\mu = 0.2607$ (day^{-1}), however, the exponential distribution in this case has a lower matching accuracy at the level of $MSE = 0.0208$ and $\rho = 0.9609$. The distributions were approximated by the least squares method. Appendix B presents the maximum likelihood estimation method for estimating failure and repair rates and compares it with the results of the least squares method.

Due to the absence of censored observations in the dataset to estimate the empirical value of the CDF of variable k, Benard's approximation was applied. Table 3 summarizes the empirical values of variable k. The empirical data was collected based on incoming demand for transportation service delivery in the system. In the analyzed transport system, this is carried out on the basis of the relevant documents, which indicate the accurate time (hour and day) of starting a task by a vehicle, the route of travel, and the expected time of completing the task. Based on the collected data, the necessary number of vehicles for each day of the system operation process was determined. The largest number of observations were recorded in the range $k \in [0, 11]$. Fig. 6 shows the empirical CDF values with approximation by normal and logistic distributions. These distributions are selected to describe the variable k due to the good fit to the cumulative distribution function. For systems with a relatively frequent small task stream, normal and logistic distributions are particularly useful for accurate mapping of this phenomenon.

Table 4 shows the results of the approximation of the cumulative distribution function k. Both distributions analyzed are defined by two parameters: ϕ (mean, location) and σ (standard deviation, scale). As with the cumulative distribution functions of time-to-failure and time-to-repair, two meters were used to measure the matching of approximated distributions to empirical values. The Pearson correlation coefficient ρ as well as MSE achieved better values for logistic distribution. This implies the validity of the implementation of logistic distribution of variable k in the developed simulation model developed.

4.1.2. CTMC analysis

CTMC analysis was performed for a transport system composed of n homogeneous vehicles, with $n \in [1, 19]$. Thus, 19 such systems were considered to check the ergodic probabilities of states for multiple configurations. Based on Eq. (4), interstate transition intensity matrices were developed on the assumption that the intensities of failure λ and repair μ of each component take values estimated in Section 4.1.1. Fig. 7 shows the results of calculations performed according to Eqs. (8) and (9) and using MATLAB software.

In all variants of the transport system analyzed, the most probable is state $S = n$. This means that the most likely event is a system with all vehicles operable. This indicates a high ratio of repair intensity to failure intensity. However, as the number of components increases, the ergodic probability of state $S = n - 1$, which for $n = 19$ reaches 0.2473, with the probability of $S = n$ at 0.7071 also increases.

4.1.3. Simulations

Simulations were performed for all variants of the analyzed system. For each of them, the number of iterations corresponds to 10,000 (days)

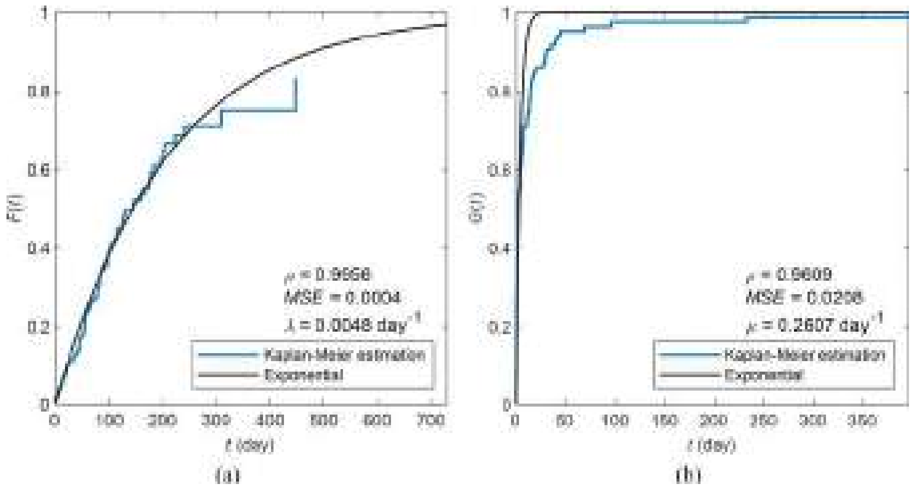

Fig. 5. Approximation of CDFs: (a) – time to failure, (b) – time to repair.

Table 3
Empirical values of variable k.

Value of variable k	Number of observations	Value of variable k	Number of observations
0	131	10	42
1	204	11	38
2	134	12	16
3	99	13	10
4	101	14	7
5	74	15	5
6	66	16	2
7	73	17	0
8	50	18	0
9	45	19	0

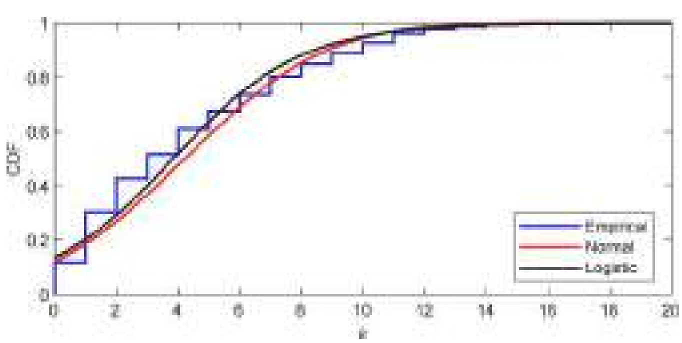

Fig. 6. Approximation of CDF for variable k.

of the operation process. Fig. 8 shows the results of the simulated process for a system of 10 vehicles. The number of operable components was compared with the number of components necessary for the reliable operation of the system. The number k for 10,000 iterations was sampled once and then collated with the CTMC simulation results. For most iterations of the simulation, the k-out-of-10 system had from 7 to 10 operable components.

4.1.4. Availability and TPM

The simulation results were used to calculate indicators A_S and TPM. Fig. 9 shows the availability of the system depending on the number of vehicles in the transport system. A significant increase in the A_S indicator is observed in the range of the number of components from 1 to 8, and for $n = 10$ an acceptable level of availability was achieved, that is, $A_S = 0.9557$. For the current situation, in which the system is composed of 19 vehicles, the availability is at the level of $A_S = 0.9993$. Thus, reducing the number of components by 9, i.e. ca. 47 %, results in a decrease in availability of 0.0436 only.

Furthermore, the availability indicators A_S obtained using the simulation model were compared with the results of the probabilistic approach and are shown graphically in Fig. 9. A detailed comparison of the indicator for a system consisting of 119 components, together with the derogations, is shown in Table 5. The largest difference was achieved for the k-out-of-5 system and was 0.0075. Very similar results obtained on the basis of both approaches indicate the validity of assumptions made and the correctness of calculations and simulations performed.

Fig. 10 shows a box plot of $TPM(i)$ for systems of 119 components. The central value for each of the systems under consideration means the median value of $TPM(i)$ for single iterations. For the k-out-of-4 system the median $TPM(i)$ is 1. This means that its availability meets the condition $A_S > 0.50$. Points marked with red markers indicate outliers and the black line indicates TPM averages for the system. The largest increase in the average value of the indicator was observed in the range of the number of components from 1 to 7.

The k-out-of-10 system obtained TPM of 0.9912, which compared to $TPM = 0.9999$ for the k-out-of-19 system is a satisfactory result. Therefore, in a system with an increase in the number of components from 10 to 19, i.e. by 90 %, there is an increase in the TPM value of less than 1.0 ‰. Once the system has reached the optimum number of components, it does not generate significant benefits associated with increasing its structure.

4.2. Sensitivity analysis

Sensitivity analysis is aimed at determining the impact of individual

Table 4
Estimation of CDF parameters (for variable k).

Distribution	CDF	Parameters	Estimation	Pearson Correlation ρ	MSE
Normal	$K(k) = \frac{1}{2}\left[1 + \mathrm{erf}\left(\frac{k-\phi}{\sigma\sqrt{2}}\right)\right]$	ϕ – mean σ – standard deviation	$\phi = 4.2115$ $\sigma = 3.6044$	0.9757	0.0049
Logistic	$K(k) = \frac{1}{1+\exp(-(k-\phi)/\sigma)}$	ϕ – location σ – scale	$\phi = 3.8344$ $\sigma = 2.0762$	0.9791	0.0036

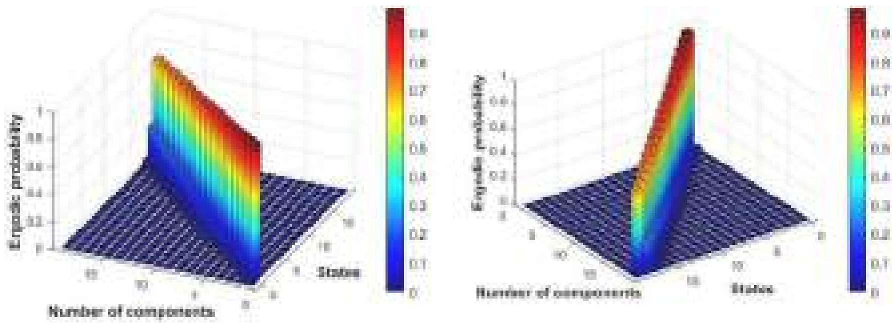

Fig. 7. Ergodic probabilities of states in CTMC.

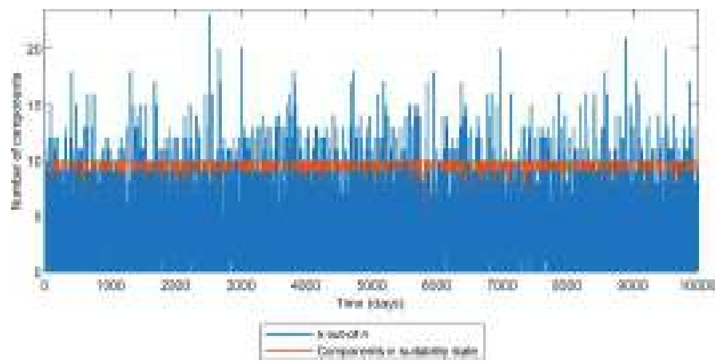

Fig. 8. Simulation results for a system of 10 components.

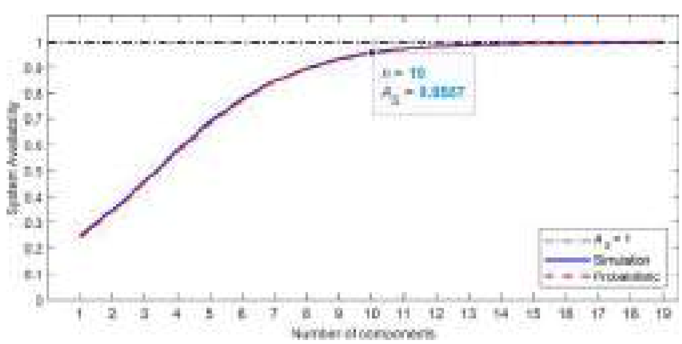

Fig. 9. Availability of a system of 119 components.

parameters on the model's output values, which for the proposed approach are indicators A_S and *TPM*. This allows the determination of the risk of system availability and performance reduction. In the first step, the sensitivity to failure and repair intensities was analyzed. The variability of these parameters can be due to system operation dynamics, a decrease (increase) in the technical potential of the maintenance and repair base, intensification of operational processes, and possible inaccuracies in estimating their values during model creation. It was assumed that the simulations would cover the range of changes in the parameters λ and μ which are the products of the estimated values of these parameters and the elements of vector **W** (35):

$$\mathbf{W} = [0.1\ \ 0.2\ \ 0.3\ \ 0.4\ \ 0.5\ \ 0.6\ \ 0.7\ \ 0.8\ \ 0.9\ \ 1\ \ 2\ \ 3\ \ 4\ \ 5\ \ 6\ \ 7\ \ 8\ \ 9\ \ 10]. \tag{35}$$

From a risk assessment point of view, this range warrants a forecast horizon wide enough to ensure the safe and reliable operation of the system. Fig. 11(a) shows the availability of the *k*-out-of-10 system with assumed variability of operational process parameters. With the current repair potential, measured by the repair intensity $\mu = 0.2607$ (day^{-1}), maintained, even a tenfold increase in the failure intensity λ did not cause a significant decrease in the indicator *AS,* which amounted to about. 0.90. In turn, with a tenfold decrease in the intensity of repair and increase in the failure intensity, the A_S indicator reached approximately 0.50. However, it should be noted that this is an extreme scenario of events with a low probability of implementation.

Table 5
System availability – comparing the results of probabilistic and simulation approaches.

Number of components	Approaches		Error
	Probabilistic	Simulation	
1	0.2438	0.2488	0.0050
2	0.3410	0.3469	0.0059
3	0.4536	0.4574	0.0038
4	0.5708	0.5773	0.0065
5	0.6804	0.6879	0.0075
6	0.7730	0.7780	0.0050
7	0.8448	0.8467	0.0019
8	0.8969	0.8961	−0.0008
9	0.9329	0.9323	−0.0006
10	0.9570	0.9557	−0.0013
11	0.9727	0.9704	−0.0023
12	0.9827	0.9823	−0.0004
13	0.9891	0.9896	0.0005
14	0.9932	0.9933	0.0001
15	0.9957	0.9955	−0.0002
16	0.9973	0.9970	−0.0003
17	0.9983	0.9980	−0.0003
18	0.9990	0.9989	−0.0001
19	0.9993	0.9993	0.0000

Fig. 11(b) shows the sensitivity of indicator *TPM* to change in parameters λ and μ. The performance of the system, as well as its availability while maintaining the current level of repair intensity, shows a high resistance to the increase in failure intensity. The *TPM* value drops below 0.90 for such extreme variants as e.g.: $\lambda = 0.0192$ (day^{-1}) and $\mu = 0.0261$ (day^{-1}) (coefficients 4 and 0.1, respectively), or $\lambda = 0.0384$

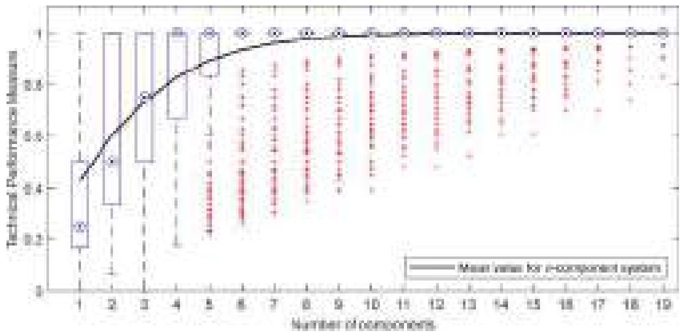

Fig. 10. *TPM* values of a system of 1 to 19 components.

(day^{-1}) and $\mu = 0.052$ (day^{-1}) (coefficients 8 and 0.2, respectively).

The second step of the sensitivity analysis is to determine the reliabilities and efficiencies with changing dynamics of the task stream entering the system. For the analyzed case study, the system dynamics description was reflected by the logistic distribution, which for the present situation takes the values of the location and scale parameters equal to, respectively, $\phi = 4.2115$ and $\sigma = 3.6044$. As for the first step, the range of parameter variability included the products of the estimated values and the elements of vector **W** (35). Ultimately, 361 points of space were identified, on the basis of which the plane of indicator value changes depending on the logistics distribution parameters was determined. The results are presented in Fig. 12(a) and (b).

Both indicators A_S and *TPM* are significantly sensitive to the location parameter ϕ, especially at small σ values. For example, for $\sigma = 1.0381$ the system availability decreases from 0.9191 to 0.2441 with ϕ increasing from 7.6688 to 11.5032. However, the same change in the location parameter when $\sigma = 2.0762$, reduces system availability from 0.7730 to 0.3587. For *TPM* there is a similar property, however, due to the nature of the continuous values of the performance indicator for individual iterations, changes in its average values are smaller.

4.3. Case study no. 2

The study involved 50 Iveco Stralis vehicles, which, according to the structure of road transport of the Polish Armed Forces, are classified as general purpose heavy vehicles [84]. They were put into operation in 2003 and are designed to transport cargo in bulk, on pallets or in containers over long distances. Can work with up to 19,000 kg trailers [86].

Table 6 lists the costs of truck purchase, repair and maintenance. The general assumptions and cost characteristics of major and minor repairs are the same as described in case study no. 1. The main components of the total cost of an object include the cost of purchase and major repair; however, they are incurred at large intervals. The purchase interval was determined on the basis of the operational potential assumed for trucks operated in the Polish Armed Forces. Based on the displayed values of

Table 6
Costs of trucks purchase, repair and maintenance.

Type of cost	Value (USD)	Interval (years)
Purchase	101 900	20
Major repair	60 700	10
Minor repair	1 400	0.76
Maintenance	1 340	1
Average cost	14 347.11 (USD/year)	

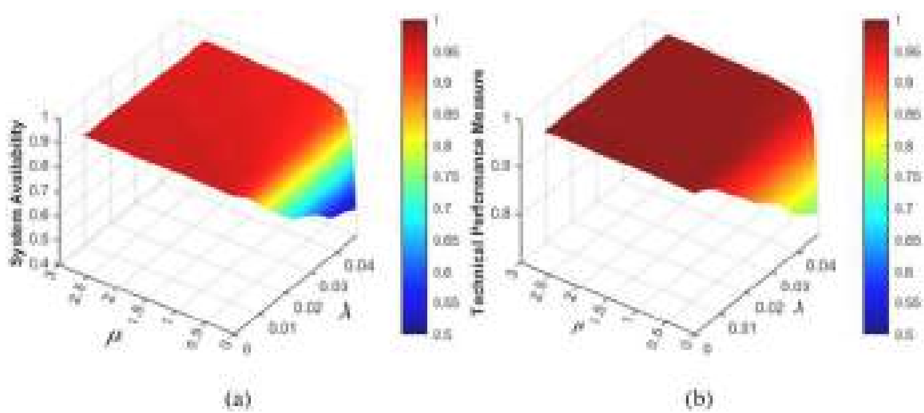

Fig. 11. Sensitivity analysis of: (a) – availability and (b) – *TPM* for the *k*-out-of-10 system.

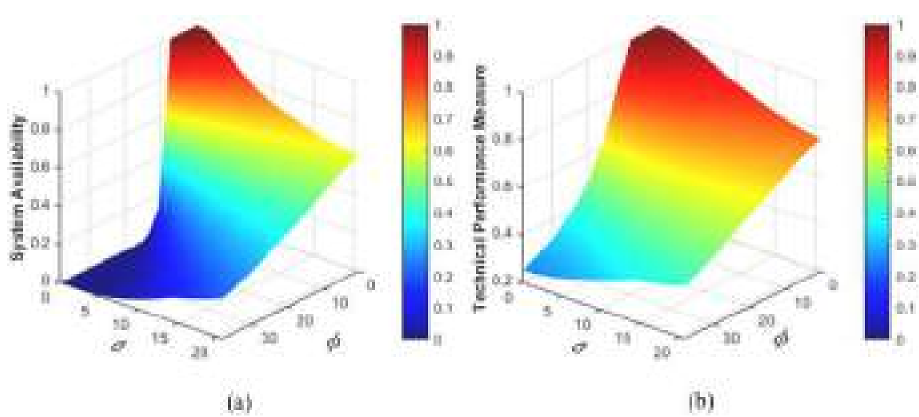

Fig. 12. Sensitivity analysis of: (a) – availability and (b) – *TPM* for the *k*-out-of-10 system.

costs and time intervals, the average annual cost of operating one technical object was calculated at $ 14,347.11.

4.3.1. Parameters estimation

To estimate the parameters of case study 2, similar methods were used as for case study 1. Fig. 13 the cumulative distribution functions of empirical damage and repair were estimated and the empirical data were matched to the exponential distribution. The failure process intensity of Iveco Stralis vehicles is constant $\lambda = 0.0037$ (day^{-1}), with the distribution matching accuracy determined by $MSE = 0.0025$ and of Pearson's correlation coefficient $\rho = 0.9940$. Intensity of the repair process intensity $\mu = 0.1317$ (day^{-1}). The exponential distribution has a slightly lower (but satisfactory) matching accuracy than that of the fault process. It was estimated as $MSE = 0.0326$ and $\rho = 0.9527$. The distributions were approximated by the least squares method.

Table 7 summarizes the empirical values of variable k. The smallest number of observations were recorded in the range $k \in [20,50]$. This indicates high structural redundancy of the system, manifested by the large number of backup components. Fig. 14 shows the empirical CDF values with approximation by normal and logistic distributions for variable k. The empirical cumulative distribution function for $k = 0$ is equal to 0.1584, which means that the system is in a downtime condition for more than 15 % of the observation. In accordance with the estimated values shown in Table 8, MSE reached similar values. Pearson correlation coefficient ρ reached higher values for the normal distribution. Therefore, it is reasonable to implement the normal distribution of variable k to the developed simulation model.

4.3.2. CTMC analysis

In case study 2, the CTMC analysis was performed for a transport system composed of n homogeneous vehicles, with $n \in [1, 50]$. Assuming that the intensities of failure λ and repair μ of each component take the values estimated in Section 4.2.1, on the basis of Eq. (4), interstate transition intensity matrices were developed. Fig. 15 shows the results calculated according to Eqs. (8) and (9).

As the number of components increases, also the ergodic probability of state $S = n - 1$ increases, and the ergodic probability of state $S = n$ decreases. If the number of components in the system $n > 35$, then $\Pr(S = n - 1) > \Pr(S = n)$. For $n = 50$, the system achieves the highest ergodic probabilities of the states, respectively: $\Pr(S = 50) = 0.2502$, $\Pr(S = 49) = 0.3515$, $\Pr(S = 48) = 0.2419$, $\Pr(S = 47) = 0.1087$. On the basis of the ergodic probabilities, the expected values of the number of operable components in the system were calculated.

Table 7
Empirical values of variable k.

Value of variable k	Number of observations	Value of variable k	Number of observations	Value of variable k	Number of observations
0	190	17	26	34	2
1	73	18	28	35	0
2	48	19	20	36	0
3	27	20	11	37	0
4	38	21	13	38	1
5	30	22	8	39	2
6	34	23	10	40	0
7	51	24	12	41	1
8	51	25	5	42	0
9	43	26	10	43	0
10	56	27	7	44	0
11	55	28	3	45	0
12	53	29	1	46	0
13	49	30	2	47	0
14	44	31	5	48	0
15	49	32	4	49	0
16	34	33	0	50	0

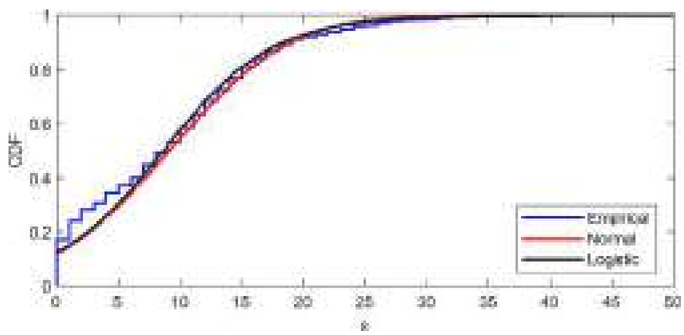

Fig. 14. Approximation of CDF for variable k.

4.3.3. Simulations

Simulation analyzes were performed for all variants of the system analyzed. Fig. 16 shows the results of the process for a system of 23 vehicles. The number of operable components was compared with the number of components necessary for the reliable operation of the system. Variable k sampling was performed once for 10,000 iterations. The values obtained were compared with the results of CTMC simulations. For most iterations of the simulation, the k-out-of-23 system had between 20 and 23 operable components.

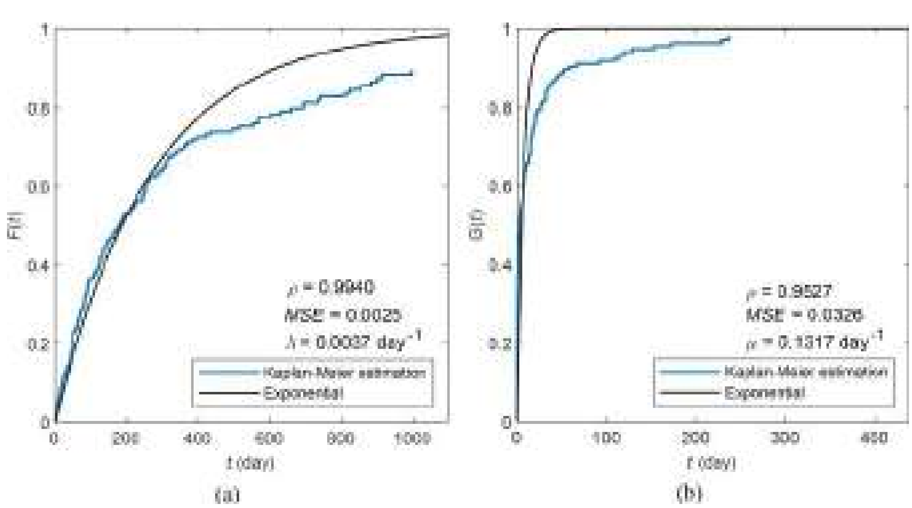

Fig. 13. Approximation of CDFs: (a) – time to failure, (b) – time to repair.

Table 8
Estimation of CDF parameters (for variable k).

Distribution	CDF	Parameters	Estimation	Pearson Correlation ρ	*MSE*
Normal	$K(k) = \frac{1}{2}\left[1 + \text{erf}\left(\frac{k-\phi}{\sigma\sqrt{2}}\right)\right]$	ϕ – mean σ – standard deviation	$\phi = 9.1323$ $\sigma = 7.6943$	0.9901	0.0020
Logistic	$K(k) = \frac{1}{1+\exp(-(k-\phi)/\sigma)}$	ϕ – location σ – scale	$\phi = 8.6307$ $\sigma = 4.4144$	0.9897	0.0019

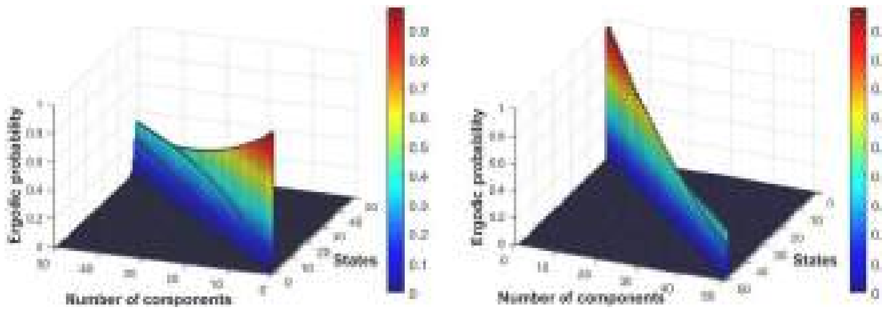

Fig. 15. Ergodic probabilities of states in CTMC.

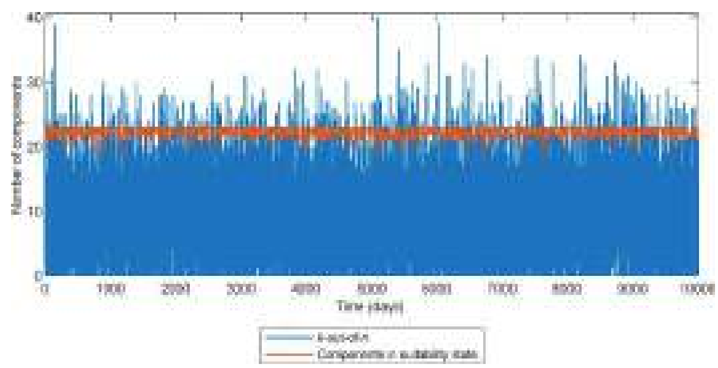

Fig. 16. Simulation results for a system of 23 components.

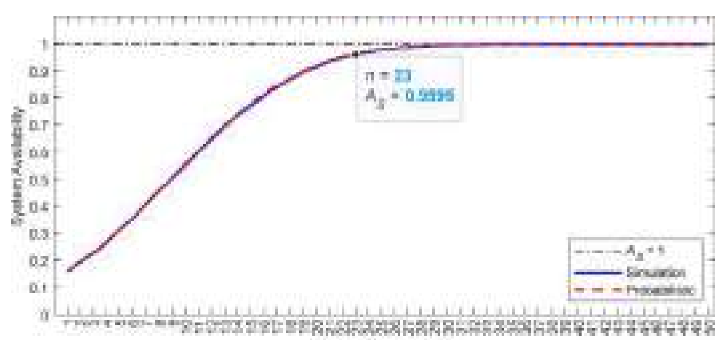

Fig. 17. Availability of a system of 1 to 50 components.

4.3.4. Availability and TPM

Based on the simulation values estimated in Section 4.2.3, the indicators A_S and *TPM* were calculated. Fig. 17 shows the availability of the tested transport system depending on the number of vehicles that make up it. A significant increase in A_S is observed in the range of the number of components from 1to 24, and for $n = 23$ an acceptable level of availability was achieved, i.e. $A_S = 0.9595$. For a full test sample of 50 vehicles, system availability $A_S = 1$. Thus, reducing the number of components by 27, i.e. ca. 54 %, results in a decrease in availability of 0.0405 only.

Fig. 17 shows a summary of the availability indicator A_S results for the probabilistic and simulation models. A detailed comparison of the indicator for a system of 1 to 50 components, together with the derogations, is shown in Table 9. The largest difference was achieved for the k-out-of-16 system and was 0.0083. The mean absolute error was equal to 0.0018, indicating very similar results achieved using both approaches.

Fig. 18 shows a box plot of *TPM*(i) for systems of 1to 50 components. Condition $A_S > 0.50$ is satisfied for the k-out-of-9 system, when the *TPM* (i) median is 1. Points marked with red markers indicate outliers and the

Table 9
System availability – comparing the results of probabilistic and simulation approaches.

Number of components	Approaches		Error
	Probabilistic	Simulation	
1	0.1598	0.1577	−0.0021
2	0.1925	0.1914	−0.0011
3	0.2290	0.2262	−0.0028
4	0.2691	0.2661	−0.0030
5	0.3123	0.3115	−0.0008
6	0.3583	0.3562	−0.0021
7	0.4065	0.4069	0.0004
8	0.4561	0.4589	0.0028
9	0.5063	0.5033	−0.0030
10	0.5565	0.5506	−0.0059
11	0.6057	0.6021	−0.0036
12	0.6532	0.6461	−0.0071
13	0.6985	0.6944	−0.0041
14	0.7408	0.7361	−0.0047
15	0.7799	0.7720	−0.0079
16	0.8153	0.8070	−0.0083
17	0.8469	0.8399	−0.0070
18	0.8747	0.8701	−0.0046
19	0.8987	0.8962	−0.0025
20	0.9192	0.9154	−0.0038
21	0.9364	0.9349	−0.0015
22	0.9506	0.9480	−0.0026
23	0.9621	0.9595	−0.0026
24	0.9714	0.9688	−0.0026
25	0.9786	0.9780	−0.0006
26	0.9843	0.9831	−0.0012
27	0.9886	0.9877	−0.0009
28	0.9918	0.9921	0.0003
29	0.9942	0.9947	0.0005
30	0.9960	0.9965	0.0005
31	0.9972	0.9973	0.0001
32	0.9981	0.9981	0.0000
33	0.9988	0.9986	−0.0002
34	0.9992	0.9995	0.0003
35	0.9995	0.9996	0.0001
36	0.9997	0.9997	0.0000
37	0.9998	0.9997	−0.0001
38	0.9999	0.9997	−0.0002
39	0.9999	0.9997	−0.0002
40	1.0000	0.9999	−0.0001
41÷50	1.0000	1.0000	0.0000

black line indicates *TPM* averages for the system. The largest increase in the average value of the indicator was observed in the 1 to 20 range of the number of components. For over 41 components, there were no outliers, and *TPM* = 1.

The k-out-of-23 system obtained a *TPM* of 0.9947, which, compared with *TPM* = 1 for the k-out-of-50 system, is a satisfactory result. Thus, in a system where the number of components has increased from 23 to 50, that is, by 117 %, the *TPM* value has increased by approximately 0.5.

4.3.5. Sensitivity analysis

Sensitivity was analyzed by determining the impact of the A_S and *TPM* indicators in accordance with Section 4.1.5.

From a risk assessment point of view, this range warrants a forecast horizon wide enough to ensure the safe and reliable operation of the system. Fig. 19(a) shows the availability of the k-out-of-23 system with assumed variability of operational process parameters. With the current repair potential, measured by repair intensity $\mu = 0.1317$ (day^{-1})), maintained, even a tenfold increase in failure intensity λ did not cause a significant decrease in the indicator A_S which was approximately 0.86. Additionally, if the intensity of the failure will remain at the estimated level $\lambda = 0.0037$ (day^{-1}), even with a 50 % reduction in the repair potential ($\mu = 0.0657$ (day^{-1})), the system will operate with availability $A_S > 0.95$. It is worth noting that the system availability reaches above 0.50 even in the case of a five-fold decrease in the repair potential with a simultaneous ten-fold increase in the failure intensity.

Fig. 19(b) shows the sensitivity of the *TPM* indicator to the change in parameters λ and μ. The behavior of the system was assessed at the current level of repair intensity and changes in failure intensity. The *TPM* decreases to 0.97 with a ten-fold increase in parameter λ.

If parameters ϕ and σ are less than the estimates listed in Table 8, then the availability of the system reaches values in the range [0.9595, 1]. In the case of an increase in the average ϕ and decrease in σ, indicator A_S is rapidly decreasing. This effect was observed especially when changing parameter ϕ from 18.2646 to 27.3969. For the observation, where ϕ decreases, the system availability shows relatively low sensitivity to large σ increases. For the average, which is the product of the estimated value ϕ and the coefficient from the range [0.1, 0.9] and the standard deviation, which is the product of the estimated value σ and the coefficient from the range [2,10], the indicator $A_S \in [0.5818, 0.9224]$. If ϕ and σ are greater than the estimates in Table 8, the system availability is in the range [0, 0.9595]. However, the decrease in indicator A_S is not as big as at an increase in the average ϕ and decrease in σ. The sensitivity analysis shown in Fig. 20 thus indicates that the system availability is more susceptible to increases in the average ϕ of the task inflow to the system, rather than changes in the parameter σ that determines the inflow variability dynamics.

5. Discussion

The main objective of this study was to analyze the availability and performance of k-out-of-n structured systems operated with varying intensity.

Using simulation methods and a probabilistic approach, the values of the availability indicator A_S were calculated for systems consisting of 1 to 19 components for case study 1 and from 1 to 50 components for the case study 2. The results obtained for both cases, despite the difference in their numbers, are similar. This is indicated by the mean absolute percentage error (MAPE) of 0.44 (%) for case study 1 and 0.32 (%) for

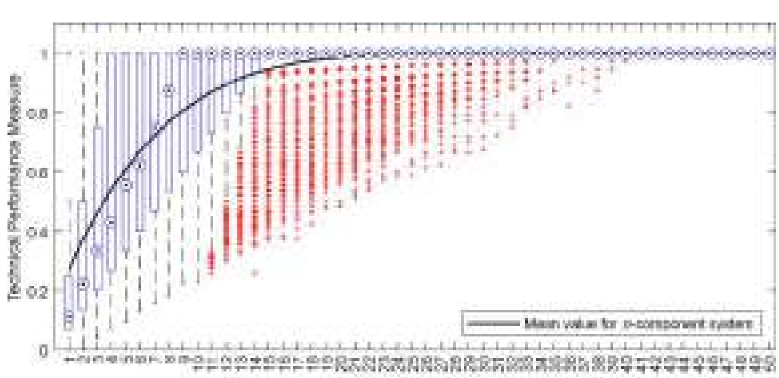

Fig. 18. *TPM* of a system of 1 to 50 components.

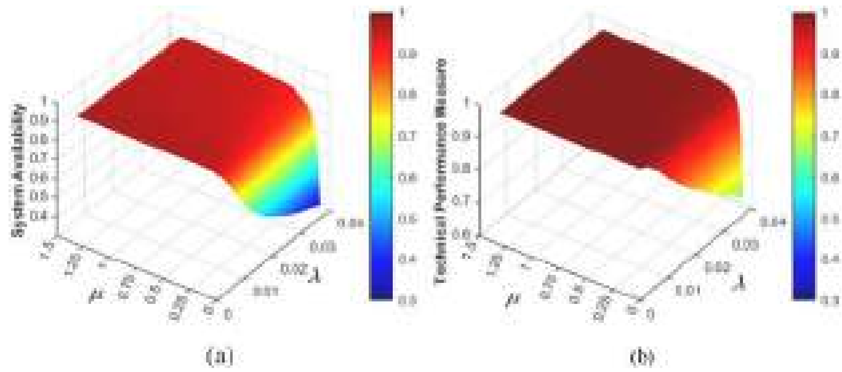

Fig. 19. Sensitivity analysis of failure and repair rates: (a) – availability and (b) – *TPM* for the *k*-out-of-23 system.

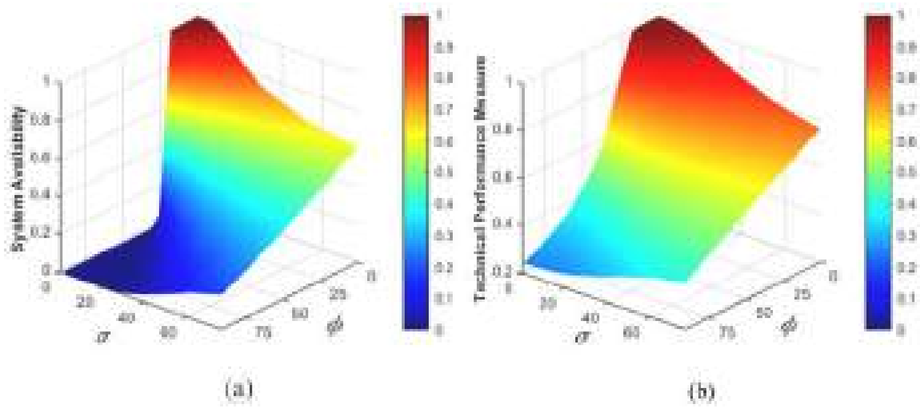

Fig. 20. Sensitivity analysis of *k* CDF parameters: (a) – availability and (b) – *TPM* for the *k*-out-of-23 system.

case study 2, respectively. The validation of the proposed models has demonstrated their availability, which is the basis for their use in the analysis and assessment of availability. Furthermore, in accordance with the intended purpose of this article for both systems, based on the availability indicator $A_{S,}$ the optimal number of components is 10 vehicles (for case study 1) and 23 vehicles (for case study 2).

For systems operating with variable performance, the use of indicator *TPM* more accurately reflects their actual performance. Optimized systems show relatively little susceptibility to changes in the failure and repair intensities. However, their availability and performance are much more sensitive to changes in the distribution parameters of the task input to the system. Therefore, this conclusion constitutes an extension of the properties of the *k*-out-of-*n* system properties formulated by Rykov et al. [26] and proven using the Markov chain method of complementary variables.

Fig. 21 presents a cost analysis for all variants considered of *k*-out-of-*n* structures for the transport systems tested. The curves represent the ratio of the increase in indicators A_S and *TPM* to the costs incurred annually in extending the structure of the system by one component. The *TPM* increment to increase in the costs incurred decreases and for the optimal number of components reaches a value close to zero. A_S increment to increase in the costs incurred is not monotonous. In case study 1

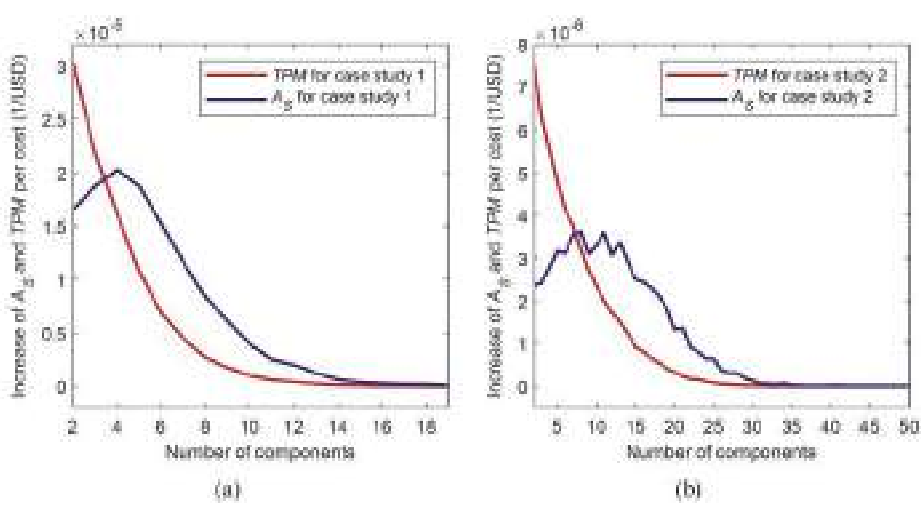

Fig. 21. Increase in A_S and *TPM* per cost: (a) for case study 1 and (b) for case study 2.

(Fig. 21(a)) it reached maximum for the k-out-of-4 structure of 2.03×10^{-5} (1/USD). This means the greatest increase in availability to the costs incurred, with the expansion of the three-element system by a fourth component. In case study 2 (Fig. 21(b)) the k-out-of-(5÷13) structures achieved the largest increases in availability to costs at a level above 3×10^{-6} (1/USD). Therefore, over a certain number of components in the system, increasing the structure loses its economic rationale.

The average costs of building and operating a real system (without infrastructure and labor expenses) are $ 112,324.40/year and $ 717,355.30/year. After the optimization, they were significantly reduced to $ 59,118.10/year for case study 1 and $ 329,983.40 year for case study 2, respectively. This means a reduction of 47 (%) and 54 (%), respectively. It should be noted that the economic gains from system optimization are disproportionately greater than the small availability losses of 4.36 (%) and 4.05 (%) and the insignificant performance losses of 0.87 (%) and 0.52 (%). Optimizing the structure of redundant systems has a direct impact on reducing costs and increasing the economic performance of the system. The proposed model is therefore relevant not only to safety, but also to financing of that safety. In the long run, it has an impact on the country's economy.

6. Conclusions and future works

Previous publications on the research problem herein discussed have so far concerned systems operating with constant intensity, which required a certain and constant number of operable components for their proper operation. In practice, the task inflow to the system (especially a military system) can significantly vary, and the variability is described with appropriate probabilistic distributions. The models presented by other authors are not applicable in the analysis of such cases.

In this publication, the problem of the k-out-of-n redundant system is analyzed that is made up of components that are homogeneous and repairable with exponential characteristics of times to failure and repair times. It was assumed that at a given time, k components are operated, and the other objects $(n - k)$ are in hot-standby mode. A two-state model has been proposed for the component operation, and an $(n + 1)$ - state model for a system composed of n components. System transition from state $S = m$ depends solely on the timing of independent failure and repair processes. If the time of occurrence of the next failure is shorter than the time of repair of the failed component, then the system transits to $S = m - 1$, otherwise it will be in state $S = m + 1$.

The presented redundancy strategy is a tool for effectively increasing the reliability of systems and ensuring that tasks are carried out successfully. Managers must have current knowledge of the technical condition of the objects, the objectives to be achieved, the constraints, and the resources available for use. This information is essential for rational and cost-effective planning of system operations. To maintain a high readiness indicator, managers should continuously diagnose the redundant system and assign tasks to individual system components. One way to do this is to allocate task prioritization to the units with the smallest reserve of resurgence. The results of the cost analysis carried out indicate that from a certain level of the number of components in the system, increasing the structure is no longer economically justified. Therefore, optimizing the structure of the system can significantly reduce the costs of its operation. Furthermore, the dynamics of changes in the incoming task streams should be monitored on a continuous process. Changes in the parameters of the task stream volume distributions determine the need to adjust the optimal level of redundancy in the system. The novelty, which is a contribution to science, is the development of original probabilistic and simulation models based on CTMC for the reliability analysis of systems operating with variable intensity. The probabilistic approach is an extension of dependencies for classical structures k-out-of-n known in the literature. The simulation model based on MC methods assumes sampling of cumulative distribution functions of times to damage and repair times for CTMC and sampling of the cumulative distribution function of variable k. The availability indicator A_S and performance indicator *TPM* obtained using probabilistic and simulation approaches, for two case studies are similar, which testifies to the universality of the proposed method and thus the credibility of the developed models. As the above examples show, optimizing the system structure taking into account the assumed levels of availability and performance also reduces costs. For this reason, the ratio of system availability and performance gains to costs, depending on the number of components, was analyzed. It was shown that for the optimal number of components, a slight decrease in the A_S and *TPM* indicators is disproportionate to significantly minimize costs, which becomes especially important during the crisis and war.

Sensitivity analysis was used to assess the risk of system operation from changes in input parameters. Variability of parameters results from the intensity of operational processes, the technical potential of the maintenance and repair base, and the dynamics of the flow of tasks. The models developed showed insensitivity to changes in failure and repair intensities with high susceptibility to variable k distribution parameters.

The next step of future research can be the application of the proposed approach to solving RAP problems for systems and subsystems with variable operational intensity. If the number of components in a technical system is constant, they can be allocated across subsystems in order to determine the optimal levels of availability and performance of the subsystems under test.

CRediT authorship contribution statement

Mateusz Oszczypała: Conceptualization, Methodology, Software, Validation, Formal analysis, Investigation, Resources, Data curation, Writing – original draft, Writing – review & editing, Visualization. **Jakub Konwerski:** Conceptualization, Methodology, Software, Validation, Formal analysis, Investigation, Resources, Data curation, Writing – original draft, Writing – review & editing, Visualization. **Jarosław Ziółkowski:** Data curation, Formal analysis, Writing – review & editing, Supervision, Project administration. **Jerzy Małachowski:** Formal analysis, Writing – review & editing, Project administration, Funding acquisition.

Declaration of Competing Interest

The authors declare that they have no known competing financial interests or personal relationships that could have appeared to influence the work reported in this paper.

Data availability

Data will be made available on request.

Acknowledgments

The authors acknowledge the Military University of Technology for the financial support (research project UGB 22-835) in this study.

Appendix A

Table A1
Acronyms.

Acronyms	Details
BIUGF	Binary Indicator Universal Generating Function
CBPS	Common bus performance sharing
CDF	Cumulative distribution function
CTMC	Continuous Time Markov Chain
EMC	Expected mission cost
FMC	Finite Markov Chain
FMCI	Finite Markov Chain Imbedding
GA	Genetic Algorithm
HFE	Hybrid Full Enumeration
MAPE	Mean Absolute Percentage Error
MC	Monte Carlo
MCMC	Markov Chain Monte Carlo
MOEA	Multi-objective Evolutionary Algorithm
MSE	Mean Squared Error
MSP	Mission Success Probability
MTBF	Mean Time Between Failures
NPPs	Nuclear Power Plants
NRGA	Non-dominated Ranked Genetic Algorithm
NSGA-II	Non-dominated Sorting Genetic Algorithm II
PM	Preventive maintenance
PR	Preventive replacement
RAP	Redundancy Allocation Problem
TPM	Technical Performance Measure
UGF	Universal Generating Function

Table A2
Notations.

Notations	Details
λ	Failure rate
μ	Repair rate
t	Time
T_S	Simulation time
n	Number of components in the system
$X(i)$	Stochastic process
$k(j)$	Minimum number of working components in j-th iteration (day)
$T(i)$	Time of state transition
$S(t)$	State of system in time t
a, b	Random values from the uniform distribution on the interval (0, 1)
p	Availability of each component
q	Unavailability of each component
t_f	Time to failure
t_r	Time to repair
$\mathbf{\Lambda}_\mathrm{C}$	Transition intensity matrix for the component
$\mathbf{\Lambda}_\mathrm{S}$	Transition intensity matrix for the system
$\mathbf{\Lambda}_\mathrm{T}$	Tensor of intensity matrices $\mathbf{\Lambda}_\mathrm{S}$
$\mathbf{P}(0)$	Initial probabilities of states
$F(t)$	CDF of time to failure (unreliability function)
$G(t)$	CDF of time to repair
$K(k)$	CDF of variable k
ϕ, σ	Distribution parameters of variable k
ρ	Pearson correlation
$A_S(i)$	System Availability for i th iteration
A_S	Mean value of System Availability
$TPM(i)$	Technical Performance Measure for i th iteration
TPM	Mean value of Technical Performance Measure
$\mathbf{W}$	Vector of coefficients for sensitivity analysis

Appendix B

The maximum likelihood estimation for lifetime and repair times with censored data can be calculated using the following formula [87]:

$$L(\theta, X) = \prod_{i=1}^{n} f(x_i, \theta)^{\delta_i} [1 - F(x_i, \theta)]^{1-\delta_i}, \tag{b-1}$$

where:

$$\delta_i = \begin{cases} 1 & \text{if } x_i \text{ is complete data} \\ 0 & \text{if } x_i \text{is censored data} \end{cases}. \tag{b-2}$$

For an exponential distribution with parameter λ, the Eq. (b-1) can be described as:

$$L(\lambda, X) = \prod_{i=1}^{n} \left(\lambda e^{-\lambda x_i}\right)^{\delta_i} \left(e^{-\lambda x_i}\right)^{1-\delta_i}, \tag{b-3}$$

and using the natural logarithm, the Equation (b-3) can be transformed into the formulas:

$$\ln L(\lambda, X) = \sum_{i=1}^{n} [(\ln\lambda - \lambda x_i)\cdot\delta_i + (-\lambda x_i)\cdot(1-\delta_i)], \tag{b-4}$$

$$\ln L(\lambda, X) = \ln\lambda \sum_{i=1}^{n} \delta_i - \lambda \sum_{i=1}^{n} x_i. \tag{b-5}$$

If number of complete data is equal to c, the Eq. (b-5) is reduced to the formula:

$$\ln L(\lambda, X) = c\ln\lambda - \lambda \sum_{i=1}^{n} x_i. \tag{b-6}$$

Differentiating on both sides by λ and comparing to 0, the estimator of the exponential distribution parameter is determined as follows:

$$\frac{\partial \ln L(\lambda, X)}{\partial \lambda} = \frac{c}{\lambda} - \sum_{i=1}^{n} x_i = 0, \tag{b-7}$$

$$\hat{\lambda} = \frac{c}{\sum_{i=1}^{n} x_i}. \tag{b-8}$$

Table B1 presents the results of the estimation of failure and repair rates using the least squares method and the maximum-likelihood estimation. In all two case studies for failure and repair rates, the results obtained by the least squares method were a better fit to the empirical data.

Table B1
The results of estimating failure and repair rates using least squares method (LSM) and maximum likelihood estimation (MLE).

Param.	Case study no. 1						Case study no. 2					
	LSM			MLE			LSM			MLE		
	Value (day^{-1})	ρ	*MSE*	Value (day^{-1})	ρ	*MSE*	Value (day^{-1})	ρ	*MSE*	Value (day^{-1})	ρ	*MSE*
λ	0.0048	0.9956	0.0004	0.0044	0.9952	0.0009	0.0037	0.9940	0.0025	0.0029	0.9849	0.0059
μ	0.2607	0.9609	0.0208	0.0676	0.9171	0.0701	0.1317	0.9527	0.0326	0.0399	0.9269	0.0717

References

[1] Qin S, Wang BX, Tsai TR, Wang X. The prediction of remaining useful lifetime for the Weibull k-out-of-n load-sharing system. Reliab Eng Syst Saf 2023;233:109091. https://doi.org/10.1016/j.ress.2023.109091.
[2] Pham H. Handbook of reliability engineering. editor. London ; New York: Springer; 2003.
[3] Sharifi M, Taghipour S, Abhari A. Inspection interval optimization for a k-out-of-n load sharing system under a hybrid mixed redundancy strategy. Reliab Eng Syst Saf 2021;213:107681. https://doi.org/10.1016/j.ress.2021.107681.
[4] Tarełko W. Redundancy as a way increasing reliability of ship power plants. Mech Rev 2017;1:56–61. https://doi.org/10.15199/148.2017.11.11.
[5] Abouei Ardakan M, Zeinal Hamadani A. Reliability optimization of series–parallel systems with mixed redundancy strategy in subsystems. Reliab Eng Syst Saf 2014; 130:132–9. https://doi.org/10.1016/j.ress.2014.06.001.
[6] Zhang J, Lv H, Hou J. A novel general model for RAP and RRAP optimization of k-out-of-n:g systems with mixed redundancy strategy. Reliab Eng Syst Saf 2023;229: 108843. https://doi.org/10.1016/j.ress.2022.108843.
[7] Gao S. Reliability analysis and optimization for a redundant system with dependent failures and variable repair rates. Math Comput Simul 2023;208:637–59. https://doi.org/10.1016/j.matcom.2023.02.001.
[8] Saberzadeh Z, Razmkhah M, Amini M. Bayesian reliability analysis of complex k -out-of- n : ℓ systems under degradation performance. Reliab Eng Syst Saf 2022: 109020. https://doi.org/10.1016/j.ress.2022.109020.
[9] Guo L, Li R, Wang Y, Yang J, Liu Y, Chen Y, et al. Availability for multi-component k-out-of-n: g warm-standby system in series with shut-off rule of suspended animation. Reliab Eng Syst Saf 2023:109106. https://doi.org/10.1016/j.ress.2023.109106.
[10] Zhao X, Liu H, Wu Y, Qiu Q. Joint optimization of mission abort and system structure considering dynamic tasks. Reliab Eng Syst Saf 2023;234:109128. https://doi.org/10.1016/j.ress.2023.109128.
[11] Gao H, Cui L, Chen J. Reliability modeling for sparsely connected homogeneous multistate consecutive-k-out-of-n: g systems. IEEE Trans Syst Man Cybern, Syst 2021;51:1844–54. https://doi.org/10.1109/TSMC.2019.2906550.
[12] Peiravi A, Nourelfath M, Zanjani MK. Redundancy strategies assessment and optimization of k-out-of-n systems based on Markov chains and genetic algorithms. Reliab Eng Syst Saf 2022;221:108277. https://doi.org/10.1016/j.ress.2021.108277.
[13] El-Ghamry E, Muse AH, Aldallal R, Mohamed MS. Availability and reliability analysis of a k-Out-of-n warm standby system with common-cause failure and fuzzy failure and repair rates. Math Probl Eng 2022;2022:1–11. https://doi.org/10.1155/2022/3170665.
[14] Zhang T, Xie M, Horigome M. Availability and reliability of k-out-of-(M+N):g warm standby systems. Reliab Eng Syst Saf 2006;91:381–7. https://doi.org/10.1016/j.ress.2005.02.003.
[15] Gong M, Liu H, Peng R. Redundancy allocation of mixed warm and cold standby components in repairable K-out-of-N systems. Proc Inst Mech Eng Part O J Risk Reliab 2020;234:696–707. https://doi.org/10.1177/1748006X20921306.
[16] Zheng J, Okamura H, Dohi T. Reliability importance of components in a real-time computing system with standby redundancy schemes. Int J Math Eng Manag Sci 2018;3:64–89. https://doi.org/10.33889/IJMEMS.2018.3.2-007.
[17] Gao H, Cui L, Chen J. Reliability modeling for sparsely connected homogeneous multistate consecutive-k-Out-of-n: g systems. IEEE Trans Syst Man Cybern, Syst 2021;51:1844–54. https://doi.org/10.1109/TSMC.2019.2906550.
[18] Bian L, Wang G, Liu P. Reliability analysis for k-out-of-n(G) systems subject to dependent competing failure processes. Comput Ind Eng 2023;177:109084. https://doi.org/10.1016/j.cie.2023.109084.

[19] Wu C, Pan R, Zhao X, Cao S. Reliability evaluation of consecutive-k-out-of-n: f systems with two performance sharing groups. Comput Ind Eng 2021;153:107092. https://doi.org/10.1016/j.cie.2020.107092.

[20] Wu C, Zhao X, Wang S, Song Y. Reliability analysis of consecutive-k-out-of-r-from-n subsystems: f balanced systems with load sharing. Reliab Eng Syst Saf 2022;228:108776. https://doi.org/10.1016/j.ress.2022.108776.

[21] Tian-yuan Y, Lin-lin L, He-wei P, Yuan-zi Z. Bayesian Networks based approach to enhance GO methodology for reliability modeling of multi-state consecutive-k-out-of-n: f system. Reliab Eng Syst Saf 2023;229:108828. https://doi.org/10.1016/j.ress.2022.108828.

[22] El-Damcese MA, El-Sodany NH. Reliability and sensitivity analysis of the k-out-of-n:g warm standby parallel repairable system with replacement at common-cause failure using Markov model. J Stat Appl Probab 2015;5:16. https://doi.org/10.18576/jsap/050316.

[23] Bogatyrev AV, Bogatyrev VA, Bogatyrev SV. The probability of timeliness of a fully connected exchange in a redundant real-time communication system. In: Proceedings of the wave electronics and its application in information and telecommunication systems (WECONF). IEEE; 2020. p. 1–4. https://doi.org/10.1109/WECONF48837.2020.9131517.

[24] Jafari M. Optimal redundant sensor configuration for accuracy increasing in space inertial navigation system. Aerosp Sci Technol 2015;47:467–72. https://doi.org/10.1016/j.ast.2015.09.017.

[25] Xiahou T., Zheng Y.X., Liu Y., Chen H. Reliability modeling of modular k-out-of-n systems with functional dependency: a case study of radar transmitter systems. reliability engineering & system safety 2023:109120. 10.1016/j.ress.2023.109120.

[26] Rykov VV, Sukharev MG, Itkin VY. Investigations of the potential application of k-out-of-n systems in oil and gas industry objects. JMSE 2020;8:928. https://doi.org/10.3390/jmse8110928.

[27] Berrade MD, Scarf PA, Cavalcante CAV, Dwight RA. Imperfect inspection and replacement of a system with a defective state: a cost and reliability analysis. Reliab Eng Syst Saf 2013;120:80–7. https://doi.org/10.1016/j.ress.2013.02.024.

[28] Zhang C, Li Q, Liu Y. Optimal replacement policy with minimal repair and preventive maintenance of an aircraft structure subjected to corrosion. Soft Comput 2020;24:375–84. https://doi.org/10.1007/s00500-019-03919-2.

[29] Lin B, Wu J, Lin R, Wang J, Wang H, Zhang X. Optimization of high-level preventive maintenance scheduling for high-speed trains. Reliab Eng Syst Saf 2019;183:261–75. https://doi.org/10.1016/j.ress.2018.11.028.

[30] Cheng C, Yang J, Li L. Reliability evaluation of a k-out-of-n(G)-subsystem based multi-state phased mission system with common bus performance sharing subjected to common cause failures. Reliab Eng Syst Saf 2021;216:108003. https://doi.org/10.1016/j.ress.2021.108003.

[31] Vallarino CR, Elsey KJ. Choosing from redundant designs of power systems using system outage rate and cost. Microelectron Reliab 1996;36:1269–74. https://doi.org/10.1016/0026-2714(96)00160-6.

[32] Maktoubian J, Ansari K. An IoT architecture for preventive maintenance of medical devices in healthcare organizations. Health Technol 2019;9:233–43. https://doi.org/10.1007/s12553-018-00286-0.

[33] Him LC, Poh YY, Pheng LW. IoT-based predictive maintenance for smart manufacturing systems. In: Proceedings of the Asia-pacific signal and information processing association annual summit and conference (APSIPA ASC). IEEE; 2019. p. 1942–4. https://doi.org/10.1109/APSIPAASC47483.2019.9023106.

[34] Lu J, Yi H, Li X, Balakrishnan N. Joint reliability of two consecutive-(1,l)or (2,k)-out-of-(2,n): f type systems and its application in smart street light deployment. Methodol Comput Appl Probab 2023;25:33. https://doi.org/10.1007/s11009-023-09984-3.

[35] Wang W, Scarf P, Smith M. On the application of a model of condition-based maintenance. J Oper Res Soc 2000;51(11):1218–27. https://doi.org/10.1057/palgrave.jors.2601042.

[36] Rykov V, Kochueva O, Farkhadov M. Preventive maintenance of a k-out-of-n system with applications in subsea pipeline monitoring. JMSE 2021;9:85. https://doi.org/10.3390/jmse9010085.

[37] Rochlin G.I., Porte T.R.L., Roberts K.H. The self-designing high-reliability organization: aircraft carrier flight operations at sea 1987;40.

[38] Eslami Baladeh A, Taghipour S. Reliability optimization of dynamic k-out-of-n systems with competing failure modes. Reliab Eng Syst Saf 2022;227:108734. https://doi.org/10.1016/j.ress.2022.108734.

[39] Jia H, Ding Y, Xing L, Liu D. Reliability of dynamic k-out-of-n systems with coupling components in power transmission systems. In: Proceedings of the Asia-pacific international symposium on advanced reliability and maintenance modeling (APARM). IEEE; 2020. p. 1–6. https://doi.org/10.1109/APARM49247.2020.9209545.

[40] Xu D, Tian Y, Shi J, Wang D, Zhang M, Li H. Reliability analysis and optimal redundancy for a satellite power supply system based on a new dynamic k-out-of-n: g model. Reliab Eng Syst Saf 2023;236:109317. https://doi.org/10.1016/j.ress.2023.109317.

[41] Lin C, Cui L, Coit D, Lv M. An approximation method for evaluating the reliability of a dynamic k-out-of-n:f system subjected to cyclic alternating operation conditions. Proc Inst Mech Eng Part O J Risk Reliab 2017;231:109–20. https://doi.org/10.1177/1748006X16689541.

[42] Wang C, Wang S, Xing L, Guan Q. Efficient performability analysis of dynamic multi-state k-out-of-n: g systems. Reliab Eng Syst Saf 2023;237:109384. https://doi.org/10.1016/j.ress.2023.109384.

[43] Wang C, Xing L, Su Y, Guan Q, Tang B, Hu Y. Reliability analysis of dynamic voting phased-mission systems. Reliab Eng Syst Saf 2023;232:109085. https://doi.org/10.1016/j.ress.2022.109085.

[44] Wang C, Xing L, Yu J, Guan Q, Yang C, Yu M. Phase reduction for efficient reliability analysis of dynamic k-out-of-n phased mission systems. Reliab Eng Syst Saf 2023;237:109349. https://doi.org/10.1016/j.ress.2023.109349.

[45] Chang CC. Optimal maintenance policy for a k-out-of-n system with replacement first and last. Ann Oper Res 2023. https://doi.org/10.1007/s10479-023-05236-2.

[46] Oszczypała M, Ziółkowski J, Małachowski J. Analysis of light utility vehicle readiness in military transportation systems using Markov and semi-Markov processes. Energies 2022;15:5062. https://doi.org/10.3390/en15145062.

[47] Oszczypała M, Ziółkowski J, Małachowski J. Modelling the operation process of light utility vehicles in transport systems using Monte Carlo simulation and semi-Markov approach. Energies 2023;16:2210. https://doi.org/10.3390/en16052210.

[48] Dembinska A. On reliability analysis of k-out-of-n systems consisting of heterogeneous components with discrete lifetimes. IEEE Trans Rel 2018;67:1071–83. https://doi.org/10.1109/TR.2018.2837080.

[49] Sharifi M, Taghipour S. Optimal inspection interval for a k-out-of-n system with non-identical components. J Manuf Syst 2020;55:233–47. https://doi.org/10.1016/j.jmsy.2020.03.007.

[50] Chen Y, Yu X, Li Y. A failure mechanism cumulative model for reliability evaluation of a k-out-of-n system with load sharing effect. IEEE Access 2019;7:2210–22. https://doi.org/10.1109/ACCESS.2018.2852730.

[51] Sharifi M, Taghipour S, Abhari A. Condition-based optimization of non-identical inspection intervals for a k-out-of-n load sharing system with hybrid mixed redundancy strategy. Knowl Based Syst 2022;240:108153. https://doi.org/10.1016/j.knosys.2022.108153.

[52] Ling X, Wei Y. Optimal Allocation of randomly selected redundancies to k–out–of–n system with independent but nonidentical components. IEEE Access 2020;8:88464–73. https://doi.org/10.1109/ACCESS.2020.2993198.

[53] Poonia PK, Sirohi A, Kumar A. Cost analysis of a repairable warm standby k-out-of-n: g and 2-out-of-4: g systems in series configuration under catastrophic failure using copula repair. Life Cycle Reliab Saf Eng 2021;10:121–33. https://doi.org/10.1007/s41872-020-00155-8.

[54] Levitin G, Xing L, Dai Y. Optimal operation and maintenance scheduling in m-out-of-n standby systems with reusable elements. Reliab Eng Syst Saf 2021;211:107582. https://doi.org/10.1016/j.ress.2021.107582.

[55] Wu H, Li YF, Bérenguer C. Optimal inspection and maintenance for a repairable k-out-of-n: g warm standby system. Reliab Eng Syst Saf 2020;193:106669. https://doi.org/10.1016/j.ress.2019.106669.

[56] Fyffe DE, Hines WW, Lee NK. System reliability allocation and a computational algorithm. IEEE Trans Reliab 1968;R-17:64–9. https://doi.org/10.1109/TR.1968.5217517.

[57] Eshraghniaye Jahromi A, Feizabadi M. Optimization of multi-objective redundancy allocation problem with non-homogeneous components. Comput Ind Eng 2017;108:111–23. https://doi.org/10.1016/j.cie.2017.04.009.

[58] Kuiti MR, Hazra NK, Finkelstein M. A note on the stochastic precedence order between component redundancy and system redundancy for k -out-of- n systems. Commun Stat Theory Methods 2022;51:5003–11. https://doi.org/10.1080/03610926.2020.1831539.

[59] Zhang Y. Optimal allocation of active redundancies in weighted k -out-of- n systems. Stat Probab Lett 2018;135:110–7. https://doi.org/10.1016/j.spl.2017.12.002.

[60] Sharifi M, Moghaddam TA, Shahriari M. Multi-objective redundancy allocation problem with weighted-k-out-of-n subsystems. Heliyon 2019;5:e02346. https://doi.org/10.1016/j.heliyon.2019.e02346.

[61] Hamdan K, Tavangar M, Asadi M. Optimal preventive maintenance for repairable weighted k-out-of-n systems. Reliab Eng Syst Saf 2021;205:107267. https://doi.org/10.1016/j.ress.2020.107267.

[62] Chen Z, Zhao T, Jiao J, Ren F. Availability analysis and optimal design of multistate weighted ${k}$ -out-of- ${n}$ systems with component performance requirements. IEEE Access 2018;6:51547–55. https://doi.org/10.1109/ACCESS.2018.2865933.

[63] Levitin G, Xing L, Huang HZ. Dynamic availability and performance deficiency of common bus systems with imperfectly repairable components. Reliab Eng Syst Saf 2019;189:58–66. https://doi.org/10.1016/j.ress.2019.04.007.

[64] Wang C, Xing L, Amari SV, Tang B. Efficient reliability analysis of dynamic k-out-of-n heterogeneous phased-mission systems. Reliab Eng Syst Saf 2020;193:106586. https://doi.org/10.1016/j.ress.2019.106586.

[65] Bisht V, Singh SB. Lz-transform approach to evaluate reliability indices of multi-state repairable weighted K-out-of-n systems. Qual Reliab Eng Int 2023:1–15. https://doi.org/10.1002/qre.3279.

[66] Zheng M, Lin J, Xia T, Liu Y, Pan E. Joint condition-based maintenance and spare provisioning policy for a K-out-of-N system with failures during inspection intervals. Eur J Oper Res 2023. https://doi.org/10.1016/j.ejor.2023.01.011.

[67] Ziółkowski J, Borucka A. Markov model in logistic management of enterprise. J Konbin 2016;38:271–90. https://doi.org/10.1515/jok-2016-0027.

[68] Ziółkowski J, Małachowski J, Oszczypała M, Szkutnik-Rogoż J, Lęgas A. Modelling of the military helicopter operation process in terms of readiness. Def Sci J 2021;71:602–11. https://doi.org/10.14429/dsj.71.16422.

[69] Franko C, Tutuncu GY. Signature based reliability analysis of repairable weighted k-out-of-n:g systems. IEEE Trans Rel 2016;65:843–50. https://doi.org/10.1109/TR.2015.2499959.

[70] Ugurlu OF, Kumral M. Reliability-based performance analysis of mining drilling operations through Markov chain Monte Carlo and mean reverting process simulations. Simulation 2020;96:593–604. https://doi.org/10.1177/0037549720923751.

[71] Wang J, Gao X, Cao R, Sun Z. A multilevel monte carlo method for performing time-variant reliability analysis. IEEE Access 2021;9:31773–81. https://doi.org/10.1109/ACCESS.2021.3059663.
[72] Wu H, Zhu Z, Du X. System reliability analysis with autocorrelated kriging predictions. J Mech Des 2020;142:101702. https://doi.org/10.1115/1.4046648.
[73] Zhao Y, Tang Y, Li W, Yu J. Composite power system reliability evaluation based on enhanced sequential cross-entropy Monte Carlo simulation. IEEE Trans Power Syst 2019;34:3891–901. https://doi.org/10.1109/TPWRS.2019.2909769.
[74] NO-06-A102. Materiel – general technical requirements, test and inspection methods – reliability requirements 2021.
[75] Sears, T.B. Taylor, E.P. Technical performance measurement handbook 1984.
[76] Selech J, Andrzejczak K. An aggregate criterion for selecting a distribution for times to failure of components of rail vehicles. Maint Reliab 2019;22:102–11. https://doi.org/10.17531/ein.2020.1.12.
[77] Kaplan EL, Meier P. Nonparametric estimation from incomplete observations. J Am Stat Assoc 1958;53:457–81. https://doi.org/10.1080/01621459.1958.10501452.
[78] Oszczypała M, Ziółkowski J, Małachowski J. Reliability analysis of military vehicles based on censored failures data. Appl Sci 2022;12:2622. https://doi.org/10.3390/app12052622.
[79] Xu K, Xie M, Tang LC, Ho SL. Application of neural networks in forecasting engine systems reliability. Appl Soft Comput 2003;2:255–68. https://doi.org/10.1016/S1568-4946(02)00059-5.
[80] Chen KY. Forecasting systems reliability based on support vector regression with genetic algorithms. Reliab Eng Syst Saf 2007;92:423–32. https://doi.org/10.1016/j.ress.2005.12.014.
[81] Moura M das C, Zio E, Lins ID, Droguett E. Failure and reliability prediction by support vector machines regression of time series data. Reliab Eng Syst Saf 2011;96:1527–34. https://doi.org/10.1016/j.ress.2011.06.006.
[82] Rajpal PS, Shishodia KS, Sekhon GS. An artificial neural network for modeling reliability, availability and maintainability of a repairable system. Reliab Eng Syst Saf 2006;91:809–19. https://doi.org/10.1016/j.ress.2005.08.004.
[83] Misra KB. Handbook of performability engineering. editor. London: Springer London; 2008. https://doi.org/10.1007/978-1-84800-131-2.
[84] Ministry of National Defence. Manual on managing the equipment of the tank and car service DU-4.22.2(A). Bydgoszcz: Ministry of National Defence; 2019.
[85] Ministry of National Defence,. HONKER 2000 light utility vehicle data sheet 2005.
[86] Ministry of National Defence. Iveco Stralis AT 260S35Y/P heavy duty general purpose vehicle data sheet 2004.
[87] Ferreira L.A., Silva J.L. Parameter estimation for Weibull distribution with right censored data using EM algorithm. EiN 2017;19:310–5. 10.17531/ein.2017.2.20.

IEEE Access

Received 3 July 2024, accepted 21 August 2024, date of publication 26 August 2024, date of current version 30 October 2024.

Digital Object Identifier 10.1109/ACCESS.2024.3450076

RESEARCH ARTICLE

Copula-Based Reliability Analysis of Vehicles Based on Censored Failures Data Using Reliability Importance Measures

MATEUSZ OSZCZYPAŁA, JAKUB KONWERSKI, JAROSŁAW ZIÓŁKOWSKI, AND JERZY MAŁACHOWSKI

Institute of Mechanics and Computational Engineering, Faculty of Mechanical Engineering, Military University of Technology, 00-908 Warsaw, Poland

Corresponding author: Jarosław Ziółkowski (jaroslaw.ziolkowski@wat.edu.pl)

This work was supported in part by the Military University of Technology under Grant UG B 22-713.

ABSTRACT The reliability of modern vehicles is a current research problem described in many scientific publications. Currently, the literature includes studies on the reliability of vehicles as technical objects, focusing on the one-dimensional domain of the reliability function. However, failures are the result of the wear and aging of the vehicle components, which should be considered in terms of the operation time of operation and the amount of work performed. Therefore, this paper aims to develop a novel two-dimensional copula-based reliability model with respect to vehicle operating time and mileage. The relationship between the two dimensions was determined to be monotonic using Kendall's tau. The vehicle was considered as a series system consisting of seven main subsystems with independent failure processes. The marginal cumulative distribution functions of time and mileage between failures were estimated on the empirical data. The best-fitted approximated marginal distributions were chosen based on the Cramer-von Mises statistics. Weak links in the reliability structure were identified using modified Birnbaum, criticality, and Barlow-Proschan importance measures. The most failing subsystems turned out to be: the engine, transmission system, and electrical installation.

INDEX TERMS Reliability, copula function, component importance, vehicles, series system, censored data.

I. INTRODUCTION

As the automotive industry develops and modern vehicles become more technologically advanced, the importance of ensuring a high level of reliability of their components increases. Reliability tests are conducted during the design and testing of new concepts and during the operation of finished units. Importantly, ensuring real working conditions translates into the credibility of the research carried out [1], [2]. For this reason, operational tests, although expensive, are the best source of information about the product. The results of such research may be useful in determining the maintenance strategy and determining the direction of changes in future modifications. Additionally, vehicle subsystem reliability tests are also important from an economic point of view, as failures and unplanned downtimes can lead to costly repairs and a decrease in the efficiency of the transport system. Therefore, vehicle subsystem reliability tests are extremely important both for manufacturers and users [3], [4].

The segment of vehicles used in the military area deserves special attention. Military vehicles are used not only to drive on public roads but also off-road. For this reason, they require greater attention to certain systems such as suspension, chassis, and steering. The increase in wear on certain elements of these systems translates into their failure rate, which, in turn, negatively affects operational readiness. Therefore, the key aspect in this case is to determine the reliability of the individual vehicle subsystems and then to indicate the appropriate intervals to replace worn parts. The discussion of military vehicle reliability modeling is motivated by the growing need to provide military transport systems with tools for a reliable assessment of the potential of transport means. Additionally,

The associate editor coordinating the review of this manuscript and approving it for publication was Xiao-Sheng Si.

the identification of ''weak links'' of vehicles can be useful in operational prevention, minimizing the risk of costly failures and unscheduled long-term unscheduled downtimes in fleet operations.

The reliability of vehicles can be related to their lifetime and to the distance traveled, called mileage. As the operating time increases, the mileage of the vehicle increases. Thus, some positive monotonic relationship is observed. Furthermore, the operating time determines the aging process of the vehicles, while the amount of work done affects the degradation of their mechanisms. The probabilistic determination of reliability only in relation to one of these dimensions does not fully describe the failure rate of vehicles. For this reason, the implementation of two-dimensional copulas for a probabilistic reliability model was proposed. This study aims to:

1) identify the main vehicle subsystems important for reliability,
2) develop a copula-based reliability model for each subsystem and the entire system,
3) modify the reliability importance measures for the copula-based reliability model,
4) identify the most failing and most reliable subsystems in the vehicle.

The main scientific contribution of this paper is as follows:

1) An innovative model of vehicle reliability as a series system composed of seven subsystems with independent failures was developed,
2) An approach based on Archimedean copulas was proposed to analyze the reliability of vehicle subsystems in the two-dimensional domain of the implementation of a random variable defining the intervals between successive failures,
3) Marginal cumulative distribution functions (cdfs) were determined on the basis of empirical data using the Kaplan-Meier estimator and then approximated by the least squares method as probabilistic distributions of continuous random variables,
4) Cramér-von Mises statistics were used to select the best-fit copula for the empirical data,
5) Reliability importance measures were modified and used to identify ''weak links'' in the series reliability structure of the vehicle based on the copula-based model.

The proposed approach has never been used in previous works on vehicle reliability modeling, which is one of the original achievements of this study. Furthermore, in terms of the development of theoretical knowledge, three main reliability importance measures were modified to evaluate subsystems based on the model using bivariate probabilistic copulas.

The paper is divided into six sections. Section I provides an introduction to the assumptions and the scope of this paper. Section II includes a review of the literature, taking into account the achievements of scientists in the field of vehicle reliability modeling, with reference to the methods of analysis and assessment of the importance of components in the reliability structure of technical systems. Section III presents the assumptions for the model and a description of the approach based on copula theory and reliability importance measures. The main subsystems installed in the vehicle were identified along with its reliability structure. Section IV presents the results of the research and reliability analyzes conducted for the light utility vehicle case study. The discussion of the results obtained, along with a reference to the current state of knowledge in the scientific literature, is presented in Section V. In the last part, conclusions were formulated and directions for further research were indicated.

II. LITERATURE REVIEW

From the perspective of reliability theory, a motor vehicle can be considered a simple technical object or a system composed of subsystems, systems, mechanisms, and components. In the publications [5], [6], light utility vehicles were taken as a case study of research on the reliability of simple objects. Using probabilistic and stochastic methods, as well as artificial neural networks, the authors determined individual and cumulative reliability characteristics. However, it should be noted that the determined probabilistic relationships referred to one-dimensional random variables. Ivanovic [7] presented a different approach, who built the vehicle reliability model as a series system, and then applied the Lagrange multiplier method for the reliability design and the allocation of new vehicles. Lolas and Olatunbosun [8] developed models based on artificial neural networks to predict vehicle reliability based on first inspection information. The preventive maintenance strategy for military trucks was optimized by Barde et al. [9], using reinforcement learning and Monte Carlo simulations. The truck reliability structure was composed of eight heterogeneous components, i.e. tire, transmission, wheel, coupling, motor, brake, steering wheel and shifting gears. Reliability characteristics (time to failure) of individual components were described using Weibull distributions. Due to the complexity of modern cars, many scientists focus only on selected systems when researching them. Popovic et al. [10] performed failure mode and effects analysis (FMEA) and failure mode, effects, and critical analysis (FMECA) for the transmission system. Yi et al. [11] presented research on power shift steering transmission for a heavy military vehicle using the goal-oriented (GO) method, fault tree, and Monte Carlo simulation. In the field of electric vehicles, Shu et al. [12] built a motor controller damage model using the Fault Tree (FT) analysis.

A copula-based approach is used to study the reliability of technical systems with dependent component failures [13]. Fang et al. [14] conducted reliability analysis of systems with correlated degradation processes with Wiener, Gamma and IG marginal distributions. Archimedean copulas (Gumbel, Clayton, Frank, and Joe) were applied to two real-world case studies: LED lamp and polymer material. Gu et al.

[15] implemented Frank, normal, and t copulas to model the reliability of series, parallel, and series-parallel structures with dependent component failures in the time domain. Based on the failure data of the crank and connecting rod mechanism of a diesel engine, the reliability models were estimated using the maximum likelihood estimation method and evaluated using the squared Euclidean distance. In turn, Mahmoudi et al. [16] carried out research on the weighted k-out-of-n systems, in which the random lifetimes of the components are dependent. Using Archimedean copulas and the Marshall-Olkin algorithm, they showed slight differences between the values of the copulas. The results demonstrated that the system reliability increases with increasing dependence on random variables in the reliability model. Increased probability, weight, and component reliability leads to increased system reliability and Birnbaum reliability importance. The effectiveness of Archimedean copulas with appropriate parameter estimation was demonstrated by a study conducted by Yang et al. [17] for constant and time-varying copulas. This is also confirmed by the results obtained by Zheng and Zhang [18] in case studies of a series-parallel system, bridge system, and 13-component system.

In addition, the copula approach is also extremely useful for technical objects whose reliability is affected by interdependent factors. In the case of vehicles, this approach was presented by Wu [19] who proposed the use of asymmetric copulas of two-dimensional random variables to describe the age tail dependence between the pair and usage. Copula-based model determine the vehicle reliability in terms of physical time and the amount of work done. In the case of wind turbine gearbox, Luo et al. [20] developed a reliability model considering the monotonic relationship of wind speed and main shaft rotation speed. Thus, the copula-based reliability model can also be used for systems with independent component failures that are affected by interdependent factors.

Birnbaum used the concept of importance measures for the first time in 1969 [21]. The Birnbaum importance measure (BIM) characterizes the rate of decline in the reliability of the system in relation to the decline in the reliability of the component analyzed. Therefore, an improvement in the reliability of an element of the highest importance causes the greatest increase in the reliability of the system [22]. In reliability engineering, importance measures are used to prioritize weak components (or states) of the system. There are many important measures relating to the reliability, productivity, security, and efficiency of systems. They are widely used as decision support indicators in reliability studies, risk analysis, and maintenance optimization. The literature distinguishes reliability importance measures, lifetime importance measures, and structure importance measures. The reliability importance measures depend on the structure of the system and the reliability of the components over a specific and fixed period of time. The history of developments in the field of reliability importance was discussed by Ku and Zhu [23] and Amrutkar et al. [24]. They discuss their definitions, probabilistic interpretations, properties, computations, and comparability.

Using BIM, Miziula and Navarro [25] investigated the copula representation to propose and study an extension of the classic Birnbaum component importance measure to the case of dependent components. By arranging the dependent components in a given system structure, the performance of the system can be improved. In addition, using Birnbaum's measure of importance, it is possible to calculate both the lifetime dependency ratio of the entire system and the lifetime of a single component or the lifetime of two systems with the same components. However, Dui et al. [26] presented the measures of importance with regard to changing the sequence of components to optimize the structure of the system in its life cycle.

Since the introduction of reliability importance measures by Birnbaum, many new importance measures have been developed. Griffith [27], by generalizing Birnbaum's importance measures, formalized the performance of the system through its expected utility and studied the impact of improving components on its performance. Eryilmaz and Bozbulut [28] extended the Birnbaum method with the Barlow-Proschan importance measure (BPIM) and determined the contribution of the component and the importance of the components in the system. Nguyen et al. [29], utilizing Birnbaum structural importance and Monte Carlo simulation, presented an optimization of the maintenance and inventory strategy. Wu and Coolen [30], introduced a new importance measure based on costs, taking into account the expenses incurred to maintain the system and its components over a finite time frame. While Si et al. [31] proposed an integrated importance measure (IIM) to evaluate the impact of changing components on the system performance. Ramirez-Marquez and Coit [32] presented a composite measure of importance to identify and locate components according to their impact on maintaining the reliability rates of multi-state systems. Dui et al. [33] proposed new importance measures to analyze the degree of impact of external factors on system performance. In [34] the marginal reliability importance measures used to determine the change in system reliability in relation to changes in system reliability of a particular element are discussed. In a recent paper by Dui et al. [35] a multi-criteria measure of validity multi-criteria importance measures (MCIM) was presented to identify the weakest components in complex engineering systems. The correlation between different criteria was also analyzed.

The multi-type component assignment problem (MCAP) was addressed by Qiu et al. [36]. The authors proposed a new mathematical model of two types of components (TCAP), which assumes that a particular position can be assigned to at least one type of component. A two-stage approach containing three assignment strategies and two exchange strategies was proposed to solve the TCAP. Zhu et al. [37], by examining MCAP, proposed a novel algorithm for variance-based analysis of the importance of correlated input variables, which can be used as an effective tool to deal with the analysis of correlated input uncertainties. Chen et al. [38] analyzed the criticality of components with continuous-time degradation. The reliability models for the components are described by the Wiener process model based on degradation data. Six importance measures were proposed to identify critical components and the dependencies between them were indicated. Do and Berenguer [39] examined the levels of information and economic dependencies between components in the system structure and proposed a time-dependent importance measure based on state for multicomponent systems. The reliability-based importance measure can be used as an indicator to make maintenance decisions. In addition, it provides the ability to increase system reliability rates by knowing the current state of all components and minimizing the likelihood of system failures and the costs during task execution.

The present work addresses the modeling of vehicle reliability to identify weak links in the reliability structure. The works published in recent years referred to the failure analysis of vehicles as simple technical objects [40]. In this area, statistical methods have been used to determine reliability in the mileage domain [5] and stochastic methods based on semi-Markov processes in the operating time domain [6]. However, vehicle failures may result from a number of causes, including degradation of cooperating components, which is influenced by the amount of work performed and aging factors acting during operation. Therefore, the present study aims to determine the synergistic influence of multiple factors in the two-dimensional domain of vehicle lifetime and mileage. Furthermore, vehicle reliability structure have usually been limited to selected components in a single system or mechanism, such as the transmission system [10], motor controller in electric vehicles [12], and engine components [41]. The motivation for this study was to fill the methodological gap of developing a vehicle reliability model that can identify the most crucial subsystems from the perspective of their failure rate as a function of the amount of work performed and operational time. The results achieved by Wu [19] indicate the usefulness of the copula function in describing vehicle reliability taking into account age and usage. This approach was extended to analyze subsystems in the vehicle structure. In addition, previous reliability importance measures have been applied to reliability models in the time domain of operation. Thus, in order to identify the weakest links in a vehicle system from a copula-based model, Birnbaum, criticality, and Barlow-Proschan importance measures were adapted to reliability functions with a two-dimensional time and mileage domain. This represents a new approach in the field of reliability engineering.

The copula theory-based probabilistic model is appropriate for analyzing the reliability of technical machinery and systems in terms of operating time and amount of work. The dimensions of random variables that determine the interval of correct operation must have continuous marginal distributions. Reliability importance measures can only be calculated for systems with a precisely defined reliability structure. Furthermore, it is crucial that individual subsystems within the system fail independently of each other. These limitations are the main determinants of the applicability of the developed method.

III. METHODOLOGY AND MODELLING FRAMEWORK

The following assumptions were made in the conducted research:

1) Failures of individual subsystems are independent processes,
2) The vehicle is a technical system with a series reliability structure, therefore failure of any subsystem leads to its unsuitability,
3) The intensity of vehicle usage is defined as the distance traveled expressed in kilometers (km),
4) The failure processes of each subsystem are described by two-dimensional random variables (t_i, l_i) that specify the time and mileage between the successive failures,
5) Dimensions of random variables (t_i, l_i) are dependent,
6) In a situation where the subsystem worked properly from the last failure until the end of the observation of its operation process, the data at this stage are censored,
7) All vehicles in the fleet undergo periodic maintenance following the same schedule.

The assumptions adopted identify the area of vehicle reliability and the applicability of the developed methodology. Assumptions 1 and 2 define the vehicle's technical system in which subsystems fail independently and whose failure leads to the failure of the entire vehicle. The rationality and applicability of this approach were demonstrated by Ivanovic [7] and Barde et al. [9]. Assumptions 3-6 refer to the method of monitoring the condition of vehicle subsystems and indicate the two-dimensional domain of the correct operating resource and the two basic factors that influence the damage process. The relationship between vehicle operating time and mileage results from the technical and organizational conditions of transport fleets. The monotonic relationship between time and usage was demonstrated by Wu [19]. Furthermore, the possibility of right-censored data is the result of the finite observation time of the empirical operation process, which is often encountered in reliability research [5], [42].

Due to the two-dimensionality of the random variable determining the interval between subsequent failures of vehicle subsystems, the use of standard statistical methods and stochastic models based on Markov and semi-Markov processes is inappropriate. Statistical methods are not able to reflect the monotonic relationship between vehicle operating time and mileage. In contrast, Markov/semi-Markov models are only useful in the operating time domain. For this reason, and based on conclusions from research carried out by other authors, an approach based on copula function was proposed.

A. COPULA APPROACH

The copula approach is used to describe the probability of the execution of a multivariate variable or several variables with specific relationships between them [43], [44]. The copula is a multidimensional distribution function and its marginals have uniform distributions throughout the section [0, 1]:

$$C : [0,1]^d \to [0,1], \tag{1}$$

and has the following properties:

1) for all $u, v \in [0, 1]$ the following dependencies occur (2)-(3):

$$C(u,0) = C(0,v) = 0, \tag{2}$$

$$C(u,1) = u \text{ and } C(1,v) = v, \tag{3}$$

2) for all $u_1, u_2, v_1, v_2 \in [0, 1]$ such as $u_1 \leq u_2$ and $v_1 \leq v_2$ the following dependency occurs (4):

$$C(u_2, v_2) - C(u_2, v_1) - C(u_1, v_2) + C(u_1, v_1) \geq 0. \tag{4}$$

According to Sklar's theorem [14], [45], if $X = (X_1, X_2, \ldots, X_d)^T$ is a random vector with continuous marginal cumulative distribution functions (cdfs) $F_1(x_1), F_2(x_2), \ldots, F_d(x_d)$, then there exists a d-dimensional copula $C(\cdot)$:

$$\begin{aligned} C(u_1, u_2, \ldots, u_d) &= C(F_1(x_1), F_2(x_2), \ldots, F_d(x_d)) \\ &= \Pr(X_1 \leq x_1, X_2 \leq x_2, \ldots, X_d \leq x_d), \end{aligned} \tag{5}$$

where $u_j = F_j(x_j)$, $1 \leq j \leq d$, $j \in \aleph$.

By calculating the partial derivative of order n from expression (5) the joint probability density function (pdf) is obtained, which takes the form [46]:

$$\begin{aligned} f(x_1, x_2, \ldots, x_d) &= \frac{\partial^d F(x_1, x_2, \ldots, x_d)}{\partial x_1 \partial x_2 \ldots \partial x_d} \\ &= c(u_1, u_2, \ldots, u_d) \prod_{j=1}^{d} f_j(x_j), \end{aligned} \tag{6}$$

where $c(u_1, u_2, \ldots, u_d)$ is a n-dimensional copula density function and $f_j(x_j)$ is the marginal pdf of x_j.

According to the assumptions adopted, the vehicle operation process is carried out in terms of physical time and the amount of work performed, measured by mileage. For this reason, bivariate Archimedean copulas have been proposed to define the probabilistic model of its reliability. Table 1 presents the functions with parameter ranges θ and the relationships between the parameter θ and Kendall's tau for the Frank, Clayton, and Gumbel copulas [47], [48].

Kendall's tau (τ) is a measure of the monotonic relationship between two random variables, defined as the difference in probabilities:

$$\begin{aligned} \tau = &\Pr\left\{(X_{1i} - X_{1j})(X_{2i} - X_{2j}) > 0\right\} \\ &- \Pr\left\{(X_{1i} - X_{1j})(X_{2i} - X_{2j}) < 0\right\}, \end{aligned} \tag{7}$$

or as the expected value of the signum function [49]:

$$\tau = \mathrm{E}\left\{\mathrm{sign}(X_{1i} - X_{1j})(X_{2i} - X_{2j})\right\}. \tag{8}$$

where (X_1, X_2) is the bivariate random variable and (X_{1i}, X_{2i}), (X_{1j}, X_{2j}) are independent realizations from (X_1, X_2).

There are several estimators of Kendall's tau, and one of the most widely used is estimator (9), which for complete data with n is compatible with the dependency [50], [51]:

$$\hat{\tau} = \binom{n}{2}^{-1} \sum_{1 \leq i \leq j \leq n} a_{ij} b_{ij}. \tag{9}$$

where:

$$a_{ij} = \begin{cases} 1 & \text{if} \quad X_{1i} < X_{1j} \\ -1 & \text{if} \quad X_{1i} > X_{1j}, \end{cases} \tag{10}$$

$$b_{ij} = \begin{cases} 1 & \text{if} \quad X_{2i} < X_{2j} \\ -1 & \text{if} \quad X_{2i} > X_{2j}, \end{cases} \tag{11}$$

or with modification proposed by Kendall [52]:

$$a_{ij} = \begin{cases} 1 & \text{if } X_{1i} < X_{1j} \\ 0 & \text{if } X_{1i} = X_{1j} \\ -1 & \text{if } X_{1i} > X_{1j}, \end{cases} \tag{12}$$

$$b_{ij} = \begin{cases} 1 & \text{if } X_{2i} < X_{2j} \\ 0 & \text{if } X_{2i} = X_{2j} \\ -1 & \text{if } X_{2i} > X_{2j}. \end{cases} \tag{13}$$

If $a_{ij}b_{ij} = 1$ the pair (X_{1i}, X_{2i}), (X_{1j}, X_{2j}) is concordant, whereas if $a_{ij}b_{ij} = -1$ it is considered discordant [50]. Kendall's tau estimator represented by Equations (9), (11) and (13) is valid if all realizations of the two-dimensional variable are uncensored data. Otherwise, the estimator can be used [49], [53], [54]:

$$\hat{\tau}_{cens} = \frac{\sum_{i,j} \tilde{a}_{ij} \tilde{b}_{ij}}{\left(\sum_{i,j} \tilde{a}_{ij}^2 \sum_{i,j} \tilde{b}_{ij}^2\right)^{\frac{1}{2}}}, \tag{14}$$

where:

$$\tilde{a}_{ij} = \begin{cases} 1 & \text{if } T_{1i} > T_{1j} \text{ and } \left(\delta_{1i}, \delta_{1j}\right) = (0,1) \text{ or } (1,1) \\ -1 & \text{if } T_{1i} < T_{1j} \text{ and } \left(\delta_{1i}, \delta_{1j}\right) = (1,0) \text{ or } (1,1) \\ 0 & \text{otherwise}, \end{cases} \tag{15}$$

and

$$\tilde{b}_{ij} = \begin{cases} 1 & \text{if } T_{2i} > T_{2j} \text{ and } \left(\delta_{2i}, \delta_{2j}\right) = (0,1) \text{ or } (1,1) \\ -1 & \text{if } T_{2i} < T_{2j} \text{ and } \left(\delta_{2i}, \delta_{2j}\right) = (1,0) \text{ or } (1,1) \\ 0 & \text{otherwise}, \end{cases} \tag{16}$$

whereby if C_{ij} is the moment of completion of the observation of the stochastic process, then T_{ij} and δ_{ij} can be determined using the appropriate minimum value X_{ij} and C_{ij} and indicator function $\mathbf{1}(\cdot)$ [55]:

$$T_{ij} = \min\left(X_{ij}, C_{ij}\right), \tag{17}$$

TABLE 1. Summary of the adopted bivariate copulas.

Copula	Copula function	Range of θ	Relationship between τ and θ
Frank	$C(u_1,u_2)=-\frac{1}{\theta}\ln\left(1+\frac{(e^{-\theta u_1}-1)(e^{-\theta u_2}-1)}{e^{-\theta}-1}\right)$	$\theta\in(-\infty,0)\cup(0,\infty)$	$\tau=1+\frac{4}{\theta}\left[\left(\int_0^\theta\frac{t}{e^t-1}dt\right)-1\right]$
Clayton	$C(u_1,u_2)=\left[\max\left\{u_1^{-\theta}+u_2^{-\theta}-1,0\right\}\right]^{-\frac{1}{\theta}}$	$\theta\in(-1,0)\cup(0,\infty)$	$\theta=\frac{2\tau}{1-\tau}$
Gumbel	$C(u_1,u_2)=\exp\left(-\left((-\ln u_1)^\theta+(-\ln u_2)^\theta\right)^{\frac{1}{\theta}}\right)$	$\theta\in[1,\infty)$	$\theta=\frac{1}{1-\tau}$

$$\delta_{ij}=\mathbf{1}\left(X_{ij}\leq C_{ij}\right)\quad\text{for } i=1,2 \text{ and } j=1,2,\ldots,d. \tag{18}$$

According to the research performed by Genest et al. [56] the appropriate way to assess the fit of the copula $C_{\theta n}\left(\hat{\mathrm{U}}_i\right)$ to the empirical data is the Cramér-von Mises statistics:

$$S_n=\int_{[0,1]^d}\tilde{C}_n(\mathbf{u})^2dC_n(\mathbf{u})=\sum_{i=1}^{n}\left\{C_n\left(\hat{\mathrm{U}}_i\right)-C_{\theta n}\left(\hat{\mathrm{U}}_i\right)\right\}^2, \tag{19}$$

wherein $C_n(\mathbf{u})$ and $\tilde{C}_n(\mathbf{u})$ fulfill the dependencies (20) and (21) [57], [58]:

$$\begin{aligned}C_n(\mathbf{u})&=\frac{1}{n}\sum_{i=1}^{n}\mathbf{1}\left(\hat{\mathrm{U}}_i\leq\mathbf{u}\right)\\&=\frac{1}{n}\sum_{i=1}^{n}\mathbf{1}\left(U_{i1}\leq u_1,\ldots,U_{id}\leq u_d\right),\mathbf{u}\in[0,\ 1]^d,\end{aligned} \tag{20}$$

$$\tilde{C}_n(\mathbf{u})=\sqrt{n}\left\{C_n(\mathbf{u})-C_{\theta n}(\mathbf{u})\right\},\mathbf{u}\in[0,1]^d, \tag{21}$$

where $\hat{\mathrm{U}}_i$ are empirical observations of the realization of a random variable.

B. MARGINAL DISTRIBUTION

The estimation of the cumulative distribution function of the marginal distribution of random variables t and l is based on empirical damage data obtained from real technical systems. If the observation of the operation process is limited in time and part of the data are censored. For the right-censored data the Kaplan-Meier estimator [59] is used, however, for the interval-censored and left-censored data Turnbull [60] proposed a modification of this estimator. The Kaplan-Meier estimator determines the empirical values of the subsystem unreliability function in the time and mileage domains according to formulas (22) and (23):

$$\hat{F}(t)=1-\prod_{i:t_i\leq t}\left(1-\frac{z_i}{Z_i}\right), \tag{22}$$

$$G(l)=1-\prod_{i:l_i\leq l}\left(1-\frac{z_i}{Z_i}\right), \tag{23}$$

where z_i is the number of objects that failed when the value t_i or l_i was reached, Z_i is the number of objects that worked correctly until the value reached t_i or l_i.

However, the copula function requires continuous probabilistic distributions. To meet this requirement, probabilistic distributions are approximated by determining their parameters based on the estimated values using the non-linear least squares method. This work takes into account four selected parametric probability distributions often used in reliability research to approximate the reliability function $F(t)$ in the time domain and $G(l)$ in the mileage domain:

1) Exponential with rate parameter λ

$$F(t)=1-e^{-\lambda t}\text{ and } G(l)=1-e^{-\lambda l}, \tag{24}$$

2) Weibull with scale parameter α and shape parameter β

$$F(t)=1-e^{-\left(\frac{t}{\alpha}\right)^\beta}\text{ and } G(l)=1-e^{-\left(\frac{l}{\alpha}\right)^\beta}, \tag{25}$$

3) Normal with mean μ and standard deviation σ

$$F(t)=\frac{1}{2}\left[1+\mathrm{erf}\left(\frac{t-\mu}{\sigma\sqrt{2}}\right)\right]\text{ and } G(l)=\frac{1}{2}\left[1+\mathrm{erf}\left(\frac{l-\mu}{\sigma\sqrt{2}}\right)\right], \tag{26}$$

4) Gamma with shape parameter k and scale parameter θ

$$F(t)=\frac{1}{\Gamma(k)}\gamma\left(k,\frac{t}{\theta}\right)\text{ and } G(l)=\frac{1}{\Gamma(k)}\gamma\left(k,\frac{l}{\theta}\right). \tag{27}$$

The reliability functions $R(t)$ and $R(l)$ are the complements of the cdfs $F(t)$ and $G(l)$, respectively, to 1.

C. RELIABILITY MODELING

The reliability of the technical system is characterized by its ability to operate properly under assumed operating conditions. In mathematical terms, the reliability function $R:t\rightarrow[0,1]$ is the probability of the event that the device will work without failure from time 0 to t [61], [62]:

$$R(t)=\Pr(T>t),t\geq 0. \tag{28}$$

Equation (28) applies to the reliability modeling in the time domain. In fact, for a comprehensive analysis of the failure rate of systems, it is appropriate to refer to the probability of failure in a multidimensional domain. The influence of physical and chemical factors, including, above all, the corrosion of metal parts and the loss of elasticity of rubber elements, causes aging wear. In turn, tribological processes are the main cause of the wear of the surface layer. As a result of static and dynamic friction, abrasive, adhesive, and fatigue wear occur. For this reason, it is appropriate to map the damage process in the field of physical time and the amount of work done by the device.

In the series reliability structure, the failure of one subsystem (component) results in the unsuitability transition to the state of the entire technical system [63], [64], [65]. The series system diagram is presented in Fig. 1. It was assumed that the two-dimensional random variable (t_i, l_i) determines the time and mileage between successive failures of this subsystem. The reliability function $R_s(\mathbf{T}, \mathbf{L})$ of the series system with independent subsystem failures is equal to the product of reliability $R_i(t_i, l_i)$ of all its subsystems [66], [67], which is represented by Equation (29):

$$R_s(\mathbf{T}, \mathbf{L}) = \prod_{i=1}^{m} R_i(t_i, l_i),$$
$$\mathbf{T} = \{t_i : 1 \le i \le m\}, \ \mathbf{L} = \{l_i : 1 \le i \le m\}. \quad (29)$$

The sum of the values of the subsystem reliability and unreliability function is equal to 1, therefore, using the relation (30):

$$R_i(t_i, l_i) = 1 - Q_i(t_i, l_i) = 1 - C_i(F_i(t_i), G_i(l_i)), \quad (30)$$

the function $R_s(\mathbf{T}, \mathbf{L})$ can be presented in relation to a copula of a two-dimensional random variable defining the intervals between successive component failures:

$$R_s(\mathbf{T}, \mathbf{L}) = \prod_{i=1}^{m} (1 - C_i(F_i(t_i), G_i(l_i))),$$
$$\mathbf{T} = \{t_i : 1 \le i \le m\}, \ \mathbf{L} = \{l_i : 1 \le i \le m\}. \quad (31)$$

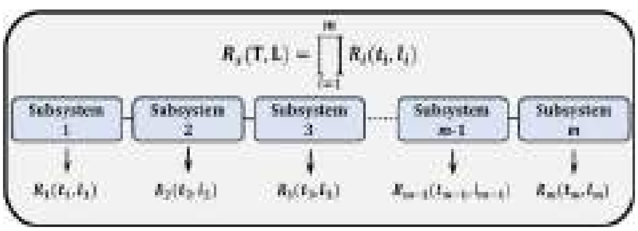

FIGURE 1. Series system of vehicle reliability.

In the analyzes carried out, the vehicle is considered a technical system composed of seven basic subsystems presented in Table 2. Subsystem 1 consists of the engine, together with the cooling system and the fuel supply system. The torque generated as a result of the conversion of chemical energy into mechanical energy is transferred from the engine to the drive system (transmission system), which is identified as Subsystem 2. From the point of view of the proper implementation

TABLE 2. Subsystems of vehicle system reliability.

Subsystem	Description
Subsystem 1	Engine
Subsystem 2	Transmission system
Subsystem 3	Brake system
Subsystem 4	Steering system
Subsystem 5	Suspension
Subsystem 6	Electrical installation
Subsystem 7	Vehicle bodywork

of the basic vehicle functions and the safety of its use, the following subsystems are important: brake system, steering system, suspension system, and electrical system. Maintaining the appropriate properties of the vehicle bodywork is necessary, firstly, to satisfy road traffic regulations, while in the case of military vehicles, the vehicle bodywork also serves as a protective shield for the personnel inside during combat operations.

D. RELIABILITY IMPORTANCE MEASURES

Determining the importance of components in terms of reliability in a technical system is carried out using reliability importance measures. Severity measures are commonly used in technical systems engineering to identify components that significantly influence the reliability and safety behavior. Generally, the importance of a component depends on the value of the reliability function and the location of the component in the reliability structure. In this subsection, the most common reliability measures are presented along with their adaptation to the copula-based approach. At the same time, it was assumed that the validity of the subsystems will be determined for the situation in which $t_i = t_j$ and $l_i = l_j$ for $\forall(i, j) \in \{1, \ldots, m\}$. This means that all subsystems have the same value of the variable (t_i, l_i) at the beginning of the observation of the exploitation process. This is a necessary assumption for simplifying the analysis because its absence implies an infinite number of possible combinations of variable values (t_i, l_i).

The primary measure of the importance of independent components in complex systems is the Birnbaum Importance Measure (BIM). The value of this measure indicates the impact of individual components on the reliability of the entire system. The BIM of the i-th component [21], which is part of a system composed of m components, is defined as follows:

$$I_i^B(t) = \frac{\partial R_s(t)}{\partial R_i(t)}. \quad (32)$$

BIM stands for the value of the loss of system reliability in the event of loss of suitability by the i-th component. However, the disadvantage of this indicator is that it does not take into account the current level of reliability of the components. Therefore, two components may have similar

BIM values, although their actual reliability levels may differ significantly [68].

For a series system, Equation (32) takes the following form:

$$I_i^B(t) = \frac{\partial R_s(t)}{\partial R_i(t)} = \frac{\partial \left(\prod_{j=1}^{m} R_j(t) \right)}{\partial R_i(t)} = \prod_{\substack{j=1 \\ j \neq i}}^{m} R_j(t), \tag{33}$$

where for the reliability function $R_s(\mathbf{T}, \mathbf{L})$ determined by means of two-dimensional copulas in accordance with formula (31), the relationship is as follows:

$$\begin{aligned} I_i^B(t, l) &= \frac{\partial R_s(\mathbf{T}, \mathbf{L})}{\partial R_i(t, l)} = \frac{\partial \left(\prod_{j=1}^{m} R_s(\mathbf{T}, \mathbf{L}) \right)}{\partial R_i(t, l)} \\ &= \prod_{\substack{j=1 \\ j \neq i}}^{m} R_j(t, l) = \prod_{\substack{j=1 \\ j \neq i}}^{m} \left(1 - C_j\left(F_j(t), G_j(l)\right)\right). \end{aligned} \tag{34}$$

An extension of BIM is the criticality importance measure (CIM), which expresses the probability that the i-th component caused damage to the system, knowing that the system was in a state of failure. The i-th component may not be the only damaged component, but with many unsuitable components it is the last damaged component. The CIM takes component failure into account and is expressed by the following formula:

$$I_i^{CR}(t) = I_i^B(t) \frac{Q_i(t)}{Q_S(t)}, \tag{35}$$

where $Q_i(t)$ is a function of the unreliability of the i-th component, and $Q_s(t)$ is a function of the system unreliability.

For a series system, Equation (35) takes the form of Equation (36), as shown at the bottom of the next page. For the reliability function $R_s(\mathbf{T}, \mathbf{L})$ and the unreliability function $Q_s(\mathbf{T}, \mathbf{L})$ determined by means of two-dimensional copulas in accordance with the Equation (31), the relationship takes the form of Equation (37), as shown at the bottom of the next page.

The Barlow-Proschan importance measure (BPIM) is an indicator that describes the probability that the failure of the i-th component occurs simultaneously with the system failure. It is a weighted average of Birnbaum measures, dependent on the unreliability of the i-th component at the moment t, calculated according to the formula [69]:

$$I_i^{BP} = \int_0^\infty I_i^B(t) \cdot q_i(t)\, dt, \tag{38}$$

where $q_i(t)$ is the pdf of the time to failure of i-th component. For a series system, Equation (38) takes the following form:

$$I_i^{BP} = \int_0^\infty I_i^B(t) \cdot q_i(t)\, dt = \int_0^\infty \left(\prod_{\substack{j=1 \\ j \neq i}}^{n} R_j(t) \right) \cdot q_i(t)\, dt, \tag{39}$$

where for the reliability function $R_s(\mathbf{T}, \mathbf{L})$ and the pdf function $q_i(t, l)$ determined by means of two-dimensional copulas according to formula (31), the relationship is according to Equation (40), as shown at the bottom of the next page.

A characteristic feature of BPIM is its independence from the operating time and other variables that determine the amount of work done by the system.

E. DESCRIPTION OF RESEARCH

The reliability modeling framework of the proposed approach based on Archimedean copulas and reliability importance measures applied to vehicles is presented using the flowchart in Fig. 2. The first step is to collect an appropriate database of failures of individual subsystems, on the basis of which the marginal cdfs estimation is made. Then, the approximation is performed with known probabilistic distributions, which are selected on the basis of the determination coefficient R^2. For the development of copulas, Kendall's tau values are needed to calculate the parameter θ. Matching the determined copulas to the empirical values is carried out using Cramer-von Mises statistics. Based on the best matching copulas, a vehicle reliability model is built and analyzed in terms of subsystem reliability measures

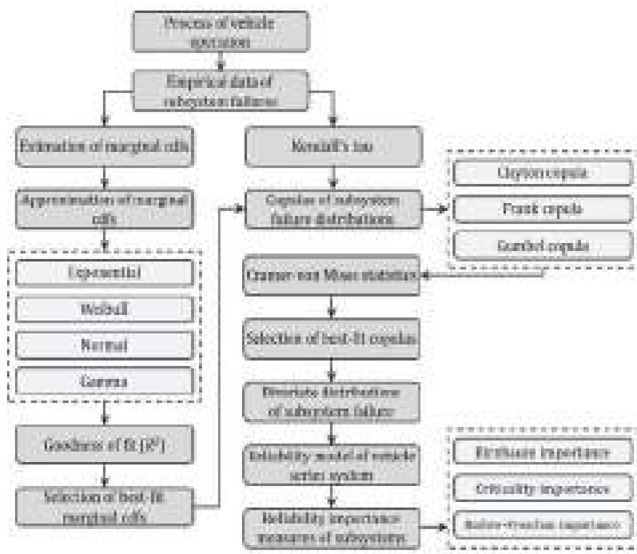

FIGURE 2. Flowchart of the proposed vehicle reliability modeling framework.

IV. RESULTS

This section presents the results of operational tests, measurements, and their analysis in terms of application of the copula theory to develop reliability characteristics and components importance measures. The subject of the research was the Honker 2000 light utility vehicles operated by military transport units. These vehicles are used to transport people and small cargo up to 1,000 kg both on public roads and off-road. Damage data was collected using a set of 55 vehicles operated for a period of five years (01/01/2017 – 12/31/2021). The collected data are under Type I censoring, as an operating process of 5 years was observed, and vehicle subsystems that did not fail during this period or whose last failure did not coincide with the end of the observation period are treated as right-censored data. A total of 575 failure intervals were collected in the two-dimensional time and mileage domain.

A. MARGINAL CDFS ESTIMATION AND APPROXIMATION

Marginal cdfs in the time domain and in the mileage domain are presented in the form of step plots in Fig. 3 and Fig. 4. In both domains, the most defective were: Subsystem 1 (engine with cooling and fuel supply system), Subsystem 2 (transmission system and wheels) and Subsystem 6 (electrical installation). For the remaining subsystems, the range of estimated marginal cdfs values was much narrower because of longer lifetimes, which in a significant percentage were censored observations. Furthermore, it should be noted that the similar shapes of the marginal cdfs for the time and mileage domains confirm the dimension dependence of the random variable measuring the failures of the vehicles studied.

Empirical values of marginal cdfs were used to determine continuous least squares distributions. Using MATLAB software, exponential, Weibull, normal, and gamma distributions were determined. The assessment of the matching with the empirical data was carried out on the basis of the determination coefficient R^2. Table 3 includes the parameter values of individual distributions approximated for each subsystem in terms of Time Between Failures (TBF) and Mileage Between Failures (MBF). For each two-dimensional random variable (t_i, l_i), two distributions were selected to best describe its marginal cdfs (the closest R^2 to 1). In total, seven Weibull distributions, four exponential distributions,

$$I_i^{CR}(t) = I_i^B(t)\frac{Q_i(t)}{Q_s(t)} = \frac{\partial\left(\prod_{j=1}^{m} R_j(t)\right)}{\partial R_i(t)} \cdot \frac{Q_i(t)}{1-\prod_{j=1}^{m} R_j(t)} = \left(\prod_{\substack{j=1 \\ j\neq i}}^{m} R_j(t)\right) \cdot \frac{Q_i(t)}{1-\prod_{j=1}^{m} R_j(t)} \tag{36}$$

$$\begin{aligned} I_i^{CR}(t,l) = I_i^B(t,l)\frac{Q_i(t,l)}{Q_s(\mathbf{T},\mathbf{L})} &= \left(\prod_{\substack{j=1 \\ j\neq i}}^{m} R_j(t,l)\right) \\ \cdot \frac{Q_i(t,l)}{1-\prod_{j=1}^{m} R_j(t,l)} &= \left(\prod_{\substack{j=1 \\ j\neq i}}^{m} \left(1-C_j\left(F_j(t), G_j(l)\right)\right)\right) \cdot \frac{C_i\left(F_i(t), G_i(l)\right)}{1-\prod_{j=1}^{m}\left(1-C_j\left(F_j(t), G_j(l)\right)\right)} \end{aligned} \tag{37}$$

$$\begin{aligned} I_i^{BP} &= \int_0^\infty\int_0^\infty I_i^B(t,l)\cdot q_i(t,l)\,dtdl = \int_0^\infty\int_0^\infty \left(\prod_{\substack{j=1 \\ j\neq i}}^{n} R_j(t,l)\right)\cdot q_i(t,l)\,dtdl \\ &= \int_0^\infty\int_0^\infty \left(\prod_{\substack{j=1 \\ j\neq i}}^{n} \left(1-C_j\left(F_j(t), G_j(l)\right)\right)\right)\cdot c_i\left(F_i(t), G_i(l)\right)\cdot f_i(t)\cdot g_i(l)\,dtdl \end{aligned} \tag{40}$$

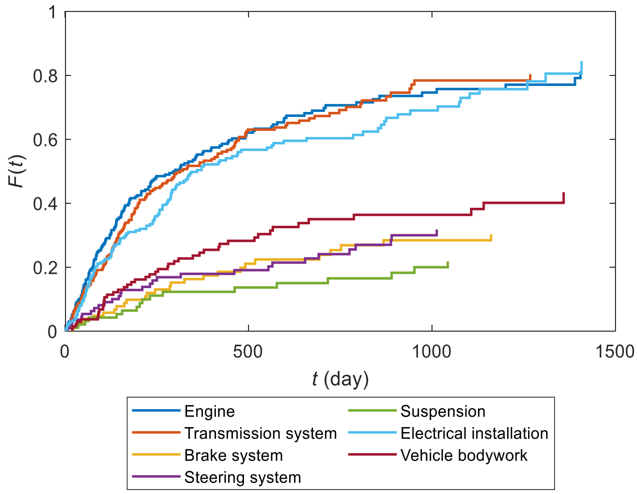

FIGURE 3. The Kaplan-Meier estimation for marginal cdfs of the time dimension.

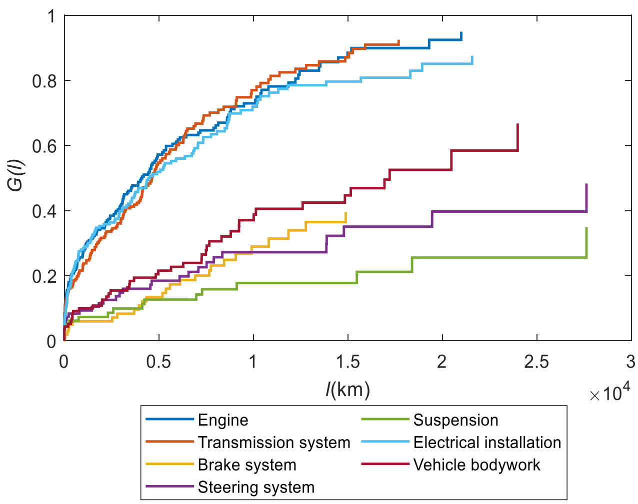

FIGURE 4. The Kaplan-Meier estimation for marginal cdfs of the mileage dimension.

and three gamma distributions were selected. However, none of the marginal distributions of variables t_i and l_i was best matched to the normal distribution. Furthermore, to confirm the applicability of the approximated marginal distributions to describe the reliability of the subsystem, the p-values were calculated using the Kolmogorov-Smirnov test. The p-values obtained for the selected marginal distributions were above the assumed significance level of 0.05.

Based on the approximated marginal cdf, expected values and standard deviations (SD) were determined for all variables t_i and l_i. The calculation results are presented in Table 4. High SD values in relation to the expected values of each variable indicate a strong dispersion of the realization of the random variables defining the failures of vehicle subsystems. In operational practice, this means that it is difficult to precisely estimate the intervals of periodic maintenance and preventive replacement of worn parts with new ones before the damage occurs.

B. COPULAS OF SUBSYSTEM FAILURES

For the empirical damage data, a measure of the monotonic relationship between the two dimensions of the variable (time and mileage) was calculated. Kendall tau values were assigned to each of the vehicle's seven subsystems. The smallest dependencies occurred for engine and transmission system subsystems and amounted to respectively $\tau_1 = 0.5928$ and $\tau_2 = 0.5804$. For the remaining subsystems, the monotonic dependencies are stronger and amount to more than 0.60. Scatter plots and Kendall's tau for all subsystems are presented in Fig. 5. High levels of dependence between time and mileage of the implementation of random variables describing vehicle damage confirm the validity of using copulas for modeling reliability.

Based on the developed marginal distributions (marginal cdfs) of two-dimensional random variables as presented in Table 3, and monotonic dependencies, calculated as Kendall's tau, three Archimedean copulas were determined for all subsystems. Assessment of the fit of the copulas to the empirical data was carried out using the Cramér-von Mises statistics. The calculation results are presented in Table 5. The smaller the statistics value S_n the better the copula is matched to the empirical distribution function of a two-dimensional variable. Clayton copulas are the best match for all vehicle subsystems.

Table 6 presents the marginal cdfs and the parameter values θ of the Clayton copulas for the seven vehicle subsystems. The Clayton copulas are probabilistic reliability models for the two-dimensional domain of vehicle operation.

C. RELIABILITY OF SUBSYSTEMS

The reliability functions $R_i(t_i, l_i)$ of the individual subsystems were determined using the Eq. (30), based on the best matching copulas. Fig. 6 presents the waveforms of the functions $R_i(t_i, l_i)$ using counter plots in the time range $t_i \in [0, 2 \times 10^3]$ (day) and mileage $l_i \in [0, 3 \times 10^4]$ (km). The analyzed ranges fully cover the domains of known marginal cdfs values of all subsystems. The developed graphs are a graphical representation of the probability of correct operation of the subsystem for a two-dimensional variable that specifies the physical time and mileage of the vehicle since the last failure of the subsystem. The fastest decrease in the value of the reliability function in the analyzed range occurs to Subsystem 1 - engine, Subsystem 2 - transmission system, and Subsystem 6 - electrical system. On the other hand, Suspension 5, Suspension, is has a high level of reliability, reaching for $t_5 = 2 \times 10^3$ (day) and $l_5 = 3 \times 10^4$ (km) the value of $R_5(t_5, l_5) = 0.7396$.

D. RELIABILITY OF VEHICLE

The reliability of the vehicle within the meaning of the assumptions adopted in the study is the reliability of a series system consisting of seven main subsystems. Knowing the mathematical relationships that describe the reliability

TABLE 3. Marginal cdfs of time between failures and mileage between failures.

Subsystem	Distribution	Dimension: Time (day) Parameters	Time R^2	Time p-value	Mileage (km) Parameters	Mileage R^2	Mileage p-value
Engine	Exponential	$\lambda = 2.319\times10^{-3}$	0.9206	0.3084	$\lambda = 1.758\times10^{-4}$	0.8634	0.0014
	Weibull	$\alpha = 575.6, \beta = 0.7381$	0.9710	0.3854	$\alpha = 7.285\times10^{3}, \beta = 0.7061$	0.9435	0.0481
	Normal	$\mu = 517.6, \sigma = 514.3$	0.7034	0.0002	$\mu = 6.779\times10^{3}, \sigma = 6.361\times10^{3}$	0.7720	0.0003
	Gamma	$k = 0.6904, \theta = 932.9$	0.9505	0.1881	$k = 0.6204, \theta = 1.348\times10^{4}$	0.9450	0.0661
Transmission system	Exponential	$\lambda = 2.081\times10^{-3}$	0.9601	0.7787	$\lambda = 1.611\times10^{-4}$	0.9365	0.0116
	Weibull	$\alpha = 597.4, \beta = 0.8043$	0.9782	0.6801	$\alpha = 7.318\times10^{3}, \beta = 0.7468$	0.9594	0.0896
	Normal	$\mu = 518.8, \sigma = 481.3$	0.7563	0.0012	$\mu = 6.537\times10^{3}, \sigma = 5721$	0.8408	0.0116
	Gamma	$k = 0.7752, \theta = 821.9$	0.9660	0.3944	$k = 0.6570, \theta = 1.241\times10^{4}$	0.9646	0.1196
Brake system	Exponential	$\lambda = 4.264\times10^{-4}$	0.9083	0.9357	$\lambda = 3.372\times10^{-5}$	0.9782	0.7537
	Weibull	$\alpha = 6324, \beta = 0.6687$	0.8946	0.7537	$\alpha = 7.196\times10^{4}, \beta = 0.6323$	0.8985	0.9357
	Normal	$\mu = 2.05\times10^{3}, \sigma = 1.328\times10^{3}$	0.5244	0.0996	$\mu = 2.654\times10^{4}, \sigma = 1.794\times10^{4}$	0.5808	0.3290
	Gamma	$k = 0.6425, \theta = 9.657\times10^{3}$	0.8702	0.7537	$k = 0.5904, \theta = 1.237\times10^{5}$	0.8963	0.9357
Steering system	Exponential	$\lambda = 4.331\times10^{-4}$	0.8328	0.3929	$\lambda = 3.082\times10^{-5}$	0.8079	0.2053
	Weibull	$\alpha = 6.873\times10^{3}, \beta = 0.5941$	0.9516	0.9578	$\alpha = 9.420\times10^{4}, \beta = 0.5562$	0.9205	0.5494
	Normal	$\mu = 1.898\times10^{3}, \sigma = 1.258\times10^{3}$	0.6400	0.2391	$\mu = 2.525\times10^{4}, \sigma = 1.653\times10^{4}$	0.7117	0.1110
	Gamma	$k = 0.5601, \theta = 1.220\times10^{4}$	0.9374	0.8080	$k = 0.5169, \theta = 1.809\times10^{5}$	0.9243	0.5494
Suspension	Exponential	$\lambda = 2.668\times10^{-4}$	0.8169	0.5026	$\lambda = 1.769\times10^{-5}$	0.7673	0.3433
	Weibull	$\alpha = 1.347\times10^{4}, \beta = 0.6272$	0.8963	0.7810	$\alpha = 1.199\times10^{5}, \beta = 0.8293$	0.5502	0.1549
	Normal	$\mu = 2.612\times10^{3}, \sigma = 1534$	0.5633	0.2754	$\mu = 3.874\times10^{4}, \sigma = 2.082\times10^{4}$	0.4240	0.0590
	Gamma	$k = 0.6042, \theta = 2.084\times10^{4}$	0.8801	0.7810	$k = 0.8139, \theta = 1.433\times10^{5}$	0.5467	0.1549
Electrical installation	Exponential	$\lambda = 1.712\times10^{-3}$	0.9371	0.6866	$\lambda = 1.565\times10^{-4}$	0.8270	0.0004
	Weibull	$\alpha = 705.1, \beta = 0.7952$	0.9792	0.4727	$\alpha = 8.478\times10^{3}, \beta = 0.6281$	0.9595	0.2665
	Normal	$\mu = 589.8, \sigma = 519.1$	0.7714	0.0005	$\mu = 7.890\times10^{3}, \sigma = 7.823\times10^{3}$	0.7432	0.0016
	Gamma	$k = 0.7558, \theta = 997.6$	0.9702	0.3786	$k = 0.5452, \theta = 1.9\times10^{4}$	0.9550	0.2665
Vehicle bodywork	Exponential	$\lambda = 6.365\times10^{-4}$	0.8531	0.8345	$\lambda = 4.577\times10^{-5}$	0.9545	0.2924
	Weibull	$\alpha = 2.778\times10^{3}, \beta = 0.7321$	0.9250	0.8345	$\alpha = 2.912\times10^{4}, \beta = 0.8533$	0.9396	0.4355
	Normal	$\mu = 1373, \sigma = 975.1$	0.6331	0.0503	$\mu = 1.781\times10^{4}, \sigma = 1.1\times10^{4}$	0.8002	0.1123
	Gamma	$k = 0.7073, \theta = 3.970\times10^{3}$	0.9034	0.6669	$k = 0.8157, \theta = 3.657\times10^{4}$	0.9404	0.4355

functions $R_i(t_i, l_i)$ for the subsystems, it is possible to define the vehicle reliability function $R_s(\mathbf{T}, \mathbf{L})$ as the product of the values $R_i(t_i, l_i)$ according to formula (29). Fig. 7 presents in a graphic form the function $R_s(\mathbf{T}, \mathbf{L})$ in time ranges $t_i \in [0, 5 \times 10^2]$ (day) and mileage $l_i \in [0, 5 \times 10^3]$ (km). The calculations were performed assuming that all elements of the time vector since the last failure $\mathbf{T}$ and the mileage vector since the last failure $\mathbf{L}$ are equal. This is justified from the point of view of reliability analysis of a new or completely overhauled vehicle. However, in the operating practice of the vehicle in use, there are different values of t_i and l_i. For this reason, determining the likelihood of correct operation should be performed individually for each vehicle on the basis of mathematical relationships.

E. RELIABILITY IMPORTANCE MEASURES FOR VEHICLES

Tables 7 and 8 present the results of the subsystem importance analysis for the reliability of the vehicle's system structure. The calculations were carried out for 35 points of the two-dimensional domain of time and mileage, respectively, for the values of 100, 200, 300, 400, 500 (day) and 1000, 2000, 3000, 4000, 5000, 10,000, 20,000 (km). As the value of any dimension of the random variable (t_i, l_i) increases, the BIM decreases, which is related to the monotonicity of the reliability function $R_i(t_i, l_i)$ and $R_s(\mathbf{T}, \mathbf{L})$.

Using BIM and CIM measures, it is possible to prioritize subsystems in order of importance for vehicle reliability. For the case study, the classification according to BIM and CIM was the same in all 35 measurement points, as evidenced

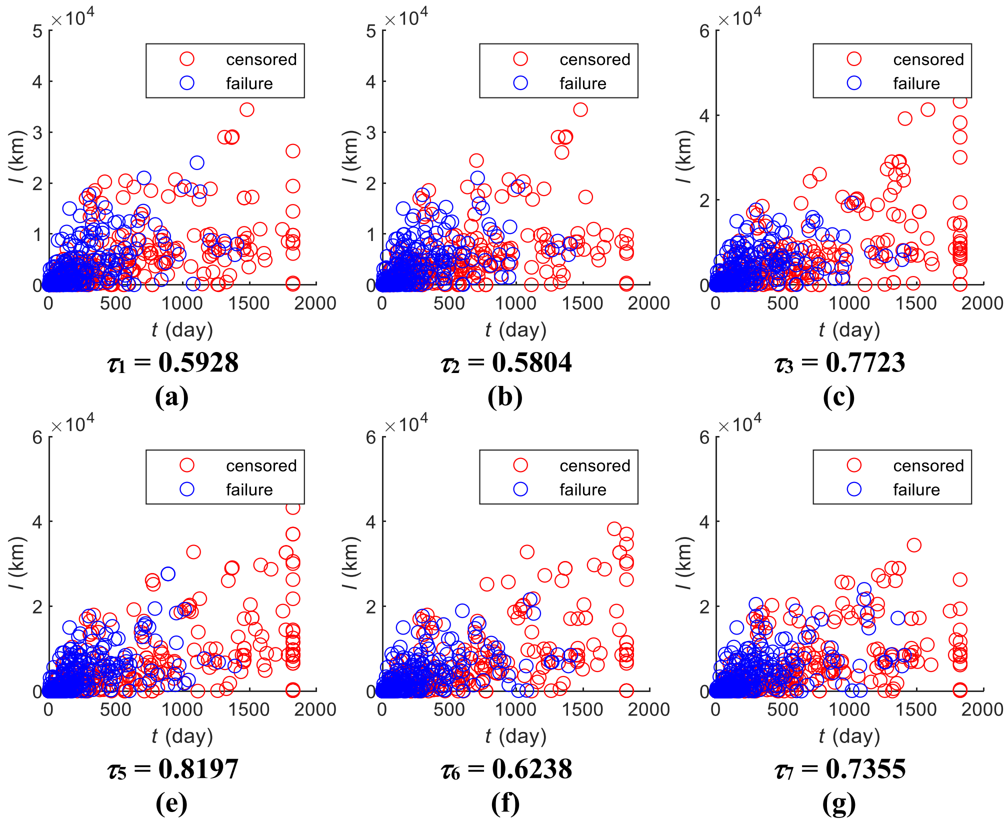

FIGURE 5. Scatter plots and Kendall's tau of measured bivariate failures data: (a) – engine, (b) – transmission system, (c) – brake system, (d) – steering system, (e) – suspension, (f) – electrical installation, (g) – vehicle bodywork.

TABLE 4. Expected values and standard deviations of time and mileage between failures of the subsystems.

Subsystem	Time (day)		Mileage (km)	
	Expected value	SD	Expected value	SD
Engine	694.58	682.04	8362.99	10 617.59
Transmission system	674.28	646.63	8153.37	10 058.99
Brake system	2345.22	2345.22	29 655.99	29 655.99
Steering system	10 476.24	9942.85	93 507.21	130 059.43
Suspension	19 176.19	18 611.53	56 529.11	56 529.11
Electrical installation	802.35	772.71	12 048.86	11 699.42
Vehicle bodywork	3375.86	3319.02	21 848.37	21 848.37

TABLE 5. Cramér-von mises statistics results for archimedean copulas.

Subsystem	Clayton	Frank	Gumbel
Engine	2.2284	5.4211	2.2675
Transmission system	1.8166	4.7568	1.8807
Brake system	0.4844	1.2213	0.5750
Steering system	0.5490	1.3350	0.6501
Suspension	0.4555	0.7811	0.4842
Electrical installation	1.9999	5.2025	2.0957
Vehicle bodywork	0.9331	2.2488	1.0820

by the value of the Spearman-rho rank correlation coefficient equal to 1. Thus, both measures of the importance of reliability yielded convergent results. On this basis, the most important subsystems in terms of reliability were determined, which achieved the highest BIM and CIM values for a given point in the two-dimensional domain of the reliability function.

The results are presented in Fig. 8. For 29 points, the most important subsystem turned out to be Subsystem 1 (engine). In turn, for the remaining 6 points, Subsystem 6 (electrical installation) had the most negative impact on vehicle reliability. It is worth highlighting that the electrical system is the most important for low mileage values at increasing values of operation time. The reason for this is the characteristics of aging processes in which non-tribological factors, such as chemical and electrochemical corrosion, play a significant role. On the other hand, the reduction in engine reliability occurs more significantly for the increasing vehicle mileage.

Fig. 9 shows the subsystems with the lowest BIM and CIM values, which correspond to the least important components of the technical system. For 30 measurement points, Subsystem 5 (suspension) turned out to be the most reliable, while

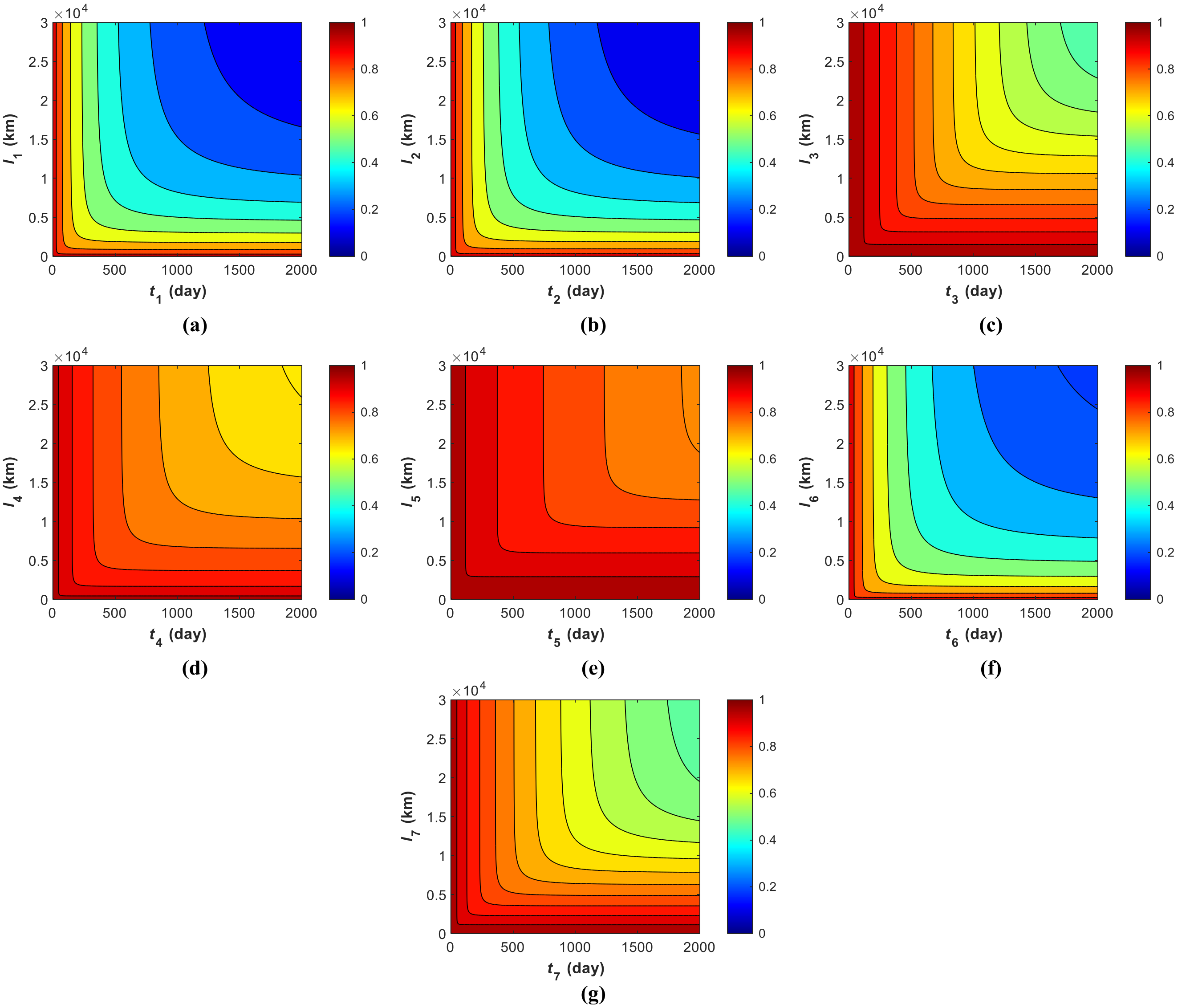

FIGURE 6. Two-dimensional reliability function of: (a) – engine, (b) – transmission system, (c) – brake system, (d) – steering system, (e) – suspension, (f) – electrical installation, (g) – vehicle bodywork.

TABLE 6. Marginal distributions and parameters for clayton copulas.

Subsystem	Marginal cdfs		Copula parameter (θ)
	Time (day)	Mileage (km)	
Engine	Weibull	Gamma	2.2675
Transmission system	Weibull	Gamma	1.8807
Brake system	Exponential	Exponential	0.5750
Steering system	Weibull	Gamma	0.6501
Suspension	Weibull	Exponential	0.4842
Electrical installation	Weibull	Weibull	2.0957
Vehicle bodywork	Weibull	Exponential	1.0820

for the remaining 5 points, Subsystem 3 (brake system) was the most reliable.

The BIM and CIM indicators determine the importance of a component for specific values of time and mileage, and therefore do not clearly indicate the ''weakest links'' in the reliability structure for the entire domain of reliability functions. For this reason, the BPIM measures were calculated to identify the subsystems that most significantly increase the unreliability of the light utility vehicle. The results of the calculations are presented in Fig. 10. The highest BPIM value was obtained for engine. Next in terms of reliability priority were transmission system and electrical installation with BPIM values relatively lower (by 5.68% and 8.91% respectively) compared to the engine. The impact of the remaining subsystems on the vehicle reliability can be described as insignificant, due to their BPIM values in the range of 0.04 – 0.10. It should be noted, however, that the presented considerations refer to the situation in which the times

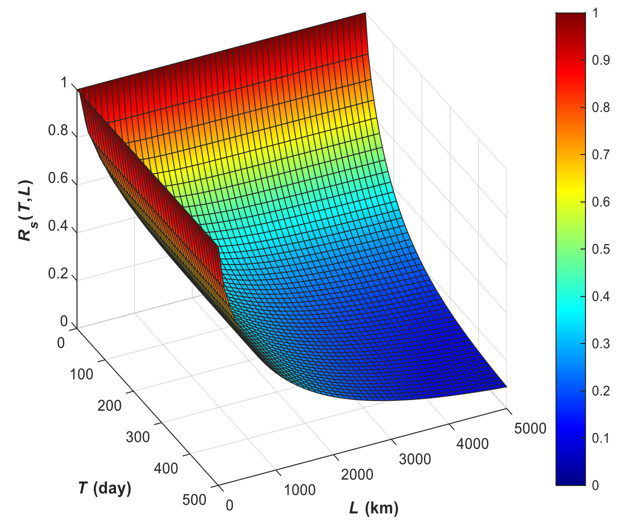

FIGURE 7. Vehicle two-dimensional reliability function.

T (day) \ L (km)	1000	2000	3000	4000	5000	10 000	20 000
500	6	6	1	1	1	1	1
400	6	6	1	1	1	1	1
300	6	1	1	1	1	1	1
200	6	1	1	1	1	1	1
100	1	1	1	1	1	1	1

FIGURE 8. Subsystems with the highest BIM and CIM values (1 – engine, 6 – electrical installation).

T (day) \ L (km)	1000	2000	3000	4000	5000	10 000	20 000
500	5	5	5	5	5	5	5
400	5	5	5	5	5	5	5
300	5	5	5	5	5	5	5
200	5	5	5	5	5	5	5
100	5	5	3	3	3	3	3

FIGURE 9. Subsystems with the lowest BIM and CIM values (3 – brake system, 5 – suspension).

and mileages since the last failure for all subsystems are equal.

V. DISCUSSION

The copula-based approach allows modeling the reliability of systems with dependent component failures or systems with independent failures in a multidimensional failure rate domain with monotonically dependent dimensions. For the analyzed case study of light utility vehicles, a model based

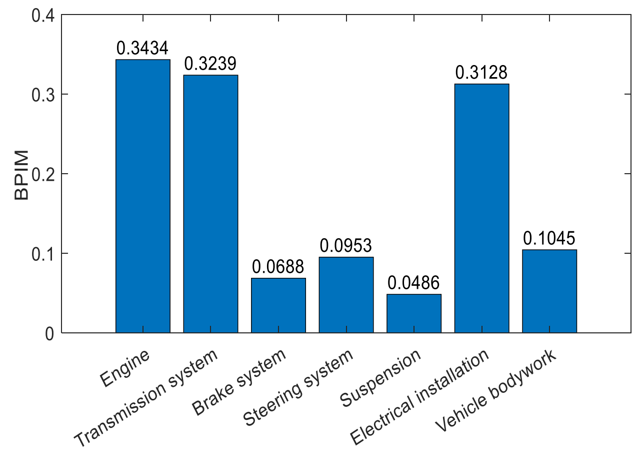

FIGURE 10. BPIM values for the vehicle subsystems.

on the Clayton copula in the series reliability structure of the technical system was developed. The identification of the elements of the structure was carried out at the level of seven basic subsystems of the vehicle. Detailing the structure to the level of mechanisms and individual components is possible mainly for theoretical considerations. For practical reliability analysis, it may be difficult to apply for two reasons. First, collecting an appropriate empirical database on damage to each mechanism or its components requires a large number of vehicles for testing and a long period of observation of the operation process. However, conducting laboratory tests for such a number of vehicles would generate high costs, disproportionate to the results obtained. The second aspect is the computational complexity of an overly detailed model, which would require a large computational power. For this reason, it should be noted that the proposed approach is a compromise between the accuracy of mapping the reliability of the vehicle and its subsystems and the time (and costs) of operational tests and the need for advanced computational support (dedicated computer software). Reliability modeling based on operational tests is a reliable source of information about a given facility or technical system. Conducting this type of research often requires large financial and technical expenditures, and the observation of the empirical exploitation process is relatively time-consuming, which is a certain limitation of the proposed approach. The difficulty in implementing two-dimensional copulas and the reliability importance measures calculated on their basis lies in the computational complexity of the developed method, especially for systems composed of many components (subsystems). In addition, the term marginal cdfs implies the need to collect a large amount of empirical data on damage. For this reason, the research presented in this article was carried out at the level of vehicle subsystems. Determining the reliability characteristics at the level of systems, mechanisms, or individual parts would require a significant increase in the size of the research sample and extending the period of operational testing.

TABLE 7. Results of BIM.

Subsystem	Time (day)	Birnbaum importance measure						
		Mileage (km)						
		1000	2000	3000	4000	5000	10 000	20 000
Engine	100	0.5891	0.5222	0.5044	0.4997	0.4976	0.4947	0.4937
	200	0.5371	0.4092	0.3535	0.3295	0.3189	0.3054	0.3010
	300	0.5243	0.3741	0.2966	0.2544	0.2322	0.2038	0.1951
	400	0.5195	0.3593	0.2722	0.2202	0.1887	0.1443	0.1317
	500	0.5171	0.3517	0.2595	0.2026	0.1660	0.1075	0.0918
Transmission system	100	0.5773	0.5077	0.4886	0.4831	0.4807	0.4770	0.4757
	200	0.5288	0.4003	0.3439	0.3193	0.3082	0.2935	0.2885
	300	0.5168	0.3674	0.2902	0.2481	0.2257	0.1966	0.1872
	400	0.5123	0.3536	0.2674	0.2158	0.1845	0.1401	0.1270
	500	0.5101	0.3466	0.2555	0.1993	0.1631	0.1051	0.0892
Brake system	100	0.4996	0.4284	0.4077	0.4011	0.3980	0.3933	0.3917
	200	0.4428	0.3180	0.2661	0.2420	0.2305	0.2139	0.2082
	300	0.4288	0.2825	0.2148	0.1791	0.1593	0.1306	0.1210
	400	0.4235	0.2675	0.1918	0.1499	0.1252	0.0868	0.0746
	500	0.4209	0.2598	0.1797	0.1344	0.1069	0.0619	0.0482
Steering system	100	0.5197	0.4448	0.4235	0.4168	0.4136	0.4086	0.4070
	200	0.4633	0.3314	0.2757	0.2508	0.2390	0.2219	0.2161
	300	0.4489	0.2959	0.2227	0.1840	0.1633	0.1341	0.1244
	400	0.4434	0.2805	0.1996	0.1541	0.1273	0.0879	0.0756
	500	0.4407	0.2726	0.1873	0.1385	0.1086	0.0616	0.0480
Suspension	100	0.4921	0.4253	0.4086	0.4025	0.3994	0.3947	0.3931
	200	0.4358	0.3086	0.2585	0.2375	0.2271	0.2109	0.2053
	300	0.4220	0.2737	0.2054	0.1708	0.1528	0.1259	0.1167
	400	0.4167	0.2590	0.1829	0.1412	0.1173	0.0817	0.0702
	500	0.4142	0.2516	0.1713	0.1262	0.0992	0.0568	0.0442
Electrical installation	100	0.5808	0.5023	0.4802	0.4734	0.4702	0.4653	0.4636
	200	0.5411	0.4022	0.3402	0.3125	0.2997	0.2815	0.2753
	300	0.5316	0.3733	0.2900	0.2443	0.2198	0.1863	0.1753
	400	0.5278	0.3612	0.2690	0.2137	0.1802	0.1314	0.1167
	500	0.5259	0.3549	0.2579	0.1980	0.1597	0.0978	0.0803
Vehicle bodywork	100	0.5060	0.4442	0.4259	0.4195	0.4163	0.4114	0.4097
	200	0.4482	0.3260	0.2775	0.2554	0.2442	0.2272	0.2212
	300	0.4340	0.2894	0.2226	0.1877	0.1686	0.1397	0.1295
	400	0.4286	0.2740	0.1987	0.1568	0.1319	0.0930	0.0801
	500	0.4260	0.2661	0.1862	0.1407	0.1127	0.0662	0.0517

Comparing the results obtained with previous research [5], [6], it is worth mentioning that the developed copula-based model determines the reliability of the vehicle in terms of physical time and vehicle mileage. On this basis, it is possible to determine the probability of failure of each subsystem for variable intensity of vehicle use. This information can be used to determine the appropriate intervals between subsequent periodic maintenance or to move from a periodic maintenance strategy to a much more economically effective proactive maintenance strategy [70], [71], [72] and condition-based maintenance [73], [74], [75]. Referring to the current state of the scientific literature, which covers the area of vehicle reliability research, it should be emphasized that the proposed approach is an innovative solution to the problem of identifying critical components in the two-dimensional domain of reliability functions.

Analysis of the reliability importance of the subsystems included in the light utility vehicle indicated the potentially weakest links of the structure that have the greatest impact on reducing the level of reliability. However, it should be noted that the most significant and least significant subsystems identified using BIM and CIM, in accordance with the adopted assumptions, refer to a situation where the times and mileage since the last failure are the same for each subsystem. However, in real operating conditions, this assumption is usually met only by a new technical object or a completely overhauled one. Therefore, the developed reliability model, based on Clayton copulas, should be applied individually to each operated vehicle, predicting the failure rate of its subsystems based on individual and current values of the time and mileage vectors $\mathbf{T} = \{t_i: 1 \leq i \leq m\}, \mathbf{L} = \{l_i: 1 \leq i \leq m\}$. BIM and CIM indicators are useful for monitoring and maintaining

TABLE 8. Results of CIM.

Subsystem	Time (day)	Criticality importance measure						
		Mileage (km)						
		1000	2000	3000	4000	5000	10 000	20 000
Engine	100	0.2044	0.1894	0.1866	0.1873	0.1879	0.1890	0.1894
	200	0.1906	0.1586	0.1434	0.1377	0.1360	0.1357	0.1358
	300	0.1874	0.1494	0.1265	0.1132	0.1066	0.1005	0.0992
	400	0.1863	0.1457	0.1195	0.1020	0.0909	0.0767	0.0734
	500	0.1858	0.1438	0.1159	0.0964	0.0827	0.0605	0.0550
Transmission system	100	0.1817	0.1647	0.1606	0.1604	0.1604	0.1607	0.1607
	200	0.1760	0.1458	0.1307	0.1245	0.1225	0.1208	0.1203
	300	0.1746	0.1403	0.1185	0.1057	0.0991	0.0923	0.0904
	400	0.1742	0.1381	0.1136	0.0969	0.0863	0.0721	0.0684
	500	0.1740	0.1370	0.1111	0.0926	0.0796	0.0579	0.0523
Brake system	100	0.0312	0.0301	0.0279	0.0272	0.0269	0.0263	0.0262
	200	0.0257	0.0287	0.0276	0.0253	0.0239	0.0218	0.0210
	300	0.0243	0.0250	0.0249	0.0236	0.0217	0.0177	0.0163
	400	0.0238	0.0233	0.0222	0.0211	0.0197	0.0147	0.0125
	500	0.0235	0.0224	0.0206	0.0191	0.0177	0.0124	0.0096
Steering system	100	0.0702	0.0579	0.0539	0.0526	0.0520	0.0510	0.0507
	200	0.0616	0.0478	0.0403	0.0365	0.0346	0.0318	0.0307
	300	0.0587	0.0431	0.0347	0.0295	0.0265	0.0218	0.0201
	400	0.0575	0.0406	0.0316	0.0259	0.0221	0.0158	0.0136
	500	0.0569	0.0393	0.0297	0.0237	0.0196	0.0121	0.0095
Suspension	100	0.0167	0.0248	0.0294	0.0294	0.0291	0.0286	0.0284
	200	0.0134	0.0153	0.0176	0.0194	0.0195	0.0181	0.0175
	300	0.0126	0.0129	0.0132	0.0137	0.0142	0.0125	0.0115
	400	0.0124	0.0120	0.0114	0.0111	0.0110	0.0092	0.0078
	500	0.0122	0.0116	0.0106	0.0098	0.0092	0.0071	0.0055
Electrical installation	100	0.1885	0.1556	0.1470	0.1446	0.1435	0.1419	0.1414
	200	0.1976	0.1486	0.1258	0.1159	0.1116	0.1059	0.1040
	300	0.1998	0.1484	0.1182	0.1012	0.0922	0.0806	0.0770
	400	0.2004	0.1482	0.1155	0.0945	0.0814	0.0628	0.0574
	500	0.2006	0.1480	0.1140	0.0912	0.0757	0.0502	0.0431
Vehicle bodywork	100	0.0436	0.0570	0.0578	0.0570	0.0565	0.0554	0.0551
	200	0.0350	0.0400	0.0427	0.0424	0.0413	0.0383	0.0371
	300	0.0332	0.0343	0.0345	0.0339	0.0326	0.0280	0.0258
	400	0.0325	0.0319	0.0305	0.0290	0.0273	0.0214	0.0184
	500	0.0321	0.0307	0.0284	0.0262	0.0240	0.0170	0.0133

vehicle components. The most critical subsystems should be constantly monitored, and maintenance must be performed at key points to ensure vehicle reliability. Subsystems with the highest BIM and CIM values have the greatest impact on vehicle failure rate, and therefore it is necessary to focus on determining the appropriate intervals between periodic maintenance and replacement of worn elements with new ones before damage occurs.

The use of BPIM made it possible to determine the reliability importance of subsystems in the structure of light utility vehicles for the entire area of the time and mileage domain. In the case of the Honker 2000 vehicle, the key subsystems are the engine, transmission system, and electrical system. Furthermore, the analysis of reliability importance can be the basis for determining the direction to introduce improvements and modifications to newly produced vehicles, which are modernized versions of the facilities currently operated. The BPIM indicator identifies subsystems that should be improved during the design process for upgraded versions of vehicles.

VI. CONCLUSION AND FUTURE WORKS

In conclusion, this paper proposes a copula-based approach to modeling vehicle reliability. The vehicle has been described as a series reliability structure composed of seven essential subsystems. Failures of these subsystems are independent stochastic processes described in the two-dimensional domain of time and mileage. The intensity of operation measured by the mileage affects the damage resulting from the processes of tribological wear, while the operating time is a factor that generates damage in the form of physical aging and corrosion. Vehicle mileage increases with time of use, and the monotonic relationship of these two values was determined using Kendall tau. Three Archimedean copulas were considered, the matching of which to empirical data was determined using the Cramer-von Mises statistics. It was found that for each subsystem, the most accurate reliability model is the Clayton copula.

The importance of reliability was determined using BIM, CIM, and BPIM based on the reliability function of the series system. The BIM and CIM indicators have been defined based on selected pairs of time and mileage values. For all points analyzed in the two-dimensional domain, the reliability hierarchy of the subsystem was the same, determined on the basis of the Spearman rank correlation coefficient equal to 1. The most failing subsystems according to BIM and CIM were the engine and electrical installation, and the most reliable were the brake system and suspension. The BPIM indicator determines the importance of a component not only for a selected argument but for the entire domain of the reliability function. The results obtained are convergent and indicate that the engine, transmission system, and electrical installation are the subsystems that have the greatest impact on reducing vehicle reliability.

The proposed approach to vehicle reliability modeling is a useful tool for identifying the ''weak links''. Determining the importance of the system components can be a valuable guide in planning and optimizing service intervals related to specific components of the reliability structure. Such a solution may bring benefits in the form of a reduction in the system failure rate and a reduction in costs. In addition, it should be emphasized that in the case of vehicles, the two-dimensional copula-based reliability function is a more reliable description of the probability of correct operation.

As a subject for further research, the implementation of the proposed approach to vehicle reliability modeling and the identification of the ''weak links'' at the level of mechanisms and individual components should be considered. The implementation of such research requires the collection of a database from a long period of observation of the empirical exploitation process and a very large research sample. In addition, an increase in the number of independent components in the system implies an increase in computational complexity, especially in the case of determining the BPIM value.

CREDIT AUTHORSHIP CONTRIBUTION STATEMENT

Mateusz Oszczypała: Conceptualization, methodology, software, validation, formal analysis, investigation, resources, data curation, writing—original draft preparation, writing—review and editing, and visualization.

Jakub Konwerski: Resources, data curation, writing—original draft preparation, and writing—review and editing.

Jarosław Ziółkowski: Formal analysis, writing—review and editing, supervision, and project administration.

Jerzy Małachowski: Formal analysis, writing—review and editing, project administration, and funding acquisition.

REFERENCES

[1] X. Wu and H. Li, ''The reliability work in fuel cell vehicle's road test,'' in *Proc. IEEE Int. Conf. Veh. Electron. Saf.*, Dec. 2006, pp. 481–484, doi: 10.1109/ICVES.2006.371639.

[2] X. Zhao, V. Robu, D. Flynn, K. Salako, and L. Strigini, ''Assessing the safety and reliability of autonomous vehicles from road testing,'' in *Proc. IEEE 30th Int. Symp. Softw. Rel. Eng. (ISSRE)*, Oct. 2019, pp. 13–23, doi: 10.1109/ISSRE.2019.00012.

[3] A. Tajibaev, B. Ibragimov, S. Narziev, and M. Alimov, ''The economic aspect of the reliability of vehicles,'' Presented at the 3rd Int. Sci. Conf. Construct. Mech., Hydraul. Water Resour. Eng., Tashkent, Uzbekistan, 2023, Art. no. 060009, doi: 10.1063/5.0115527.

[4] M. Farhadi, M. Shahrokhi, and S. H. A. Rahmati, ''Developing a supplier selection model based on Markov chain and probability tree for a k-out-of-N system with different quality of spare parts,'' *Rel. Eng. Syst. Saf.*, vol. 222, Jun. 2022, Art. no. 108387, doi: 10.1016/j.ress.2022.108387.

[5] M. Oszczypała, J. Ziółkowski, and J. Małachowski, ''Reliability analysis of military vehicles based on censored failures data,'' *Appl. Sci.*, vol. 12, no. 5, p. 2622, Mar. 2022, doi: 10.3390/app12052622.

[6] M. Oszczypała, J. Ziółkowski, and J. Małachowski, ''Semi-Markov approach for reliability modelling of light utility vehicles,'' *Eksploatacja I Niezawodnośc-Maintenance Rel.*, vol. 25, no. 2, Mar. 2023, Art. no. 161859, doi: 10.17531/ein/161859.

[7] G. Lvanovic, ''The reliability allocation application in vehicle design,'' *Int. J. Vehicle Design*, vol. 24, no. 2, pp. 274–286, 2000, doi: 10.1504/ijvd.2000.005186.

[8] S. Lolas and O. Olatunbosun, ''Prediction of vehicle reliability performance using artificial neural networks,'' *Exp. Syst. Appl.*, vol. 34, no. 4, pp. 2360–2369, May 2008, doi: 10.1016/j.eswa.2007.03.014.

[9] S. R. A. Barde, S. Yacout, and H. Shin, ''Optimal preventive maintenance policy based on reinforcement learning of a fleet of military trucks,'' *J. Intell. Manuf.*, vol. 30, no. 1, pp. 147–161, Jan. 2019, doi: 10.1007/s10845-016-1237-7.

[10] P. Popovic, G. Ivanovic, R. Mitrovic, and A. Subic, ''Design for reliability of a vehicle transmission system,'' *Proc. Inst. Mech. Eng., D, J. Automobile Eng.*, vol. 226, no. 2, pp. 194–209, Feb. 2012, doi: 10.1177/0954407011416175.

[11] X.-J. Yi, B. S. Dhillon, J. Shi, H.-N. Mu, and Z. Zhang, ''A new reliability analysis method for vehicle systems based on goal-oriented methodology,'' *Proc. Inst. Mech. Eng., D, J. Automobile Eng.*, vol. 231, no. 8, pp. 1066–1095, Jul. 2017, doi: 10.1177/0954407016671276.

[12] X. Shu, Y. Guo, H. Yang, H. Zou, and K. Wei, ''Reliability study of motor controller in electric vehicle by the approach of fault tree analysis,'' *Eng. Failure Anal.*, vol. 121, Mar. 2021, Art. no. 105165, doi: 10.1016/j.engfailanal.2020.105165.

[13] L. Yang, X. Zhang, Z. Lu, Y. Fu, D. Moens, and M. Beer, ''Reliability evaluation of a multi-state system with dependent components and imprecise parameters: A structural reliability treatment,'' *Rel. Eng. Syst. Saf.*, vol. 250, Oct. 2024, Art. no. 110240, doi: 10.1016/j.ress.2024.110240.

[14] G. Fang, R. Pan, and Y. Hong, ''Copula-based reliability analysis of degrading systems with dependent failures,'' *Rel. Eng. Syst. Saf.*, vol. 193, Jan. 2020, Art. no. 106618, doi: 10.1016/j.ress.2019.106618.

[15] Y.-K. Gu, C.-J. Fan, L.-Q. Liang, and J. Zhang, ''Reliability calculation method based on the copula function for mechanical systems with dependent failure,'' *Ann. Oper. Res.*, vol. 311, no. 1, pp. 99–116, Apr. 2022, doi: 10.1007/s10479-019-03202-5.

[16] E. Mahmoudi, R. S. Meshkat, and H. Torabi, ''Copula-based reliability for weighted-k-out-of-n systems having randomly chosen components of m different types,'' *IEEE Trans. Rel.*, vol. 71, no. 2, pp. 630–639, Jun. 2022, doi: 10.1109/TR.2021.3074472.

[17] C. Yang, X. Gu, and F. Zhao, ''Reliability analysis of degrading systems based on time-varying copula,'' *Microelectron. Rel.*, vol. 136, Sep. 2022, Art. no. 114628, doi: 10.1016/j.microrel.2022.114628.

[18] Y. Zheng and Y. Zhang, ''Reliability analysis for system with dependent components based on survival signature and copula theory,'' *Rel. Eng. Syst. Saf.*, vol. 238, Oct. 2023, Art. no. 109402, doi: 10.1016/j.ress.2023.109402.

[19] S. Wu, ''Construction of asymmetric copulas and its application in two-dimensional reliability modelling,'' *Eur. J. Oper. Res.*, vol. 238, no. 2, pp. 476–485, Oct. 2014, doi: 10.1016/j.ejor.2014.03.016.

[20] Z. Luo, C. Liu, and S. Liu, "A novel fault prediction method of wind turbine gearbox based on pair-copula construction and BP neural network," *IEEE Access*, vol. 8, pp. 91924–91939, 2020, doi: 10.1109/ACCESS.2020.2994077.
[21] Z. W. Birnbaum, "On the importance of different components in a multicomponent system," in *Multivariate Analysis-II*. New York, NY, USA: Academic Press, 1969, pp. 581–592.
[22] H. Pham, *Handbook of Reliability Engineering*. New York, NY, USA: Springer, 2003.
[23] W. Kuo and X. Zhu, "Some recent advances on importance measures in reliability," *IEEE Trans. Rel.*, vol. 61, no. 2, pp. 344–360, Jun. 2012, doi: 10.1109/TR.2012.2194196.
[24] K. P. Amrutkar and K. K. Kamalja, "An overview of various importance measures of reliability system," *Int. J. Math., Eng. Manage. Sci.*, vol. 2, no. 3, pp. 150–171, Sep. 2017, doi: 10.33889/ijmems.2017.2.3-014.
[25] P. Miziula and J. Navarro, "Birnbaum importance measure for reliability systems with dependent components," *IEEE Trans. Rel.*, vol. 68, no. 2, pp. 439–450, Jun. 2019, doi: 10.1109/TR.2019.2895400.
[26] H. Dui, S. Si, and R. C. M. Yam, "Importance measures for optimal structure in linear consecutive-k-out-of-n systems," *Rel. Eng. Syst. Saf.*, vol. 169, pp. 339–350, Jan. 2018, doi: 10.1016/j.ress.2017.09.015.
[27] W. S. Griffith, "Multistate reliability models," *J. Appl. Probab.*, vol. 17, no. 3, pp. 735–744, Sep. 1980, doi: 10.2307/3212967.
[28] S. Eryilmaz and A. R. Bozbulut, "Computing marginal and joint Birnbaum, and Barlow–Proschan importances in weighted-k-out-of-n: G systems," *Comput. Ind. Eng.*, vol. 72, pp. 255–260, Jun. 2014, doi: 10.1016/j.cie.2014.03.025.
[29] K.-A. Nguyen, P. Do, and A. Grall, "Joint predictive maintenance and inventory strategy for multi-component systems using Birnbaum's structural importance," *Rel. Eng. Syst. Saf.*, vol. 168, pp. 249–261, Dec. 2017, doi: 10.1016/j.ress.2017.05.034.
[30] S. Wu and F. P. A. Coolen, "A cost-based importance measure for system components: An extension of the Birnbaum importance," *Eur. J. Oper. Res.*, vol. 225, no. 1, pp. 189–195, Feb. 2013, doi: 10.1016/j.ejor.2012.09.034.
[31] S. Si, H. Dui, X. Zhao, S. Zhang, and S. Sun, "Integrated importance measure of component states based on loss of system performance," *IEEE Trans. Rel.*, vol. 61, no. 1, pp. 192–202, Mar. 2012, doi: 10.1109/TR.2011.2182394.
[32] J. E. Ramirez-Marquez and D. W. Coit, "Composite importance measures for multi-state systems with multi-state components," *IEEE Trans. Rel.*, vol. 54, no. 3, pp. 517–529, Sep. 2005, doi: 10.1109/TR.2005.853444.
[33] H. Dui, S. Si, S. Wu, and R. C. M. Yam, "An importance measure for multistate systems with external factors," *Rel. Eng. Syst. Saf.*, vol. 167, pp. 49–57, Nov. 2017, doi: 10.1016/j.ress.2017.05.016.
[34] H. Dui, L. Chen, and J. Li, "Importance analysis in two kinds of redundant systems: K-out-of-n and consecutive k-out-of-n: F systems," *Adv. Mech. Eng.*, vol. 11, no. 1, pp. 1–13, Jan. 2019, doi: 10.1177/1687814018819248.
[35] H. Dui, X. Wei, and L. Xing, "A new multi-criteria importance measure and its applications to risk reduction and safety enhancement," *Rel. Eng. Syst. Saf.*, vol. 235, Jul. 2023, Art. no. 109275, doi: 10.1016/j.ress.2023.109275.
[36] S. Qiu, X. Ming, M. Sallak, and J. Lu, "A Birnbaum importance-based two-stage approach for two-type component assignment problems," *Rel. Eng. Syst. Saf.*, vol. 218, Feb. 2022, Art. no. 108051, doi: 10.1016/j.ress.2021.108051.
[37] X. Zhu, Y. Fu, T. Yuan, and X. Wu, "Birnbaum importance based heuristics for multi-type component assignment problems," *Rel. Eng. Syst. Saf.*, vol. 165, pp. 209–221, Sep. 2017, doi: 10.1016/j.ress.2017.04.018.
[38] R. Chen, C. Zhang, S. Wang, E. Zio, H. Dui, and Y. Zhang, "Importance measures for critical components in complex system based on copula hierarchical Bayesian network," *Rel. Eng. Syst. Saf.*, vol. 230, Feb. 2023, Art. no. 108883, doi: 10.1016/j.ress.2022.108883.
[39] P. Do and C. Bérenguer, "Conditional reliability-based importance measures," *Rel. Eng. Syst. Saf.*, vol. 193, Jan. 2020, Art. no. 106633, doi: 10.1016/j.ress.2019.106633.
[40] A. Borucka, "Three-state Markov model of using transport means," in *Proc. 18th Int. Sci. Conf. Bus. Logistics Modern Manag.*, Osijek, Croatia, 2018, pp. 3–19.
[41] K. Wifvat, J. Kumerow, and A. Shemyakin, "Copula model selection for vehicle component failures based on warranty claims," *Risks*, vol. 8, no. 2, p. 56, Jun. 2020, doi: 10.3390/risks8020056.
[42] J. Selech and K. Andrzejczak, "An aggregate criterion for selecting a distribution for times to failure of components of rail vehicles," *Eksploatacja I Niezawodność-Maintenance Rel.*, vol. 22, no. 1, pp. 102–111, Mar. 2020, doi: 10.17531/ein.2020.1.12.
[43] F. L. Spizzichino, "On the probabilistic meaning of copula-based extensions of fuzzy measures. Applications to target-based utilities and multi-state reliability systems," *Fuzzy Sets Syst.*, vol. 354, pp. 1–19, Jan. 2019, doi: 10.1016/j.fss.2018.01.011.
[44] F. Sun, N. Wang, X. Li, and W. Zhang, "Remaining useful life prediction for a machine with multiple dependent features based on Bayesian dynamic linear model and copulas," *IEEE Access*, vol. 5, pp. 16277–16287, 2017, doi: 10.1109/ACCESS.2017.2735966.
[45] Y. Zhao, Q. Liu, J. Kuang, K. Xie, and W. Du, "Modeling multivariate dependence by nonparametric pair-copula construction in composite system reliability evaluation," *Int. J. Electr. Power Energy Syst.*, vol. 124, Jan. 2021, Art. no. 106373, doi: 10.1016/j.ijepes.2020.106373.
[46] P. Wang, Z. Lu, K. Zhang, S. Xiao, and Z. Yue, "Copula-based decomposition approach for the derivative-based sensitivity of variance contributions with dependent variables," *Rel. Eng. Syst. Saf.*, vol. 169, pp. 437–450, Jan. 2018, doi: 10.1016/j.ress.2017.09.012.
[47] M. B. Ghalibaf, "Relationship between Kendall's tau correlation and mutual information," *Revista Colombiana de Estadística*, vol. 43, no. 1, pp. 3–20, Jan. 2020, doi: 10.15446/rce.v43n1.78054.
[48] Y. Liu and Y. Chen, "Dynamic reliability evaluation of high-speed train gearbox based on copula function," *IEEE Access*, vol. 10, pp. 51792–51803, 2022, doi: 10.1109/ACCESS.2022.3174043.
[49] Y. Kim, J. Lim, and D. Park, "Testing independence of bivariate interval-censored data using modified Kendall's tau statistic," *Biometrical J.*, vol. 57, no. 6, pp. 1131–1145, Nov. 2015, doi: 10.1002/bimj.201300162.
[50] J.-J. Hsieh, "Estimation of Kendall's tau from censored data," *Comput. Statist. Data Anal.*, vol. 54, no. 6, pp. 1613–1621, Jun. 2010, doi: 10.1016/j.csda.2010.01.015.
[51] D. Beaudoin, T. Duchesne, and C. Genest, "Improving the estimation of Kendall's tau when censoring affects only one of the variables," *Comput. Statist. Data Anal.*, vol. 51, no. 12, pp. 5743–5764, Aug. 2007, doi: 10.1016/j.csda.2006.09.044.
[52] M. G. Kendall, *Rank Correlation Methods. in Rank Correlation Methods*. London, U.K.: Griffin, 1962.
[53] W. Wang and M. T. Wells, "Estimation of Kendall's tau under censoring," *Statistica Sinica*, vol. 10, no. 4, pp. 1199–1215, 2000.
[54] L. Lakhal, L.-P. Rivest, and D. Beaudoin, "IPCW estimator for Kendall's tau under bivariate censoring," *Int. J. Biostatistics*, vol. 5, no. 1, pp. 1–20, Jan. 2009, doi: 10.2202/1557-4679.1121.
[55] I. D. Ha, "ML estimation using Poisson HGLM approach in semi-parametric frailty models," *J. Korean Data Inf. Sci. Soc.*, vol. 27, no. 5, pp. 1389–1397, Sep. 2016, doi: 10.7465/jkdi.2016.27.5.1389.
[56] C. Genest, B. Rémillard, and D. Beaudoin, "Goodness-of-fit tests for copulas: A review and a power study," *Insurance, Math. Econ.*, vol. 44, no. 2, pp. 199–213, Apr. 2009, doi: 10.1016/j.insmatheco.2007.10.005.
[57] S. Mukherjee, Y. Lee, J.-M. Kim, J. Jang, and J.-S. Park, "Construction of bivariate asymmetric copulas," *Commun. Stat. Appl. Methods*, vol. 25, no. 2, pp. 217–234, Mar. 2018, doi: 10.29220/csam.2018.25.2.217.
[58] I. Kojadinovic and J. Yan, "Modeling multivariate distributions with continuous margins using the copula R package," *J. Stat. Softw.*, vol. 34, no. 9, pp. 1–20, 2010, doi: 10.18637/jss.v034.i09.
[59] E. L. Kaplan and P. Meier, "Nonparametric estimation from incomplete observations," *J. Amer. Stat. Assoc.*, vol. 53, no. 282, pp. 457–481, Jun. 1958, doi: 10.1080/01621459.1958.10501452.
[60] B. W. Turnbull, "The empirical distribution function with arbitrarily grouped, censored and truncated data," *J. Roy. Stat. Soc. Ser. B, Stat. Methodol.*, vol. 38, no. 3, pp. 290–295, Jul. 1976.
[61] M. Catelani, L. Ciani, and M. Venzi, "Sensitivity analysis with MC simulation for the failure rate evaluation and reliability assessment," *Measurement*, vol. 74, pp. 150–158, Oct. 2015, doi: 10.1016/j.measurement.2015.07.003.
[62] M. Oszczypała, J. Konwerski, J. Ziółkowski, and J. Małachowski, "Reliability analysis and redundancy optimization of k-out-of-n systems with random variable K using continuous time Markov chain and Monte Carlo simulation," *Rel. Eng. Syst. Saf.*, vol. 242, Feb. 2024, Art. no. 109780, doi: 10.1016/j.ress.2023.109780.
[63] B. Jafary, A. Mele, and L. Fiondella, "Component-based system reliability subject to positive and negative correlation," *Rel. Eng. Syst. Saf.*, vol. 202, Oct. 2020, Art. no. 107058, doi: 10.1016/j.ress.2020.107058.

[64] Z. Ye, Z. Cai, F. Zhou, J. Zhao, and P. Zhang, "Reliability analysis for series manufacturing system with imperfect inspection considering the interaction between quality and degradation," *Rel. Eng. Syst. Saf.*, vol. 189, pp. 345–356, Sep. 2019, doi: 10.1016/j.ress.2019.05.005.

[65] S. Qiu and X. Ming, "A fuzzy universal generating function-based method for the reliability evaluation of series systems with performance sharing between adjacent units under parametric uncertainty," *Fuzzy Sets Syst.*, vol. 424, pp. 155–169, Nov. 2021, doi: 10.1016/j.fss.2020.08.013.

[66] S. Li, X. Chi, and B. Yu, "An improved particle swarm optimization algorithm for the reliability–redundancy allocation problem with global reliability," *Rel. Eng. Syst. Saf.*, vol. 225, Sep. 2022, Art. no. 108604, doi: 10.1016/j.ress.2022.108604.

[67] S. Ahmadi, S. Moosazadeh, M. Hajihassani, H. Moomivand, and M. M. Rajaei, "Reliability, availability and maintainability analysis of the conveyor system in mechanized tunneling," *Measurement*, vol. 145, pp. 756–764, Oct. 2019, doi: 10.1016/j.measurement.2019.06.009.

[68] J. F. Espiritu, D. W. Coit, and U. Prakash, "Component criticality importance measures for the power industry," *Electric Power Syst. Res.*, vol. 77, nos. 5–6, pp. 407–420, Apr. 2007, doi: 10.1016/j.epsr.2006.04.003.

[69] F. Yalcin and C. Franko, "Computing Birnbaum and Barlow–Proschan importance measures using system signature," *Commun. Statist.-Theory Methods*, vol. 51, no. 23, pp. 8446–8457, Dec. 2022, doi: 10.1080/03610926.2021.1986536.

[70] E. C. Fitch, *Proactive Maintenance for Mechanical Systems*. Amsterdam, The Netherlands: Elsevier, 2013.

[71] T. Wu, X. Ma, L. Yang, and Y. Zhao, "Proactive maintenance scheduling in consideration of imperfect repairs and production wait time," *J. Manuf. Syst.*, vol. 53, pp. 183–194, Oct. 2019, doi: 10.1016/j.jmsy.2019.09.011.

[72] C. Senthil and R. Sudhakara Pandian, "Proactive maintenance model using reinforcement learning algorithm in rubber industry," *Processes*, vol. 10, no. 2, p. 371, Feb. 2022, doi: 10.3390/pr10020371.

[73] A. Prajapati, J. Bechtel, and S. Ganesan, "Condition based maintenance: A survey," *J. Quality Maintenance Eng.*, vol. 18, no. 4, pp. 384–400, Oct. 2012, doi: 10.1108/13552511211281552.

[74] E. Quatrini, F. Costantino, G. Di Gravio, and R. Patriarca, "Condition-based maintenance—An extensive literature review," *Machines*, vol. 8, no. 2, p. 31, Jun. 2020, doi: 10.3390/machines8020031.

[75] E. Ingemarsdotter, M. L. Kambanou, E. Jamsin, T. Sakao, and R. Balkenende, "Challenges and solutions in condition-based maintenance implementation—A multiple case study," *J. Cleaner Prod.*, vol. 296, May 2021, Art. no. 126420, doi: 10.1016/j.jclepro.2021.126420.

MATEUSZ OSZCZYPAŁA received the M.Eng. degree in logistics with movement and transportation specialization from the Military University of Technology, Warsaw, Poland, in 2017, where he is currently pursuing the Ph.D. degree with the Faculty of Mechanical Engineering. He is a Senior Engineer with the Faculty of Mechanical Engineering, Military University of Technology. His research interests include artificial neural networks, reliability modeling, and optimization.

JAKUB KONWERSKI received the M.Eng. degree in mechanical engineering with military logistics specialization from the Military University of Technology, Warsaw, Poland, in 2011, where he is currently pursuing the Ph.D. degree with the Faculty of Mechanical Engineering. His research interests include reliability, availability, and maintenance of systems modeling.

JAROSŁAW ZIÓŁKOWSKI received the Ph.D. degree, in 2004. He is currently with the Faculty of Mechanical Engineering, Military University of Technology, Warsaw, Poland. His research interests include reliability, mathematical analysis, transportation, and optimization methods.

JERZY MAŁACHOWSKI is currently the Dean of the Faculty of Mechanical Engineering, Military University of Technology, Warsaw. He has been a participant (manager/contractor) in several national and international projects focused on scientific, development, and implementation work. He is constantly cooperating with numerous scientific and academic units in Europe and the USA. He belongs to five scientific societies and reviews publications in more than 70 JCR-listed scientific journals. He is the author/co-author of more than 600 publications. His research interests include the computer methods of mechanics, biomedical engineering, and advanced computer engineering. He was a recipient of NATO and the U.S. Research Council Foundation Grants.